

USDOT Spectrum Sharing Test Report:

Effects of Unlicensed-National Information Infrastructure-3 (U-NII-3) Devices on Dedicated Short-Range Communications (DSRC)



January 2020 DRAFT Version 0.5

Prepared for:

U.S. Department of Transportation
Intelligent Transportation Systems Joint Program Office
1200 New Jersey Avenue, SE
Washington, D.C. 20590



U.S. Department of Transportation

Notice

This document is disseminated under the sponsorship of the Department of Transportation in the interest of information exchange. The United States Government assumes no liability for the contents or use thereof.

The United States Government does not endorse products or manufacturers. Trade or manufacturers' names appear herein solely because they are considered essential to the objective of this report.

REPORT DOCUMENTATION PAGE		<i>Form Approved</i> <i>OMB No. 0704-0188</i>
Public reporting burden for this collection of information is estimated to average 1 hour per response, including the time for reviewing instructions, searching existing data sources, gathering and maintaining the data needed, and completing and reviewing the collection of information. Send comments regarding this burden estimate or any other aspect of this collection of information, including suggestions for reducing this burden, to Washington Headquarters Services, Directorate for Information Operations and Reports, 1215 Jefferson Davis Highway, Suite 1204, Arlington, VA 22202-4302, and to the Office of Management and Budget, Paperwork Reduction Project (0704-0188), Washington, DC 20503.		
1. AGENCY USE ONLY (Leave blank)	2. REPORT DATE March 2020	3. REPORT TYPE AND DATES COVERED Test Report, 2015-2020
4. TITLE AND SUBTITLE USDOT Spectrum Sharing Test Report: Effects of Unlicensed-National Information Infrastructure-3 (U-NII-3) Devices on Dedicated Short-Range Communications (DSRC)		5a. FUNDING NUMBERS
6. AUTHOR(S) U.S. DOT/Office of the Assistant Secretary for Technology and Research (OST-R): James Arnold (OST-R) Jeffrey Bellone (Volpe National Transportation Systems Center) Alan Chachich (Volpe National Transportation Systems Center) Walton Fehr (Volpe National Transportation Systems Center) Jingsi Shaw (Volpe National Transportation Systems Center) Suzanne M. Sloan (Volpe National Transportation Systems Center) Evan Sullivan (Volpe National Transportation Systems Center) U.S. DOT/Federal Highway Administration: Volker Fessmann (FHWA) U.S. DOT/Intelligent Transportation Systems Joint Program Office: Jonathan B. Walker (ITS JPO) U.S. DOT/National Highway Traffic Safety Administration: Steve Stasko (NHTSA)		5b. CONTRACT NUMBER None
7. PERFORMING ORGANIZATION NAME(S) AND ADDRESS(ES) U.S. Department of Transportation Office of the Assistant Secretary for Research and Technology John A Volpe National Transportation Systems Center 55 Broadway Cambridge, MA 02142-1093 And U.S. Department of Transportation Office of the Assistant Secretary for Research and Technology Federal Highway Administration National Highway Traffic Safety Administration 1200 New Jersey Ave, S.E. Washington, D.C. 20590 And U.S. Department of Transportation Turner-Fairbank Highway Research Center 6300 Georgetown Pike McLean, VA 22101		8. PERFORMING ORGANIZATION REPORT NUMBER TBD
9. SPONSORING/MONITORING AGENCY NAME(S) AND ADDRESS(ES) U.S. Department of Transportation Intelligent Transportation Systems Joint Program Office Washington, DC 1200 New Jersey Avenue, SE Washington, DC 20590		10. SPONSORING/MONITORING AGENCY REPORT NUMBER N/A
11. SUPPLEMENTARY NOTES		

None			
12a. DISTRIBUTION/AVAILABILITY STATEMENT None		12b. DISTRIBUTION CODE None	
13. ABSTRACT (Maximum 200 words) This document reports the results of testing to characterize the existing radio frequency signal environment. Specifically, the USDOT's test plan sought to identify the interference impacts to transportation's 5.9 GHz Dedicated Short-Range Communications (DSRC) operations from today's unlicensed Wi-Fi devices (known as unlicensed national information infrastructure devices operating in the third 5GHz band, or U-NII-3 devices) if they were to operate in the 5850-5925 MHz band and adjacent bands. In order to accomplish this work the USDOT developed the capability to evaluate proposed band sharing mechanisms via laboratory and field testing, noting that the ability to test wireless systems at full scale and high speed is challenging and unique. As per Congressional direction provided to the USDOT, the FCC, and the National Telecommunications and Information Administration (NTIA) in 2015, the results are intended to provide data to deployment scale modeling by NTIA and allow further collaboration with the FCC to provide Congress with factual information on the impacts to DSRC operations from unlicensed devices in the band. A planned follow-on Phase II will use the results of testing documented in this report to form a baseline for testing UNII-4 devices with sharing mechanisms proposed to mitigate these interference impacts.			
14. SUBJECT TERMS DSRC, U-NII, ITS, Dedicated Short-Range Communications, Unlicensed National Information Infrastructure, Intelligent Transportation Systems, Radio Frequency Interference, V2V, V2I, V2X, IEEE 802.11, Wi-Fi Access Points, wireless testing		15. NUMBER OF PAGES 150	
		16. PRICE CODE N/A	
17. SECURITY CLASSIFICATION OF REPORT Unclassified	18. SECURITY CLASSIFICATION OF THIS PAGE Unclassified	19. SECURITY CLASSIFICATION OF ABSTRACT Unclassified	20. LIMITATION OF ABSTRACT Unlimited

NSN 7540-01-280-5500

Standard Form 298 (Rev. 2-89)
Prescribed by ANSI Std. Z39-18
298-102

Version History

Version				Approval	
#	Author/editor	Date	Changes	By	Date
0	Chachich	9/20/2018	Incomplete Draft – included inputs from framework exercise. Updated URLs in the Introduction.		
0.1	Chachich	6/6/2019	Wrote chapters 1-5 and started chapters 6-10 incorporating inputs from Walt Fehr, Jim Arnold, Chris Henry, Steve Oates and Jim Buxton. Created table of contents.		
0.2	Buxton, Fehr	7/10/2019	Supplied new material for chapter 4 and made edits		
0.3	Chachich	11/22/2019	Chapter 10 analysis of building tests, begin chapter 7 description of testing, corrections to chapters 1-5.		
0.4	Chachich	11/31/2019	New material for chapters 6 & 7. Created tables of figures and tables. Added adjacent channel field measurements to chapter 9.		
0.5	Bellone	1/15/2020	Proofread and edit		
0.6	Sloan	3/11/2020	Prepared for publication as a draft.		

SI* (MODERN METRIC) CONVERSION FACTORS					
APPROXIMATE CONVERSIONS TO SI UNITS					
Symbol	When You Know	Multiply By	To Find	Symbol	
LENGTH					
in	inches	25.4	millimeters	mm	
ft	feet	0.305	meters	m	
yd	yards	0.914	meters	m	
mi	miles	1.61	kilometers	km	
AREA					
in²	square inches	645.2	square millimeters	mm ²	
ft²	square feet	0.093	square meters	m ²	
yd²	square yard	0.836	square meters	m ²	
ac	acres	0.405	hectares	ha	
mi²	square miles	2.59	square kilometers	km ²	
VOLUME					
fl oz	fluid ounces	29.57	milliliters	mL	
gal	gallons	3.785	liters	L	
ft³	cubic feet	0.028	cubic meters	m ³	
yd³	cubic yards	0.765	cubic meters	m ³	
NOTE: volumes greater than 1000 L shall be shown in m³					
MASS					
oz	ounces	28.35	grams	g	
lb	pounds	0.454	kilograms	kg	
T	short tons (2000 lb)	0.907	megagrams (or "metric ton")	Mg (or "t")	
oz	ounces	28.35	grams	g	
TEMPERATURE (exact degrees)					
°F	Fahrenheit	5 (F-32)/9 or (F-32)/1.8	Celsius	°C	
ILLUMINATION					
fc	foot-candles	10.76	lux	lx	
fl	foot-Lamberts	3.426	candela/m ²	cd/m ²	
FORCE and PRESSURE or STRESS					
lbf	poundforce	4.45	newtons	N	
lbf/in²	poundforce per square inch	6.89	kilopascals	kPa	

*SI is the symbol for the International System of Units. Appropriate rounding should be made to comply with Section 4 of ASTM E380. (Revised March 2003)

DRAFT

SI* (MODERN METRIC) CONVERSION FACTORS				
APPROXIMATE CONVERSIONS FROM SI UNITS				
Symbol	When You Know	Multiply By	To Find	Symbol
LENGTH				
mm	millimeters	0.039	inches	in
m	meters	3.28	feet	ft
m	meters	1.09	yards	yd
km	kilometers	0.621	miles	mi
AREA				
mm²	square millimeters	0.0016	square inches	in ²
m²	square meters	10.764	square feet	ft ²
m²	square meters	1.195	square yards	yd ²
ha	hectares	2.47	acres	ac
km²	square kilometers	0.386	square miles	mi ²
VOLUME				
mL	milliliters	0.034	fluid ounces	fl oz
L	liters	0.264	gallons	gal
m³	cubic meters	35.314	cubic feet	ft ³
m³	cubic meters	1.307	cubic yards	yd ³
mL	milliliters	0.034	fluid ounces	fl oz
MASS				
g	grams	0.035	ounces	oz
kg	kilograms	2.202	pounds	lb
Mg (or "t")	megagrams (or "metric ton")	1.103	short tons (2000 lb)	T
g	grams	0.035	ounces	oz
TEMPERATURE (exact degrees)				
°C	Celsius	1.8C+32	Fahrenheit	°F
ILLUMINATION				
lx	lux	0.0929	foot-candles	fc
cd/m²	candela/m ²	0.2919	foot-Lamberts	fl
FORCE and PRESSURE or STRESS				
N	newtons	0.225	poundforce	lbf
kPa	Kilopascals	0.145	poundforce per square inch	lbf/in ²

*SI is the symbol for the International System of Units. Appropriate rounding should be made to comply with Section 4 of ASTM E380. (Revised March 2003)

Table of Contents

List of Figures	x
List of Tables.....	xxii
List of Abbreviations.....	xxiv
Preface.....	1
Executive Summary	4
1. Introduction	8
2. Goals and Objectives	14
2.1 USDOT Goals	14
2.2 Desired Outcomes.....	14
2.3 Analysis Plan Objectives.....	14
2.4 Progress.....	15
3. Description of DSRC devices under test.....	20
3.1 Cohda DSRC Devices	21
3.2 DSRC Traffic Generation.....	23
4. Description of the UNII testbed.....	40
4.1 UNII testbed	41
4.2 Wi-Fi Traffic Generation.....	47
4.3 Characterization of Wi-Fi	54
4.4 Inter-packet gap versus channel loading	69
5. Description of Facilities.....	79
5.1 Lab – ATEC (APG)	79
5.2 Lab – ARL (APG).....	80
5.3 Lab – CERDEC (APG)	81
5.4 Mobile Facilities – ATEC (APG).....	82
5.5 Field Site – Zone 1 & Zone 2 at Phillips Army Airfield (APG).....	83
5.6 Field Site – ATEF Course (APG).....	86
5.7 Field Site – Dynamometer Test Facility (APG)	86
5.8 Field Site – Perryman Test Area (APG).....	87
5.9 Lab – NTIA (ITS-Boulder)	90
5.10 Field Site – Table Mountain (ITS-Boulder)	91
6. Calibrations and Preparatory Measurements	94

6.1	Power Calibrations	95
6.2	Antenna Characterization and Calibrations	102
6.3	Surrogate U-NII-4 Setup and Verification	113
6.4	DSRC Setup and Verification	116
6.5	Baseline Environmental Signal Data Collection	120
7.	Description of Testing	124
7.1	Baseline Testing	127
7.2	Interference Testing.....	144
7.3	DSRC Band Background Noise Level Analysis	152
7.4	Detectability Analysis between DSRC and U-NII-4 devices.....	153
8.	Description of Data Collection, Processing and Analysis	154
8.1	Data Collection.....	154
8.2	Data Analysis.....	156
9.	Test Results	166
9.1	Baseline Measurements.....	167
9.2	Packet Collision	206
9.3	Packet suppression via EDCA	228
9.4	Impact on signal-to-noise	230
9.5	Out-of-channel interference.....	232
9.6	UNII in vehicle	244
10.	Environmental Variation.....	245
10.1	Building tests.....	245
10.2	Effect of Foliage	331
10.3	Precipitation and pavement condition	333
11.	Comparison with other published results.....	335
12.	Lessons Learned	335
13.	Conclusions	335
14.	Potential next steps.....	335
15.	References	335
Appendix A: DSRC Terminology		337
Appendix B: Mapping this report to the test plan.....		339
Appendix C: Clear Channel Access Mechanism		340
C.1	First excerpt to explain what happens in the time between packets:	340

C.2 Second excerpt to explain EDCA parameters: 342

Appendix D: Experimental License345

Appendix E: Radio Calibrations345

Appendix F: Antenna Patterns345

Appendix G: DSRC Baselines345

Appendix H: Surrogate UNII-4 Testbed Baselines.....345

Appendix I: Sensitivity Testing345

Appendix J: Effect of the Wi-Fi inter-packet space distribution on interference346

Appendix K: Adjacent Channel Sensitivity and Interference.....346

Appendix L: Transmission Suppression and EDCA configurations.....346

Appendix M: EDCA channel access whitepaper346

Appendix N: DSRC Radio Density Study.....346

Appendix O: Outdoor Access Point Interference Data.....347

Appendix P: Indoor Access Point Interference Data.....347

Appendix Q: Wi-Fi In-Vehicle Access Point Interference Data347

Appendix R: High Closing Speed near Access Point Interference Data347

Appendix S: Maximum Range DSRC and UNII Data348

Appendix T: 40 DSRC Radio Interference Data.....348

Appendix U: Interference Data under Rain, Snow, and Pavement wet versus dry348

List of Figures

Figure 1-1: DSRC Channel Plan in the ITS Band 9

Figure 1-2: DSRC channel number designations for both 10 and 20MHz channels 9

Figure 1-3: Proposed U-NII-4 band (“NEW”)..... 10

Figure 1-4: Proposed U-NII-4 Wi-Fi channel overlap with the DSRC band 12

Figure 2-1. Progress on Phase 1 Spectrum Test Objectives 19

Figure 3-1 Cohda Mk V OBU (left) and RSU (right) 22

Figure 3-2. OSI model of wireless communication 23

Figure 3-3. OSI model details 25

Figure 3-4. 802.11 data frame..... 26

Figure 3-5. GUI created by ATC to interface with the Cohda DSRC radios 28

Figure 3-6. Arada from Safety Pilot Model Deployment..... 32

Figure 3-7. Cohda MK5 test device in “BSM” mode 33

Figure 3-8. Cohda MK5 test device in “Test” mode 35

Figure 3-9. Structure of the 802.11a Preamble 36

Figure 3-10. Timing of the OFDM PLCP Preamble 36

Figure 3-11. Components of the OFDM PLCP Preamble..... 36

Figure 3-12. Decomposition of the 802.11a PLCP frame 37

Figure 3-13. IEEE 802.11ac PPDU 38

Figure 4-1. Surrogate U-NII-4 Testbed diagram 41

Figure 4-2. Surrogate U-NII-4 Testbed photo 42

Figure 4-3. Surrogate U-NII-4 Testbed Access Point components 43

Figure 4-4. Surrogate U-NII-4 Testbed traffic generating components 44

Figure 4-5. Surrogate U-NII-4 Testbed Client inside (backside) 46

Figure 4-6. Surrogate U-NII-4 Testbed Client inside (antenna or front side)..... 47

Figure 4-7. Detailed Surrogate U-NII-4 Testbed diagram 49

Figure 4-8. Mathematical illustration of Uniform spacing, which is a Periodic distribution 50

Figure 4-9. Mathematical illustration of a Poisson distribution 50

Figure 4-10. Illustration of Periodic and Poisson distributions 51

Figure 4-11. Periodic distribution, 2% load, 96 pps 52

Figure 4-13. Periodic dist., 5% load, 241 pps 52

Figure 4-15. Periodic dist., 10% load, 482 pps 53

Figure 4-17. Periodic dist., 30% load, 1446 pps Figure 4-18. Poisson dist., 30% load, 1446 pps 53

Figure 4-19. Test location at Turner Fairbank Highway Research Center 55

Figure 4-20. Screenshot of AirPcap graphical user interface (GUI) 55

Figure 4-21. About windows of the MetaGeek capture tools used..... 56

Figure 4-22. Sample of streaming HD video 57

Figure 4-23. Interval of background management activity..... 58

Figure 4-24. Interval of intermittent management activity..... 58

Figure 4-25. Interval of bursty management activity 58

Figure 4-26. Sample of multiple streaming HD videos..... 59

Figure 4-27. Interval of background management activity..... 59

Figure 4-28. Interval of intermittent management activity..... 59

Figure 4-29. Interval of bursty management activity 60

Figure 4-30. iPad speed test..... 60

Figure 4-31. Channel 153 beacons and probes..... 60

Figure 4-32. Channel 149 beacons and probes..... 60

Figure 4-33. Channel 36 beacon and probe data..... 61

Figure 4-34. Channel 40 beacon and probe data..... 61

Figure 4-35. Channel 44 beacon and probe data..... 61

Figure 4-36. Channel 48 beacon and probe data..... 61

Figure 4-37. Apple laptop viewing Internet video 61

Figure 4-38. MotoX laptop viewing Internet video..... 61

Figure 4-39. Windows laptop viewing Internet video..... 62

Figure 4-40. Voice over IP session..... 62

Figure 4-41. Apple Facetime session..... 62

Figure 4-42. Apple Siri session 62

Figure 4-43. Access point streaming ultra HD video to a Smart TV 62

Figure 4-44. Everything in the lab running at the same time 63

Figure 4-45. Same devices 5 minutes later 63

Figure 4-46. UNII testbed beacons and probes..... 64

Figure 4-47. UNII testbed beacons and probes with DSRC..... 64

Figure 4-48. 2% Poisson UNII traffic load on channel 165 65

Figure 4-49. 2% Poisson UNII traffic load on channel 173 with DSRC 65

Figure 4-50. 5% Poisson UNII traffic load on channel 165 65

Figure 4-51. 5% Poisson UNII traffic load on channel 173 with DSRC 66

Figure 4-52. 10% Poisson UNII traffic load on channel 165 66

Figure 4-53. 10% Poisson UNII traffic load on channel 173 with DSRC 66

Figure 4-54. 20% Poisson UNII traffic load on channel 165 67

Figure 4-55. 20% Poisson UNII traffic load on channel 173 with DSRC 67

Figure 4-56. 30% Poisson UNII traffic load on channel 165 67

Figure 4-57. 30% Poisson UNII traffic load on channel 173 with DSRC 67

Figure 4-58. 70% Poisson UNII traffic load on channel 165 68

Figure 4-59. 70% Poisson UNII traffic load on channel 173 with DSRC 68

Figure 4-60. 100% Poisson UNII traffic load on channel 165 68

Figure 4-61. 100% Poisson UNII traffic load on channel 173 with DSRC 68

Figure 4-62. Measured gaps between UNII packets for various loadings 71

Figure 4-63. Packet splitting (1500 byte data at 10% load) 74

Figure 4-64. Wi-Fi management packets 75

Figure 4-65. Data packets NOT split (1400 byte data, 10% load) 76

Figure 4-66. Data packets and acknowledgements (300 byte data, 10% load)..... 77

Figure 4-67. Comparison of packet length at a 10% traffic loading..... 78

Figure 5-1. ATC high bay lab and Figure 5-2. ATC signal analysis..... 80

Figure 5-3: Measuring antenna patterns in large anechoic chamber..... 81

Figure 5-4 Data van outside and Figure 5-5 Data van workstations 82

Figure 5-6. ATC Mobile Field Office and Figure 5-7. MFO Inside 83

Figure 5-8: Zone 1 on Runway at Aberdeen Proving Ground 84

Figure 5-9: ATEF Test Track and Runways at Aberdeen Proving Ground 85

Figure 5-10. Dyno course with foliage and Figure 5-11. Dyno course foliage down 86

Figure 5-12: Dynotrack at Aberdeen Proving Ground 87

Figure 5-13. View down the Perryman site 3 mile straightaway 88

Figure 5-14: Test tracks at Aberdeen Proving Ground 89

Figure 5-15: Lab testing at NTIA ITS-Boulder 90

Figure 5-16: RF Backplane Testbed at NTIA ITS-Boulder 91

Figure 5-17: Table Mountain Field Measurement Site 92

Figure 5-18. Rohn Model 25G towers with PVC RSU mounting pole 93

Figure 5-19: Typical View of Table Mountain Measurement Site 93

Figure 6-1. ARL Power calibration diagram..... 96

Figure 6-2. RF Enclosures for calibration at ITS Boulder..... 97

Figure 6-3: Sample transmit calibration plot of a DSRC radio made at ARL 98

Figure 6-4: Sample receive calibration plot of a DSRC radio made at ARL 99

Figure 6-5. Sample calibration plot of a DSRC radio made at ITS-Boulder 100

Figure 6-6: Azimuthal antenna pattern of a vehicle DSRC antenna..... 104

Figure 6-7: Elevation antenna pattern of a vehicle DSRC antenna 105

Figure 6-8: Antenna pattern measurement on test vehicle in a CERDEC anechoic chamber 106

Figure 6-9: Vendor shark-fin antenna opened and Figure 6-10: Black whip antenna 106

Figure 6-11: Three antenna patterns, two shark fins (blue and red) and one whip (brown) 107

Figure 6-12: Variability in azimuth patterns across the vehicle mounted antennas used 108

Figure 6-13: Variability in elevation patterns across the vehicle mounted antennas used..... 109

Figure 6-14: DSRC azimuthal antenna patterns, RSU (blue) and OBU (orange) 110

Figure 6-15: DSRC elevation antenna patterns, RSU (blue) and OBU (orange) 110

Figure 6-16: VSWR measurement for a black whip antenna 112

Figure 6-17: Passenger van equipped for RF data collection..... 121

Figure 7-1: Research Activity Dependencies..... 121

Figure 7-2. DSRC Baseline Test Illustration 128

Figure 7-3. Surrogate U-NII-4 Baseline Test Illustration 128

Figure 7-4. UNII baselining – client on 18’ tripod, access point in white vehicle at Perryman test track 129

Figure 7-5. Phillips Army Airfield test facilities, Zone 1 at the left. Zone 2 at the right..... 130

Figure 7-7. Zone 2 – looking toward Zone 1 131

Figure 7-8. Test vehicles and tower at Table Mountain 138

Figure 7-9: Noise level comparison of Table Mountain versus Aberdeen Proving Grounds 141

Figure 7-10: RSSI comparison of Table Mountain versus Aberdeen Proving Grounds..... 142

Figure 7-11: Packet loss comparison of Table Mountain versus Aberdeen Proving Grounds..... 142

Figure 7-12: Wi-Fi stability affected by movement in the environment 143

Figure 7-13. Interferer set up as outdoor access point and client at Zone 1..... 145

Figure 7-14. Outdoor Access Point 146

Figure 7-15: Representative Outdoor Access Point scenario 146

Figure 7-16. Indoor Access Point 147

Figure 7-17: Representative indoor access point scenario 148

Figure 7-18. In-Vehicle access point 149

Figure 7-19: In-Vehicle Equipment 150

Figure 7-20: Representative example of unlicensed Devices Transmitting in a Vehicle 150

Figure 7-21. High speed V2V near access point 151

Figure 7-22. Multiple access points 152

Figure 8-3: RSSI and noise plot..... 159

Figure 8-4: Signal-to-noise ration plot 160

Figure 8-5: Packet error rate plot..... 161

Figure 9-1. Heights, Angles and Distances for the Two-Ray Model..... 168

Figure 9-2. Two-Ray Model showing RSSI null positions as a function of vehicle height and frequency (V2V case) 169

Figure 9-3. Two-Ray Model showing RSSI null positions from an RSU as a function of vehicle height (I2V case) 170

Figure 9-4. Two-Ray Model showing RSSI null positions as a function of equal RSU antenna heights (I2I case)..... 171

Figure 9-5. Two-Ray Model showing RSSI I2V null positions over a long range 172

Figure 9-6. Two-Ray Model showing RSSI I2V null positions over a short range..... 173

Figure 9-7. Effect of DSRC antenna elevation 174

Figure 9-8. Typical Zone 1 Baseline RSSI and noise level 175

Figure 9-9. Typical Zone 1 Baseline Signal-to-Noise ratio (SNR) 175

Figure 9-10. Typical Zone 1 Baseline Packet Error Rate (PER) 176

Figure 9-11. Typical Zone 1 Baseline gap analysis 176

Figure 9-12. Typical Zone 1 Baseline cumulative gap analysis..... 177

Figure 9-13. Typical Zone 1 Baseline radio count 177

Figure 9-14. Typical Zone 1 Baseline transmit latency (time between sends) 178

Figure 9-15. Typical Zone 1 Baseline geographical distribution of PER 178

Figure 9-16. Unclean Zone 1 V2V Baseline RSSI and noise level..... 179

Figure 9-17. Unclean Zone 1 V2V Baseline PER 179

Figure 9-18. Unclean Zone 1 Baseline gap analysis 180

Figure 9-19. Typical Perryman Baseline RSSI and noise level 180

Figure 9-20. Typical Perryman Baseline Signal-to-Noise ratio (SNR) 181

Figure 9-21. Typical Perryman Baseline Packet Error Rate (PER) 181

Figure 9-22. Typical Perryman Baseline gap analysis..... 182

Figure 9-23. Typical Perryman Baseline cumulative gap analysis..... 182

Figure 9-24. Typical Perryman Baseline geographical distribution of PER 183

Figure 9-25. Typical ATEF Baseline RSSI and noise level (EIRP=25 dBm) 184

Figure 9-26. Typical ATEF Baseline Signal-to-Noise ratio (EIRP=25 dBm)..... 185

Figure 9-27. Typical ATEF Baseline Packet Error Rate (EIRP=25 dBm)..... 186

Figure 9-28. Typical ATEF Baseline gap analysis (EIRP=25 dBm)..... 187

Figure 9-29. Typical ATEF Baseline cumulative gap analysis (EIRP=25 dBm)..... 188

Figure 9-30. Typical ATEF Baseline geographical distribution of PER (EIRP=25 dBm) 189

Figure 9-31. Recoil Avenue Baseline RSSI and noise level (EIRP=25 dBm) 190

Figure 9-32. Recoil Avenue Baseline geographical distribution of PER (EIRP=25 dBm) 192

Figure 9-33. Recoil Avenue Baseline Signal-to-Noise ratio (EIRP=25 dBm) 193

Figure 9-34. Recoil Avenue Baseline Packet Error Rate (EIRP=25 dBm) 194

Figure 9-35. Recoil Avenue Baseline gap analysis (EIRP=25 dBm)..... 195

Figure 9-36. Recoil Avenue Baseline cumulative gap analysis (EIRP=25 dBm) 196

Figure 9-37. Mulberry Point Baseline RSSI and noise level (EIRP=25 dBm)..... 197

Figure 9-38. Mulberry Point Baseline geographical distribution of PER (EIRP=25 dBm) 198

Figure 9-39. Mulberry Point Baseline Signal-to-Noise ratio (EIRP=25 dBm)..... 199

Figure 9-40. Mulberry Point Baseline Packet Error Rate (EIRP=25 dBm) 200

Figure 9-41. Mulberry Point Baseline gap analysis (EIRP=25 dBm) 201

Figure 9-42. Mulberry Point Baseline cumulative gap analysis (EIRP=25 dBm) 202

Figure 9-43. Wet Dynamometer Course Baseline RSSI and noise level..... 203

Figure 9-44. Wet Dynamometer Course Baseline Signal-to-Noise ratio (SNR)..... 203

Figure 9-45. Wet Dynamometer Course Baseline Packet Error Rate (PER) 204

Figure 9-46. Wet Dynamometer Course Baseline gap analysis 204

Figure 9-47. Wet Dynamometer Course Baseline cumulative gap analysis 205

Figure 9-48. Wet Dynamometer Course Baseline geographical distribution of PER 205

Figure 9-49. Bounding case: EIRPs, UNII=5 dBm, DSRC=25 dBm, UNII at 70% load 206

Figure 9-50. Bounding case: UNII traffic load at 20% 207

Figure 9-51. DSRC power increases range in the face of interferer..... 208

Figure 9-52. DSRC EIRP=15 dBm PER (left) and RSSI (right) both reveal the interferer’s deepest ground-bounce null. 208

Figure 9-53. DSRC power decreases gaps in the face of interferer but still significant 209

Figure 9-54. DSRC power decreases gaps in the face of interferer but still significant 209

Figure 9-55. Packet error rate increases as UNII power increases (DSRC EIRP=25 dBm)..... 210

Figure 9-56. Distribution of safety critical gaps worsens as UNII power increases (DSRC EIRP=25 dBm)..... 210

Figure 9-57. Proportion of safety critical gaps worsens as UNII power increases (DSRC EIRP=25 dBm)..... 210

Figure 9-58. Interference to DSRC levels out for Wi-Fi traffic loads above 30% 211

Figure 9-59. Packet Error Rate (PER) increases Wi-Fi traffic load 212

Figure 9-60. Safety critical gaps increase with Wi-Fi traffic load 213

Figure 9-61. Comparison of PER interference to DSRC by 1400 byte (solid) and 1500 byte (broken) Wi-Fi packets (V2V DSRC EIRP=25 dBm, UNII EIRP=17 dBm) 214

Figure 9-62. Comparison of PER interference to DSRC by 1400 byte (solid) and 300 byte (dashed) Wi-Fi packets (V2V DSRC EIRP=25 dBm, UNII EIRP=35 dBm) 215

Figure 9-63. Safety critical gaps worse with smaller with Wi-Fi packets 217

Figure 9-64 Comparison of Periodic and Poisson induced DSRC Packet Error Rate for 2% traffic load 219

Figure 9-65. Comparison of Periodic and Poisson induced DSRC Packet Error Rate for 3% traffic load 219

Figure 9-66. Comparison of Periodic and Poisson induced DSRC Packet Error Rate for 5 % traffic load 220

Figure 9-67. Comparison of Periodic and Poisson induced DSRC Packet Error Rate for 1 0% traffic load 221

Figure 9-68. Comparison of Periodic and Poisson induced DSRC Packet Error Rate for 15% traffic load 222

Figure 9-69. Comparison of Periodic and Poisson induced DSRC Packet Error Rate for 20% traffic load 222

Figure 9-70. Comparison of Periodic and Poisson induced DSRC Packet Error Rate for 30% traffic load 223

Figure 9-71. DSRC Packet Error Rate caused by Periodic distribution Wi-Fi traffic as a function of traffic load 224

Figure 9-72. DSRC Packet Error Rate caused by Poisson distribution Wi-Fi traffic as a function of traffic load 225

Figure 9-73. Comparison of the DSRC Packet Error Rates induced by Periodic and Poisson distributions as a function of traffic load vehicle driving away..... 226

Figure 9-74. Interference to DSRC [EIRP=20 dBm] by UNII [EIRP=20 dBm, 10% Poisson traffic] 227

Figure 9-75 Same thing but more frequently with serious gaps close in (50-100m) UNII EIRP at 17 dBm..... 228

Figure 9-76. Interference by CCA suppression to DSRC handheld transmitting near a Wi-Fi handheld..... 229

Figure 9-77. Interference by CCA suppression to full power DSRC transmitting near a Wi-Fi handheld..... 229

Figure 9-78. PER due to packet suppression increasing with UNII transmit power 230

Figure 9-79. Safety critical gaps due to packet suppression increasing with UNII transmit power 230

Figure 9-80. DSRC RSSI and noise as UNII interferer power increases 231

Figure 9-81. DSRC Signal-to-Noise as UNII interferer power increases 231

Figure 9-82 Block Diagram of Test Configuration 233

Figure 9-83. Receiver Sensitivity based on Packet Error Rate 235

Figure 9-84 Packet Completion rate for Channel 178..... 236

Figure 9-85. AWGN and Recorded DSRC impact on PER. 237

Figure 9-86, AWGN from channels 174, 176, and 178..... 238

Figure 9-87. S/J for UNII into DSRC channel 172..... 239

Figure 9-88. Packet error rate from adjacent channel interference, I2V 240

Figure 9-89. Gap analysis of adjacent channel interference, I2V 241

Figure 9-90. Geographical distribution of Packet error rate from adjacent channel interference, I2V .. 242

Figure 9-91. Geographical distribution of PER from adjacent channel interference, I2V close up 243

Figure 9-92. Signal-to-Noise ratio with adjacent channel interference, I2V 244

Figure 10-1. Filled cinderblock fire tower at ATEF 246

Figure 10-2. Aerial view of the fire tower near the ATEF test track. 246

Figure 10-3a. V2I Baseline PER departing 247

Figure 10-4a. View south from fire tower..... 248

Figure 10-5. RSSI and noise power plots, V2I, UNII EIRP=36 dBm, approaching Cinderblock building ... 249

Figure 10-6. Signal-to-Noise plots, V2I, UNII EIRP=36 dBm, approaching Cinderblock building 249

Figure 10-7. Packet Error Rate plots, V2I, UNII EIRP=36 dBm, approaching Cinderblock building..... 250

Figure 10-8. Packet gap plots, V2I, UNII EIRP=36 dBm, approaching Cinderblock building 251

Figure 10-9. Summary of packet gaps, V2I, UNII EIRP=36 dBm, approaching Cinderblock building 252

Figure 10-10. Geographical distribution of PER, V2I, UNII EIRP=36 dBm, approaching Cinderblock building 252

Figure 10-11. Comparing RSSI plots approaching and departing the fire tower, V2I EIRP=25 dBm 253

Figure 10-12. Geographical distribution of PER, V2I, UNII EIRP=36 dBm, departing Cinderblock building 254

Figure 10-13. Comparing packet gaps, V2I EIRP=25 dBm, UNII EIRP=31 dBm, Cinderblock building 254

Figure 10-14. Packet Error Rate plots, V2I, UNII EIRP=8 dBm, approaching Cinderblock building..... 255

Figure 10-15. Packet gap plots, V2I, UNII EIRP=8 dBm, approaching Cinderblock building 256

Figure 10-16. Effect of UNII power on packet gaps, V2I EIRP=25 dBm, approaching Cinderblock building 257

Figure 10-17. Comparing V2V and V2I RSSI plots both approaching and departing the fire tower, DSRC EIRP=25 dBm. Shows the complexity in simple power measurements due to multipath scatterers in the environment. 258

Figure 10-18. Comparing V2V and V2I PER, DSRC=25dBm, UNII EIRP=8 dBm, approaching Cinderblock building 259

Figure 10-19. Comparing V2V and V2I Packet gap distribution, DSRC=25dBm, UNII EIRP=8 dBm, approaching Cinderblock building 260

Figure 10-20. Comparing V2V and V2I Aggregate packet gap distribution, DSRC=25dBm, UNII EIRP=8 dBm, approaching Cinderblock building..... 261

Figure 10-21. Brick building with the surrogate UNII-4 interferer set up outside..... 262

Figure 10-22. Brick building with the surrogate UNII-4 interferer set up inside 262

Figure 10-23. Layout of the brick building tests..... 263

Figure 10-24: The start point, RSU, and environment west of the brick building. 264

Figure 10-25. Packet Error Rate, I2V, UNII EIRP=35 dBm, 70% load, passing brick building shows effect of windows 265

Figure 10-26. Packet Error Rate, I2V, UNII EIRP=35 dBm, 10% load, passing brick building shows effect of windows with light Wi-Fi traffic 265

Figure 10-27. Packet Error Rate, I2V, UNII EIRP=35 dBm, 10% load, passing brick building shows effect of windows with light Wi-Fi traffic 267

Figure 10-28. Packet Error Rate, I2V UNII outside, UNII EIRP=35 dBm, at short range..... 268

Figure 10-29. Packet Error Rate, I2V, UNII EIRP=8 dBm, 10% load, passing brick building shows effect of windows with light Wi-Fi traffic at very low power 269

Figure 10-30. Packet gap distribution, I2V, UNII EIRP=35 dBm, 10% load, passing brick building shows that large PER correlates with large packet gaps 270

Figure 10-31. Correlation between PER and Packet gap distribution, I2V, UNII EIRP=35 dBm, 10% load, UNII inside brick building with windows..... 271

Figure 10-32. PER and Packet gap distribution, UNII EIRP=35 dBm, 10% load, drive by brick building with windows when mobile was transmitting (V2I) vs receiving (I2V)..... 272

Figure 10-33 Time between transmissions, UNII EIRP=35 dBm, 10% load, drive by brick building with windows when mobile was transmitting (V2I) vs receiving (I2V)..... 273

Figure 10- 34. RSSI and noise power plots, I2V, UNII EIRP=35 dBm, 70% load, approaching Brick building 274

Figure 10-35. Signal-to-Noise plots, I2V, UNII EIRP=35 dBm, 70% load, approaching Brick building..... 275

Figure 10- 36. Packet Error Rate plots, I2V, UNII EIRP=35 dBm, 70% load, approaching Brick building . 275

Figure 10-37. Packet gap plots, I2V, UNII EIRP=35 dBm, 70% load, approaching Brick building..... 276

Figure 10-38. Summary of packet gaps, I2V, UNII EIRP=35 dBm, 70% load, approaching Brick building 277

Figure 10-39. Geographical distribution of PER, I2V, UNII EIRP=35 dBm, 70% load, approaching Brick building 277

Figure 10-40. Geographical distribution of PER, I2V, UNII EIRP=35 dBm, 70% load, departing Brick building 278

Figure 10-41. Comparing RSSI plots as UNII traffic load changed, UNII EIRP=35 dBm, I2V EIRP=25 dBm, approaching Brick building 279

Figure 10-42. Comparing SNR plots as UNII traffic load changed, UNII EIRP=35 dBm, I2V EIRP=25 dBm, approaching Brick building 280

Figure 10-43. Comparing PER plots as UNII traffic load changed, UNII EIRP=35 dBm, I2V EIRP=25 dBm, approaching Brick building 281

Figure 10-44. Comparing safety critical gaps as UNII traffic load changed, UNII EIRP=35 dBm, I2V, DSRC EIRP=25 dBm, approaching Brick building 282

Figure 10-45. Summary of consecutive packet gaps as UNII traffic load changed, UNII EIRP=35 dBm, V2I EIRP=25 dBm, approaching Brick building..... 283

Figure 10-46. Geographical distribution of PER, approaching Wood building as UNII traffic load changed, UNII EIRP=35 dBm, V2I EIRP=25 dBm, approaching Brick building..... 284

Figure 10-47. I2V versus V2I, approaching Brick building, UNII inside building with traffic load of 70%, UNII EIRP=35 dBm, DSRC EIRP=25 dBm..... 285

Figure 10-48. I2V versus V2I, approaching Brick building, UNII inside building with traffic load of 10%, UNII EIRP=35 dBm, DSRC EIRP=25 dBm..... 286

Figure 10-49. Sensitivity to UNII power, approaching Brick building, UNII traffic load of 10%, UNII EIRP=35 dBm, I2V 287

Figure 10-50. Sensitivity to UNII power, approaching Brick building, UNII traffic load of 10%, UNII EIRP=35 dBm, V2V EIRP=25 dBm..... 288

Figure 10-51. PER and gaps, V2V versus V2I, approaching Brick building, UNII inside building with traffic load of 70%, UNII EIRP=35 dBm, DSRC V2V and V2I EIRP=25 dBm, mobile transmitter..... 290

Figure 10-52. PER and gaps, V2V versus V2I, approaching Brick building, UNII inside building with traffic load of 10%, UNII EIRP=35 dBm, DSRC V2V and V2I EIRP=25 dBm, mobile transmitter..... 291

Figure 10-53. Deployment versus high power scenarios, RSSI, approaching Brick building, UNII traffic load of 10%, I2V 293

Figure 10-54. Deployment versus high power scenarios, SNR, approaching Brick building, UNII traffic load of 10%, I2V 294

Figure 10-55. Deployment versus high power scenarios, PER, approaching Brick building, UNII traffic load of 10%, I2V 295

Figure 10-56. Deployment versus high power scenarios, Gaps, approaching Brick building, UNII traffic load of 10%, I2V 296

Figure 10-57. Summary of consecutive packet gaps in the deployment and high power scenarios, approaching Brick building, UNII traffic load of 10%, I2V..... 297

Figure 10-58. Deployment versus high power scenarios, Geographical distribution of PER, approaching Brick building, UNII traffic load of 10%, I2V..... 298

Figure 10-59 Wood building outside..... 299

Figure 10-61. PER Baselines for RSU to WVV (mobile), EIRP = 25 dBm..... 300

Figure 10-62. RSSI Baselines for RSU to WVV (mobile), EIRP = 25 dBm 301

Figure 10-63. West side PER I2V and V2V Baselines, EIRP = 25 dBm..... 302

Figure 10-64. Comparing low and high power V2V Baselines 303

Figure 10-65. RSSI and noise power plots, I2V, UNII EIRP=35 dBm, approaching Wood building 304

Figure 10-66. Signal-to-Noise plots, I2V, UNII EIRP=35 dBm, approaching Wood building..... 304

Figure 10-67. Packet Error Rate plots, I2V, UNII EIRP=35 dBm, approaching Wood building..... 305

Figure 10-68. Packet gap plots, I2V, UNII EIRP=35 dBm, approaching Wood building 306

Figure 10-69. Summary of packet gaps, I2V, UNII EIRP=35 dBm, approaching Wood building 307

Figure 10-70. Geographical distribution of PER, I2V, UNII EIRP=35 dBm, approaching Wood building.. 307

Figure 10-71. Geographical distribution of PER, I2V, UNII EIRP=35 dBm, departing Wood building 308

Figure 10-72. Comparing RSSI plots as UNII traffic load changed, UNII EIRP=35 dBm, I2V EIRP=25 dBm..... 309

Figure 10-73. Comparing SNR plots as UNII traffic load changed, UNII EIRP=35 dBm, I2V EIRP=25 dBm..... 310

Figure 10-74. Comparing PER plots as UNII traffic load changed, UNII EIRP=35 dBm, I2V EIRP=25 dBm..... 311

Figure 10-75. Comparing safety critical gaps as UNII traffic load changed, UNII EIRP=35 dBm, I2V EIRP=25 dBm 312

Figure 10-76. Summary of consecutive packet gaps as UNII traffic load changed, UNII EIRP=35 dBm, I2V EIRP=25 dBm 313

Figure 10-77. Geographical distribution of PER, approaching Wood building as UNII traffic load changed, UNII EIRP=35 dBm, I2V EIRP=25 dBm 314

Figure 10-78. V2V versus V2I, approaching Wood building, UNII inside building with traffic load of 10%, UNII EIRP=35 dBm, V2V and V2I EIRP=25 dBm..... 315

Figure 10-79. Comparing minimum and maximum interferer: RSSI and noise power plots, I2V, UNII EIRP=35 dBm, approaching Wood building 317

Figure 10-80. Comparing minimum and maximum interferer: Signal-to-Noise plots, I2V, UNII EIRP=35 dBm, approaching Wood building 318

Figure 10-81. Comparing minimum and maximum interferer: Packet Error Rate plots, I2V, UNII EIRP=35 dBm, approaching Wood building 319

Figure 10-82. Comparing minimum and maximum interferer: Packet gap plots, V2I, UNII EIRP=35 dBm, approaching Wood building 320

Figure 10-83. Comparing minimum and maximum interferer: Summary of packet gaps, V2I, UNII EIRP=35 dBm, approaching Wood building 322

Figure 10-84. Comparing minimum and maximum interferer: Geographical distribution of PER, V2I, UNII EIRP=35 dBm, approaching Wood building 323

Figure 10-XXX1: Cinderblock attenuation 325

Figure 10-XXX2: Brick attenuation 326

Figure 10-XXX3: Wood attenuation 327

Figure 10-XXX4: RF transmission through Cinderblock..... 328

Figure 10-XXX5: RF transmission through Brick..... 329

Figure 10-XXX5: RF transmission through Wood 330

Figure 10-XXX1 Dynamometer course with dry foliage 332

Figure 10-XXX2 Dynamometer course after the foliage had fallen 333

Figure 10-YYY1. Snow at Perryman and Figure 10-YYY2. Testing in snowstorm 334

Figure C-1. Breakdown of Interframe Spacing..... 340

Figure C-2: Depiction of 802.11 default EDCA parameters..... 343

List of Tables

Table 3-1. Test radio identifiers	22
Table 3-2. Wireless glossary.....	26
Table 3-3: 802.11p DSRC Modulation Options	29
Table 4-1 Inter-packet gaps of initial UNII loadings.....	70
Table 4-2 Inter-packet gaps including additional UNII loadings	71
Table 4-3 Measured Inter-packet gaps	72
Table 4-4 Calculated inter-packet gaps for 1400 byte data frames.....	75
Table 4-5 Calculated inter-packet gaps for 300 byte data frames.....	77
Table 6-1: Power Calibration Runs for Transmitters.....	101
Table 6-2: Antenna Pattern Calibration Data Collection Matrix	102
Table 6-3: OBU antenna data collected	111
Table 6-4: RSU antenna data collected	111
Table 6-5: Surrogate U-NII-4 Modulation Data Collection Matrix	114
Table 6-6: 802.11ac Modulation Options and Data Rates	115
Table 6-7: DSRC Radio Modulation Data Collection Matrix.....	117
Table 6-8: 802.11p DSRC Modulation Options	119
Table 6-9: Mobile Data Collection Platform Equipment.....	121
Table 6-10: RF Environmental Data Collection Matrix.....	123
Table 7-1. Factors important to schedule estimation.....	125
Table 7-2 Radio data collected.....	132
Table 7-3: Radiated Power Levels Selected for Analysis.....	135
Table 7-4. Key hardware and equipment used in the testing.....	138
Table 8-1 Key Performance Metrics.....	155
Table 9-1. Ballpark Packet Error Rates above baseline at select distances as Wi-Fi traffic increases (from Fig 9-59)	213
Table 9-2. Example noise contribution from a single co-channel Wi-Fi radio	232
Table 9-3. Definitions for Figure 9-82	234
Table 9-4. Signal to Jamming for AWGN in dB	238
Table 9-5. Signal to Jamming for Recoded DSRC in dB.	238
Table 9-6. Signal to Jamming for UNII channels in dB	239

Table 10-1: Comparing USDOT building interference attenuation with NIST construction material RF measurements..... 324

Table C-1: Packet Data Types..... 342

Table C-2: Summary of Recommended EDCA Parameters..... 344

DRAFT

List of Abbreviations

Abbreviation	Term
AP	Access Point
BER	Bit Error Rate
BSM	Basic Safety Message – Messages from OBUs containing vehicle data including GPS location coordinates
C/I	Carrier-to-Interference ratio
C/J	Carrier-to-Jammer ratio
CCA	Clear Channel Assessment – mechanism by which radios listen and do not attempt to transmit until the channel is clear of transmissions from other radios.
CCH	Control Channel (Channel 178 in the DSRC band)
CCTV	Closed Circuit Television
CFR	Code of Federal Regulations
Client	Device that uses a wireless link to connect to an AP to reach a network
CVHT	Cooperative Vehicle-Highway Testbed (outdoor test facility at TFHRC)†
dB	Decibel
dBi	Decibel (referenced to isotropic, that is an antenna radiating equally in all directions)
dBm	Decibel referenced to 1 milliwatt
DSRC	Dedicated Short Range Communication
EDCA	Enhanced Distributed Channel Access – a way to prioritize messages that try to access the channel at the same time. See Appendix B.
EIRP	Equivalent Isotropic Radiated Power
EVM	Error Vector Magnitude (signal quality)
FCC	Federal Communications Commission
FHWA	Federal Highway Administration
FLETC	Federal Law Enforcement Training Center†
FSS	Fixed Satellite Service
GHz	Giga-Hertz (1 billion cycles per second) – unit of frequency
GPS	Global Positioning System
Handheld DSRC	Portable DSRC – DSRC radio in a handheld device such as a smartphone or tablet computer
IEEE	Institute of Electrical and Electronic Engineers
ISM	Industrial, Scientific and Medical – devices radiating non-communication RF energy
ITS	Institute for Telecommunication Sciences
ITS	Intelligent Transportation Systems
kHz	Kilohertz (1000 cycles per second) – unit of frequency
km	Kilometer (1000 meters) – unit of distance
LAN	Local Area Network

Abbreviation	Term
LTE	Long Term Evolution – 4 th generation cellphone technology standard
m	Meter – unit of distance
MAP	Message that defines the geometry of an intersection. A companion to SPaT.
MHz	Mega-Hertz (1 million cycles per second) – unit of frequency
mph	Miles per hour
MUTCD	Manual of Uniform Traffic Control Devices
mW	Milliwatt (1 thousandths of a Watt, 0.001W) – unit of power
NPRM	Notice of Proposed Rule Making
NTIA	National Telecommunications and Information Administration
NTIA/ITS	National Telecommunications And Information Administration/Institute for Telecommunication Sciences
OBE	On-board Equipment – Electronic equipment in a vehicle that includes an OBU
OBU	Onboard Unit – DSRC radio mounted in a vehicle
Octet	8 bit byte
OFDM	Orthogonal Frequency Division Multiplexing
PAN	Personal Area Network
PER	Packet Error Rate
QAM	Quadrature Amplitude Modulation
QPSK	Quadrature Phase Shift Keying
Rec, Rx	Receive
RF	Radio Frequency
RSE	Roadside Equipment – Traffic equipment near a road, may contain an RSU
RSSI	Receive Signal Strength Indicator
RSU	Roadside Unit – DSRC radio mounted to fixed or moveable but not mobile infrastructure
RTK	Real Time Kinematic
S/J	Signal-to-Jammer ratio,
S/N	Signal-to-Noise ratio
SAE	Society of Automotive Engineers
SPaT	Signal Phase and Timing – Data from a traffic signal controller giving signal status and the timing of upcoming state changes in all directions.
TFHRC	Turner Fairbank Highway Research Center
Tx	Transmit
U-NII	Unlicensed National Information Infrastructure
V2I	Vehicle-to-Infrastructure
V2V	Vehicle-to-Vehicle
VSG	Vector Signal Generator
VSWR	Voltage Standing Wave Ratio or Return Loss (measures energy reflected back to the source due to imperfect impedance matching)
V-TTSS	Vehicle Technology Test Support System
W	Watt – unit measure of power

Abbreviation	Term
WAN	Wide Area Network
Wi-Fi	Wireless Fidelity

† Candidate site described in the test plan but not used.

DRAFT

Preface

In 1991, the Intermodal Surface Transportation Efficiency Act (ISTEA) introduced, for the first time, the concept of an intermodal transportation management system.¹ To expand on this concept, the Transportation Equity Act for the 21st Century (TEA-21) was created and passed in 1998. TEA-21 highlighted the importance of the role of technology in maintaining efficient and interoperable transportation systems by providing funding and policy support for Intelligent Transportation Systems (ITS) technologies and applications. Responsibility for coordinating safe ITS evolution falls upon the ITS Joint Program Office (ITS JPO), a component of the Office of the Assistant Secretary of Transportation for Research and Technology (OST-R), of the U.S. Department of Transportation (USDOT).²

TEA-21 asked the Federal Communications Commission (FCC) and USDOT to consider spectrum needs as pertaining to the operation of intelligent transportation systems. The FCC responded in 1999 by allocating 75 MHz of spectrum in the 5.9 GHz band (5.850-5.925 GHz) for dedicated short-range communications-based technologies.³ These technologies support dynamic, low latency vehicle-to-vehicle (V2V), vehicle-to-infrastructure (V2I), and vehicle-to-other devices and systems (V2X) communication exchanges at high vehicle speeds and within short distances (300 meters). It is configured to meet the unique needs of high-speed data exchange among moving vehicles and with roadway infrastructure or mobile devices in a manner necessary for supporting critical safety applications without compromising personal privacy or facilitating the tracking of traveler whereabouts. By allocating this band to transportation, users gain maximum benefit from interoperability whereby all participating technologies have to “speak” the same language and “hear” each other on the same communications medium.

DSRC is both a broadcast and a two-way short- to medium-range wireless communications capability, which permits rapid and reliable data transmission essential for communications-based active safety applications.⁴ It is a Wi-Fi derivative communications technology developed to meet specialized needs for transportation environments and for crash-avoidance safety. It has been through appropriate, robust testing that is necessary to prove that a technology is sufficiently mature to be used in critical safety-of-life situations. It is also proven to coexist and function in band of the spectrum with few other primary users. The original 5.9 GHz channel plan was designed to accommodate efficiently all user needs while

¹ Public Law 102-240, Part B, § 6051 et seq., web, available at <https://www.congress.gov/bill/102nd-congress/house-bill/2950>, accessed September 20, 2018.

² Public Law 112-141, Division E, Title III, Intelligent Transportation Systems Research, web, available at <http://www.gpo.gov/fdsys/pkg/PLAW-112publ141/pdf/PLAW-112publ141.pdf>, accessed September 20, 2018.

³ See <https://www.fcc.gov/wireless/bureau-divisions/mobility-division/dedicated-short-range-communications-dsrc-service>, accessed September 20, 2018.

⁴ ITS website, Connected Vehicle Fact Sheets, available at https://www.its.dot.gov/factsheets/pdf/CV_Brochure.pdf and https://www.its.dot.gov/factsheets/pdf/JPO_HowCVWork_v3.pdf, accessed September 20, 2018.

optimizing spectrum use. Sound engineering practice was used to determine the guard intervals⁵ and maximum transmit power levels assigned to each channel.

Connected Vehicle crash-avoidance warning applications enabled by short-range communications with non-line-of-sight capabilities offer the Nation an opportunity to achieve a transformation in transportation. The incorporation of this communications capability within vehicle sensor systems permits data on emerging threats and roadway hazards to be gathered from multiple external sources (i.e., other vehicles, infrastructure, or portable devices) and fused with on-board data. Because of the dedicated nature and low latency configuration of DSRC, safety-critical alerts and warnings can be provided to drivers in time to allow for an appropriate response to prevent a crash. The National Highway Traffic Safety Administration (NHTSA) estimates that an initial set of V2V and V2I safety applications have the potential to address 83 percent of light vehicle crashes involving unimpaired drivers.⁶

Since 2009, collision avoidance applications increasingly are available in many vehicles and offered by many vehicle manufacturers. Most of these applications rely upon sensor-based technologies (e.g., cameras, and motion, speed, or directional sensors).⁷ Collision avoidance can be greatly enhanced by using communications-based connected vehicle technologies operating in the 5.9 GHz band to expand the vehicle field of view and increase confidence in threat detection. By using communications-based strategies, collision avoidance applications can offer additional safety by alerting drivers of potential collisions that are not visible to existing sensor-based technologies (such as detecting potential collisions around buildings or other blind intersections) and by augmenting the range and object recognition capability of radar or camera based systems.

A potential conflict with Unlicensed National Information Infrastructure devices emerges.

On June 28, 2010, a Presidential Memorandum directed the Secretary of Commerce to work with the FCC to identify and make available 500 megahertz of spectrum over the next ten years for wireless broadband use. The National Telecommunications and Information Administration (NTIA) Policy and Plans Steering Group (PPSG) comprised of Federal agency members (including the Department of Defense) recommended adding the 5350-5470 MHz and 5825-5925 MHz bands to the bands under consideration, the latter of which overlaps with the ITS radio spectrum. On February 22, 2012, the President signed the Middle Class Tax Relief and Job Creation Act of 2012 (the “Act”) into law. Title VI of the Act includes a provision that requires the Assistant Secretary of Commerce (through NTIA), in

⁵ The guard intervals are defined by the IEEE 802.11 standard and determine resistance to multipath.

⁶ Results from Frequency of Target Crashes for IntelliDrive Safety Systems, Najm, W., J. Koopmann, S. Smith, and J. Brewer, October 2010, DOT HS 811 381. See:

<https://www.nhtsa.gov/DOT/NHTSA/NVS/Crash%20Avoidance/Technical%20Publications/2010/811381.pdf>

(last accessed September 20, 2018); and “Vehicle-to-Vehicle Communications: Readiness of V2V Technology for Application.” NHTSA Report DOT HS 812 014, August 2014, p. 17, web, available at

www.nhtsa.gov/staticfiles/rulemaking/pdf/V2V/Readiness-of-V2V-Technology-for-Application-812014.pdf, accessed September 20, 2018.

⁷ ITS Joint Program Office factsheet, “How Connected Vehicles Work,” web, available at www.its.dot.gov/factsheets/pdf/JPO_HowCVWork_v3.pdf, accessed September 20, 2018.

consultation with the DOD and other impacted agencies, to evaluate spectrum-sharing technologies and the risk to users if Unlicensed-National Information Infrastructure (U-NII) wireless broadband devices were allowed to operate in these bands.⁸

The most common example of a U-NII device is a Wi-Fi device that operates without a license in specific bands, and which has no interference protection. These include laptops, computers, printers, smartphones, tablets, televisions, and any of the emerging “smart” or “connected” devices increasingly found in the home and office – thermostats, lightbulbs, security cameras, and appliances—and increasingly used outdoors as people carry their internet and connectivity with themselves as they travel. Current FCC rules prohibit these devices from interfering with *licensed* devices operating within their authorized frequency bands. If these types of U-NII devices are allowed to operate in the 5.9 GHz DSRC band and it is later found that they cause harmful interference, it may cause unintended consequences (such as additional crashes) and it may be impossible to remove them.

The path toward coexistence with U-NII devices lies through analysis.

The purpose of the USDOT Spectrum Sharing analysis is to develop test procedures, establish test sites, and perform the necessary analyses to evaluate coexistence between DSRC and U-NII devices. This “USDOT Spectrum Test Report” presents the results of the first phase of testing the impacts of unlicensed devices on DSRC communications to address the department’s four high-level goals that seek to identify and resolve any potential conflicts.

⁸ 47 U.S.C. § 1453, web, available at <http://www.gpo.gov/fdsys/pkg/USCODE-2013-title47/pdf/USCODE-2013-title47-chap13-subchapIV-sec1453.pdf>.

Executive Summary

This report details the testing and corresponding results from the USDOT’s “baseline” testing of DSRC performance in the presence of unlicensed devices within a real-world setting. The USDOT completed this testing as part of a three-phased effort in partnership with the Federal Communications Commission (FCC) and the National Telecommunications and Information Administration (NTIA). The USDOT continues to research approaches for efficiently utilizing the 5.9 GHz Safety Band without sacrificing the safety benefits promised by DSRC technology. As part of that effort, the USDOT will build on the findings of this work to identify sharing mechanisms that have the potential to allow unlicensed devices to operate alongside DSRC within the 5.9 GHz band.

The USDOT conducted tests to measure and understand interference to DSRC by Wi-Fi transmitters in the same channel and in an adjacent channel. We tested a wide range of conditions and scenarios, which generated numerous results. We summarize the most significant results in this executive summary. Further results that will be of interest to researchers, developers and other agencies are contained in the body of the report and appendices.

The most significant finding from our test results is that Wi-Fi access points cause significant interference to DSRC communications when located 100 meters or more away, even if operating an access point inside a building or on an adjacent channel. This represents a consequential impact to safety given that DSRC was designed to provide situational awareness in a safety zone defined by a 300-meter radius around a vehicle. Co-channel sharing with Wi-Fi or any unlicensed radio service with similar power and duty cycle as Wi-Fi will not be possible without a robust and reliable sharing mechanism that defers to the high priority safety messages. Similarly, a reallocation of channels would need to provide guard bands to protect both radio services from adjacent channel interference from the other.

The testing focused mostly on co-channel radio performance; however, testing also revealed some preliminary findings on adjacent channel interference. The USDOT’s Phase 2 DSRC-UNII-4 Sharing testing (in collaboration with FCC and NTIA) will build on these initial results to understand better the impacts of reallocating the band or sharing the band with UNII devices. .

Outcomes: The desired outcomes of the DSRC-UNII testing were:

1. Generate experimental data from individual devices for models of potential interference at deployment scale (hundreds to thousands of devices in range).
2. Define bounding cases where no sharing may be possible, where unrestricted sharing may be possible, and exploring any zone in between where design choices and regulation impact the potential for sharing.
3. Understand interference mechanisms well enough to shed light on possible ways to mitigate them.
4. Create the technical grounding for USDOT to analyze to the effects of spectrum sharing.

Key findings:

- **Co-channel interference** from a weak outdoor Wi-Fi access point with minimal power (50 times less than the DSRC power) and a light traffic load (10%) caused untenable interference as far as 300 meters from the access point.
 - Putting the weak access point inside a wooden building reduced the interference but it was still untenable 100 meters from the building.
 - Putting the weak access point inside a brick or filled-cinderblock building mitigated the interference.
 - If the building had windows, the interference when the vehicle was exposed to the access point through a window as it drove by was the same as if the access point was outside, that is, untenable.
- **Co-channel interference** from a strong outdoor Wi-Fi access point at high power (EIRP=36 dBm), highly loaded (70%) opposite DSRC running at 4 times higher power than would be deployed (EIRP=25 dBm) caused untenable interference at least 800 meters from the access point.
 - Putting the strong access point in a wooden building made no difference. It was untenable at all ranges.
 - Putting the strong access point in a brick or filled-cinderblock building reduced interference but it was still untenable to at least 200 meters and significant to 800 meters.
- Interference was far more sensitive to the traffic load transmitted by the Wi-Fi than the power level. As noted above, even the weakest power level was enough to cause interference, so the number of Wi-Fi packets in the air and the space between them, which is determined by the loading, is what mattered most.
- A regular periodic distribution of Wi-Fi traffic caused about 10-20% more packet errors than a more random Poisson distribution. We provide data that can be used to scale between tests using easier to control periodic Wi-Fi traffic and those using more realistic Poisson traffic.
- Actual interference during deployment would be bounded by these high power-high load, and low power-low load cases. That means real-world interference will be something in between these particular measurements. It is unlikely to be less or more than the extent described here.
- **Adjacent channel interference** from a Wi-Fi access point at high power (EIRP=36 dBm) but moderate traffic load (15%) caused significant interference 200 meters from DSRC.
- Interference from Wi-Fi in an **adjacent channel** typically resulted in significant packet errors 200-350 meters away for traffic loads of 15% and higher. This interference included gaps in the DSRC traffic greater than half of a second, which US DOT deems safety critical. For traffic loads less than 15%, the packet errors were more likely to cluster in gaps of missing BSMs less than

half of a second long. Those may, or may not, be safety critical depending on the sensitivity of the safety application and level of channel congestion.

- DSRC was designed to provide situational awareness in a safety zone defined by a 300 meter radius around a vehicle. Even operating an access point in a building or on an adjacent channel still causes interference 100 meters or more away so would have a significant impact on safety. Co-channel sharing with Wi-Fi or any unlicensed radio service with similar power and duty cycle as Wi-Fi will not be possible without a robust and reliable sharing mechanism that defers to the high priority safety messages. Similarly, a reallocation of channels would need to provide guard bands to protect both radio services from adjacent channel interference from the other.
- The DSRC receiver is far more susceptible to interference from Wi-Fi than the DSRC transmitter. Most of the interference measured, especially at the long ranges was due to packets corrupted at the receiver.
- **Suppression of DSRC** transmissions happened only at much shorter ranges (25-75 meters) and was far less than interference to a receiver at the same distance from the Wi-Fi. Because the 10 MHz DSRC and the 20 MHz Wi-Fi radios do not recognize each other's packets, their clear channel access mechanisms only kick in at the much less sensitive energy-detect threshold.
- **Suppression of DSRC** transmissions might be more significant if DSRC was operating in the 20 MHz channels. Both DSRC and Wi-Fi are based on the same 802.11 protocols so they could detect each other's symbols. That detection has a more sensitive detection threshold. In that case, they would be likely to suppress each other's transmissions much further out.

The work undertaken by the USDOT is unique in several aspects. To date, only a small amount of work on radio interference to DSRC under such dynamic conditions has been performed and published. Our interference measurements were made over the air in real environments at full scale, in real-time, with vehicles closing at speeds as high as 100 mph. Moreover, tests were conducted in both "RF clean" open environments on tracks as long as three miles, as well as conducted both inside and outside buildings constructed of different materials in complex multipath environments and with foliage under different weather conditions.

The following points summarize what is unique about this USDOT contribution.

- The USDOT over-the-air (OTA) testing is at large-scale and in diverse environments. Through our partnership with the Army we have line-of-sight, open-air test tracks up to three miles long, line-of-sight tracks one-mile-and-one-half long in densely forested terrain, and we tested in buildings constructed of various materials and in a suburban environment.
- Our results do not depend entirely on simulations and include real-world effects. Our results include propagation effects that are too complicated for existing wireless models at our frequencies. In fact, our data can be used to develop or validate propagation models. We are using real, off-the-shelf equipment.

- Our focus has been on safety of life for the public as the highest priority. This is appropriate for our role as the government agency charged with protecting the traveling public.
- Our goal was to describe the onset and development of interference to make clear the problems that must be solved in order to make sharing possible. That way, those that want to share can decide if they can take that challenge on. Furthermore, this work helps regulators better understand the risks they have to manage. We make a large body of data available here that achieves that goal.
- We treated the two radio services as an interactive system with mutual feedback and characterized both.
- We developed a custom sniffer that can monitor both DSRC and Wi-Fi signals at the same time.
- The experience and capabilities we developed to do this work leave us well positioned to measure and analyze the impact of other emerging wireless technologies to transportation systems in real over-the-air environments.

DRAFT

USDOT Spectrum Sharing Test Report

I. Introduction

The Federal Communications Commission (FCC) allocated 75 MHz of spectrum in 1999 for use by Dedicated Short Range Communications (DSRC) to support Intelligent Transportation Systems (ITS).⁹ This spectrum (5850-5925 MHz) is referred to as the “DSRC band” or “ITS band” interchangeably. The allocation for DSRC is a co-primary allocation shared with the Fixed Satellite Service (FSS) as the other non-government primary allocation. Federal use on a primary basis is for radiolocation (i.e. radar) operation. In addition, there is a secondary Amateur allocation for the entire band. Unlicensed as well as Industrial, Scientific, and Medical (ISM) operations are permitted in the 5850-5875 MHz portion of the band.¹⁰ Figure 1-1 illustrates the DSRC band, and Figure 1-2 illustrates the channel plan established in the FCC Report and Order.

There are no sharing mechanisms established for the DSRC band. Testing and analysis conducted in the mid-to-late 1990’s demonstrated compatible operation between an early implementation of DSRC, FSS, and government radar systems.^{11, 12, 13, 14} DSRC devices operating too close to radar installations or FSS ground stations may suffer interference. DSRC devices may also suffer interference from users of the

⁹ FCC Report and Order “Amendment of Parts 2 and 90 of the Commission’s Rules to Allocate the 5.850-5.925 GHz Band to the Mobile Service for Dedicated Short Range Communications of Intelligent Transportation Services,” FCC 99-305, released October 22, 1999.

¹⁰ Per FCC Part 15.249

¹¹ “Measured Occupancy of 5850-5925 MHz and Adjacent 5-GHz Spectrum in the United States,” NTIA Technical Report TR-00-373, December 1999, <http://www.its.bldrdoc.gov/publications/2404.aspx>, Accessed September 20, 2018.

¹² “Electromagnetic compatibility testing of a dedicated short-range communication system,” NTIA Technical Report TR-98-352, July 1998, available at http://www.its.bldrdoc.gov/publications/download/dsrc_rpt.pdf, accessed September 20, 2018.

¹³ “Electromagnetic compatibility testing of a dedicated short-range communication system that conforms to the Japanese standard,” NTIA Technical Report TR-99-359, November 1998, available at http://www.its.bldrdoc.gov/publications/download/99-359_ocr.pdf, accessed September 20, 2018.

¹⁴ To avoid interference from co-channel radars, DSRC frequency assignments need to be coordinated with local radar assignments to avoid co-channel operations at short separation distances.

adjacent bands below 5850 MHz and above 5925 MHz. In each of these cases, co-primary band users are to work out interference issues amongst themselves if they arise.

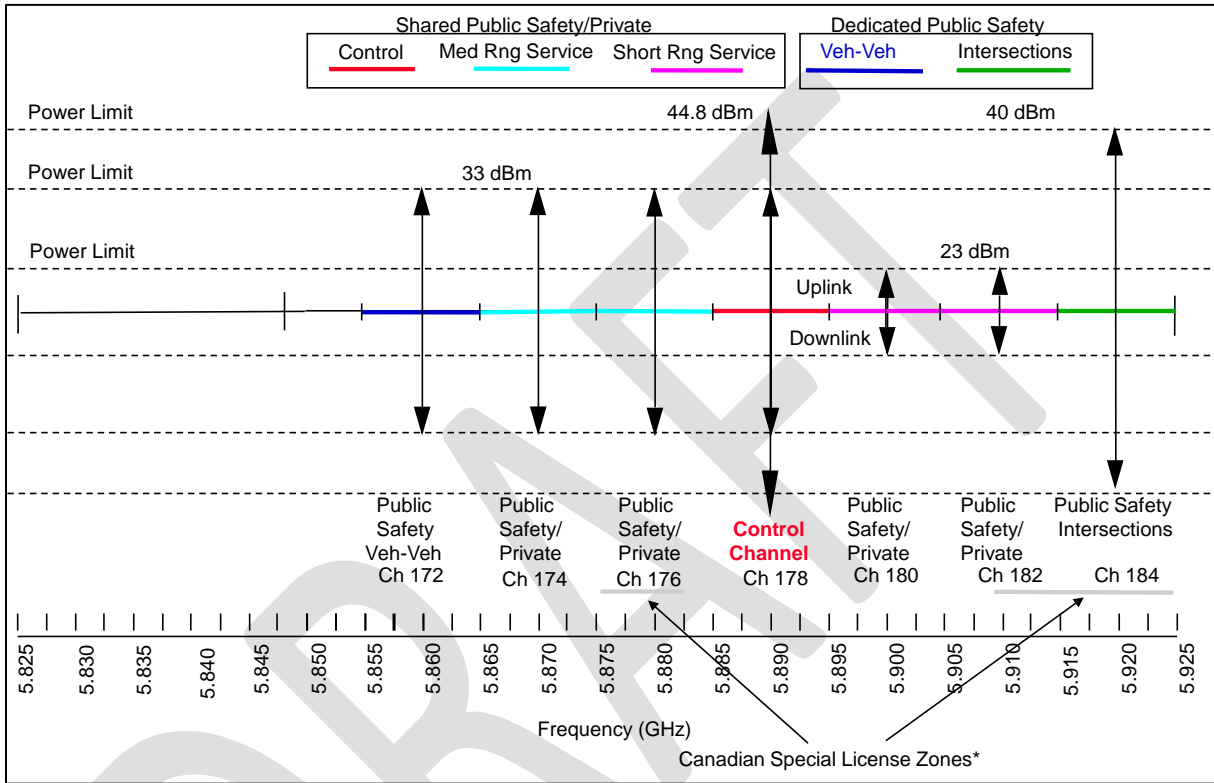


Figure 1-1: DSRC Channel Plan in the ITS Band^{15 16}

5.850 GHz		CH175			CH181			5.925 GHz
5850-5855	CH172	CH174	CH176	CH178	CH180	CH182	CH184	
5 MHz	5855-5865 Service	5865-5875 Service	5875-5885 Service	5885-5895 Service	5895-5905 Service	5905-5915 Service	5915-5925 Service	
	10 MHz							

Figure 1-2: DSRC channel number designations for both 10 and 20MHz channels¹⁷

¹⁵ DSRC Tutorial, Rockwell Collins, 2003.

¹⁶ Note that the DSRC Channel plan allows for two 20 MHz channels to be formed as well. Channels 174 and 176 can be combined to form 20 MHz channel 175 and Channels 180 and 182 can be combined to form 20 MHz channel 181.

¹⁷ From FCC-03-324A1, page 19

In a more recent notice, the FCC solicited input for a proposed rule to open up more bandwidth for unlicensed Wi-Fi devices using 20, 40, 80, or 160MHz channels defined by the 802.11ac standard (Figure 1-3).¹⁸ (DSRC devices are based on the 802.11p standard. The primary difference is that the 802.11p standard allows 10MHz channels.) The proposed new U-NII-4 band overlaps the DSRC band (indicated in purple in Figure 1-3). That means DSRC devices would share the band with an uncontrolled number of unlicensed 802.11ac devices if an adequate sharing method can be found. Such a sharing mechanism would have to give deference to the DSRC devices since they are primary users of the band and unlicensed devices are not allowed to interfere with primary users.¹⁹ Figure 1-4 gives a close up view of the proposed sharing in the DSRC band.

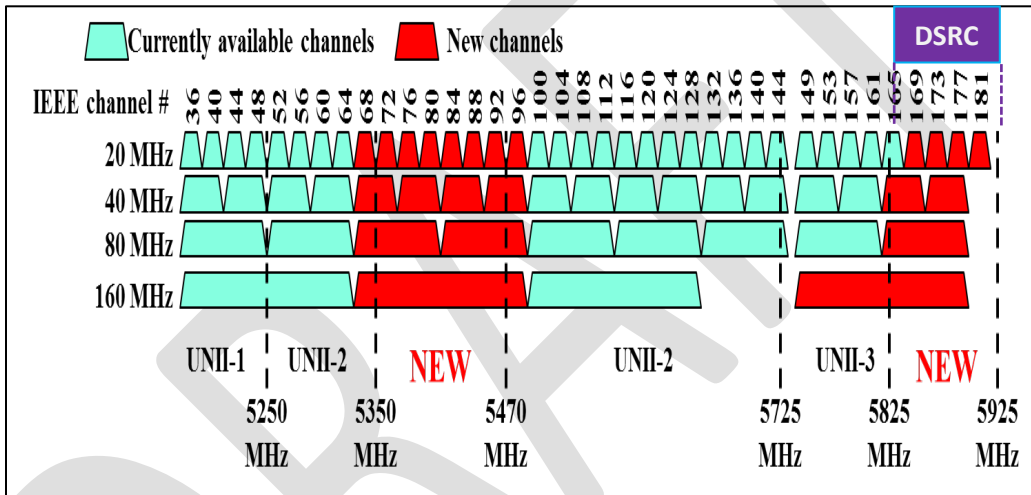


Figure 1-3: Proposed U-NII-4 band (“NEW”)

Though the impetus for creating the U-NII-4 band comes from desire to provide more bandwidth for 802.11ac Wi-Fi devices, a rule considered by the FCC would permit sharing by any unlicensed device in the band that complied with FCC Part 15²⁰ rules for the band. One example is License Assisted Access (LAA) also known as LTE-U (for unlicensed) which looks to offload cellular LTE data traffic onto the unlicensed bands. Others include unmanned aircraft system (UAS) downlinks, other forms of video streaming, wireless backhaul concepts, and any new application that might be devised in the future.

This work investigated 802.11ac as the first, but not only, unlicensed device that may be examined. We started with 802.11ac because commercial devices are available for the U-NII-3 band that can be adjusted in frequency to act as surrogates for potential U-NII-4 devices well enough to investigate interference, (but not mitigation). We will incorporate other unlicensed devices, including potential U-

¹⁸ FCC Notice of Proposed Rulemaking (NPRM) 13-22, (Docket 13-49), February 20, 2013, proposes revising Part 15 of the Commission’s Rules to Permit Unlicensed National Information Infrastructure (U-NII) Devices in the 5 GHz Band, to operate within the majority of the 5.850 to 5.925 GHz frequency band, designated as the U-NII-4 band.

¹⁹ See 47 CFR §2.1, “Terms and definitions” and 47 CFR §15.5, “General conditions of operation.”

²⁰ <https://www.fcc.gov/media/radio/low-power-radio-general-information#PART15>.

NII-4 devices with mitigation, into our analysis in a later phase since they were not available during this Phase 1 work. By potential U-NII-4 devices, we mean devices designed and programmed to share the band with DSRC.

The following terminology is used to describe unlicensed devices in this report:

<u>Term</u>	<u>Definition</u>
U-NII-3	Off-the-shelf devices operating in 5 GHz bands, particularly 5725-5850 GHz that are programmed for the U-NII-3 rules set by the FCC. These devices were both examined to see how much energy they leak into the DSRC band seen by DSRC devices as out-of-band interference and programmed to operate in the 5850-5925 GHz band for this baseline testing. ²¹ (see “surrogate U-NII-4 definition below).
U-NII-4	Placeholder for rules to allow unlicensed devices into 5850-5925 MHz, including the DSRC band. There are several proposals but these rules have not been written. This test effort considered proposed ideas in the absence of a rule.
Surrogate U-NII-4	U-NII-3 devices modified to operate at the higher frequencies of the DSRC band but using the U-NII-3 rules.
Potential U-NII-4	Devices built for the purpose of operating unlicensed in the DSRC band, including rechannelization devices and detect-and-vacate devices. The USDOT team has begun to investigate devices in Fall of 2019. The devices operate by rules the designer proposes that the FCC may adopt if they write a U-NII-4 rule. Their proposed rules must mitigate interference with DSRC.
Unlicensed device	Any device operating under FCC Part 15. Includes, but is not limited to U-NII devices.

²¹ We note that the recent FCC proposed rulemaking proposes a scenario that allows U-NII-3 devices to operate up to 5895 MHz with a proposed DSRC channel (180) in operation with no guard band. Details can be found at docket 19-138; see https://www.fcc.gov/ecfs/search/filings?limit=25&proceedings_name=19-138&q=19%5C-138&sort=date_disseminated,DESC.

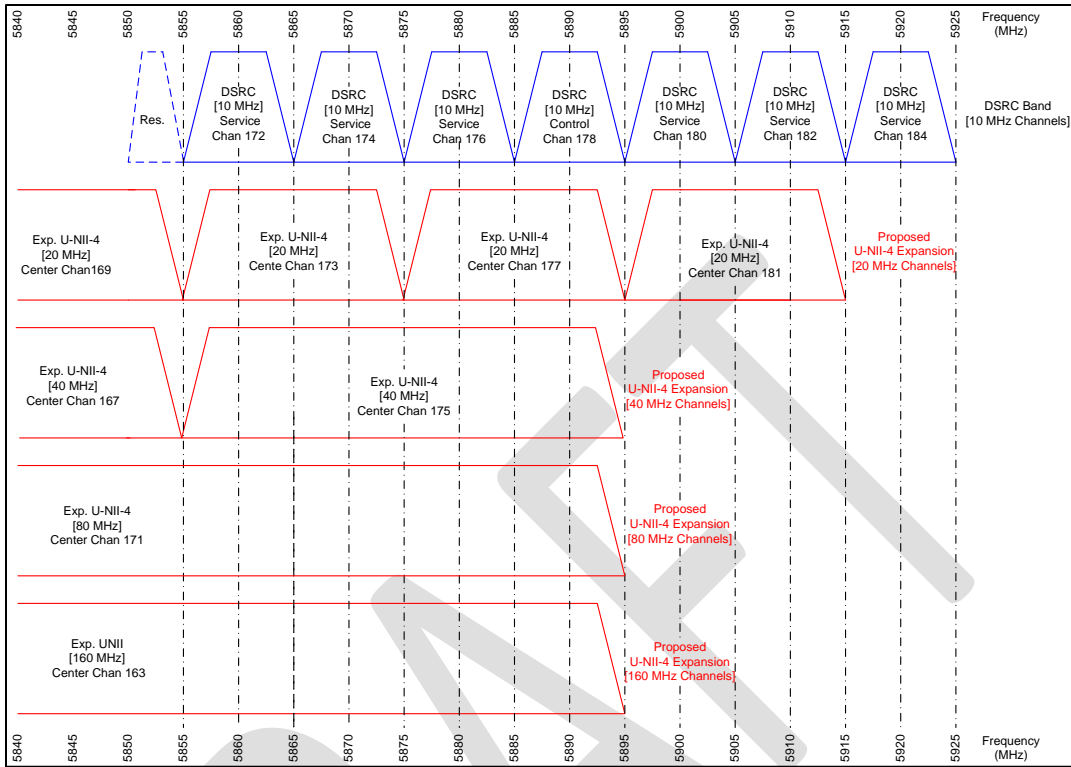


Figure 1-4: Proposed U-NII-4 Wi-Fi channel overlap with the DSRC band²²

The USDOT concern is focused on anything that disrupts DSRC communications. By this definition then, Radio Interference can take three forms:

- First: the increase in ambient noise level due to unlicensed devices transmitting in or near the DSRC band. In this case, the ability to receive weak signals from distant transmitters would be reduced.
- Second: when two or more packets from different sources enter a receiver at the same time. In that case, the receiver may accurately interpret only one, or likely none, of the incoming message packets. Those messages are transmitted but lost.
- Third: when the Clear Channel Assessment (CCA) mechanism causes a radio to suppress and not send its message because it hears another source already transmitting on the channel. A secondary or unlicensed user preventing a primary user from transmitting in this way is considered to be interfering with the primary user's ability to communicate by the USDOT. Messages are not received because they are prevented from being sent.

²² Source: Rockwell Collins

The USDSOT needs to understand the impacts of unlicensed devices operating in the DSRC band in order to provide recommendations through the NTIA to the FCC. The FCC may use these inputs to make decisions that will avoid interference with and ensure reliable operation of DSRC as well as ensure highly available access to the DSRC band. This report provides the USDOT's first bench and lab measurements,²³ field measurements, simulation and analysis.²⁴ The initial guidance for this work is described in the USDOT Spectrum Sharing Analysis Plan.²⁵ That document describes the required equipment, facilities and preparatory activities; and specifies a series of tests starting with baseline tests to understand normal unimpeded device operation and finishing with several potential interference scenarios with DSRC devices communicating in the presence of Wi-Fi signals. This report conveys the results of that work.

The following sections first list the goals and objectives; then describe equipment, facilities and testing before providing test results, analysis, and conclusions. Numerous appendices contain data that support the results and conclusions.

²³ "Bench test" is defined here as a component test that verifies that a device is working properly. "Lab test" is defined as indoor performance and interference testing.

²⁴ Existing interference models have not been applied to the DSRC environment. Data is needed in order to adapt and verify those models for use in this band.

²⁵ https://www.its.dot.gov/research_archives/connected_vehicle/pdf/DSRC_Analysis_Planv4Dec2017.pdf.

2. Goals and Objectives

2.1 USDOT Goals

The overarching goal driving the USDOT in this work is to ensure safe, reliable, and on-demand access to the 5850-5925 MHz spectrum allocation for Connected Vehicle Vehicle-to-Everything (V2X) transportation applications and operations. The Department cares about spectrum access to ensure that our nation has the safest, most efficient and modern transportation system in the world. Without the spectrum access, V2X applications will not be able to support public-benefit V2X services that reduce automobile crashes, injuries, and save lives; provide faster and safer public safety response; and address system inefficiencies such as congestion. To achieve that, the USDOT seeks to attain the following specific goals:

1. Understand the impacts of unlicensed devices operating in the 5.9 GHz band.
2. Develop the capability to evaluate proposed band sharing mechanisms.
3. Define requirements necessary for sharing mechanisms to prevent interference.
4. Collaborate with the National Telecommunications and Information Administration (NTIA) and the FCC to provide Congress with results on impacts to DSRC operations from proposed sharing mechanisms.

2.2 Desired Outcomes

To serve these goals the desired outcomes of this analysis boil down to four things.

1. Measured data from individual devices to be inputs for models of potential interference at deployment scale (hundreds to thousands of devices in range).
2. Defining bounding cases where no sharing may be possible, where unrestricted sharing may be possible, and exploring any zone in between where design choices and regulation impact the potential for sharing.
3. Understanding of interference mechanisms to shed light on possible ways to mitigate them.
4. Technical grounding for USDOT policy related to spectrum sharing.

2.3 Analysis Plan Objectives

The following objectives were set out to help the USDOT achieve those goals. Each activity described in the analysis plan addressed one or more of the following objectives.

1. Develop the capability to do accurate and relevant experimental evaluations of band sharing and interference between unlicensed devices and DSRC devices.
2. Characterize the existing radio frequency (RF) signal environment in and near the DSRC band.
3. Measure the effect of unlicensed devices on the background noise level.
4. Measure the impact that unlicensed device transmissions have on receiving DSRC messages.
5. Measure DSRC suppression caused by Clear Channel Assessment (CCA) of DSRC devices in the presence of unlicensed device transmissions.
6. Measure other impacts on DSRC channel quality of unlicensed device transmissions (e.g., S/N, PER, transmission delay, etc.).
7. Determine the minimum received power levels at which DSRC and unlicensed devices can sense one another.
8. Investigate how interference and detection (determined in the previous objectives) varies if the channel width of the overlapping unlicensed device transmission changes.
9. Measure the impact of DSRC operations on unlicensed device performance, recognizing that the two radios may form an interactive system.
10. Investigate mitigation possibilities once potential U-NII-4 devices designed and programmed to share the band with DSRC are available.

Each of these objectives is described more fully in the USDOT Analysis Plan²⁶.

2.4 Progress

Progress on the objectives made during Phase 1 is summarized below and in Figure 2-1.

2.4.1 Develop the capability to do accurate and relevant experimental evaluations of band sharing and interference between unlicensed devices and DSRC devices

Accomplished. The USDOT acquired equipment, set up test facilities, trained personnel, and established partnerships to make the measurements needed to explore possible interference.

2.4.2 Characterize existing RF signal environment in the DSRC band

Accomplished. The USDOT had measurements made of existing background noise levels and interference from existing transmitters to set the baseline values in order to see what changes when DSRC devices and unlicensed transmitters operate in or near the band. This included out-of-band as well as in-band transmitters since energy can leak between channels. Since use of the spectrum can change, it may be prudent to survey the band again in the future.

²⁶ https://www.its.dot.gov/research_archives/connected_vehicle/pdf/DSRC_Analysis_Planv4Dec2017.pdf.

2.4.3 Measure the effect of unlicensed devices on the background noise level

Background noise level limits the range that DSRC safety applications can function. As noise increases, range decreases, until it is too short for the applications to warn the driver. The first step in considering possible band sharing is to measure how much the noise level increases due to unlicensed devices transmitting in and near the band. The NTIA/ITS will input these measurements into models to examine noise level in full deployment scenarios of DSRC and unlicensed devices. That means aggregating the energy that many unlicensed devices would leak into the band, including those out of range and those operating in adjacent channels. The effect on noise level will be much higher with hundreds or thousands of transmitters out of range but still adding energy to the noise floor compared to the number of devices that will be examined under this plan. Because signal-to-noise ratio (S/N) limits the range at which connected vehicle safety applications can work, higher noise level means a smaller S/N, hence less range. With NTIA/ITS models, we can estimate the effect on safety range both in our measurement scenarios and at deployment scales.

2.4.4 Measure the impact of unlicensed transmissions on the receipt of DSRC messages that are transmitted

Accomplished. The USDOT measured packet collisions in DSRC devices that prevented them from receiving Basic Safety Messages (BSMs) caused by Wi-Fi signals from a surrogate UNII-4 device in a range of different conditions.

2.4.5 Measure DSRC suppression caused by Clear Channel Assessment (CCA) of DSRC devices in the presence of unlicensed device transmissions

Accomplished. The USDOT measured conditions in which a surrogate UNII-4 device caused a DSRC device to suppress its transmissions because it sensed that the channel was busy when the other device did not. The measurements were taken in the field as well as the lab.

2.4.6 Measure other impacts on DSRC channel quality of unlicensed transmissions (e.g., S/N, PER, etc.)

Accomplished. The USDOT collected other channel quality metrics during tests of DSRC communications in the presence of a surrogate UNII-4 transmitter. These other metrics include Received Signal Strength Indicator (RSSI), signal-to-noise ratio, packet error rate (PER), latency and gaps between packet completions. These measurements help to better understand potential interference.

2.4.7 Determine the energy levels at which DSRC and U-NII-4 devices can sense one another

DSRC receivers are highly sensitive and can sense energy in the range of -95 to -104 dBm. To separate a signal from noise, receivers typically need the signal to be 7 dB above the noise floor. Since atmospheric noise provides a noise floor of -104 dBm in a 10 MHz channel the best DSRC receiver sensitivity should be -97 dBm. If unlicensed devices do not have similar or better sensitivity, they will not hear DSRC

devices that hear them. The result is that the unlicensed devices will think the channel is clear when it is not. At the same time, the more sensitive DSRC devices will hear the unlicensed devices and suppress their own transmissions. By preventing the DSRC transmissions, the unlicensed devices would directly interfere with a primary user of the band, a violation of §15.5 of the FCC Rules. Comparing receiver sensitivities with range will indicate the potential for this kind of interference.

2.4.8 Investigate how interference and detection (determined in the previous objectives) varies if the bandwidth of the overlapping unlicensed transmission changes

This objective will be met through Phase 2 testing, because the surrogate UNII-4 testbed did not allow the control of transmission parameters (e.g. power, modulation, data rate, etc.) when operated with bandwidths wider than 20 MHz. Because Wi-Fi always includes management frames at 20 MHz, even when operating at higher bandwidths, we may have measured the worst case conditions. As shown in Figure 1-3, the U-NII-4 band can overlap the 10 MHz DSRC channels with 20, 40, 80 and 160 MHz U-NII-4 channels. When the same energy is spread over a wider channel, the amount of energy available to interfere in the 10 MHz channel is less. Even if data transmitted in the wider U-NII-4 channels does not interfere, accompanying 20 MHz management frames might interfere anyway.

Others have found that the wider Wi-Fi channels cause less co-channel interference for the reasons described above, but cause greater adjacent channel interference because of their much wider transmission masks.²⁷ That means their power tapers off more gradually at the band edges. Other options (Software Defined Radio (SDR), Amateur radio equipment, and commercial devices overseas) are available to examine wider bandwidths if necessary in Phase 2. This objective will determine if such conditional sharing might be possible.

2.4.9 Measure the impact of DSRC operations on unlicensed device performance recognizing that the two radios may form an interactive system

Accomplished. The impact of DSRC devices on the surrogate UNII-4 testbed was measured.

Processors and logic are central to modern radios. Therefore, two radios that can affect decisions made by the other form an interactive system. That is especially true when they follow the same rule set, IEEE 802.11 in this case. Studying a single component does not surface the deleterious modes that can occur

²⁷ Vehicle-to-Vehicle Communications Research Project (V2V-CR), DSRC and Wi-Fi Baseline Cross-channel Interference Test and Measurement Report, -Pre-Final Version-, December 2019, Produced by Crash Avoidance Metrics Partners LLC in response to Cooperative Agreement Number DTNH22-14-H-00449 , U.S. Department of Transportation National Highway Traffic Safety Administration, https://www.nhtsa.gov/sites/nhtsa.dot.gov/files/documents/v2v-cr_dsrc_wifi_baseline_cross-channel_interference_test_report_pre_final_dec_2019-121219-v1-tag.pdf.

when two components interact, even when both follow their component-oriented rules correctly. It is well known that component-based analysis fails to capture important system behaviors.²⁸

In addition, measuring the effect of DSRC devices on the operation of unlicensed devices will allow the USDOT to evaluate the credibility of claims made for unlicensed device operation. It will allow the USDOT to evaluate the feasibility of proposed deployment scenarios. This knowledge would better position the USDOT for its collaboration with the FCC and reporting to Congress. Such understanding may also allow the USDOT to develop a sharing mechanism that is more likely to be complied with by unlicensed users.

2.4.10 Investigate mitigation possibilities once potential U-NII-4 devices designed and programmed to share the band with DSRC are available

Not done. No proposed UNII4 devices from industry that included mitigation methods were forthcoming from industry during Phase 1.

Objectives	Comments
1) Develop USDOT RF test capability	Accomplished
2) Characterize existing interference	Accomplished
3) Measure effect on RF background noise	Analysis In Progress
4) Measure interference to receiving BSMs	Accomplished
5) Measure suppression of BSM transmissions	Accomplished
6) Measure impacts to channel quality	Accomplished
7) Determine the minimum detection levels	Analysis In Progress

²⁸ For example, “there does not exist any versatile model even today for the reliability assessment of component based software.” <https://waset.org/publications/10004282/suitability-of-black-box-approaches-for-the-reliability-assessment-of-component-based-software->.

8) Measure effect of UNII-channel width

UNII-4 testbed did not allow the control of transmission parameters with bandwidths wider than 20 MHz—examining in Phase 2 testing

9) Measure impact to UNII Wi-Fi of DSRC

Accomplished

10) Investigate mitigation possibilities

Focus of Phase 2 testing

Figure 2-1. Progress on Phase 1 Spectrum Test Objectives

DRAFT

3. Description of DSRC devices under test

To understand the impact of unlicensed devices operating in the DSRC band we created a relatively multipath-free test environment with DSRC communications and then added signals from potentially interfering devices. To begin developing our processes for measuring interference, we procured a set of DSRC devices to create a communication environment where changes in DSRC communication could be observed in the presence of possible interferers. The DSRC devices needed to be capable of creating realistic DSRC activity and provide a means of observing and recording the DSRC activity – both transmissions and receptions - in order to test with realistic interfering signals.

This chapter describes the DSRC devices and DSRC signals down to the most fundamental level. The first section describes the hardware. The second section explains the DSRC signals and how they are generated. It starts with a basic description of the IEEE 802.11a protocol that both DSRC and Wi-Fi are based on. This information applies to the following chapter on UNII Wi-Fi signals as well. The section continues with a description of the interface used to control the radios, a description of the modulation options, a description of the shell scripts that applied commands to the radio during tests, and lastly a detailed description of the data frames as sent over the air, including all the overhead bits.

Key chapter takeaways

- 1) The DSRC radios used in testing were Cohda Mk V.
- 2) DSRC and Wi-Fi signals are both based on the IEEE 82.11a protocol. The OSI model describes how the data is transformed before it reaches the antenna and transformed in reverse upon entering a receiving antenna.
- 3) For interference testing we are primarily concerned with the bottom two layers of the protocol, the physical layer (PHY) and the data link layer (LLC & MAC).
- 4) The physical layer turns the data into symbols (representing one or more bits) that are added to an RF carrier, modulated, and then pushed to the amplifier, then antenna, and over the air. It does the reverse on reception.
- 5) The data link layer assembles and disassembles the components of the frame that is transmitted by adding or removing all the overhead bits involved with conveying and securing the data component over the air between radios.
- 6) Above this would be the safety applications that create or use the data, which were out of scope since those applications are proprietary and not available. Moreover, interference operates directly at the physical layer. Our data can be applied by others to study the performance of their safety applications.

- 7) DSRC safety messages are transmitted using $\frac{1}{2}$ QPSK modulation but there are several other modulation options available that might be better for shorter range, higher data rate operations that have not been explored by the DSRC community. We looked at interference to a higher order modulation as well.
 - 8) We created our own graphical user interface and test scripts to conduct the tests to reduce the operator error inherent in the command line interface that came with the off-the-shelf devices, when performing data logging and control.
 - 9) We used a special test frame rather than actual BSMs so that all the frames were identical, easing diagnosis of RF issues in the field. In addition, it would not be possible for the radios to interact with commercial DSRC, which is now on the road in deployment sites around the country. Such interactions would introduce errors into our results.
 - 10) This better suited our objective, which was to measure interference to the signals over-the-air and not the performance of BSMs and safety applications
 - 11) The chapter ends with a detailed tutorial on 802.11a data frames, especially how the preambles are structured. This is central to potential mitigation, in particular, understanding how unlicensed devices would have to detect DSRC signals in order to defer.
-

3.1 Cohda DSRC Devices

Cohda Wireless devices were chosen because they had the combination of abilities to create controllable, realistic DSRC activity and the ability to provide the transmission and reception logging needed to conduct test sequences. We used MK5 generation OBU's²⁹ and RSU's³⁰.

²⁹ https://cohdawireless.com/wp-content/uploads/2018/08/CW_Product-Brief-sheet-MK5-OBU.pdf

³⁰ https://cohdawireless.com/wp-content/uploads/2018/08/CW_Product-Brief-sheet-MK5-RSU.pdf



Figure 3-1 Cohda Mk V OBU (left) and RSU (right)

Table 3-1. Test radio identifiers

Radio ID	Make/Model	Type	IP Address	MAC Last 4	Test site
Radio 1	Cohda/Mark 5	OBU	169.254.155.224	9BE0	APG
Radio 2	Cohda/Mark 5	RSU	169.254.88.176	58B0	ITS-Boulder
Radio 3	Cohda/Mark 5	RSU	169.254.80.208	50D0	APG
Radio 4	Cohda/Mark 5	OBU	169.254.57.140	398C	APG
Radio 5	Cohda/Mark 5	OBU	169.254.59.32	3B20	ITS-Boulder
Radio 6	Cohda/Mark 5	OBU	169.254.155.52	9B34	ITS-Boulder
Radio 7	Cohda/Mark 5	OBU	169.254.156.20	9C14	ITS-Boulder
Radio 8	Cohda/Mark 5	OBU	169.254.156.16	9C10	ATC
Radio 9	Cohda/Mark 5	RSU	169.254.18.72	1248	FHWA spare
Radio 10	Cohda/Mark 5	RSU	169.254.88.184	58B8	FCC

3.2 DSRC Traffic Generation

3.2.1 Wireless traffic basics

Wireless traffic starts as data generated by a human or machine application at the highest level. This data is handed down to a more basic layer, which adds information to the package of information for the function that layer performs. It is passed down again and again, increasing in size, eventually reaching the physical layer which prepares the information for transmission over some media. That is over the air for wireless but this model applies to transmission over wires and fiber as well. This is conceptually illustrated by Figure 3-2.

The physical layer at the receiver acquires the package of information and uses the information added by the transmitter's physical layer to demodulate and prepare the information for the next layer up. In this case, that is the data link layer. It uses information provided by the data link layer of the transmitter to prepare the data for the next layer up and so on until the information arrives as intended for the receiver's end use.

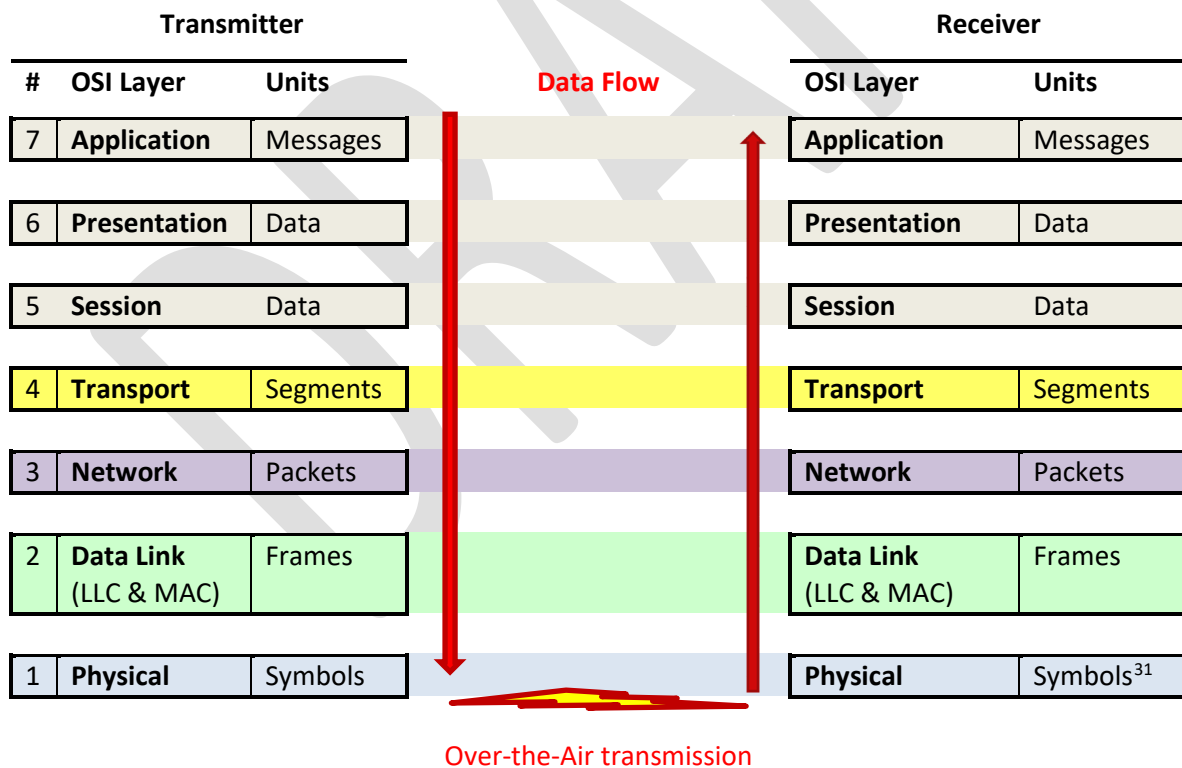


Figure 3-2. OSI model of wireless communication

³¹ An OFDM medium actually sends symbols over the air. Each symbol represents one or more bits depending on the Modulation Coding Scheme.

Figure 3-3 provides a more detailed definition of what happens at each layer with example protocols. Often the functions of layers 5, 6 and 7 are accomplished by one higher “merged” layer. Not all of these higher level functions are necessary in all circumstances either. A key point to note is that the wireless protocols that define Wi-Fi and DSRC essentially govern layers 1 and 2. The next two layers above are for communications in a network.

While these layers are irrelevant to broadcast messages like basic safety messages, DSRC is also capable of peer-to-peer communications and operating in that mode would employ the functions of layers 3 and 4. Protocols most relevant to DSRC are in boldface.

The multilayered OSI model is useful conceptually but how it is manifested in actuality looks different at the data packet level. Figure 3-4 shows that each of these vertical layers appears as horizontal growth before and sometimes after the initial data package. This shows the data bits added by Wi-Fi and DSRC at the physical (blue) and data link (green) layers to the package handed down from the higher layers (white). We will refer back to this figure when discussing the data frames used in the Phase 1 testing. Table 3-2 contains a glossary of wireless terms that will help with understanding that material as well.

DRAFT

#	OSI Layer	Units	Functions	Protocols	Equipment	
7	Application	Messages	Services that affect end user applications. Select channel & network, message format, human-machine interface	DNS, DHCP, FTP , HTTP , IMAP, LDAP, POP3, RTP, RTSP, SSH , SIP, SMTP , Telnet, TFTP, SFTP		
6	Presentation	Data	Coding into 1s and 0s, encryption, compression	JPEG, MIDI, MPEG, PICT, TIFF, GIF, XML, HTTPS, SSL, TLS, JSON		
5	Session	Data	Authentication, permissions, session restoration	NetBIOS, NFS, PAP, SCP, SQL, ZIP		
4	Transport	Segments	Splits files into data packets or groups of packets and checks that they are sent and received correctly, end-to-end error control	TCP, UTP, UDP		IP
3	Network	Packets	Addressing, routing, switching	IP Addresses (IPv4, IPv6), ICMP, IGMP, IPsec, IPX, RIP	Routers, switches	
2	Data Link (LLC & MAC)	Frames (control, data, and mgt)	Channel access (CSMA/CA), Addressing, frame Validation, error detection, security, flow control on physical link, radio resource mgt, mobility mgt, message prioritization	ARP, ATM, CDD, CDP, FDDI, FRAME RELAY, HDLC, MPLS, PPP, STP, Token Ring, MAC addresses	Switches	WiFi
1	Physical	Bits	Put bits into the air, wire or fiber. Take bits from the air, wire or fiber.	Bluetooth, USB, RJ45, Ethernet, DSL, ISDN, 802.11 (Wi-Fi & DSRC), OFDM modulation	Hubs, cables, fiber, radios, antennas	

Figure 3-3. OSI model details

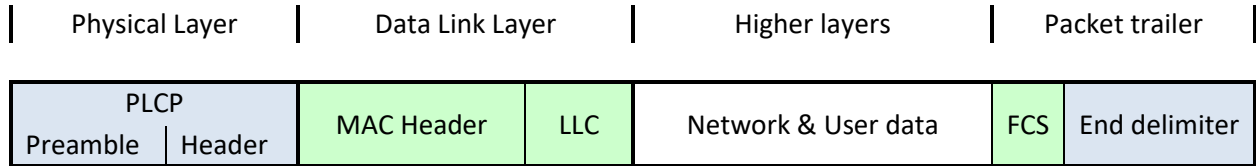


Figure 3-4. 802.11 data frame

Table 3-2. Wireless glossary

Term	Meaning	Notes
LLC	Logical Link Control	
MAC	Medium Access Control	
PLCP	Physical Layer Convergence Protocol	
PPDU	PLCP Protocol Data Unit	
PSDU	PLCP Service Data Unit	The package of data transferred between the physical and data link layers. The same package is called PSDU at the physical layer and MPDU at the data link layer.
MPDU	MAC Protocol Data Unit	Name for the PSDU at the data link layer level.
OFDM	Orthogonal Frequency Division Multiplexing	
D-BPSK	Differential-Binary Phase Shift Keying	A form of modulating the RF carrier by shifting the phase of the waveform.
DSAP	Destination Service Access Point	
SNAP	Subnetwork Access Protocol	
SFD	Start Frame Delimiter	Breaks the pattern of bits in the preamble letting the radio know an 802.11 frame is coming in and to start decoding now.

3.2.2 DSRC radio interface

DSRC radio traffic was generated using Linux shell scripts provided by Cohda and modified by personnel at the Aberdeen Proving Ground to work with a test management user interface that was also developed by the Aberdeen Proving Ground using National Instruments' Labview (Figure 3-5). The user interface provided a convenient way for a test operator to select devices and operating conditions as well as coordinate the creation and retrieval of log files.

DSRC radio traffic and radio log data was generated by Cohda Wireless MK5 devices. Linux shell scripts, provided by Cohda and modified by ATC, were utilized to control DSRC transmission parameters and logging of received signals. Various parameters and variables in the shell scripts had to be modified from one test run to another. Initially this was executed through Linux command line commands. However, this process was inefficient and prone to human error.

ATC developed a graphical user interface (GUI), using National Instruments LabVIEW, to reduce human error and increase test efficiency (Figure 3-5). The GUI provided a convenient way for test operators to select various MK5 devices, control the operating conditions of those devices, as well as coordinate the creation, retrieval, viewing and storing of test log files. The GUI was capable of controlling up to four Cohda MK5 devices.

The GUI steps operators through setup of test scenario parameters and then individually through configuration of each MK5 device used for the particular test. The interface provides operators with real-time feedback of connectivity to the DSRC radios. The GUI uses the MK5 configuration settings to programmatically modify the Linux shell scripts on each device.

When test runs are completed, the GUI programmatically transfers test logs from the DSRC radios to the computer hosting the interface. Once the files have transferred the GUI then parses and plots the log data. This enables operators and test personnel to assess the quality of the test run and identify any anomalies prior to the next test run.

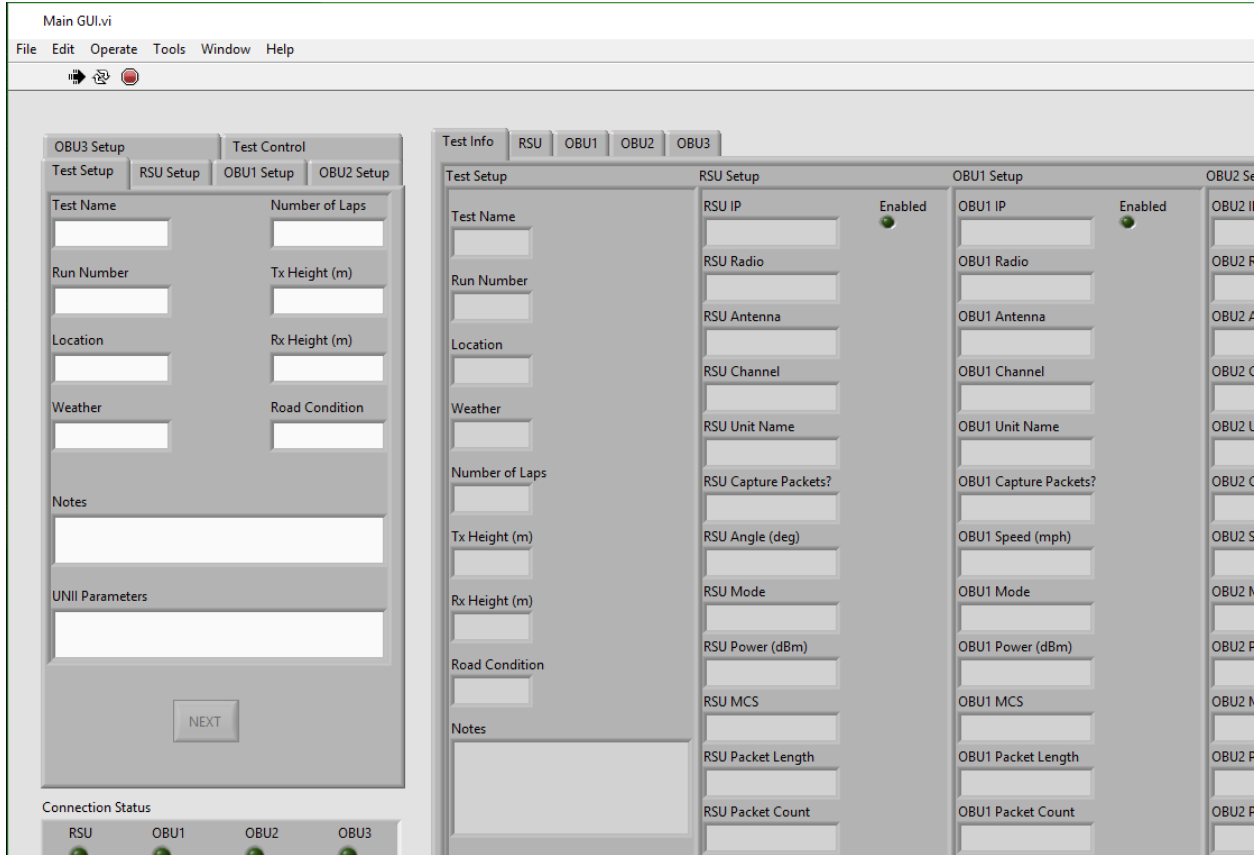


Figure 3-5. GUI created by ATC to interface with the Cohda DSRC radios

3.2.3 Modulation Options

In Figure 3-5, one of the user selectable boxes for the RSU and OBU that is not obvious is MCS. That stands for modulation and coding scheme. It is an index that sets how the radio will modulate the RF signal. Table 3-3 shows the modulation options permitted for DSRC by the 802.11p standard. The basic safety messages and most testing of DSRC has used ½QPSK in 10 MHz channels, highlighted in yellow in the table.

Table 3-3: 802.11p DSRC Modulation Options³²

Modulation	Coding rate (R)	Coded bits per subcarrier (N_{BPSC})	Coded bits per OFDM symbol (N_{CBPS})	Data bits per OFDM symbol (N_{DBPS})	Data rate (Mb/s) (20 MHz channel spacing)	Data rate (Mb/s) (10 MHz channel spacing)	Data rate (Mb/s) (5 MHz channel spacing)
BPSK	1/2	1	48	24	6	3	1.5
BPSK	3/4	1	48	36	9	4.5	2.25
QPSK	1/2	2	96	48	12	6	3
QPSK	3/4	2	96	72	18	9	4.5
16-QAM	1/2	4	192	96	24	12	6
16-QAM	3/4	4	192	144	36	18	9
64-QAM	2/3	6	288	192	48	24	12
64-QAM	3/4	6	288	216	54	27	13.5

3.2.4 Cohda Test Shell Scripts

Cohda Wireless MK5 devices are delivered with built in functions and Linux shell scripts that allow users to test the transmission and reception of DSRC radio traffic.

Transmit control: The primary function for controlling and executing DSRC radio transmissions is the *fieldtest-tx* function. This function controls transmit parameters such as; radio device, antenna port, channel, power, modulation, packet length, packet rate, number of packets, and log directory. The Cohda provided shell script *starttx.sh* provides variables that can be modified for each transmit parameter that is part of the *fieldtest-tx* function. This script also executes the *fieldtest-tx* function.

Receive control: The primary function for controlling DSRC radio reception is *llc rcap*. This function controls receive parameters such as radio device and log directory. The Cohda provided shell script *startrx.sh* provides variables that can be modified for each receive parameter that is part of the *llc rcap* function. This script also executes the *llc rcap* function.

ATC and Cohda collaborated on two new shell scripts that would interact more efficiently with the ATC developed DSRC GUI. The first script, *start_fieldttest_atc_5.sh*, combines the ability to modify *fieldtest-tx* and *llc rcap* variables as well as selectively execute each function. This script also adds diagnostic logging that tracks parameters of the MK5 device such as firmware version, radio configuration, and Global Positioning System (GPS) status.

³² IEEE 802.11-2012 wireless standard, Table 18—Modulation –dependent parameters, 3/29/2012, p1590.

The second script, *kill_fieldtest_atc_2.sh*, provides a means to stop, or kill, the Linux processes running on the DSRC devices as a result of the *fieldtest-tx* and *llc rcap* functions. This script ensures that no additional, or ‘zombie’, processes are running in the background the next time the functions are executed.

3.2.5 Cohda Over-the-Air Frames

The test shell scripts use Cohda-unique test frames to emulate the behavior of typical DSRC over-the-air transmissions. Below is are sample packet capture dissections of frame headers showing that the physical and MAC layer properties are the same as DSRC WSMP frames up to the link layer. They show these are OFDM modulated wireless signals and look the same whether they are DSRC, a 10 MHz Wi-Fi channel, or some other OFDM-based signal. Differences at the higher level layers are not important for measuring the effects of RF interference.

Figure 3-6 is a packet capture tool frame dissection presentation of an actual BSM from an Arada DSRC radio used in the Safety Pilot Model Deployment testing in Ann Arbor, Michigan. Figure 3-7 is the frame dissection from one of our Cohda Mark 5 radio transmitting actual BSMs in BSM mode. Figure 3-8 is the Cohda Mark 5 test frame used in our interference testing.

To make the differences stand out, everything that is identical between the Arada and Cohda BSM frames are shown in black text. The higher level information of interest is on a white background and everything else is on gray to deemphasize it. Information in the frames that are not identical is shown in red text. Where the Cohda Test frame differs from the Cohda BSM frame that text is in hot pink.

Most of these difference marked in red and pink are expected and have no bearing on the testing. This is mostly differing identifiers, locations, time stamps and message sizes which you would expect in captured transmissions from different radios at different places and times.

The significant differences to note are the red text that is highlighted in yellow. Those are the designators that indicate the frame type, Quality of Service (QoS) control, and message priority.

Arada from Safety Pilot Model Deployment

```

No.      Time          Source                Destination            Protocol Length
Latitude Longitude TemporaryID DSecond  Info
1 0.000000000 Mingjong_7b:9f:0a Broadcast              SAE J2735r200911
143                                           License not valid or expired

Frame 1: 143 bytes on wire (1144 bits), 143 bytes captured (1144 bits) on interface 0
Radiator Header v0, Length 42
  Header revision: 0
  Header pad: 0
  Header length: 42
  Present flags
    . . . . .1 = TSFT: True
    . . . . .1 = Flags: True
    . . . . .1 = Rate: True
    . . . . .1 = Channel: True
    . . . . .0 = FHSS: False
    . . . . .1 = dBm Antenna Signal: True
    . . . . .0 = dBm Antenna Noise: False
    . . . . .0 = Lock Quality: False
    . . . . .0 = TX Attenuation: False
    . . . . .0 = dB TX Attenuation: False
    . . . . .0 = dBm TX Power: False

```

```

.....1..... = Antenna: True
.....0..... = dB Antenna Signal: False
.....0..... = dB Antenna Noise: False
.....1..... = RX flags: True
.....0..... = Channel+: False
.....0..... = HT information: False
.....1..... = A-MPDU Status: True
.....0..... = VHT information: False
...0 0000 00... = Reserved: 0x00000000
...0..... = Radiotap NS next: False
...0..... = Vendor NS next: False
0..... = Ext: False
MAC timestamp: 2294771578
Flags: 0x10
....0... = CFP: False
....0... = Preamble: Long
....0... = WEP: False
....0... = Fragmentation: False
...1... = FCS at end: True
...0... = Data Pad: False
...0... = Bad FCS: False
0... = Short GI: False
Data Rate: 6.0 Mb/s
Channel frequency: 5860 [A 172]
Channel type: 802.11p (0x4140)
....0... = Turbo: False
....0... = Complementary Code Keying (CCK): False
....1... = Orthogonal Frequency-Division Multiplexing (OFDM): True
....0... = 2 GHz spectrum: False
....1... = 5 GHz spectrum: True
....0... = Passive: False
....0... = Dynamic CCK-OFDM: False
....0... = Gaussian Frequency Shift Keying (GFSK): False
...0... = GSM (900MHz): False
...0... = Static Turbo: False
...1... = Half Rate Channel (10MHz Channel Width): True
0... = Quarter Rate Channel (5MHz Channel Width): False
SSI Signal: -59 dBm
Antenna: 1
RX flags: 0x0000
....0... = Bad PLCP: False
GPS information (39 28 26.7719 N, 76 7 43.9558 W)
Latitude: 394741033 39.4741033 (39 28 26.7719 N)
Longitude: -761288766-76.1288766( 76 7 43.9558 W)
IEEE 802.11 QoS Data, Flags: .....C
Type/Subtype: QoS Data (0x0028)
Frame Control Field: 0x8800
....00 = Version: 0
....10.. = Type: Data frame (2)
1000... = Subtype: 8
Flags: 0x00
....00 = DS status: Not leaving DS or network is operating in AD-HOC mode (To DS: 0 From DS: 0)
(0x00)
....0... = More Fragments: This is the last fragment
....0... = Retry: Frame is not being retransmitted
...0... = PWR MGT: STA will stay up
...0... = More Data: No data buffered
...0... = Protected flag: Data is not protected
...0... = Order flag: Not strictly ordered
.000 0000 0000 0000 = Duration: 0 microseconds
Receiver address: Broadcast (ff:ff:ff:ff:ff:ff)
Destination address: Broadcast (ff:ff:ff:ff:ff:ff)
Transmitter address: Mingjong_7b:9f:0a (00:15:0f:7b:9f:0a)
Source address: Mingjong_7b:9f:0a (00:15:0f:7b:9f:0a)
BSS Id: Broadcast (ff:ff:ff:ff:ff:ff)
Fragment number: 0
Sequence number: 185
Frame check sequence: 0x8b965ba1 [correct]
[Good: True]
[Bad: False]
Qos Control: 0x0022
....0010 = TID: 2
[....010 = Priority: Spare (Background) (2)]
....0... = QoS bit 4: Bits 8-15 of QoS Control field are TXOP Duration Requested
....01... = Ack Policy: No Ack (0x0001)
....0... = Payload Type: MSDU
0000 0000... = TXOP Duration Requested: 0 (no TXOP requested)
Logical-Link Control
DSAP: SNAP (0xaa)
1010 101. = SAP: SNAP
....0... = IG Bit: Individual

```

```

SSAP: SNAP (0xaa)
1010 101. = SAP: SNAP
.... ..0 = CR Bit: Command
Control field: U, func=UI (0x03)
Organization Code: Encapsulated Ethernet (0x000000)
Type: (WAVE) Short Message Protocol (WSM) (0x88dc)
WSMP IEEE 1609.3r2010 PSID: (32) (Channel: 172) (Data Rate: 6 Mb/s) (TX Power: 14)
IEEE 1609.2-v2-d9.3 2011
SAE J2735r200911

```

Figure 3-6. Arada from Safety Pilot Model Deployment

Cohda MK5 test device in "BSM" mode

No.	Time	Source	Destination	Protocol	Length
Latitude	Longitude	TemporaryID	DSecond	Info	
1					
0.000000000		CohdaWir_01:39:8e	Broadcast	LLC	139
		U, func=Unknown; DSAP 0x88	Individual, SSAP 0xdc	Command	

Frame 1: 139 bytes on wire (1112 bits), 139 bytes captured (1112 bits) on interface 0
Radiator Header v0, Length 42
Header revision: 0
Header pad: 0
Header length: 42
Present flags

-1 = TSFT: True
-1 = Flags: True
-1 = Rate: True
-1 = Channel: True
-0 = FHSS: False
-1 = dBm Antenna Signal: True
-0 = dBm Antenna Noise: False
-0 = Lock Quality: False
-0 = TX Attenuation: False
-0 = dB TX Attenuation: False
-0 = dBm TX Power: False
-1 = Antenna: True
-0 = dB Antenna Signal: False
-0 = dB Antenna Noise: False
-1 = RX flags: True
-0 = Channel+: False
-0 = HT information: False
-1 = A-MPDU Status: True
-0 = VHT information: False
- ..0 0000 00.. = Reserved: 0x00000000
- ..0.. = Radiotap NS next: False
- ..0.. = Vendor NS next: False
- 0... = Ext: False

MAC timestamp: 5254738423
Flags: 0x10

-0 = CFP: False
-0 = Preamble: Long
-0 = WEP: False
-0 = Fragmentation: False
-1 = FCS at end: True
-0 = Data Pad: False
-0 = Bad FCS: False
-0 = Short GI: False

Data Rate: 6.0 Mb/s
Channel frequency: 5860 [A 172]
Channel type: 802.11p (0x4140)

-0 = Turbo: False
-0 = Complementary Code Keying (CCK): False
-1 = Orthogonal Frequency-Division Multiplexing (OFDM): True
-0 = 2 GHz spectrum: False
-1 = 5 GHz spectrum: True
-0 = Passive: False
-0 = Dynamic CCK-OFDM: False
-0 = Gaussian Frequency Shift Keying (GFSK): False
-0 = GSM (900MHz): False
-0 = Static Turbo: False
-1 = Half Rate Channel (10MHz Channel Width): True
-0 = Quarter Rate Channel (5MHz Channel Width): False

SSI Signal: -55 dBm
Antenna: 1

```

RX flags: 0x0000
.... .0. = Bad PLCP: False
GPS information (Unavailable), (Unavailable)
Latitude: 900000001 90.0000001 (Unavailable)
Longitude: 1800000001 (Unavailable)
IEEE 802.11 QoS Data, Flags: .....C
Type/Subtype: QoS Data (0x0028)
Frame Control Field: 0x8800
.... .00 = Version: 0
.... 10.. = Type: Data frame (2)
1000 ... = Subtype: 8
Flags: 0x00
.... .00 = DS status: Not leaving DS or network is operating in AD-HOC mode (To DS: 0 From DS: 0)
(0x00)
.... .0.. = More Fragments: This is the last fragment
.... 0... = Retry: Frame is not being retransmitted
...0 .... = PWR MGT: STA will stay up
..0. .... = More Data: No data buffered
.0.. .... = Protected flag: Data is not protected
0... .... = Order flag: Not strictly ordered
.000 0000 0000 0000 = Duration: 0 microseconds
Receiver address: Broadcast (ff:ff:ff:ff:ff:ff)
Destination address: Broadcast (ff:ff:ff:ff:ff:ff)
Transmitter address: CohdaWir_01:39:8e (04:e5:48:01:39:8e)
Source address: CohdaWir_01:39:8e (04:e5:48:01:39:8e)
BSS Id: Broadcast (ff:ff:ff:ff:ff:ff)
Fragment number: 0
Sequence number: 531
Frame check sequence: 0xba390ace [correct]
[Good: True]
[Bad: False]
QoS Control: 0x0022
.... .010 = TID: 2
[.... .010 = Priority: Spare (Background) (2)]
.... .0... = QoS bit 4: Bits 8-15 of QoS Control field are TXOP Duration Requested
.... .01. .... = Ack Policy: No Ack (0x0001)
.... .0... = Payload Type: MSDU
0000 0000 .... = TXOP Duration Requested: 0 (no TXOP requested)
Logical-Link Control
DSAP: Unknown (0x88)
1000 100. = SAP: Unknown
.... .0 = IG Bit: Individual
SSAP: Unknown (0xdc)
1101 110. = SAP: Unknown
.... .0 = CR Bit: Command
Control field: U, func=Unknown (0x0B)
Data (64 bytes)
0000 03 0f 01 ac 10 01 0c 04 01 a0 00 10 33 30 31 80 .....301.
0010 01 02 81 26 43 2e 7c 0e 21 40 d8 17 87 47 d1 d2 ...&C.]!@...G..
0020 9f a7 84 ff 12 ff ff ff ff 45 dc 27 85 05 00 8c .....E.'....
0030 00 1e 14 00 af 00 00 32 c1 a4 a2 04 80 02 01 00 .....2.....
Data: 030f01ac10010c0401a000103330318001028126432e7c0e...
[Length: 64]

```

Figure 3-7. Cohda MK5 test device in “BSM” mode

Cohda MK5 test device in “Test” mode

No.	Time	Source	Destination	Protocol	Length
Latitude	Longitude	TemporaryID	DSecond	Info	
1					
0.000000000		CohdaWir_01:39:8c	Broadcast	LLC	374
I, N(R)=109, N(S)=96; DSAP 0x88 Individual, SSAP 0xb6 C					
ommand					
Frame 1: 374 bytes on wire (2992 bits), 374 bytes captured (2992 bits) on interface 0					
Radiotap Header v0, Length 42					
Header revision: 0					
Header pad: 0					
Header length: 42					
Present flags					
.....1 = TSFT: True					
.....1. = Flags: True					
.....1.. = Rate: True					

DRAFT

```

.....1... = Channel: True
.....0... = FHSS: False
.....1... = dBm Antenna Signal: True
.....0... = dBm Antenna Noise: False
.....0... = Lock Quality: False
.....0... = TX Attenuation: False
.....0... = dB TX Attenuation: False
.....0... = dBm TX Power: False
.....1... = Antenna: True
.....0... = dB Antenna Signal: False
.....0... = dB Antenna Noise: False
.....1... = RX flags: True
.....0... = Channel+: False
.....0... = HT information: False
.....1... = A-MPDU Status: True
.....0... = VHT information: False
...0 0000 00.. = Reserved: 0x00000000
..0... = Radiotap NS next: False
..0... = Vendor NS next: False
0... = Ext: False
MAC timestamp: 7267802560
Flags: 0x10
...0... = CFP: False
...0... = Preamble: Long
...0... = WEP: False
...0... = Fragmentation: False
...1... = FCS at end: True
..0... = Data Pad: False
..0... = Bad FCS: False
0... = Short GI: False
Data Rate: 6.0 Mb/s
Channel frequency: 5860 [A 172]
Channel type: 802.11p (0x4140)
...0... = Turbo: False
...0... = Complementary Code Keying (CCK): False
...1... = Orthogonal Frequency-Division Multiplexing (OFDM): True
...0... = 2 GHz spectrum: False
...1... = 5 GHz spectrum: True
...0... = Passive: False
..0... = Dynamic CCK-OFDM: False
...0... = Gaussian Frequency Shift Keying (GFSK): False
...0... = GSM (900MHz): False
..0... = Static Turbo: False
..1... = Half Rate Channel (10MHz Channel Width): True
0... = Quarter Rate Channel (5MHz Channel Width): False
SSI Signal: -52 dBm
Antenna: 1
RX flags: 0x0000
...0... = Bad PLCP: False
GPS information (Unavailable), (Unavailable)
Latitude: 900000001 90.0000001 (Unavailable)
Longitude: 1800000001 (Unavailable)
IEEE 802.11 QoS Data, Flags: .....C
Type/Subtype: QoS Data (0x0028)
Frame Control Field: 0x8800
...0... = Version: 0
...10... = Type: Data frame (2)
1000... = Subtype: 8
Flags: 0x00
...0... = DS status: Not leaving DS or network is operating in AD-HOC mode (To DS: 0 From DS: 0)
(0x00)
...0... = More Fragments: This is the last fragment
...0... = Retry: Frame is not being retransmitted
...0... = PWR MGT: STA will stay up
..0... = More Data: No data buffered
..0... = Protected flag: Data is not protected
0... = Order flag: Not strictly ordered
.000 0000 0000 0000 = Duration: 0 microseconds
Receiver address: Broadcast (ff:ff:ff:ff:ff:ff)
Destination address: Broadcast (ff:ff:ff:ff:ff:ff)
Transmitter address: CohdaWir_01:39:8c (04:e5:48:01:39:8c)
Source address: CohdaWir_01:39:8c (04:e5:48:01:39:8c)
BSS Id: Broadcast (ff:ff:ff:ff:ff:ff)
Fragment number: 0
Sequence number: 118
Frame check sequence: 0x1df01a82 [correct]
[Good: True]
[Bad: False]
Qos Control: 0x0020
...0000 = TID: 0
[...000 = Priority: Best Effort (Best Effort) (8)]

```

```

.....0.... = QoS bit 4: Bits 8-15 of QoS Control field are TXOP Duration Requested
.....01.... = Ack Policy: No Ack (0x0001)
.....0.... = Payload Type: MSDU
0000 0000 .... = TXOP Duration Requested: 0 (no TXOP requested)
Logical-Link Control
  DSAP: Unknown (0x88)
    1000 100. = SAP: Unknown
    ....0... = IG Bit: Individual
  SSAP: Unknown (0xb6)
    1011 011. = SAP: Unknown
    ....0... = CR Bit: Command
Control field: I, N(R)=109, N(S)=96 (0xDAC0)
Data (298 bytes)
0000 0c 14 5c 19 29 d2 00 00 00 76 17 87 4c 19 d2 9f ..\.)...v..L...
0010 9f e7 78 ce 00 01 5c 19 29 de 00 03 0d 40 00 00 ..x...\.)...@..
0020 00 82 00 00 00 01 00 00 00 76 29 01 99 60 5a 01 .....v)...Z.
0030 39 dc a9 20 a2 bb 87 04 1c b1 e0 52 e5 96 e5 08 9...R....
0040 ad 76 4a 24 3c a3 41 64 f9 cf 19 46 ac 45 c3 6b .vJ$<.Ad...F.E.k
0050 22 86 74 67 0e 32 62 6a 09 ba 68 51 49 94 5c 55 ".tg.2bj..hQI.\U
0060 30 9c bc 09 a5 ef 7f 6e bd e3 4d 52 a0 5e ec 5e 0.....n..MR.^.^
0070 83 9b 0d 20 06 b1 3d 5f 33 b7 27 4b e7 f2 1b 3a ... =_3.'K...:
0080 da 02 21 4e 86 54 be 0f 0d 6c 37 11 0b a2 91 34 ..!N.T...l7...4
0090 2c a6 a9 6d 49 21 82 6e 5d 4a 22 5d c0 ac 37 74 ,..mI!.n]J"..7t
00a0 e5 97 b5 22 55 64 80 6f bc ea f6 5a 28 b7 a0 2d ... "Ud.o...Z(..-
00b0 4d 24 16 51 52 85 9f 2f 7a 25 65 0e 1f 8d d7 6e M$.QR../z%e...n
00c0 0a e1 68 41 e0 6c 57 65 ef 82 d0 16 21 a1 ba 53 ..hA.lWe....!..S
00d0 bc f2 ca 0b 95 b6 ed 0c f0 1e 50 78 d8 4f 60 0a .....Px.O`
00e0 c6 ca 6f 7a 92 c8 f8 7b 5d 11 ac 7f 46 92 87 14 ..oz...{]...F...
00f0 2d bf 66 51 c1 8a 4e 77 d8 8d 17 47 8c 68 69 17 -.fQ...Nw...G.hi.
0100 98 fe ee 0e ad 17 d5 31 90 0c e8 48 55 e7 f9 1f .....1...HU...
0110 77 82 ef 36 fd 6f 77 65 3b ee fc 37 e2 71 6c 63 w..6.`we?...7.qlc
0120 41 c1 a0 44 8e 61 65 3f 00 00 A..D.ae?...
Data: 0c145c1929d20000007617874c19d29f9fe778ce00015c19...
[Length: 298]

```

Figure 3-8. Cohda MK5 test device in “Test” mode

Cohda uses an Ethertype designated for experimental protocol development (0x88b6) rather than the Ethertype designated for WSMP use by DSRC (0x88dc)³³ so that the frames will not be misinterpreted by other devices that may be nearby. That also allows each packet to be identical rather than vary in size as a vehicle moves to facilitate data analysis.

The comparison shows that any mitigation method based on detecting 10 MHz BSMs may need to look far up the protocol stack, perhaps to the logical link control. Note that these differences, which will distinguish a DSRC frame from a Wi-Fi frame, appear near the end of the frame header. Methods based strictly on the pattern of the first few bits in the preamble may be inadequate.

Figure 3-9 illustrates what a frame looks like in time, essentially taking Figure 3-4 to the bit level. This is the same preamble identified in the frame captures in Figures 3-6, 3-7 and 3-8 (roughly 38 lines down in grey). It is the OFDM PLCP preamble.

Figure 3-10 explicitly shows the timing of the symbols. The preamble consists of 10 short 0.8 microsecond symbols followed by a guard interval then two long training symbols all fit into the first 16 microseconds. Each short training symbol consists of 12 subcarriers and each long training symbol

³³ <http://www.netconfcentral.org/modules/ietf-ethertype>.

consists of 53 subcarriers. Figure 3-11 further describes the components of the preamble. The point of the preamble is to let the receiver know that an 802.11 frame is arriving (Sync) and when to start decoding.

Figure 3-12 Decomposes the entire PLCP frame, including the preamble. Refer to Table 3-2 to decode all of the acronyms.

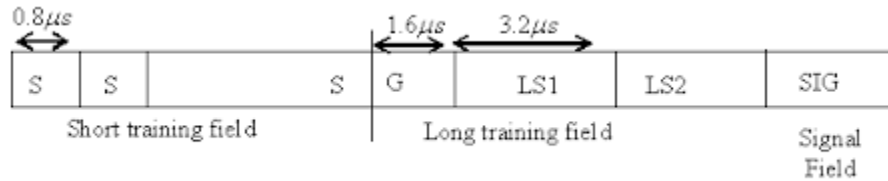


Figure 6: PLCP preamble of the IEEE 802.11a burst

Figure 3-9. Structure of the 802.11a Preamble

The OFDM training structure (PLCP Preamble)

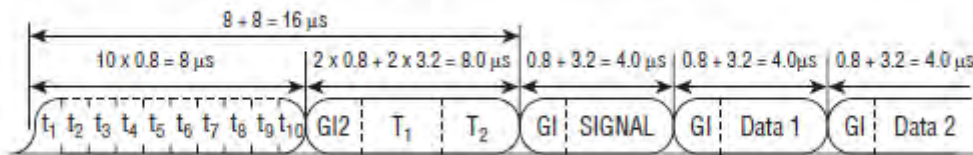
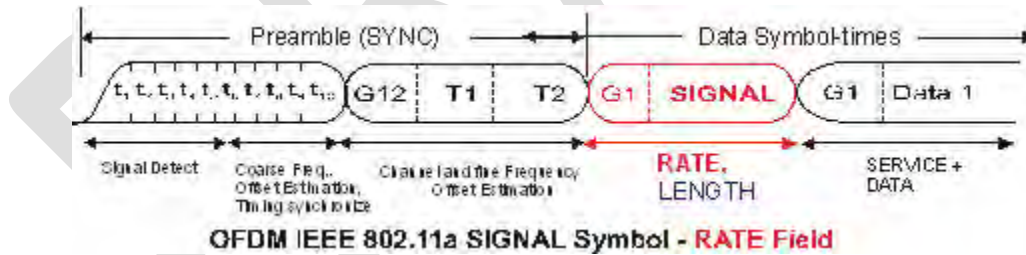


Figure 3-10. Timing of the OFDM PLCP Preamble



OFDM IEEE 802.11a SIGNAL Symbol - RATE Field

Figure 3-11. Components of the OFDM PLCP Preamble

Physical Layer Standards

- PLCP for 802.11a based on OFDM
- Three basic frame components: Preamble, header, and data

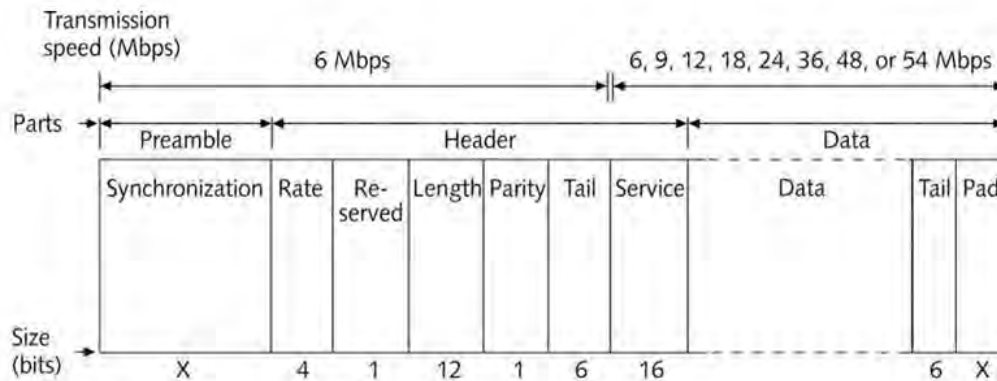


Figure 4-18: 802.11a PLCP frame

CWNA Guide to Wireless LANs, Second Edition

54

Figure 3-12. Decomposition of the 802.11a PLCP frame

The key thing to note is the PLCP Header which follows the preamble. The PLCP header tells the receiver three things

1. Which OFDM modulation to use for the rest of the frame (data rate).
2. Length of time required to transmit the packet
3. Parity check bit to protect against errors in the previous bits of the header.

The receiver must have this in order to demodulate and decode everything that follows, which is much of what shows up in the frame captures above (Figures 3-6, 3-7 and 3-8).

This preamble distinguishes the 802.11a derived frames from the legacy DSSS (Direct Sequence Spread Spectrum) and FSSS (Frequency Select Spread Spectrum (e.g., 802.11 b)

As with other 802.11 standards, there is a Physical Layer Convergence Protocol, PLCP and this defines a PLCP Protocol Data Unit, PPDU. For 802.11ac, this has been defined to be backward compatible with 802.11a and 802.11n which may also use the 5.8 GHz unlicensed ISM band.

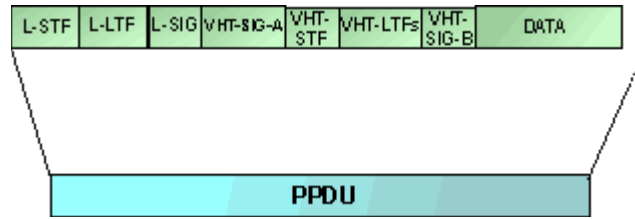


Figure 3-13. IEEE 802.11ac PPDU

There are various fields within the PPDU frame structure:

- **L-STF:** This short training field is two symbols in length and it is transmitted for backwards compatibility with previous versions of 802.11. The field is duplicated over each 20 MHz sub-band with phase rotation. The subcarriers are rotated by 90° or 180° in some sub-bands to reduce the peak to average power ratio.
- **L-LTF:** This is a legacy long training field, and is two symbols long. It has many of the same properties as the L-STF including the transmission criteria, being transmitted in sub-bands and those of phase rotation.
- **L-SIG:** This field is one symbol long and it is transmitted in BPSK. Like the L-STF and L-LTF it is a legacy field.
- **VHT-SIG-A:** VHT means Very High Throughput for protocols added as 802.11 evolved to achieve higher data throughput. This is an 802.11ac field and consists of one symbol transmitted in BPSK and a second in QBPSK, i.e. BPSK rotated by 90°. This mode of transmission enables auto-detection of a VHT transmission. The field contains information to enable the receiver to interpret correctly the later data packets. Information including the bandwidth, number of MIMO streams, STBC used, guard interval, BCC or LDPC coding, MCS, and beam-forming information.
- **VHT-STF - VHT Short Training Field:** This 802.11ac field is one symbol long and is used to improve the gain control estimation for MIMO operation.
- **VHT-LTF - VHT Long Training Field:** The long training fields may include 1, 2, 4, 6, or 8 VHT-LTFs. The mapping matrix for 1, 2, or 4 VHT-LTFs is the same as in 802.11n whereas the 6 and 8 VHT-LTF combinations have been added for 802.11ac.
- **VHT-SIG-B:** This field details payload data including the length of data and modulation coding scheme for the multi-user mode. Bits are repeated for each 20 MHz sub-band

Simply measuring the pattern of the preamble in whatever form may not sufficiently not distinguish the type of 802.11 signal. Note that 802.11ac begins with an identical preamble to be compatible with legacy 802.11 systems. Can a detect-and-vacate scheme quickly distinguish high priority DSRC signals from other 802.11a-type signals with just the first two training fields? Or will it take more time and processing further up the stack to know when to vacate?

There two other 802.11 legacy preambles for DSSS and FSSS systems plus three additional preambles for 802.11n which were intended to boost throughput. Any Wi-Fi receiver may have to decode more header information than the preamble to identify and adjust to the different flavors of 802.11 (including

DSRC) on the same channel. If so, will the necessary detect capability be inherent in future Wi-Fi devices anyway?

These captures also show something similar for mitigation via re-channelization, which needs to recognize and give DSRC safety messages priority. That information is again far up the protocol stack near the end of the capture meaning that a Wi-Fi receiver must process much of the frame or only operate with Background priority all of the time on channels shared with DSRC. That implies different operating rules for Wi-Fi radios when transmitting on a channel shared with DSRC versus when transmitting on other UNII channels.

Detection is going to be an important functionality for any of the sharing schemes that have been proposed.

DRAFT

4. Description of the UNII testbed

This section describes the UNII testbed where testing activities occurred. In order to simulate the proposed UNII-4 band, a Wi-Fi software development kit (SDK) for UNII-3 devices was modified to operate in the DSRC band using UNII-3 rules. For purposes of this report, we call this a “surrogate UNII-4 device.” Actual UNII-4 industry devices were not available for testing.

This chapter has four parts. The first two describe the UNII testbed and how it generated wireless traffic. The third part describes measurements of real Wi-Fi in order to learn how to simulate realistic interfering signals. The fourth part examines how loading and modulation affect inter-packet gaps, hence the opportunities for BSMs to avoid collision.

Key chapter takeaways

- 1) Industry devices that operated by potential UNII-4 rules proposed to the FCC were not available to the USDOT in Phase 1.
- 2) We created a surrogate UNII-4 device using an off-the-shelf UNII-3 Wi-Fi device. We modified it to transmit in the DSRC band using UNII-3 rules.
- 3) We tested with two kinds of Wi-Fi interference signals.
- 4) The Periodic distribution, which sends packets out at a fixed and essentially constant rate, or uniform inter-packet spacing. It provided more precise control over the interfering signal when we needed it.
- 5) The Poisson distribution, which has a randomly varying inter-packet spacing with a shorter average spacing than Periodic, but the distribution randomly includes some much longer inter-packet gaps. This provides an interfering signal much more like actual Wi-Fi in the wild.
- 6) We measured signals from actual Wi-Fi devices to understand how they manifest over the air.
- 7) We discovered a constant flow of periodic management frames even when no data is being transmitted. This is how Wi-Fi devices find and are controlled by access points.
- 8) Management frames tend to be short but are transmitted at the highest power. They tend to always be present on a 20 MHz channel even when the data is being sent on a wider channel.
- 9) We discovered Wi-Fi data signals are highly complex and “bursty” in nature. That means even for applications like streaming video, which might appear constant or steady, the data is downloaded in periodic intense bursts.

- 10) What matters most for interference is the opportunities provided for BSMs to pass between Wi-Fi frames without colliding with one. These gaps are controlled by the data rate (which is determined by the modulation), the percent traffic load (100% meaning constant transmission with no idle time between packets) and packet size.
- 11) Our calculations, confirmed by our measurements, show that for traffic loadings greater than 30% the inter-packet gap will be too small for BSMs to slip in between. Poisson traffic presents worse interference than Periodic at low loadings due to its smaller average gap, but less interference at high loads due to the small tail of random larger gaps.
-

4.1 UNII testbed

The surrogate UNII-4 device used in our testing consists of modified Wi-Fi radios, each connected to a Raspberry Pi computer via an Ethernet cable (Figures 4-1 through 4-6). The Raspberry Pi feeds data traffic to the radio to be transmitted and logs the data traffic received by the radio.

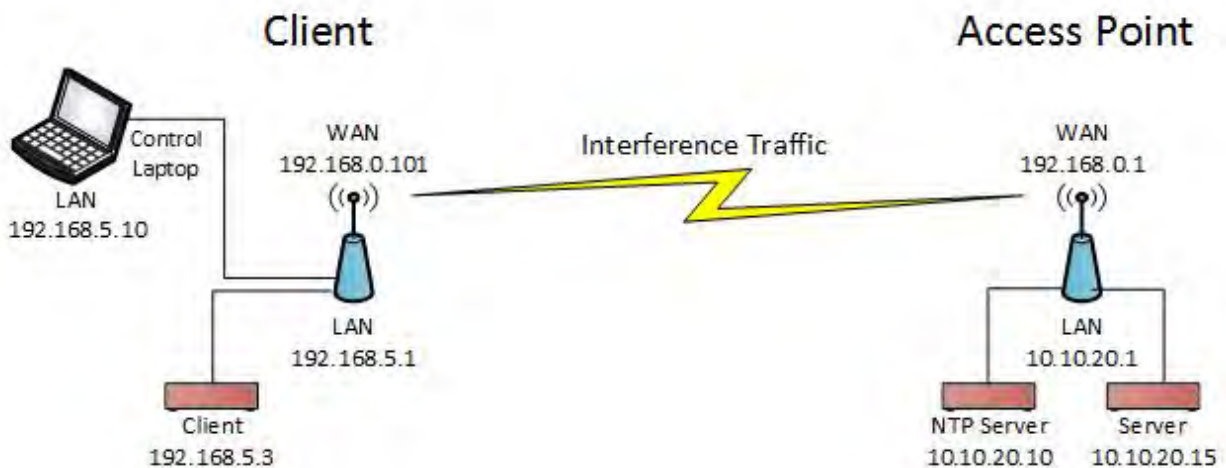


Figure 4-1. Surrogate U-NII-4 Testbed diagram

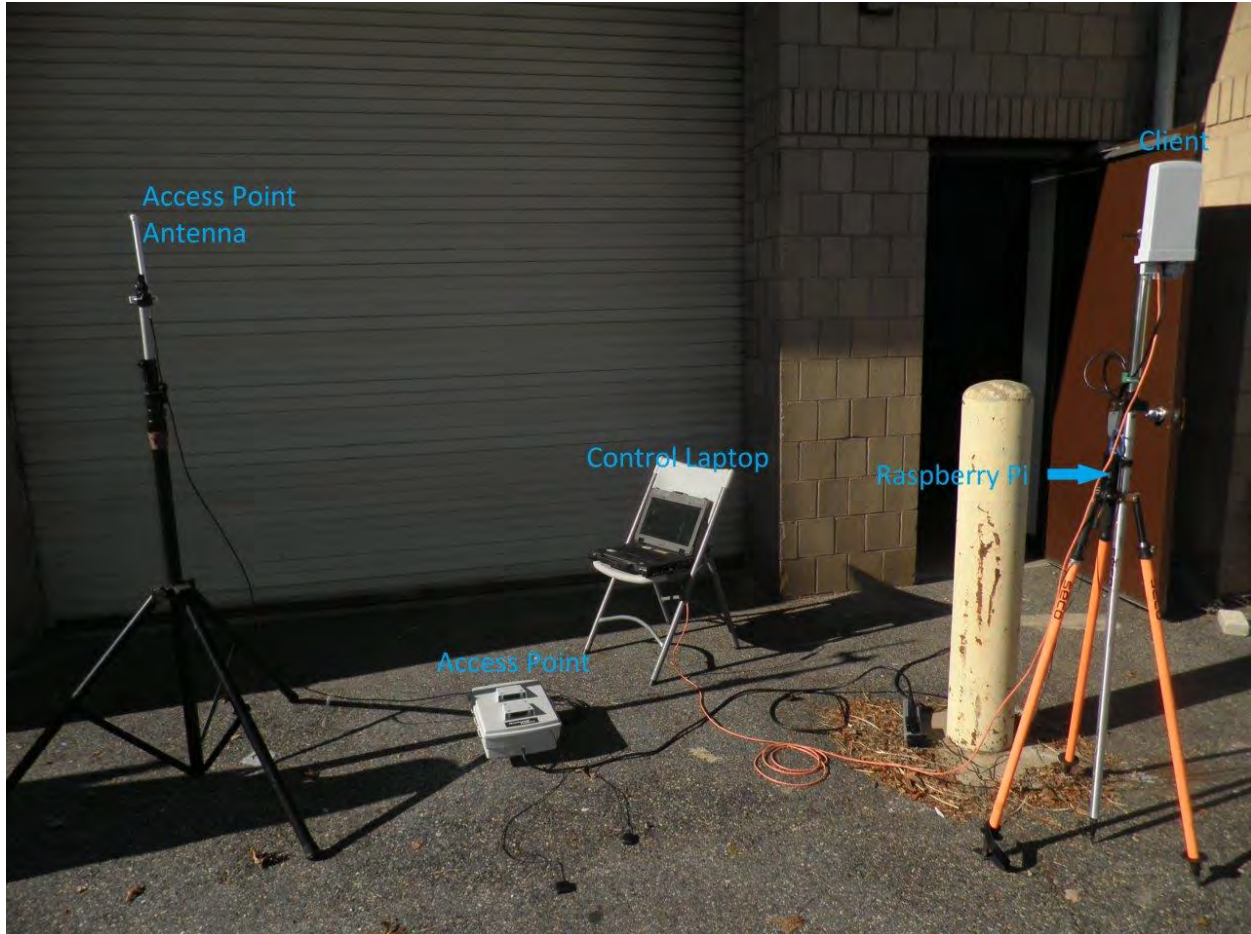


Figure 4-2. Surrogate U-NII-4 Testbed photo

We used open source software developed by the Naval Research Laboratory called Multi-Generator (MGEN) to create the data traffic that was input to the Wi-Fi radio. MGEN provides the ability to perform IP network performance tests and measurements using UDP and TCP IP traffic. The toolset generates real-time traffic patterns so that the network can be loaded in a variety of ways. The generated traffic can also be received and logged for analyses. Script files are used to drive the generated loading patterns over the course of time. These script files can be used to emulate the traffic patterns of unicast and/or multicast UDP and TCP IP applications. The tool set can be scripted to dynamically join and leave IP multicast groups. MGEN log data can be used to calculate performance statistics on throughput, packet loss rates, communication delay, and more. MGEN currently runs on various Unix-based (including MacOS X) and WIN32 platforms.³⁴

We found that when set to operate by 802.11ac rules, we could not control the transmission parameters of data frames as required by the test plan. The Wi-Fi radios would constantly change power, modulation, channel bonding in real-time to optimize reception being sensitive to any movement in the environment. In order to be certain that channel size, power, modulation and data rate would remain

³⁴ MGEN User's and Reference Guide Version 5.0, <https://downloads.pf.itd.nrl.navy.mil/docs/mgen/>.

as commanded for a data run we had to switch to the 802.11a mode. This allowed us to fix the transmission parameters but limited us to testing with 20 MHz channels.

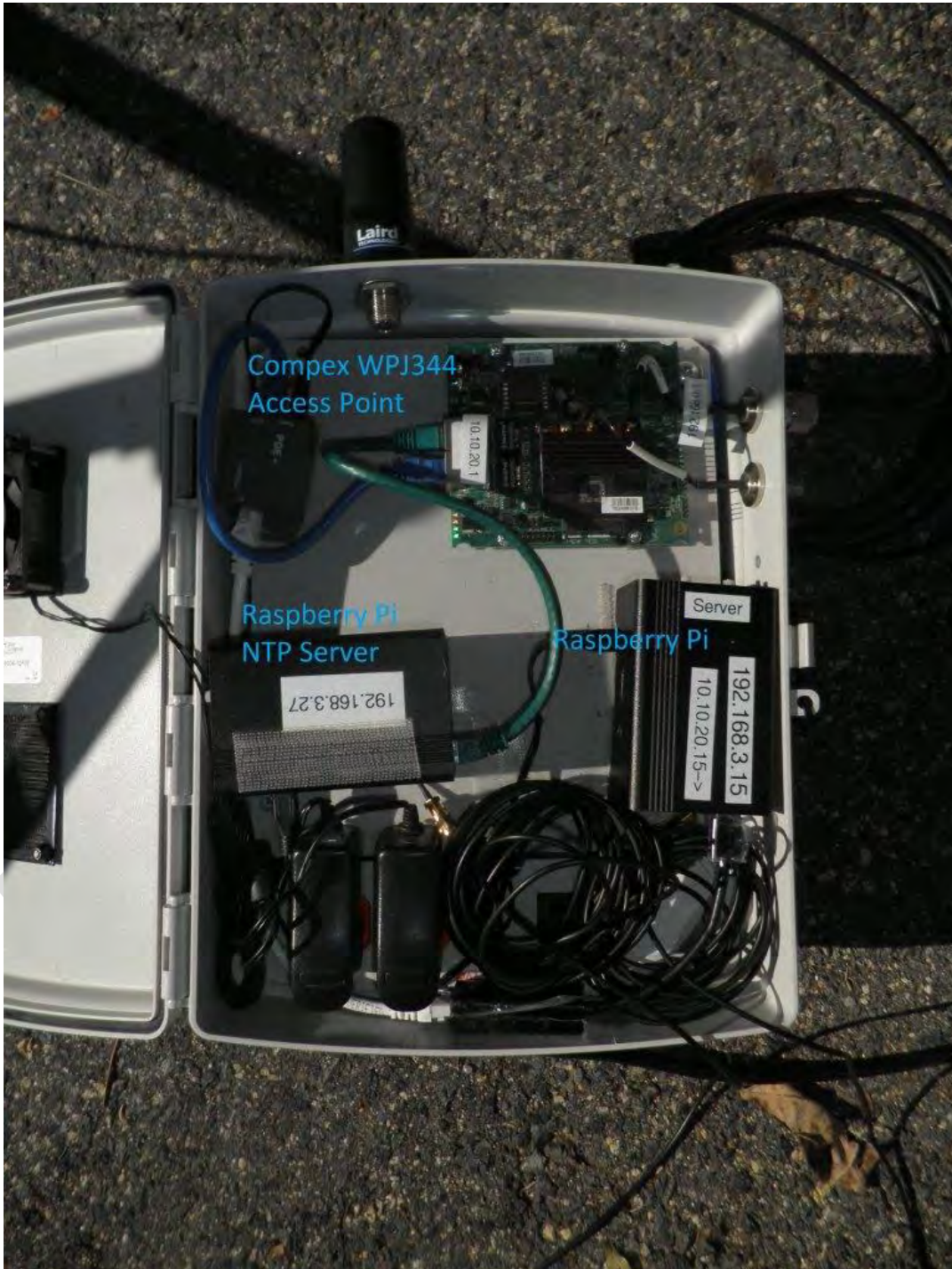


Figure 4-3. Surrogate U-NII-4 Testbed Access Point components

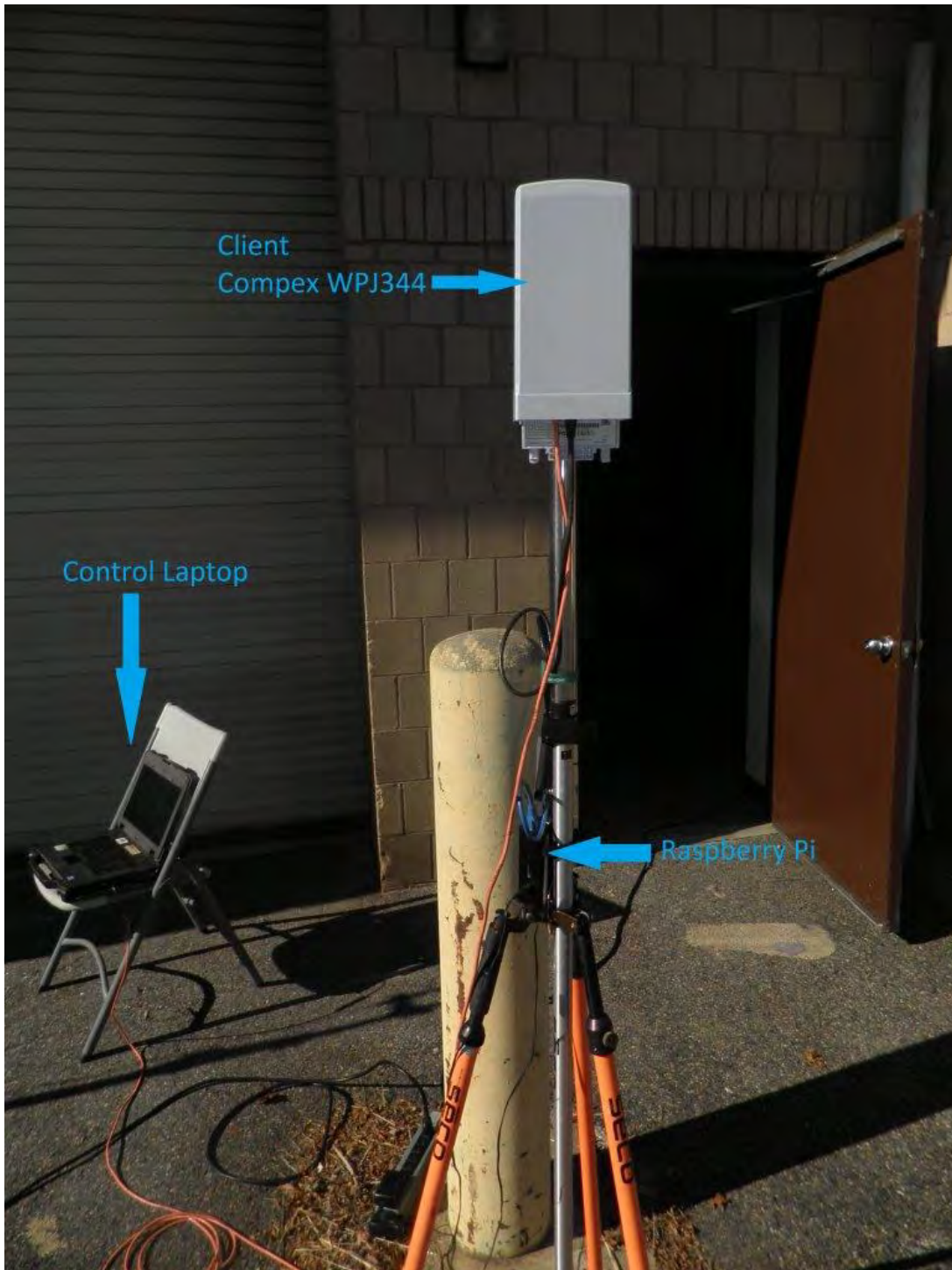


Figure 4-4. Surrogate U-NII-4 Testbed traffic generating components

DRAFT





Figure 4-5. Surrogate U-NII-4 Testbed Client inside (backside)

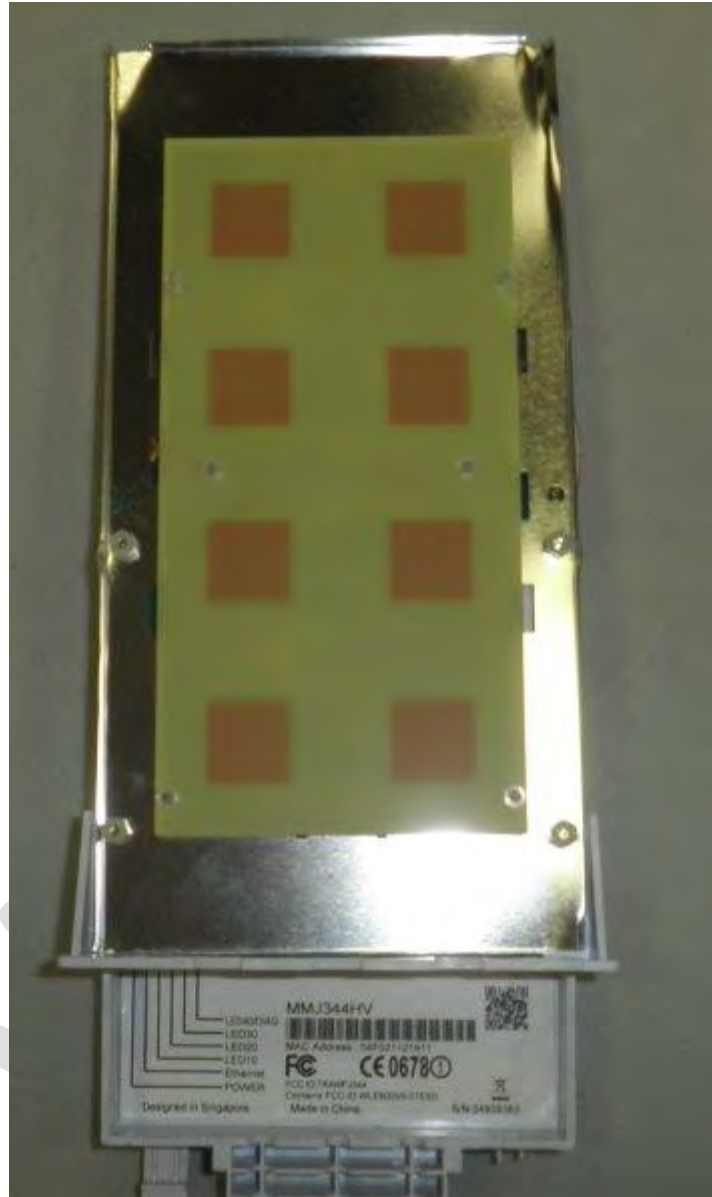


Figure 4-6. Surrogate U-NII-4 Testbed Client inside (antenna or front side)

4.2 Wi-Fi Traffic Generation

This section describes how Wi-Fi traffic was generated within the UNII testbed. First, the components required to generate the traffic are described, and then the techniques used. The client, server, and the NTP server (colored red in Figure 4-1 above) are Raspberry Pi single board computers. The server adds header information to the payload then transmits network traffic to the Access Point via wired Ethernet at which point the Access Point adds 802.11 radio tap header information and transmits the data to the

Station over the air. The Station then forwards this data to the client Raspberry Pi where the network packet information is written to a CSV file.

4.2.1 Traffic Generation Mechanism

In our configuration, the client Raspberry Pi is strictly a receiver for the MGEN network data. That data is stored in a CSV file and contains transmit time, receive time, packet sequence ID, packet size, and GPS coordinates of where the packet was transmitted from. The server Raspberry Pi handles all the network packet creation and transmission. Simple scripts are created using a specific syntax that contain start, stop, modification commands, flow number, the protocol to be used, source port, destination IP address, destination port, flow profile, packet rate, and packet size. All transmissions used UDP as the protocol and were primarily only in one direction, from the Access Point to the Station, simulating a stream or download.

The following is an example of a script that was used to command a channel usage of 20 percent with a $\frac{3}{4}$ QAM 64 modulation scheme inputting 1400 byte packets³⁵.

```
0.0 ON 1 UDP SRC 5001 DST 192.168.0.101/5001 PERIODIC [964 1400]
```

Periodic flow profile takes the packet rate, splits it equally over a second and repeats it every second until the script is commanded to stop. A packet rate of 964 would send a packet about once every millisecond. There are 802.3 and 802.11 mechanisms in the network such as CSMA/CD (Carrier Sense Multiple Access/Collision Detection) for Ethernet and Clear Channel Access or CSMA/CA (Collision Avoidance) for Wi-Fi that would cause the periodicity to vary slightly.

Figure 4-7 is a more detailed diagram of the testbed and shows more explicitly where the MGEN data traffic is generated and how it gets to the radios.

³⁵ $\frac{3}{4}$ QAM-64 modulation produces a data rate of 54 Mbps. 54 Mbps * 20% load = 10.8 Mbps.
 $10,800,000 \text{ bps} / (1400 \text{ octets/packet} * 8 \text{ bits/octet}) = 964 \text{ packets/sec}$
 $1/964 = 0.00104 \text{ sec/packet}$ or 1.04 ms between packets

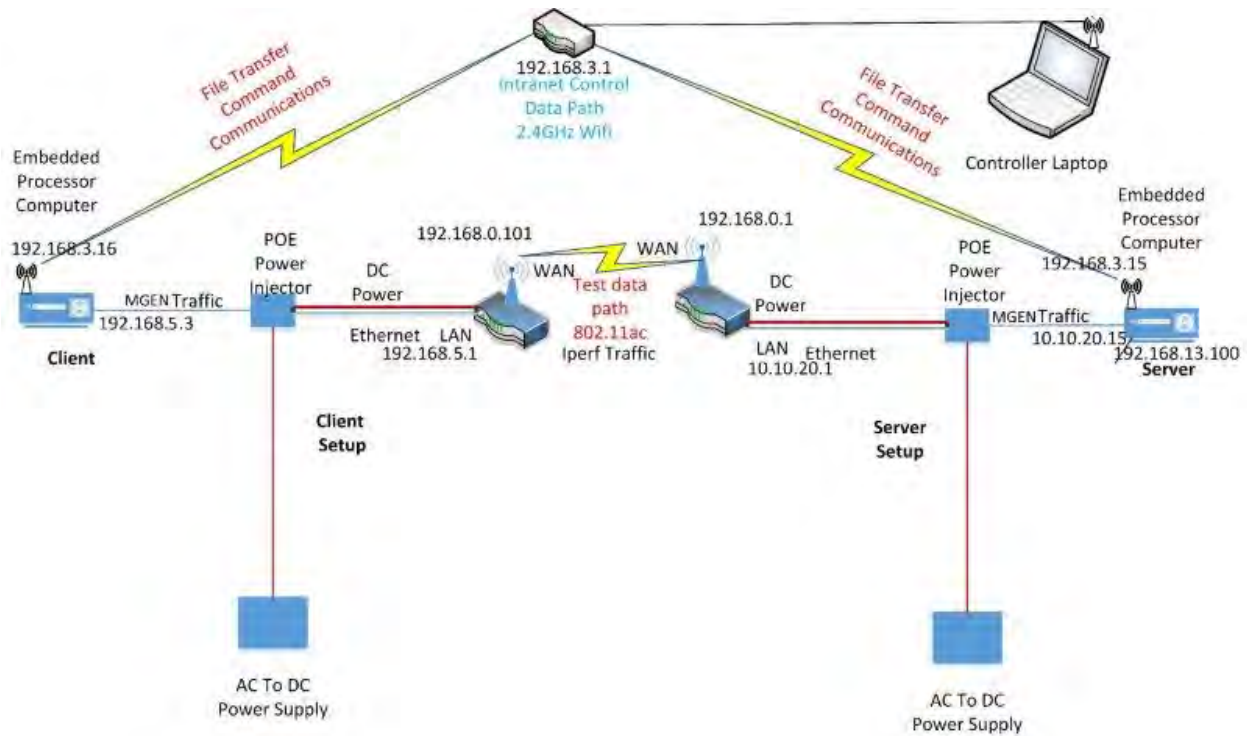


Figure 4-7. Detailed Surrogate U-NII-4 Testbed diagram

4.2.2 Packet distribution

Most network traffic generation was accomplished using a **periodic** function due to its predictability. A **Poisson** distribution was used in early and much later tests since it is a better model of real world message traffic. MGEN provides other distribution functions that were not employed in this work.

As shown in Figure 4-8, in a periodic or uniform distribution, all the values and the average are the same. On the other hand, you can see in Figure 4-9 the data is spread out asymmetrically in a Poisson distribution. But unlike a Gaussian where the median and average values are the same, that is in the middle of a symmetrical distribution, in a Poisson distribution the average value will be less than the median with a small fraction of samples being much higher than the rest due to the long tail to the right. In this example, the median value is 5 but the average would be more like 3.

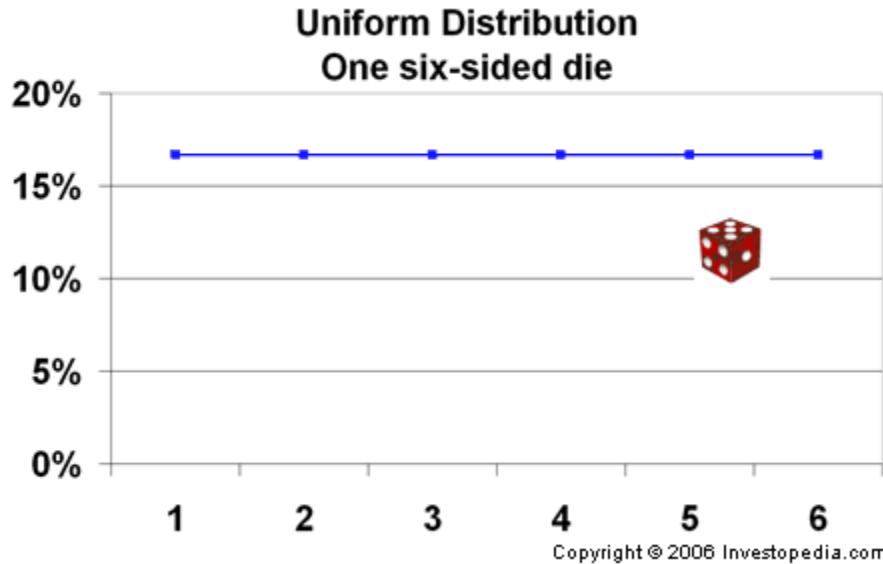


Figure 4-8. Mathematical illustration of Uniform spacing, which is a Periodic distribution

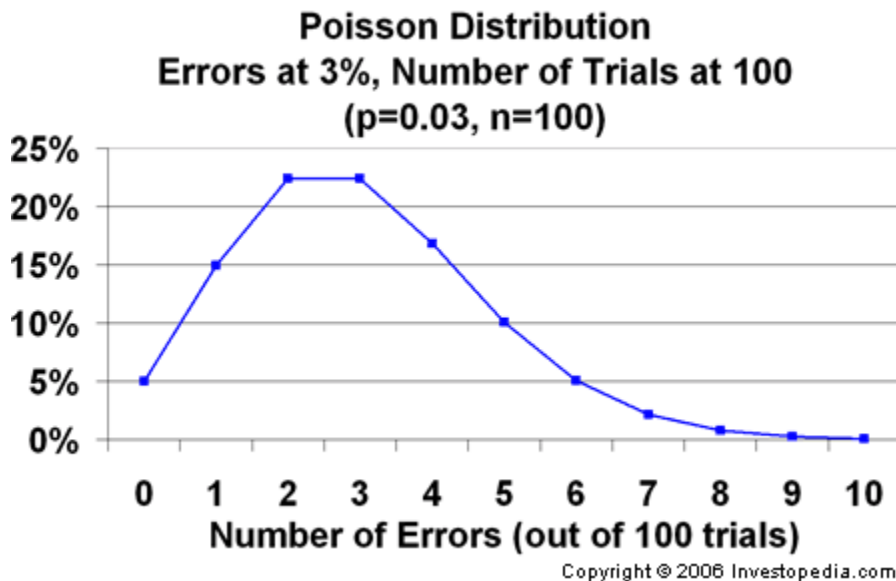


Figure 4-9. Mathematical illustration of a Poisson distribution

For radio traffic, the periodic distribution means that the time between packets is the same. It allowed us a more calibrated control of interference where we needed it to understand the interference. The Poisson distribution allowed us to generate traffic that captured the randomness in real Wi-Fi traffic when desired. The majority of gaps between packets would be less than the periodic distribution at the same traffic load, but there a few longer gaps in between packets as well. Figure 4-10 is a simple

cartoon that may more intuitively illustrate the difference between these distributions if imagined as two picket fences and the BSM a red ball you are trying to throw through them.

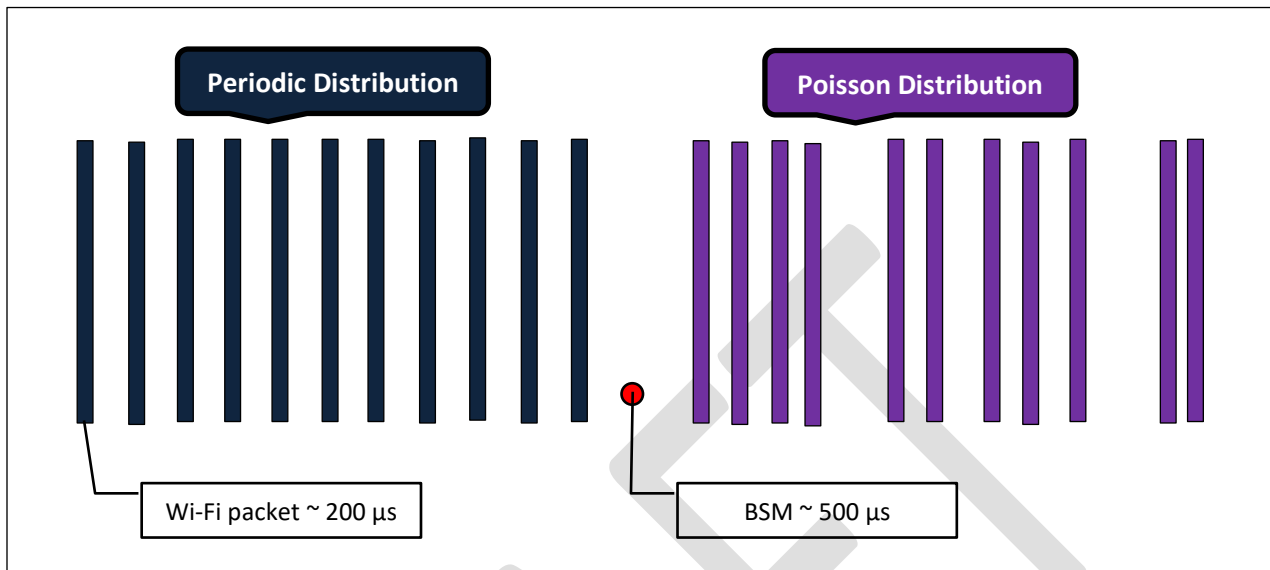


Figure 4-10. Illustration of Periodic and Poisson distributions

The difference is further illustrated by Figures 4-11 to 4-18 below. They are plots of measured transmissions from the UNII testbed with a modulation of $\frac{3}{4}$ QAM-64. That is a data rate of 54 Mbps if loaded at 100%. These plots are for much lower loadings that would be typical of real deployed Wi-Fi. The load percentage and actual packets per second (pps) are given in the figure titles.

Each plot is 1 second of data (x-axis). The data plotted on the y-axis is the time between the transmit time of consecutive packets. This time includes the 1400 byte data frame which is roughly 207 microseconds. The red dashed line in all the plots is the approximate average for the periodic distribution. The gap available for BSMs to slip through would be this time minus the 207 microseconds occupied by the Wi-Fi data.

If you aggregate the 1 second of data in time, the distribution is the vertical slice. So all the points of the periodic distribution are very close to the single point of the average as expected. The Poisson distribution has more points at shorter times than the periodic distribution average (the blunt end of the distribution), with the long tail of the Poisson containing fewer points but stretching upward to much longer times between packets. The Poisson approximates the randomness in real traffic.

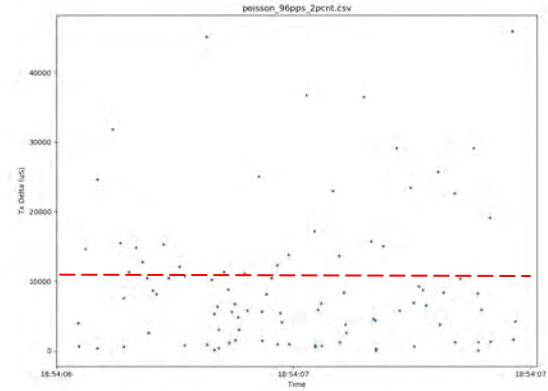
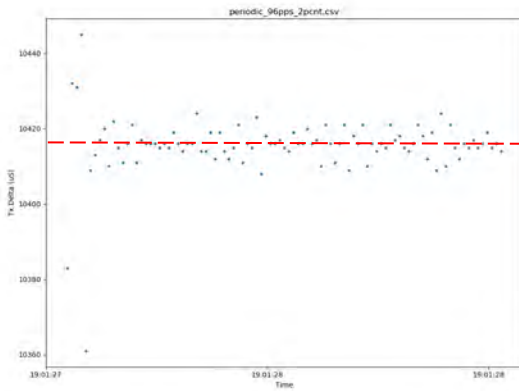


Figure 4-11. Periodic distribution, 2% load, 96 pps **Figure 4-12. Poisson distribution, 2% load, 96 pps**

Key points to note in Figures 4-11 and 4-12, 2% loading: Periodic gaps available to BSMs are roughly 10400 – 200 microseconds or 10,200 microseconds. That is plenty of opportunity for BSMs roughly 500 microseconds long to miss colliding with a Wi-Fi packet. The majority of the inter-packet gaps in the Poisson transmission are shorter and some are too short for BSMs to pass in between. So even though light loading, Poisson at two percent should interfere a bit more with DSRC traffic than periodic gaps.

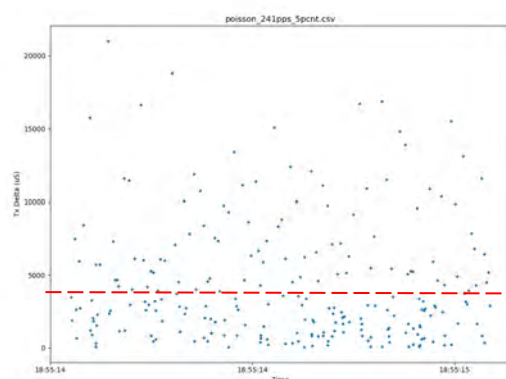
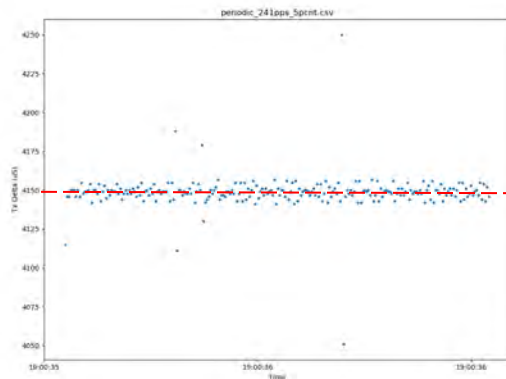


Figure 4-13. Periodic dist., 5% load, 241 pps **Figure 4-14. Poisson dist., 5% load, 241 pps**

Key points to note in Figures 4-13 and 4-14, 5% loading: Periodic gaps available to BSMs are roughly 4150 – 200 microseconds or 3,950 microseconds. Those gaps are still roughly 8 times the size of a BSM. The majority of the inter-packet gaps in the Poisson transmission are shorter and some too short for BSMs to pass in between. So again, Poisson at 5 percent should interfere more with DSRC traffic than periodic gaps.

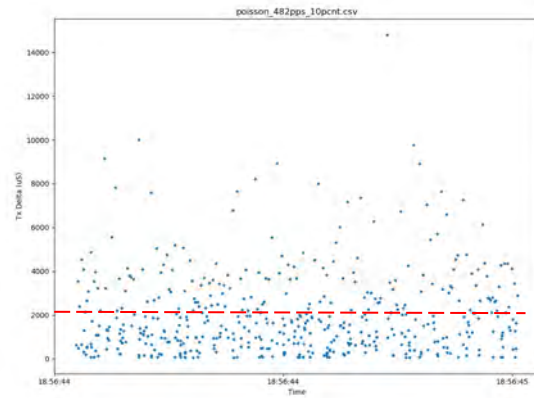
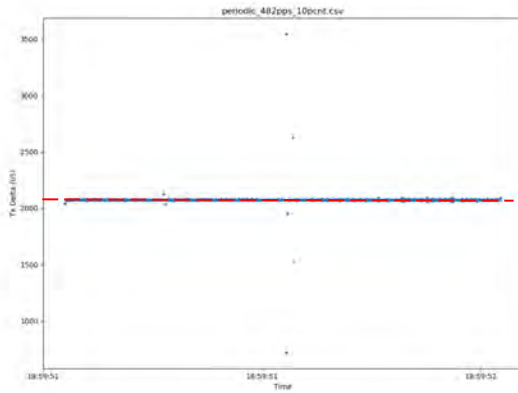


Figure 4-15. Periodic dist., 10% load, 482 pps **Figure 4-16. Poisson dist., 10% load, 482 pps**

Key points to note in Figures 4-15 and 4-16, 10% loading: Periodic gaps available to BSMs are roughly 2000 – 200 microseconds or 1,800 microseconds. At 3 to 4 times the size of a BSM these gaps still provide opportunity for BSMs but packet collisions are more likely. The majority of the inter-packet gaps in the Poisson transmission are again shorter and many too short for BSMs to pass in between. There are also some gaps much longer too, so Poisson at 10 percent load should interfere similarly with DSRC traffic as periodic.

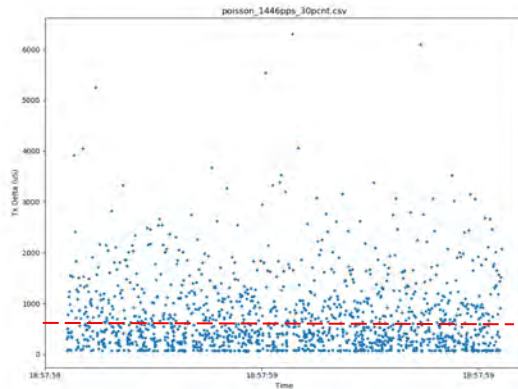
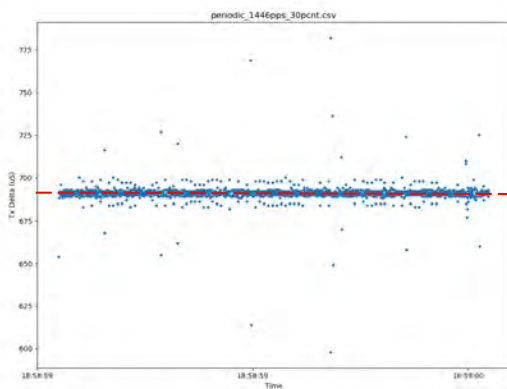


Figure 4-17. Periodic dist., 30% load, 1446 pps **Figure 4-18. Poisson dist., 30% load, 1446 pps**

Key points to note in Figures 4-17 and 4-18, 30% loading: Periodic gaps available to BSMs are roughly 690 – 200 microseconds or 490 microseconds. With the gaps now being the same size or smaller than the BSMs packet collisions and interference are highly likely. At loadings of 30% or higher, the periodic distribution becomes a brick wall to DSRC traffic. The majority of the inter-packet gaps in the Poisson transmission are again shorter but the long gaps provided by the long tail of the distribution now provide more opportunity for BSMs to leak through than the periodic distribution. So Poisson at 30 percent and higher loads should interfere with DSRC traffic but less so than the periodic distribution.

The data above demonstrates how the periodic distribution allowed us a more calibrated control of interference where we needed it to understand the interference. The Poisson distribution allowed us to generate traffic that captured the randomness in real Wi-Fi traffic when desired.

4.3 Characterization of Wi-Fi

In order to generate interference signals that would represent real Wi-Fi we made a series of measurements to characterize actual Wi-Fi devices. Wi-Fi is complex in its operation. The original research plan assumed that Wi-Fi was predictable with controllable behaviors such as modulation code settings and scheduling on a fixed channel.

We decided that we would not learn as much as needed if we forced Wi-Fi to operate like DSRC. We needed a more realistic set of scenarios to ensure that we understood what a vehicle is experiencing while driving through a Wi-Fi environment and that we needed to conduct experiments to characterize Wi-Fi operations in a naturalistic sense.

We started by trying to develop the information needed to establish repeatable test cases to use when we wanted to investigate operating DSRC and Wi-Fi in the same spectrum. We tried to find information about the typical operating pattern for Wi-Fi from Internet sources and experts such as the FCC, NTIA and people from industry we know. No ready test cases or standard performance test cases for a Wi-Fi installation were available to the public.

Most test cases are proprietary, as FCC only requires Wi-Fi to work properly in terms of radio performance, not medium performance. Private companies use their own experts to figure out how to ensure that their product does not interfere while still working properly.

Also, note that Wi-Fi is not a fully interoperable environment—it is up to individuals setting up Local Area Networks (LANs) to decide when the basic interoperability meets their needs. Newer generations of the service may not be able to use all of their features if older generation devices are part of the LAN

4.3.1 Turner Fairbank Location

We investigated commercial-off-the-shelf windows-based tools that can capture Wi-Fi activity. We found a location at the Federal Highway Administration's (FHWA) Turner Fairbank Highway Research Center where we could set up Wi-Fi activity and observe it without inadvertently observing Wi-Fi activity from the general public or other businesses (Figure 4-19). It was also isolated enough to not have competing Wi-Fi installations confusing our observations.

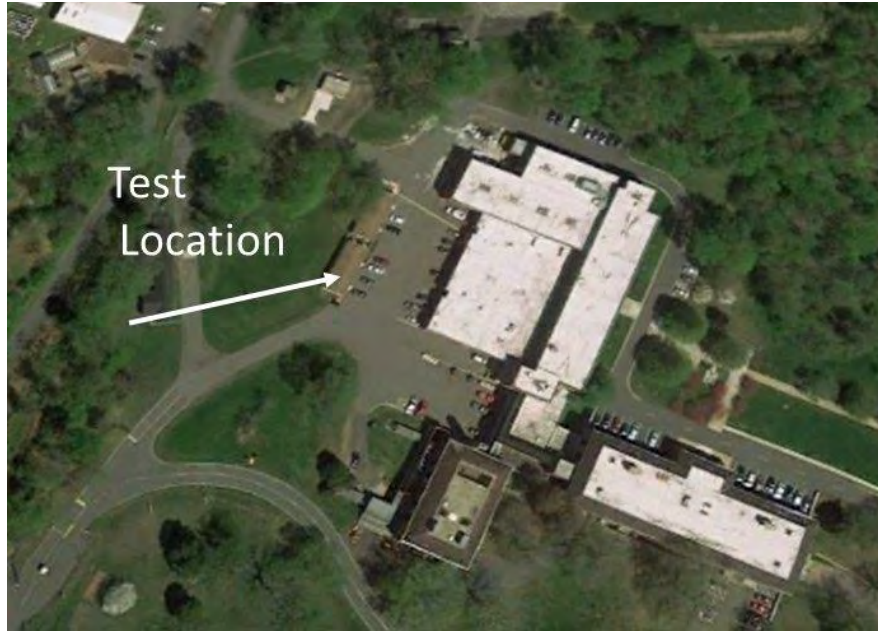


Figure 4-19. Test location at Turner Fairbank Highway Research Center
We bought several COTS Wi-Fi packet capture tools and a collection of consumer devices that use Wi-Fi.

- AirPCAP Nx capture adapter

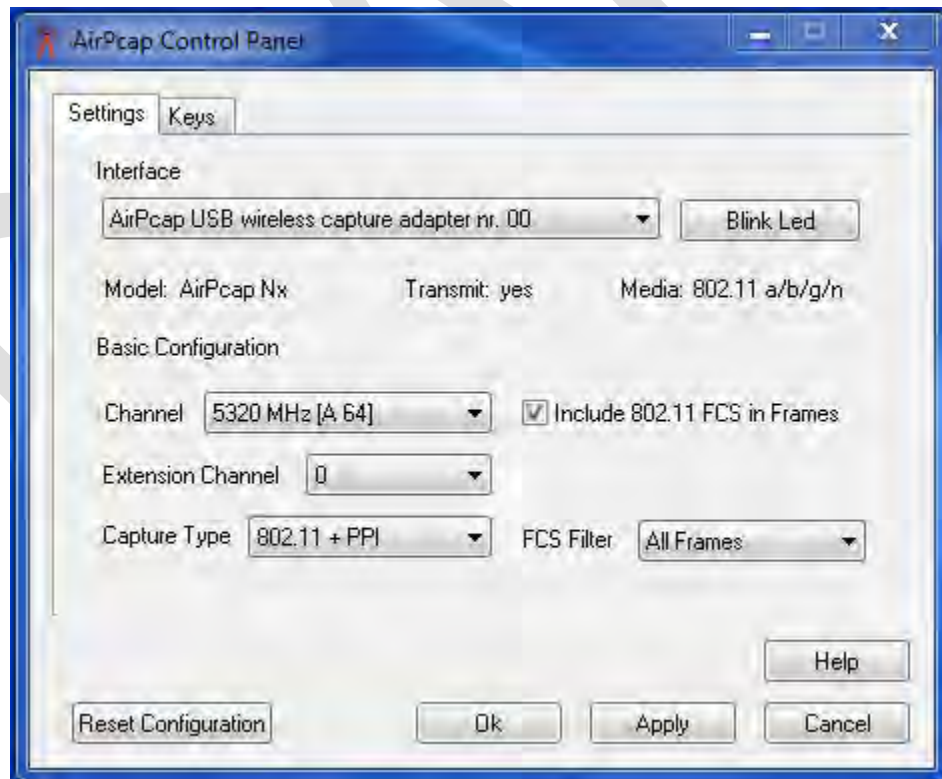


Figure 4-20. Screenshot of AirPcap graphical user interface (GUI)

- EyePA and inSSIDer analysis tools



Figure 4-21. About windows of the MetaGeek capture tools used

- CentOS 7 Linux distribution with tcpdump packet capture feature
- 3M DSRC packet capture tool modified to capture 20MHz 802.11a channel activity in the proposed U-NII-4 band

All of the packet captures from all of the tools were in standard .pcap file formats. These files could then be analyzed using the EyePA tool. All of the visualizations below were generated with that tool.

We set them up at the test site at Turner Fairbank. Consumer devices included: up-to-date laptops (2015 or newer Wi-Fi interfaces) (Windows and Apple based), cellphone handsets (Android and Apple), voice-interactive services on devices (Siri, etc.) as these are a server-based (internet-based) and require prompt Wi-Fi interaction, devices that enable streaming 4K ultra HD video, VOIP, collaborative web conferencing, browser-based videos, and regular internet-based Wi-Fi activities.

We started by measuring the ambient environment. It was very quiet after we shut down carried-in devices being used by people present in the building we were using. The ambient level of activity with one Wi-Fi access point operating was established. Then, devices were turned on one-at-a time to look at the individual contributions to the Wi-Fi medium using the sniffer tools.

The first trials showed us the basic pattern of air time usage and revealed details about the various frame types and interframe spacings that are used in Wi-Fi. Two key conclusions:

- A lot of these things that people envision being large users of the capacity of the medium are actually “bursty” in nature....not continuous use. Like BIG gulps rather than a lot of little sips. Typical observations would be a burst of activity followed by a pause. Then another burst of

activity and pause, this pattern repeating continually. These were notched-type patterns. We need to recreate that behavior in our scenarios for Wi-Fi operation. We have technical details to do so.

- Interframe spacing—number of different ones used in Wi-Fi.
 - Standard interframe spaces when one device finishes using the medium and the rest of devices decide who gets to use it next. MEDIUM ACCESS INTERVAL in 802.11 environment. Space between frames—similar to DSRC. Nearly 100 microseconds when the CCA process is working, such as when two devices or applications are competing for access.
 - Wi-Fi ALSO has small spaces that bracket the frames for transmission without the expected CCA between the frames, such as when ACK frames are sent from a receiver to a sender. More on order of 1-5 microseconds.

When Wi-Fi, particularly the 802.11ac version, is operating, it does not stick with one modulation coding scheme or one channel-width. Management and control happens on the 20 MHz channel (primary channel) with data transport taking place on wider, bonded channels made up of multiple adjacent 20MHz channels—40-80 MHz wide—that associates with the primary channel. The wider channel is the integration of the adjacent 20 MHz channels. The control channel is often, but not always, the lowest frequency 20 MHz channel of the combination. Our devices could only measure a channel width so could see the control frames but not data itself on the wider channels.

The trials at Turner Fairbank lead us to the concept of looking for opportunities for DSRC devices to transmit if they happened to be sharing the same spectrum allocation (based on energy detection).

4.3.2 Typical Activity

We want to characterize typical Wi-Fi activity so we can find realistic test cases to use during interference testing. We observed three typical behavior elements in naturalistic Wi-Fi operation – constant activity, spikes of activity, and bursts of activity. The following plots were generated by the EyePA tool. They show time on the horizontal axis and percent of channel capacity used on the vertical axis.

Trial on channel 66, one Ultra 4x HD streaming session, for reference

4.3.2.1 Observing Control activity on 20MHz channel 66.

Data was being sent on a wider channel was not observed.

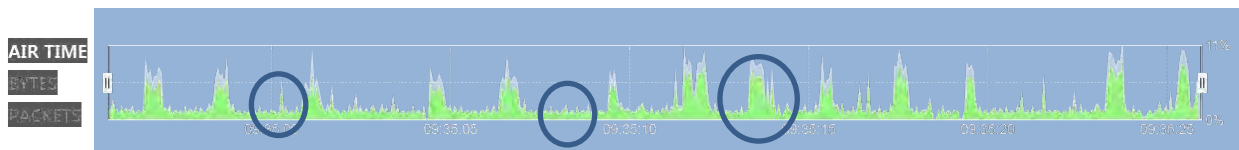


Figure 4-22. Sample of streaming HD video

Figure 4-22 shows the three typical behavior elements during a 30-second capture taken while a single 4x Ultra HD stream was in use. (The x-axis is time and the y-axis is percent of time that there are is observable Wi-Fi activity in the channel.) The three behavior elements are:

1. The background level of activity that consists of beacons from the access point, probes from potential station devices, and low-level application service data exchanges, (see blue circles in Figure 4-22 above).



Figure 4-23. Interval of background management activity

Figure 4-23 focuses on the middle blue circle in Figure 4-22. It shows that during a 1-second interval of background-level activity, there were 48 mostly management frames sent with the average time between frame starts being 22 milliseconds. Management frames tend to be short with lengths of less than 100 bytes. At the modulation coding schemes used, they would be several 10's of microseconds long. Therefore, the opportunity for BSMs to pass through this traffic without collision would mostly depend on the data frames. These management frames should present little interference.

2. Spikes of activity when an application is serviced



Figure 4-24. Interval of intermittent management activity

Figure 4-24 focuses on the left blue circle in Figure 4-22. During a 0.33 second interval of spike-type activity, there were there were 31 mostly management frames with an average time between frame starts of 17 milliseconds. Again, 0.5 ms BSMs should have little trouble getting through gaps over 16 ms long between the short management frames.

3. Bursts of streaming video activity.



Figure 4-25. Interval of bursty management activity

Figure 4-25 focuses on the right blue circle in Figure 4-22. During a 0.5-second interval of burst-type activity, there were 576 data and management frames with an average time between frame starts of 830 microseconds. Measurements described in section 9.1.5 below show that this burst of activity would block most DSRC during the interval.

4.3.2.2 Trial on channel 165 with an 802.11a MCS forced, like several Ultra 4x HD streaming sessions

Control and data are on 20MHz channel 165.

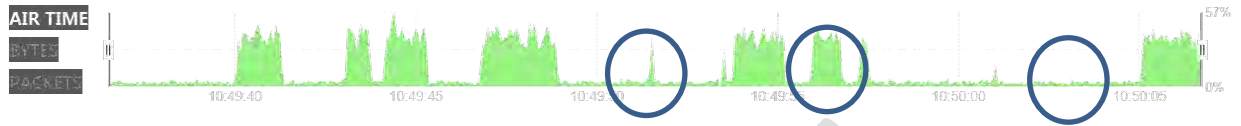


Figure 4-26. Sample of multiple streaming HD videos

1. The background level of activity that simulates beacons from the access point, probes from potential station devices, and low-level application service data exchanges, (see blue circles in Figure 4-26 above).



Figure 4-27. Interval of background management activity

Figure 4-27 focuses on the right blue circle in Figure 4-26. During a 0.75 second interval of background-level activity, there were 275 mostly management-like frames sent with the average time between frame starts of 3 milliseconds.

2. Spikes of activity when an application is serviced

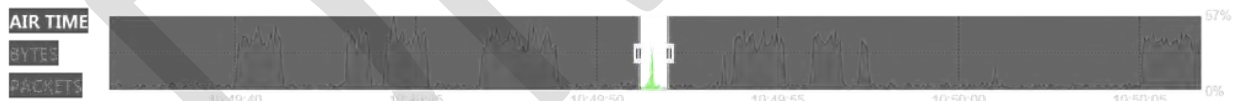


Figure 4-28. Interval of intermittent management activity

Figure 4-28 focuses on the left blue circle in Figure 4-26. During the 0.65 second interval examined, a series of 240 data frames (with corresponding acknowledgement frames sent back) were sent to a particular device servicing an unknown application.

3. Bursts of streaming video activity.



Figure 4-29. Interval of bursty management activity

Figure 4-29 focuses on the middle blue circle in Figure 4-26.

During a 0.65 second interval of burst-type activity, there were 2244 data and management-like frames with an average time between frame starts of 330 microseconds. It would be impossible for a 500 microsecond long BSM to fit through any gaps between packets in this interval.

The first group of files (above) was a survey of the U-NII-3 group of channels for background type activities.

4.3.2.3 Additional Wi-Fi Device Characterizations

Channel 149 iPad speed test – Channel 149 was monitored while a speed test was conducted on an iPad device. The plot shows both the upload and download phases of the test. The speed test was conducted using a consumer-grade application. At most it caused activity that only used 30% of the channel capacity. More complete utilization can be seen further on in the report when better tools were used to generate the over-the-air traffic.

Channel 149 iPad speed test – Channel 149 was monitored while a speed test was conducted on an iPad device. The plot shows both the upload and download phases of the test.

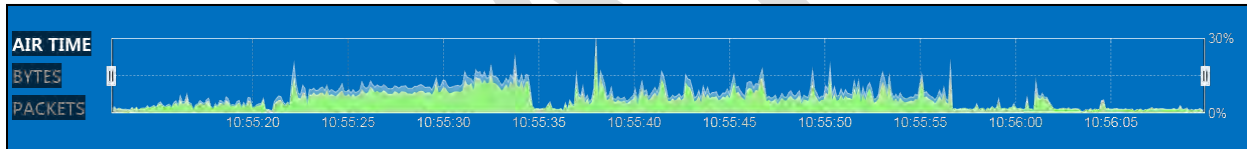


Figure 4-30. iPad speed test

Channel 153 beacon and probe – Activity on Channel 153 was observed. One device was probing and the access points did something. A number of malformed frames were observed that were probably from the adjacent channel 149.

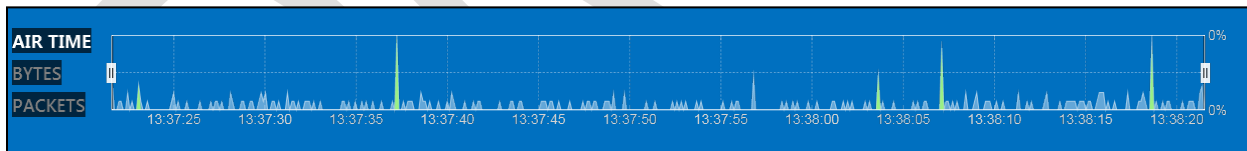


Figure 4-31. Channel 153 beacons and probes

Channel 149 beacon and probe – Activity on channel 149 was observed. A steady amount of activity that occupied 1 to 3% of the airtime was observed.

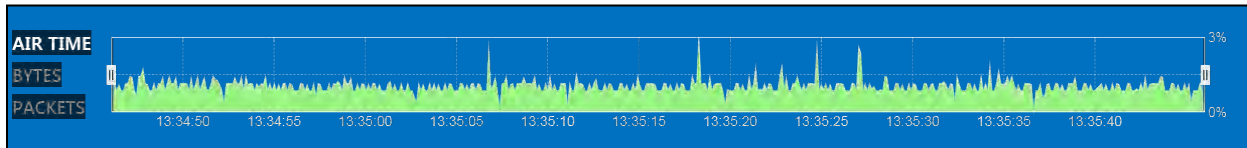
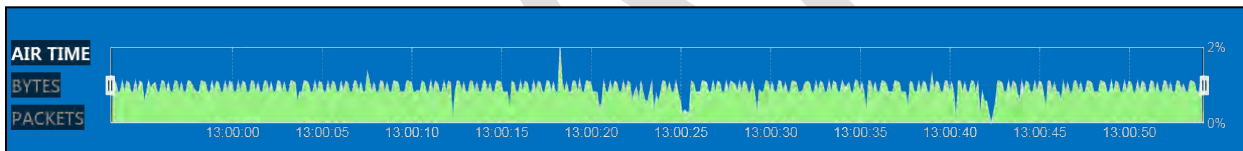
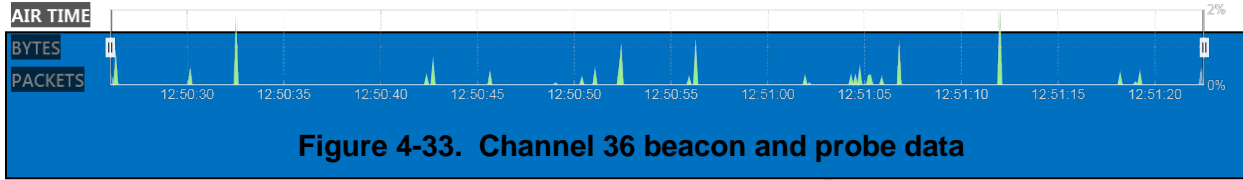


Figure 4-32. Channel 149 beacons and probes

4.3.2.4 Background activity on UNII-1 channels

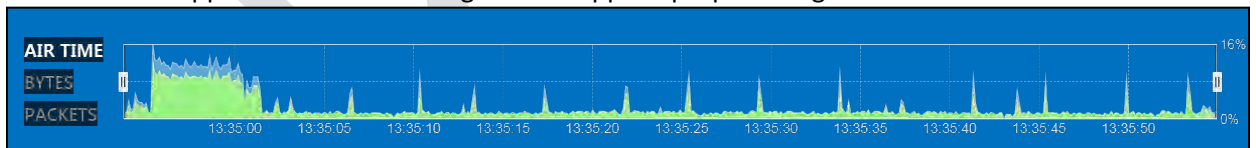
The next group of files was a survey of some of the U-NII-1 group of channels for background activity. SSIDs are advertised on Channel 36.



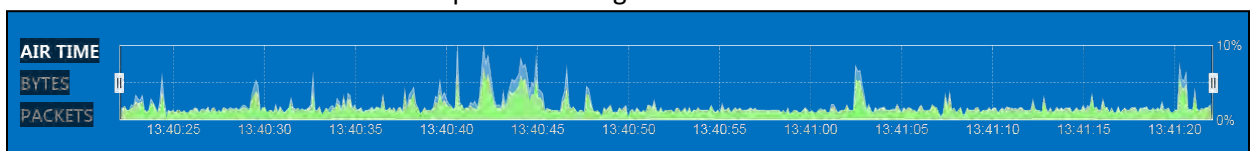
4.3.2.5 Typical Consumer Devices

The next group of plots is of typical consumer activity one-device-at-a-time.

Channel 149 Apple browser streaming video – Apple laptop viewing Internet video



Channel 149 Motorola MotoX smart phone viewing Internet video



Channel 149 Windows laptop browser video

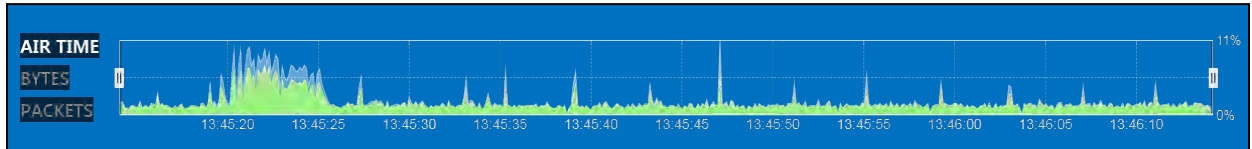


Figure 4-39. Windows laptop viewing Internet video

Channel 149 MotoX voip – voice over IP session

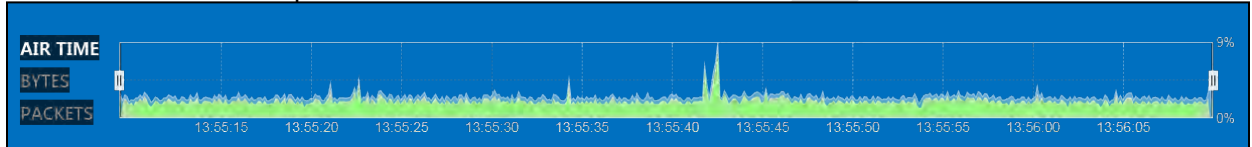


Figure 4-40. Voice over IP session

Channel 149 Apple facetime -- two people on the same LAN

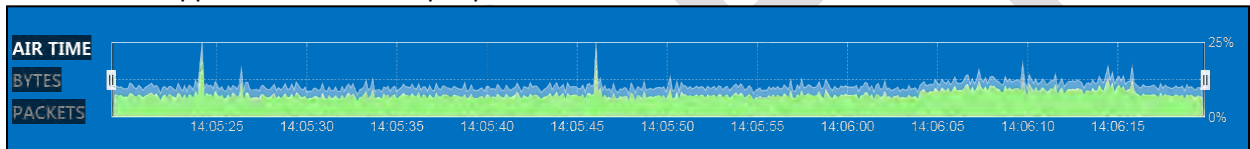


Figure 4-41. Apple Facetime session

4.3.2.6 Natural Wi-Fi

The next two images illustrate the spikey and repetitive nature of real Wi-Fi traffic.

Channel 149 talking with Apple Siri

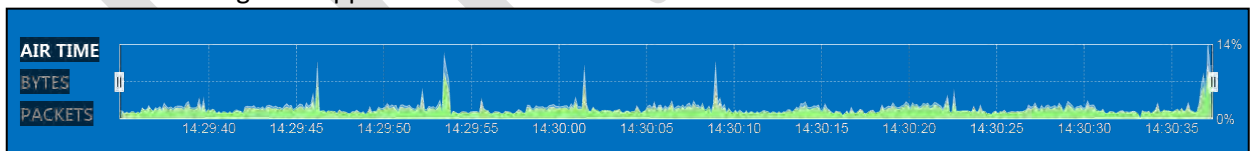


Figure 4-42. Apple Siri session

Channel 149 streaming ultra HD to a smart TV

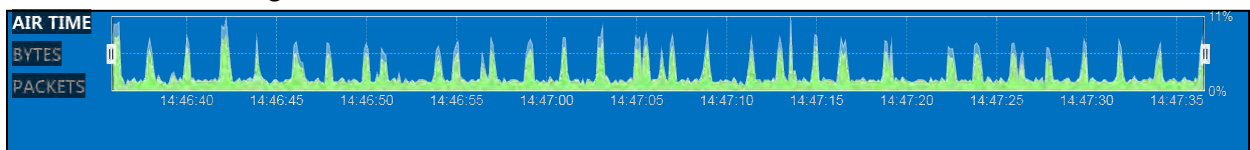


Figure 4-43. Access point streaming ultra HD video to a Smart TV

4.3.2.7 Complexity of Natural Wi-Fi

These last two data captures illustrate the complexity due to the unpredictability of multiple applications obscuring the spikey regularity of individual Wi-Fi transmitters in the wild.

Channel 149 everything in the lab running at the same time

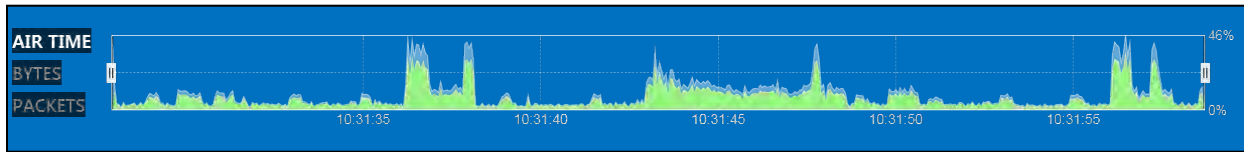


Figure 4-44. Everything in the lab running at the same time

Channel 149 everything in the lab running at the same time five minutes later

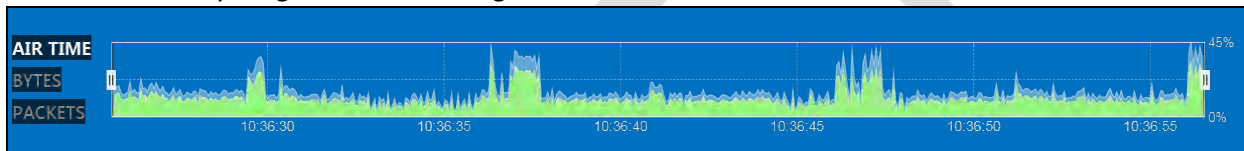


Figure 4-45. Same devices 5 minutes later

4.3.3 Specific Captures of Simulated DSRC and Wi-Fi Activities.

The DSRC signals in the data captured below, also with the EyePA tool, was generated with a Cohda OBU transmitting in the 10 MHz DSRC channel 172. The UNII Wi-Fi signals were generated with our UNII testbed operating with a modulation of $\frac{3}{4}$ QAM-64, hence at a 54 Mbps data rate, transmitting in the overlapping 20 MHz UNII channel 173 or adjacent channel 165. The UNII packet size was 1400 bytes so 100% traffic loading transmitted 4821 frames per second.³⁶ **The key result of this activity is the observation that the transmissions from our surrogate UNII testbed qualitatively resemble the actual Wi-Fi traffic that we measured in the field.**

4.3.3.1 Background spectrum activity

Figure 4-46 shows the spectrum with the UNII testbed turned on but not transmitting any data. The frames in the figure are just the beacons sent by the access point and probes sent by the client. Note how they are transmitted as a highly regular periodic distribution.

³⁶ Frames per second = { (Max Data Rate [bps]/8 [bits/byte]) / 1400 bytes per frame } * load %

At 10% load, the output would be [(54,000,000 bps)/8 bits/byte] /1400 bytes/frame] *0.10 = 482 fps

Measured: Channel 165 54MB/s actual management frame background activity

Beacon Frames: 109 sent, 100 % received

(A skip in sequence numbers was noted but further investigation indicated that the access point transmitter double incremented one time for an unknown reason.)

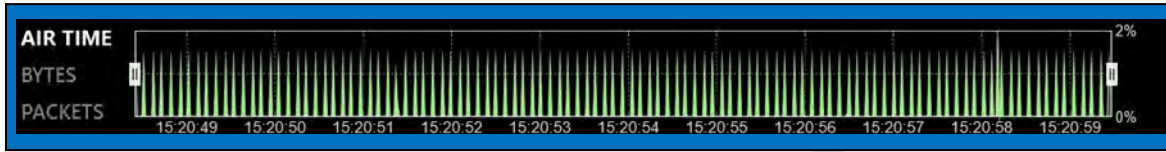


Figure 4-46. UNII testbed beacons and probes

Figure 4-47 is the same UNII background but with the DSRC radio turned on. The larger square DSRC frames periodically stepping on the more frequent and narrow UNII management frames is obvious. Neither radio hears the other well enough for the CCA mechanism to step in and get either to back off. The gap between the beginning of one DSRC frame to the beginning of the next is 50 ms but because the sniffer sometimes would lose one signal or the other during the collisions in the receiver complete frames were not always captured obscuring that timing somewhat.

Measured: Channel 173 54MB/sec actual management background and DSRC on channel 172

Beacon Frames: 159 sent, 100 % received

DSRC: 20.1 frames/sec

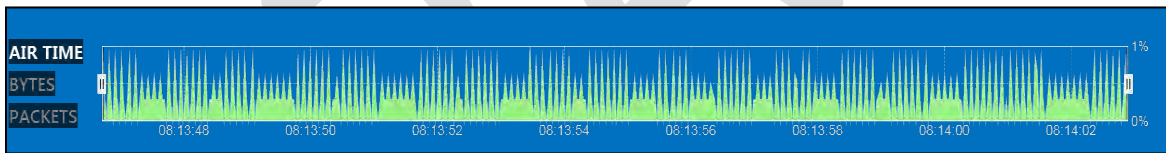


Figure 4-47. UNII testbed beacons and probes with DSRC

4.3.3.2 Spectrum with UNII data transmission as well as background management activity

The following data captures show the spectrum as the traffic load from the UNII testbed is increased, often on top of the DSRC signal.

Figure 4-48 shows the UNII testbed transmitting a **2% traffic load** (96 frames per second) at the 54 Mbps data rate. Compare to the plots in section 4.3.2 above and note the similarity to the data bursts.

Measured: Channel 165 54MB/sec 2% Poisson – 96 fps

Beacon Frames: sent, 100 % received

QOS Data: 1140 sent, 100 % received (There were several cases where the transmitting device in the U-NII4 Test Bed repeated sequence numbers for an unknown reason.)

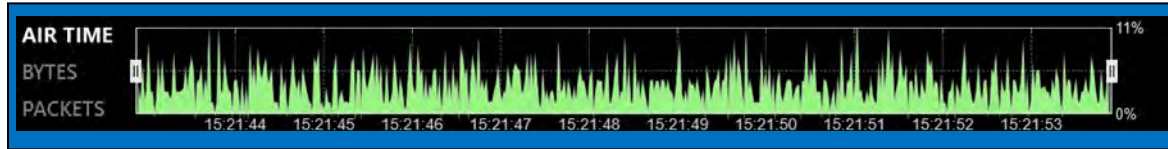


Figure 4-48. 2% Poisson UNII traffic load on channel 165

Figure 4-49 shows essentially the same thing but with the addition of the 20Hz DSRC signals.

Measured: Channel 173 54MB/sec 2% Poisson – 96 fps

Beacon Frames: 142 sent, 100 % received

QOS Data: 1385 sent, 95.7 % received 4.3% missed

DSRC: 20.1 frames/sec

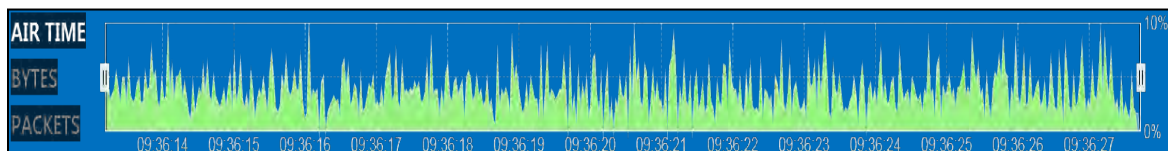


Figure 4-49. 2% Poisson UNII traffic load on channel 173 with DSRC

Figure 4-50 shows the UNII testbed transmitting a **5% traffic load** (241 frames per second) at the 54 Mbps data rate without DSRC, and Figure 4-51 with DSRC.

Measured: Channel 165 54MB/sec 5% Poisson – 241 fps

Beacon Frames: 108 sent, 100 % received (One sequence number was skipped but the beacons were sent at the correct interval.)

QOS Data: 2605 sent, 100 % received

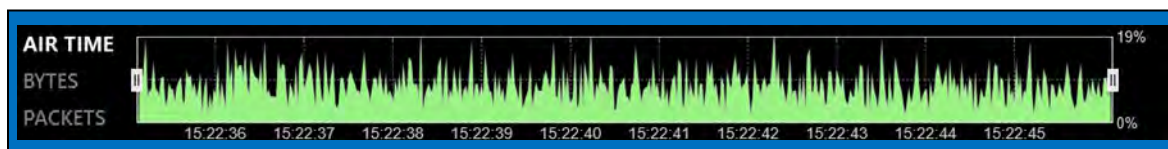


Figure 4-50. 5% Poisson UNII traffic load on channel 165

Measured: Channel 173 54MB/sec 5% Poisson – 241 fps
Beacon Frames: 110 sent, 100% received
QOS Data: 2562 sent, 96.3% received 3.7% missed
DSRC: 20.1 frames/sec

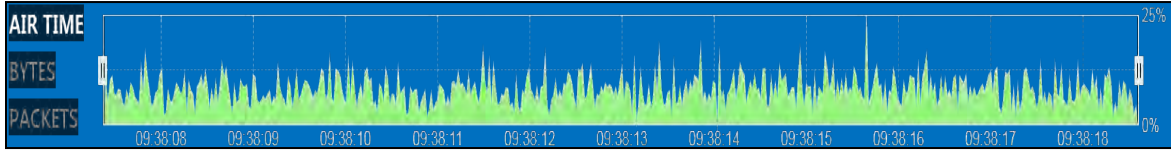


Figure 4-51. 5% Poisson UNII traffic load on channel 173 with DSRC

Figure 4-52 shows the UNII testbed transmitting a **10% traffic load** (482 frames per second) without DSRC, and Figure 4-53 with DSRC.

Measured: Channel 165 54MB/sec 10% Poisson – 482 fps
Beacon Frames: 105 sent, 100% received
QOS Data: 5240 sent, 100% received

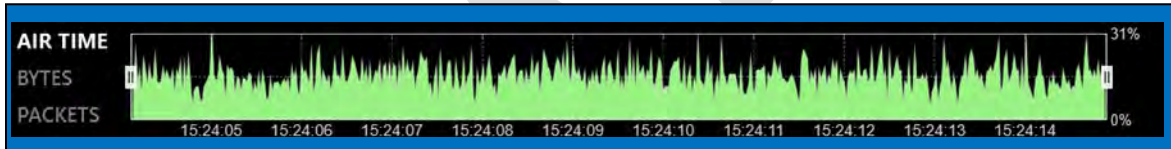


Figure 4-52. 10% Poisson UNII traffic load on channel 165

Measured: Channel 173 54MB/sec 10% Poisson – 482 fps
Beacon Frames: 118 sent, 100% received
QOS Data: 5563 sent, 95.4% received 4.6% missed
DSRC: 19.8 frames/sec

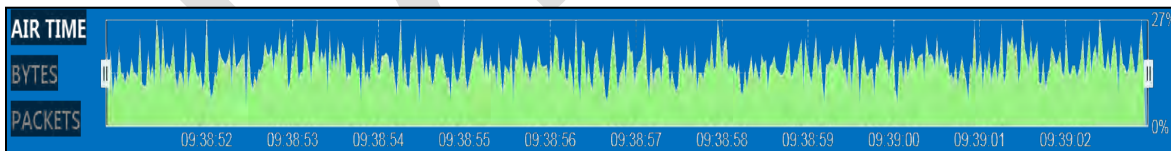


Figure 4-53. 10% Poisson UNII traffic load on channel 173 with DSRC

Figure 4-54 shows the UNII testbed transmitting a **20% traffic load** (964 frames per second) without DSRC, and Figure 4-55 with DSRC.

Measured: Channel 165 54MB/sec 20% Poisson – 964 fps

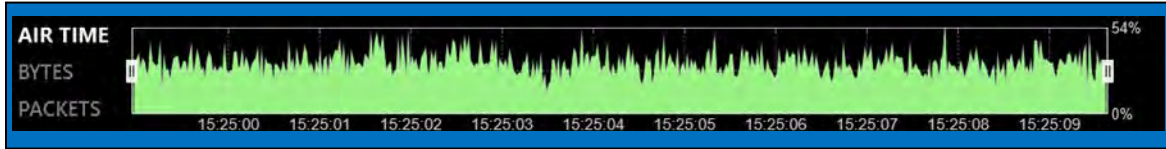


Figure 4-54. 20% Poisson UNII traffic load on channel 165

Measured: Channel 173 54MB/sec 20% Poisson – 964 fps

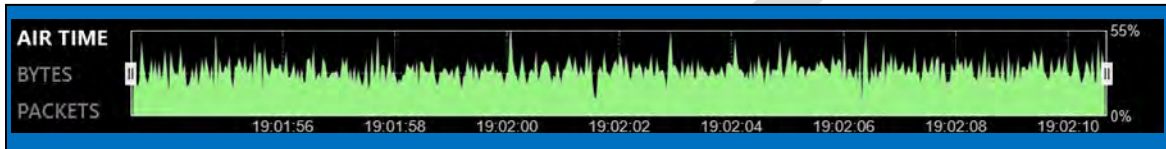


Figure 4-55. 20% Poisson UNII traffic load on channel 173 with DSRC

Figure 4-56 shows the UNII testbed transmitting a **30% traffic load** (1446 frames per second) without DSRC, and Figure 4-57 with DSRC.

Measured: Channel 165 54MB/sec 30% Poisson – 1446 fps

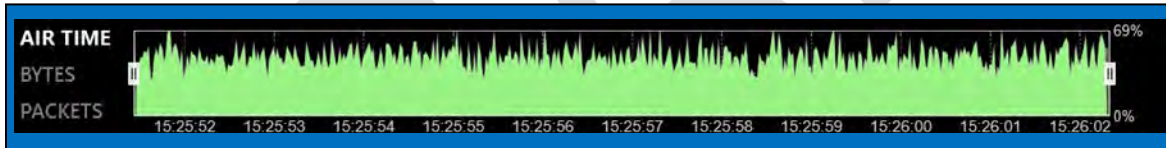


Figure 4-56. 30% Poisson UNII traffic load on channel 165

Measured: Channel 173 54MB/sec 30% Poisson – 1446 fps



Figure 4-57. 30% Poisson UNII traffic load on channel 173 with DSRC

Figure 4-58 shows the UNII testbed transmitting a **70% traffic load** (3375 frames per second) without DSRC, and Figure 4-59 with DSRC.

Measured: Channel 165 54MB/sec 70% Poisson – 3375 fps

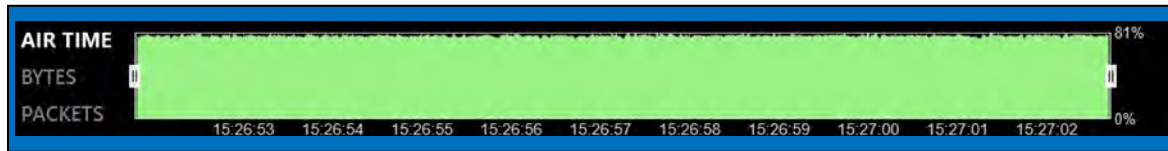


Figure 4-58. 70% Poisson UNII traffic load on channel 165

Measured: Channel 173 54MB/sec 70% Poisson

Beacon Frames: 100 sent, 99% received
QOS Data: 23166 sent, 95.8 % received 4.1% missed (For 0.3 seconds near the beginning of the capture, no frames were recorded because of an unknown reason.)
DSRC: 18.9 frames/sec

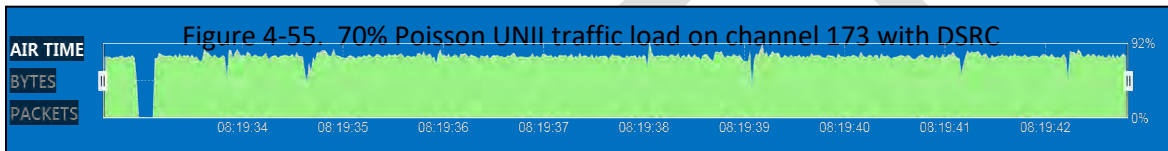


Figure 4-59. 70% Poisson UNII traffic load on channel 173 with DSRC

Figure 4-60 shows the UNII testbed transmitting a **100% traffic load** (4821 frames per second) without DSRC, and Figure 4-61 with DSRC.

Measured: Channel 165 54MB/sec 100% Poisson – 4821 fps

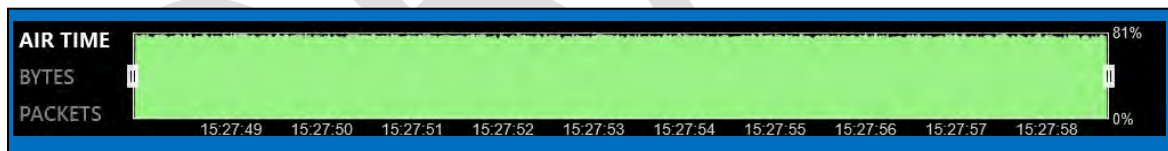


Figure 4-60. 100% Poisson UNII traffic load on channel 165

Measured: Channel 173 54MB/sec 100% Poisson – 4821 fps

Beacon Frames: 115 sent, 100% received
QOS Data: 26196 sent, 92.6% received 7.4% missed
DSRC: 14.6 frames/sec

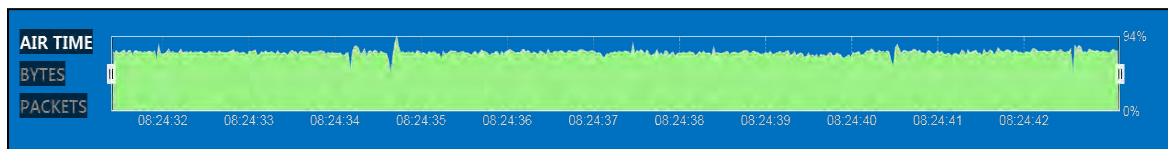


Figure 4-61. 100% Poisson UNII traffic load on channel 173 with DSRC

As shown in the measurements at Turner Fairbank, single devices may occupy a few percent or less bandwidth for less than a second at a time in bursts. But 10 to 100 of such devices could easily be in range of a DSRC device and not hear each other as hidden nodes. So testbed generated Wi-Fi traffic at higher loads essentially represents environments with multiple UNII Wi-Fi devices in the band. Also, note the similarity between the actual Wi-Fi and generated Poisson traffic.

4.4 Inter-packet gap versus channel loading

Setting the modulation of the surrogate UNII testbed would determine the maximum data rate. For example, setting the modulation to ¼QAM-64 sets the maximum data rate of 54 Mbps per the 802.11a standard. At 100% loading the UNII sends out 54 Mbps. To achieve the loadings of 70, 30 and 2% we just multiply 54 Mbps times these fractions and specify those data rates in the MGEN input to the Wi-Fi radio. For example, set to 30% loading, the UNII testbed generates $54 * 0.3$ or 16.2 Mbps.

In our initial sensitivity tests using these loadings (2, 30, 70 and 100%) the results were not sensitive to load except at two percent. That is because how the energy that makes up a channel busy percentage is distributed makes a difference; in particular, what the resulting gaps are between packets.

4.4.1 Inter-Packet Gaps

We started by setting the data packet size from MGEN to 1500 bytes, the largest Message Transport Unit (MTU) for 802.11a.³⁷ We can calculate the average inter-packet gap available for BSMs to enter the receiver unobstructed.³⁸ Table 4-1 shows the data rates and inter-packet gaps for the UNII Wi-Fi traffic loads we tested. Note that these calculations are based only on the data sent and do not include all the Wi-Fi management frames (like probes, beacons, requests-to-send [RTS], acknowledgements [ACK], etc.), which further reduce the gaps available for BSMs to slip through.

³⁷ We simulate 802.11ac 20 MHz channels using 802.11a since this setting of the testbed allows us to control other transmission variables for a 20 MHz channel. For example to hold the modulation, channel width and power constant. Set to 802.11ac the testbed automatically adjusts all the transmission variables in real-time to optimize the WLAN communications so that it is not possible to test sensitivity of interference to the transmission variables.

³⁸ 1500 bytes/packet * 8 bits/byte = 12,000 bits/packet. So for the 30% load case:

$$54,000,000 \text{ bits/sec} / 12,000 \text{ bits/packet} = 1350 \text{ packets/sec}$$

$1/1350 \text{ packets/sec} = 0.00074 \text{ sec}$ or 0.74 ms/packet, this is the average time between packet start times. We must subtract the time taken up by the packet to calculate the inter-packet gap.

$$\text{Packet length in time: } 12,000 \text{ bits/packet} / 54,000,000 \text{ bits/sec} = .00022 \text{ sec or } 0.22 \text{ ms.}$$

$$\text{Inter-packet gap: } 0.74\text{ms} - 0.22 \text{ ms} = 0.52 \text{ ms}$$

Table 4-1 Inter-packet gaps of initial UNII loadings

Modulation = ¾QAM-64	Peak data rate = 54 Mbps	Packet size = 1500 bytes	Byte size = 8 bits/byte	Packet duration = 0.22 ms
Traffic Load (%)	Data Rate (Mbps)	Packets/sec	Seconds/packet (ms)	Average Inter-packet gap (ms)
100	54	4500	0.22	0
70	37.8	3150	0.32	0.1
30	16.2	1350	0.74	0.5
2	1.1	90	11.1	10.9

Since Basic Safety Messages (BSMs) are on the order of 0.5 ms long, it is obvious that they can't squeeze through the gaps presented by 30, 70 and 100% traffic loadings (shaded pink in the table). This table explains why only the 2% loading showed any effect on interference. All the other loadings presented maximum interference.

One way to conceive this effect is to imagine the 30% load case to be a picket fence between the DSRC receiver and DSRC transmitter. In this case, the space between pickets would be 5 inches. Imagine trying to throw balls through the fence that are themselves 4-5 inches in diameter without touching a picket. Then shrink the space between pickets for the 70% load case. Clearly, no ball can get through. Loadings above the red line in Table 4-1 can be expected to generate interference that allows no significant quantity of BSMs through. This conclusion is indeed what measurements in the field demonstrated.

Therefore, our interference measurements provided a true result.

The problem is that except for 2% load we did not test any other loadings that interference might be sensitive to. So in that respect, what appears to be a lack of sensitivity is actually an artifact of our choosing to test mostly loadings of 30% and higher. Hence our measurements were true but the results were an artifact of our choices.

4.4.2 Additional Traffic Loadings

We added traffic loadings to the test protocol that would be more likely to show how interference to DSRC could be influenced by the traffic loading of a Wi-Fi device. Table 4-2 calculates the expected gaps or opportunities for BSMs of these additional loadings. Note the agreement with the measured Periodic distribution inter-packet gaps shown in section 4.2.2 above.

Table 4-2 Inter-packet gaps including additional UNII loadings

Modulation = ¼QAM-64	Peak data rate = 54 Mbps	Packet size = 1500 bytes	Byte size = 8 bits/byte	Packet duration = 0.22 ms
				Average
Traffic Load (%)	Data Rate (Mbps)	Packets/sec	Seconds/packet (ms)	Inter-packet gap (ms)
100	54	4500	0.22	0
70	37.8	3150	0.32	0.1
30	16.2	1350	0.74	0.5
20	10.8	900	1.1	0.9
10	5.4	450	2.2	2.0
5	2.7	225	4.4	4.2
3	1.6	135	7.4	7.2
2	1.1	90	11.1	10.9

We confirmed these calculations with time-domain measurements on a spectrum analyzer. Figure 4-62 shows clearly how the spectrum congests as the Wi-Fi traffic increases. Each x-axis division in the time-domain pulse plots is 25 ms (i.e., block is 250 ms wide). A BSM needs a gap of ~0.5 ms. The x-axis for the spectrograms below in the figure spans frequency from 5.81 to 5.82 GHz centered on 5.865 GHz. The y-axis is time from zero at the bottom up to 250 ms. These plots also show how the gaps vary.

UNII CH173 PL 1500 with Varying Loads – IQ Data

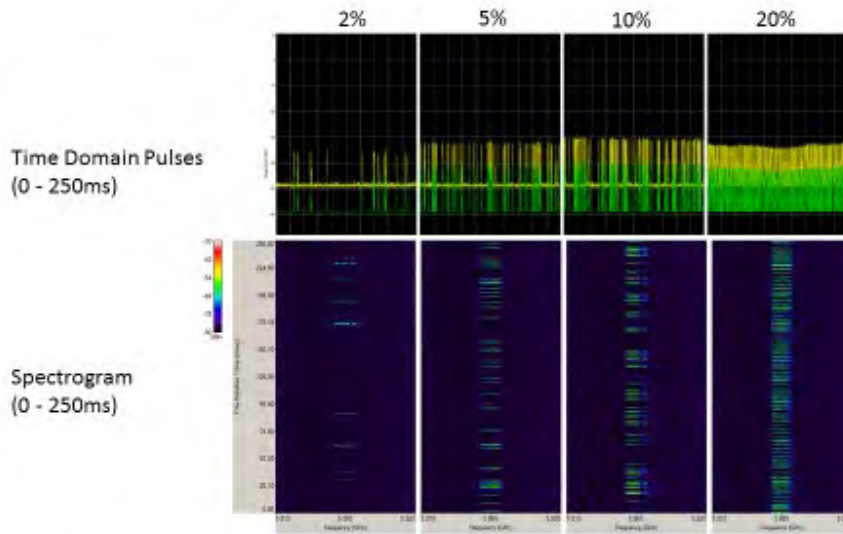


Figure 4-62. Measured gaps between UNII packets for various loadings

To confirm our calculations we measured 10 seconds of I-Q data for traffic loadings listed in Table 4-2. A statistical analysis by Spectro-X software shows that our calculations overestimated the opportunities for BSMs by roughly a factor of 2 since our calculation assumes a regular periodic transmission but the traffic generation was actually a random Poisson transmission.

The measured data in Figure 4-13 above confirms this. In Figure 4-13 (5% load) the measured space between packet start times is 4.2 ms, the same as calculated in Table 4-3. You can also see that the average of the Poisson spacing in the data in Figure 4-14 on the right is about 1.8 ms, which is consistent with the Spectro-X data in the measured average column of Table 4-3.

Similarly, the measured 10% periodic spacing of the data in Figure 4-15 above is 2.0 ms, the same as calculated in Table 4-3. The average for the Poisson spacing in Figure 4-16 looks to be 0.8 ms, which is the same as measured in the Spectro-X data in Table 4-3.

As previously described, when the periodic distribution spacing is smaller than a BSM the tiny variability, calculated and measured, does not allow space for BSMs to slip through leading to worst case interference for that loading. But even though the average spacing of Poisson traffic at the same percent loading is roughly half the periodic spacing, the much larger gaps that randomly show up still allow for some BSMs to get through for high loadings. The 20% load case in Table 4-3 is a perfect example. Notice that the maximum gap was almost 5 times as wide as a BSM though the average space is smaller than a BSM.

Concerning our field measurements, Table 4-3 shows that any sensitivity of interference to UNII load must be for loadings less than 20% using our surrogate U-NII-4 testbed. This explains the lack of sensitivity above 30% load. These results are consistent with the independent measurements shown in section 4.2.2 above.

Table 4-3 Measured Inter-packet gaps

Modulation = ¾QAM-64	Peak data rate = 54 Mbps	Packet size = 1500 bytes	Byte size = 8 bits/byte	Packet duration = 0.22 ms
Traffic Load (%)	Calculated average Inter-packet gap (ms)	Measured Average (ms)	inter-packet gaps Maximum (ms)	Minimum (ms)
100	0			
70	0.1			
30	0.5			
20	0.9	0.4	2.4	0.016
10	2.0	0.8	19	0.043
5	4.2	1.8	30	0.016
3	7.2	3.0	63	0.00032
2	10.9	4.0	62	0.00012

4.4.3 Sensitivity to Packet Length

Another finding is how the gaps, and essentially the interference, were affected by the selected packet length.

4.4.3.1 1500-byte packets

We selected data packet size in the internet protocol to be 1500 bytes long. But the Wi-Fi wireless protocol adds header bytes to the frame, causing it to exceed the 1500-byte Message Transfer Unit limit. As a result every packet was split into two packets, doubling the number of data packets and management packets. We realized there were more packets transmitted than we intended when looking at the data shown in Figure 4-63³⁹ below.

In the time-domain plot at the top of 4-63 you see a large packet in the middle, which is a data packet. (That the packet is data is verified by the IQ display to lower right that shows it is at QAM-64 modulation, which is the high-speed modulation used for data transfer.) Shortly after (to the right) is a much shorter packet which is an acknowledgement (ACK). Then after a gap is another short data packet, which is the rest of the 1500-byte packet that didn't fit into the first frame. An ACK packet follows the remainder packet as well. These additional gaps and packets reduce the gap between the large data packets, hence reducing the opportunity for a BSM to slip through.

The top trace in 4-64 shows management frames also not included in my calculation, which was based on data packets alone. (The IQ display to lower right that shows these packets have BPSK modulation that is used for management and control packets.)

These figures show why the actual measured gaps available for BSMs, which include all of these other packets, are even smaller than our calculations estimated.

³⁹ Captured by a calibrated Tektronix 60120B Real-time Signal Analyzer. The same instrument was used for all the figures in this section.

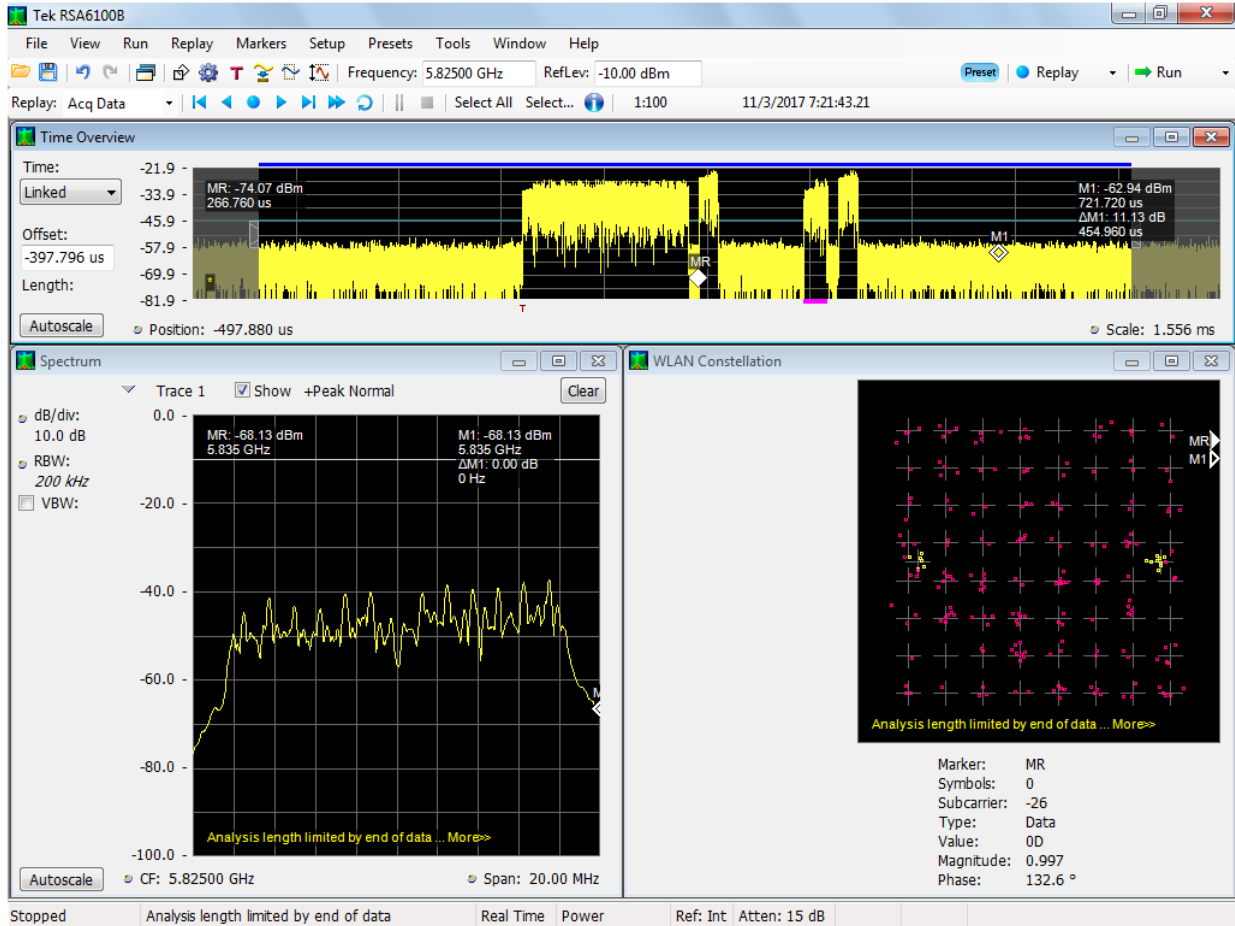


Figure 4-63. Packet splitting (1500 byte data at 10% load)

Therefore, our 1500-byte UNII packets represent complicated mixed Wi-Fi traffic that includes large, small, and split data packets with numerous management packets throughout.

4.4.3.2 1400-byte packets

To better replicate streaming video that would aggregate the data within the 1500 byte MTU limit, to minimize the number of management packets, we programmed MGEN to generate data in packets of 1400 bytes to allow the header and data to travel within one frame. With the data packets not being split, the number of packets was greatly reduced. Table 4-4 calculates slightly smaller inter-packet gaps for 1400-byte packets (compared to Table 4-2). These smaller gaps between data packets are more than offset by much fewer remainder packets and management packets to get in the way, as can be seen by comparing 4-63 and Figure 4-65.

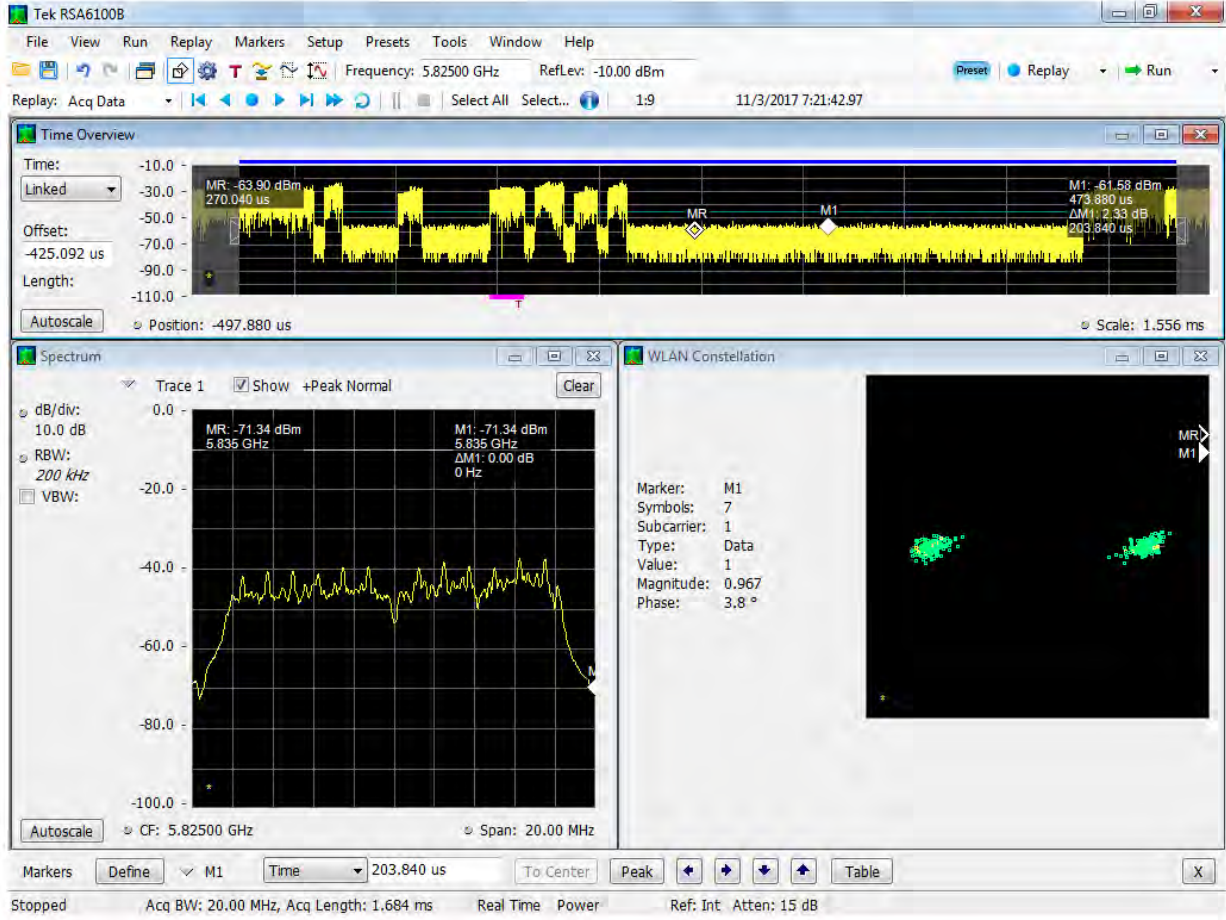


Figure 4-64. Wi-Fi management packets

Table 4-4 Calculated inter-packet gaps for 1400 byte data frames

Traffic Load (%)	Data Rate (Mbps)	Packets/sec	Seconds/packet (ms)	Average Inter-packet gap (ms)
100	54	4821	0.21	0
70	37.8	3375	0.30	0.9
30	16.2	1446	0.69	0.48
20	10.8	964	1.0	0.83
10	5.4	482	2.1	1.9
5	2.7	241	4.2	3.9
3	1.6	145	6.9	6.7
2	1.1	96	10.4	10.2

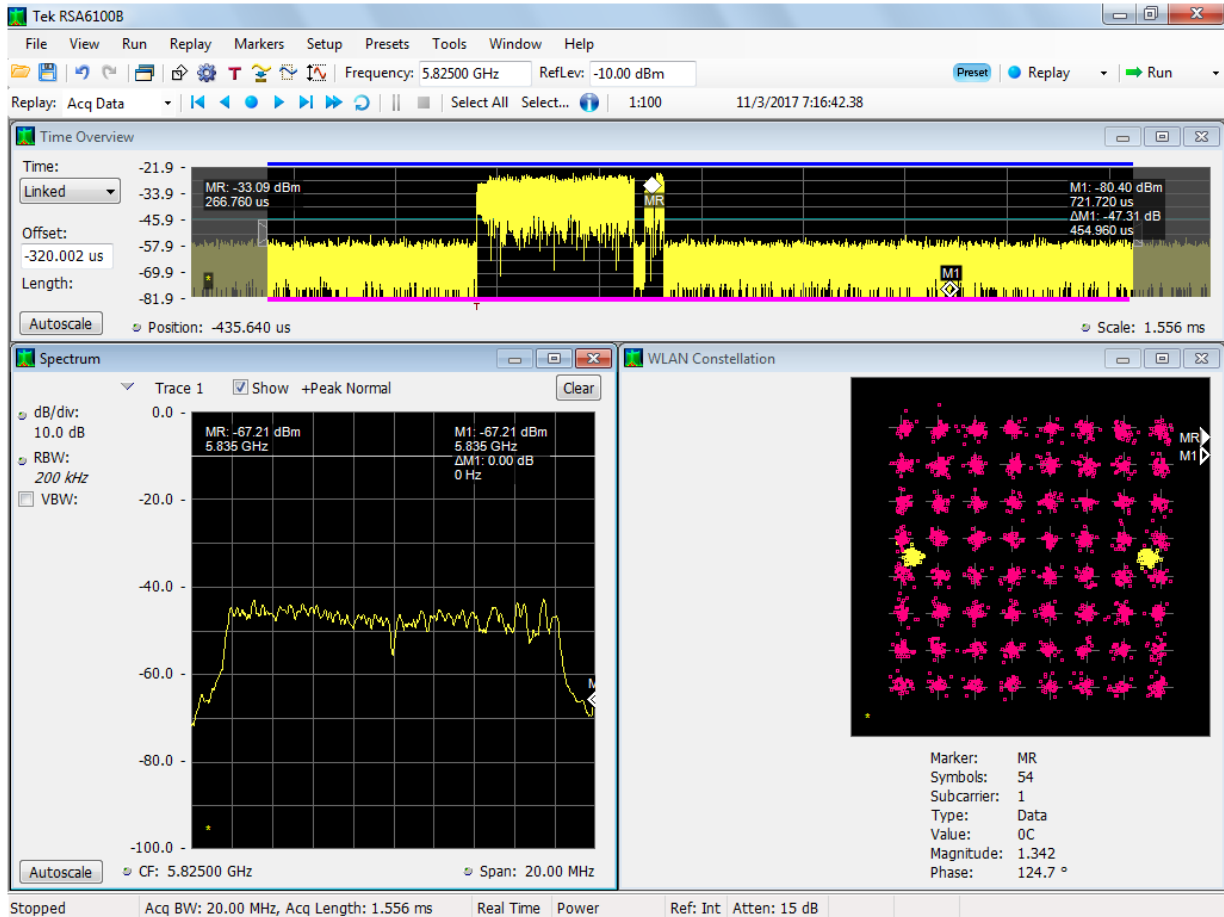


Figure 4-65. Data packets NOT split (1400 byte data, 10% load)

4.4.3.3 300-byte packets

To simulate the much shorter data packets that might be more typical of text-like data messages we tested with 300-byte data packets as well. Table 4-5 shows that calculated inter-packet gaps predict fewer opportunities for BSMs (compared to Table 4-2 and Table 4-4). Figure 4-66 shows the actual gaps in this 300-byte traffic including the acknowledgement packets.

Table 4-5 Calculated inter-packet gaps for 300 byte data frames

Modulation = ¼QAM-64	Peak data rate = 54 Mbps	Packet size = 300 bytes	Byte size = 8 bits/byte	Packet duration = 0.04 ms
				Average
Traffic Load (%)	Data Rate (Mbps)	Packets/sec	Seconds/packet (ms)	Inter-packet gap (ms)
100	54	22500	0.04	0
70	37.8	15750	0.06	0.02
30	16.2	6750	0.15	0.1
20	10.8	4500	0.22	0.2
10	5.4	2250	0.44	0.4
5	2.7	1125	0.89	0.8
3	1.6	675	1.5	1.4
2	1.1	450	2.2	2.2

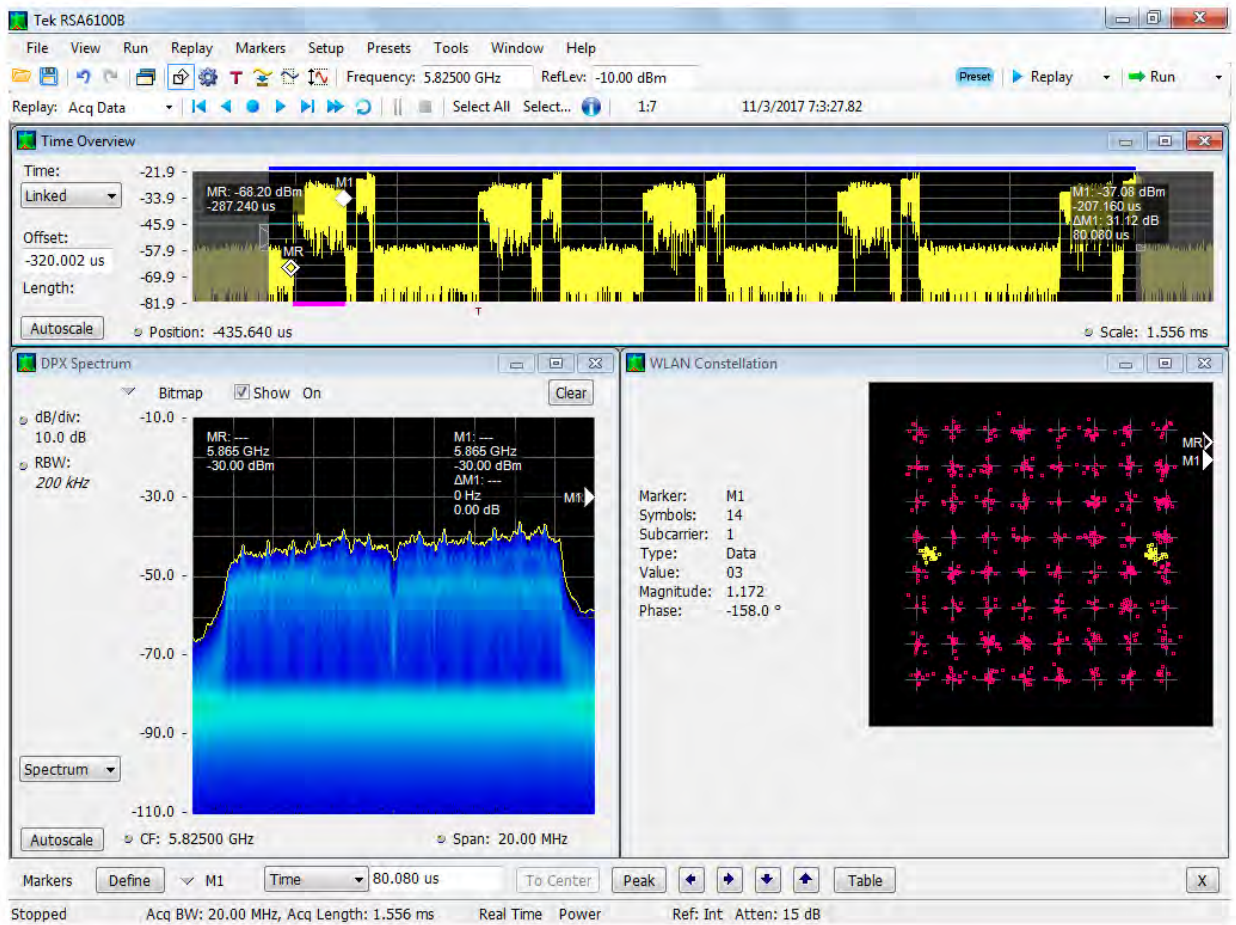


Figure 4-66. Data packets and acknowledgements (300 byte data, 10% load)

Figure 4-67 directly compares the three packet lengths in the time-domain. Note that a division in the time-domain plots is 3 ms and a BSM is about 0.5 ms or one-sixth of a division to visualize the different levels of interference presented to DSRC.

Based on the calculations, pushing the same quantity of data in 300 byte Wi-Fi packets should be more disruptive than the other packets lengths tested and the 1400 byte packets, the least disruptive. A first look at results in the field, in particular interrupted BSM sequence numbers, indicates that the greatest interference was caused by the 300-byte traffic stream. We did not observe the expected consistent difference between 1400-byte and 1500-byte traffic streams. Perhaps the difference in inter-packet space available for BSMs was smaller than the experimental variations in the field. The remainder packet and second acknowledgement may follow the initial packet too closely to encroach on the inter-packet gaps as much we thought. See Section 9.1.4.

UNII CH165 10% Load with Varying PL – IQ Data

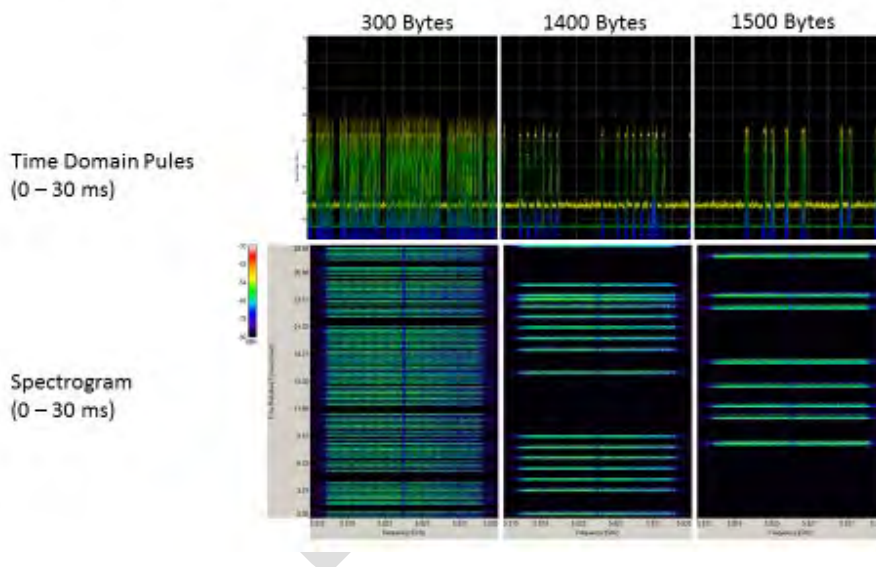


Figure 4-67. Comparison of packet length at a 10% traffic loading

5. Description of Facilities

Several sites were considered or used briefly in the early developmental part of the program. They are described in detail in the USDOT Analysis Plan.⁴⁰ The most significant results in this report were made at the facilities listed below. The first eight sites are at the Army's Aberdeen Proving Ground (APG) in Aberdeen, Maryland and the last two are NTIA ITS facilities in Boulder, Colorado.

Key chapter takeaways

- 1) We used laboratory facilities to calibrate, checkout and troubleshoot components.
 - 2) We calibrated antennas in anechoic chambers.
 - 3) We selected most outdoor test courses that had minimal multipath reflection.
 - 4) The longest course provided a 3-mile line of site.
 - 5) Other sites provided the opportunity to test environmental effects like wet and dry foliage; and being inside and outside different types of buildings.
-

5.1 Lab – ATEC (APG)

The Army Test and Evaluation Command (ATEC) has skilled personnel on base available to support the analysis. The ATEC subordinate organization, the US Army Aberdeen Test Center (ATC) there has a full suite of RF instrumentation including instrumented vehicles and RF listening stations that are mobile and located around the airfield test site to detect spurious emissions.

Building 5014 on the Post has a dedicated high bay enclosed garage area with a GPS repeater that is well suited for instrumentation installation, daily checkout and troubleshooting/maintenance of the vehicle mounted DSRC radios should it become necessary (Figure 5-1). A suite of RF instrumentation tailored specifically to monitor over the air transmissions and ambient RF environment is available in this lab facility (Figure 5-2)). The centerpiece of the instrumentation is the RSA 6120B from Tektronix. It is a real-time swept spectrum analyzer capable of receiving, displaying and recording a 110MHz portion of the spectrum at the command of the operator. The entire DSRC band as well as adjacent UNII 3 and UNII 4 Wi-Fi signals become available with a 100% probability of intercept. The RSA is augmented with a Rhode & Schwarz HE600 antenna. Also available is a high fidelity 16 bit I and Q recording system capable of playback through a KEYSIGHT E8267D Vector Signal Generator.

⁴⁰ https://www.its.dot.gov/research_archives/connected_vehicle/pdf/DSRC_Analysis_Planv4Dec2017.pdf.

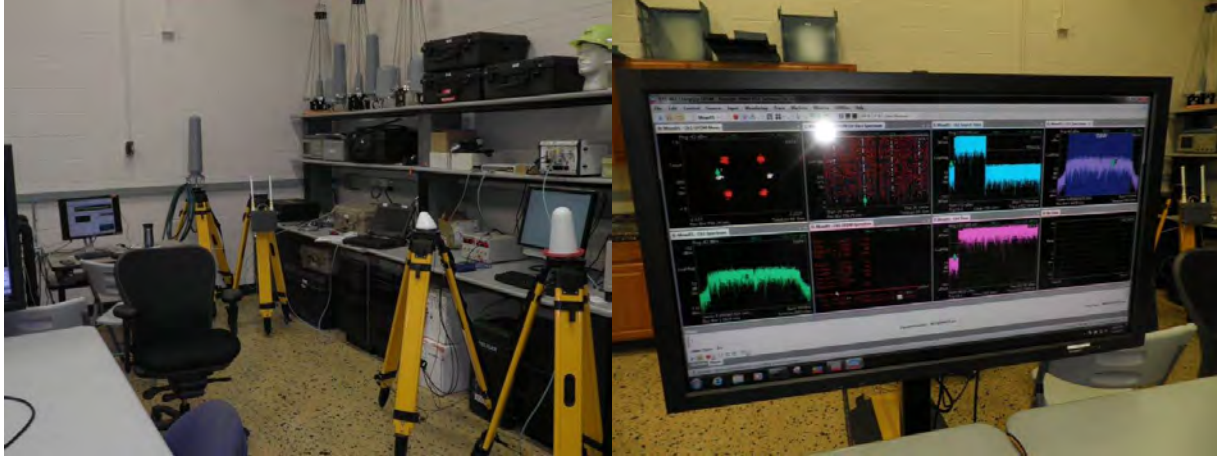


Figure 5-1. ATC high bay lab

Figure 5-2. ATC signal analysis

5.2 Lab – ARL (APG)

The Communications Electronic Warfare Branch (CEW) falls within the hierarchy of the US Army Research Laboratory (ARL), Survivability and Lethality Analysis Directorate (SLAD). CEW maintains an RF lab that has been operating since the 1970s and provides vulnerability assessments of transceivers in a controlled laboratory environment. They test with regularly calibrated state-of-the-art electronic measurement equipment. That equipment includes RF signal generators, power meters, real-time signal analyzers, spectrum analyzers, network analyzers and a wide array of passive RF components.

In order to generate repeatable results, antennas are never used in the lab. Radios are connected via high quality coaxial cables, attenuators, splitters, and so on. Because radios are often not sealed against RF either escaping or entering their cases, radios under test are placed in an RF enclosure, reducing stray RF power by about 110 dB. The final product of a vulnerability assessment is a report detailing procedure, equipment, and interpretation of results, converting raw laboratory data into actionable information.

Fielding a system begins with design, development, and prototyping. CEW is a signals-oriented test and evaluation lab that becomes involved in the radio acquisition process after a prototype exists. Typically, their role is to quickly feed vulnerability information back to the design update process. Most radios that come to the lab are for some form of electronic warfare (EW). Because EW typically is not taught in universities, new CEW engineers usually get 6 to 12 months of specialized training.

Data acquisition during testing is traditionally a tedious process of adjusting equipment and recording results, while gradually degrading the RF channel. To alleviate this, CEW has written software to automate the data acquisition process. That also offers the further advantage of statistical confidence. Interfering signals can be mathematically generated both by the same software or recorded, edited and replayed. The latter is helpful when studying the response of a transmitter to a signal its receiver

recognizes. ARL performed the transmit-and-receive calibrations, sensitivity measurements, and lab-based interference testing for USDOTs DSRC and surrogate UNII-4 devices.

5.3 Lab – CERDEC (APG)

In addition, the Army’s Communications-Electronics Research, Development and Engineering Center (CERDEC), is also located at APG. Within CERDEC is the RF-Electromagnetic Compatibility and Antenna Test Laboratory (REMCAT Lab). REMCAT Lab has small and large anechoic chambers capable of measuring the patterns of antennas including those mounted on vehicles. The large chamber has a 10 meter turntable rated to over 70 tons and can measure patterns of antennas on vehicles as large as tanks. Antenna patterns can be measured at frequencies from 400 MHz to 18 GHz with over 100 dB of isolation.

REMCAT Lab measured antenna patterns of our devices on vehicles in a large anechoic chamber (Figure 5-3) and on large metal plates in a smaller internal anechoic chamber. The antenna patterns allow us to correct our over-the-air (OTA) measurements for the orientation between two radio devices and for irregularities in antenna patterns when necessary. The antenna measurements also factor into the uncertainty around the RF measurements.

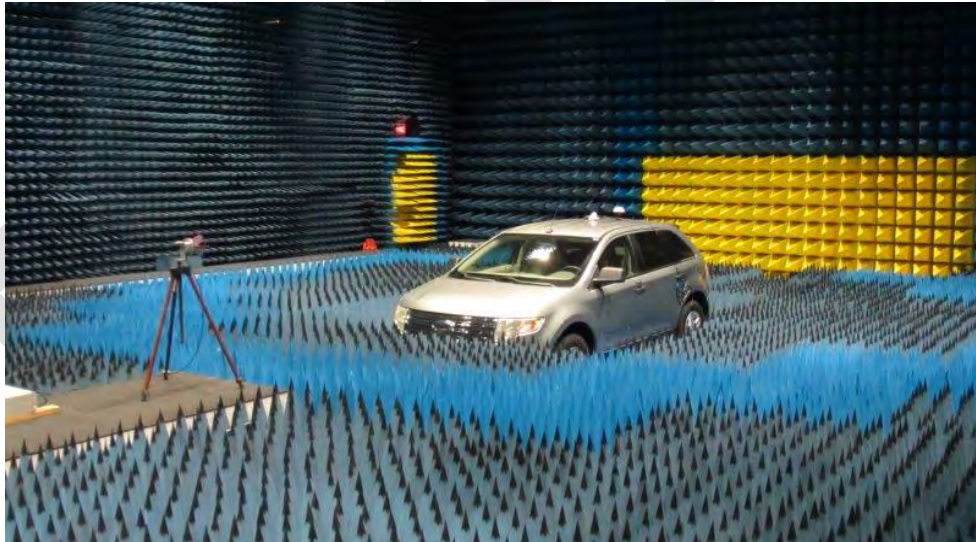


Figure 5-3: Measuring antenna patterns in large anechoic chamber

5.4 Mobile Facilities – ATEC (APG)

In addition to the laboratory, ATEC has two mobile RF data collection facilities that can be moved between test locations. The first is a data collection van and the second is a mobile field office, both described below.

The ATC owned Mobile Recording System (MRS) vehicle is a specially modified 2500 series Dodge Sprinter van (Figure 5-4). It serves as a small mobile office and data collection vehicle. It is outfitted with dual side-by-side workstations each with a dedicated 30" monitor (Figure 5-5). An equipment rack houses a Tektronix 6120B Real Time Spectrum Analyzer and a hi-fidelity 16 bit I and Q recorder. A rack mounted Cisco switch provides for connectivity to the systems under observation and provides Operator 1 with a LABVIEW GUI interface to remotely control DSRC radio parameters and transfer data files. Operator 2 is connected primarily to the roof top radome.

The radome provides two additional swept spectrum analyzers to allow background emission monitoring over the DSRC band and adjacent RF frequencies. Any nearby unwanted RF interference can be identified and located with the Angle of Arrival Direction Finding ability built into the radome electronics. The electronics are powered by an RF-quiet 3 KW diesel generator. ATC has two identical Sprinters. Both were at our disposal.

The van also provided comfortable refuge from the elements for the researchers. There are scenarios purposely written into the plan to provide data points in adverse climatic conditions. Aberdeen Proving Ground proudly boasts itself to be a research facility replicating 85% of the climate and terrain in the world. The DSRC Research was conducted here on a year around basis. The vans were deployed at the APG field sites described below.



Figure 5-4 Data van outside



Figure 5-5 Data van workstations

Field Research was also augmented by ATC's Mobile Field Office (MFO). It is a 53' commercial trailer outfitted to act as a deployable field office (Figure 5-6). Two on board diesel generators make it completely stand alone. It has a small conference room, 12 workstations with monitors and an assortment of communication and network electronics including a satellite dish (Figure 5-7). Creature comforts include a refrigerator, coffee pot and microwave. It served as a mobile Command Post and data collection facility at the Perryman field site described below.



Figure 5-6. ATC Mobile Field Office

Figure 5-7. MFO Inside

5.5 Field Site – Zone 1 & Zone 2 at Phillips Army Airfield (APG)

The Aberdeen Proving Ground in Maryland has numerous vehicle test tracks and a very large, physically isolated, active airfield. Two of the runways at Phillips Army Airfield are unused at this time, and offer long, flat paved surfaces in clear terrain with few nearby sources of multiple path reflection (see Figure 5-8). The Zone 1 runway is 3600 feet long and Zone 2 is 2800 feet in length. The closed runways offer a benign RF environment that is suitable for interference analysis.

Most short range measurements were taken at Zone 1, which was formerly runway 17-35. Zone 2 was formally runway 8-26. This fortunate happenstance created a natural 90 degree intersection which proved useful in the overall research scenario. The numeric identifier of the runways denotes the direction of travel in degrees (relative to magnetic North) on the paved surface.

There are no utilities at Zone 1 so all power and lighting is provided by a towed generator, portable generators, test vehicles or an RF data collection van that has to be driven onto the site and removed each day. The runways must be clearable within 5 minutes to allow for emergency landings. Another part of the Airfield complex is the perimeter road known as ATEF and it is described below.



Figure 5-8: Zone 1 on Runway at Aberdeen Proving Ground

DRAFT

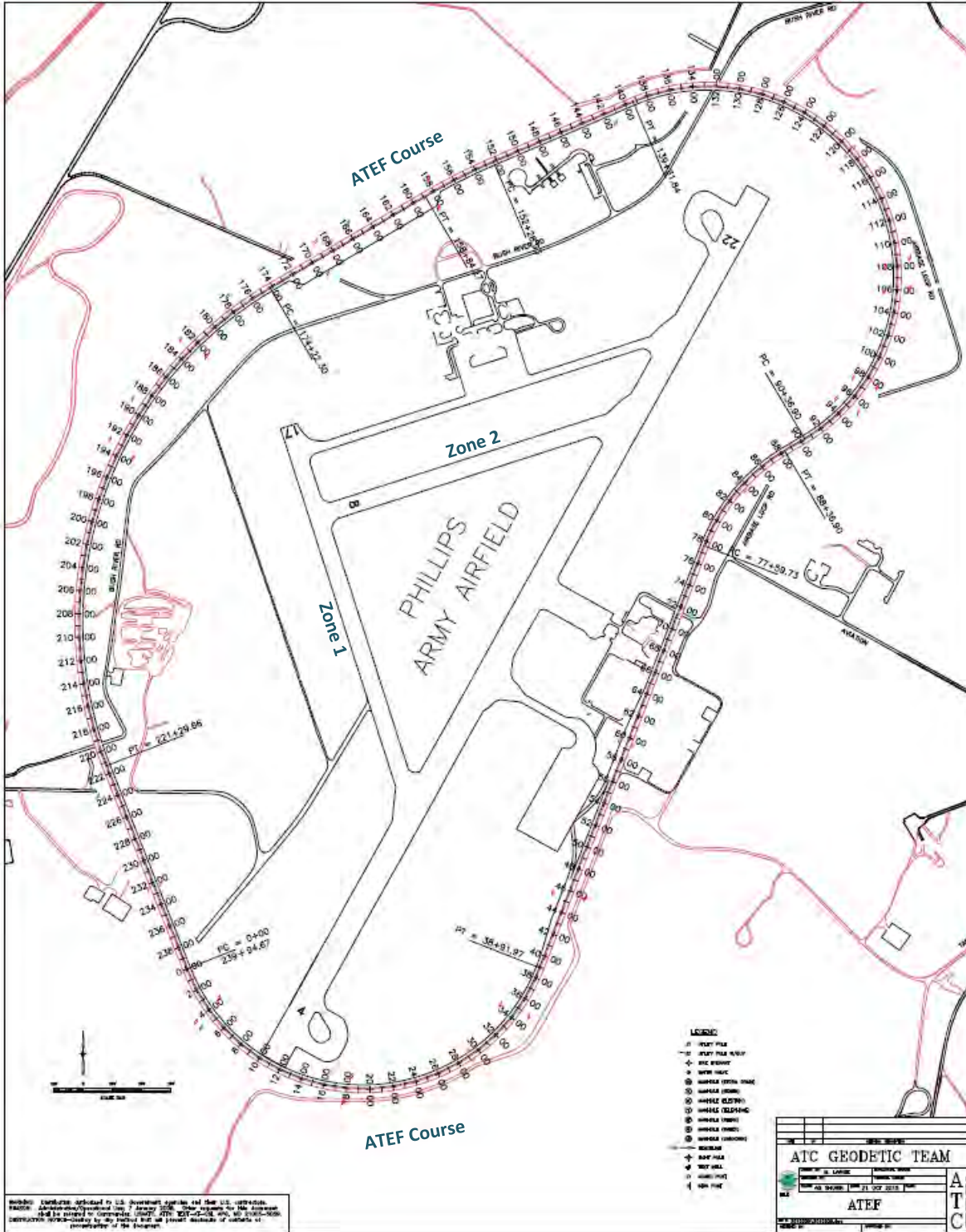


Figure 5-9: ATEF Test Track and Runways at Aberdeen Proving Ground

5.6 Field Site – ATEF Course (APG)

The Automotive Technology Evaluation Facility (ATEF) is designed to allow for sustained high speed testing of automotive systems. The primary feature is a 4.54 mile triple oval test track with wide sweeping turns (Figure 5-9). It consists of two paved lanes with a continually marked center line and is complemented by a concentric outer perimeter gravel roadway.

We used this private highway around the airfield and nearby buildings for some of our tests. There are 21 RSUs installed around ATEF. These networked RSU's were under the control of the ATC engineers at all times. It created a managed, controlled and repeatable DSRC environment for our research effort. The close proximity of permanent buildings lent themselves to become excellent venues for research scenarios utilizing the UNII-3 and 4 interference devices.

5.7 Field Site – Dynamometer Test Facility (APG)

The Dynamometer Course is specifically designed for heavy mobile dynamometer testing of a full range of wheeled and tracked military and commercial vehicles (Figure 5-12). The course itself covers some 126.9 acres and offers a straight, bituminous concrete roadway, level within 0.1 percent, is 1 mi long and 17 ft. wide with oval turnarounds at both ends. Unlike the other sites, this track is hemmed in by dense woods most of the way so it provides a foliage-heavy environment in contrast to the open track at Zone 1 (Figure 5-10). The preponderance of the foliage is deciduous trees. The course provided an excellent venue to obtain data points in a rural environment. Research was conducted in the summer season with maximum foliage evident. Data was collected in both wet and dry conditions. Identical research scenarios were conducted in the fall, at a time with minimum foliage present (Figure 5-11). Winter operations afforded an opportunity to see the effects of snow cover on our DSRC research.



Figure 5-10. Dyno course with foliage

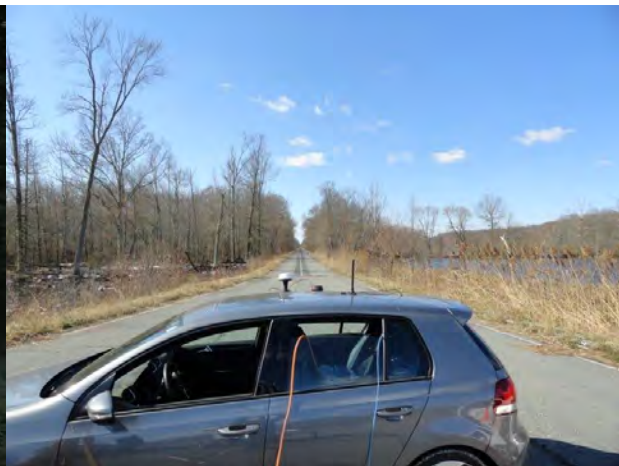


Figure 5-11. Dyno course foliage down

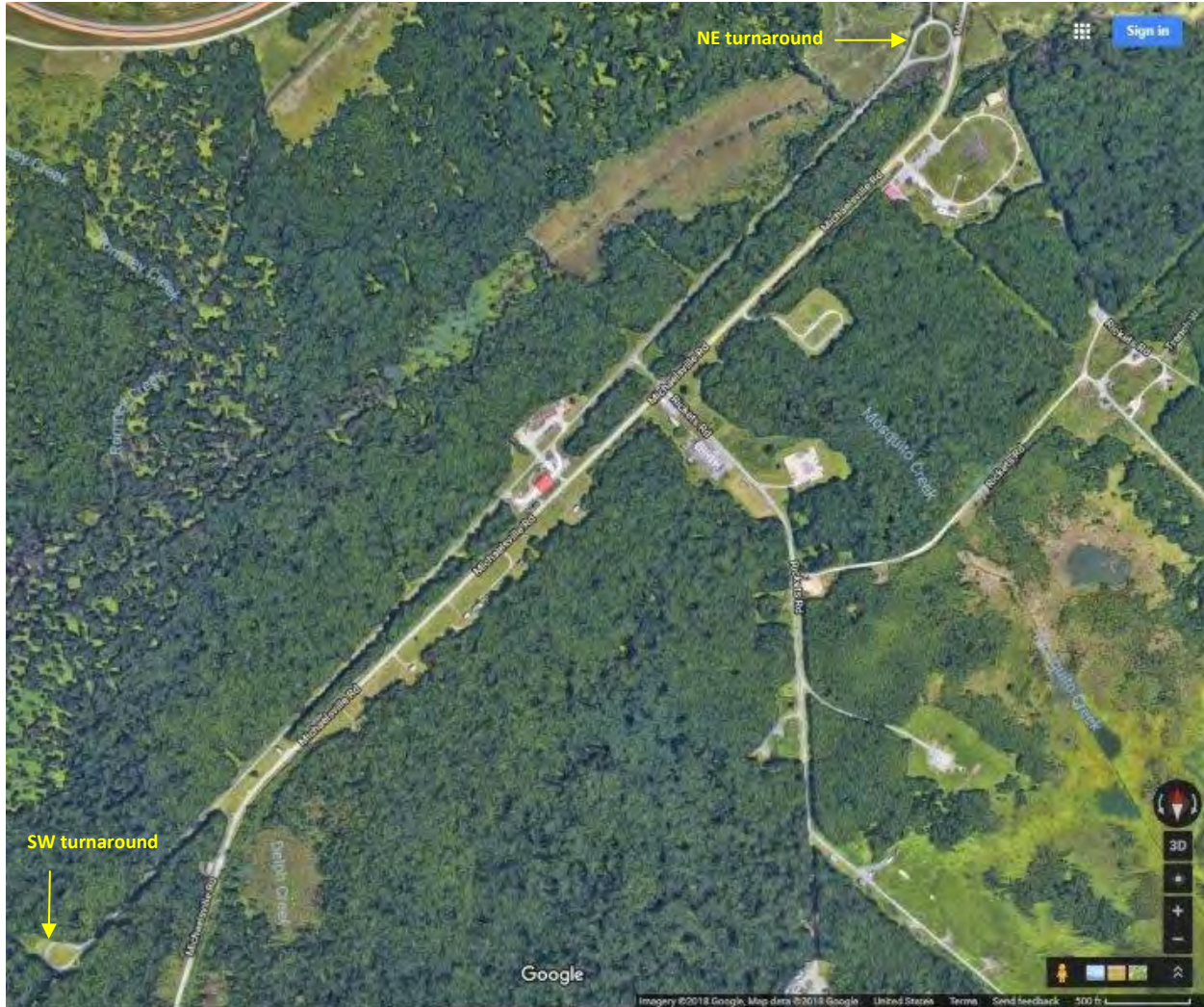


Figure 5-12: Dynotrack at Aberdeen Proving Ground

5.8 Field Site – Perryman Test Area (APG)

The Perryman Test Area (PTA) is an automotive test site with multiple courses suited for a full range of test activities. A tailored mix of testing on the courses supports the assessment of automotive system performance, endurance, and reliability under a variety of operating conditions. The long flat open expanse of real estate and paved surface at this facility was very attractive to the research project.

The Paved Course at PTA is a paved straightaway almost 3 miles long that varies from 2 to almost 5 lanes wide. It is relatively flat with maximum change in elevation of 14 feet along the entire course. It is the only facility with a line-of-sight longer than the maximum ranges of the DSRC and surrogate UNII-4 radios (Figure 5-13). Hence, it is the place where we could determine those maximum ranges.

It is also open space with a minimal number of nearby potential multipath scatters in the form of occasional light poles, range targets, and tenth of mile markers. This very long and open course was also ideal for the research scenarios with the UNII-3 and UNII-4 interference devices. Set up at the 1 ½ mile marker, the DSRC equipped vehicles were able to simulate approach and passing a stationary Interference Access Point starting outside its radio range. This site was also valuable for testing interference to DSRC vehicles approaching each other at highway speeds.

Figure 5-14 shows Perryman along with the other test tracks at APG. The red R's indicate where the RSU was usually set up during testing at each of the test tracks.

Unlike Zone 1, Perryman has fixed power and communications infrastructure. Often tests were performed operating out of the RF van as at Zone 1 but some of the time the Mobile Field Office (MFO) instrumentation trailer was present. At those times we operated from the trailer which provided shelter, power, Wi-Fi, lighting, conference room space, chairs, desk space, and external monitors.



Figure 5-13. View down the Perryman site 3 mile straightaway



Figure 5-14: Test tracks at Aberdeen Proving Ground

5.9 Lab – NTIA (ITS-Boulder)

The Institute for Telecommunication Sciences (ITS) is the research and engineering laboratory of the National Telecommunications and Information Administration (NTIA), an agency of the Department of Commerce (DoC). This Boulder Laboratory at ITS serves as a principal federal resource for the conduct of basic research on the nature of radio waves. ITS works with Government agencies and private organizations to explore, understand, and improve the use of telecommunications technologies and principles; investigate and invent new technologies; and overcome telecommunications challenges.

NTIA ITS-Boulder assembled a lab facility for bench testing DSRC and surrogate UNII-4 devices. Figure 5-15 shows the test equipment which includes: Two shielded enclosures, Keysight MXG Signal Generator, Keysight PXA Signal Analyzer, RF Backplane for interference signal injection, switch driver for switching the RF switches on the backplane, various power supplies, various precision RF cables, radio frequency network analyzer, and power meters. Several laptops are also included for RSU and OBU device control and data collection. The MXG Signal Generator can simulate interference signals and noise signals. Various waveforms can be simulated in software and loaded into the MXG signal generator.



Figure 5-15: Lab testing at NTIA ITS-Boulder

ITS-Boulder created an RF backplane for calibration devices and using circuits of attenuators and dividers to simulate what to expect in the outdoor testing. See Figure 5-16. You can see the link between DSRC radios established with the chain at the bottom using variable attenuators to simulate range. Interfering signals can be introduced at the top and directed into the DSRC devices below. The MXG is a signal generator and can produce Gaussian noise. The output to the PXA measures the simulated OTA signals.

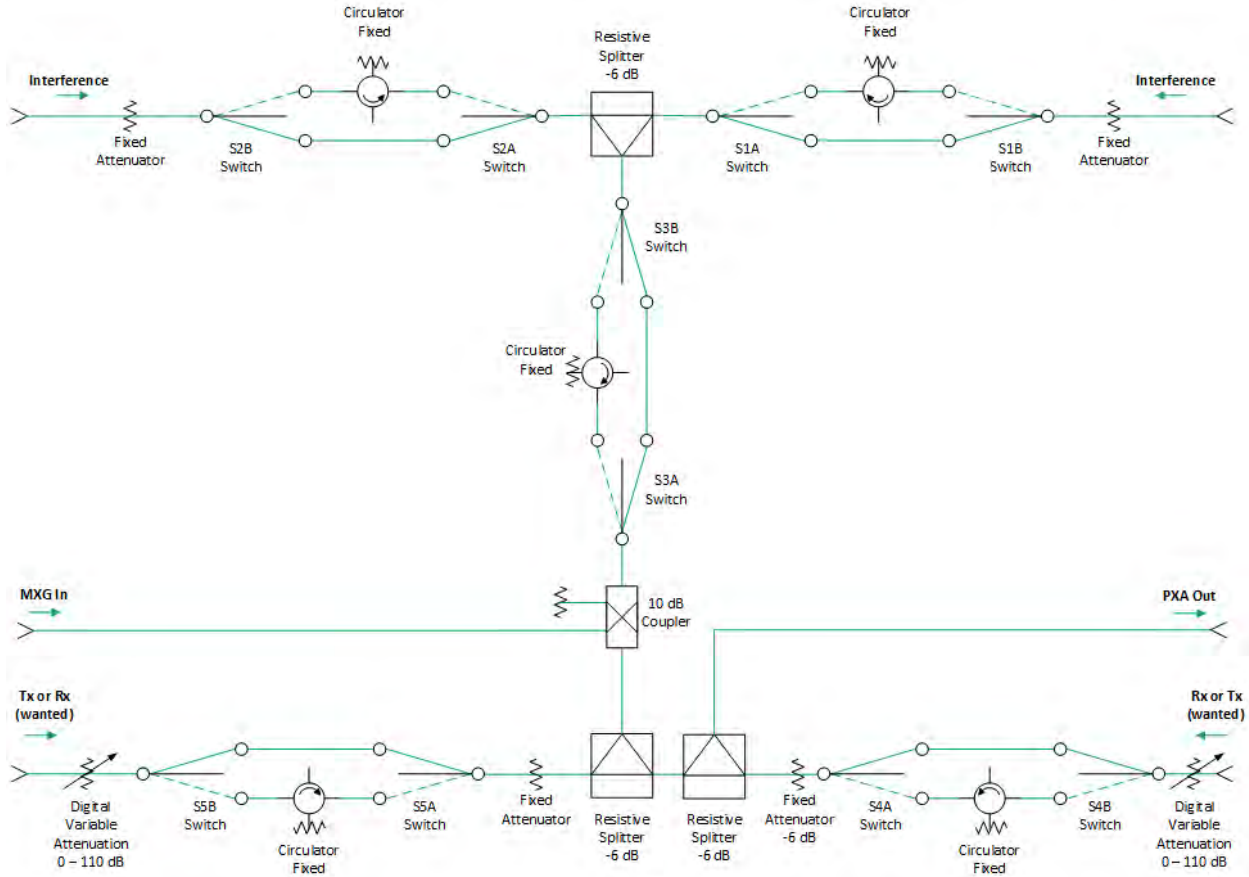


Figure 5-16: RF Backplane Testbed at NTIA ITS-Boulder

5.10 Field Site – Table Mountain (ITS-Boulder)

The Table Mountain Field Site and Radio Quiet Zone is operated by the Institute for Telecommunications Sciences (ITS). It offers flat, open terrain with few reflectors that might cause unanticipated multipath and long, straight stretches of gravel road suitable for investigating mobile line of sight communications. (See Figure 5-17.)

The Table Mountain Field Site is located north of Boulder, Colorado and extends about 4 kilometers (2.5 miles) north-south by 2.4 kilometers (1.5 miles) east-west, an area of approximately 1,800 acres. The site is designated as a Radio Quiet Zone where the magnitude of external signals is restricted by state law and federal regulation to minimize radio frequency interference to sensitive projects. Site power distribution is by means of buried lines to avoid interference.



Figure 5-17: Table Mountain Field Measurement Site

As a flat-topped butte with uniform 2% slope, Table Mountain is uniquely suited for radio experiments. Table Mountain is elevated above the surrounding community so that the perimeter edges of the mesa provide significant diffraction attenuation to signals emanating from the surrounding community. Lack of perimeter obstructions on Table Mountain and the relatively homogeneous ground, facilitates studying outdoor radiation patterns from bare antennas or antennas mounted on structures. Table Mountain is a state-of-the-art facility for research into radio spectrum usage and occupancy. Radio quiet restrictions ensure that no signal incident on the mesa overpowers any other signals.

ITS constructed a tower structure to mount the RSU 18 feet (5.5 meters) high above the ground for testing V2I DSRC links. The tower structure consists of two Rohn Model 25G towers that are 19 feet high (Figure 5-18). A three-inch diameter PVC cross member connects the two towers and provides hardware

for mounting the RSU at various heights above ground. Two winches and cables provide the capability to provide RSU antenna continuous elevations above ground from less than a meter up to 5.5 meters.



Figure 5-18. Rohn Model 25G towers with PVC RSU mounting pole



Figure 5-19: Typical View of Table Mountain Measurement Site

6. Calibrations and Preparatory Measurements

It is essential to calibrate devices in the lab to know what they are actually doing in the field. This prevents mistakenly believing measurements show interference when they actually result from peculiarities or flaws in a device under test. Calibration also indicates the uncertainties around the measured values. It is important to know which differences are significant and which are not. Our most significant calibrations were of radio transmit and received powers and the antenna patterns. An additional activity was an RF survey to measure signals from sources already in the band as an “environmental calibration.”

Key chapter takeaways

- 1) We characterized the DSRC and UNII radios in the lab to determine how actual powers transmitted and received compared to the commanded power levels. This allows us to correct data to remove imperfections due to device behavior.
- 2) The lab testing required that at least one radio needed to be in an isolation chamber because of the large amount of RF energy these devices leak. In essence, when they are close to each other, the devices communicate with each other via energy leaked over the air even without antennas.
- 3) We characterized antennas used in the testing by measuring return loss and antenna patterns. Return loss can be used to correct power measurements for losses from reflected energy at the connector. Antenna patterns, measure how the antenna’s sensitivity varies with direction. They can be used to correct for power lost due to the orientation of the two antennas. Orientation matters since the antenna patterns are not perfect spheres.
- 4) The antenna measurements showed us that our initial vendor provided antennas were unsuitable for a test program. We replaced them with an antenna that performed better in our tests. In particular, its patterns were much more consistent, regular, and repeatable.
- 5) We selected an antenna with minimal variation so that radio interference would be easier to identify in our measurements. It is a better antenna than one would select to simulate DSRC performance on commercial automobiles. Our focus is radio interference, not DSRC performance.
- 6) In order to hold the control variables of our surrogate U-NII-4 device steady we had to limit our interference testing to Wi-Fi on 20 MHz channels. Otherwise the device varied those parameters on its own in real-time.

- 7) We created a means to control and log data from the radios (detailed in Chapter 3). Data that was not logged by the radios was recorded by our GUI, screenshots from a vector analyzer, and manually.
 - 8) When necessary we collected additional diagnostic information with our DSRC/UNII packet sniffer.
 - 9) We selected two modulations for operating DSRC: $\frac{1}{2}$ QPSK (the default standard) and $\frac{3}{4}$ QAM-64 (a more vulnerable modulation that would be used for short range, high data rate applications).
 - 10) We selected two modulations for operating the UNII Wi-Fi interferer: $\frac{1}{2}$ BPSK (typical of management frames and when the radios sense a high level of RF noise) and $\frac{3}{4}$ QAM-64 (a moderately high and typical Wi-Fi data rate).
 - 11) We found other transmissions in the band during a background survey along highways, near FSS sites, and near a rocket test.
-

6.1 Power Calibrations

6.1.1 Purpose

The purpose of calibrating or characterizing the devices used in testing is to ensure that imperfections in a device are not misinterpreted as test results. It is important to understand the sensitivity between the commanded transmit power and the actual transmit power so test parameters can be set properly and recorded accurately. If the actual transmit power is not the same as the commanded transmit power, then the commanded power can be adjusted to achieve the desired transmit power or the results can be corrected if the power was more or less than intended. If a gap between commanded and actual transmit power exists and is not corrected, the difference is at least a key component in the uncertainty analysis.

Similarly, calibrating the received power is important to understand if any corrections need to be made to remove bias in the receiver. That allows any remaining deviation in the received power to be attributed only to external sources of interference (environment and interfering radio). Environmental interference, mostly due to multipath reflections, is removed by subtracting baseline measurements from the data. Baseline measurements are made using the DSRC radios with all Wi-Fi devices turned off. Baseline measurements will be described in chapter 7 and will be prevalent in the data analyses of chapters 9 and 10.

Subtracting baseline data from interference data can be done by software processing of the data or by simply comparing the baseline and interference plots visually. The former is necessary for precise quantitative results but the latter is often sufficient to gauge the extent of interference, especially when a baseline is “clean,” that is, showing little or no interference.

ARL performed most of the power calibrations of the DSRC radios and the surrogate UNII-4 testbed. ITS-Boulder calibrated the DSRC radios in their possession as well.

ARL used a Keysight N1911A power meter, calibrated to NIST standards that samples 100 million samples per second to take at least 1500 measurements per second. The sensor uncertainty is +/- 0.2 dB (4.7%). They used MGEN to generate UDP packets, which contain a time stamp and sequence number.

The meter was set up to report one value after averaging 5 readings (about 4 ms). The software pauses 100 ms between measurements, and repeats 30 times, that is, for 3 seconds so each data point represents a little under 150 raw readings. The whole process was automated with software scripts. Figure 6-1 is a schematic of the test set up.

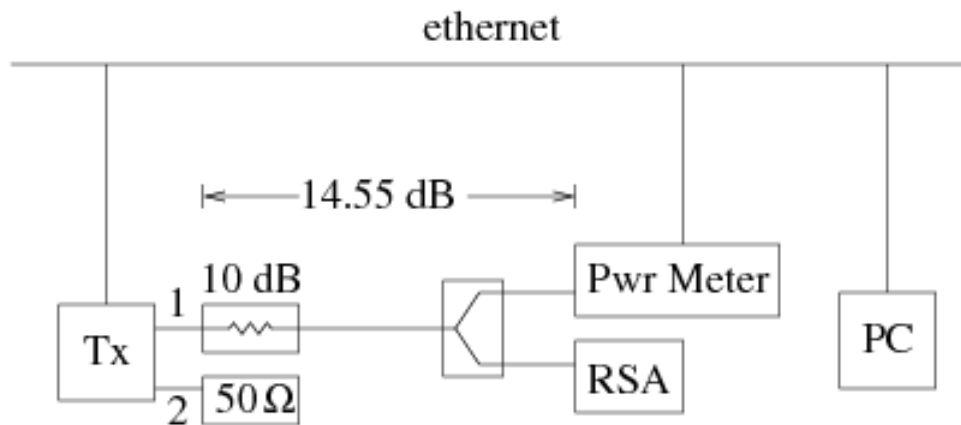


Figure 6-1. ARL Power calibration diagram

ARL looked at the effect of changing certain variables on the power calibrations. Variables tested included channel selection, modulation and packet length. Calibrations included measurements of both transmit power and receiver sensitivity.

ITS-Boulder used a different instrument (PXA) for their calibrations that was also automated. The power levels were selected randomly until all 40 power levels were measured rather than stepping up or down incrementally. The process was repeated 30 times and the resulting average provided the calibration curve for the radio. Figure 5-16 (within Chapter 5) is the schematic for the RF backplane, which was used for the calibration. Figure 6-2 shows the RF isolation enclosures they used to prevent radiation leakage (EMI) from causing errors in the measurements.

Both labs accounted for the insertion and return losses in the passive components, cables and connectors in their test fixtures.

The outputs of the calibration process were calibration tables that can be used to correct measurements from the field and to generate plots of that calibration data. Figures 6-3 and 6-4 are sample calibration curves from ARL and Figure 6-5 presents a sample calibration from ITS-Boulder.



Figure 6-2. RF Enclosures for calibration at ITS Boulder

Power Calibration 169.254.61.132: MK2MCS_R12QPSK-400B

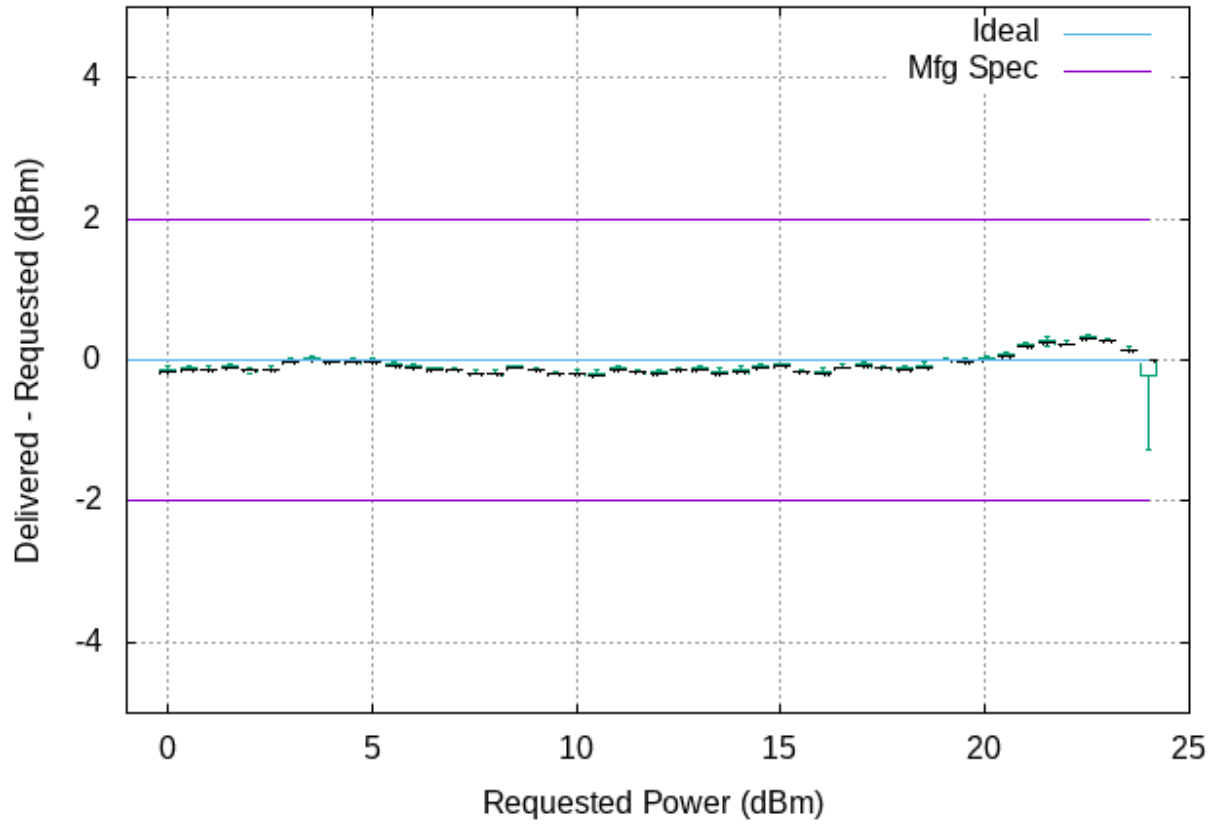


Figure 6-3: Sample transmit calibration plot of a DSRC radio made at ARL

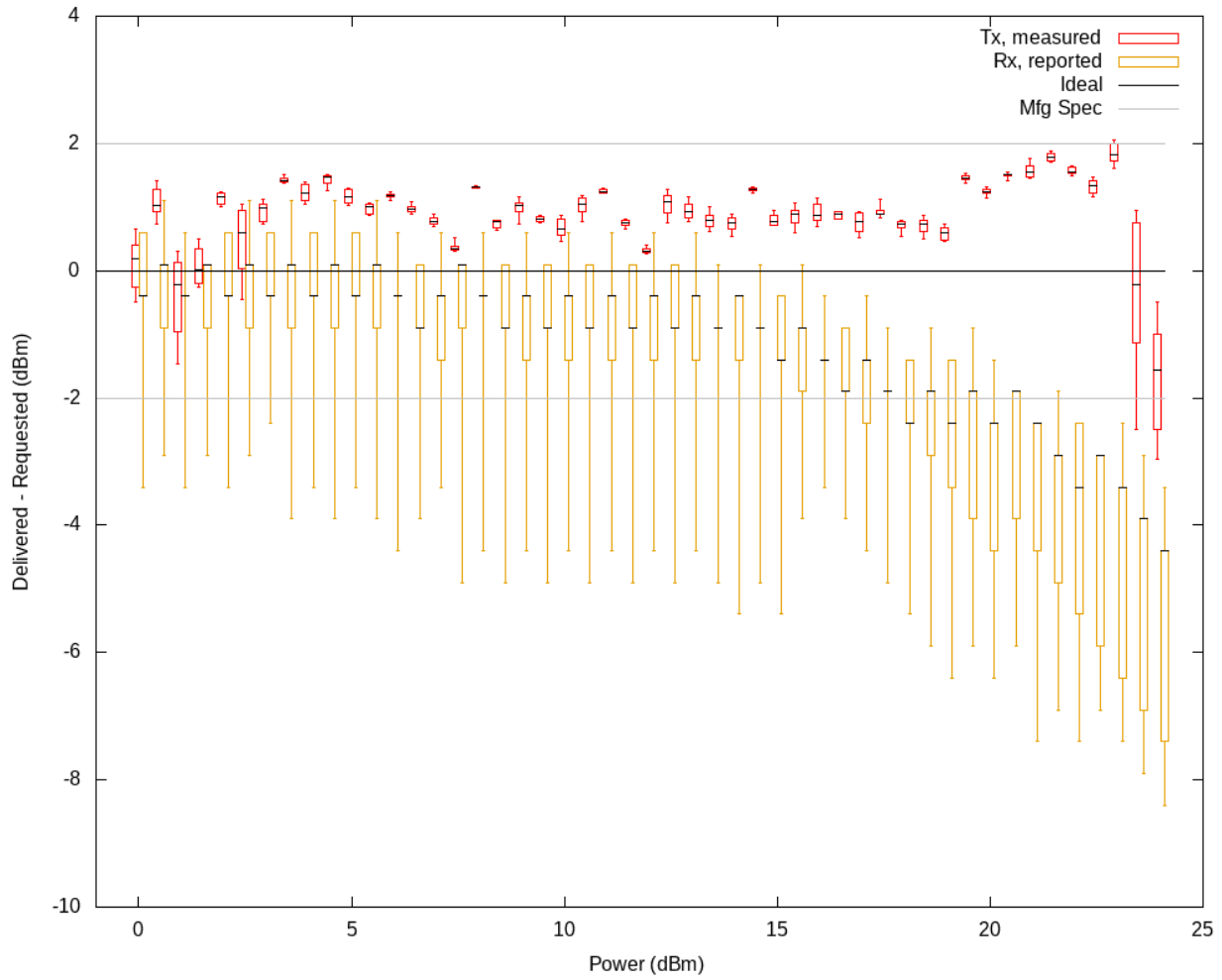


Figure 6-4: Sample receive calibration plot of a DSRC radio made at ARL

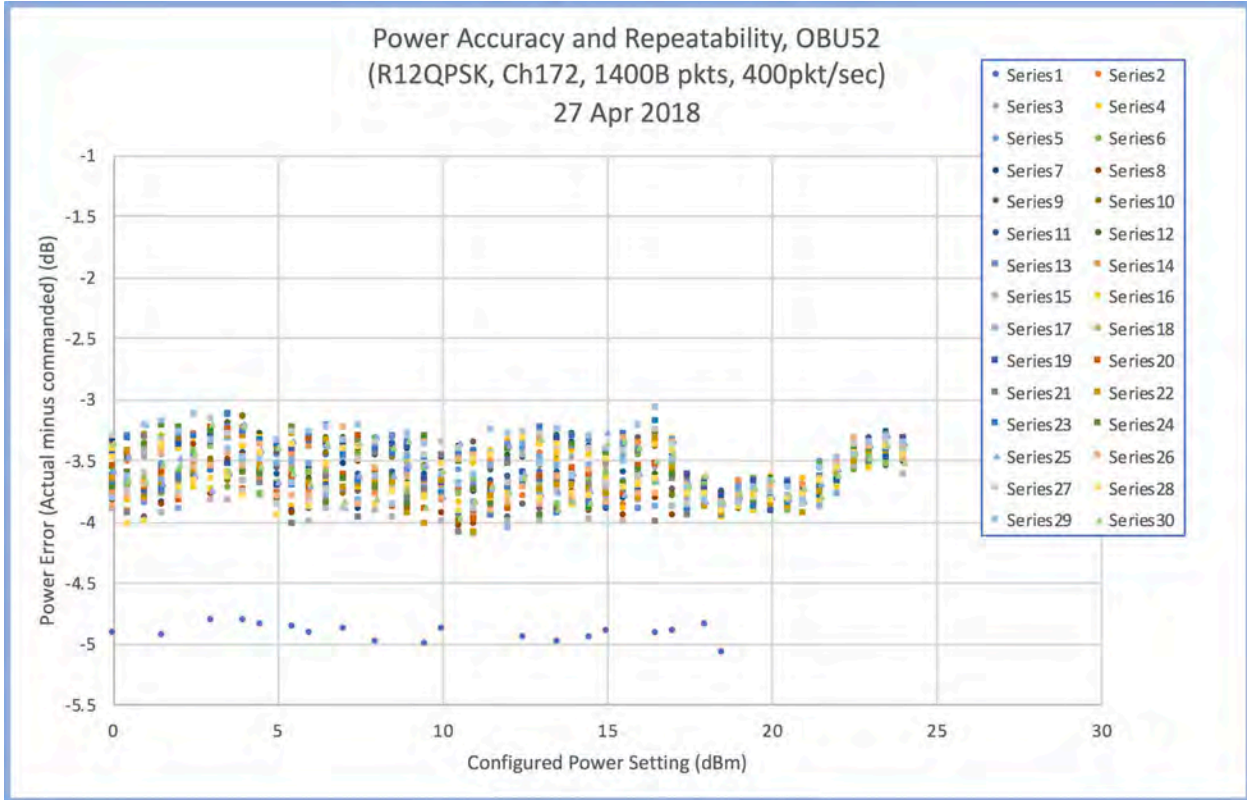


Figure 6-5. Sample calibration plot of a DSRC radio made at ITS-Boulder

6.1.2 Activities

We initially calibrated over a range of variables (Table 6-1) including bandwidth, channel number, modulation and packet size. Where little difference was observed we streamlined the permutations for subsequent calibrations and recalibrations. Table 6-1 lists the permutations of the calibration measurements. Note that we did not calibrate DSRC at 20 MHz as planned because a 20 MHz DSRC radio was not available at time of testing.

Table 6-1: Power Calibration Runs for Transmitters

Device	Bandwidth (MHz)	Channel Number (DSRC and U-NII band)	Modulation	Power measured by spectrum analyzer (dBm)	Packet Sizes (octets)
IEEE 802.11p DSRC Transmitters	10	172 174, 176, 178,	½BPSK, ¼BPSK, ½QPSK, ¼ QPSK, ½QAM-16, ¼QAM-16, ⅔QAM-64, ¼QAM-64	0 to 24 dBm in 0.5 dBm increments	400 and 1500
IEEE 802.11ac U-NII-3 & 4 Transmitters	20	169, 173, 177	Same	1 dB increments from 0 to 30 dBm	1500

DSRC power was calibrated in increments of 0.5 dB because that was the smallest control increment of the DSRC radios. Initial measurements suggested limiting the transmit powers used for the interference analysis. Commercial DSRC equipment available at time of testing did not support transmit powers up to the maximum limits allowed by the FCC (shown in chapter 1, Figure 1-1). For example, for channel 172 the specified limits are 28.8 dBm transmitter power out and 33 dBm EIRP (which includes antenna gain and cable losses). The SAE J2945 standard specifies 20 dBm as the maximum radiated power (or EIRP). Moreover, initial measurements at Aberdeen have shown ranges exceeding 300 meters even at 0 dBm transmit power (or ~5 dBm EIRP assuming the typical gain of DSRC test antenna is 6 dBi with ~1 dB of cable loss). That means in order to reduce self-interference and channel congestion, deployed DSRC may very well operate with lower radiated power than anticipated by the standard. Therefore, we made most measurements with the following four transmit powers:

- 20 dBm (EIRP ~ 25 dBm),
- 15 dBm (EIRP ~ 20 dBm),
- 10 dBm (EIRP ~ 15 dBm),
- 0 dBm (EIRP ~5 dBm).

These values bracket the reliable operating range of the DSRC radios from minimum to maximum and also provide data to match the SAE J2945 benchmark (EIRP=20 dBm), and a midpoint.

We did not find commercially available DSRC hardware that could achieve the maximum EIRPs for channels 178 and 184 (44.8 and 40 dBm). Instead, we tested with EIRPs in the field of 25 dBm. We did not use higher gain antennas to try to achieve larger EIRPs in those channels as intended due to time constraints. Moreover, interference to the lower power BSMs and the resulting impact to safety applications was our primary concern.

6.2 Antenna Characterization and Calibrations

6.2.1 Purpose

The antennas needed to be calibrated so that the variable gain of the antenna patterns can be removed from the over-the-air signal power measurements between the DSRC and U-NII radios under test. This lets us more accurately recognize and measure multipath and interference.

6.2.2 Description

None of the antennas used in the analysis were perfectly isotropic, that is radiating or receiving equally in all directions. That means the antenna is more sensitive at some elevation and some azimuthal angles than others. This introduces a systematic error into the power measured between a transmitter and a receiver due to energy that is not received simply due to the changing orientation of the antennas. An antenna pattern measures this change in sensitivity with angle.

Using the antenna patterns of the two antennas (transmit and receive), power measurements between two radios can be corrected to provide the same result as if the communications occurred with perfectly isotropic antennas. By removing the result of antenna imperfections, the remaining variations in power must be the result of other phenomena such as range, multipath and interference. Not correcting for the patterns can mask these other phenomena. Often power variation or errors are incorrectly attributed to these other phenomena when they are actually due to a null or lobe in an antenna pattern.

Accurate antenna calibration requires a specialized facility and expertise in antenna measurement. We used anechoic chambers and experts at CERDEC as described on chapter 5.

6.2.3 Equipment

- Mobile and fixed antennas for DSRC devices that will be used in the tests.
- Mobile and fixed antennas for unlicensed devices that will be used in the tests
- Standard gain horn calibrated for the 5-6 GHz band.
- Precision rotational positioners with 360 degree movement around at least one axis.
- Anechoic chamber, open air range or near field probe calibrated or characterized for the 5-6 GHz band.
- Vector signal analyzer.

6.2.4 Data Collected

Table 6-2: Antenna Pattern Calibration Data Collection Matrix

Device/Parameter	Range	Resolution	Notes
Instrument configuration			
Vector analyzer model, ID			
Instrumentation uncertainties			

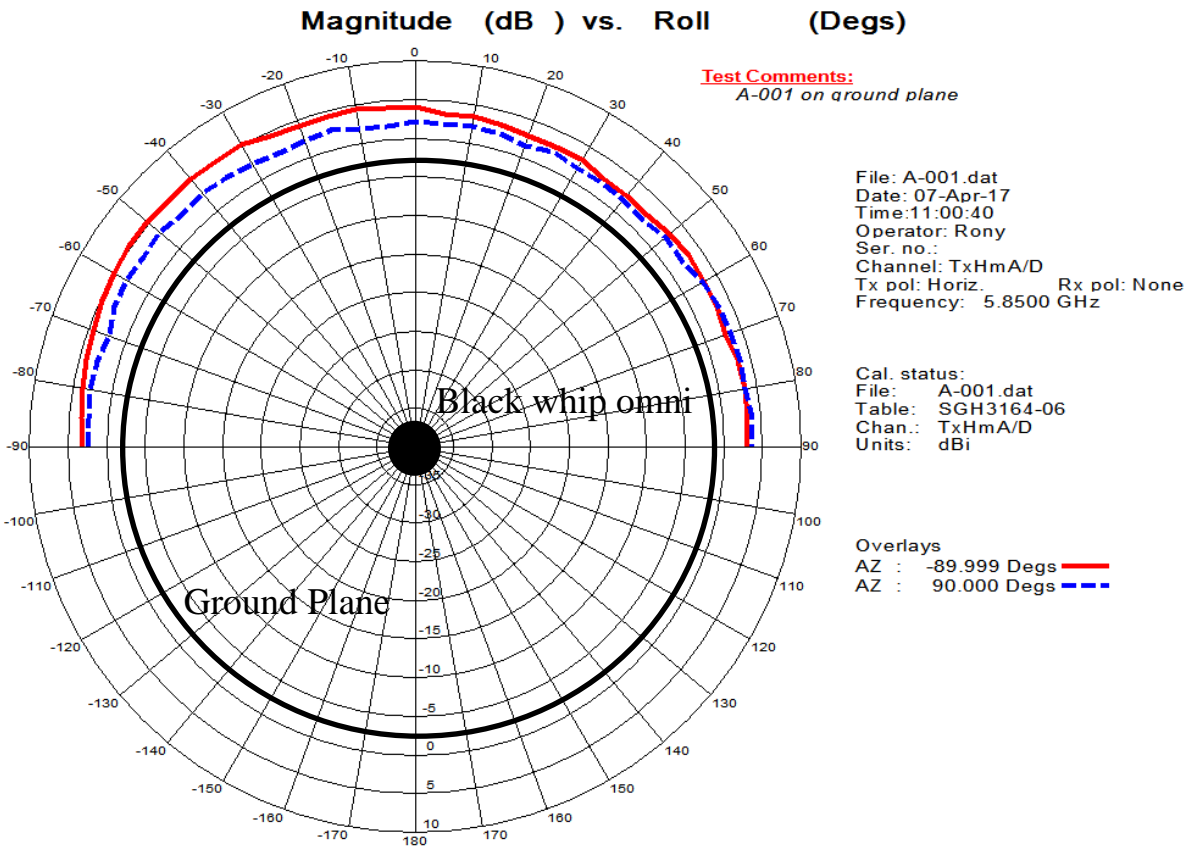
Device/Parameter	Range	Resolution	Notes
Transmitted power setting			
Transmitted modulation	CW		
Antenna configuration			
Type, model, ID			
Reference points for front and up			
Antenna height	variable		May be varied to get elevation angle
Reference antenna height			
Gain of reference antenna			
Antenna pattern identifier			
Polarization	Vertical		Horizontal can also be measured
Antenna measurements			
Frequency	5-7 GHz		
Return loss (VSWR)			
Transmitted RF power			
Received RF power			
Received signal phase			
Antenna azimuthal angle	0-360°	1°-5°	
Antenna elevation angle	±45°	1°-2°	

6.2.5 Test Activities

For each antenna, we measured the return loss across the frequencies of interest (5-7 GHz) to ensure that the antenna was resonant at the proper frequencies and in good working order. An antenna connector with a defective center pin was discovered by this process.

Next, we measured the antenna power while rotating the antenna about one axis, then incremented the other angle and repeated. Then we increment the frequency and repeat the cycle over again. The CERDEC instrumentation was fast enough that frequency could be swept during the rotation eliminating the need for a separate iteration for frequency.

Figures 6-6 and 6-7 are sample plots of the antenna patterns for one of the vehicle-mounted antennas. Figure 6-6 shows how the radiated or received energy is distributed azimuthally (horizontally). The solid red line is the data from the lower part of the plot. We flipped it on top of the data in the upper half to make any asymmetry or differences easier to see. For example, you can see that the gain along a bearing of -130° is about 2 dB greater than the direction of -40°. Other than this slight distortion, this is a nice clean pattern with almost no ripple.



959 Spectrum
ORBIT/FR

Figure 6-6: Azimuthal antenna pattern of a vehicle DSRC antenna

Figure 6-7 shows how the energy is distributed vertically for four different frequencies in the DSRC band. It is clear that frequency changes across the band are too small to affect the pattern of this antenna. It also shows that the gain is constant for about 10 degrees of the main beam. That is from the horizon at 90° up to 80° (and the horizon behind at -90° up to -80°).

The antennas were mounted in the center of a three-foot diameter metal plate to approximate a vehicle mounting and to keep all edges in the far field (with respect to the size of the wavelength). Energy seen below the horizon is due to diffraction around the edge of the plate but note that it quickly becomes 100 times less power than main beam.

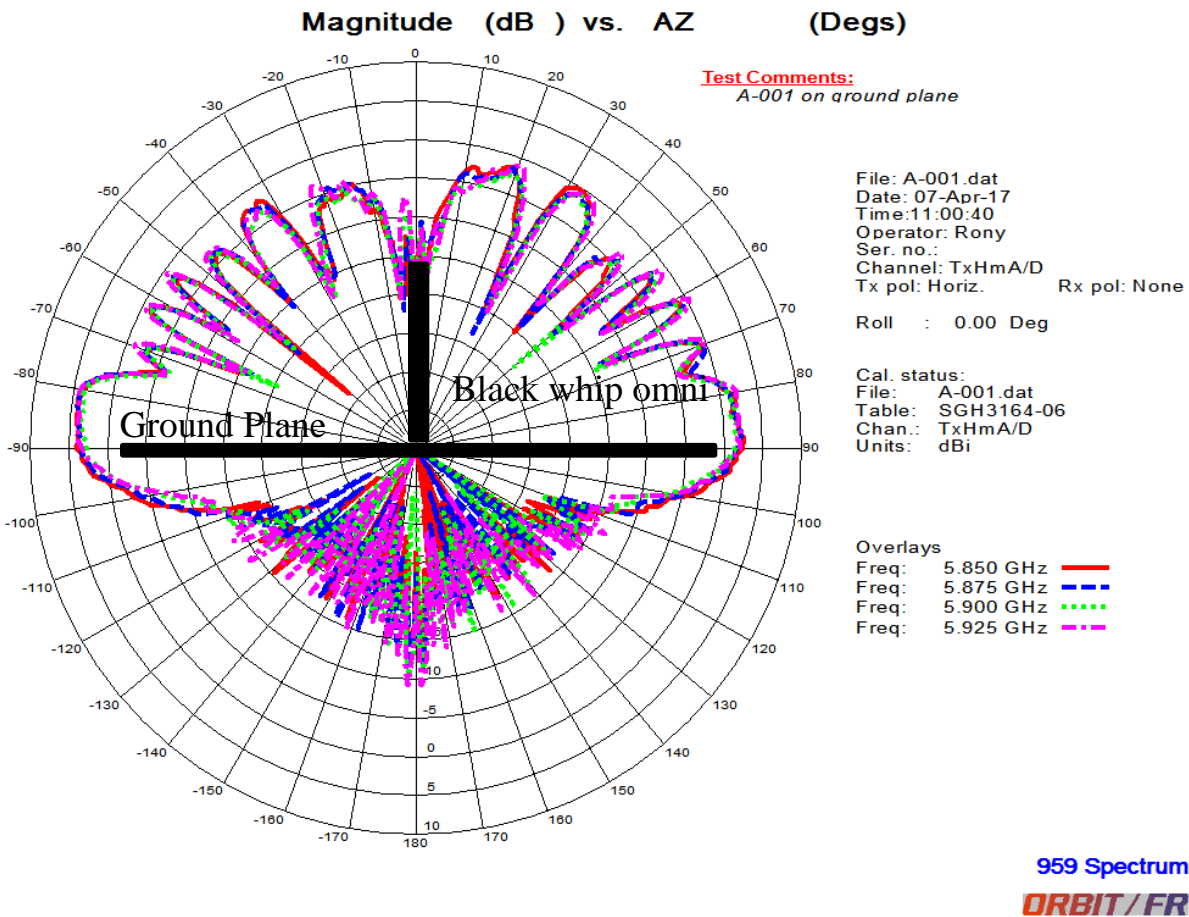


Figure 6-7: Elevation antenna pattern of a vehicle DSRC antenna

We conducted our initial pattern measurements in a large anechoic chamber on the test vehicles (Figure 6-8). That led us to discover that the vendor supplied shark-fin antennas (Figure 6-9) were unsuitable for any kind of measurement program.



Figure 6-8: Antenna pattern measurement on test vehicle in a CERDEC anechoic chamber



Figure 6-9: Vendor shark-fin antenna opened



Figure 6-10: Black whip antenna

Figure 6-11 compares the patterns of two shark-fin antennas with a small black whip antenna (Figure 6-10) that we procured separately. The red and blue patterns of the shark fins show extremely irregular patterns that were very inconsistent from unit to unit. This irregularity and inconsistency explained confounding signal losses that we experienced when we first went into the field. Our findings also explained problems that were being experienced by another USDOT test program for vehicle platooning

as well. Both programs changed to the black whip antenna (brown pattern) due to its much more repeatable performance.

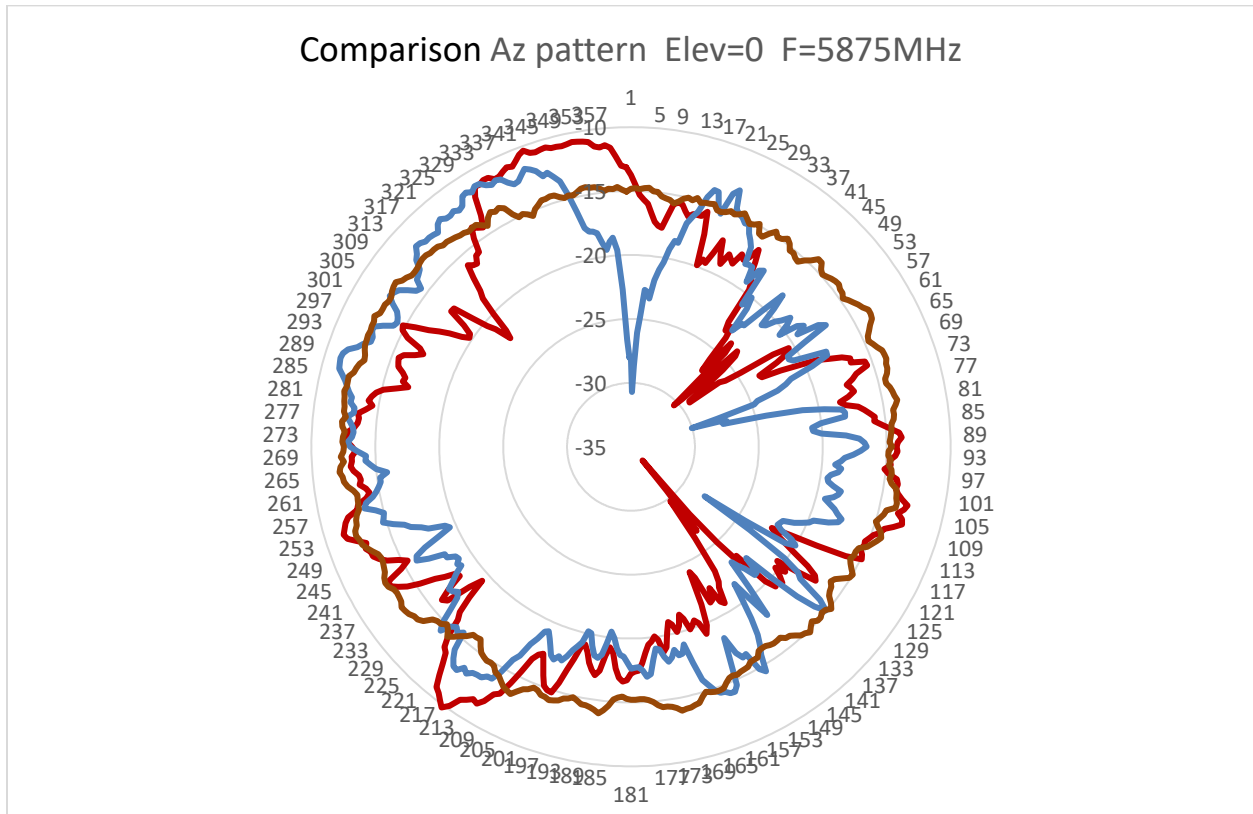


Figure 6-11: Three antenna patterns, two shark fins (blue and red) and one whip (brown)

Comparing the brown pattern measured on a vehicle in Figure 6-11 with the pattern measured on a metal plate in a smaller anechoic chamber in Figure 6-6 gives an idea of how much the curve and asymmetry of a vehicle roof perturbs the antenna pattern.

Figure 6-12 shows the azimuthal patterns for all vehicle-mounted black whip OBU antennas used for testing. The unit-to-unit variation in gain varies from zero to 5 dB, but all of the patterns are smooth, consistent and almost circular. We paired the antennas that were closest in gain when deciding which antennas to send ITS-Boulder and Aberdeen. Figure 6-13 is the same for the elevation patterns. The variation in gain is evident here as well but the pattern shape (peaks and nulls) is consistent from unit-to-unit.

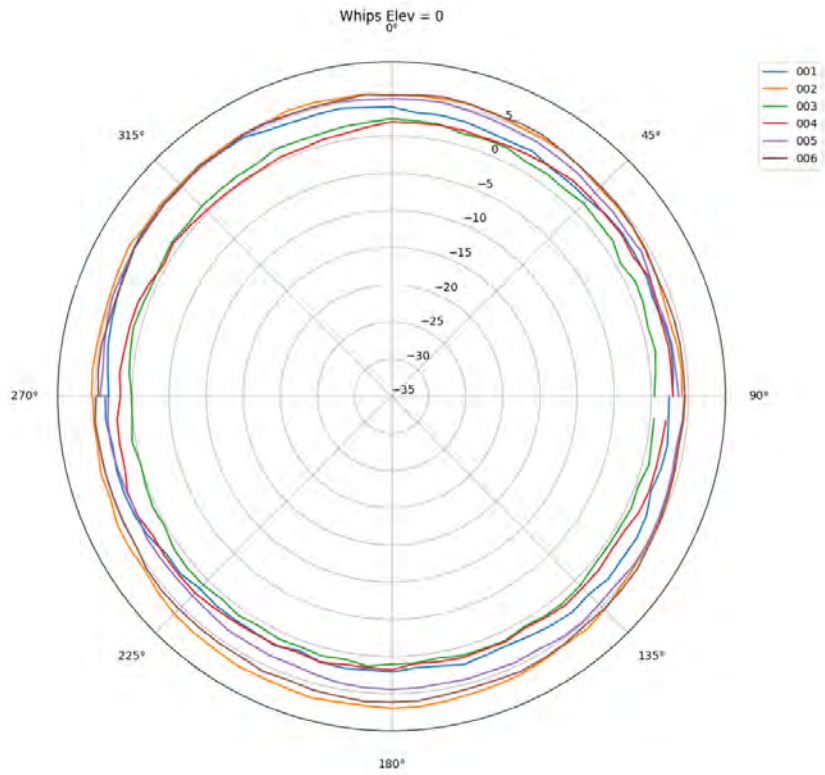


Figure 6-12: Variability in azimuth patterns across the vehicle mounted antennas used

DRAFT

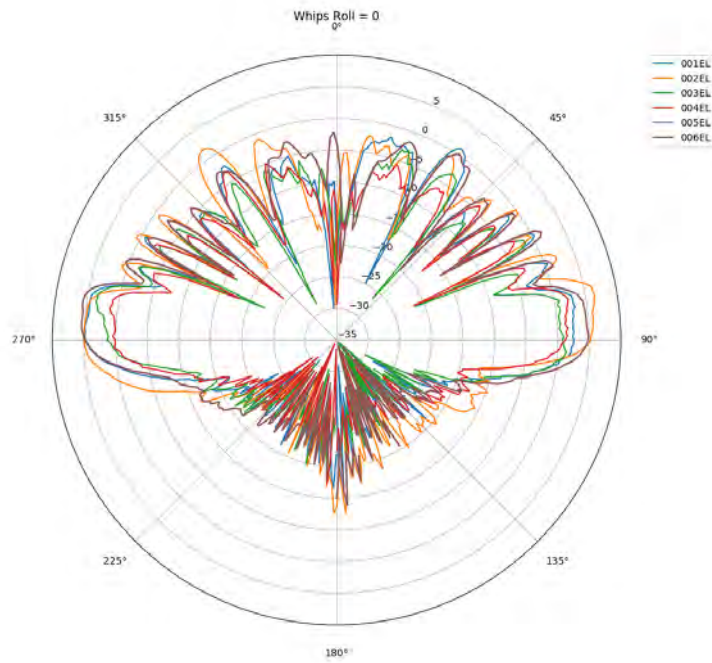


Figure 6-13: Variability in elevation patterns across the vehicle mounted antennas used

A number of other antennas were calibrated as well. Figures 6-14 and 6-15 show the azimuthal and elevation patterns, respectively, of one of the RSUs compared with the OBU antenna in Figures 6-6 and 6-7. Note that the RSU elevation pattern shows much more energy above and below the horizon because it is not sitting on a metal plate. Note also that we mounted the RSUs as they typically are mounted with the antennas pointing down. That means that in Figure 6-15, 0° points to the ground and 180° to the sky.

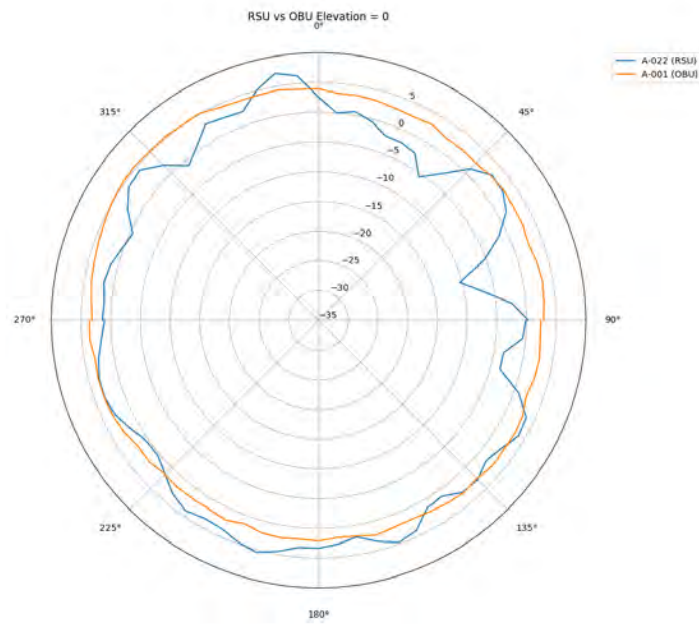


Figure 6-14: DSRC azimuthal antenna patterns, RSU (blue) and OBU (orange)

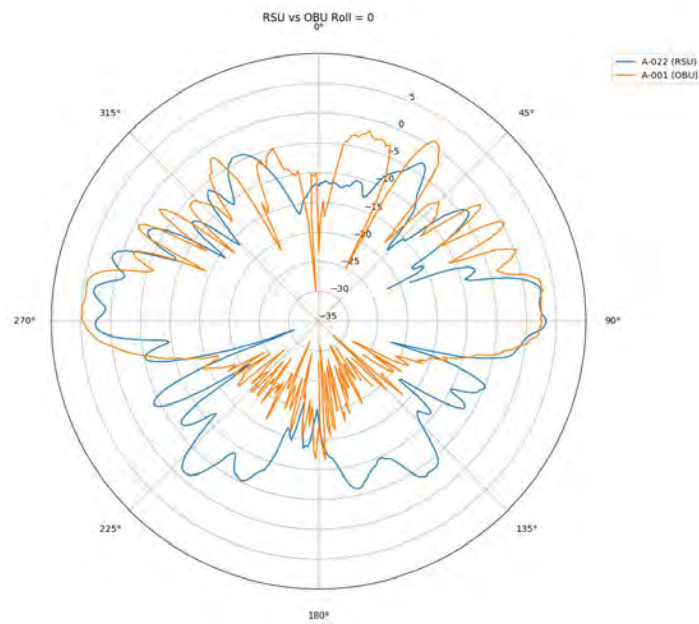


Figure 6-15: DSRC elevation antenna patterns, RSU (blue) and OBU (orange)

We have only shown azimuthal antenna patterns for the horizon and single cut elevation patterns. We measured many more patterns for each antenna so we have the data to produce a 3-D representations or examine the gain in specific directions. Our data resolution is 5° in azimuth and 1° in elevation. Table 6-3 lists antenna patterns measured for the black whip antennas and Table 6-4 lists the same for the RSUs.

Table 6-3: OBU antenna data collected

Elevation angle	Pattern	Azimuthal resolution
-5°	360° azimuthal	5°
0° (horizontal)	360° azimuthal	5°
5°	360° azimuthal	5°
10°	360° azimuthal	5°
15°	360° azimuthal	5°
20°	360° azimuthal	5°
30°	360° azimuthal	5°
45°	360° azimuthal	5°
Azimuthal cut	Pattern	Elevation resolution
0°/180°	-5° to +185° Elevation	1°
45°/225°	-5° to +185° Elevation	1°
90°/270°	-5° to +185° Elevation	1°
135°/315°	-5° to +185° Elevation	1°

Table 6-4: RSU antenna data collected

Elevation angle	Pattern	Azimuthal resolution
+10°	360° azimuthal	5°
+ 5°	360° azimuthal	5°
0° (horizontal)	360° azimuthal	5°
-5°	360° azimuthal	5°
-10°	360° azimuthal	5°
-15°	360° azimuthal	5°
-20°	360° azimuthal	5°
-25°	360° azimuthal	5°
-30°	360° azimuthal	5°
-45°	360° azimuthal	5°
Azimuthal cut	Pattern	Elevation resolution
0°/180°	+60° to +120° Elevation	1°
45°/225°	+60° to +120° Elevation	1°
90°/270°	+60° to +120° Elevation	1°
135°/315°	+60° to +120° Elevation	1°

Most of the RSU patterns were collected using non-conductive mounts, but one RSU was measured on a metal post for comparison.

Figure 6-16 shows a VSWR plot, which measures the amount of energy reflected by the antenna and its connector back to the transmitter. The markers in the upper left display the values at two frequencies in the DSRC band. The lower the VSWR the better. These values indicate a return loss of -30.7 dB or ~0.1% power reflected at 5.85 GHz and a return loss of 23.7 dB or ~0.5 % power reflected at 5.92 GHz. All of the vehicle-mounted black whip omnidirectional antennas had similarly good return loss performance.

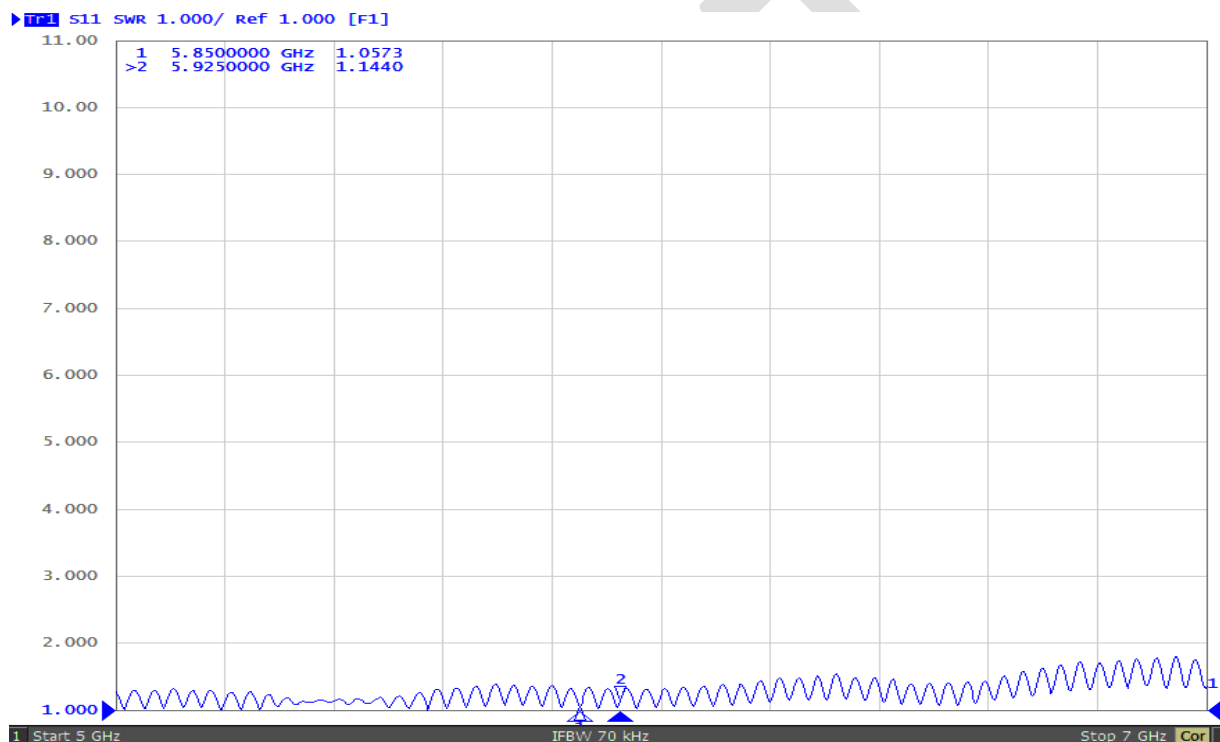


Figure 6-16: VSWR measurement for a black whip antenna

We also characterized a commercial automotive antenna and antenna for use with portable DSRC like might be put on a dashboard. Antenna pattern data will be put into an appendix.

Note that our objective was to measure RF interference and not DSRC performance. Therefore, we did not use a commercial automotive antenna due to their slightly lower gains and more irregular antenna patterns compared to the black whip. (The commercial automotive antenna that we tested was much better though than the antenna supplied by the DSRC radio vendor shown in Figure 6-9.) To hone in on differences in DSRC reception caused by Wi-Fi, we needed an antenna that was regular and consistent and so not a factor that would confound the interference measurements.

6.3 Surrogate U-NII-4 Setup and Verification

6.3.1 Purpose

It is essential to have a U-NII-4 device to study potential interference with DSRC devices. However, without the availability of proposed U-NII-4 devices from industry, we had to prepare a surrogate U-NII-4 device from commercially available U-NII-3 device Software Development Kits (SDKs).

Before using the surrogate U-NII-3 devices in testing, we needed to ensure that the modified U-NII-3 SDKs properly modeled U-NII-4 devices operating under U-NII-3 rules. We had no basis from which to create possible U-NII-4 rules since that is something the FCC would do. We do have the U-NII-3 rules written by the FCC so with the assumption that a new FCC U-NII rule would not be radically different from their previous rules this was a reasonable starting point.

This activity also identified limitations in the device that were not anticipated by the test plan.

6.3.2 Description

The U-NII-3 bands come up to the lower edge of the DSRC band. The U-NII-3 device becomes a U-NII-4 device easily enough by programming it to run at the slightly higher frequencies of the U-NII-4 band, which overlaps the DSRC band. The difference with a potential U-NII-4 device is that we have a U-NII-4 device operating under U-NII-3 rules. That will be good enough to measure interference. Examining a sharing mechanism customized for the DSRC band will require a potential U-NII-4 device operating under proposed U-NII-4 rules.

We first used a vector analyzer to verify that the modified U-NII-3 device mimicked a U-NII-4 device properly. Then we had to determine which modulations to use in the interference tests.

Because we modified production U-NII-3 radios to operate under U-NII-3 rules in the proposed U-NII-4 band, our testing occurred under the experimental license the USDOT has from the FCC (See appendix D).

6.3.3 Equipment

- U-NII-3 Wi-Fi Software Development Kits (SDKs)
- Software drivers for SDKs to operate as U-NII-4 devices
- Embedded Processor Computers (EPCs)
- Vector analyzer
- DSRC device

6.3.4 Data Collected

To verify correct surrogate U-NII-4 operation we measured the following:

- Channelization per proposed channel plan in NPRM (see Figure 1-4)
- Center frequency
- Bandwidth
- Receiver sensitivity
- Transmit emission mask
- Transmit power
- Transmit power adjustment
- Basic data transmission
- Basic sharing etiquette⁴¹
- Signal quality (error vector magnitude (EVM))
- Logging of transmitter and receiver variables specified in Table 6-5

Table 6-5: Surrogate U-NII-4 Modulation Data Collection Matrix

Device/Parameter	Notes
Vector analyzer	
Model, ID	
Receiver (client) configuration	
Antenna height	Unless cabled through an attenuator
Antenna - Azimuth	“ ”
Receiver (client) measurements	
Received channel (frequency)	
Channel bandwidth	
Received RF power	
Signal-to-Noise (S/N)	From vector Analyzer or calculated
Packet Error Rate (PER)	calculated
Packet Reception Rate (PRR)	calculated
Duty cycle or percent time channel occupied	Calculated, verified with vector analyzer
Transmitter (access point) configuration	
Antenna height	Unless cabled through an attenuator
Antenna orientation - Azimuth	“ ”
Transmitter (access point) Variables	
Transmitter channel (frequency)	
Channel bandwidth	
Transmitted power	

⁴¹ Most likely, the U-NII-3 rules that the Wi-Fi devices use to avoid interfering with each other.

Device/Parameter	Notes
Transmitted modulation	
Transmitted data rate	
Packet repetition rate	Calculated from data rate, frame size, and load
Packet size	

A graphical user interface for the UNII testbed was developed later on but most of the time the information listed in Table 6-5 was recorded manually.

6.3.5 Test Activities

Select Modulation

Table 6-6 shows that there are more possible modulations for 802.11ac than there are for 802.11p (see table 4-16). There is some overlap. If operating with the same channel width within the same channel, both devices have the potential to recognize the other and suppress messages via the more sensitive symbol detection CCA mechanism. (The energy detect mechanism is less sensitive and so less effective.)

We narrowed down to two modulations that both devices recognize using power calibrations at different modulations and testing to see if see if any modulations were more disruptive to DSRC. The modulations selected were 1/2 BPSK and 3/4 QAM-64

Table 6-6: 802.11ac Modulation Options and Data Rates

Theoretical throughput for single Spatial Stream (in Mb/s)										
MCS index	Modulation type	Coding rate	20 MHz channels		40 MHz channels		80 MHz channels		160 MHz channels	
			800 ns GI	400 ns GI	800 ns GI	400 ns GI	800 ns GI	400 ns GI	800 ns GI	400 ns GI
0	BPSK	1/2	6.5	7.2	13.5	15	29.3	32.5	58.5	65
1	QPSK	1/2	13	14.4	27	30	58.5	65	117	130
2	QPSK	3/4	19.5	21.7	40.5	45	87.8	97.5	175.5	195
3	16-QAM	1/2	26	28.9	54	60	117	130	234	260
4	16-QAM	3/4	39	43.3	81	90	175.5	195	351	390
5	64-QAM	2/3	52	57.8	108	120	234	260	468	520
6	64-QAM	3/4	58.5	65	121.5	135	263.3	292.5	526.5	585
7	64-QAM	5/6	65	72.2	135	150	292.5	325	585	650
8	256-QAM	3/4	78	86.7	162	180	351	390	702	780
9	256-QAM	5/6	N/A	N/A	180	200	390	433.3	780	866.7

Where it was possible to control modulation, early testing at 20 MHz suggested using modulations of 1/2BPSK and 3/4QAM-64. As the Wi-Fi device perceives a noisier (but not occupied) channel it employs a data rate adaptation mechanism that switches to lower MCS indexes, hence lower level modulation and lower data rate to reduce the number of retransmissions. Therefore, the Wi-Fi device will most likely be operating with 1/2BPSK when energy in a busy channel finally reaches the threshold to activate the Clear

Channel Access (CCA) mechanism. $\frac{3}{4}$ QAM-64 was the highest modulation we could set easily on the surrogate UNII-4 devices without needing to reprogram the devices between measurement runs.

We discovered that when operating in 802.11ac mode it was not possible to set and hold fixed all the control variables, like power, channel width, and modulation. The radio constantly changed these variables to optimize the communication in real-time even when the radios and the environment seemed to be sitting still and unchanging. In order to execute the controlled tests in our test plan we had to operate the radio in 802.11a mode. We could then fix these variables at the cost of being constrained to just 20 MHz channels. As a consequence, all the interference testing was done using 20 MHz channels.

6.4 DSRC Setup and Verification

6.4.1 Purpose

We tested the DSRC devices in the lab to ensure they could function as required to fulfill the test plan, identify where they could not, and identify any other limitations that required that we develop exceptions or alter the original test plan.

6.4.2 Description

We developed command programs to control the DSRC device settings so we could execute the various runs specified in the test plan. We also had to determine if the DSRC devices recorded the required transmitter and receiver data logs to measure performance well enough to identify interference. Two fundamental types of lab testing followed. We first used a vector analyzer to verify that the DSRC devices operated as required and to identify limitations. Following that, we made measurements to determine which modulations to use for the interference testing.

6.4.3 Equipment

- DSRC devices and software development kits
- Software drivers to program the DSRC devices
- Vector analyzer
- Surrogate U-NII-4 device

6.4.4 Data Collected

To verify correct DSRC radio operation we measured the following:

- Channelization per the FCC Report and Order⁴² (see Figure 1-2)
- Center frequency
- Bandwidth
- Receiver sensitivity
- Transmit emission mask
- Transmit power
- Transmit power adjustment
- Basic data transmission
- Basic sharing etiquette⁴³
- Signal quality (error vector magnitude (EVM))
- Logging of required transmit and receive variables (Table 6-7)

Table 6-7: DSRC Radio Modulation Data Collection Matrix

Device/Parameter	Logged by radio	Recorded by control GUI	Vector Analyzer screenshot	Manually recorded in GUI or notes
DSRC Receiver configuration				DSRC
Type, model, ID	MAC address	Radio Type and ID		
Antenna height		Yes		Manual
Channel		Yes		Manual
Channel bandwidth			sometimes	Defined by channel number
DSRC radio				Manual
DSRC Receiver measurements				
MAC address	Of each received packet			
Transmit packet ID (sequence number)	yes			
Received channel (frequency)	yes		sometimes	
Received Signal Strength	RSSI		sometimes	
Noise power	In the 16 μ s period after			

⁴² FCC-03-324A1, page 19

⁴³ The CCA using the 802.11p EDCA and the channelization shown in Figure 1-1.

DRAFT

Device/Parameter	Logged by radio	Recorded by control GUI	Vector Analyzer screenshot	Manually recorded in GUI or notes
	each packet reception			
Signal-to-Noise (S/N)				Calculated from RSSI and noise measurements
Packet Error Rate (PER)	1 second averages			Calculated from time stamps and packet sequence IDs
Packet transmit time	yes			
Packet receive time	yes			
Inter-packet gap			sometimes	Calculated From Tx and Rx timestamps
GPS position and time	Yes			
DSRC Transmitter(s) configuration				
Type, model, ID	MAC address	Radio Type and ID		
Antenna height		Yes		Manual
Vehicle ID or RSU		Yes		Manual
Vehicle speed				Manual
Channel (frequency)		Yes	sometimes	Manual
Channel bandwidth		Yes	sometimes	Defined by channel number
Transmit power		Yes		Manual
Transmit modulation		Yes	sometimes	Manual
Transmit data rate			sometimes	Determined from MCS index
Packet size		Yes	sometimes	Manual
Packet transmission rate		Yes	sometimes	Manual
DSRC Transmitter Variables				
MCS index	Specifies modulation & data rate			
Transmitted power	Yes		sometimes	Manual
GPS position and time	Yes			
Distance between transmitter and receiver				Calculated from GPS
Signal quality (e.g., EVM)			sometimes	

During the checkout period, we recorded all data in the table above manually. We developed the graphical user interface to address operational problems that surfaced in the field. Lab testing continued as needed for a few reasons: first, to diagnose problems that develop in the field; second, to

recalibrate after the radio vendor issues a firmware upgrade that can't be avoided. Hence, we used the GUI that we developed for the later lab work as well.

Additionally, we used our DSRC/UNII packet sniffer to collect diagnostic information when necessary and for our tests varying the EDCA parameters of the 802.11 clear channel access mechanism.

6.4.5 Analysis Activities

Select Modulation

The modulations permitted for DSRC shown in table 6-8 overlap but are not identical to the list of modulations available to Wi-Fi U-NII that are seen in table 6-6. The 802.11ac standard allows for very high throughput modulations (e.g., 256-QAM) that are not specified for other 802.11 devices in the IEEE 802.11-2012 standard.

Higher order modulations provide greater throughput but are more vulnerable to interference so operate at much lower ranges. On the other hand, most DSRC applications described to date, in particular the safety applications, require the long ranges only possible with the lower order modulations. In fact, most DSRC operations to date have used ½ QPSK at 6 Mbps.

Table 6-8: 802.11p DSRC Modulation Options⁴⁴

Modulation	Coding rate (R)	Coded bits per subcarrier (N_{BPSC})	Coded bits per OFDM symbol (N_{CBPS})	Data bits per OFDM symbol (N_{DBPS})	Data rate (Mb/s) (20 MHz channel spacing)	Data rate (Mb/s) (10 MHz channel spacing)	Data rate (Mb/s) (5 MHz channel spacing)
BPSK	1/2	1	48	24	6	3	1.5
BPSK	3/4	1	48	36	9	4.5	2.25
QPSK	1/2	2	96	48	12	6	3
QPSK	3/4	2	96	72	18	9	4.5
16-QAM	1/2	4	192	96	24	12	6
16-QAM	3/4	4	192	144	36	18	9
64-QAM	2/3	6	288	192	48	24	12
64-QAM	3/4	6	288	216	54	27	13.5

⁴⁴ IEEE 802.11-2012 wireless standard, Table 18—Modulation –dependent parameters, 3/29/2012, p1590.

Based on our measurements at Aberdeen, we selected two modulations in order to streamline the analysis activities and attain experimental results sooner: $\frac{1}{2}$ QPSK and $\frac{3}{4}$ QAM-64. The first, represents the modulation used for most DSRC testing and development and the one specified for safety applications through NHTSA analysis (6 Mbps data rate in a 10 MHz channel). The more complex modulation represents the highest data rate applications possible in the future (27 Mbps in this case) to provide a bounding case that would be more vulnerable to interference.

6.5 Baseline Environmental Signal Data Collection

6.5.1 Purpose

The purpose of the baseline environmental signal data collection was to measure background RF noise levels on roadways as well as the facilities to be used for testing. It was also to measure existing signals in the environment that include the co-primary users in the band. Those are predominantly government radars and FSS earth stations, as well as other signals and potential sources of interference that could be found opportunistically. Other signals could come from unlicensed ISM, secondary users such as amateur radio operators, and users in adjacent bands. The latter can be licensed users like FSS (satellite ground stations operating above the DSRC band) and unlicensed users (e.g., U-NII-3 wireless CCTV links) operating below the DSRC band.

The objective was to characterize the current signal environment by known emitters in the DSRC band to confirm they present no risk to connected vehicle communications or identify RF issues that should be considered before connected vehicle devices are deployed on a larger scale.

6.5.2 Description

For the baseline environmental testing, we used vehicles equipped as mobile listening stations to record RF energy in the spectrum and localize the source. Equipment included spectrum analyzers, various omni- and directional-antennas, and data recorders. Prior to the Mobile Recording System provided by ATC described in section 5.4 we equipped a passenger van as shown in Figure 6-17.

We collected background noise and signal data on representative roads in the DSRC band and adjacent bands. We collected data in the vicinity of other co-primary sources of RF like FSS stations near roads in Maryland and Virginia and a Federal tracking radar at Wallops Island.

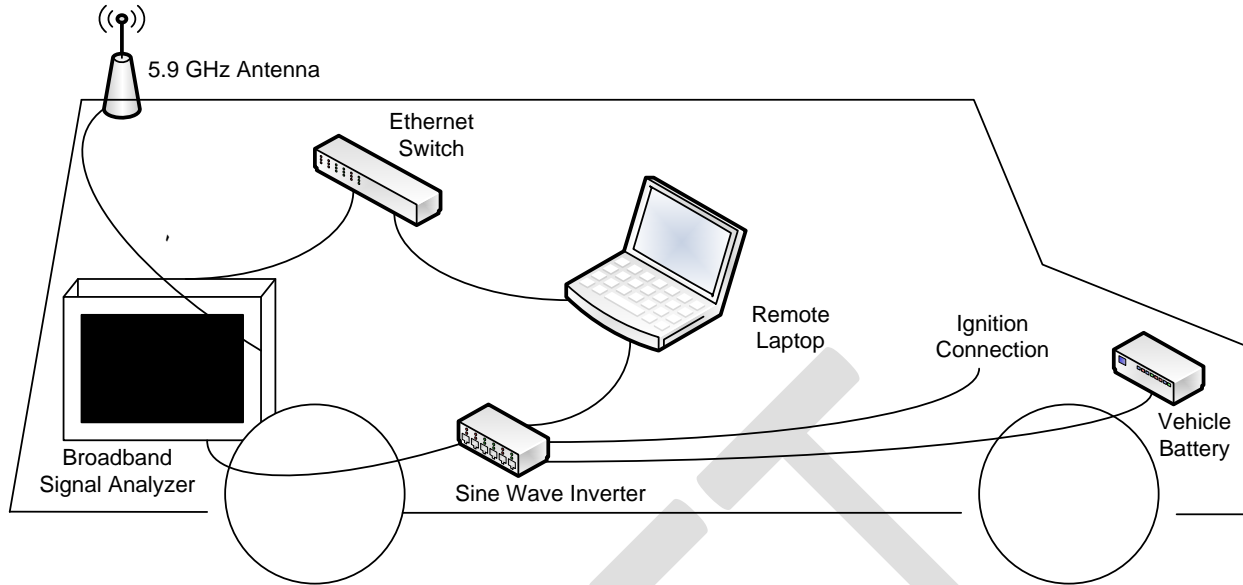


Figure 6-17. Passenger van equipped for RF data collection

6.5.3 Equipment

Table 6-9 lists equipment used in the passenger van to do the RF survey.

Table 6-9: Mobile Data Collection Platform Equipment

Equipment	Specifications	Notes
Omni-directional antenna	2-6 GHz magnetic mount Wi-Fi antenna, Mobile Mark ECOM6-5500-3C-BLK-120	Receive any signals in the environment
Handheld directional antenna	680MHz to 8GHz Log Periodic Antenna, Kaltman Creations HyperLOG 6080	Rough identification of signal source for aiming directional antennas
Directional antenna	4.9-6.5GHz, 20 degree beamwidth Single Polarization Antenna, Mars MA-WA57-3HG1B	Narrow down signal source location
Precision directional antenna	4.9-6.1GHz, 10 degree beamwidth Dual Polarization Antenna Mars MA-WA56-DP23B	To identify signal source
Precision directional antenna	4.9-6.1GHz, 7 degree beamwidth Dual Polarization Antenna Mars MA-WA55-27B, small form factor	To identify signal source
High gain horn antenna	4.9 - 7.05 GHz, 20 dB Gain Pasternack WR-159 Standard Gain Horn Antenna	Highly sensitive measurement of signals
GPS antenna	GPS Antenna - External Active Antenna - 3-5V 28dB 5 Meter SMA. Adafruit Industries 960.	Mobile GPS antenna

Equipment	Specifications	Notes
Mount for GPS antenna	Magnetic Antenna Mount 3" Hemisphere GPS P/N 720-0033-00A	GPS to determine location of the platform
Pan/Tilt/Zoom mount	FLIR D48 E-series, D48E-SS-SS-000-SS	For aiming directional antennas
DC Power supply	Converts 110-240VAC, 47-63Hz to 30VDC, FLIR PTU-APS-30V-NA	Power for PTZ mount
Power inverter	2 kilowatt Xantrex PROWatt 2000 Inverter, Model# 806-1220	Convert 12VDC vehicle power to 110VAC for the instruments
Magnetic base	Master Magnetics #07217 2.04"d Round Base Magnet	Moveable base for PTZ mount
Controller	Wireless Gamepad Controller with Vibration Feedback, Logitech pn F710	Control PTZ mount movement
Antenna switch	USB/Ethernet controlled RF Switch Matrix, 4:1 RF ports, Mini Circuits RC-1SP4T-A18	Switch antenna input to the signal analyzer
Portable Broadband Signal Analyzer	Aeroflex CS9000SM System	Spectrum analysis
Laptop		For data collection and analysis
8-port, Gigabit Ethernet Switch	Netgear GS608NA	
External Hard drive	Silicon Power 2TB Rugged Armor A80 2.5-Inch USB 3.0 Military Grade Portable	Data storage
Cable, connection and mounting hardware	Various, not described here.	Document with data collection.

6.5.4 Data Collected

We used the broadband analyzer for two general forms of data collection: measure channel power and to capture high resolutions waveform. The channel power measurement (with GPS tracking) is useful when the mobile test vehicle is in motion and continuously logging channel power on the defined channel plan. When we identified a possible source of interference we sometimes took a high-resolution measurement to try to locate it. Because the high resolution measurements generate enormous data files they were made judiciously. Table 6-10 lists variables recorded during the field measurements of potential sources of interference.

Table 6-10: RF Environmental Data Collection Matrix

Device/Variable
Spectrum analyzer configuration
Model, ID
Antenna height
Antenna orientation - Azimuth
Antenna orientation - Elevation
Other fixed settings
Spectrum analyzer measurements
Bandwidth setting
Frequency vs power plots
Spatial measurements
Speed during data collection
GPS location
Timestamp
Location on road network
Distance to co-primary transmitter
Signal identifier or label

{Section still under development}

7. Description of Testing

After completing the preparatory activities and calibrations, there were two basic parts remaining to the testing. In the first part, we made baseline measurements of the DSRC devices and the surrogate U-NII-4 testbed, separately, to understand their normal performance when not exposed to the other radio service. In the second part, we tested the performance of DSRC when exposed to transmissions from the surrogate U-NII-4 testbed in four of the five scenarios described below.

In addition, there were additional characterization testing to determine the relative sensitivity of the two radio services (DSRC and Wi-Fi).

DRAFT

Learning how long it took to execute key functions was an important first step. Table 7-1 lists factors that affected schedule estimation along with our observations in the field.

Table 7-1. Factors important to schedule estimation

	Variable	Observations
1	The time to set up and tear down specific measurement configurations	10-20 minutes typical. 30-45 minutes when operating 40 DSRC transmitters.
2	The time to make a single data collection run	<p>Variable. At Zone 1 (1600m r/t) the fastest runs were under 3 minutes and start-time to start-time to next run was as little as 5 minutes at 40 mph.</p> <p>At Perryman (6 mile r/t) typical runs at 40 mph took 10 minutes and start-time to start-time was typically 30-45 minutes. But driving only part way down the course at 50 mph the run time could be shortened to as much as 4 minutes with only 15 minutes between run start times.</p> <p>The most number of runs in a single day was 38. Typical was 15-20 but could be as few as 4 when problems developed.</p> <p>The bigger time components than physical run time are time lost to equipment malfunction, troubleshooting and correction (often rebooting radios); and viewing data and reacting to the results before deciding what parameters to set for the subsequent run. One needs to include time for these unpredictable activities when estimating schedules. That meant budgeting for 10-12 runs a day, rather than 38.</p>
3	The time required to analyze a data collection run to ensure the data collected is of high quality	<p>Analysis in the field was as short as 2-3 minutes to view the raw data and summary plots of a just completed run. This often took place during the subsequent run to avoid delaying runs.</p> <p>But this time was much longer when trying to understand unexpected results or troubleshooting inconsistent or incorrect data.</p>
4	The number of data collection runs that are needed to ensure the data is statistically significant	<p>For signal-over-distance baselining, the variation in 3 runs was similar enough to 10 runs to be adequate for most data collection runs. Over time we accumulated enough baseline runs to prove that that one baseline run a day was sufficient to demonstrate consistency with measurements from previous days.</p> <p>Typical procedure was to do a 10 mph baseline run at the beginning of each day and a 10 or 30 mph baseline at the end of each day to catch anything that may have changed to corrupt the data. Data runs were made at 30-50 mph.</p>

Key chapter takeaways

- 1) We made baseline measurements of DSRC communications without Wi-Fi interference to characterize environmental interference and imperfections in the devices.
- 2) We remove this interference from the data with the Wi-Fi interference to identify interference that is solely due to the Wi-Fi signals.
- 3) We used an independent spectrum analyzer to ensure signals over the air looked normal before a run and to monitor the background for spurious signals that might contaminate the data.
- 4) Most tests were done with DSRC EIRP's of 5, 15, 20 or 25 dBm.
- 5) We set the Wi-Fi EIRP as high as the FCC limit of 36 dBm for many of the tests, but we tested with Wi-Fi power settings as low as 5 dBm as well.
- 6) Because the calibration and baseline tests showed little difference when changing the DSRC channel, most interference tests were run with the DSRC in channel 172. Interference to other DSRC channels will be the same.
- 7) We tested 10 MHz DSRC channels. As explained in chapter 6, the Wi-Fi was limited to 20 MHz channels. The DSRC and Wi-Fi radios could only sense each other via the energy detect mechanism.
- 8) We usually tested DSRC with packet rates of ten or 400 packets/second. Varying the rate did not affect results for interference due to packet collisions in the receiver, the predominant interference that we detected.
- 9) Wi-Fi packet rate was varied to achieve desired channel loadings from two to 100%.
- 10) We measured maximum V2I ranges to 3600 meters and maximum V2V ranges to 2000m, with EIRP of 25 dBm. Wi-Fi range would be at least this far since its maximum power was ten times larger.
- 11) Individual vehicle speed ranged from 10 to 50 mph, with the maximum closing speeding between two vehicles being 100 mph.
- 12) Independent baseline measurements at ITS-Boulder in Colorado confirmed the baseline measurements at APG in Maryland.
- 13) We tested 4 scenarios. The first, outdoor access point had the mobile DSRC driving away from the static DSRC and towards and past the Wi-Fi downrange.
- 14) The second scenario, indoor access point, tested with the static DSRC near the building and the mobile DSRC driving toward, past, and away.
- 15) The third scenario, in-vehicle Wi-Fi, had the mobile DSRC driving away from the static DSRC with Wi-Fi access point and client onboard.

- 16) The fourth scenario, high speed rural, had two mobile DSRC vehicles driving toward each other and static DSRC and Wi-Fi in the middle at closing speeds up to 100 mph.
-

7.1 Baseline Testing

7.1.1 Purpose

Baseline testing measured the performance of DSRC reception in terms of power, error rate and the selected channel quality. Baseline performance metrics were captured in order to see how the metrics changed when unlicensed radios were introduced for the subsequent interference tests. Imperfect communication performance in the baseline data was due to imperfections of the radios and environmental interference, not the Wi-Fi. We needed to measure baseline imperfections to remove them from the interference data collected with the Wi-Fi operating in the presence of the DSRC devices. This activity created the reference data for subsequent analysis and inputs for NTIA/ITS models.

7.1.2 Overview

The set up for baseline testing the DSRC devices consisted of setting up two static radios, one an RSU on an 18' tower⁴⁵ and the other an OBU in a stationary vehicle parked nearby. Another OBU was installed in a mobile vehicle that drove from the position of the static radios to the end of the test track and back (Figure 7-2). The performance metrics were recorded for four permutations:

- V2V mobile transmitting, static receiving,
- V2V mobile receiving, static transmitting,
- V2I mobile transmitting,
- V2I mobile receiving, static transmitting.

Runs generally were made at either 10 mph or 30 mph. Within a single run the test vehicle would usually drive out and back one time (at Perryman) and perhaps two to four times (at Zone 1).

⁴⁵ 18 feet is midrange for the mounting heights for traffic controls allowed by the Manual of Uniform Traffic Control Devices. RSUs are often mounted on the mast arms for traffic signals.



Figure 7-2. DSRC Baseline Test Illustration

The baselines for the surrogate UNII-4 testbed were done similarly. Either the access point was put in the mobile vehicle and the client was mounted on a tripod on the track at heights of 6' and 18', or the client rode in the mobile vehicle with the access point on the track and its antenna at 6' or 18' (Figures 7-3 and 7-4).

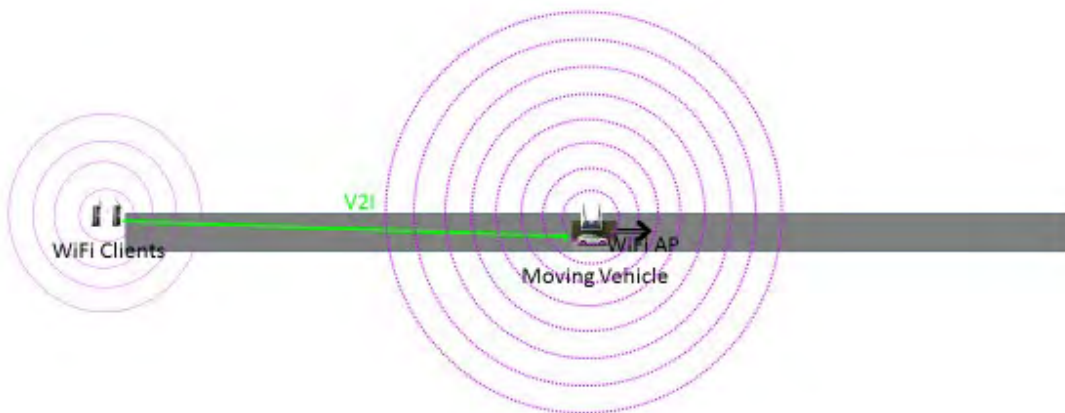


Figure 7-3. Surrogate U-NII-4 Baseline Test Illustration



Figure 7-4. UNII baselining – client on 18’ tripod, access point in white vehicle at Perryman test track

Figure 7-5 shows the location and dimensions of the Zone 1 and Zone 2 test areas at Phillips Army Airfield. The RSU (and start point for the mobile vehicle) was near the intersection of the two zones and is marked in the figure. Early baseline tests and low power interference tests were done at Zone 1 (Figure 7-6).

We did not use Zone 2 as anticipated due to signals that showed up near our band on that course from a dish antenna on the ground near the airfield tower. The airfield tower (Figure 7-7) appears as a large black dot in Figure 7-5. The suspect antenna was aimed low and directly across Zone 2.



Figure 7-5. Phillips Army Airfield test facilities, Zone 1 at the left. Zone 2 at the right.



Figure 7-6. Zone 1 - minimal sources of multipath interference



Figure 7-7. Zone 2 – looking toward Zone 1

7.1.3 Description

We obtained most DSRC metrics from log files generated in each DSRC radio. We accessed this data using proprietary software provided by the radio vendor. Table 7-2 lists the data logged by the radios and the data that was recorded manually and used for the bulk of our analysis. We used additional variables logged by the radios like *mean-time busy ratio* and statistics on various flags related to the Clear Channel Access mechanism to understand unexpected results in the field and for diagnosing problems. These additional variables are numerous and, since they didn't figure into the analysis that led to our results, they are not listed here. Each radio included a GPS receiver, which provided the location of the radio for each data record as well as a time stamp used to correlate the position with the RF measurements.

All OBU DSRC signals were received using an external antenna on the roof of the car. For baselining the UNII, the access point's isotropic antenna was mounted between and just behind the seats.

A spectrum analyzer fed by antennas on the roof of the data van monitored the background for spurious signals that could introduce error into the baseline measurements. It also provided a quality check that radios were on the air and that the signals looked normal. Screenshots from the spectrum analyzer were used to record characteristics of the DSRC and UNII signals from time to time. Those included plots of amplitude versus frequency, waterfall plots (that show amplitude versus frequency scrolling with time), amplitude versus time, and Electric Vector Magnitude plots showing the modulation of the received signal. Figure 4-66, in chapter 4, shows all of these except the waterfall plot.

Table 7-2 Radio data collected

Device/Parameter	Logged by radio	Recorded by control GUI	Vector Analyzer screenshot	Manually recorded in GUI or notes
DSRC Receiver configuration				DSRC
Type, model, ID	MAC address	Radio Type and ID		
Antenna height		Yes		Manual
Channel		Yes		Manual
Channel bandwidth			sometimes	Defined by channel number
Vehicle ID or RSU				Manual
Vehicle speed				Manual
DSRC Receiver measurements				
MAC address	Of each received packet			
Transmit packet ID (sequence number)	yes			

DRAFT

Device/Parameter	Logged by radio	Recorded by control GUI	Vector Analyzer screenshot	Manually recorded in GUI or notes
Received channel (frequency)	yes		sometimes	
Received Signal Strength	RSSI		sometimes	
Noise power	In the 16 μ s period after each packet reception			
Signal-to-Noise (S/N)				Calculated from RSSI and noise measurements
Packet Error Rate (PER)	1 second averages			Calculated from time stamps and packet sequence IDs
Packet transmit time	yes			
Packet receive time	yes			
Inter-packet gap			sometimes	Calculated From Tx and Rx timestamps
GPS position and time	Yes			
DSRC Transmitter(s) configuration				
Type, model, ID	MAC address	Radio Type and ID		
Antenna height		Yes		Manual
Vehicle ID or RSU		Yes		Manual
Vehicle speed				Manual
Channel (frequency)		Yes	sometimes	Manual
Channel bandwidth		Yes	sometimes	Defined by channel number
Transmit power		Yes		Manual
Transmit modulation		Yes	sometimes	Manual
Transmit data rate			sometimes	Determined from MCS index
Packet size		Yes	sometimes	Manual
Packet transmission rate		Yes	sometimes	Manual
DSRC Transmitter Variables				
MCS index	Specifies modulation & data rate			
Transmitted power	Yes		sometimes	Manual
GPS position and time	Yes			
Distance between transmitter and receiver				Calculated from GPS
Signal quality (e.g., EVM)			sometimes	

Device/Parameter	Logged by radio	Recorded by control GUI	Vector Analyzer screenshot	Manually recorded in GUI or notes
UNII Transmitter configuration				
Antenna height				Manual
Channel (frequency)	Yes		sometimes	Manual
Channel bandwidth	Yes		sometimes	Manual
Transmit power	Yes			Manual
Transmit modulation	Yes		sometimes	Manual
Transmit data rate				Specified by modulation
Packet size			Sometimes	Manual
Packet transmission rate			Sometimes	Calculated from data rate, packet size and loading
Traffic load percentage				Manual
GPS position and time	Yes			
Signal quality (e.g., EVM)			sometimes	
Environmental data				
Precipitation (Time, type (rain, snow, sleet, hail))				Manual - Potential for signal attenuation
Surface condition (Wet/dry/snow/ice)				Manual - May affect multipath
Wind events (Time or general condition)				If exceptional conditions – possible antenna shaking
Temperature				If exceptional

7.1.3.1 Test Variables

We varied several parameters to determine their effect on the sensitivity of DSRC to Wi-Fi radio interference. As a result, we measured baselines for all the permutations we anticipated in the interference testing. Adding another variable or value to a variable multiplies the number of runs so we made tradeoffs to try to streamline the number of runs necessary while still capturing either bounding or “typical” cases. Because of time constraints, the actual number of variables tested was less than anticipated in the original test plan. A summary of the primary variables follows.

Transmit power:

Even though the DSRC radio power calibrations measurements were made every 0.5 dB, DSRC power in most tests was one of four values shown in Table 7-3 below to keep the schedule manageable. The first column lists the setting on the radio transmitter, but the actual radiated power (EIRP) that includes antenna gain and cable loss is what matters most for comparison.

The maximum UNII test power is also listed in the table. Other lower values of UNII power were also used on occasion. Powers specified by the FCC rule and order⁴⁶ and the SAE J2945 standard are also listed for reference.

Table 7-3: Radiated Power Levels Selected for Analysis

Tested		Reference		Remarks
Tested Transmit Power (dBm)	Tested EIRP (dBm)	EIRP ⁴⁷ dBm	EIRP mW	
0	5	0	1.0	Baseline for handheld DSRC and FCC class A (15 meter range) RSUs. Test power was the lowest setting available with our hardware.
10	15	10	10	Baseline for FCC DSRC class B RSU (100 meter range)
15	20	20	100	Baseline for FCC DSRC class C RSU (400 meter range), Also the DSRC maximum power specified in SAE J2735. This tested value represents the maximum DSRC that will be found in deployment.
20	25	23	200	Allowed FCC maximum for the low power 10 MHz DSRC service channels and the 20 MHz channels. SAE J2735 specifies DSRC operation much less than the allowed FCC maximum. This tested power represents an upper bound better than will be achieved by DSRC in deployment. Any interference to this DSRC power will be untenable in deployment.
		30	1 W	Baseline for U-NII access point and close to baseline for FCC DSRC class D (1000 meter range) RSUs
30	35	33	2 W	FCC maximum for the high power DSRC service channels (all 10 MHz). The FCC maximum for Wi-Fi access points is 36 dBm so this power was used for the surrogate UNII Wi-Fi device.
		40	10 W	FCC maximum power for channel 184. Requires high gain antenna. Commercial DSRC devices not found so not tested.
		44.8	30 W	FCC maximum power for channel 178. Requires high gain antenna. Commercial DSRC devices not found so not tested.

Channel width:

Most of the baseline data collected was on three of the seven 10 MHz DSRC channels. Those were channels 172, 178 and 184. Channel 172 is representative of all the service channels and will be overlapped by U-NII-4 channels in any sharing scenario. Channel 178 allows for the highest DSRC EIRP

⁴⁶ Federal Communications Commission Report and Order FCC-03-324A1, released February 10, 2004, page A-12.

⁴⁷ The Effective Isotropic Radiated Power (EIRP) can be larger than the transmitter output power because it includes antenna gain. [EIRP = transmitter output power – cable losses + antenna gain]

(30W), and Channel 184 allows 10W signals. Because there was not a lot of difference in radio performance across these channels most of the interference testing was done on channel 172.

All UNII channels used in our testing were 20 MHz as it was the only way to maintain control of other variables like power and modulation at the same time with our surrogate UNII testbed. The channels were typically channel 173 for co-channel testing and channels 169 and 177 for adjacent channel testing.

Packet content:

Because our interest was examining radio interference rather than DSRC performance, we used identical test packets (as described in Chapter 4) rather than actual BSMs for RF consistency.

Packet length:

We selected two packet lengths for analyzing DSRC messages.

- 1) 300 bytes which is typical for a BSM.
- 2) 1500 bytes which is the maximum allowable WAVE short message size. Note that larger packets might occur when exchanging V2I data with a data warehouse.

We simulated BSMs by having the vehicle mounted OBUs transmit 300 byte packets. We simulated the larger SPaT and MAP messages by having the RSU transmit 1500 byte packets.

We generally tested with three Wi-Fi packet sizes (300, 1400 and 1500 bytes). The 300 byte packets roughly simulated applications like text messaging. The 1400 byte packets better simulate streaming video. The 1500 byte packets appear as more complicated mixed traffic over the air due to packet splitting by the radio. The packet splitting doubled the number of data frames and roughly doubled the number of management frames transmitted. Chapter 4 discusses these packet sizes, their selection and impact in greater detail.

For the same reason that we were limited to 20 MHz Wi-Fi channels, we did not test the 9000 byte and 1 million byte jumbo frames of 802.11ac as originally planned.

Modulation:

Based on the results of lab tests we selected two modulations to baseline and use in the interference testing.

- 1) $\frac{1}{2}$ QPSK – used in all currently deployed DSRC and the second most robust DSRC modulation.
- 2) $\frac{3}{4}$ QAM-64 – a modulation that would be used for high data rate applications in the future. It is one of the least robust DSRC modulations. Interference to this modulation might constrain future development of DSRC capabilities.

The UNII modulation was selected to provide the data rate necessary to achieve the desired channel loading. A higher index modulation has less range and would be more susceptible to interference from DSRC, but its interference to DSRC should be the same as a robust low index modulation since they have the same carrier power.

Data Rate:

The modulation determines the data rate, that is, bits per second as a frame is transmitted. As noted, just two DSRC modulations were tested. The UNII data rate was manipulated to achieve desired traffic load (i.e., duty cycle or band occupancy). Wi-Fi traffic load determines the size of the inter-packet gaps available for BSMs to pass through.

Frame or packet rate:

We usually operated DSRC at 10 or 400 packets/second. Ten packets/second would be typical of a deployed DSRC radio. Four hundred packets/per second was often used to simulate 40 DSRC vehicles with one radio to occupy more bandwidth. This provided higher range resolution as there were more data points in a given distance and increased the likelihood of packet collisions with the Wi-Fi.

Increasing the packet rate to simulate more vehicles works when looking at interference at the receiver, which is where most of the interference we observed occurred. This kind of scaling would be problematic when looking at interference that causes transmitter suppression since 40 DSRC radios would not operate in lockstep, but instead would back off with 40 randomly selected back-off times. The results in chapters 9 and 10 show that transmitter suppression happens at such short ranges compared to packet collisions in the receiver that we focused on the latter. As a result, the DSRC data rate wasn't a factor that mattered or biased the results.

As already noted, particularly in the discussion in chapter 4, the UNII packet rate was determined by the modulation/data rate and packet size and manipulated to occupy the desired fraction of airtime.

Range:

Range was measured from five meters until there was no measurable signal or the limit of the test facility was reached. At the higher powers, the range of both the DSRC and Wi-Fi exceeded the length of Zone 1. As result, all long range measurements had to be done at the Perryman test site.

Other variables in the original test plan included additional antenna heights and tilt angles but were dropped from testing due to time constraints. When changing a parameter resulted in insignificant variation, we reduced the number of runs with that variable to reduce the effort. Conversely, where results were more sensitive to a variable than anticipated, we added runs to increase the resolution or number of iterations of that variable as necessary. This scaling of effort was typical in the field for all testing activities to reduce effort where possible and focus attention where it seemed to matter most.

Vehicle speed along with packet rate determined the number of data points in each range bin, that is, the spatial resolution of the data. Speed also determined the time per run, hence the number of runs per day. The speeds used for various tests were determined in the field based on the tradeoff between time to collect data, fidelity of the data and safety considerations. Individual vehicle speed ranged from 10 to 50 mph, with the maximum closing speeding between two vehicles being 100 mph.



Figure 7-8. Test vehicles and tower at Table Mountain

7.1.4 Equipment

Table 7-4 lists the major equipment and hardware items used in the testing. In addition, there were various cables, GPS antennas, other antennas, Ethernet routers and switches

Table 7-4. Key hardware and equipment used in the testing

Equipment	Specifications	Notes
Omni-directional antenna	50, 5-6 GHz 6 dBi, vertical polarization, 360° azimuth angle, 25° elevation angle, Mobile Mark, ECO6-5500-WHT	To make 30 dBm EIRP U-NII-3 access point
Omni-directional antenna	Two, 5-6 GHz 9 dBi, vertical polarization, 360° azimuth angle, 12° elevation angle, Mobile Mark, ECO9-5500-WHT with lightning protection	For the VSG but also to make 33 dBm EIRP U-NII-3 access point
Omni-directional antenna	Two, 5.9-6.0 GHz 12 dBi, vertical polarization, 360° azimuth angle, 7° elevation angle, Mobile Mark, ECO12-5900-WHT	For the VSG but also to make 36 dBm EIRP U-NII-3 access point
GPS RTK antenna	A42 Antenna Kit, multi frequency, GNSS, L-Band. Hemisphere 940-2084-000	Antenna for the GPS RTK receiver

DRAFT

Equipment	Specifications	Notes
GPS antenna	GPS Antenna - External Active Antenna - 3-5V 28dB 5 Meter SMA. Adafruit Industries 960.	Mobile GPS antenna
Antenna (active)	Rohde and Schwarz HE600	Connected to RSA6120B for monitoring and recording DSRC U-NII signals
Bias Unit	Rohde and Schwarz IN600	Supplies DC bias to HE600 active antenna
Antenna cables	3 dB loss cables, 6' LMR400 Jumper NM plus RFI TRFC-11806-12 1 foot N Female to MMCX Male	Jumpers to connect the U-NII devices to the external antennas listed above.
Vector Signal Generator/Analyzer	Two Aeroflex 3070A	Generating U-NII waveforms and measuring received signals
Portable Broadband Signal Analyzer	Aeroflex CS9000SM System	Monitor spectrum to detect external signals that may interfere with measurements
Real-Time Signal Analyzer	Tektronix RSA6120B	Monitoring, recording and analyzing DSRC and U-NII signals in the field and lab
Real Time Spectrum Monitor	CRFS, Inc. RFeye Array 300	Monitoring and recording DSRC and U-NII signals in the field
Power Meter	Keysight N1911A	Measure transmitter power in the ARL lab
Vector Signal Generator w/internal I/Q AWGs	Keysight N5182B	Playback interfering signals in the ARL lab
Oscilloscope	Keysight DSOS-804A	Monitor time domain signals in the ARL lab
Real-time Signal Analyzer	Keysight UXA N9040B / Tektronix RSA 5115B	Monitor frequency domain signal in the ARL lab
RF Enclosure	ETS-Lindgren	Isolate transceiver from RF & EMI in the ARL lab
U-NII-3 Wi-Fi development kit	25 Compex, MMJ344HV6A06AFCEBRV527-B, programmed for U-NII-4 band, with integrated PoE (Power over Ethernet), 27 dBm	Surrogate U-NII-3/4 device for measuring adjacent band and in-band interference
Stationary DSRC radio	23 dBm, Cohda Wireless MK5 RSU (with integrated antennas)	DSRC RSU
Mobile DSRC radio - external antenna	Two 23 dBm, Cohda Wireless MK5 OBU, MK5 OBU CWP-OBU-MK05-WW00102	DSRC OBU to simulate OEM devices built into the vehicle
Mobile DSRC radio – integral antenna	TBD	DSRC OBU to simulate aftermarket devices

Equipment	Specifications	Notes
8-port, Power over Ethernet Switch	Transition Networks 1-1000520 8-port 10/100BASE-TX w/POE and 2-port 10/100/1000Base-T or 100/1000Base-X-SFP Combo ports, Industrial Managed Switch	Ethernet data switch to transfer data or provide power to components in the Ethernet chain: switches, cameras, DSRC devices, U-NII devices (but not the laptop)
Power supply	Transition Networks 25080 power supply for industrial converters, 48VDC @ 2.5A / AC 120V	Power source for the Power over Ethernet switch
Embedded Processor Computer (EPC)	Quad-Core 900 MHz 1GB RAM New Raspberry Pi 2 with 8 GB MicroSD Card	To generate data traffic for the surrogate U-NII-4 devices to transmit
External Hard drive	Silicon Power 2TB Rugged Armor A80 2.5-Inch USB 3.0 Military Grade Portable	Data storage
GPS RTK receiver	Eclipse R330 Receiver, L1 GPS, 10Hz, raw data. Hemisphere 940-2103-000	To generate precise time stamps (100 ns resolution) and locations (to within 5 cm)

Two Ford Edge SUVs and two Volkswagen GTI's were transferred from the USDOT Southeast Michigan test-bed project to support this testing. The vehicles included AC power inverters and cabling for data collection. Early testing at APG, for example the baselines at Zone 1, used the Ford Edges. After the SUVs were shipped to ITS-Boulder for baseline testing there, the bulk of the measurements made at APG used the VWs. The slightly higher antenna heights in the data discriminate between the SUV and sedan data.

7.1.5 Validation

A sample of the baseline runs made at APG were repeated at ITS-Boulder to confirm the results and to see how much the different environments (gravel versus paved) would change the data. Figure 7-8 shows the test vehicles and tower at Table Mountain, in Colorado. Figure 7-9 shows that both environments had relatively similar noise levels with ITS-Boulder being slightly higher (-100 dBm versus -102 dBm).

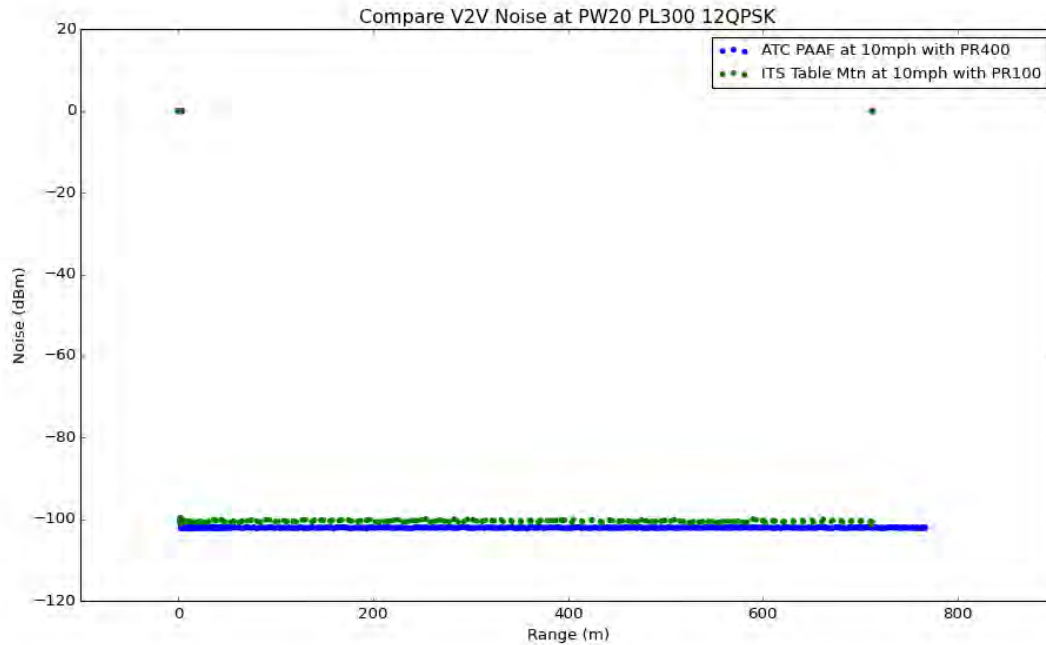


Figure 7-9: Noise level comparison of Table Mountain versus Aberdeen Proving Grounds

The received signal strength measurement of Figure 7-10 shows good agreement between the locations with one major exception. That is the highly dampened ground-bounce nulls at Table Mountain compared APG. We believe this is due to more scattering and less specular reflection from the gravel and more humid surface at Table Mountain (see Figure 7-8) compared to the paved and drier surface at Aberdeen (see Figure 7-13). Finally, the comparison between the two locations in Figure 7-11 shows similarly low packet losses of only a couple of percent.

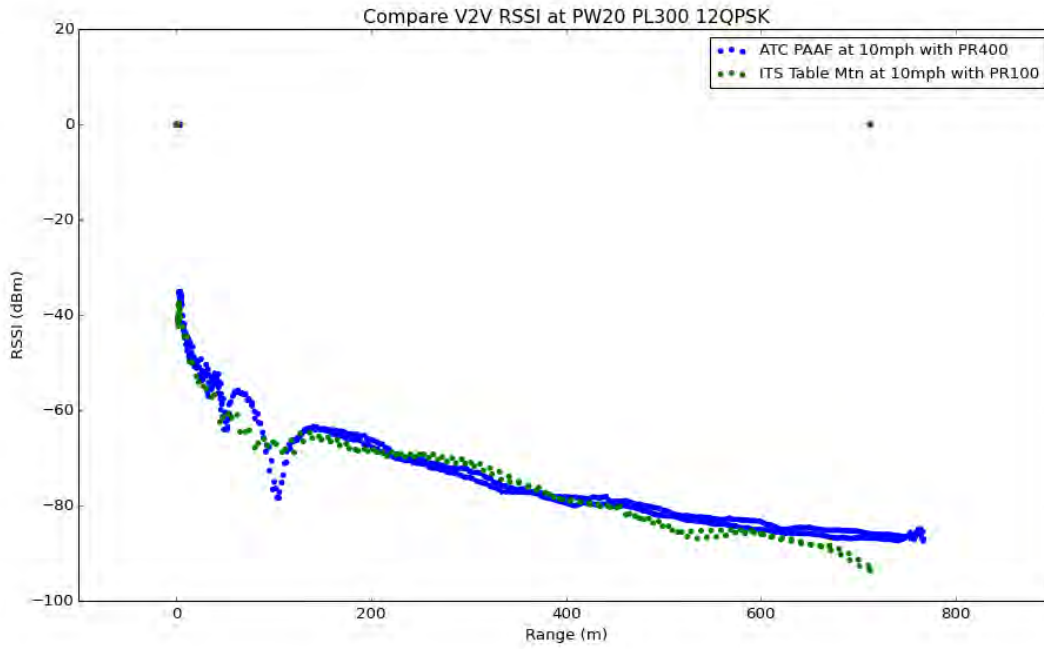


Figure 7-10: RSSI comparison of Table Mountain versus Aberdeen Proving Grounds

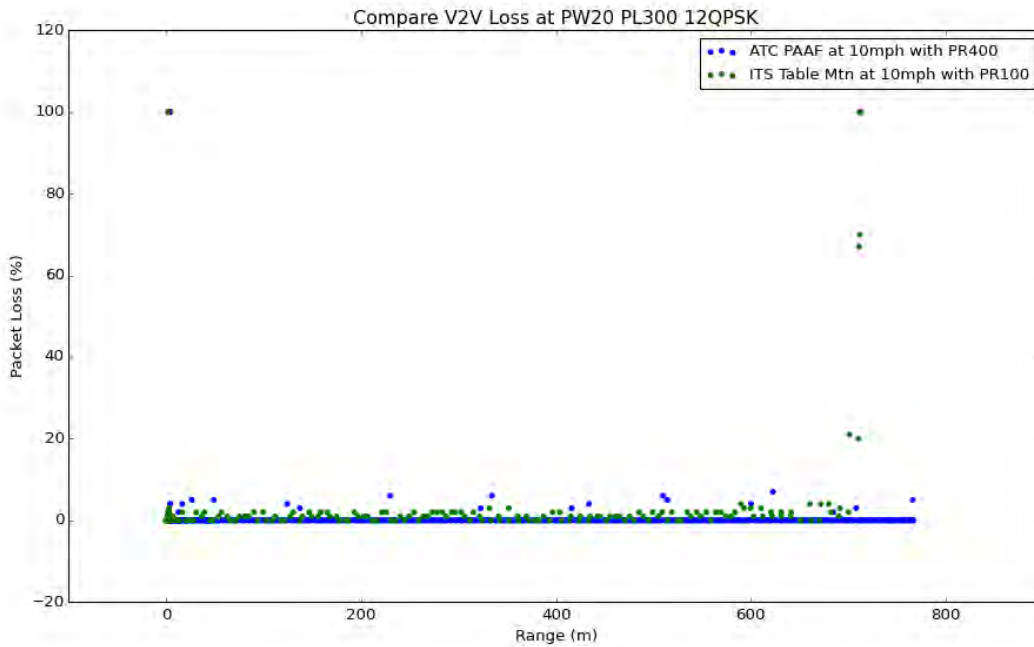


Figure 7-11: Packet loss comparison of Table Mountain versus Aberdeen Proving Grounds

7.1.6 UNII testbed stability

While investigating the repeatability of results in the field, we discovered that transmitted power from our surrogate UNII-4 testbed varied and that this variance was enhanced by movement in the environment. Figure 7-12 shows an example where the UNII power initially varied ± 3 dB with no movement in the lab. Then when people were moving around the lab (without stepping in between the access point and client) that fluctuation increased to ± 6 dB. Consistent with observations in the field it appears that the transmit power of the Wi-Fi access point will fluctuate more as the test vehicle drives by the radio. We don't believe the phenomena is simple multipath, which should only affect the receiving client and not the transmitter because this fluctuation occurs in static conditions. We are not sure if the DSRC radios are subject to the same thing as they are only broadcasting, rather than the two-way communication that occurs in W-Fi.

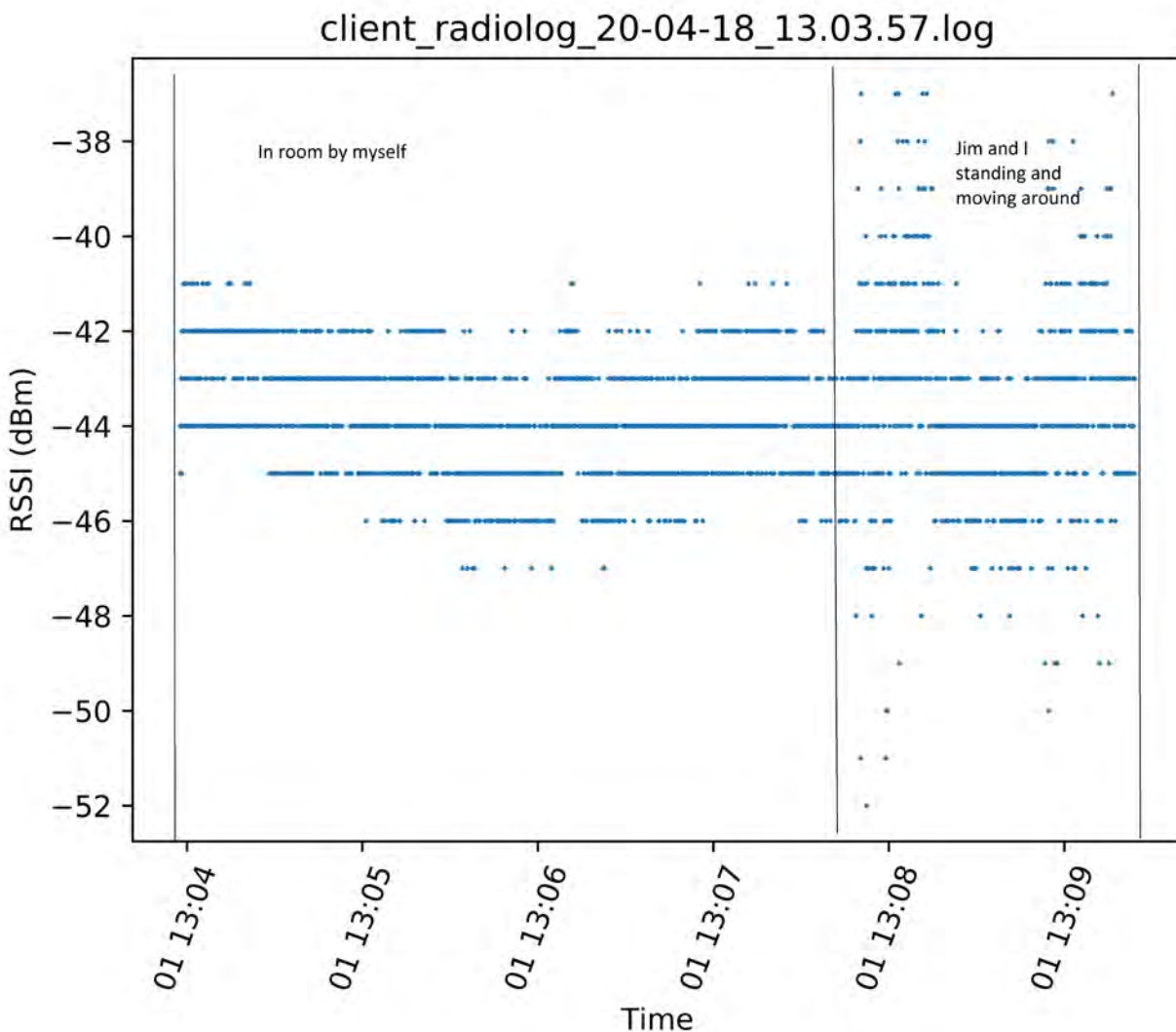


Figure 7-12: Wi-Fi stability affected by movement in the environment

{Section still under development}

7.2 Interference Testing

7.2.1 Overview

To measure the effects on DSRC communications of unlicensed U-NII-4 transmitters we endeavored to investigate anticipated real world scenarios that included OBEs communicating with the OBE's in other vehicles and with infrastructure mounted RSEs in the presence of unlicensed access points. The data demonstrates how unlicensed Wi-Fi devices interfere with DSRC devices in these common scenarios. It was also provided as input to NTIA/ITS models investigating deployment scale effects.

Potential interference depends on the many variables of actual operation for both types of devices. Since it is not possible to investigate all cases we examined specific cases that represent the most common scenarios in which these devices would be likely to interact and have potential for interference.

Scenario 1: The effect of an 802.11ac access point, externally mounted on a commercial building near an intersection, on RSE-to-OBE and OBE-to-OBE communications.

For example, a wireless CCTV camera system linked to building security.

Scenario 2: The effect of an 802.11ac access point, mounted inside a house in a residential area near an intersection, on RSE-to-OBE and OBE-to-OBE communications.

For example, a home Wi-Fi access point linking computers, printers, TVs, appliances and other smart or connected devices in the emerging Internet of Things (IoT).

Scenario 3: The effect of an 802.11ac access point and portable devices operating inside a vehicle on RSE-to-OBE and OBE-to-OBE communications.

For example, handheld devices such as tablets or smartphones that include 802.11ac Wi-Fi. The vehicle could even have its own 802.11ac access point mounted in the passenger compartment, as some automakers now offer Wi-Fi connectivity in their vehicles.

Scenario 4: The effect of an 802.11ac access point on the OBE-to-OBE communications of two vehicles approaching at high speed.

In this example, two vehicles approach one another on a rural road, where traffic and radio densities are low compared to urban and suburban scenarios. Each vehicle is traveling at high speed – perhaps 55 mph, with a combined closing speed of 110 mph. This case would be more sensitive to interference, because the loss of a single BSM exchanged between two rapidly-converging vehicles on a rural road could be a greater threat to safety than two cars slowly converging at an urban intersection.

Scenario 5: The effect of multiple 802.11ac Access points and client devices along a corridor on RSE-to-OBE and OBE-to-OBE communications.

In this example, the scale of the test is increased from a couple of devices to perhaps two dozen, in order to simulate potential real-world conditions at deployment if unlicensed devices are allowed into the 5.850 to 5.925 GHz band.



Figure 7-13. Interferer set up as outdoor access point and client at Zone 1

7.2.2 Outdoor Wi-Fi access point (scenario I)

An externally mounted unlicensed access point has the greatest ability to interfere with DSRC communications. This type of access point can be found on a commercial building, such as a Wi-Fi hub for passing client devices, to receive streaming video from CCTV surveillance cameras or to act as a building-to-building link. The DSRC communications examined are the ability of an RSU and OBU to receive BSMs from an OBU, and the OBU to receive SPaT messages from the RSU.

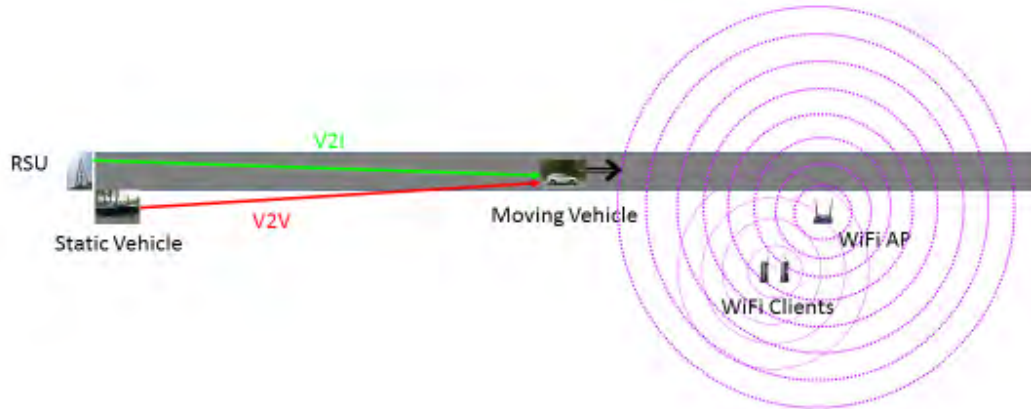


Figure 7-14. Outdoor Access Point

We staged the radio equipment to simulate a typical outdoor Wi-Fi access point near an intersection. The RSU to transmit SPaT messages was mounted on a mast at 18 feet to simulate mounting with a traffic signal at an intersection. The RSU received BSMs from the moving OBU as well. An OBU in a vehicle parked near the RSU also sent and received BSMs to/from the moving OBU (Figure 7-14). The second OBU in the moving vehicle transmitted BSMs and received SPaT messages. An example of this scenario might be a restaurant that has installed a Wi-Fi access point for customer use (Figure 7-15).

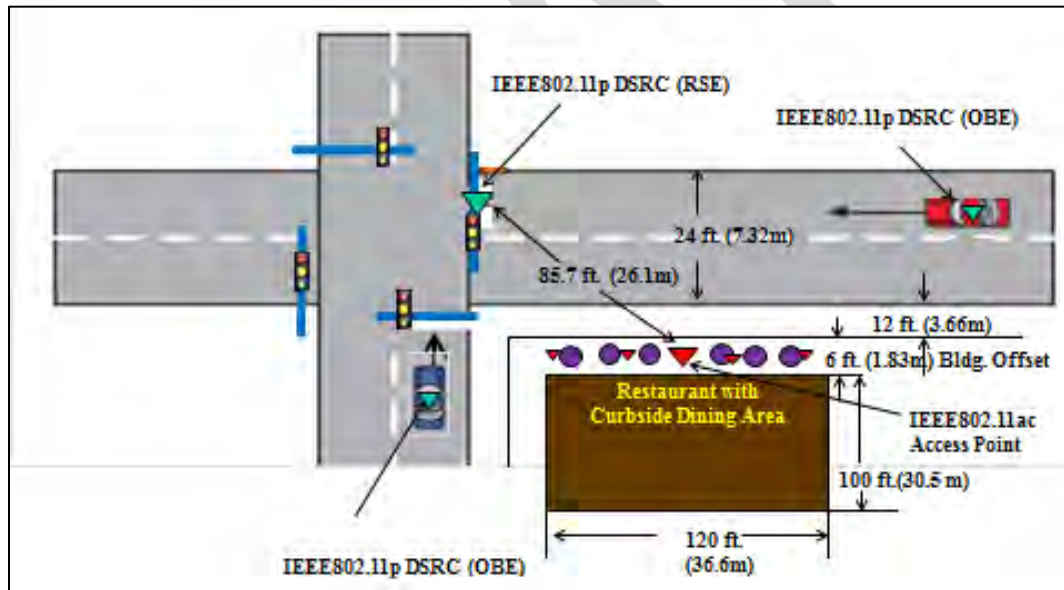


Figure 7-15: Representative Outdoor Access Point scenario

The typical data run was for the vehicle to drive away from the start point at the RSU until it was out of signal range at Perryman, or to the end of Zone 1, and then return. The Wi-Fi access point was often down range near the end of the track so the vehicle could start in a condition of zero interference. The data shows where and how interference developed between DSRC at the start point and the moving vehicle as it approached the access point.

Chapter 9 conveys some results with the rest in the appendices. Our results show the impact of unlicensed Wi-Fi operating without any mitigation or sharing techniques on the performance of DSRC communications. Some tests examined packet collisions in the moving vehicle, others packet collisions in the static DSRC, and others measured suppression of transmission from the moving vehicle as it drove by the access point.

Other tests looked at the effect of changing the potency of the Wi-Fi, such as different transmit powers, packet rates and data rates (modulations). The first run almost always was the daily baseline measurement that was used to make sure everything was working and to provide a data set for examining day-to-day repeatability and for analyzing uncertainty in the measurements.

7.2.3 Indoor Wi-Fi access point (scenario 2)

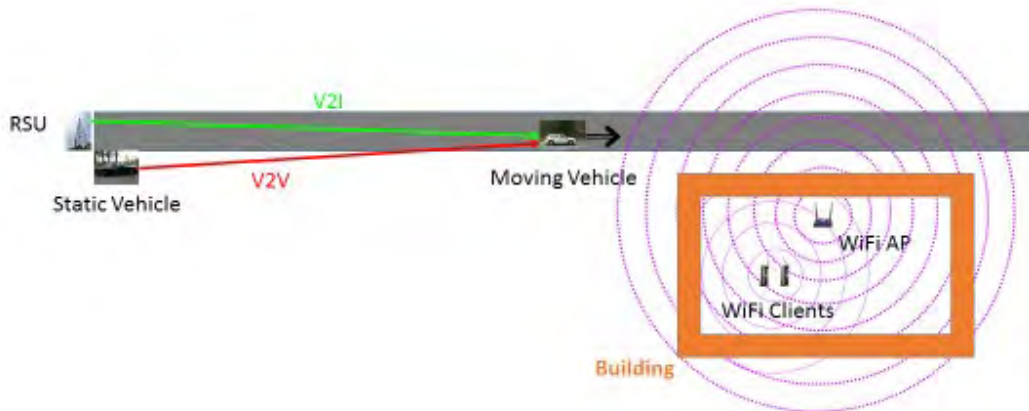


Figure 7-16. Indoor Access Point

The indoor access point tests (Figure 7-16) were conceptually the same as the outdoor access point tests with three major exceptions.

- 1) We tested with the access point inside a building as well as outside it (to compare with outdoor access point test results)
- 2) The RSU and start point were typically near the building rather than at the opposite end of the track.
- 3) The multipath environments were complex and not minimal as with the scenario 1 tests.

These differences allowed us a far richer data set with a more complete set of bounding cases. Any real interference experienced in deployment should not be worse nor better than the range of conditions that we tested. We tested with three different buildings (cinderblock, brick, and wood). See Chapter 10 for our indoor access point test results.

By putting the UNII device near the RSU and start point and having the vehicle drive away we can see how the DSRC competes with the Wi-Fi directly. That would be the case in the intersection example shown in Figure 7-15 if the access point were moved inside. Doing so in an environment full of

buildings, trees and other reflective objects that create complicated multipath environmental interference gives some idea of the RF propagation to expect in real urban and suburban environments.

Conversely, driving from the start point (where the RSU is located), with the DSRC set to its strongest power and the Wi-Fi set to its weakest power, toward the access point where the DSRC link weakens and the Wi-Fi interference strengthens in a clean multipath environment (like Figure 7-14), we could examine the balance between the two radio services and generate clean results useful for modeling and simulation.

Figure 7-17 illustrates a residential indoor access point. In the example, an indoor IEEE 802.11 access point inside a building is near an RSU and vehicles in a school zone.

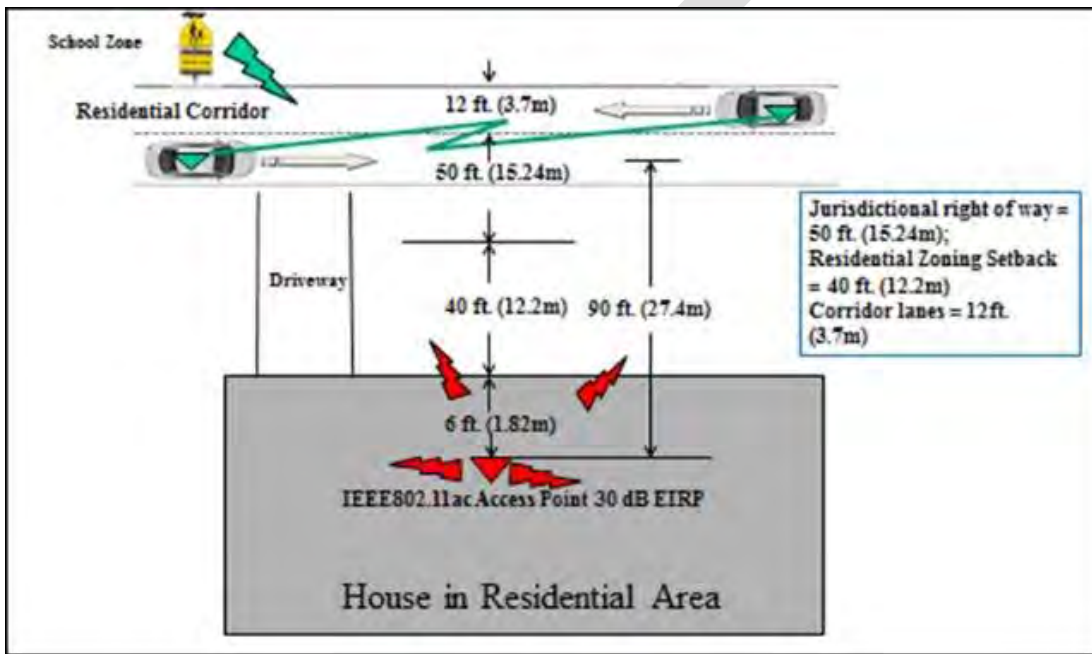


Figure 7-17: Representative indoor access point scenario

7.2.4 In-vehicle access point

This activity looked at the impact of Wi-Fi inside the vehicle on DSRC communications (Figure 7-18). The Wi-Fi might be from a built-in access point or portable unlicensed devices carried by passengers. Portable unlicensed devices inside the vehicle will communicate with an unlicensed LAN in the vehicle. Examples would be tablet computers and smartphones accessing the Internet and streaming video.

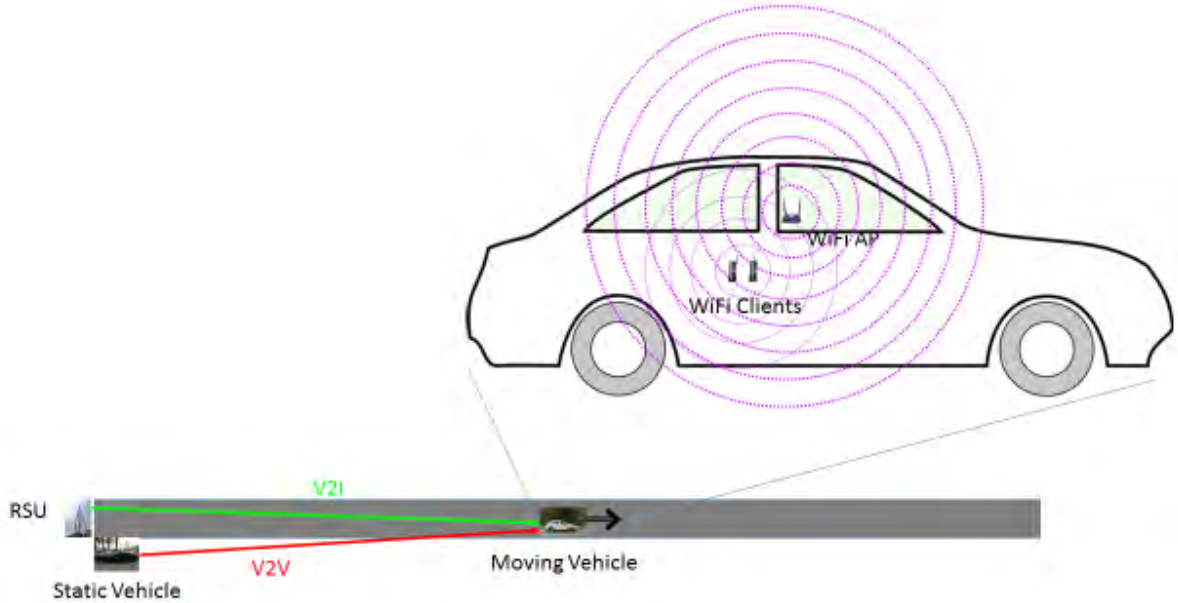


Figure 7-18. In-Vehicle access point

In this scenario, we positioned the RSU and parked one vehicle near the start of the Perryman test track. The second vehicle drove past and away from the RSU and parked vehicle with the UNII access point and client onboard as well as the DSRC OBU. The access point antenna was mounted between and just aft of the front seats (Figure 7-19). Figure 7-20 illustrates how this scenario might occur in the real-world. See chapter 9 for results.

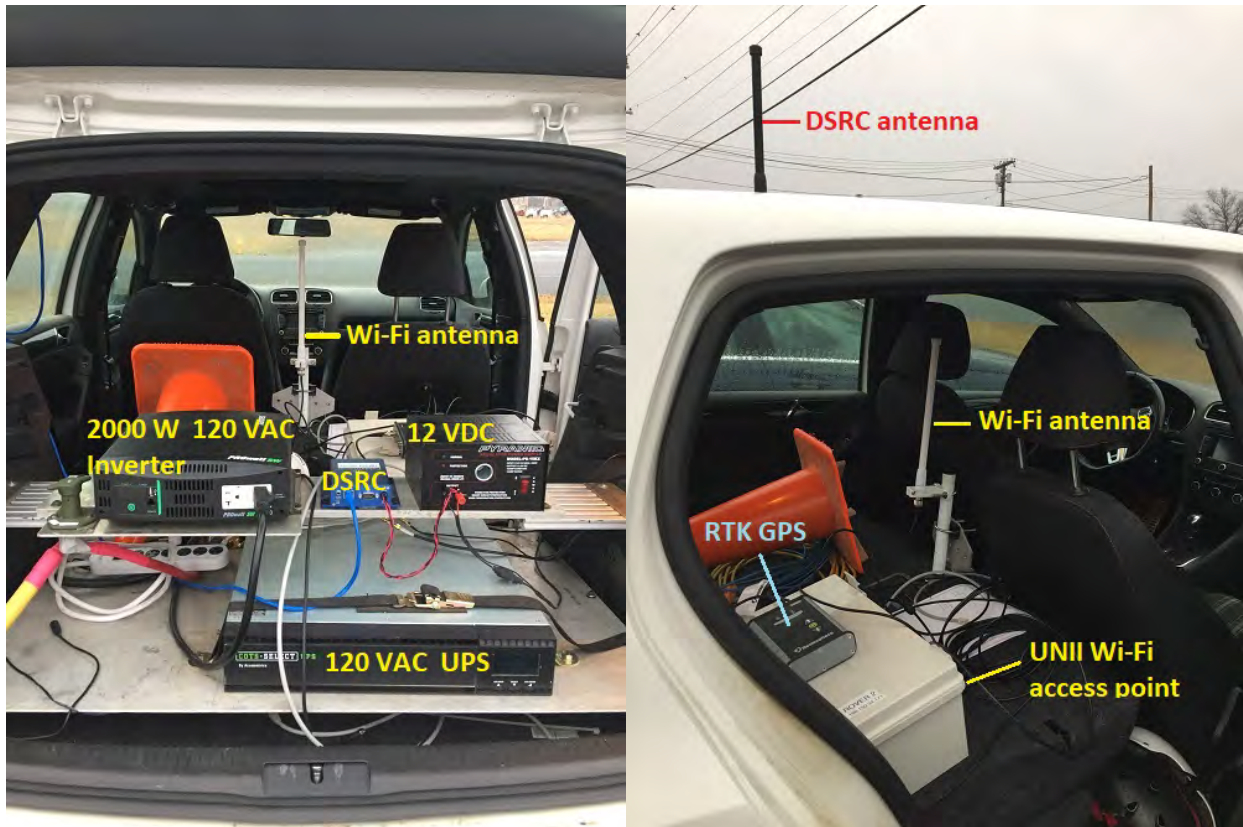


Figure 7-19: In-Vehicle Equipment

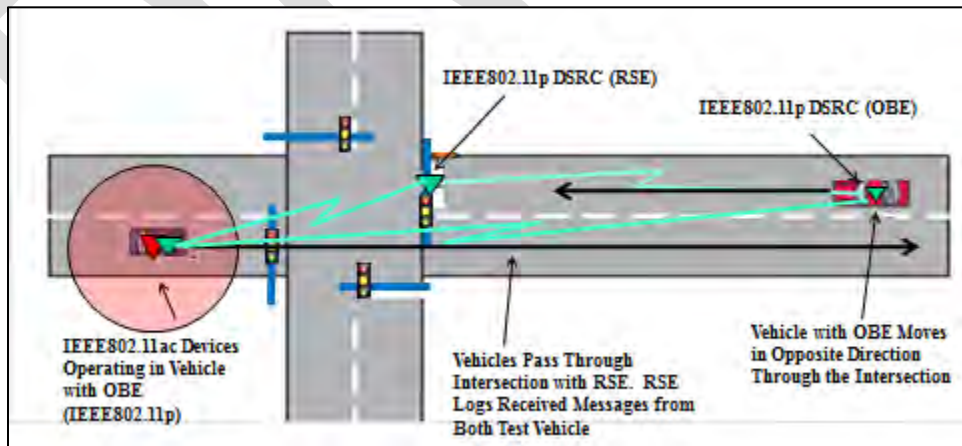


Figure 7-20: Representative example of unlicensed Devices Transmitting in a Vehicle

7.2.5 High speed approach

This activity looked at the effect of an unlicensed access point on the ability of two OBUs to communicate with an RSU, and each other, as they approach at high speed (Figure 7-21). We tested with vehicle speeds up to 50 mph, which results in a closing speed of 100 mph.

This would be the case of two vehicles driving by each other on a rural road late at night when there is no other traffic nearby. In this scenario, the density of radios is low, so signal-to-noise or energy in the band should not be an issue. Wi-Fi operation in the channel potentially interfering with BSMs in this scenario may have a greater safety impact than the more urban scenarios because the closing distance between the vehicles changes so much between BSMs. For example, with a loss of five consecutive BSMs the vehicles would close 74 feet in the half a second they were blind to each other.

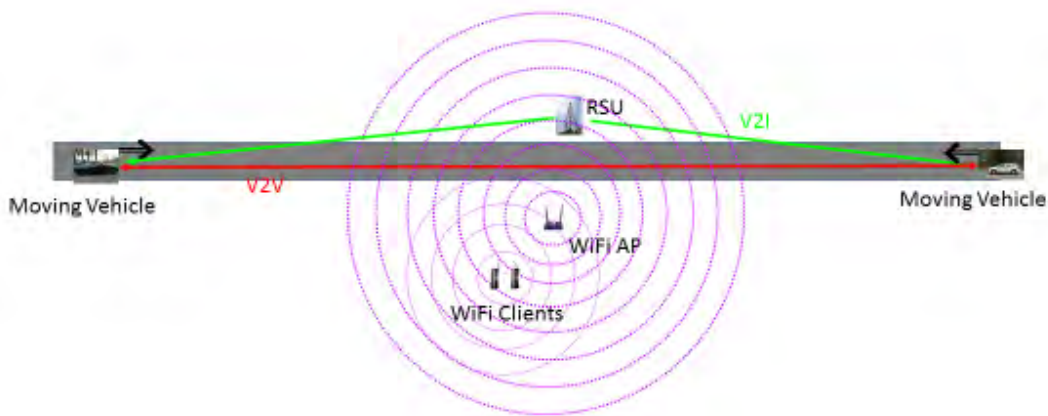


Figure 7-21. High speed V2V near access point

We positioned the RSU and the Wi-Fi access point near the center of the Perryman track. Each test vehicle was located one mile from the RSU and access point, one vehicle was located to the south and the other was located to the north. This starting distance was determined by identifying where the vehicles were out of range of each other with minimal interference from the access point. We started the vehicles at the same time. Radio operators in the vehicles communicated speed and location information between the drivers to synchronize speed so they could pass each other at the RSU. The track is marked with 0.1 mile markers. This worked well enough that we achieved this crossing to within 20 meters for most runs. See chapter 9 for results.

7.2.6 Multiple access points in a corridor

All of the other testing was device level experiments. This test was to investigate a possible deployment scenario at small scale. Similar to the first scenario, this also examines RSU-to-OBU and OBU-to-OBU communications but along a corridor with multiple unlicensed devices in operation (Figure 7-22).

We acquired 25 unlicensed devices configured to act as both access points and clients. They were to be positioned to simulate commercial, residential and personal use, as might occur along a road corridor the way unlicensed devices are typically deployed now. The results of the previous scenario testing would inform the specific positioning of the unlicensed devices for this scenario. The results could be used to validate deployment scale models developed using device level test results. We ran out of time to conduct this test when access to industry-developed, proposed UNII-4 devices became available, which initiated our Phase 2 test program. We may conduct this test in the future with our surrogate UNII-4 testbed as well as industry proposed UNII-4 Wi-Fi access points.

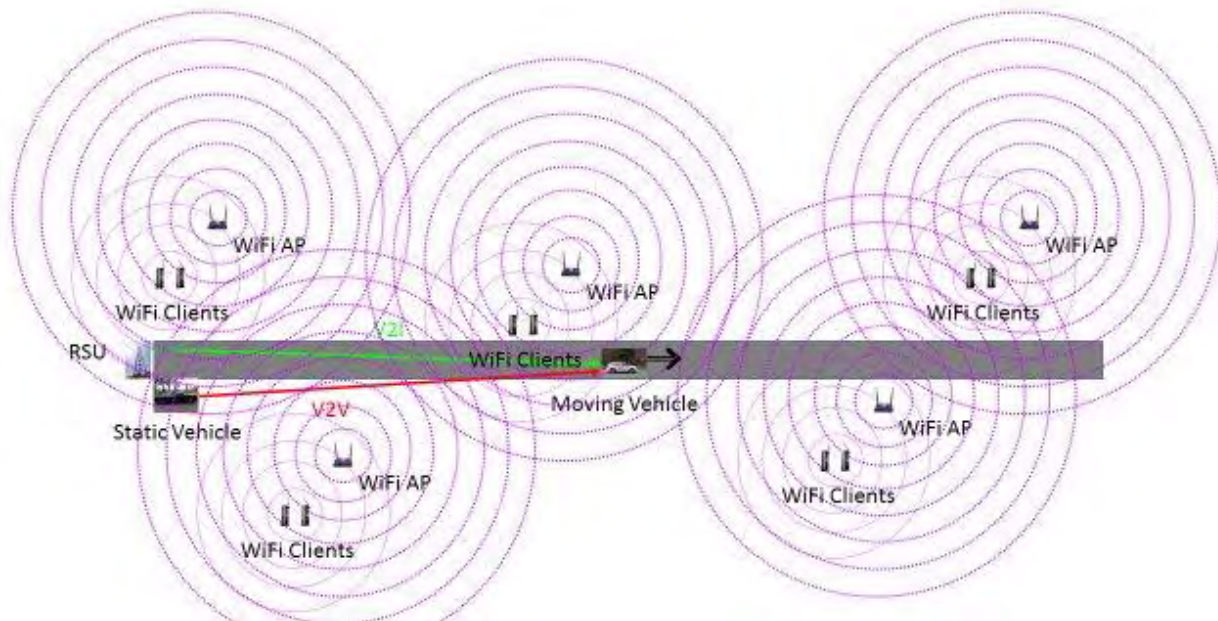


Figure 7-22. Multiple access points

In the course of making measurements for these scenarios, the work suggested other areas of discovery we did not anticipate. Moreover, opportunities to conduct tests we didn't think possible materialized that we took advantage of as well. They concern the effect of environmental conditions like weather and foliage. These additional tests and their results are described in the section 10.

7.3 DSRC Band Background Noise Level Analysis

This effort to measure ambient noise and then measure changes to the noise level in the presence of different transmitters in the same channel and in adjacent channels for a few select configurations was to look at energy injected into the band independent of modulation.

Data from these measurements established the noise levels for subsequent analysis and measured energy leaked in from adjacent bands and channels. It also was provided as an input for NTIA work on models investigating deployment scale effects.

{Section still under development}

7.4 Detectability Analysis between DSRC and U-NII-4 devices

7.4.1 Purpose

The purpose of this analysis was to see if the sensitivities of DSRC and U-NII-4 receivers are different in such a way that increases the risk of interference. The more sensitive device will hear the other and keep quiet. The less sensitive device may transmit on top of the other device when it shouldn't.

Data from this analysis would show if interference stems from different sensitivities between DSRC and unlicensed devices. It was available for use in NTIA/ITS models investigating deployment scale effects.

7.4.2 Description

We input progressively lower power signals into a DSRC receiver and a U-NII-4 receiver to determine the minimum power receivable by each. Then we similarly determined the minimum signal that will cause the CCA to suppress transmission for both types of radio. Then we operated the DSRC and U-NII-4 radios in range of each other such that the level of both the DSRC and U-NII-4 transmissions at both receivers was at a value in between the two minimum sensitivities that were determined.

Our intent was to measure channel metrics to determine if the CCA mechanism favored one type of radio over the other when they use the same EDCA (enhanced distributed channel access) parameters. But because we did not have a DSRC radio that could operate in a 20 MHz channel, we weren't able in order to see the effect the EDCA parameters on the different receiver sensitivities.

The same EDCA parameters should grant equal access. The measurement could be repeated with EDCA parameters that give priority to the DSRC communications to see if that is overwhelmed by the difference in sensitivities or can mitigate it. All of this analysis can occur in the lab.

The limited testing that we did in the lab with both radios using their default EDCA settings showed that at least with their energy-detect thresholds, meaning they sense energy but don't recognize the radio, the radios are fairly hard of hearing and have to be relatively close to be heard well enough to cause a radio to suppress its transmission.

{Section still under development}

8. Description of Data Collection, Processing and Analysis

Section 8 describes the data collection, processing, and analysis techniques used to evaluate coexistence between DSRC and U-NII devices in the 5.9 GHz safety band. Data collected and analyzed during this testing effort is used to demonstrate whether or not unlicensed devices interfere with DSRC devices in common scenarios.

Key chapter takeaways

- 1) Raw data collected from radio log files is processed using Python scripts to calculate key performance metrics and charts for interference analysis.
 - 2) The team considered different approaches for smoothing the data in order to understand the general behavior of the data as opposed to outlying readings that may not be representative of actual performance
 - 3) Definitions of key performance metrics and examples of the charts used for analysis are provided in this chapter.
-

8.1 Data Collection

Data collection and processing activities were designed to inform the analysis of whether or not unlicensed devices interfere with DSRC devices in common scenarios. Raw data was collected in the field from log files generated by the devices under test. Background noise was also measured using spectrum analyzing equipment. The log files were processed using various scripting techniques to generate the metrics under consideration for analysis.

See Section 7.2 for detail on performance metrics.

8.1.1 Baseline Data

In order to analyze the impact of unlicensed devices operating in the presence of DSRC devices, baseline tests were conducted to understand the performance of DSRC and unlicensed devices with no interference. Baseline test results provided device performance and channel quality benchmarks to compare with the results collected during interference analysis.

Performance of DSRC devices under conditions of possible interference was analyzed in comparison to the baseline results to distinguish between impacts that could be attributed to the environment, or device itself, versus impacts particular to the presence of the unlicensed device.

See section 7.1 for more detail about baseline testing.

8.1.2 Raw Data Processing

The raw data collected during each test run was processed through several Python scripts to produce outputs of plots and spreadsheets for analysis. The scripts gather relevant information from the devices to calculate performance metrics.

We obtained most of the raw data from log files generated in each DSRC radio. Table 7-2 (Chapter 7) lists the data logged by the radios and the data that was recorded manually and used for the bulk of our analysis. Each radio included a GPS receiver, which provided the location of the radio for each data record as well as a time stamp used to correlate the position with the RF measurements.

Table 8-1 lists the key performance metrics calculated using the raw data collected from the radio logs. These performance metrics were plotted against range and time to understand the potential impacts of DSRC communication relative to the distance between DSRC radios, the distance between DSRC radios and the U-NII device (interferer), and the time it took for packets to transmit between radios.

Table 8-1 Key Performance Metrics

Performance Metric	Description	Calculation
Packet Error Rate (PER)	The percentage of the packets that were transmitted but not received by the receiver	Calculated using timestamps and packet sequence numbers
Packet Completion Rate (PCR)	The percentage of the packets that were transmitted and received by the receiver	Opposite of Packet Error Rate (PER), calculated from 1 minus PER
Received Signal Strength Indicator (RSSI)	Measures the power present in a received radio signal	Measured (but used as performance metric in analysis and in Signal-to-Noise Ratio below)
Signal-to-Noise Ratio (SNR)	Measures the strength of the signal power relative to the noise level	Calculated from Received Signal Strength Indicator (RSSI) and noise measurements
Inter-packet Gap	Measures the time between packets	Calculated by comparing Transmit and Receive timestamps
Reliability	Measures the probability of dropping a certain number of packets in a row	$PAPP = 1 - (PER)^T$ where PER is Packet Error percentage, T is the timeframe in which no packets received would be considered a safety hazard, and

		t is how frequent DSRC messages are transmitted.
--	--	--

8.2 Data Analysis

Test data is used to demonstrate the amount of interference that occurs between DSRC radios in the presence of unlicensed devices. While there are several metrics that could be used to analyze radio interference, the performance metrics considered for this analysis include packet error rate (PER), signal-to-noise ratio (SNR), received signal strength (RSSI), and inter-packet gap times. These metrics were analyzed under different scenarios of range, transmit power, channel loading, and environmental settings.

The large amount of data transactions recorded every second of testing presented a challenge for analyzing the data in a meaningful way. The team considered different approaches for smoothing the data in order to understand the general behavior of the data as opposed to outlying readings that may not be representative of actual performance. This was particularly important when evaluating packet error rates. Instead of plotting the data relative to any threshold, which is yet to be specified, the data is plotted relative to a range of test PER thresholds of 5%, 25%, 75% and 95%. The team was interested in learning the distances (between the DSRC radios and interferer) at which the packet error rate crossed each of these thresholds.

The team used three approaches to fit the raw data and identify PER thresholds.

First, the team charted packet error rate relative to distance between radios and manually marked on the graph where there appeared to be a significant amount of data points that first reached the various PER thresholds of 5%, 25%, 75%, and 95%. If only one or two data points crossed one of these thresholds before returning to the general trend of the data, those points were ignored. The purpose of this manual exercise was to assign where the general trend of the data (a majority of the data points) crossed the particular threshold.

Second, the team decided to use a Savitzky-Golay filter on the data which uses different X-order equations (where X is supplied by the user) to fit the raw data. Savitzky-Golay fits adjacent subsets of points to a polynomial using the linear least squares method. From this set of adjacent localized fits, a series of coefficients is found that can be used to model the smoothed behavior of the packet error rate as it relates to distance from the UNII. The estimated PERs from the model are subsequently used to calculate where specific thresholds are crossed at 10%, 40%, 80%, and 100%. The Savitzky-Golay filter was set to fit a 5th order polynomial to subsets of nine adjacent data points as this provided the best performance in capturing the general behavior of the datasets. Figure 8-1 provides an example of how the Savitzky-Golay filter fit the data and provided color-coded markings for where the PER rate reached different thresholds.

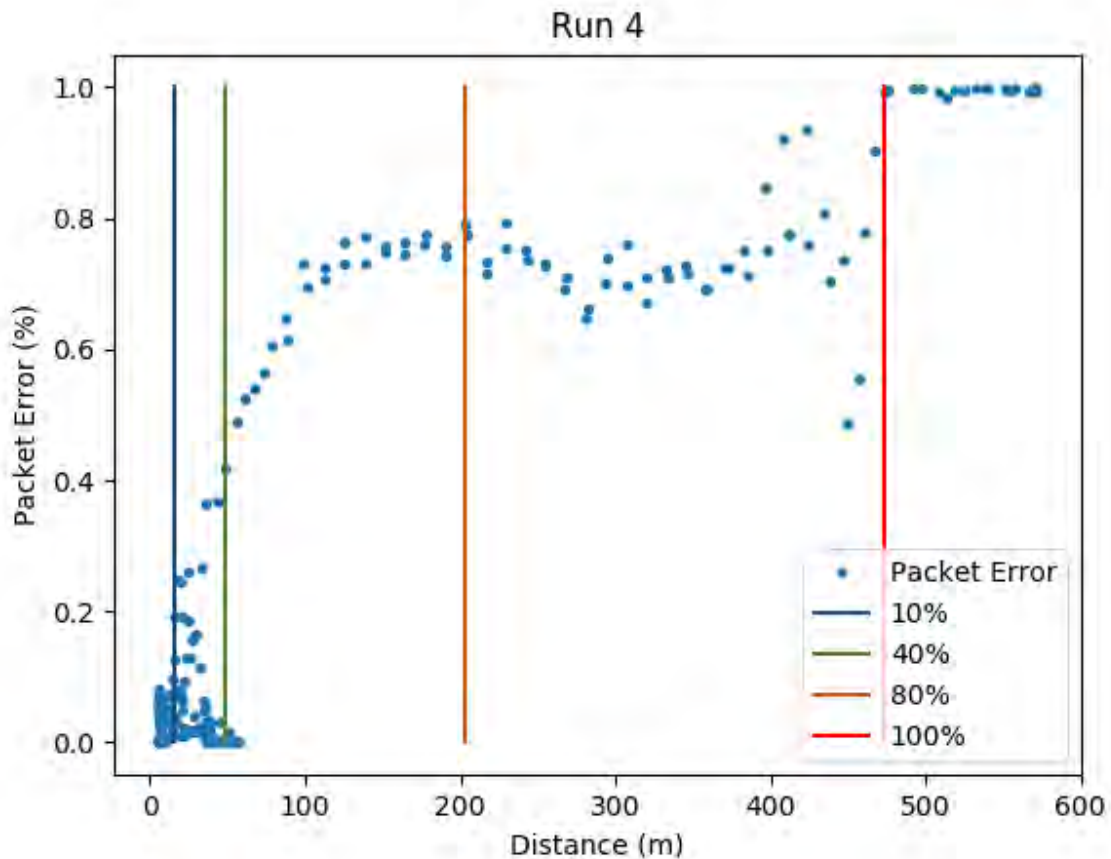


Figure 8-1: Savitzky-Golay Filtering

After experimenting with the manual and Savitzky-Golay approaches, the team decided to use a time-based rolling mean approach to fit the data and identify the PER thresholds. Since BSMs transmit every tenth of a second, the data log files are rich with time-series data for analysis. The team wanted an approach that eliminated the possibility of error from manual selection and provided a mathematical foundation for fitting the data. Upon comparing the results achieved from the rolling mean approach and the Savitzky-Golay approach, the results were very similar, as shown in Figure 8-2 (red = rolling mean, orange = Savitzky-Golay). Ultimately, it was decided that time-series data is best suited for the rolling means approach.

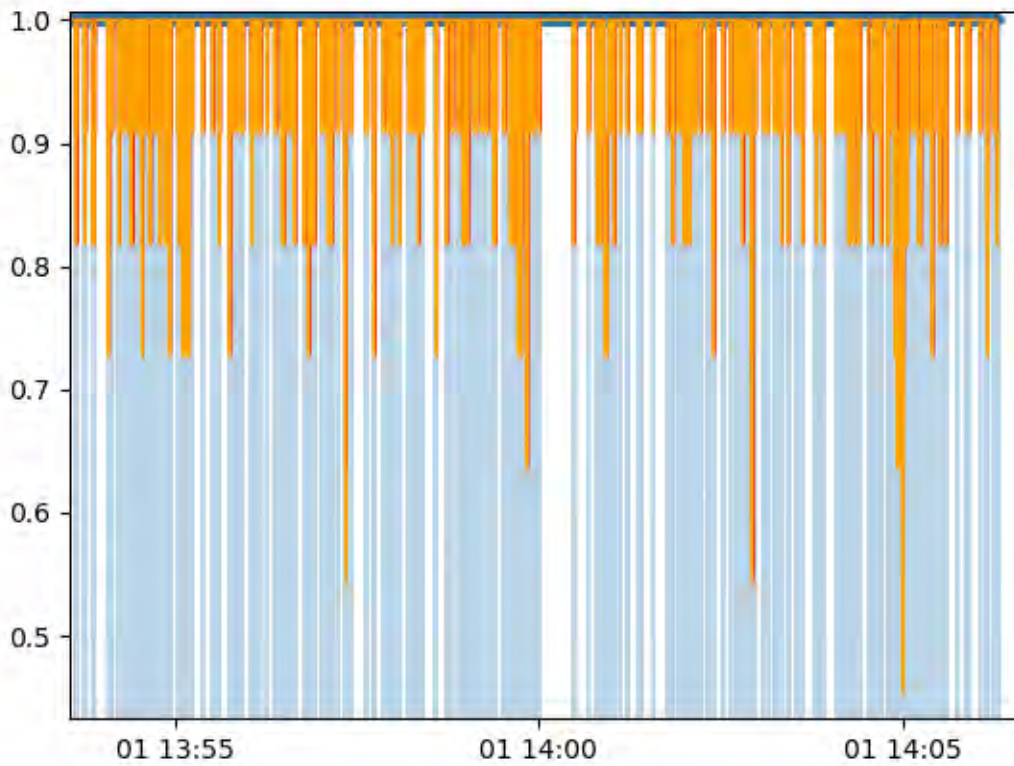


Figure 8-2: Comparison Rolling Mean vs Savitzky-Golay

The remaining sections of this chapter describe each of the plots and performance metrics used for analysis. Before describing each plot, there are a few important notes to consider:

- As mentioned earlier, in order to accommodate the large amount of data transactions recorded every second, a rolling average filter was often used for analysis. This method also filters out some of the outliers. To illustrate the approach, using a rolling average set to 500 ms with 100 ms packet transmission rate means the filter averages across the five previous points.
- The plots distinguish between incoming and outgoing paths, because each test run is designed such that a driver travels around 800 meters towards a Wi-Fi Interferer, and 800 meters back, either with another vehicle following, towards a roadside unit (RSU) sends DSRC messages, or both. When processing the raw data, the team selected the region of data points that represented incoming and outgoing paths.
- The plots used to evaluate interference are organized to show packet error rates, the inverse of packet completion rates. Instead of plotting the data relative to any threshold, which is yet to be specified, the data is plotted relative to arbitrary thresholds of 5%, 25%, 75% and 95%.

8.2.1 Received Signal Strength Indicator (RSSI) Plot

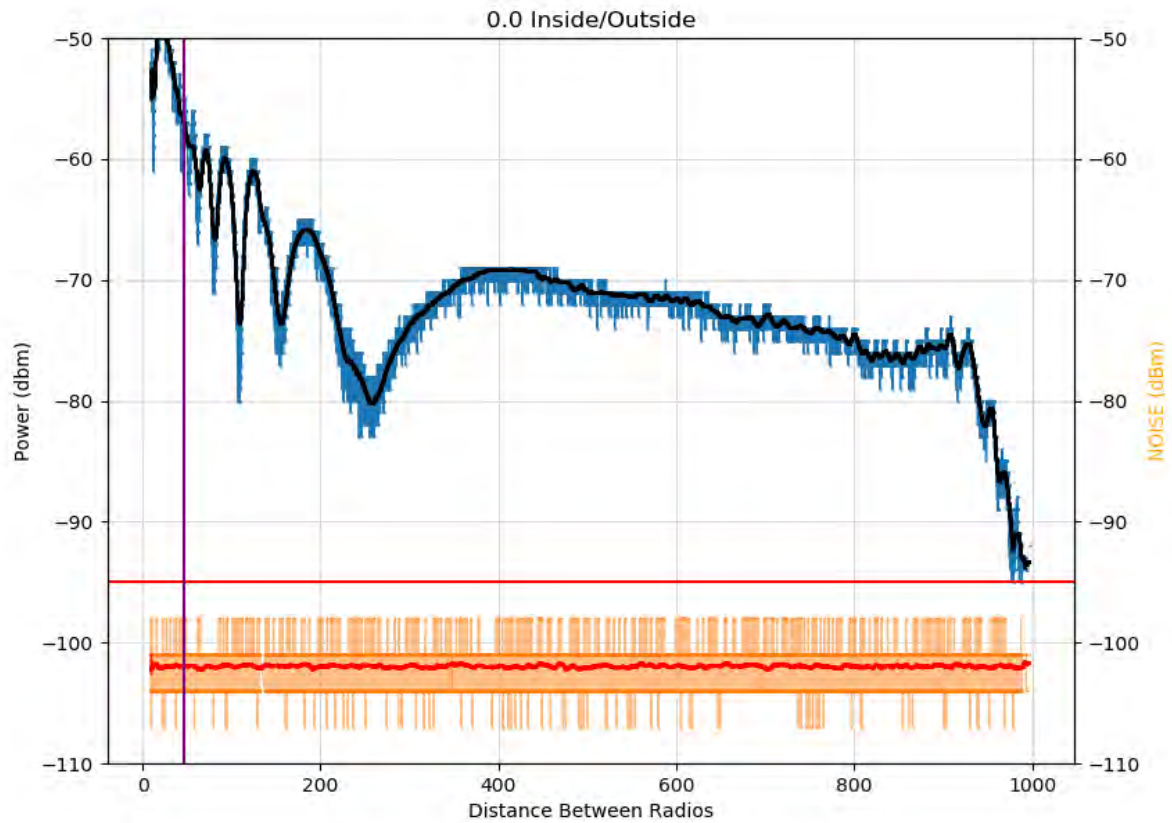


Figure 8-3: RSSI and noise plot

This Figure 8-3 shows BSM received power and noise level in relation to the distance between transmitting and receiving devices during a particular test run. The primary Y-axis displays the received power (dbm) for every BSM transmitted during a particular test run (blue line), with the black line displaying the 0.5 ms rolling average. The secondary Y-axis shows the received noise power (dbm) for each BSM (tan line), with the red line the 0.5 ms rolling average. The purple line marks the location of the Wi-Fi access point.

8.2.2 Signal to Noise Plot

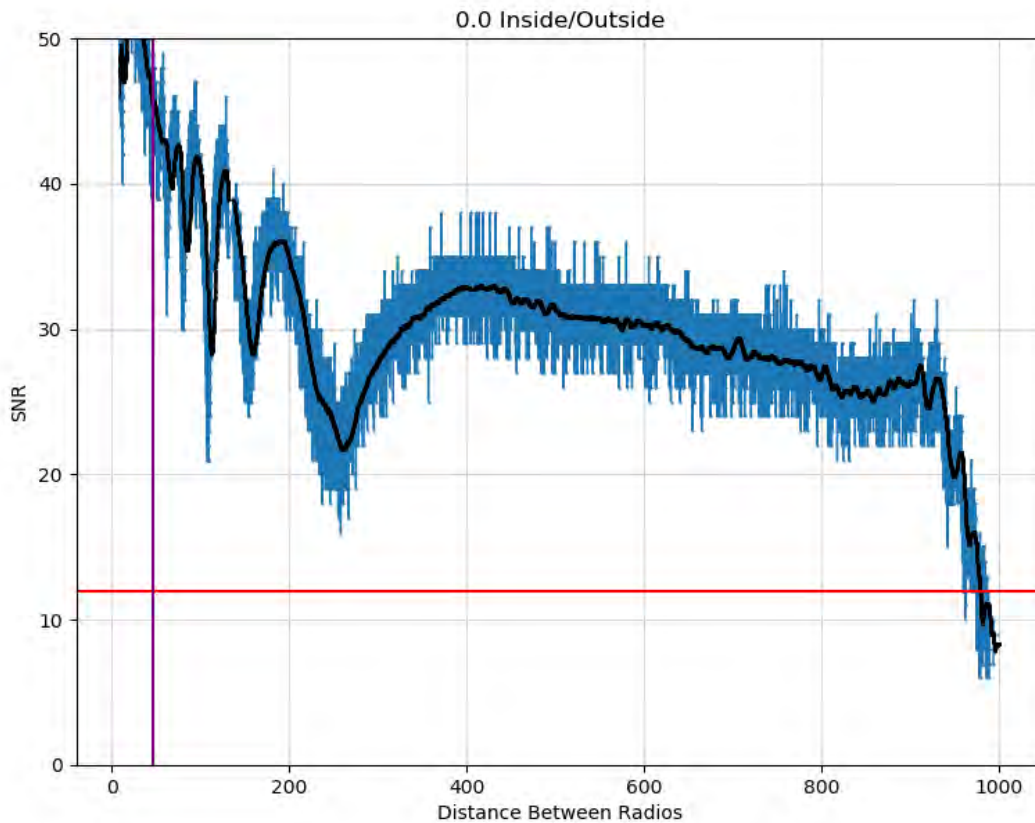


Figure 8-4: Signal-to-noise ration plot

The signal to noise plot illustrates the signal power relative to the noise power over varying distances. This plot tells how much stronger the signal is compared to the noise level; for example, when SNR=30 dBm (along the Y-axis), it means the signal is 1000 times stronger than the noise level at that particular point of distance (along the X-axis). The blue line is the signal-to-noise of every BSM, with the black line the 0.5 ms rolling average. The red line is a benchmark for the minimum SNR required for some safety applications.

8.2.3 Packet Error Rate Plot

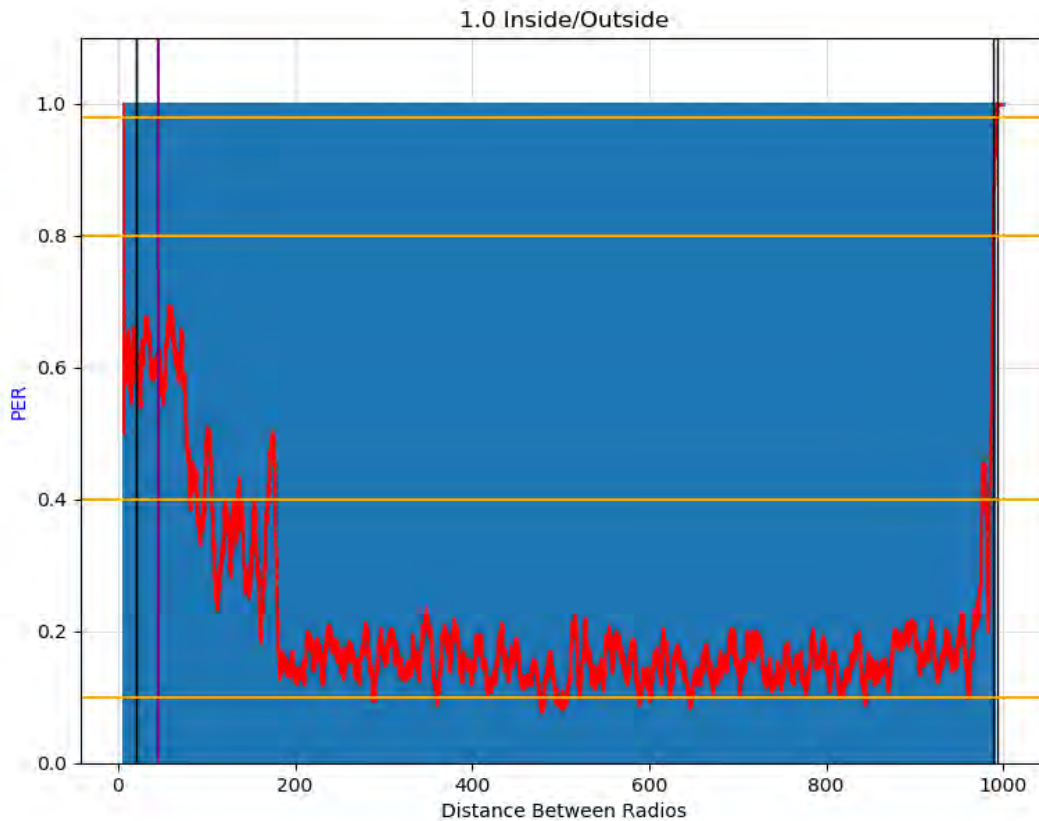


Figure 8-5: Packet error rate plot

Packet Error Rate (PER) is the percent of the packets that are transmitted but not decoded by the receiver. This means the packets are either not received or the receiver cannot decode the signal because other energy comes in at the same time. The blue line in the plot above indicates when a BSM was **not** received; the white line indicates when the BSM was received. The lines are thicker than the time of a BSM (0.5 ms) so a mix of white and blue lines may look like solid blue. The red line shows the 0.5 ms rolling average. The orange line is a benchmark for the 300-meter safety radius around the vehicle.

Packet error rate is calculated using timestamps and packet sequence numbers from the transmit and receive logs of the communicating DSRC radios under test. If a packet was transmitted and not received or decoded by the receiving device, a packet error exists. The packet error rate on the graph represents the 0.5 ms rolling average relative to the distance between the DSRC radios.

8.2.4 Gap Plot

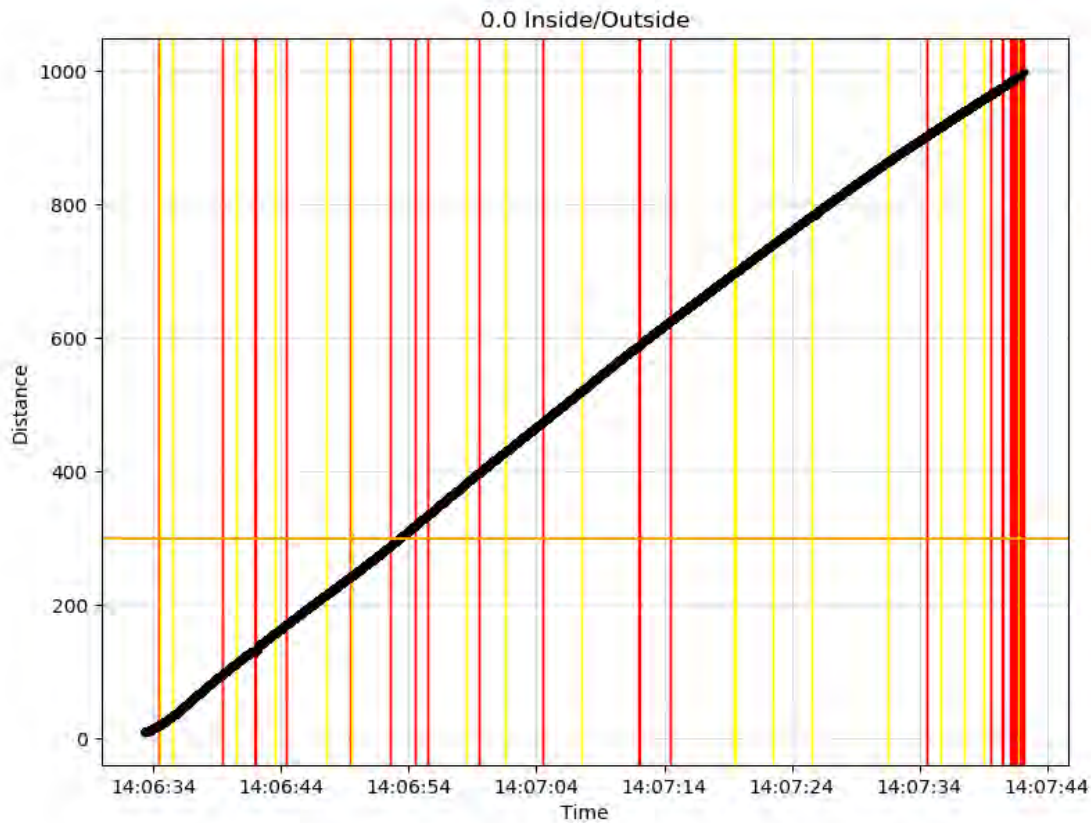


Figure 8-6: Gap Plot

The gap plot is used to understand the statistical distribution of the packet error rate. For example, if the packet error was 50%, but evenly distributed, there would be no colored lines. Half of the packets could be lost without safety implications. But if there is a clumping in the packet error rate, bigger gaps would have implications to safety even with a relatively smaller packet error rate (for example, 25% instead of 50%).

The black line shows the range of the moving vehicle relative to static DSRC radio at each point in time (y-axis = Distance, x-axis = Time). The colored lines indicate the length of the gap between consecutive BSMS: yellow indicates a gap of 300-500 ms; red indicates gaps between BSMS greater than 500 ms (which would present a safety issue). The gap plot shows where safety-critical gaps exist and how the packet error rate is distributed over time.

8.2.5 Cumulative Gap Plot

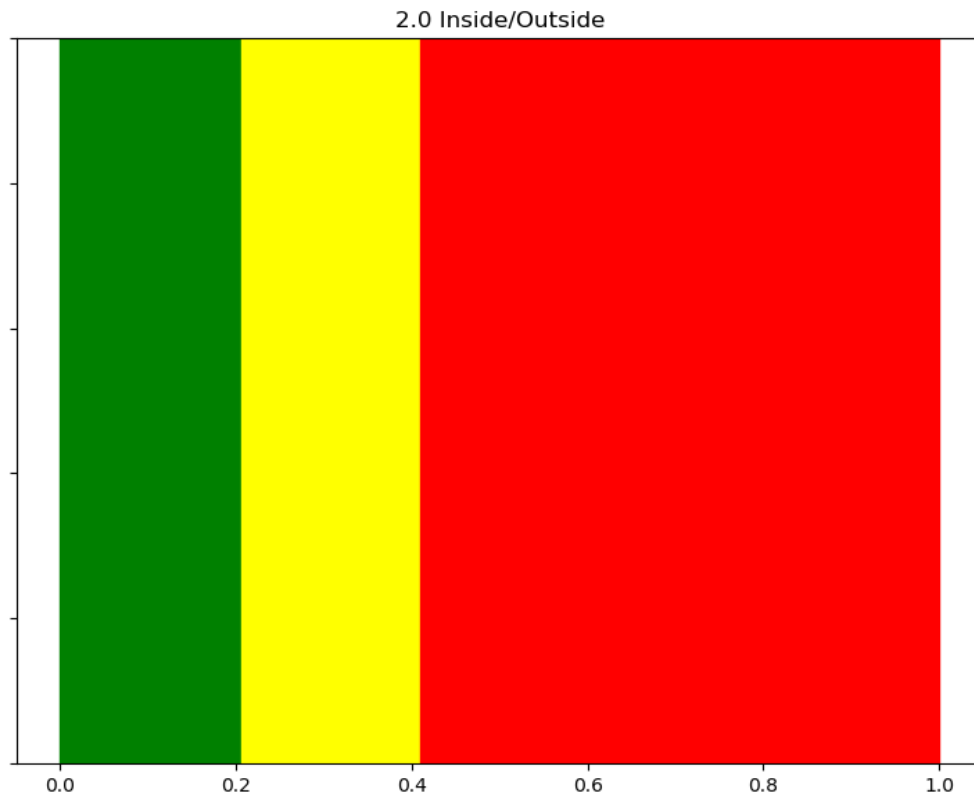


Figure 8-7: Cumulative Gap Plot

The cumulative gap plot builds off the gap plot described in section 8.2.4. Figure 8-7 shows the fraction of time during a particular run that consecutive BSMs were missed. Assuming a 10 Hz transmission rate: green if no more than two consecutive BSMs were missed; yellow if 3-5 consecutive BSMs were missed; and red if more than 5 consecutive BSMs were missed. The cumulative gap plot is created by counting the amount of packet errors within the specified buckets of time.

1.0 Inside/Outside



Figure 8-8: PER Mapped onto Geography

Figure 8-8 is a visual representation of packet error rate over a satellite image of the test track. The image in Figure 8-8 represents the outbound leg of a single test run. The color of the line indicates the packet error rate at that particular geographical point: magenta means all packets were received (PER = 0); aqua means no packets were received (PER = 100%); and the colors in-between magenta and aqua are scaled relative to the packet error rate between 0-100 percent. The static DSRC and U-NII interferer are set-up near the red dot on the image. You can see that the packet error rate is highest (aqua/blue) when the mobile vehicle is closest to the interferer; and the packet error rate improves (color changing to magenta) as the mobile vehicle moves away from the interferer. It goes to aqua suddenly as the signal is blocked by the trees. We truncated the data for analysis at this point.

{Remainder of section still under development}

DRAFT

9. Test Results

{Section still under development}

We present test results in several specific sections. The first section describes interference at the DSRC receiver, namely packet collision. Within this section we examine how interference changed as we separately varied DSRC power, Wi-Fi power, Wi-Fi traffic load, Wi-Fi packet size, and the distribution (regularity versus randomness) of the Wi-Fi traffic. The following section presents data on DSRC packet suppression at the transmitter due to Wi-Fi signals. The next section looks at the impact of interference on signal-to-noise. The section after that examines interference from energy leaked from Wi-Fi that is not in the same channel. This two-part section presents lab measurements and theory followed by our field measurements of adjacent channel interference. Lastly, we present our results when the W-Fi was inside a vehicle.

Key chapter takeaways

- 1) Increasing DSRC power 100 times in the face of high power Wi-Fi pushes the range of complete breakdown from 350 meters to 100 meters from the access point, but interference is unacceptable for safety communications 500 meters from the access point in all cases.
- 2) Wi-Fi interferes with DSRC 500 meters away even at the lowest Wi-Fi power tested (EIRP = 5 dBm). So regulating Wi-Fi power will not mitigate interference to DSRC.
- 3) The Wi-Fi traffic load is the strongest factor that controls interference to DSRC. Load of 3% may not affect safety, 20% load is untenable in any circumstance. The acceptability of Wi-Fi loading from 5-15% depends on the sensitivity of individual safety apps.
- 4) Transmitting the same volume of data in smaller Wi-Fi frame sizes made the interference worse. A 5% traffic load sent in 300 byte packets caused worse interference than a 10% load sent in 1400 byte packets.
- 5) We tested with two Wi-Fi traffic distributions. Periodic for precise control and Poisson for the random behavior more typical of real Wi-Fi traffic. Our data allows the scaling of results using Periodic distributions to estimate results for more realistic Wi-Fi traffic.
- 6) At high Wi-Fi traffic loads (20-30%), where interference is high, the Poisson PERs were roughly 15% less than Periodic. At moderate traffic loads (10-20%) Poisson PERs were roughly 10% less than Periodic. There was very little difference for lower traffic loads.

- 7) Interference results obtained using Periodic Wi-Fi traffic that are untenable, are still generally untenable when reduced 10% to approximate actual Wi-Fi traffic.
-

9.1 Baseline Measurements

We show representative baseline measurements and some of the discoveries made during the baseline measurements in this section.

9.1.1 Ground-bounce nulls

The first thing to know about RF measurements is that the receiving antenna receives RF energy from more than the direct ray from the transmit antenna. Some of the transmitted energy going in different directions reflects off objects in the environment and enters the receiving antenna as well. This energy takes a longer path than the straight line between the two antennas. That means it arrives a bit later in time so will be out of phase with the direct energy. When the path length distance causes the reflected energy to be 180 degrees out of phase it can cancel the direct energy.

Usually the reflected ray is smaller than the direct ray so though it subtracts from the signal, creating narrow nulls or dips in the received signal, it usually does not cancel it completely. We tested at Zone 1 and Perryman because there are very few objects near the range to cause this kind of multipath reflection.

The exception is the ray that bounces off the ground, which is always present. That energy is like the reflected headlights that you see at night as a car approaches you in the rain on wet pavement. You can see the headlights directly but you also see their reflection in the pavement in front of the oncoming car. Figure 9-1 illustrates the geometry used to construct a 2-ray model to predict ground-bounce nulls.

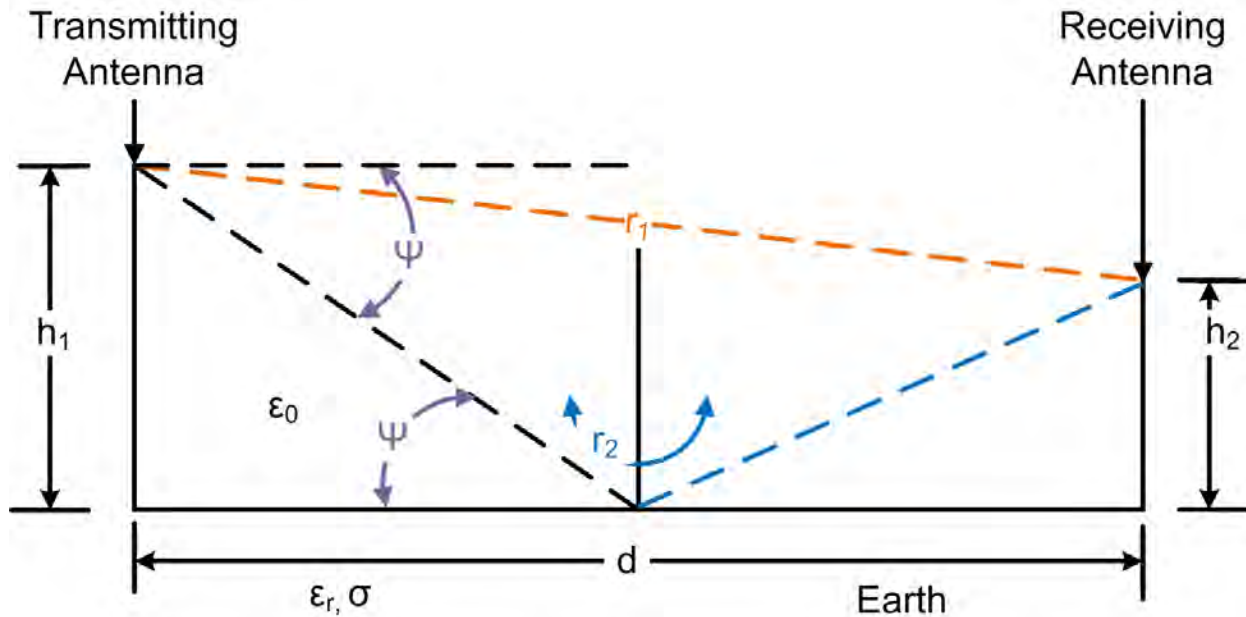


Figure 9-1. Heights, Angles and Distances for the Two-Ray Model

DSRC communications are most vulnerable in the ground-bounce null. Conversely, when in the ground-bounce null of the Wi-Fi interferer, the DSRC link gets a break from the interference.

The location and depth of the null depends on the heights of the two antennas, the range between them, and frequency of the signal, as well as the electromagnetic permittivity and conductivity of the surface.

Figure 9-2 is the plot of a 2-ray model for equal height V2V communications for three different vehicle heights and two frequencies at opposite ends of the safety band. There are three observations to make from this plot. First, the power can dip by 20 dB in a null, which means dropping to a value 100 times less before coming up again. These nulls are superimposed on the $1/\text{range-squared}$ decrease in power you would expect and see in free space. Second, the change in frequency across the entire safety band is too small to have any noticeable effect on where the nulls occur and how deep they are. Third, as the vehicle heights decrease, the location of the nulls move closer to the vehicle that isn't moving (distance zero). For example, the deepest null for two vehicle antennas two meters high occurs at a distance of 155 meters. The same null when the height is 1.57 meters occurs around 97 meters.

Received Signal vs Distance for $P_t = 20$ dBm and Equal Antenna Heights $\sigma = 0.005$ $\epsilon = 6.0$
 A Comparison of Channel 172 and 184 Null Positions OBUOBUHTRYE2.plt

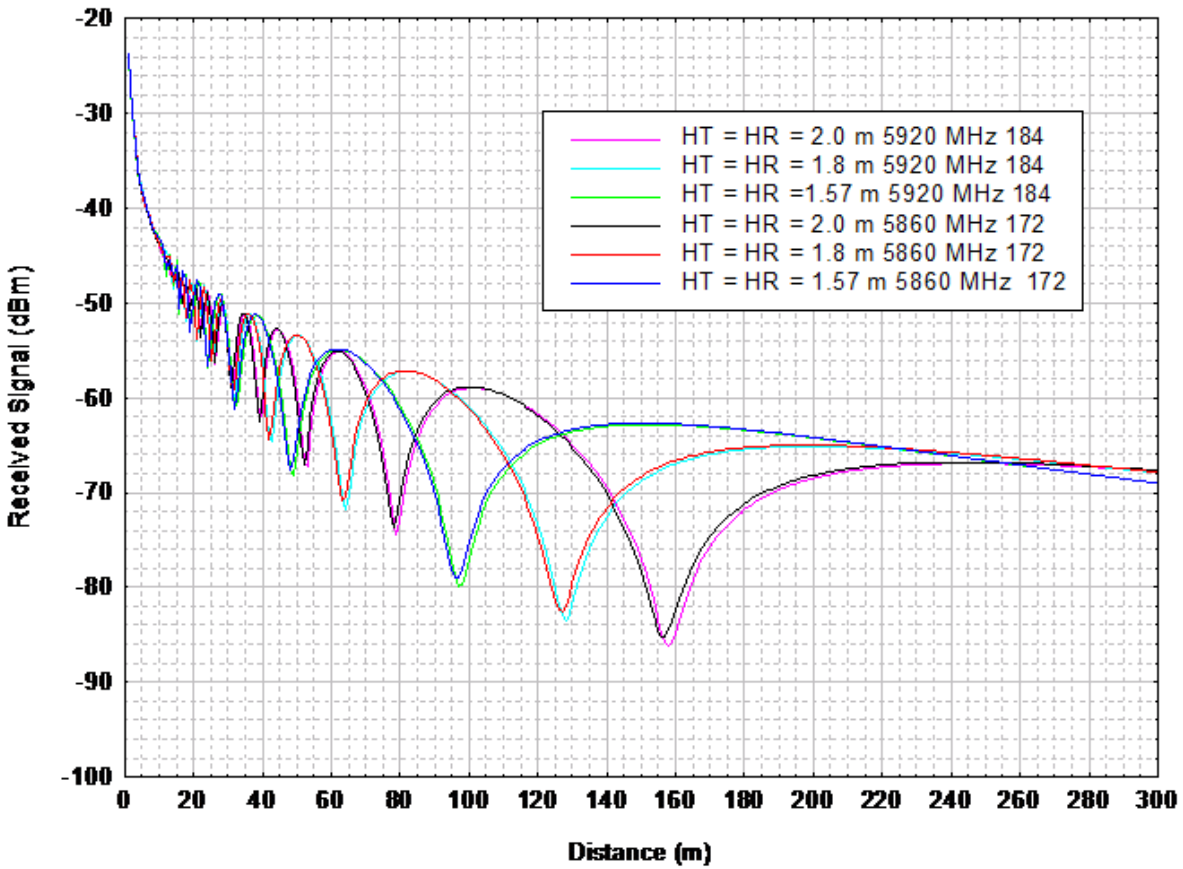


Figure 9-2. Two-Ray Model showing RSSI null positions as a function of vehicle height and frequency (V2V case)

Figure 9-3 provides similar data for the I2V case. It plots RSSI given an RSU antenna height of 5.5 meters, which is the 18 feet we used in our testing, to a selection of different vehicle heights. As in the V2V case, you can see that as the vehicle antenna height decreases, the nulls move closer to the RSU.

Received Signal vs Distance for $P_t = 20$ dBm and $H_T = 5.5$ m $\Sigma = 0.005$ $\epsilon = 6.0$ $f = 5860$ MHz
 RSUOBUVR2.plt

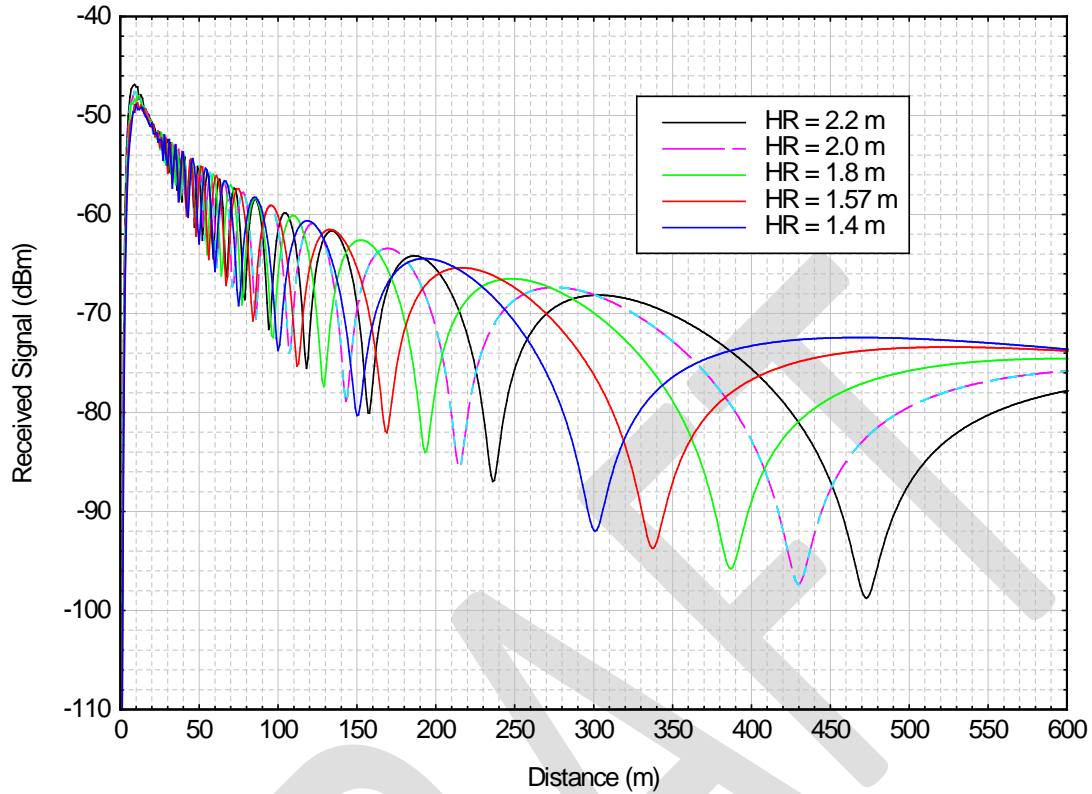


Figure 9-3. Two-Ray Model showing RSSI null positions from an RSU as a function of vehicle height (I2V case)

To be complete, Figure 9-4 is a similar plot to Figure 9-2 but for higher infrastructure antennas, essentially RSU to RSU. If you look at the green line, you can see that the effect of raising the second antenna up from 1.4 meters (blue line in Figure 9-3) to 5.5 meters (green line in Figure 9-4) moves the deep null from around 300 meters to roughly 1180 meters. So reducing antenna height moves the nulls to the left and increasing antenna height moves the nulls to the right.

Received Signal vs Distance for $P_t = 20$ dBm Equal Antenna Heights $\sigma = 0.005$ Epsilon = 6.0 $f = 5860$ MHz
 RSURSUHTHRE2.plt

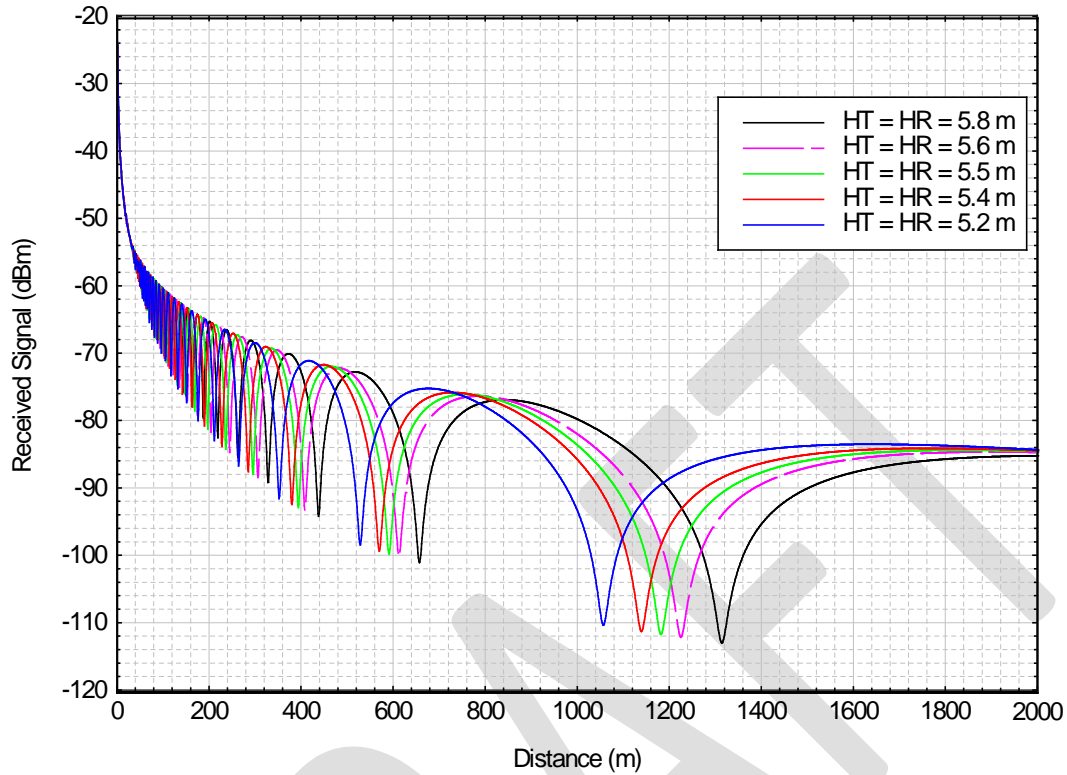


Figure 9-4. Two-Ray Model showing RSSI null positions as a function of equal RSU antenna heights (I2I case)

Back to the V2I case, because this isn't apparent in the previous figures, Figure 9-5 shows clearly over a long range that the nulls cease after a deepest and widest null and then the RSSI decreases along the inverse range-squared law expected in free space.

Received Power vs Distance for $h_t = 5.5$ m $h_r = 1.5$ m for Average Ground at 5865 MHz

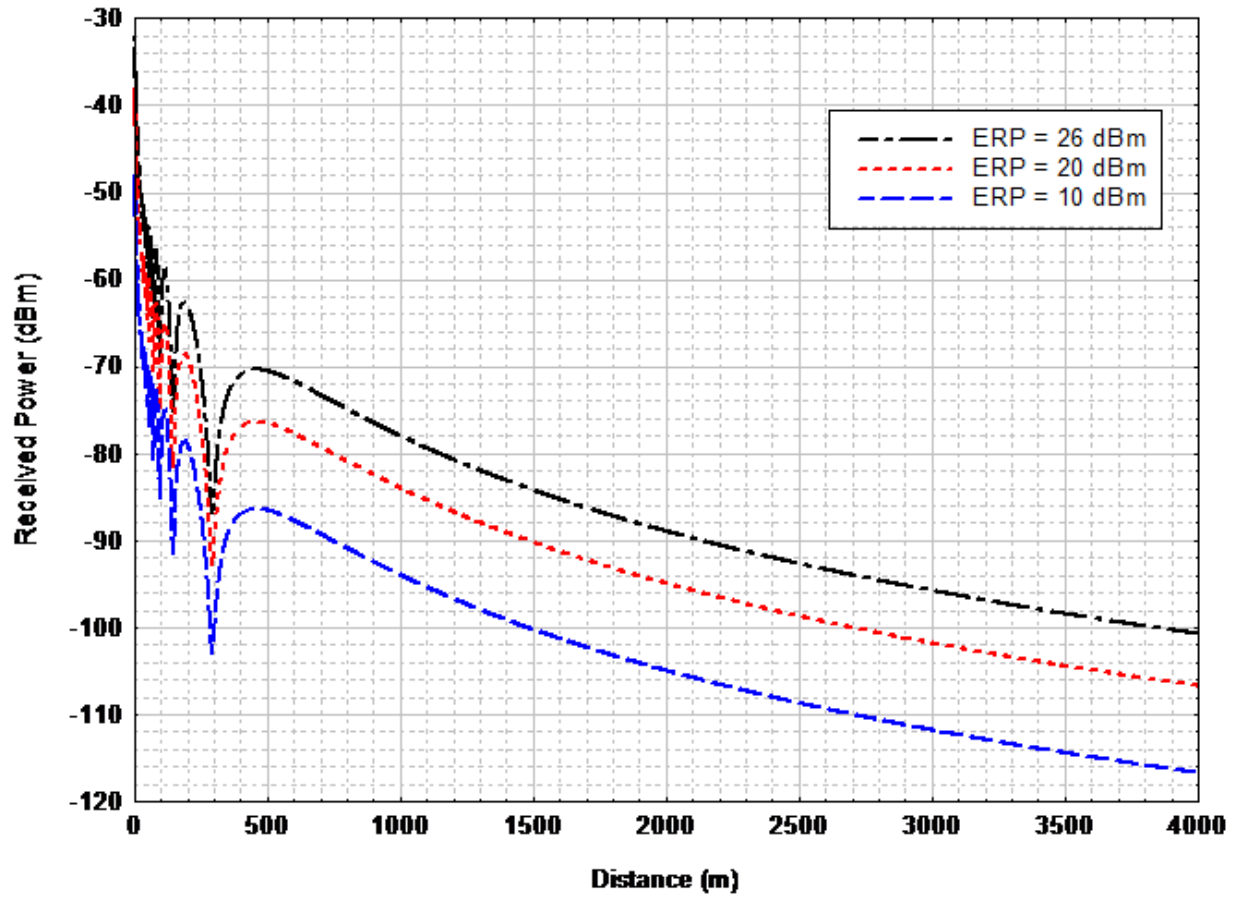


Figure 9-5. Two-Ray Model showing RSSI I2V null positions over a long range

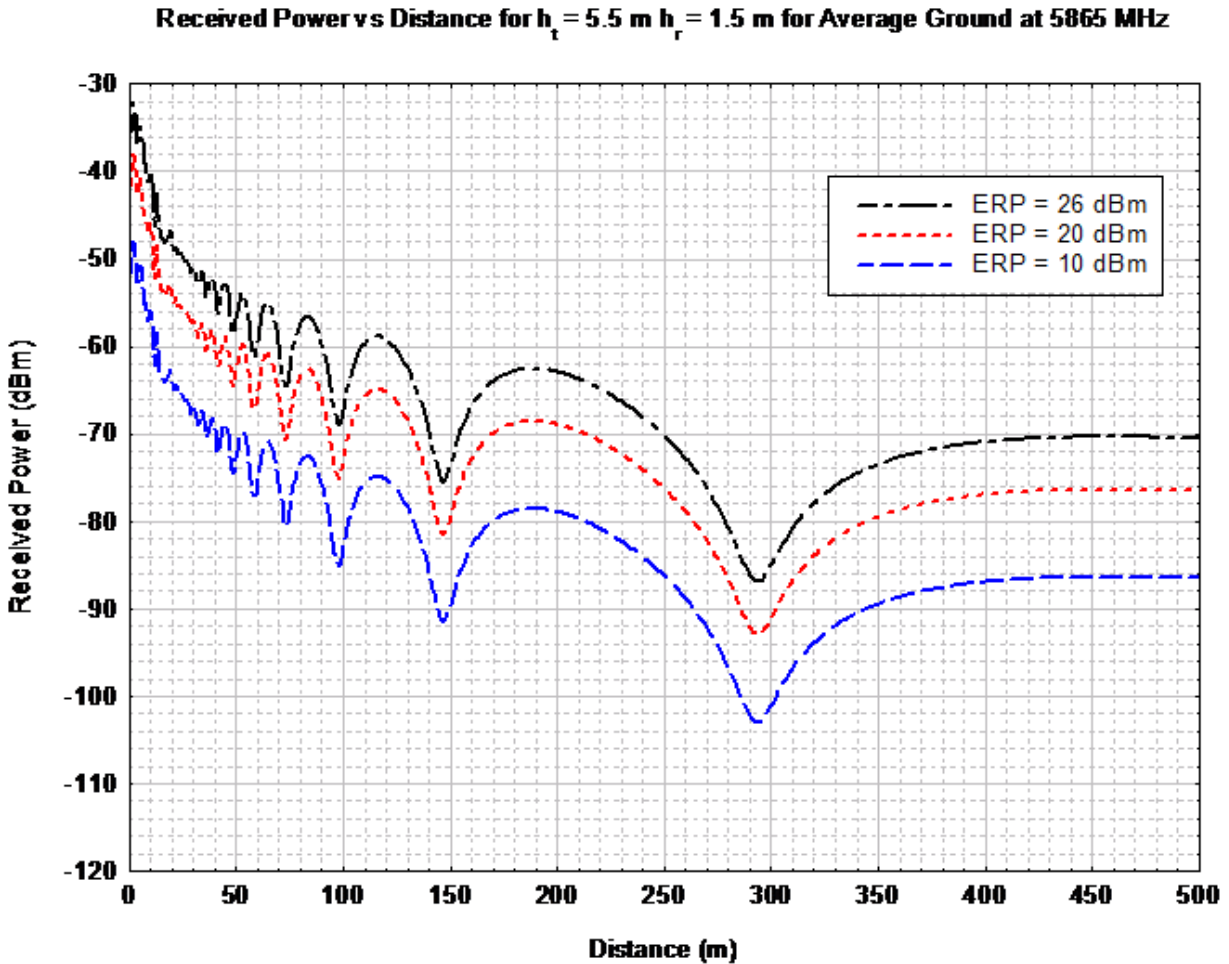
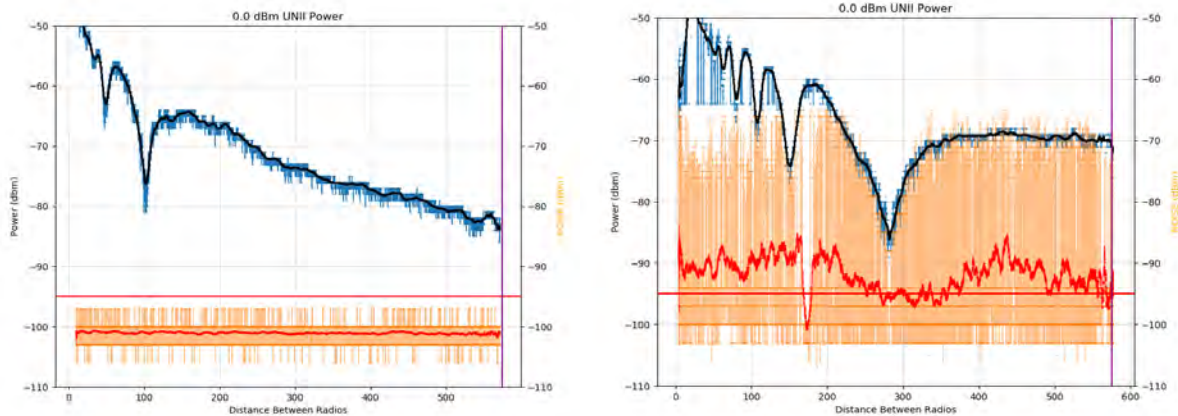


Figure 9-6. Two-Ray Model showing RSSI I2V null positions over a short range

Figure 9-6 is a close up plot of Figure 9-5 to compare with our measured baseline data in Figure 9-7. Note that the deep null just shy of 300 meters in the measured data of Figure 9-7 agrees well with the null predicted to be at 290 meters in the model data of Figure 9-6.

Similarly, the V2V null around 100 meters in Figure 9-7 agrees well with the null at 97 meters for the OBU antenna height of 1.57 meters in Figure 9-2. The antenna heights in the vehicles used in this test was indeed 1.57 meters.

In addition, Figure 9-7 shows the effect of raising antenna from 5 to 18 feet high in our field measurements. You can see that the peak ground-bounce null shifted from 100 meters to 300 meters downrange. Also, note the greater DSRC signal power at the interferer (purple line) with the higher antenna. Zone 1 was clearly not long enough to out run the radios but the much higher I2V power foreshadows the much longer range for I2V when we could out run the radios and measure maximum range at the Perryman facility.



DSRC Antenna Height 5 feet (V2V)

18 feet (I2V)

Figure 9-7. Effect of DSRC antenna elevation

Source: 20170821 Vary UNII pwr half ms avg --was UNII_powerV3.xlsx, Tab: Compare Rx at 5 vs 18 ft

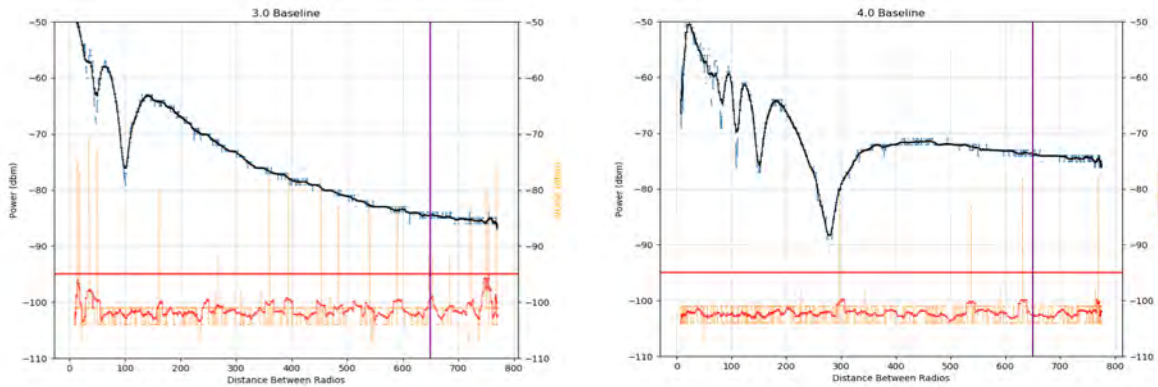
We provided a detailed treatment of the ground-bounce null here for two specific reasons. One, the plots above provide a useful reference for those that don't have the means to program such a model. Two, though the ground-bounce null is familiar to RF and microwave engineers it is apparently not familiar to many working in the wireless and automotive industries that have published results or made claims about radio performance in the safety band.

Signal strength plots over distance that do not show these nulls indicate a flaw in data collection, data processing, data presentation, or perhaps fundamental validity. The data is either wrong or it has been averaged so much, over such a long time period to make the data appear smooth that it conceals phenomena that are large enough to have an impact on safety.

The ground-bounce nulls are so predictable that we used them as a quick check that basic systems were working properly with our daily baseline run.

9.1.2 Zone I Baseline

The following figures convey baseline data taken at Zone 1 during our 40-radio tests in November 2017. These were tests where we ran 40 separate DSRC radios each transmitting at 10 Hz, to compare with the same tests using a single DSRC radio transmitting at 400 Hz. The data below is from the end of day baseline runs for both V2V and I2V.



EIRP=25 dBm:

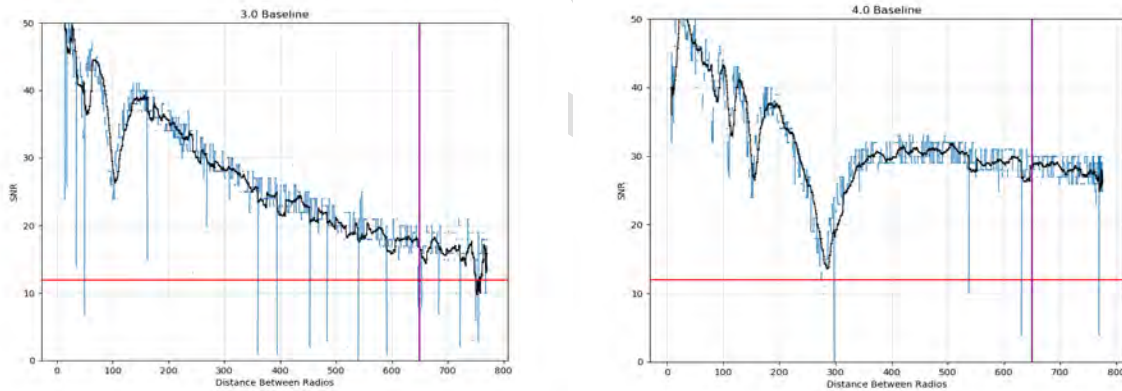
V2V

I2V

Figure 9-8. Typical Zone 1 Baseline RSSI and noise level

Source: 20171101 Vary UNII Load V2b --was exl_report_20171101 (version 1).xlsb [Autosaved], Tab: Baselines

Key points to note in Figures 9-8 and 9-9: First, the predictable nulls that immediately distinguish V2V from I2V data. Second, the noise level is around -102 dBm, which is below the -95 dBm receiver sensitivity benchmark. That benchmark is the level generally specified by DSRC radio vendors for detecting DSRC data frames. Third, the SNR stays above the 12 dB benchmark, even in the deep nulls. That benchmark indicates the minimum SNR needed by safety applications. These plots show a clean predictable RF environment.



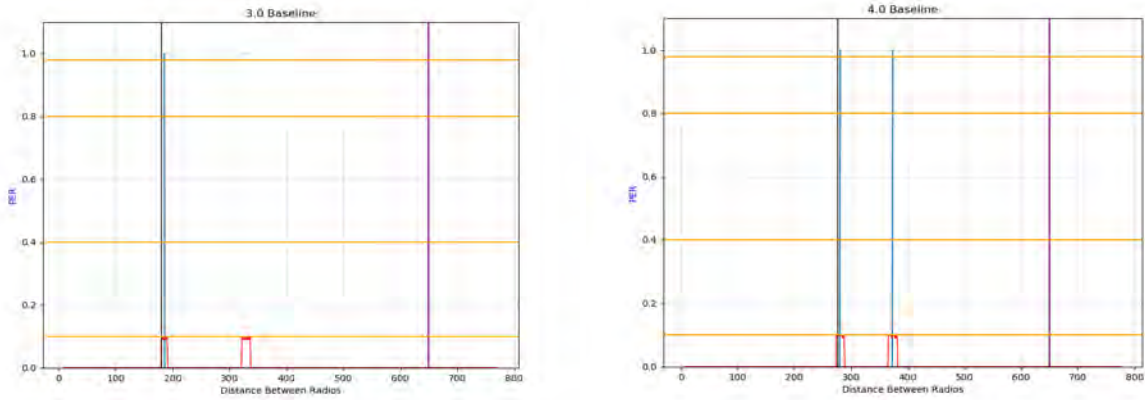
EIRP=25 dBm:

V2V

I2V

Figure 9-9. Typical Zone 1 Baseline Signal-to-Noise ratio (SNR)

Source: 20171101 Vary UNII Load V2b --was exl_report_20171101 (version 1).xlsb [Autosaved], Tab: Baselines



EIRP=25 dBm:

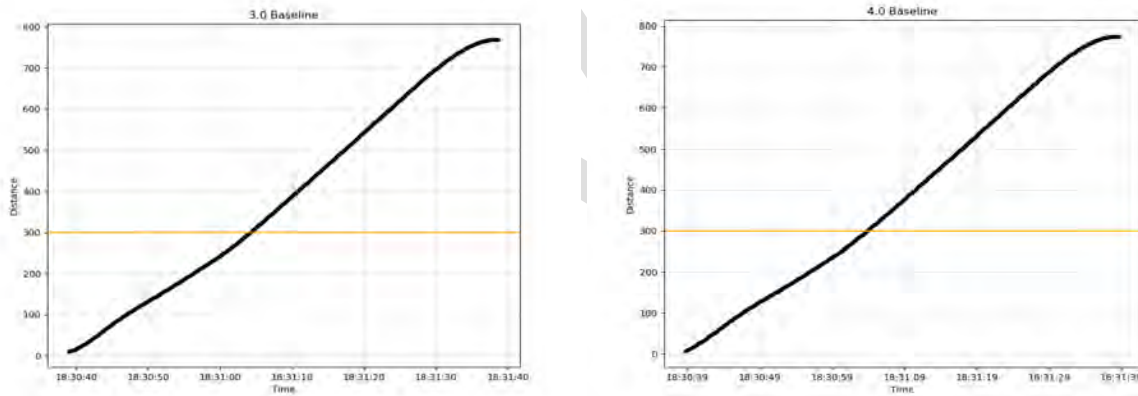
V2V

I2V

Figure 9-10. Typical Zone 1 Baseline Packet Error Rate (PER)

Source: 20171101 Vary UNII Load V2b --was exl_report_20171101 (version 1).xlsb [Autosaved], Tab: Baselines

The rare sporadic missed packets in Figure 9-VVV10 and the lack of gaps larger than 0.3s in Figures 9-11 and 9-12 show extremely little environmental interference. This would indicate that any missed packets in the interference testing that day would have been due to the UNII Wi-Fi device.



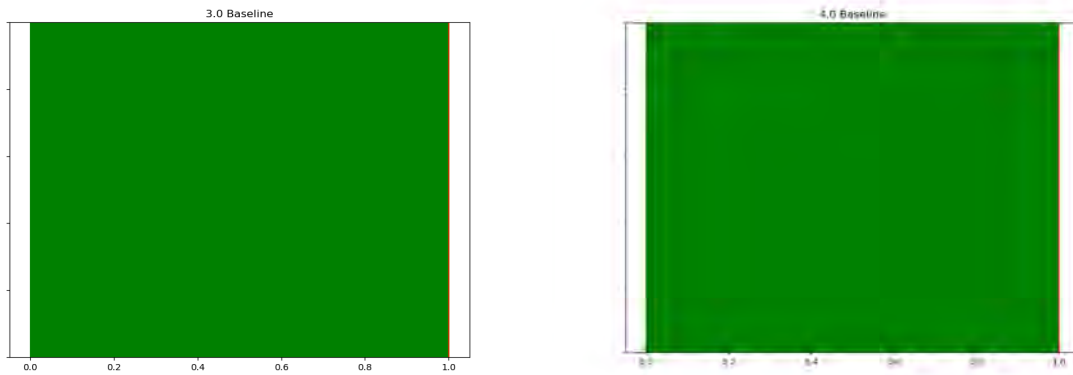
EIRP=25 dBm:

V2V

I2V

Figure 9-11. Typical Zone 1 Baseline gap analysis

Source: 20171101 Vary UNII Load V2b --was exl_report_20171101 (version 1).xlsb [Autosaved], Tab: Baselines



EIRP=25 dBm:

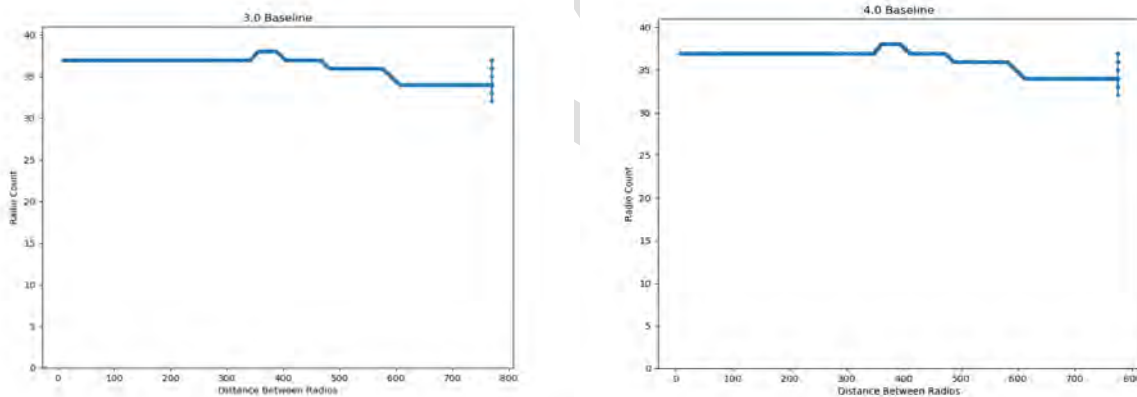
V2V

I2V

Figure 9-12. Typical Zone 1 Baseline cumulative gap analysis

Source: 20171101 Vary UNII Load V2b --was exl_report_20171101 (version 1).xlsb [Autosaved], Tab: Baselines

Figure 9-13 shows a count of radio MAC addresses received as the test vehicle drove down range. It shows that a few radios dropped out of view near the end of the range. For all other tests than the 40 radio tests, this plot shows a straight line at one radio. Therefore, we will not include it in the baseline data for the other test tracks.



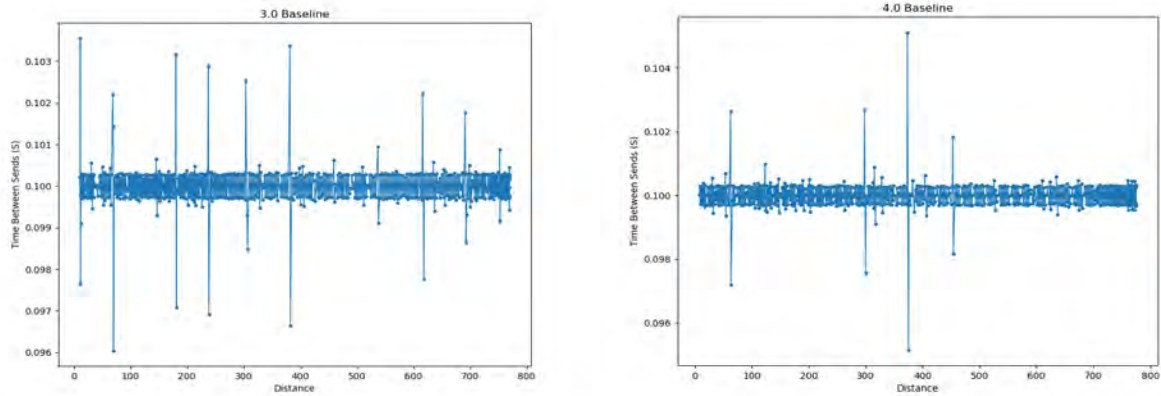
EIRP=25 dBm:

V2V

I2V

Figure 9-13. Typical Zone 1 Baseline radio count

Source: 20171101 Vary UNII Load V2b --was exl_report_20171101 (version 1).xlsb [Autosaved], Tab: Baselines



EIRP=25 dBm:

V2V

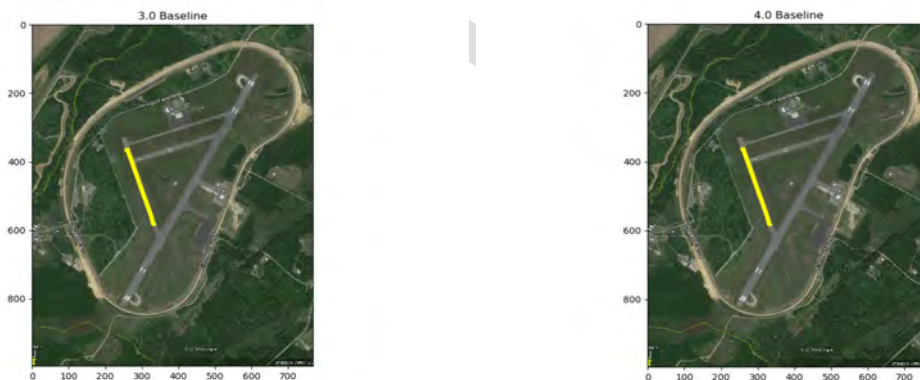
I2V

Figure 9-14. Typical Zone 1 Baseline transmit latency (time between sends)

Source: 20171101 Vary UNII Load V2b --was exl_report_20171101 (version 1).xlsb [Autosaved], Tab: Baselines

Figure 9-14 tells us how repeatable the signal transmission is. You can see that almost all packets are sent within 0.3 ms of the 100 ms period of a 10 Hz signal. Moreover, the worst outliers less than 5 ms late or early. Almost all of our data fell within this range so we will not repeat the baseline transmit latency plots for the other facilities as well.

Figure 9-15 shows PER mapped across Zone 1. This is the old color scale where yellow indicates zero PER. Locations where enough packets were lost would appear red for 100% loss.



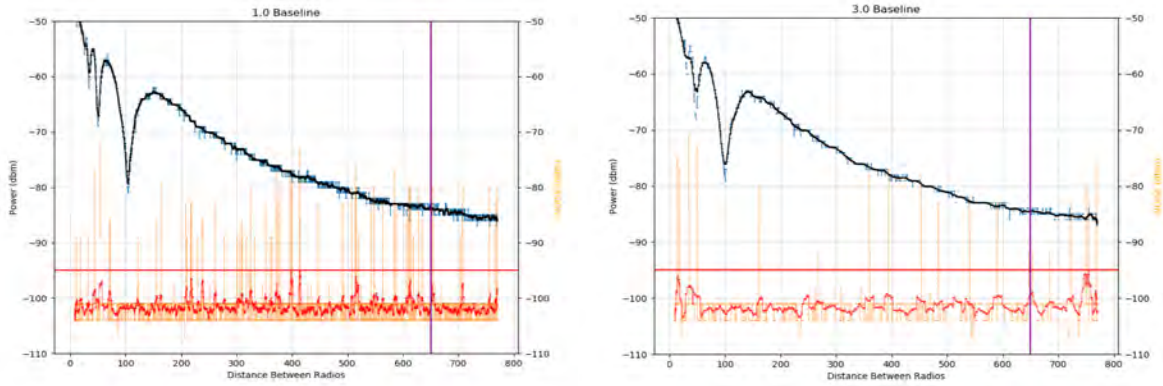
EIRP=25 dBm:

V2V

I2V

Figure 9-15. Typical Zone 1 Baseline geographical distribution of PER

Source: 20171101 Vary UNII Load V2b --was exl_report_20171101 (version 1).xlsb [Autosaved], Tab: Baselines



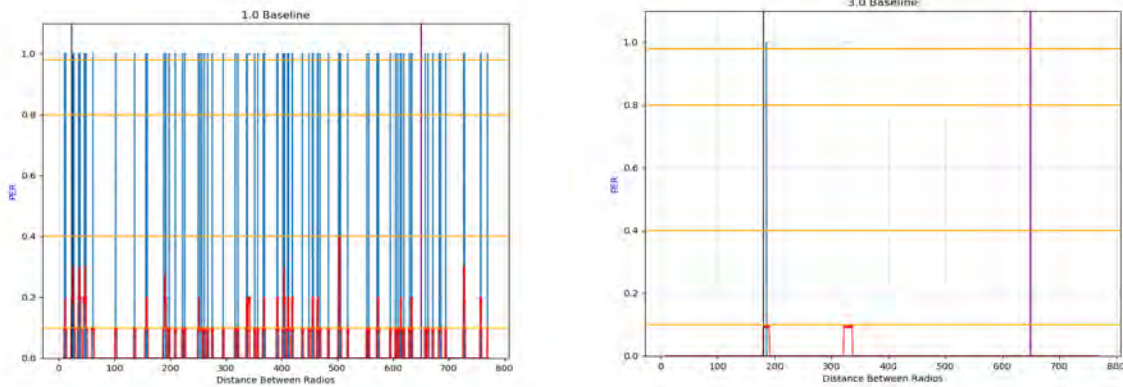
EIRP=25 dBm: First baseline

Last baseline

Figure 9-16. Unclean Zone 1 V2V Baseline RSSI and noise level

Source: 20171101 Vary UNII Load V2b --was exl_report_20171101 (version 1).xlsb [Autosaved], Tab: Baselines

Not all baseline runs were pristine. Figure 9-16 shows that something was adding noise to the equipment in the environment at the beginning of the day when we started testing (left) compared to the end of the day when we ceased (right). Figure 9-17 shows that this noise knocked some packets out but Figure 9-18 shows that only once did it knock out packets for more than half a second and only twice for 0.3-0.5 seconds. The 0.5+ second gap occurs at 500 meters where the average PER briefly peaked at 40%

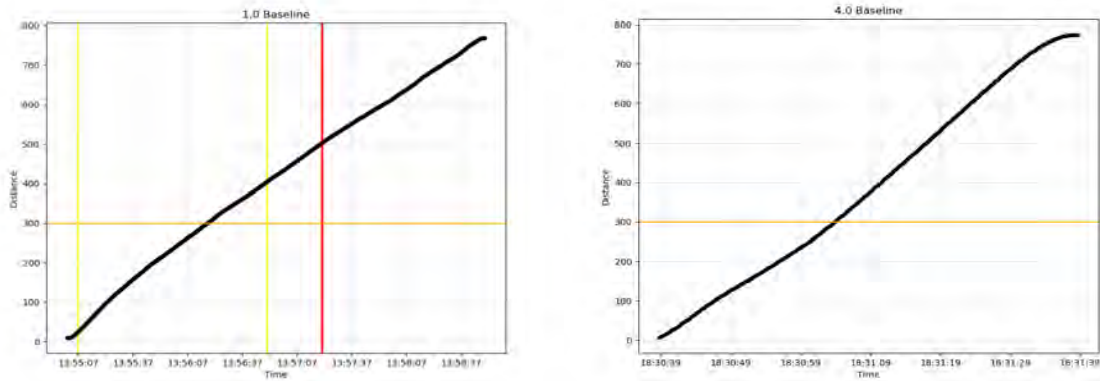


EIRP=25 dBm: First baseline

Last baseline

Figure 9-17. Unclean Zone 1 V2V Baseline PER

Source: 20171101 Vary UNII Load V2b --was exl_report_20171101 (version 1).xlsb [Autosaved], Tab: Baselines



EIRP=25 dBm:

V2V

I2V

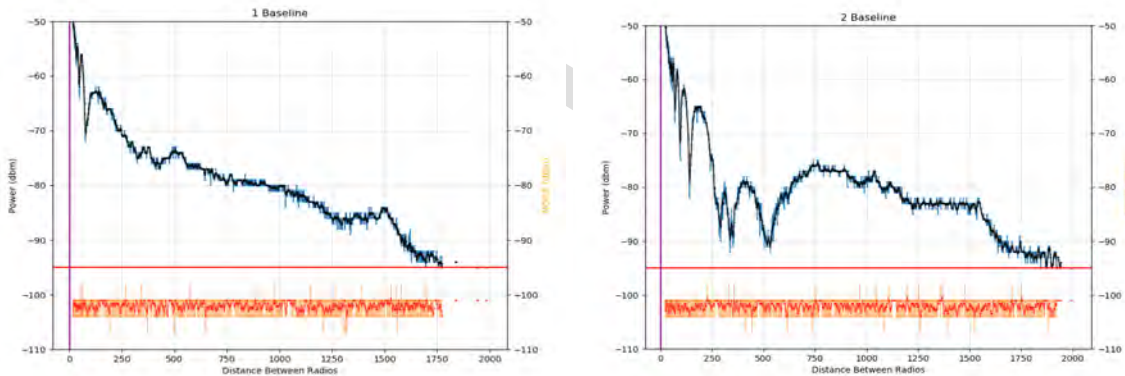
Figure 9-18. Unclean Zone 1 Baseline gap analysis

Source: 20171101 Vary UNII Load V2b --was exl_report_20171101 (version 1).xlsb [Autosaved], Tab: Baselines

On this day, the baseline measurement exposed this small amount of noise when we started but it was not enough to mask interference from the UNII device, which was far more substantial.

9.1.3 Perryman Baseline

The following figures are representative of baseline runs at the Perryman facility. This data was taken March 22, 2019 before beginning adjacent channel interference testing.



EIRP=25 dBm:

V2V

I2V

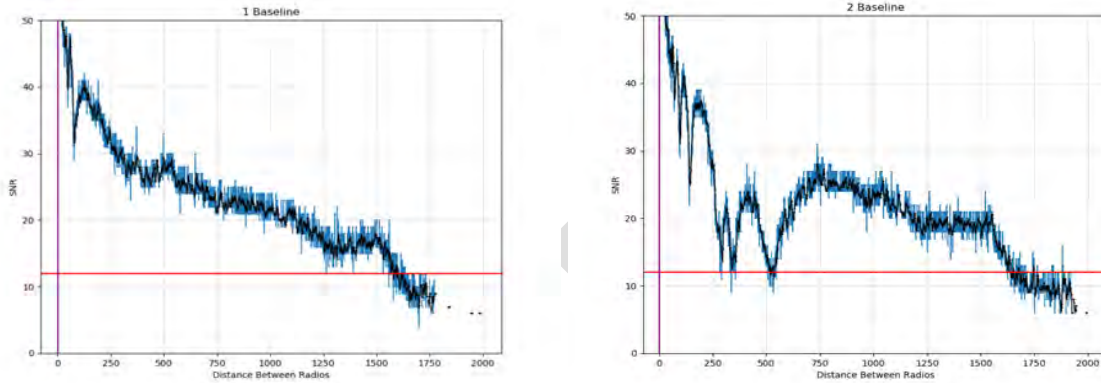
Figure 9-19. Typical Perryman Baseline RSSI and noise level

Source: 20190322 Adj channel tests away --was exl_report_away.xlsx, Tab: Baselines

Figure 9-19 shows the same -102 dBm noise level as Zone 1. Because the range is much longer than Zone 1 we can see the range of the radios. The V2V signal disappears at roughly 1750 meters and the I2V signal goes out to 2000 meters this day because we turned around the mobile DSRC in that proximity. On other days, both signals and especially the I2V signal propagated even further. Both V2V

and I2V signals remained above the -95 dBm receiver sensitivity benchmark the entire run. The shape of the RSSI curves is not as close to the ideal modelled RSSI because the elevation of the track varies slightly (by a few feet over the course of a mile).

Figure 9-20 shows that if the SNR benchmark matters the range for safety apps will be somewhat less than indicated by the RSSI plots.



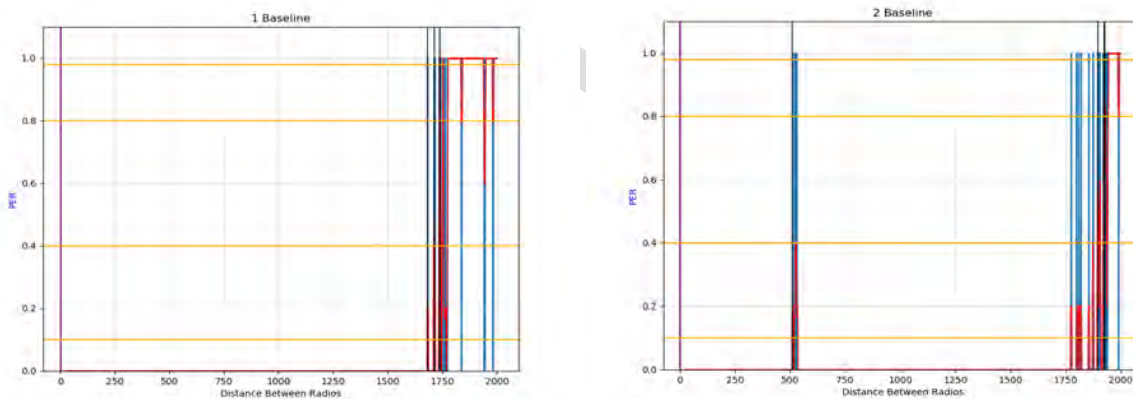
EIRP=25 dBm:

V2V

I2V

Figure 9-20. Typical Perryman Baseline Signal-to-Noise ratio (SNR)

Source: 20190322 Adj channel tests away --was exl_report_away.xlsx, Tab: Baselines



EIRP=25 dBm:

V2V

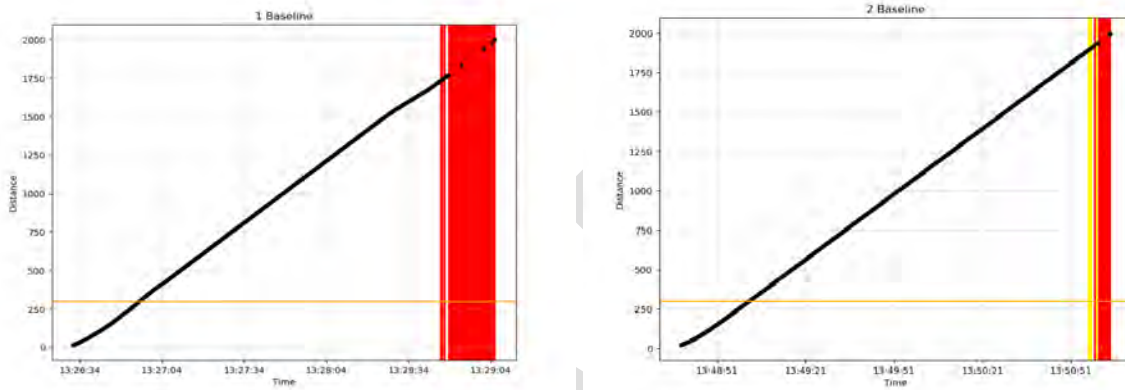
I2V

Figure 9-21. Typical Perryman Baseline Packet Error Rate (PER)

Source: 20190322 Adj channel tests away --was exl_report_away.xlsx, Tab: Baselines

Figure 9-21 shows that packet error rate is zero to the ranges shown in the RSSI plot, so not effected by SNR. The one exception occurs around 500 meters for the I2V measurement. You can see the PER jump to 40% for a very short space at the deepest null and where the SNR drops to a minimum. This is environmental interference and needs to be subtracted from the interference data or accounted for in the analysis to avoid attributing these missed packets to the Wi-Fi.

Figure 9-22 shows no significant gaps that would affect safety until the signal was lost at the end of the run. That means the lost packets at 500 meters did not create a gap in the BSM transmissions longer than 300 ms.



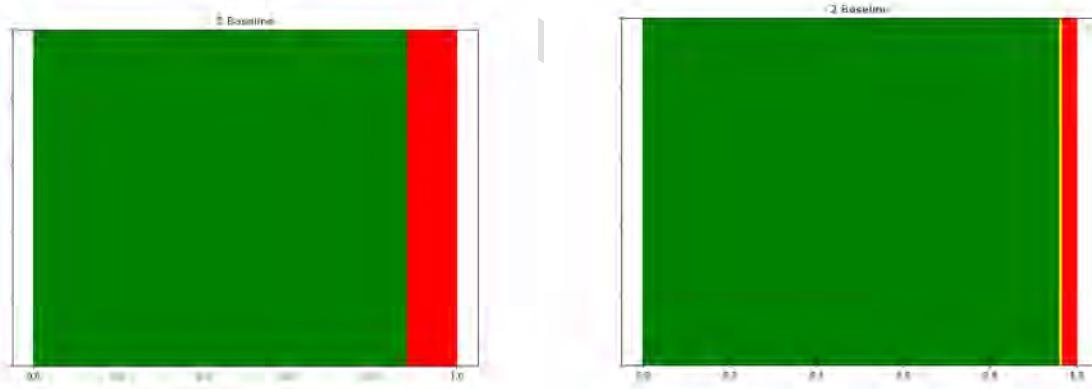
EIRP=25 dBm:

V2V

I2V

Figure 9-22. Typical Perryman Baseline gap analysis

Source: 20190322 Adj channel tests away --was exl_report_away.xlsx, Tab: Baselines



EIRP=25 dBm:

V2V

I2V

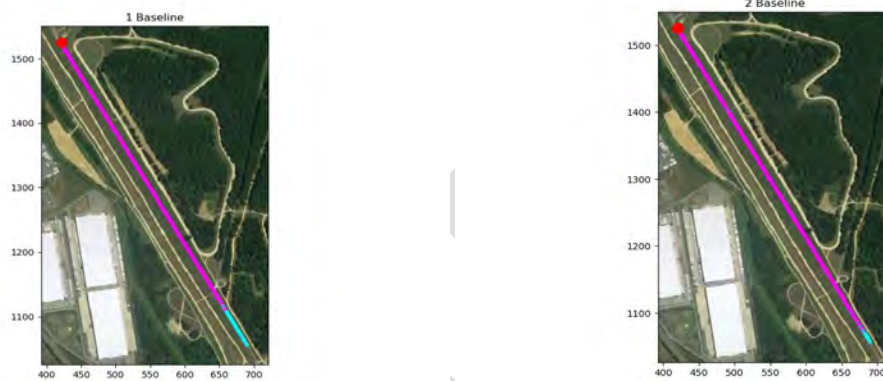
Figure 9-23. Typical Perryman Baseline cumulative gap analysis

Source: 20190322 Adj channel tests away --was exl_report_away.xlsx, Tab: Baselines

The roughly 12 percent of the V2V side of Figure 9-23 that is red shows that there were gaps greater than half a second that much of the run. That is because when this leg was selected for processing, it

included that much of the time after the signal was lost at the end. None of that 12 percent gap time has to do with interference. The same is true for the I2V side as the tiny PER that shows up around 500 meters was too brief to show up here.

Figure 9-24 conveys intuitively where the signals dropped, and how much of the run includes time without signal. Note how the proportion of aqua color in Figure 9-24 matches the proportion of red in Figure 9-23.



EIRP=25 dBm:

V2V

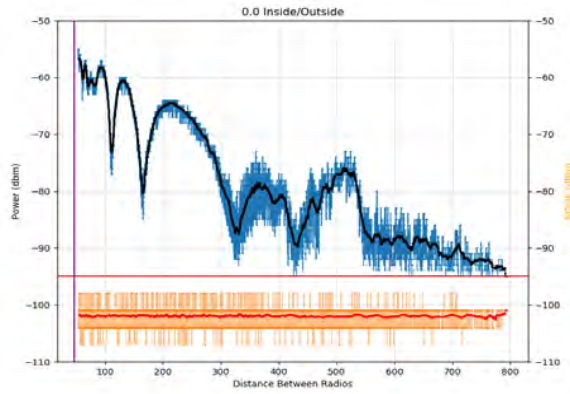
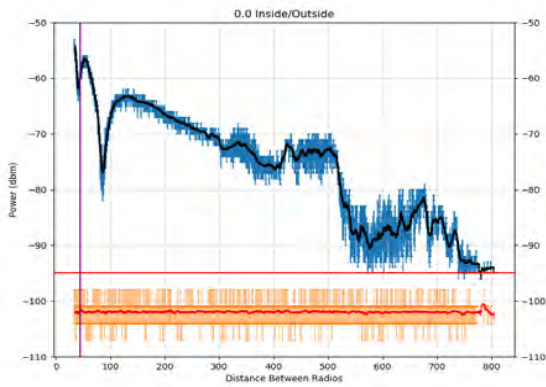
I2V

Figure 9-24. Typical Perryman Baseline geographical distribution of PER

Source: 20190322 Adj channel tests away --was exl_report_away.xlsx, Tab: Baselines

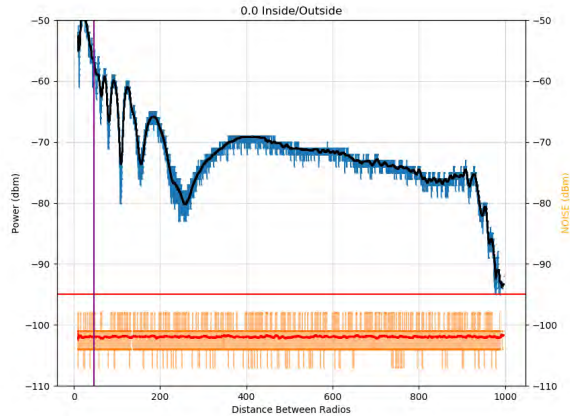
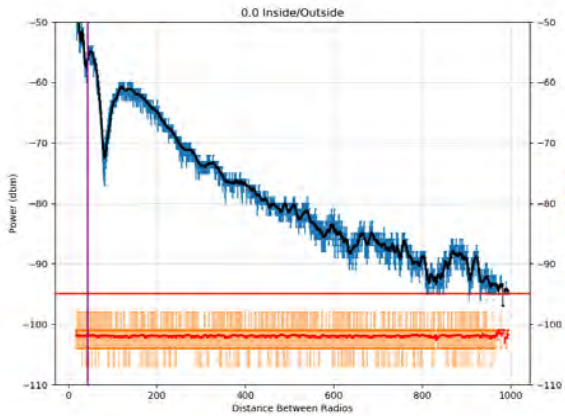
9.1.4 ATEF Baseline

The ATEF facility is a large ring track that encircles Phillips Army Airfield. This is where we tested the effect of putting the Wi-Fi inside a cinderblock building. The baseline measurements were taken only for the portion of the track where RF from the RSU and static OBU could reach. Because this was not an out and back test we need to show the baselines for both the approaching and departing data.



Approaching: V2V

I2V



Departing: V2V

I2V

Figure 9-25. Typical ATEF Baseline RSSI and noise level (EIRP=25 dBm)

Source: 20170912 Building-Cinderblock toward -- was exl_report_toward_20170912.xlsx, Tabs: V2V mobile Tx to UNII=3; V2I mobile Rx to UNII=31; and

Source: 20170912 Building-Cinderblock away -- was exl_report_away_20170912.xlsx, Tabs: V2V mobile Tx to UNII=3; V2I mobile Rx to UNII=31

In the approach plots the vehicle moves right-to-left (range decreasing). In the departure plots the vehicle moves left-to-right (range increasing). Note the same background noise level as at the other facilities (-102 dBm).

Unlike Zone 1 and Perryman the ATEF track is not a clean RF environment with trees, buildings, brick walls, and poles alongside the track in places. The multipath reflections are most obvious in the approach data in Figure 9-25. The departing direction data is a little more like Zone 1 and Perryman because that direction has more of a simple line of sight with fewer reflecting objects to create multipath. You can see how multipath reflectors in the environment add nulls and fill in the expected ground-bounce nulls to some extent making the data harder to interpret.

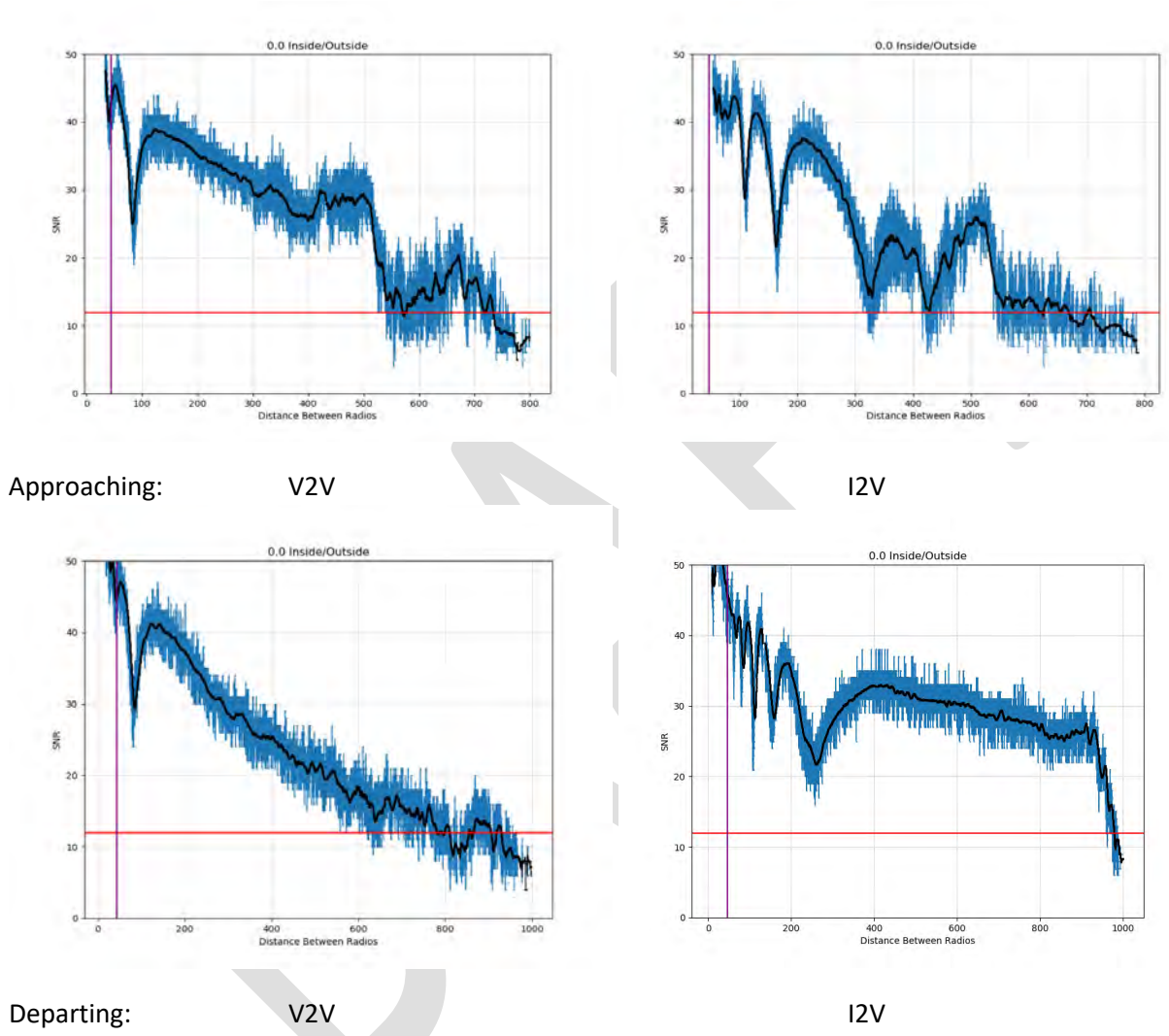
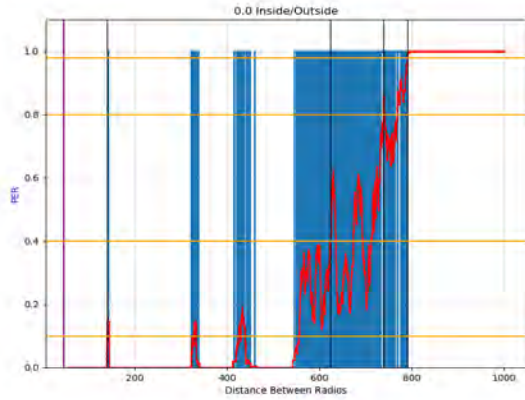
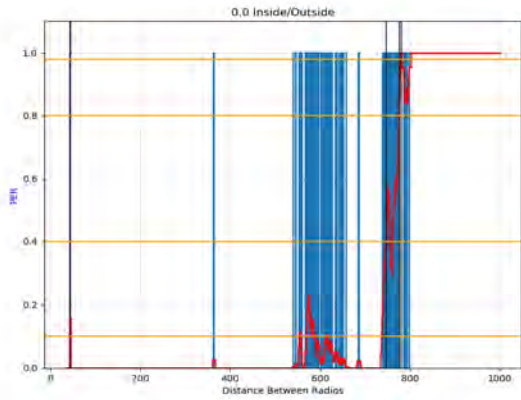


Figure 9-26. Typical ATEF Baseline Signal-to-Noise ratio (EIRP=25 dBm)

Source: 20170912 Building-Cinderblock toward -- was exl_report_toward_20170912.xlsx, Tabs: V2V mobile Tx to UNII=3; V2I mobile Rx to UNII=31; and

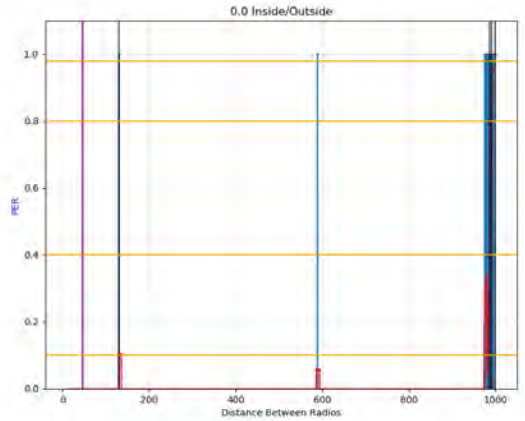
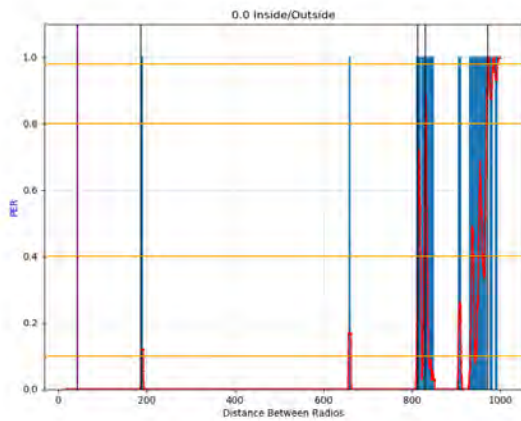
Source: 20170912 Building-Cinderblock away -- was exl_report_away_20170912.xlsx, Tabs: V2V mobile Tx to UNII=3; V2I mobile Rx to UNII=31



Approaching:

V2V

I2V



Departing:

V2V

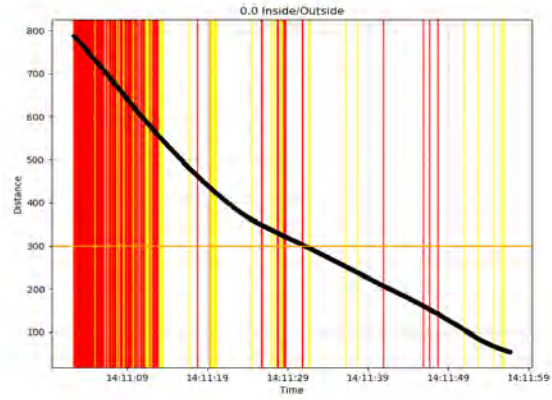
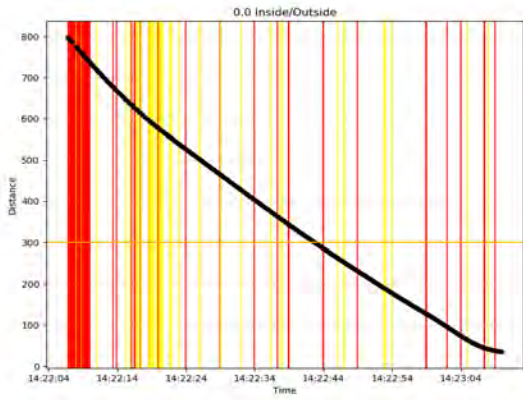
I2V

Figure 9-27. Typical ATEF Baseline Packet Error Rate (EIRP=25 dBm)

Source: 20170912 Building-Cinderblock toward -- was exl_report_toward_20170912.xlsx, Tabs: V2V mobile Tx to UNII=3; V2I mobile Rx to UNII=31; and

Source: 20170912 Building-Cinderblock away -- was exl_report_away_20170912.xlsx, Tabs: V2V mobile Tx to UNII=3; V2I mobile Rx to UNII=31

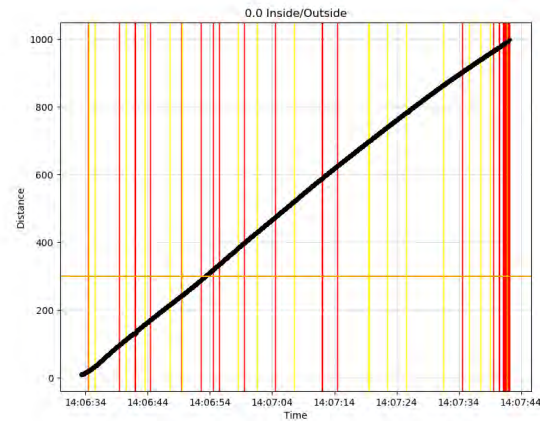
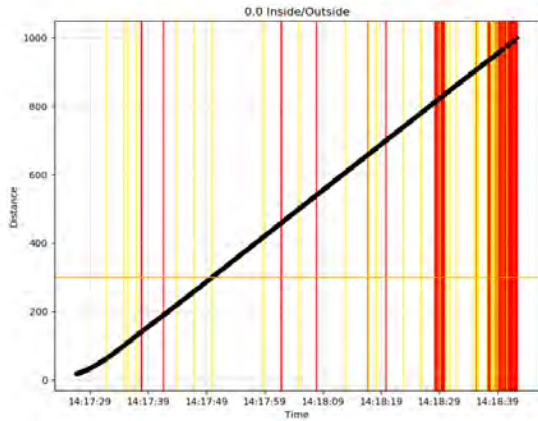
Figure 9-27 shows the departing leg to be similar to the other facilities with just a couple of locations where packets were missed until the signal was cut off by trees. The more complicated approach PER is due to signal leaking through the trees from 550-750 meters as the vehicle came around the track before it was directly in view. You can see the approach signal is completely blocked at 750 meters but it was not cut off in the departure direction until around 1000 meters.



Approaching:

V2V

I2V



Departing:

V2V

I2V

Figure 9-28. Typical ATEF Baseline gap analysis (EIRP=25 dBm)

Source: 20170912 Building-Cinderblock toward -- was exl_report_toward_20170912.xlsx, Tabs: V2V mobile Tx to UNII=3; V2I mobile Rx to UNII=31; and

Source: 20170912 Building-Cinderblock away -- was exl_report_away_20170912.xlsx, Tabs: V2V mobile Tx to UNII=3; V2I mobile Rx to UNII=31

Figure 9-28 shows that even in the 300 meter range marked by the horizontal orange line the multipath reflectors in the environment sporadically knock out BSMs in groupings large enough to cause safety critical gaps. The black line is the vehicle trajectory in time (x-axis) and space (y-axis). Where it intersects a red line a safety critical gap in the BSMs occurred (greater than 0.5 seconds). Yellow lines mark gaps that may be critical to sensitive safety applications (0.3 to 0.5 seconds). Again, this must be accounted for so that the environmental interference isn't attributed to Wi-Fi in the interference measurements.

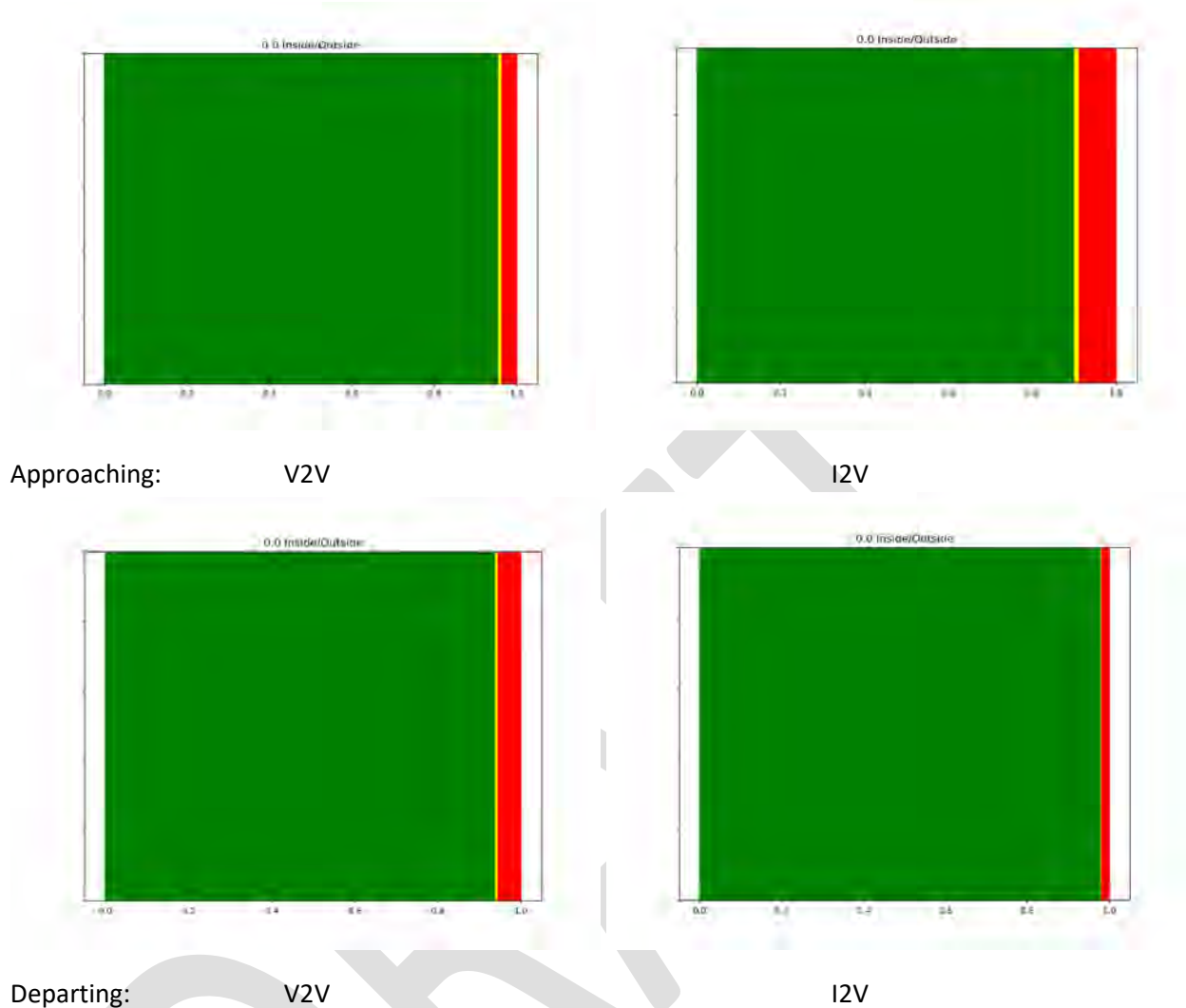
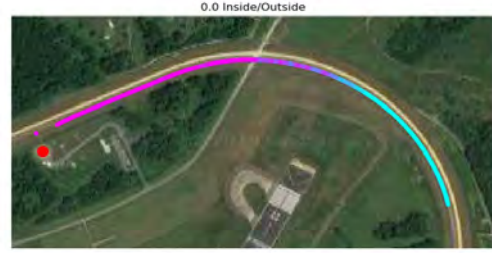
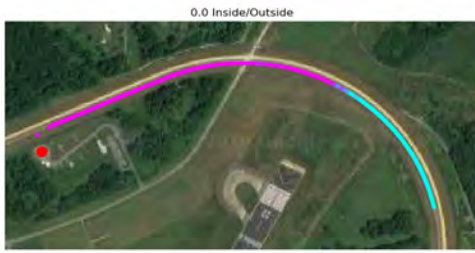


Figure 9-29. Typical ATEF Baseline cumulative gap analysis (EIRP=25 dBm)

Source: 20170912 Building-Cinderblock toward -- was exl_report_toward_20170912.xlsx, Tabs: V2V mobile Tx to UNII=3; V2I mobile Rx to UNII=31; and

Source: 20170912 Building-Cinderblock away -- was exl_report_away_20170912.xlsx, Tabs: V2V mobile Tx to UNII=3; V2I mobile Rx to UNII=31

As noted above, we must subtract the fraction of red that shows up in the Figure 9-29 plots from the equivalent interference test plots.



Approaching:

V2V

I2V



Departing:

V2V

I2V

Figure 9-30. Typical ATEF Baseline geographical distribution of PER (EIRP=25 dBm)

Source: 20170912 Building-Cinderblock toward -- was exl_report_toward_20170912.xlsx, Tabs: V2V mobile Tx to UNII=3; V2I mobile Rx to UNII=31; and

Source: 20170912 Building-Cinderblock away -- was exl_report_away_20170912.xlsx, Tabs: V2V mobile Tx to UNII=3; V2I mobile Rx to UNII=31

Figure 9-30 shows better what blocks packets in the approach. See the purple transition between full cut off (aqua) to full signal (magenta) that you do not have in the departing direction. You can see the trees that partially obstruct the signal through the curve in the approach to the DSRC and UNII radios at the red dots (small is DSRC, large is UNII). You can also see how the departure side has direct line of sight until suddenly blocked by the line of trees.

9.1.5 Wood building corridor baseline

The street where we tested with the Wi-Fi access point in and outside of a wooden building is a corridor (Recoil Avenue) with many buildings on both side generating many more multipath reflections than at ATEF. This would be more typical of an urban environment. You can see the result of these tests from February 6, 2018 in Figure 9-31. There are many small nulls as well as filling of the ground-bounce nulls making them difficult or impossible to see. (Compare to the Zone 1 data in Figure 9-8). This test was also more complicated than a simple out and back so we will show baseline departure data from both sides.

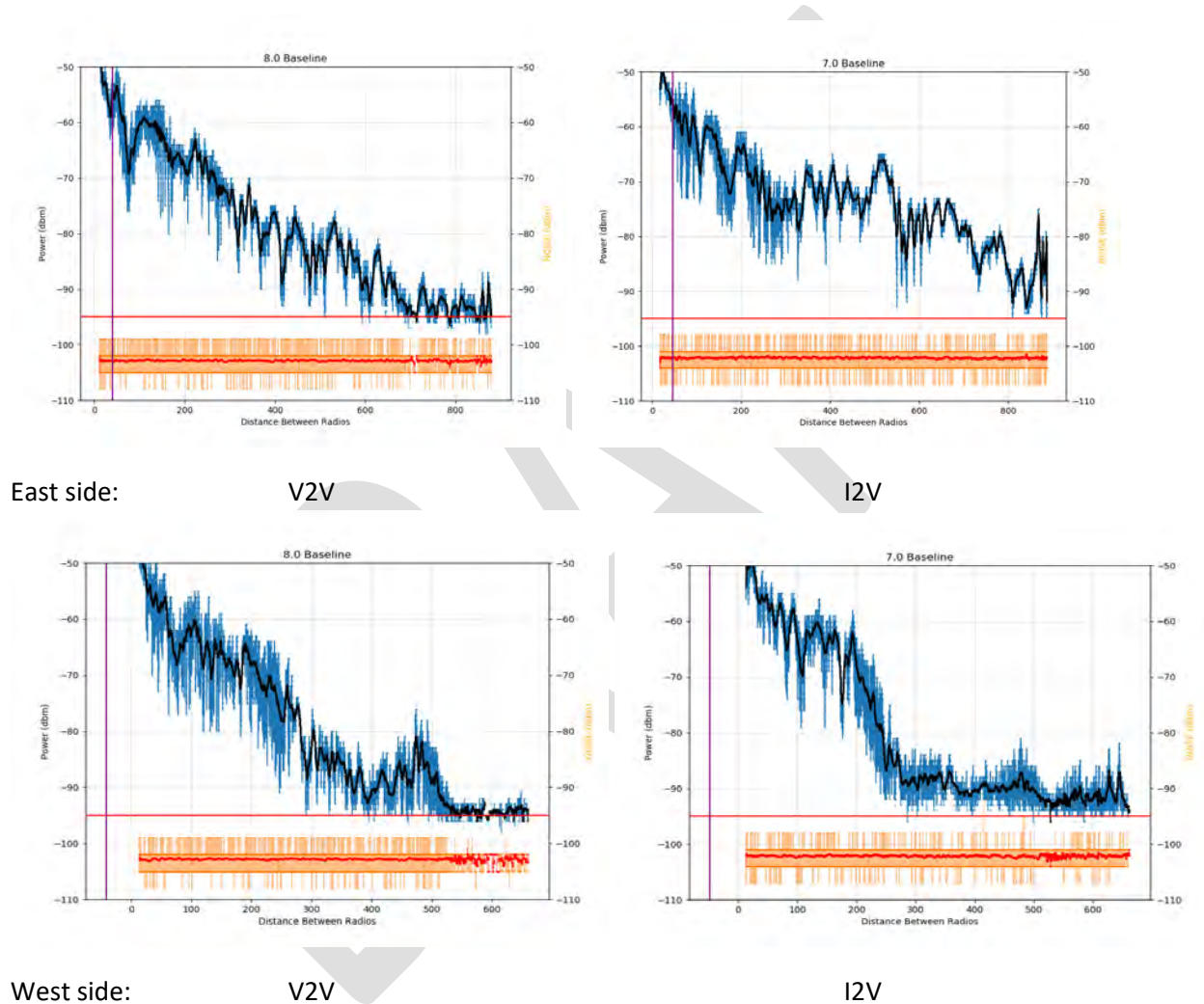


Figure 9-31. Recoil Avenue Baseline RSSI and noise level (EIRP=25 dBm)

Source: 20180206 Building-Wood E-side away V1 -- was exl_report_away_20180206_side2.xlsx, Tab: Baselines; and

Source: 20180206 Building-Wood W-side away V1 -- was exl_report_away_20180206-2.xlsx, Tab: Baselines

We present the geographical PER data first this time because understanding the topography will make it easier to understand the baselines of the interference measures.

8.0 Baseline



7.0 Baseline

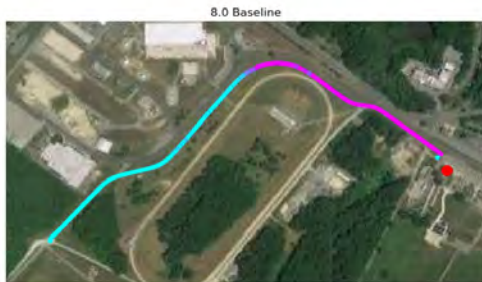


DRAFT

East side:

V2V

I2V



West side:

V2V

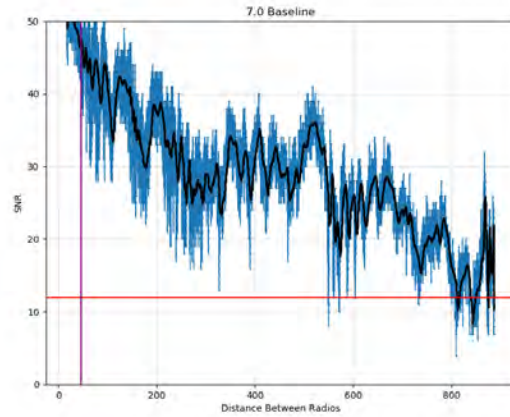
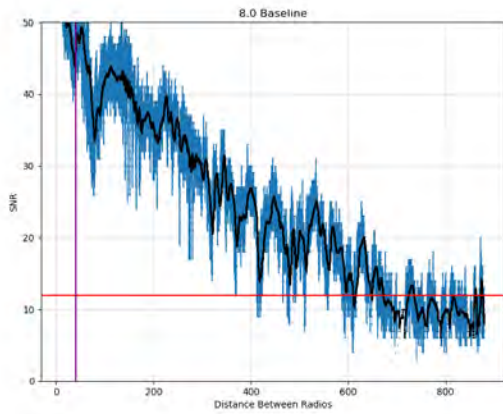
I2V

Figure 9-32. Recoil Avenue Baseline geographical distribution of PER (EIRP=25 dBm)

Source: 20180206 Building-Wood E-side away V1 -- was exl_report_away_20180206_side2.xlsx, Tab: Baselines; and

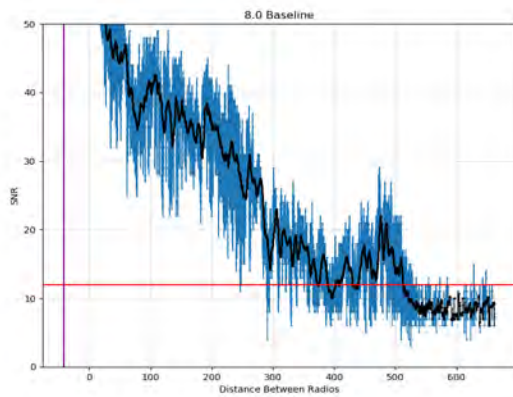
Source: 20180206 Building-Wood W-side away V1 -- was exl_report_away_20180206-2.xlsx, Tab: Baselines

Figure 9-32 shows that east of the building and static radius (red dot) is a straight drive like many Zone 1 and Perryman but with a very complex multipath environment caused by numerous buildings and vehicles. To the west, the test vehicle had to follow a curved route with trees and building obstructions. You can see that the effect on V2V was different from V2I. We examine this in detail in Chapter 10.

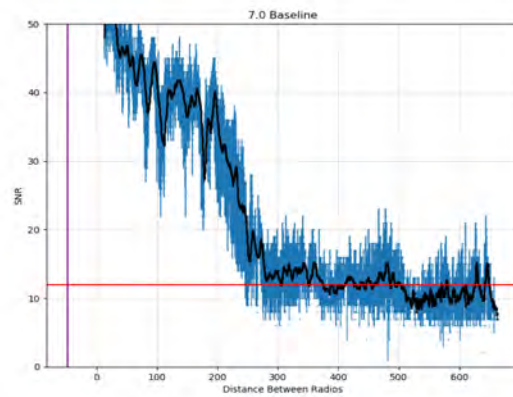


East side:

V2V



I2V



West side:

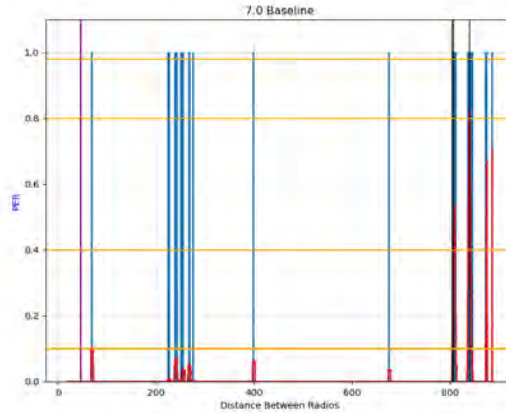
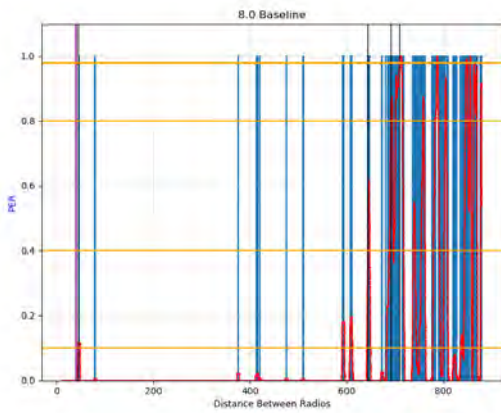
V2V

Figure 9-33. Recoil Avenue Baseline Signal-to-Noise ratio (EIRP=25 dBm)

Source: 20180206 Building-Wood E-side away V1 -- was exl_report_away_20180206_side2.xlsx, Tab: Baselines; and

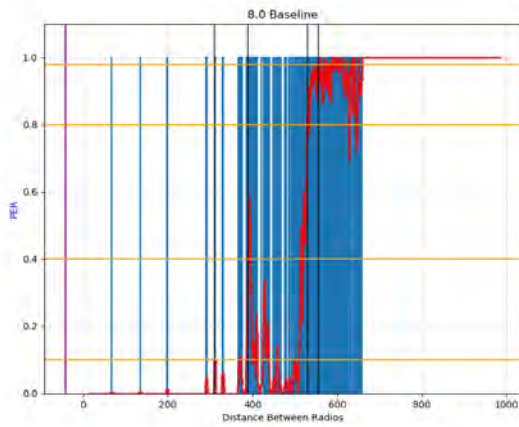
Source: 20180206 Building-Wood W-side away V1 -- was exl_report_away_20180206-2.xlsx, Tab: Baselines

As with the previous two figures Figure 9-33 shows the signal on the west side running into the trees at around 300 meters. That is even more obvious in the packet error rate plots below.

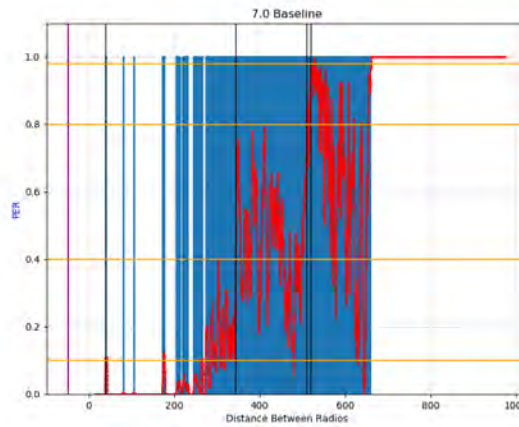


East side:

V2V



I2V



West side:

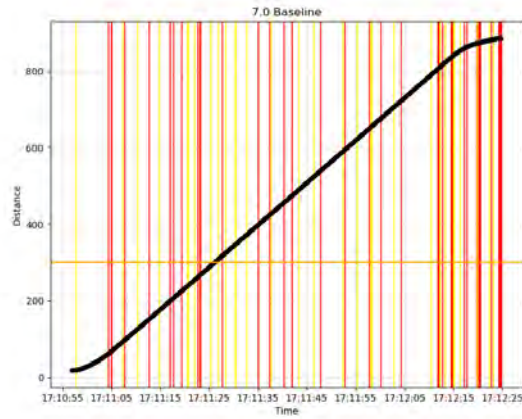
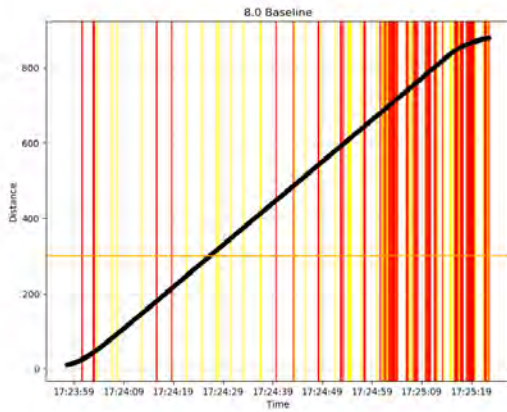
V2V

Figure 9-34. Recoil Avenue Baseline Packet Error Rate (EIRP=25 dBm)

Source: 20180206 Building-Wood E-side away V1 -- was exl_report_away_20180206_side2.xlsx, Tab: Baselines; and

Source: 20180206 Building-Wood W-side away V1 -- was exl_report_away_20180206-2.xlsx, Tab: Baselines

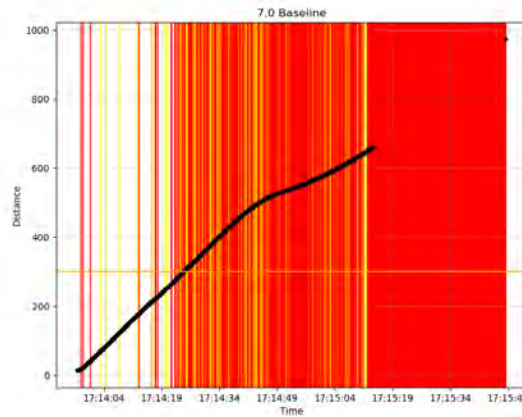
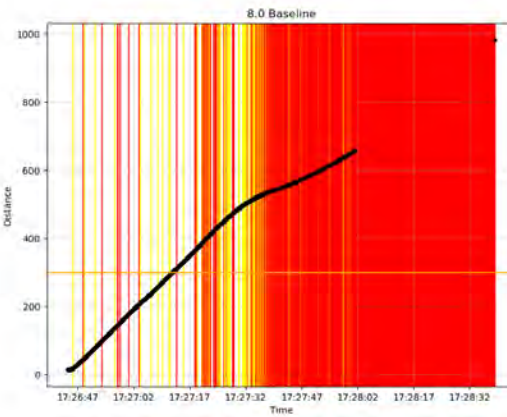
The packet errors and safety critical gaps shown in Figures 9-34 and 9-35 document the safety critical dropouts that occur due to environmental interference in a complicated environment even before adding interference from other radio services.



East side:

V2V

I2V



West side:

V2V

I2V

Figure 9-35. Recoil Avenue Baseline gap analysis (EIRP=25 dBm)

Source: 20180206 Building-Wood E-side away V1 -- was exl_report_away_20180206_side2.xlsx, Tab: Baselines; and

Source: 20180206 Building-Wood W-side away V1 -- was exl_report_away_20180206-2.xlsx, Tab: Baselines

The gap and cumulative gap analyses of Figures 9-35 and 9-36 highlight the difference between signals getting a straight shot down a street even with the multipath compared to signals obstructed by trees and buildings. Chapter 10 describes the different impact of the foliage versus the tree trunks on V2V and V2I in some detail.

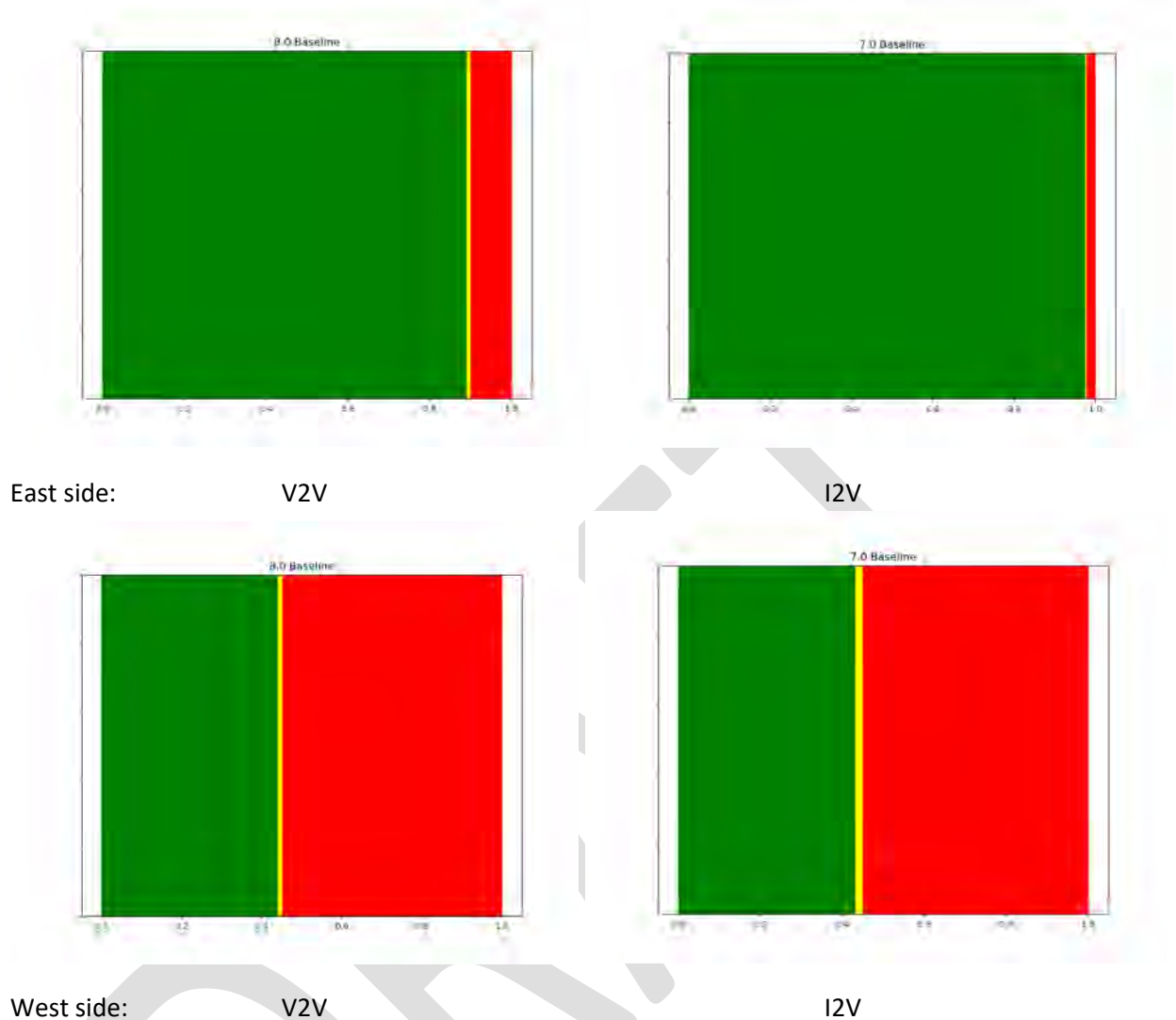


Figure 9-36. Recoil Avenue Baseline cumulative gap analysis (EIRP=25 dBm)

Source: 20180206 Building-Wood E-side away V1 -- was exl_report_away_20180206_side2.xlsx, Tab: Baselines; and

Source: 20180206 Building-Wood W-side away V1 -- was exl_report_away_20180206-2.xlsx, Tab: Baselines

9.1.6 Mulberry point baseline

The brick building tests were conducted at a training facility called Mulberry Point on February 18, 2018. It is another complicated multipath environment with buildings and vehicles along the road. The runs were analyzed in two legs. Because the RSU and zero point were at an intersection a couple hundred feet west of the building, the east-side features a drive by of the building. In Figure 9-37, the purple

vertical line marks the position of the brick building where the Wi-Fi access point will go. Zero range is the location of the RSU and static OBU. As in the other locations the noise level is -102 dBm.

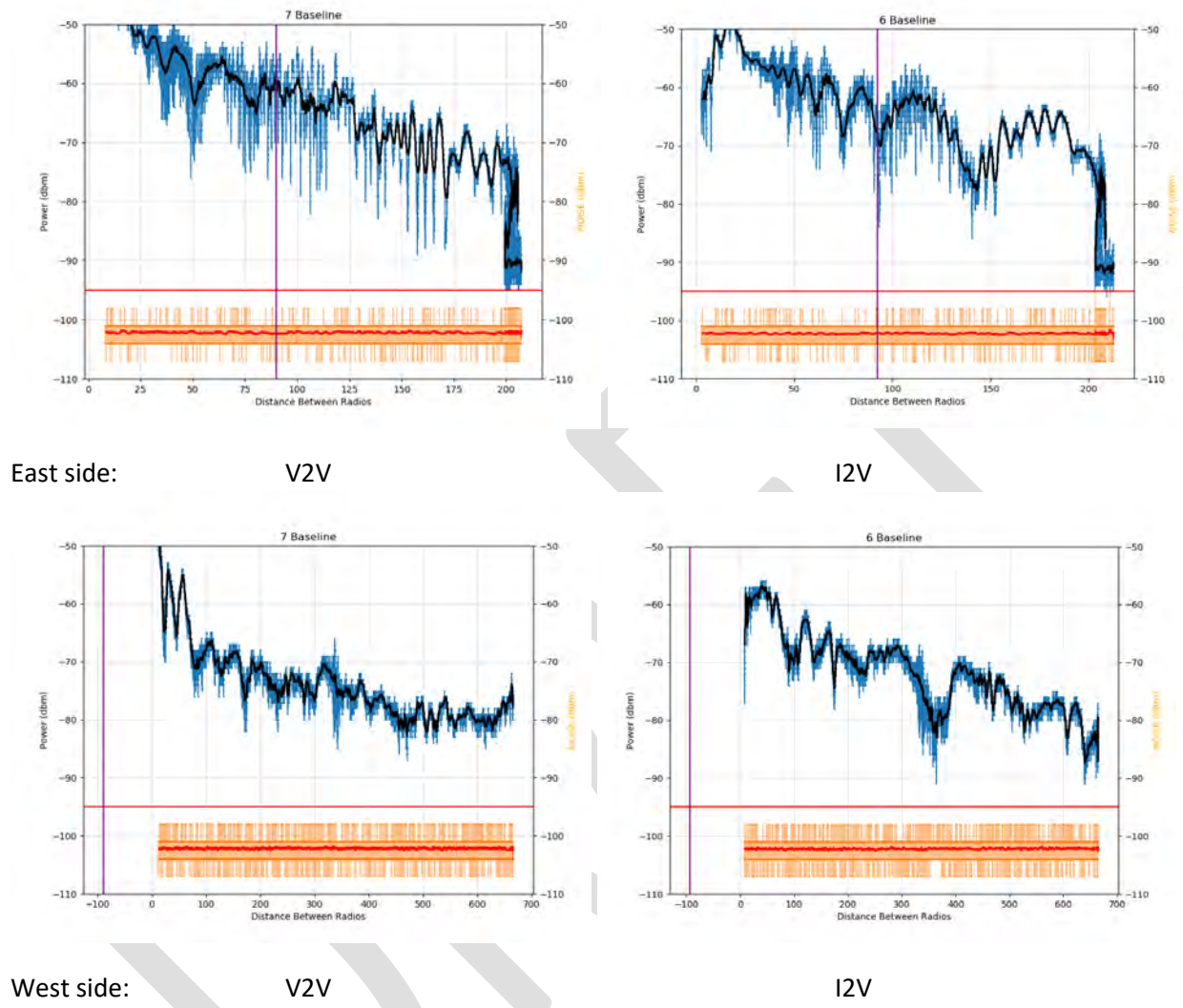


Figure 9-37. Mulberry Point Baseline RSSI and noise level (EIRP=25 dBm)

Source: 20180208 Building-Brick drive-by toward V1 was --exl_report_away_20180208_side2.xlsx, Tab: Baselines; and

Source: 20180208 Building-Brick W-side toward V1 was --exl_report_toward_20180208.xlsx, Tab: Baselines

In this case, the west-side data is like the straight shot of the east-side data at Recoil Ave. You can see how they are both more similar compared to the complicated other sides in both cases. But, also note how different the nulls in the RSSI curves are due to the different environments. To make the following plots easier to understand we show the satellite view of PER next to orient the reader before the interference metric plots.

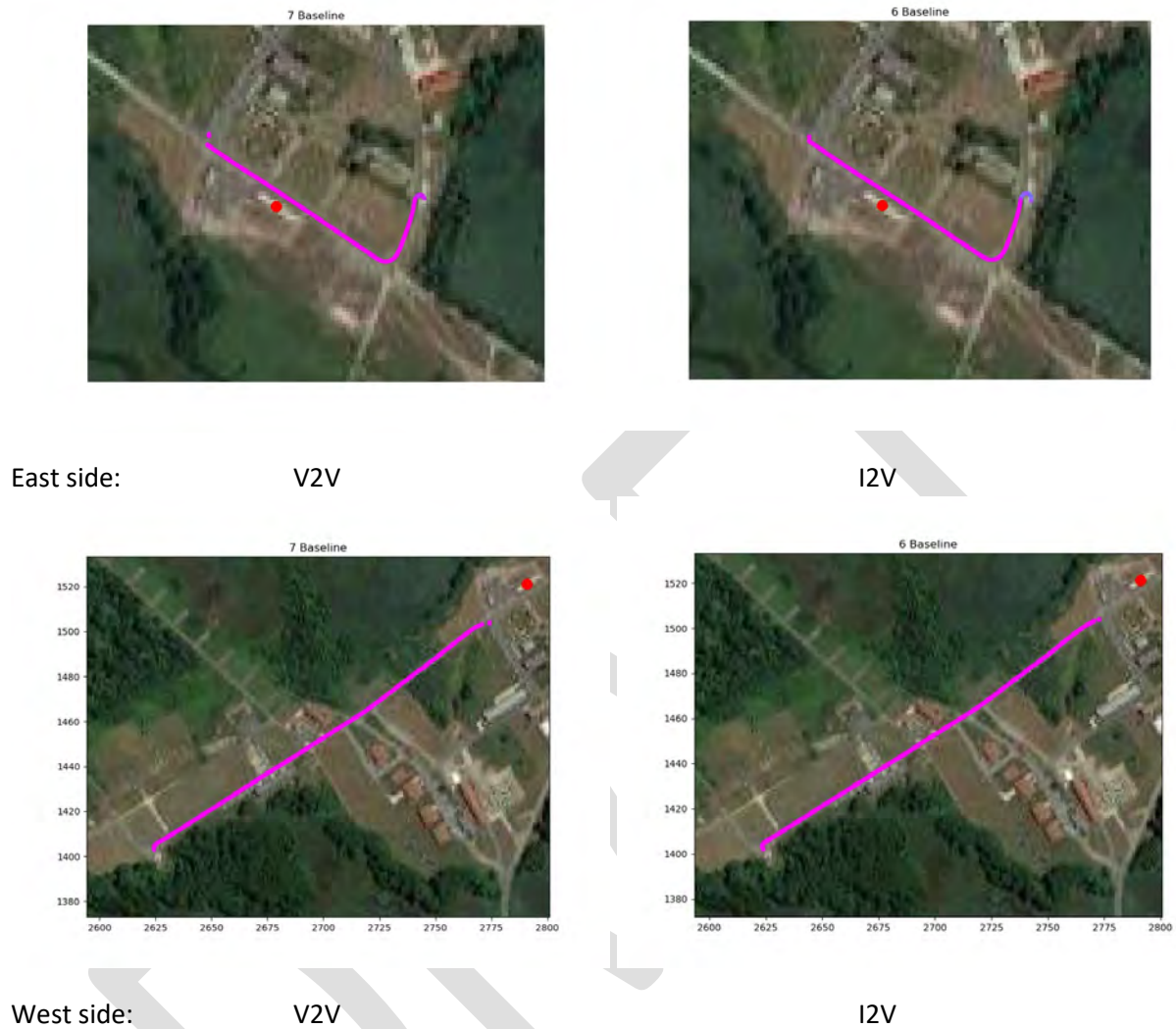
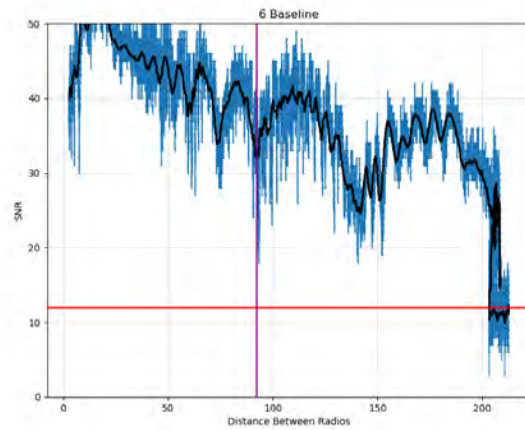
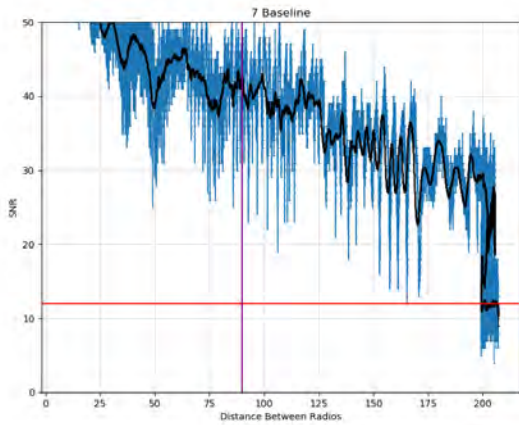


Figure 9-38. Mulberry Point Baseline geographical distribution of PER (EIRP=25 dBm)

Source: 20180208 Building-Brick drive-by toward V1 was --exl_report_away_20180208_side2.xlsx, Tab: Baselines; and

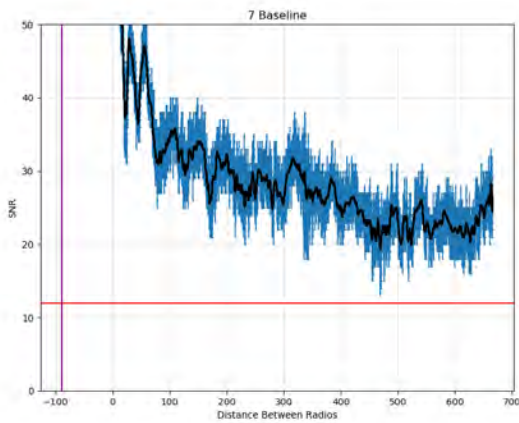
Source: 20180208 Building-Brick W-side toward V1 was --exl_report_toward_20180208.xlsx, Tab: Baselines

Figures 9-38, 9-40 and 9-41 show that even with the multipath obvious from Figure 9-37 this location caused less environmentally induce packet loss than Recoil Ave.

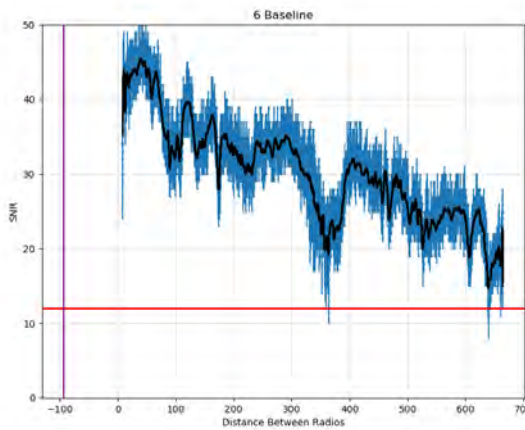


East side:

V2V



I2V



West side:

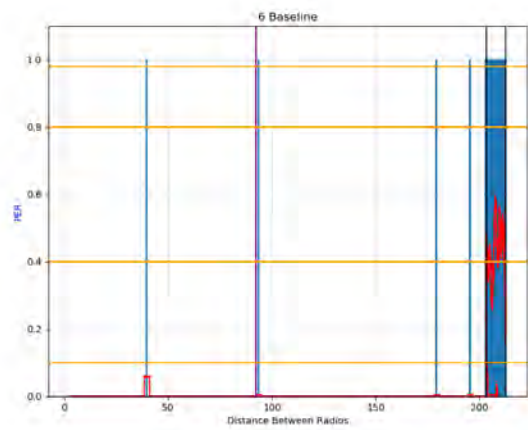
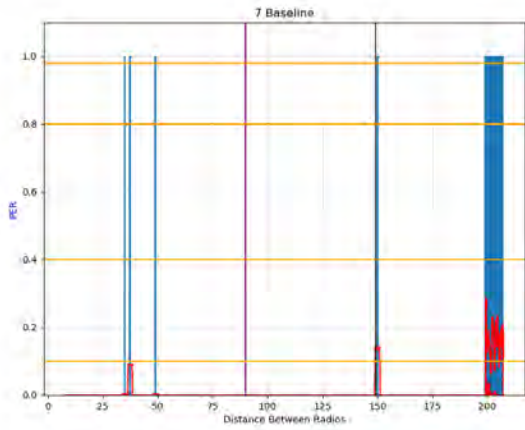
V2V

I2V

Figure 9-39. Mulberry Point Baseline Signal-to-Noise ratio (EIRP=25 dBm)

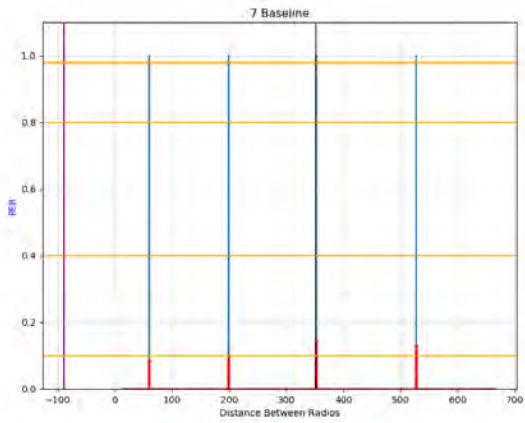
Source: 20180208 Building-Brick drive-by toward V1 was --exl_report_away_20180208_side2.xlsx, Tab: Baselines; and

Source: 20180208 Building-Brick W-side toward V1 was --exl_report_toward_20180208.xlsx, Tab: Baselines

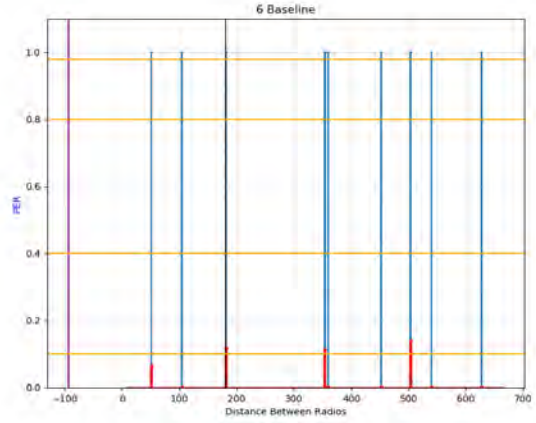


East side:

V2V



I2V



West side:

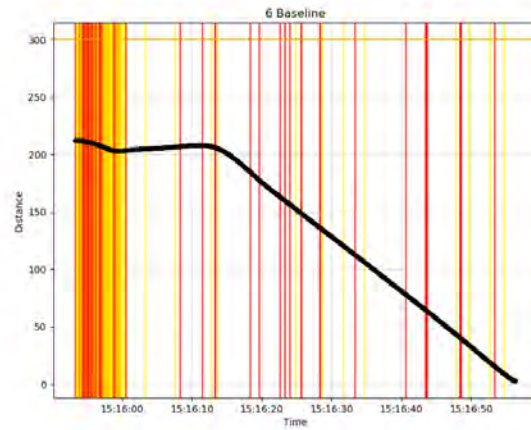
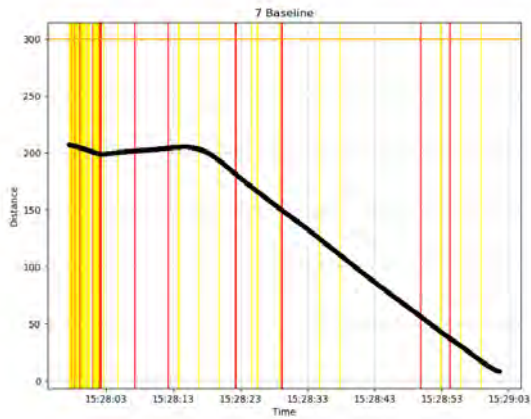
V2V

I2V

Figure 9-40. Mulberry Point Baseline Packet Error Rate (EIRP=25 dBm)

Source: 20180208 Building-Brick drive-by toward V1 was --exl_report_away_20180208_side2.xlsx, Tab: Baselines; and

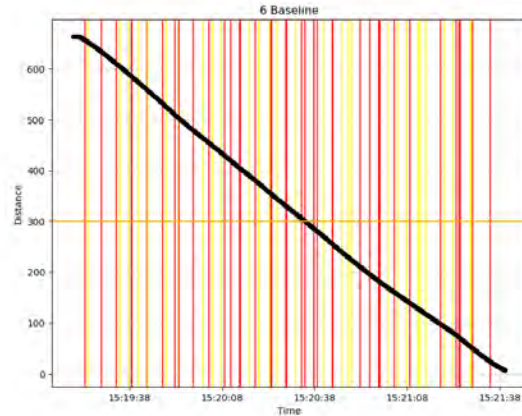
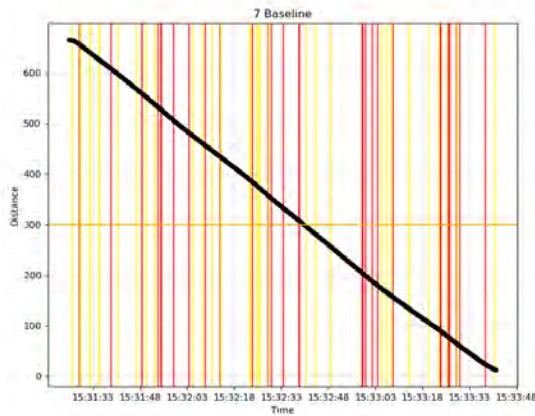
Source: 20180208 Building-Brick W-side toward V1 was --exl_report_toward_20180208.xlsx, Tab: Baselines



East side:

V2V

I2V



West side:

V2V

I2V

Figure 9-41. Mulberry Point Baseline gap analysis (EIRP=25 dBm)

Source: 20180208 Building-Brick drive-by toward V1 was --exl_report_away_20180208_side2.xlsx, Tab: Baselines; and

Source: 20180208 Building-Brick W-side toward V1 was --exl_report_toward_20180208.xlsx, Tab: Baselines

Even with fewer lost packets, Figure 9-41 shows that the losses clustered into a few safety critical gaps.

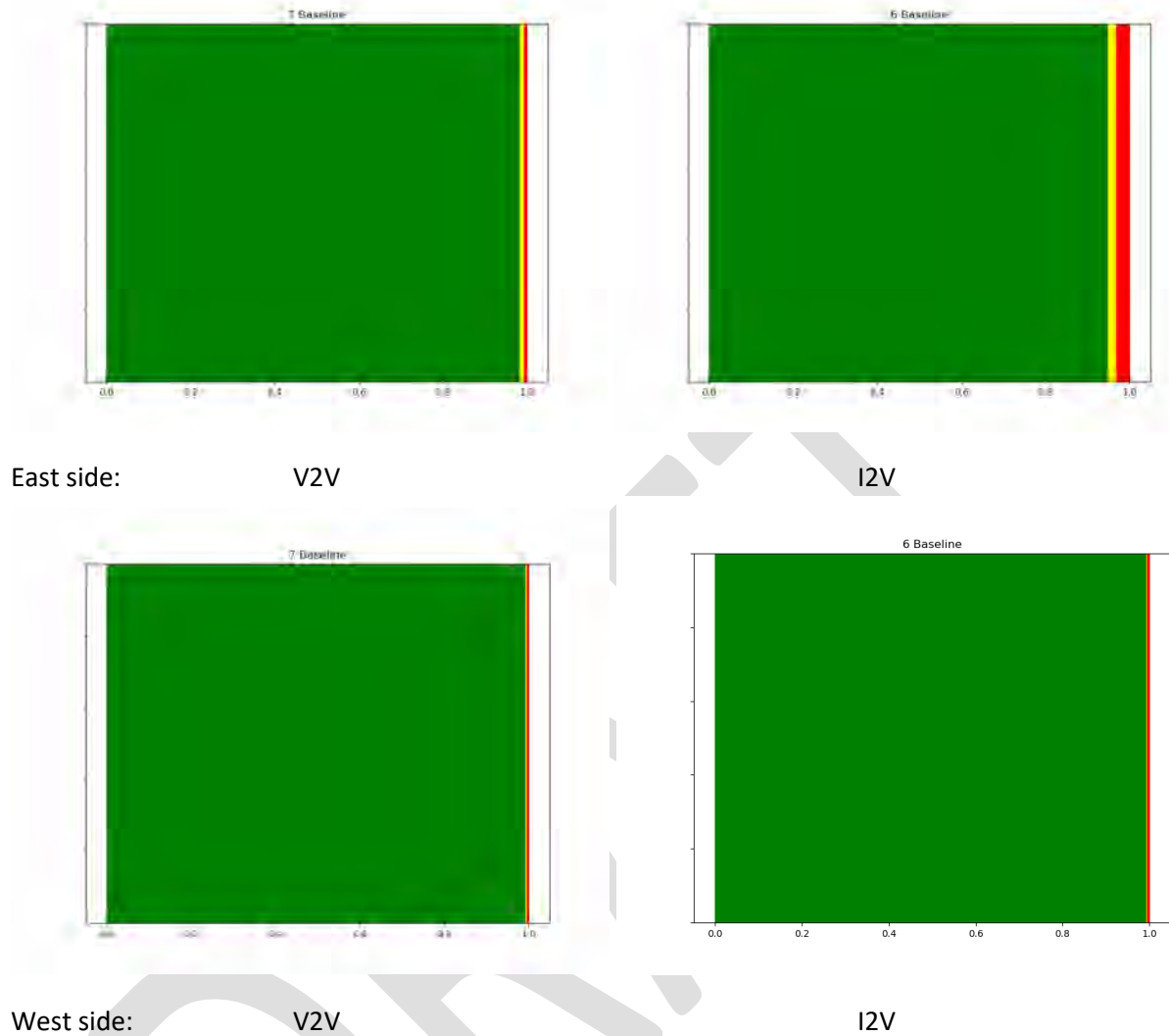


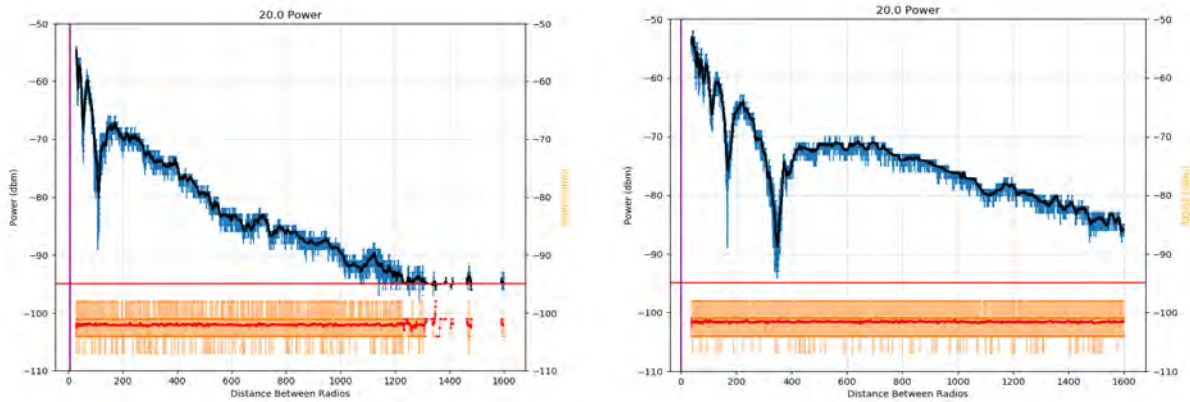
Figure 9-42. Mulberry Point Baseline cumulative gap analysis (EIRP=25 dBm)

Source: 20180208 Building-Brick drive-by toward V1 was --exl_report_away_20180208_side2.xlsx, Tab: Baselines; and

Source: 20180208 Building-Brick W-side toward V1 was --exl_report_toward_20180208.xlsx, Tab: Baselines

9.1.7 Dynamometer course

We conducted tests along a test track that was closely hemmed in by trees in three different weather conditions wet on September 13, 2017. The baseline data below was taken when the leaves and road surface were wet.



EIRP=25 dBm:

V2V

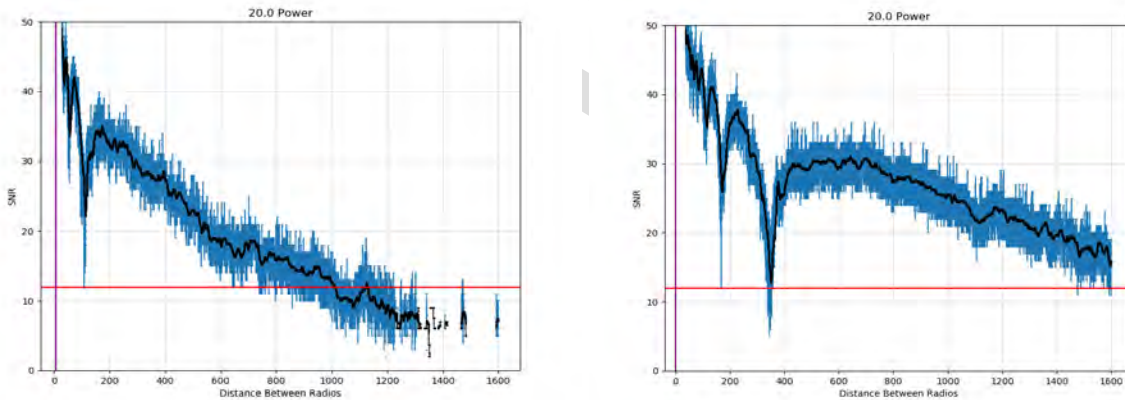
V2I

Figure 9-43. Wet Dynamometer Course Baseline RSSI and noise level

Source: 20170913 wet foliage baselines away --was exl_report_away_20170913.xlsx, Tabs: V2V mobile Tx; V2I mobile Tx

Figure 9-43 shows a less complicated environment than the sites of the building tests. It resembles more the data from the open Zone 1 and Perryman locations.

Figure 9-44 shows V2V SNR dropping below the 12 dB benchmark a while before the signal is lost. The never happens in the V2I case, except at the deepest ground-bounce null.



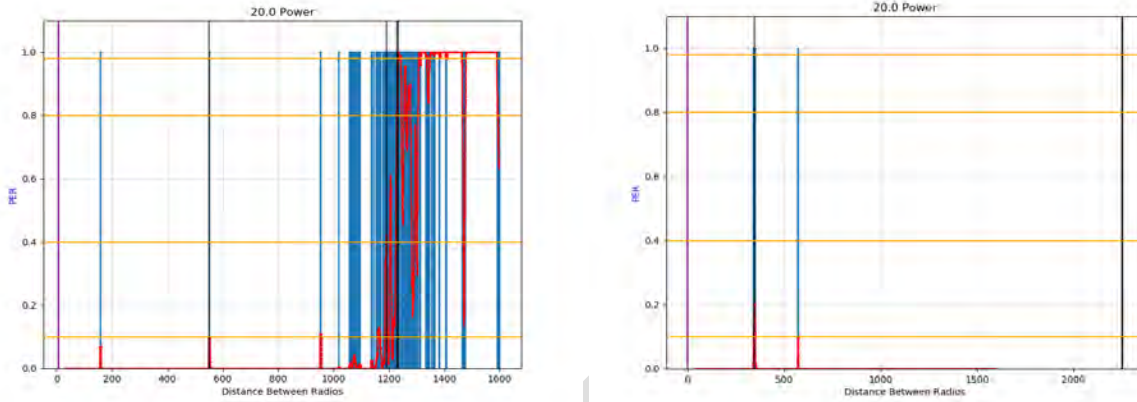
EIRP=25 dBm:

V2V

V2I

Figure 9-44. Wet Dynamometer Course Baseline Signal-to-Noise ratio (SNR)

Source: 20170913 wet foliage baselines away --was exl_report_away_20170913.xlsx, Tabs: V2V mobile Tx; V2I mobile Tx



EIRP=25 dBm:

V2V

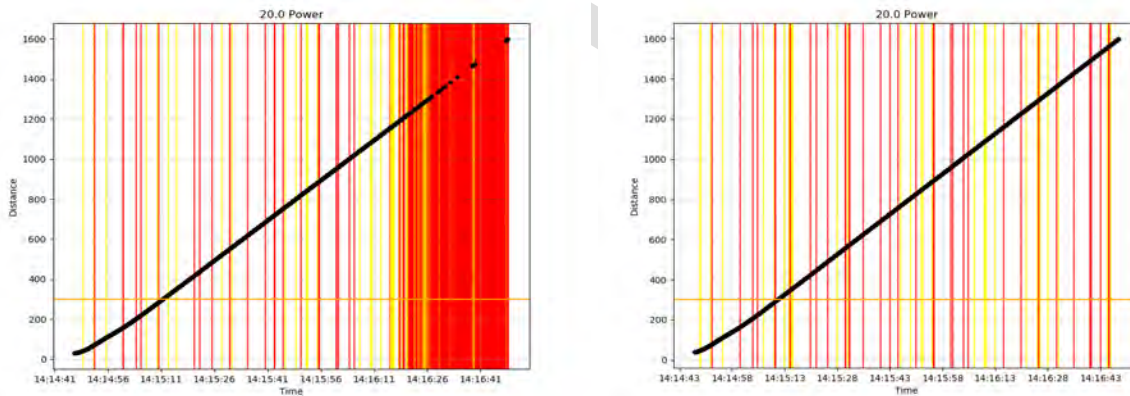
V2I

Figure 9-45. Wet Dynamometer Course Baseline Packet Error Rate (PER)

Source: 20170913 wet foliage baselines away --was exl_report_away_20170913.xlsx, Tabs: V2V mobile Tx; V2I mobile Tx

Figure 9-45 shows that packet error rate is good where the SNR is above the 12 dB benchmark. Packets were lost in the deepest V2I ground-bounce null.

Figure 9-46 shows that the packets were lost in clusters large enough for several safety critical gaps just due to the environment.



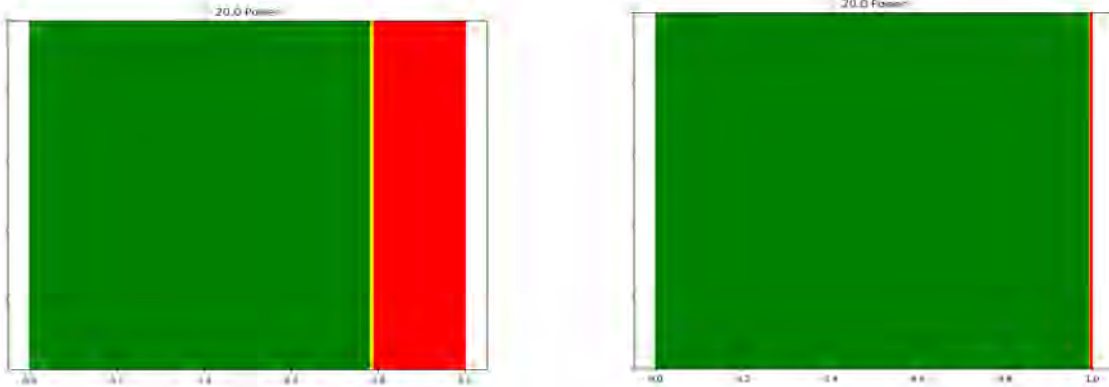
EIRP=25 dBm:

V2V

I2V

Figure 9-46. Wet Dynamometer Course Baseline gap analysis

Source: 20170913 wet foliage baselines away --was exl_report_away_20170913.xlsx, Tabs: V2V mobile Tx; V2I mobile Tx



EIRP=25 dBm:

V2V

I2V

Figure 9-47. Wet Dynamometer Course Baseline cumulative gap analysis

Source: 20170913 wet foliage baselines away --was exl_report_away_20170913.xlsx, Tabs: V2V mobile Tx; V2I mobile Tx

The roughly 21 percent of the V2V side of Figure 9-47 that is red shows that there were gaps greater than half a second that much of the run. That is because when this leg was selected for processing, it included that much of the time after the signal was lost at the end. None of that 21 percent gap time has to do with interference. The same is true for the I2V side as the tiny PER that shows up around 500 meters was too brief to show up here.

Figure 9-48 conveys intuitively where the signals dropped, and how much of the run includes time without signal. Note how the proportion of aqua color in Figure 9-48 matches the proportion of red in Figure 9-47. The red dot marks the location of the static DSRC radios.



EIRP=25 dBm:

V2V

V2I

Figure 9-48. Wet Dynamometer Course Baseline geographical distribution of PER

Source: 20170913 wet foliage baselines away --was exl_report_away_20170913.xlsx, Tabs: V2V mobile Tx; V2I mobile Tx

9.2 Packet Collision

This section examines interference at the DSRC receiver, measured in terms of packet collision.

In a minimal bounding case, DSRC was disrupted 500 meters from the interferer (when 100 meters from the other DSRC). That case was Wi-Fi with high traffic load (70%) but at the lowest power (EIRP of 5 dBm). Moreover, the DSRC was transmitting with 4 times more power than expected in actual deployment (EIRP of 25 dBm) and 100 times more higher than the Wi-Fi. See Figure 9-49. The vertical purple line at 575 meters marks the position of the Wi-Fi access point in the PER plot. The static DSRC is at zero meters range.

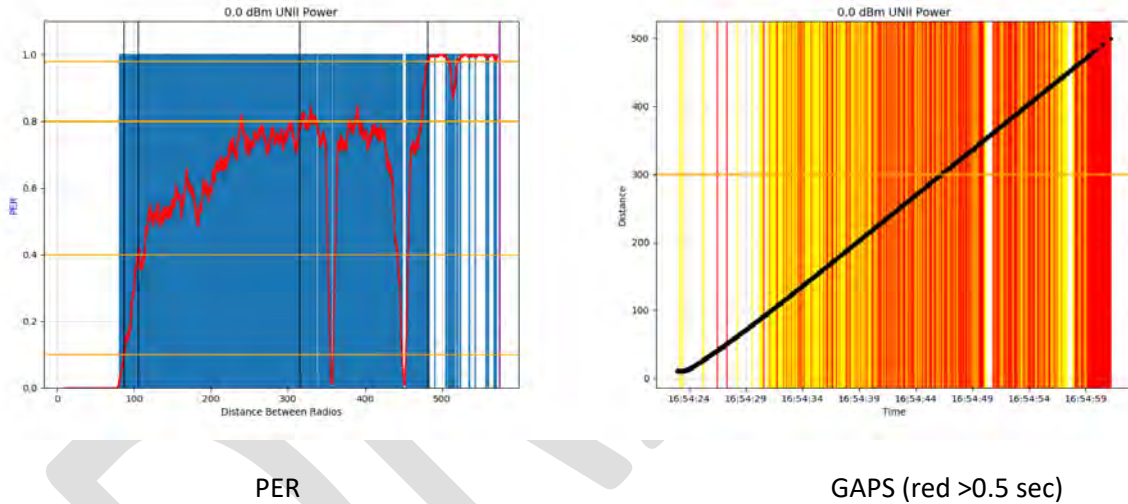


Figure 9-49. Bounding case: EIRPs, UNII=5 dBm, DSRC=25 dBm, UNII at 70% load

Source: 20170821 Vary UNII pwr half ms avg --was UNII_powerV3.xlsx, Tab: V2V mobile Rx

This means that no matter what the power of the UNII device is its packets will be strong enough collide in DSRC receivers 500 meters or more away. The severity of the interference will then be determined primary by the inter-packet spacing, that is, the traffic load of the Wi-Fi.

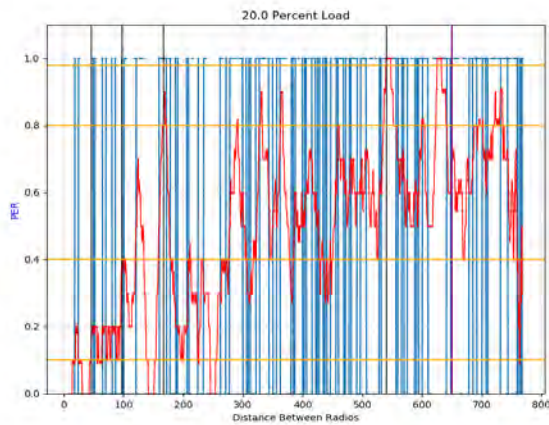
Figure 9-50 looks at a bounding case of Wi-Fi traffic load. The vertical purple line at 650 meters marks the position of the Wi-Fi access point in the PER plot. The static DSRC is at zero meters range. The mobile DSRC drove from there to the Wi-Fi access point.

With a 20% Wi-Fi traffic load the interference to DSRC 500 meters from the access point shows safety critical gaps and PER that ranges as high as 60%, which is untenable. At a range of 300 meters, the

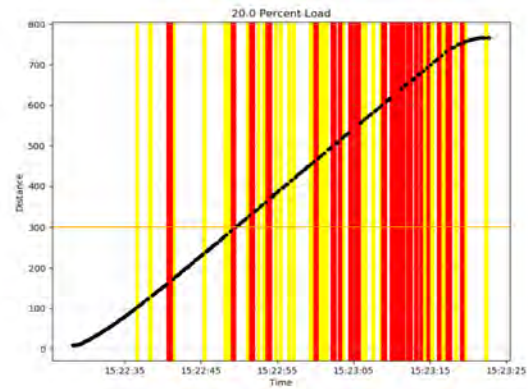
average PER is on the order of 60% and safety critical gaps are numerous and prevalent. A traffic load this high causes unacceptable interference under any circumstance.

We measured interference from traffic loads of two and three percent. Even though the packet error rates ranged as high as 20-40% the errors were distributed evenly enough that gaps of consecutively missing BSMs rarely exceeded 0.3 seconds. Traffic loading that light might not substantially affect safety.

The acceptability of Wi-Fi traffic loads in between the bounding cases of 2% and 20% depends on the sensitivity of individual safety applications to the number of consecutive BSMs lost. Sensitive applications may not be able to tolerate interference from Wi-Fi at traffic loadings of 5%. Others may work with traffic loadings of 10%.



PER



GAPS (red >0.5 sec)

Figure 9-50. Bounding case: UNII traffic load at 20%
(V2V DSRC EIRP=25 dBm, UNII EIRP=17 dBm, 1400 byte packets)

Source: 20171101 Vary UNII Load V2b --was exl_report_20171101.xls, Tab: V2V UNII PL1400

9.2.1 Effect of DSRC power

This section examines the impact of DSRC power on observed interference during testing. The signal-to-noise plots in Figure 9-51 show how increasing DSRC power increases the range at which the vehicle could receive from the RSU when exposed to Wi-Fi signals. The vehicle drove from the RSU (at range zero to the left) to the interferer on the right (marked by the vertical purple line).

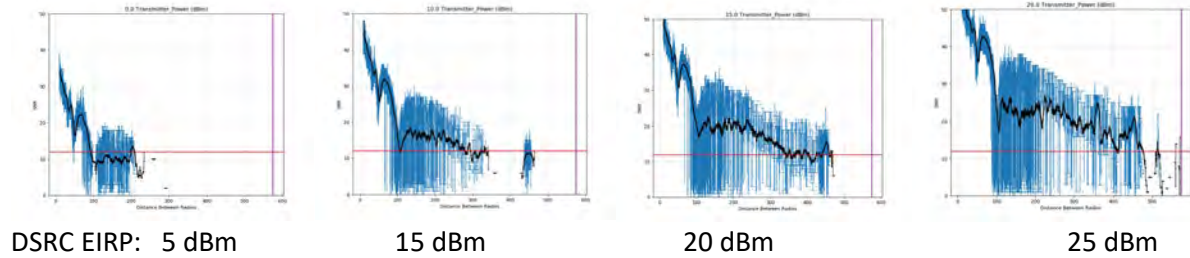


Figure 9-51. DSRC power increases range in the face of interferer

Source: 20170821 Vary DSRC pwr --was Transmitter_Power_V3.xlsx, Tab: V2V mobile Rx

Notice that the EIRP=15 dBm signal comes back for a bit about 100 meters before the interferer (located by the purple line at 575 meters). That is because the interferer’s antenna is on a tripod at an elevation of 6 feet high. Hence it has a deep ground bounce null ~100 meters away just like the DSRC. In the null, the interfering signal is greatly diminished or disappears, so the DSRC packets can be successful received until the vehicle leaves the null. The PER plot for this case (Figure 9-52) shows what happens here more clearly. You can see how the PER at 100% suddenly drops to around 10% in the null and shoots back up after leaving it.

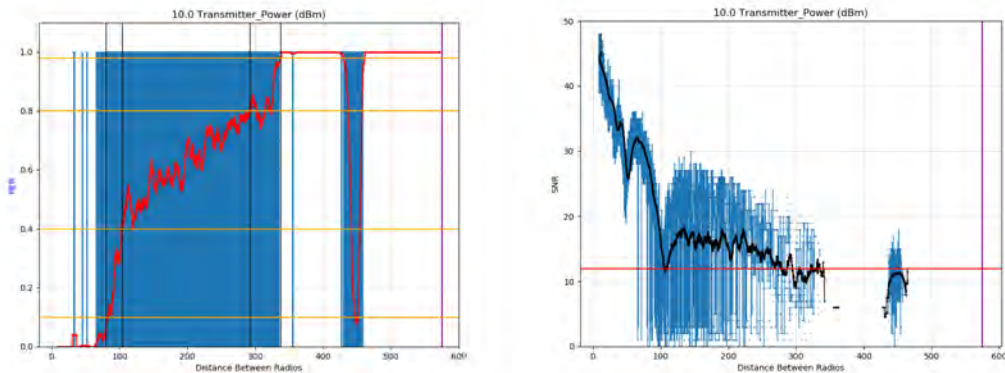


Figure 9-52. DSRC EIRP=15 dBm PER (left) and RSSI (right) both reveal the interferer’s deepest ground-bounce null.

Increasing DSRC power reduced interference but there are still significant gaps even at the highest power and the UNII at its lowest power setting (UNII CH173 0dBm 34QAM64 70% at 575m). Figure 9-53 shows the location in time and space of gaps in DSRC packet reception from 300-500 ms long (yellow) and greater than 500 ms long (red). The signal is completely lost where the black line breaks. Figure 9-54 shows what fraction of time packet gaps are smaller than these thresholds (green). This figure shows how increasing power helps performance but even at the maximum power level, less than half the DSRC packets are received without significant (yellow) and safety critical (red) gaps.

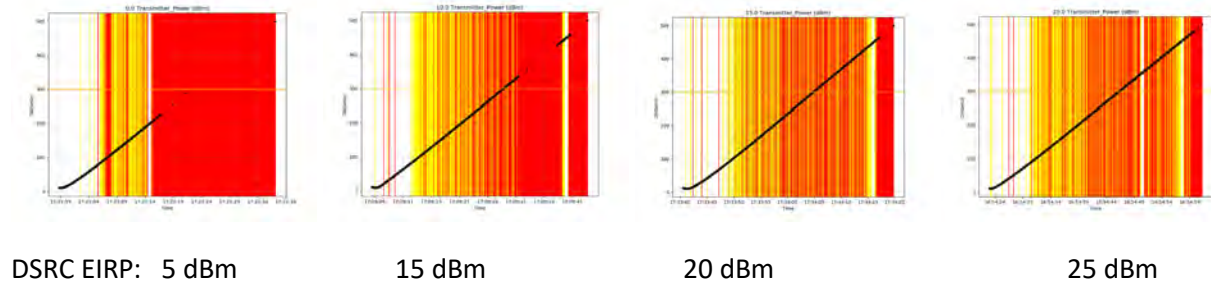


Figure 9-53. DSRC power decreases gaps in the face of interferer but still significant
 Source: 20170821 Vary DSRC pwr --was Transmitter_Power_V3.xlsx, Tab: V2V mobile Rx

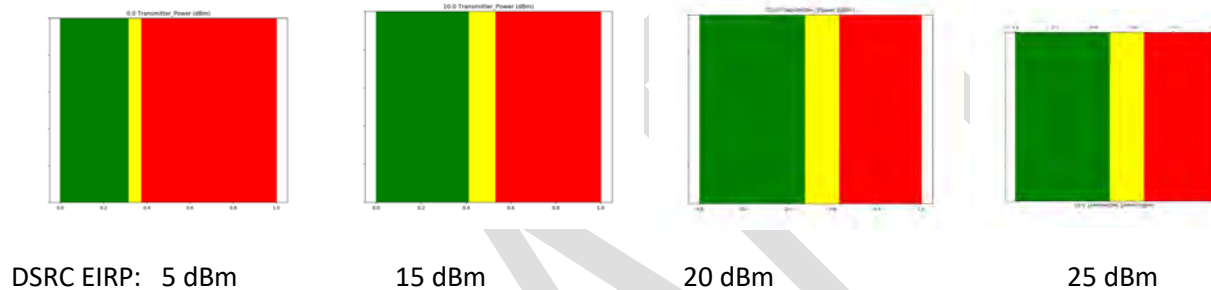
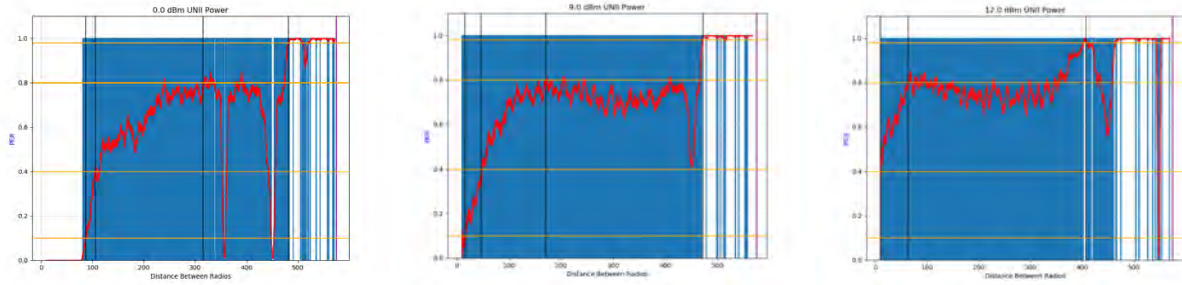


Figure 9-54. DSRC power decreases gaps in the face of interferer but still significant
 Source: 20170821 Vary DSRC pwr --was Transmitter_Power_V3.xlsx, Tab: V2V mobile Rx

9.2.2 Effect of UNII power

With DSRC transmitting at higher than specified EIRP, (that is, a transmit power of 20 dBm so EIRP of 25 dBm), increasing the transmit power of the UNII predictably increased the interference. The Wi-Fi loading was high (70%). See Figures 9-55, 9-56, and 9-57.

Two things are noteworthy. First, the level of interference that still occurred even though DSRC power was 100 times larger (UNII EIRP 5 dBm). Second, the largest UNII power in this test is still 100 times less than allowed for a Wi-Fi access point. DSRC was totally blocked roughly 100 meters from the interferer with packet rates on the order of 70% or higher as far as 400 meters from the interferer. Safety critical gaps are prevalent more than 500 meters from the interferer, even though the two DSRC radios are within 100 meters of each other at that point.



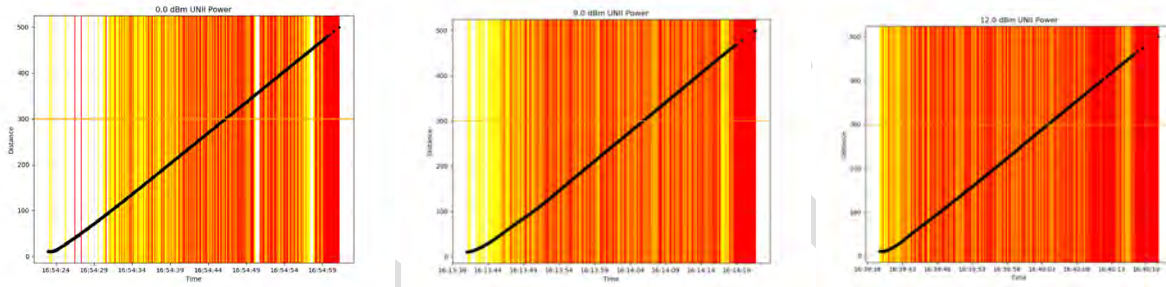
UNII EIRP: 5 dBm

14 dBm

17 dBm

Figure 9-55. Packet error rate increases as UNII power increases (DSRC EIRP=25 dBm)

Source: 20170821 Vary UNII pwr half ms avg V2 --was UNII_PowerV3.xlsx, Tab: V2V mobile Rx



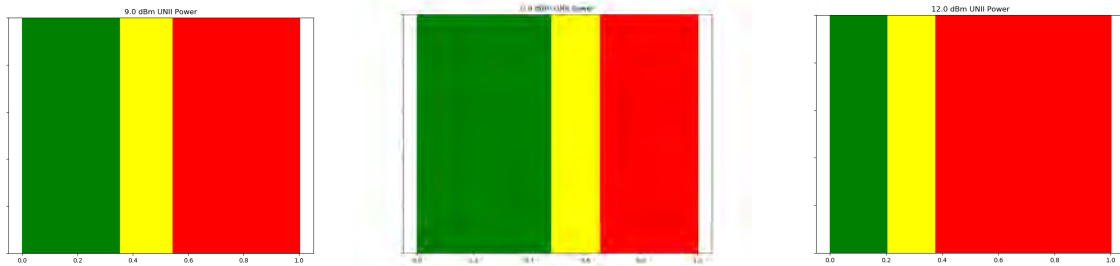
UNII EIRP: 5 dBm

14 dBm

17 dBm

Figure 9-56. Distribution of safety critical gaps worsens as UNII power increases (DSRC EIRP=25 dBm)

Source: 20170821 Vary UNII pwr half ms avg V2 --was UNII_PowerV3.xlsx, Tab: V2V mobile Rx



UNII EIRP: 5 dBm

14 dBm

17 dBm

Figure 9-57. Proportion of safety critical gaps worsens as UNII power increases (DSRC EIRP=25 dBm)

Source: 20170821 Vary UNII pwr half ms avg V2 --was UNII_PowerV3.xlsx, Tab: V2V mobile Rx

9.2.3 Effect of UNII load

All of the interference metrics tended to increase as the Wi-Fi traffic load was increased from zero to roughly 30%. Above 30% the metrics roughly held steady, confirming the analysis on inter-packet gaps in Section 4.4 . above. In the regime above 30%, with the UNII essentially offering few to no gaps large enough for a BSM to pass through, differences due to other factors like packet size became inconsistent and correlations observed at loadings from 5-30% fell apart above that range. Those things didn't matter once the DSRC traffic had no opportunities to avoid collision.

At the lowest loadings (2-5%), correlations were weak or inconsistent most likely because the gaps between packets was so large that BSMs were unlikely to collide with a Wi-Fi packet and did so very randomly. In that case, other factors didn't matter much either.

Figure 9-58, illustrates these observations with V2V data from November 2017 which shows the distance from the interferer at which the average PER exceeded 50%. You can see how this distance rapidly grows as Wi-Fi traffic load increases from 5 to 30 percent and then levels off for all higher Wi-Fi traffic loadings. The blue lines are for UNII EIRP of 17 dBm and the red are for UNII EIRP of 35 dBm showing that higher power pushed out this level of interference roughly 100 meters further. Note that greater distances are worse for DSRC.

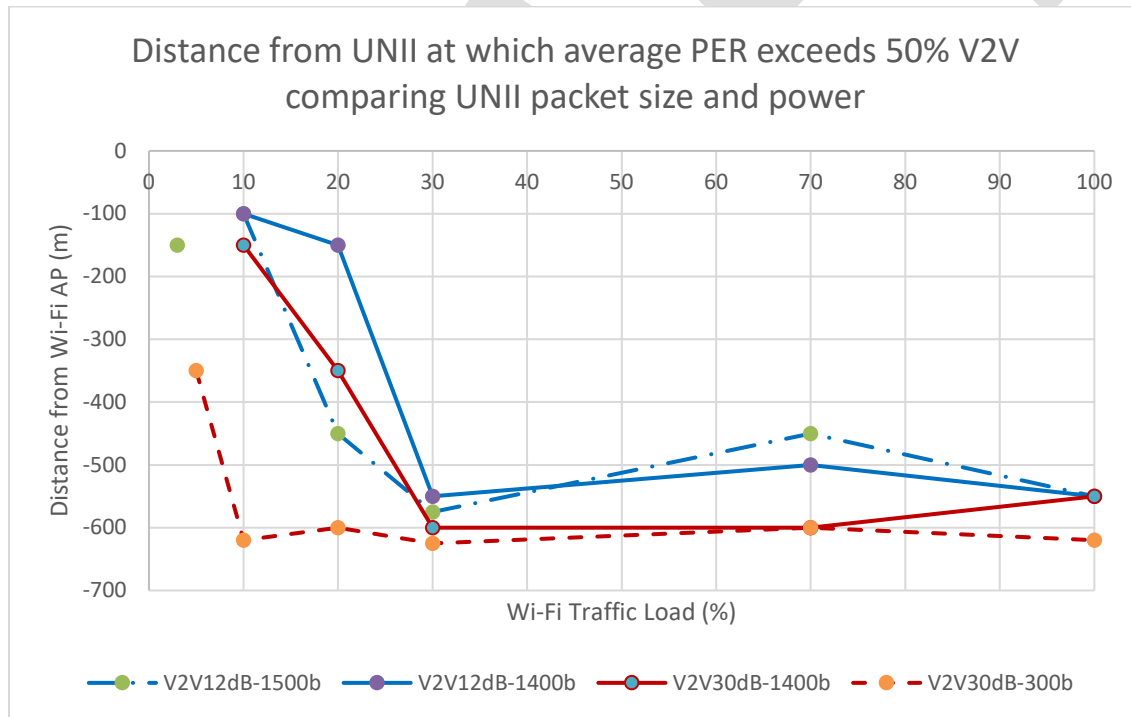


Figure 9-58. Interference to DSRC levels out for Wi-Fi traffic loads above 30%

Source: 20171101 Vary UNII Load V2b --was exl_report_20171101.xls, Tab: Plot examples

The solid lines are for 1400 byte UNII packets. The broken blue line is for 1500 byte UNII packets and the red dashed line is for 300 byte packets.

As another illustration, Figure 9-59 shows the effect of increasing the Wi-Fi traffic load on the average PER in a DSRC link. You can see regardless of line type, which conveys other factors, the strong correlation with color, which conveys loading. The thick lines are V2I data and the thin lines are V2V.

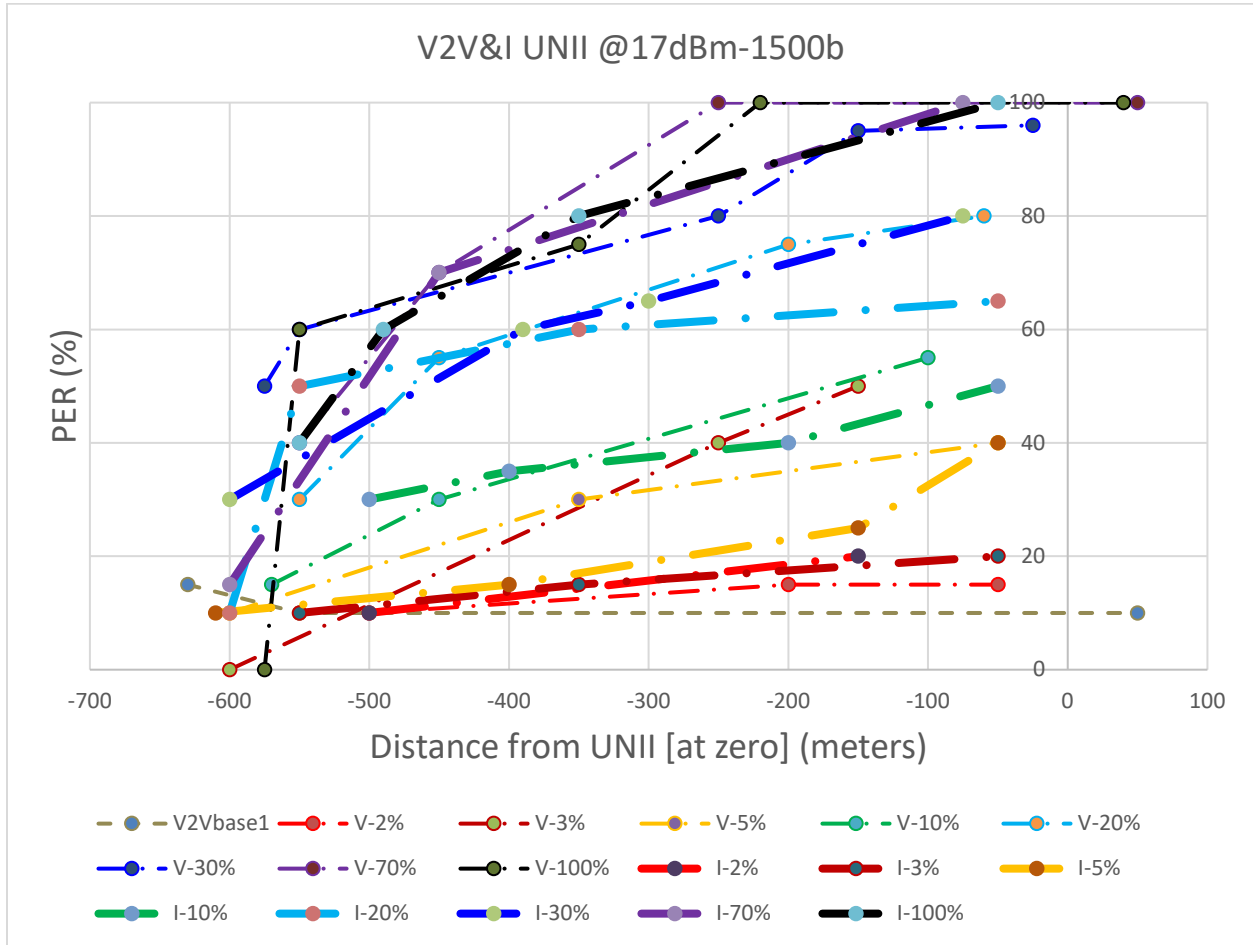


Figure 9-59. Packet Error Rate (PER) increases Wi-Fi traffic load
(V2V DSRC EIRP=25 dBm, UNII EIRP=17 dBm, 1500 byte packets)

Source: 20171101 Vary UNII Load V2b --was exl_report_20171101.xls, Tab: Plot examples

Table 9-1 is another way to look at the data in Figure 9-59 to gain insights from it. The table lists the packet error rate due to the Wi-Fi access point. The roughly 10% baseline PER has been subtracted. You can see that at very low Wi-Fi traffic loadings like two and three percent, there is interference 300 meters out but it is limited to a few percent. When the traffic consumes only 5% of the spectrum the packet collisions start to become significant. The induced error rate ranges from 5 to 30% and extends to over 500m. You can also see that as the Wi-Fi traffic load increases, both the packet error rate and the spread get larger (steeper slope to the curve). The latter point means that interference increases more rapidly as you get nearer to the access point when there is more Wi-Fi traffic.

Table 9-1. Ballpark Packet Error Rates above baseline at select distances as Wi-Fi traffic increases (from Fig 9-59)

Wi-Fi load: Distance from AP	2 & 3%	5%	10%	20%	30%	70%	100%
500 m	~0	~5%	~20%	~40%	~45%	~40%	~50%
300 m	~5%	~20%	~30%	~55%	~60%	~80%	~75%
100 m	~10%	~30%	~40%	~60%	~80%	100%	100%

Figure 9-60 provides another way to see the effect of increasing Wi-Fi traffic load on the DSRC link. You can clearly see how consecutive gaps caused by missing 3-5 BSMs (yellow) or more than 5 BSMs (red) increase as the load increases up to 30% at which point things level out. Safety critical gaps, which start to show up at the 10% load 200 meters from the access point become prevalent at 20% traffic load 400 meters from the access point, which is untenable under any circumstance.

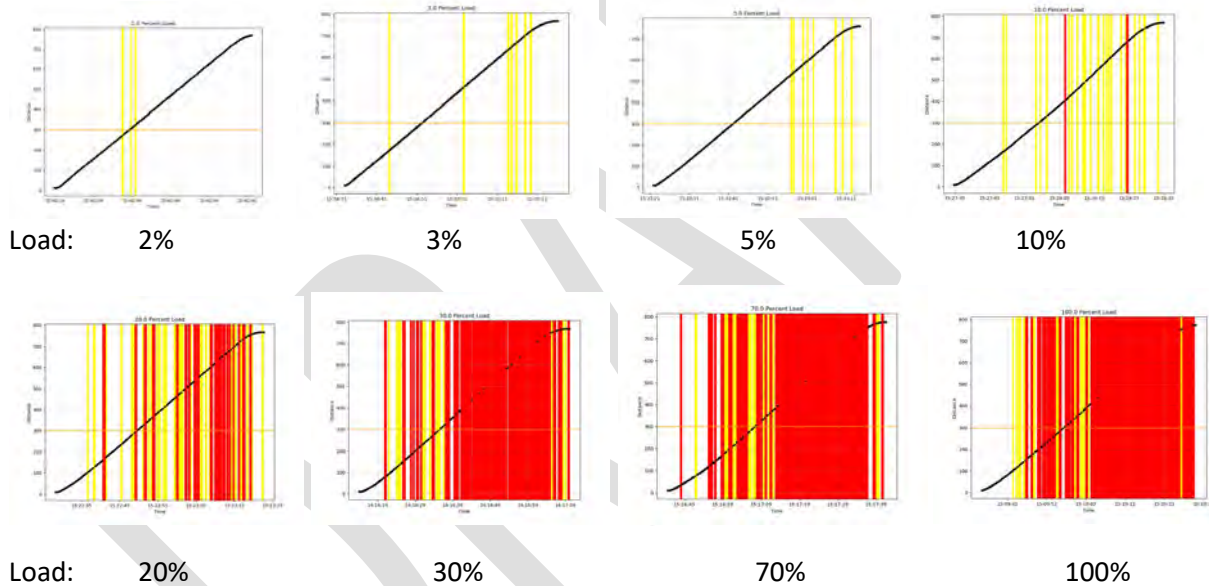


Figure 9-60. Safety critical gaps increase with Wi-Fi traffic load
(V2V DSRC EIRP=25 dBm, UNII EIRP=17 dBm, 1400 byte packets)

Source: 20171101 Vary UNII Load V2b --was exl_report_20171101.xls, Tab: V2V UNII PL1400

9.2.4 Effect of UNII packet size

In the inter-packet analysis of Section **Error! Reference source not found.**, our calculations and lab measurements show that for a given data rate, breaking it up into a 1400 byte Ethernet traffic stream should provide the largest gaps between packets, so the least interference to DSRC. The 1500 byte Ethernet stream resulted in more data packets and acknowledgments cutting into the gaps than offered by the cleaner 1400 byte packet stream. The 300 byte packets left much smaller gaps so was the most disruptive, being disruptive at lower traffic loadings than the other packet sizes.

The field measurements did not always show the 1500 byte mixed packet stream to be worse than 1400 byte packets. In Figure 9-61 the broken 1500 byte lines are not always at a higher PER than the solid 1400 byte lines of the same color (traffic load). The inconsistencies may be due to the much larger uncertainties and variation in the field measurements.

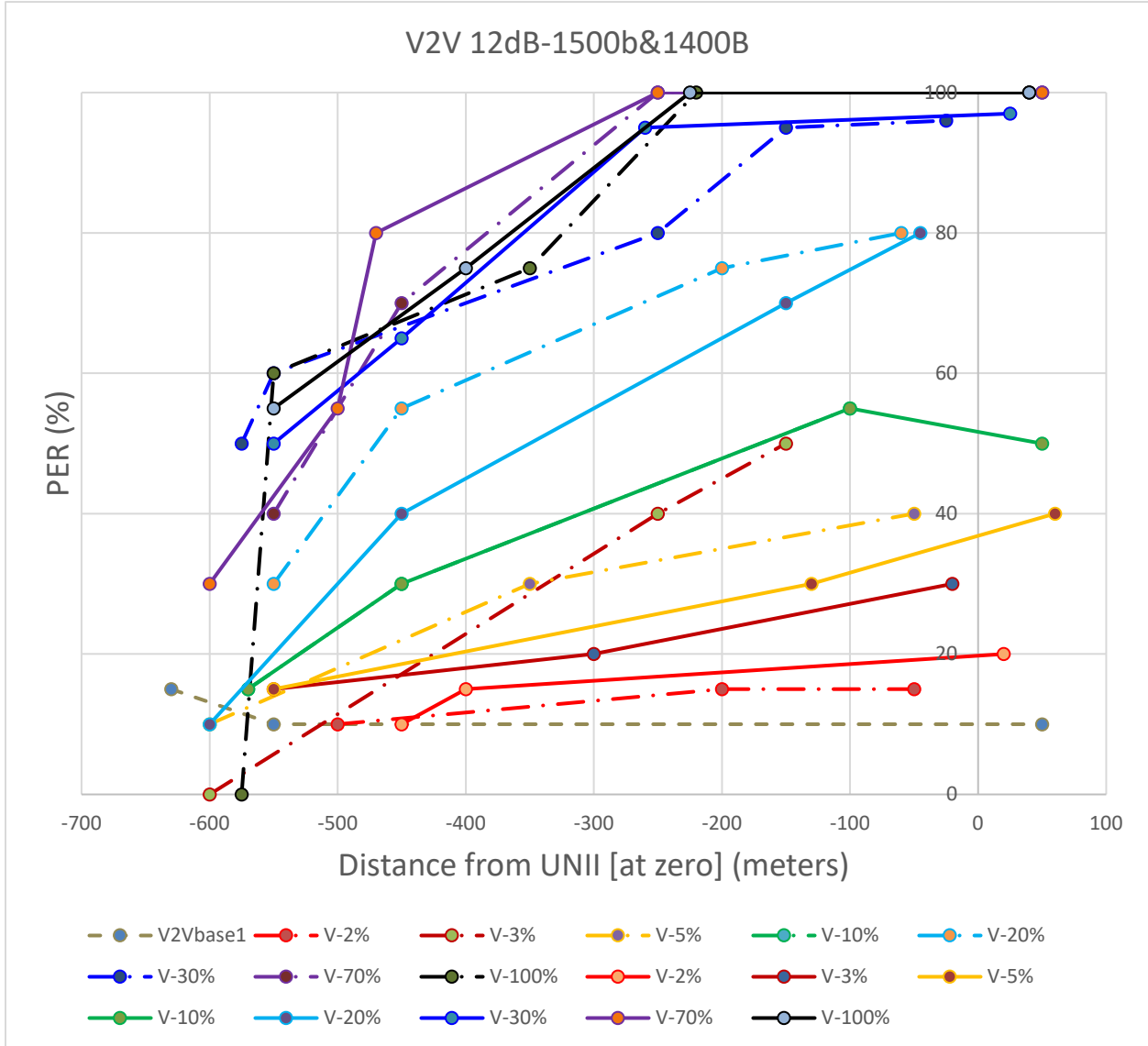


Figure 9-61. Comparison of PER interference to DSRC by 1400 byte (solid) and 1500 byte (broken) Wi-Fi packets (V2V DSRC EIRP=25 dBm, UNII EIRP=17 dBm)

Source: 20171101 Vary UNII Load V2b --was exl_report_20171101.xls, Tab: Plot examples

The 300 byte packet streams were clearly much more disruptive as shown by Figures 9-62 and 9-63 (agreeing with our predictions). Note that at a given distance from the interferer, the PER for the dashed line (300 byte) is always higher than for the solid line (1400 byte) of that same color. Color represents Wi-Fi traffic load percent.

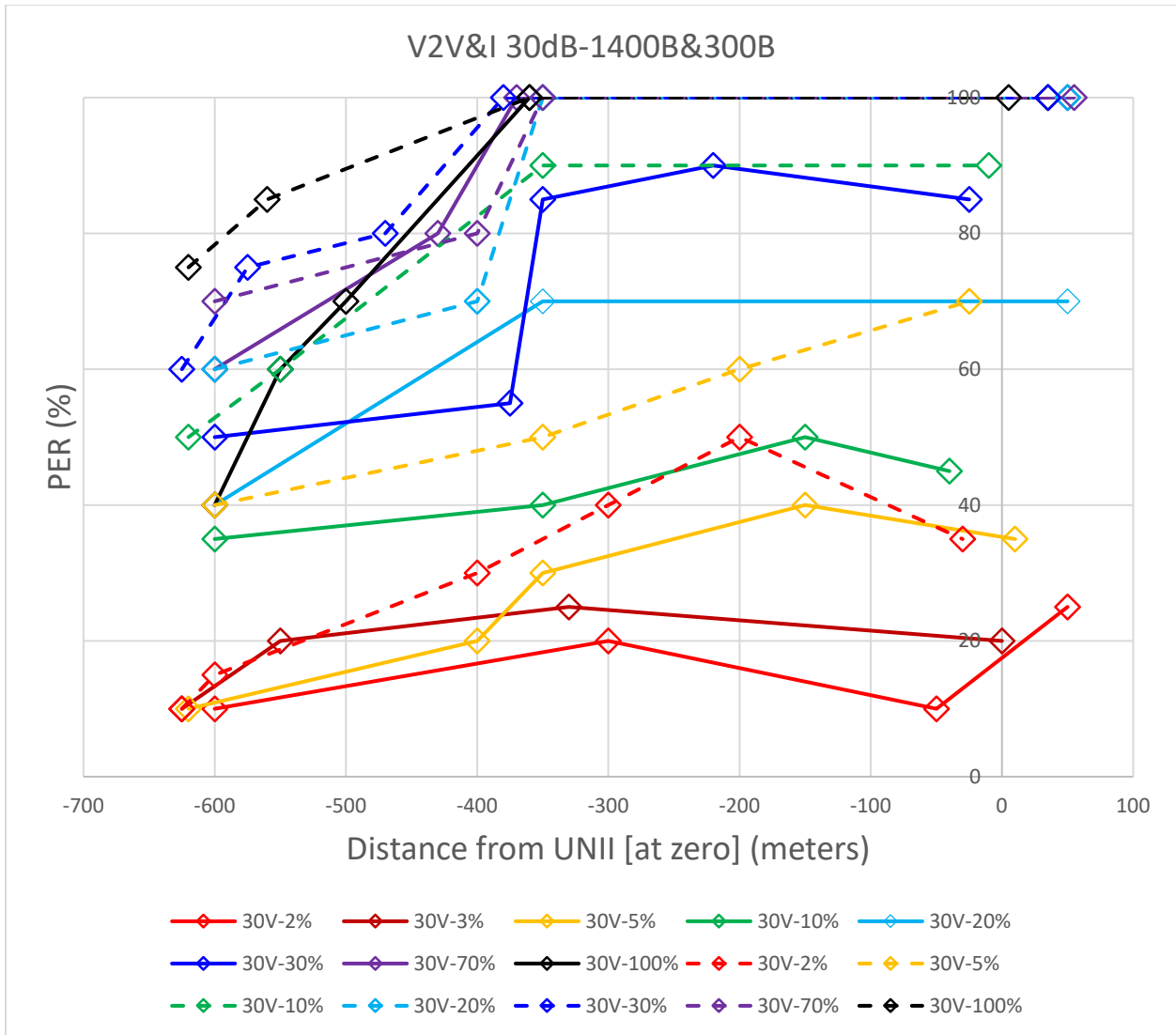


Figure 9-62. Comparison of PER interference to DSRC by 1400 byte (solid) and 300 byte (dashed) Wi-Fi packets (V2V DSRC EIRP=25 dBm, UNII EIRP=35 dBm)

Source: 20171101 Vary UNII Load V2b --was exl_report_20171101.xls, Tab: Plot examples

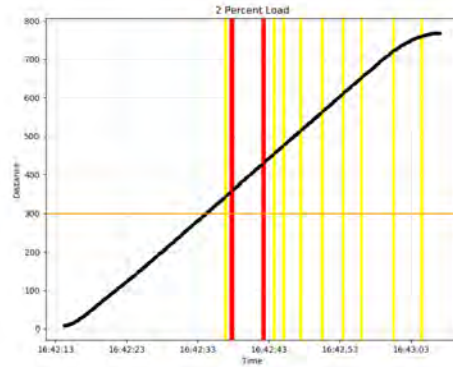
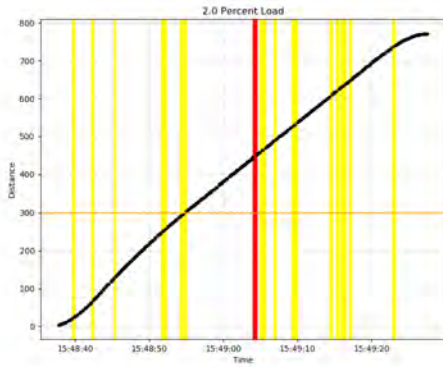
Figure 9-63 shows how the distribution of packet error rate is affected by the Wi-Fi packet size and loading. The x-axis is the time of a data run and the y-axis is distance from the start point and RSU. The time and location when 3-5 consecutive BSMs are missed are in yellow and marked in red when more than 5 BSMs are missed. We omitted the 100% loaded runs because, as noted above, they offer the same blockage as the 70% loaded runs. It is clear for every loading that the 300 byte Wi-Fi packet stream causes more safety critical gaps. Moreover, with 300 byte packets the DSRC communication becomes untenable with a 10% Wi-Fi traffic load. With a 1400 byte traffic stream that doesn't happen until between 20 and 30% Wi-Fi traffic load.

Wi-Fi Packet size:

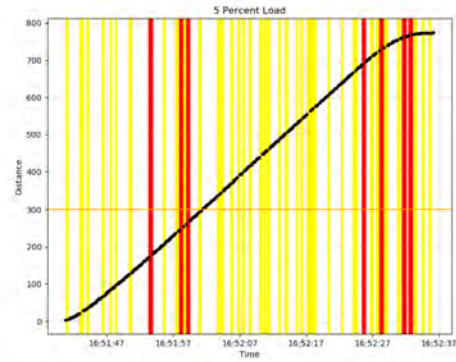
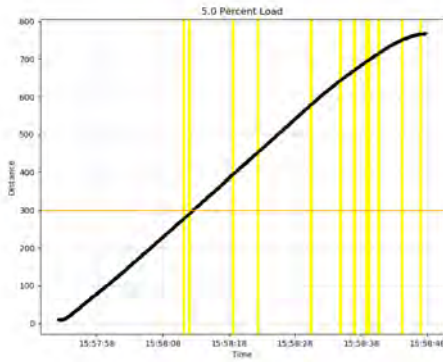
1400 bytes

300 bytes

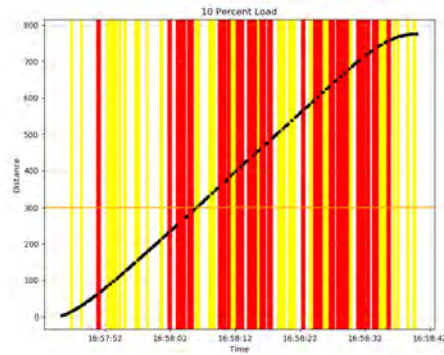
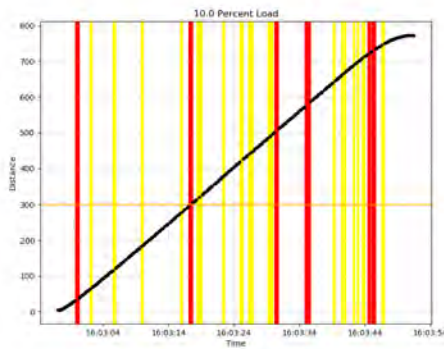
2% Load:



5% Load:



10% Load:



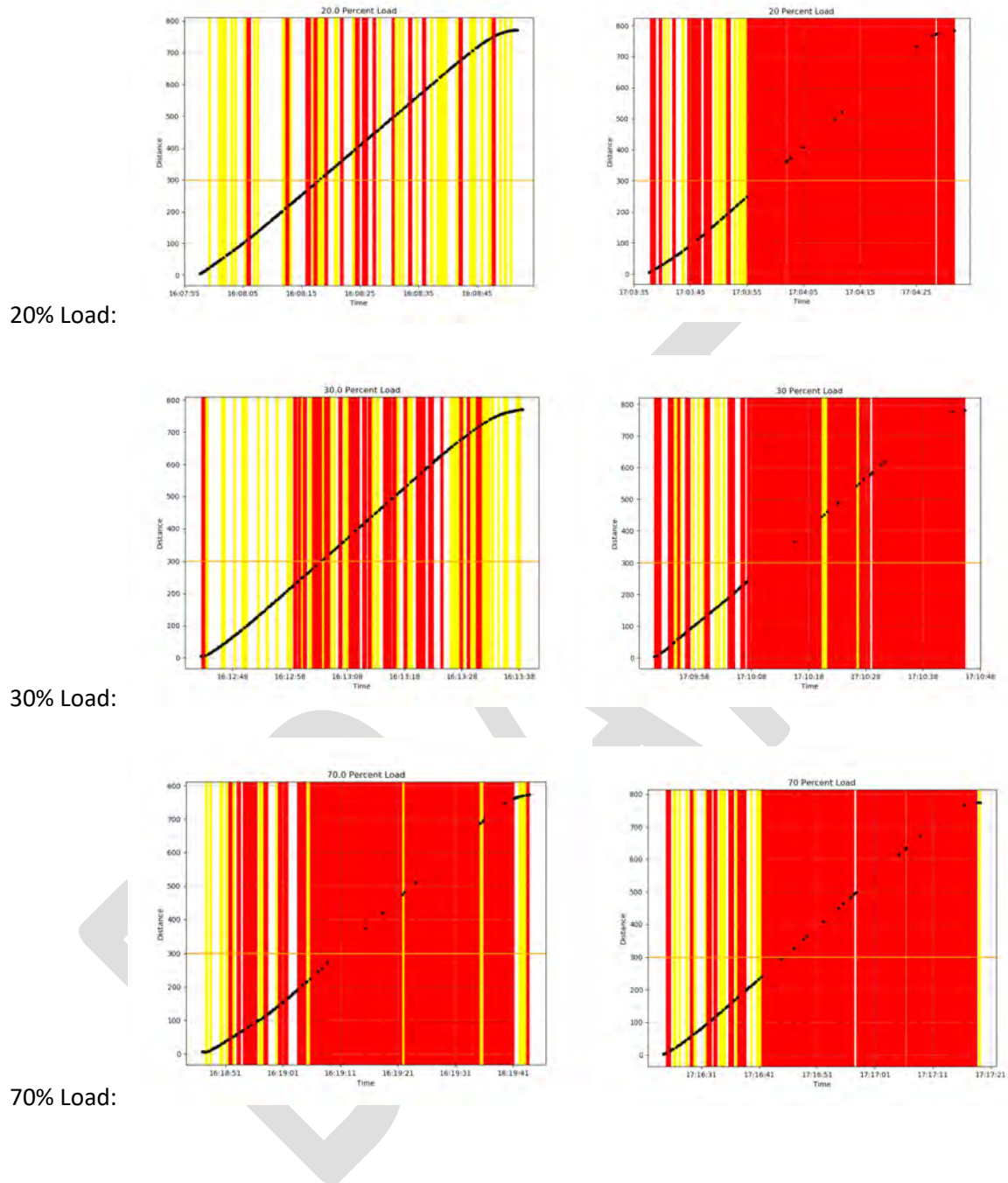


Figure 9-63. Safety critical gaps worsen with smaller with Wi-Fi packets
(V2I DSRC EIRP=25 dBm, UNII EIRP=30 dBm)

Source: Effect of packet size and loading v1b.xlsx

9.2.5 Effect of UNII traffic generation (Periodic versus Poisson)

As described in section 4.2.2 we tested with both Periodic and Poisson Wi-Fi traffic. As described in that section and section 4.4, the primary impact of the traffic distribution was the availability of inter-packet gap time for BSMs to slip through in between Wi-Fi packets. To see how well the calculations and lab measurements described in those sections translated to the interference to DSRC, we ran a series of V2V interference tests of each distribution under various traffic loads.

The fixed parameters were as follows. The transmit power of both the DSRC and UNII testbed were the same with an EIRP of 20 dBm. The DSRC devices operated on channel 172 with a repetition rate of 100 Hz. The UNII test bed operated on the overlapping 20 MHz Wi-Fi channel 173, the repetition rate governed by the loading selected for each run.

The static vehicle was the DSRC transmitter, the mobile vehicle the receiver, which drove from the static vehicle to past the UNII testbed 1600 meters or half a mile away and then came back.

Consistent with the earlier analysis in Chapter 4 and our lab measurements, Figures 9-64 and 9-65 show that at very low levels of Wi-Fi traffic the Periodic and Poisson distributions caused roughly the same interference because the inter-packet gaps were large and plentiful. The thick lines in both plots are the 3 second rolling average PER. The thinner, fainter lines are the 500 ms rolling averages which capture the variability around the 3 second averages. In this case, both the 3 second average PER (thick lines) and 500 ms average PER (thin lines) from both distributions essentially lie on top of each other. The distributions caused the same interference.

What is interesting to note though is that even at these low radio traffic levels, the UNII interferer started causing packet errors 900 meters away and they rose to 10-15% for the 2% load, and 20% PER for the 3% load for most of the 600 meters in front of the UNII testbed.

Legend for Figures 9-64-9-70

Load	Periodic		Poisson	
	0.5s avg	3s avg	0.5s avg	3s avg
30%	=====	=====	=====	=====
20%	=====	=====	=====	=====
15%	=====	=====	=====	=====
10%	=====	=====	=====	=====
5%	=====	=====	=====	=====
3%	=====	=====	=====	=====
2%	=====	=====	=====	=====

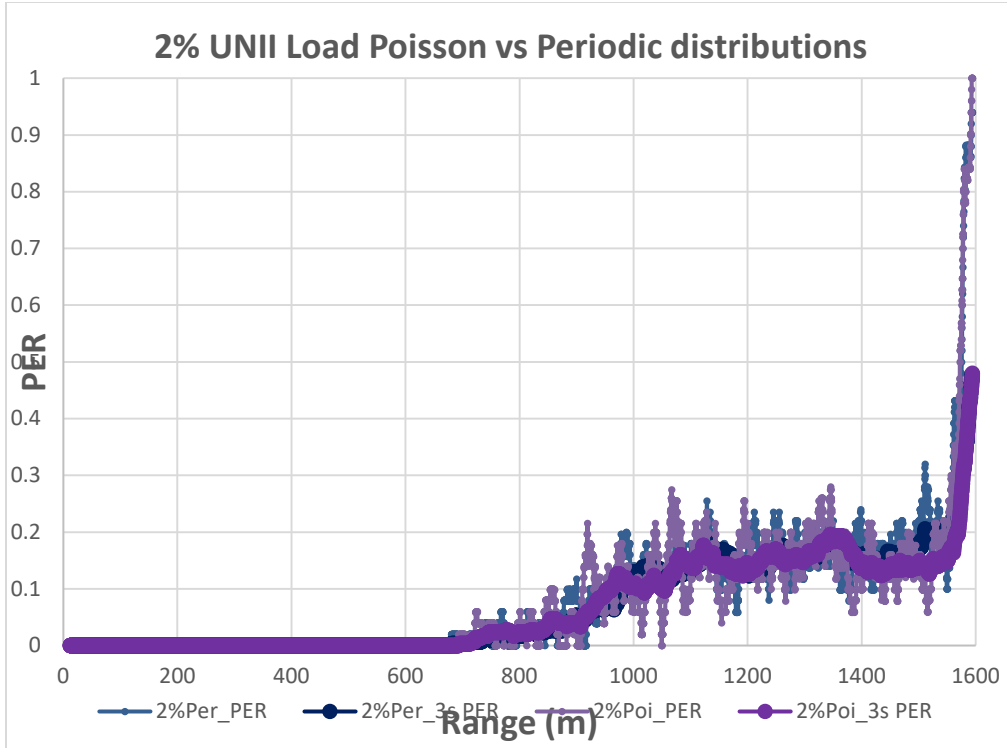


Figure 9-64 Comparison of Periodic and Poisson induced DSRC Packet Error Rate for 2% traffic load

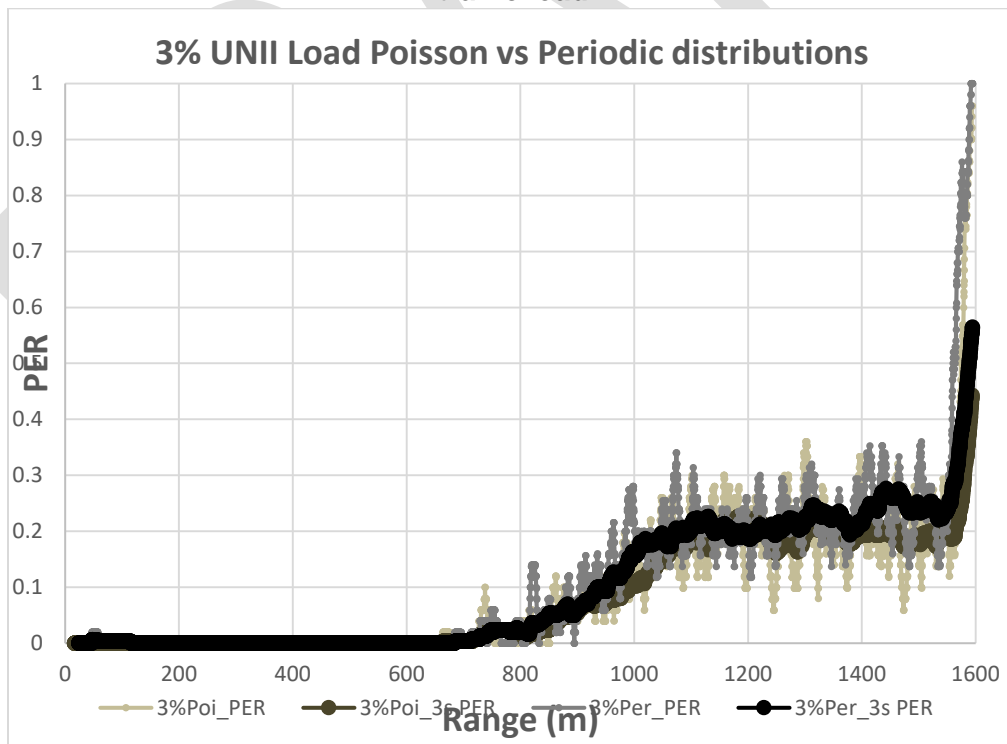


Figure 9-65. Comparison of Periodic and Poisson induced DSRC Packet Error Rate for 3% traffic load

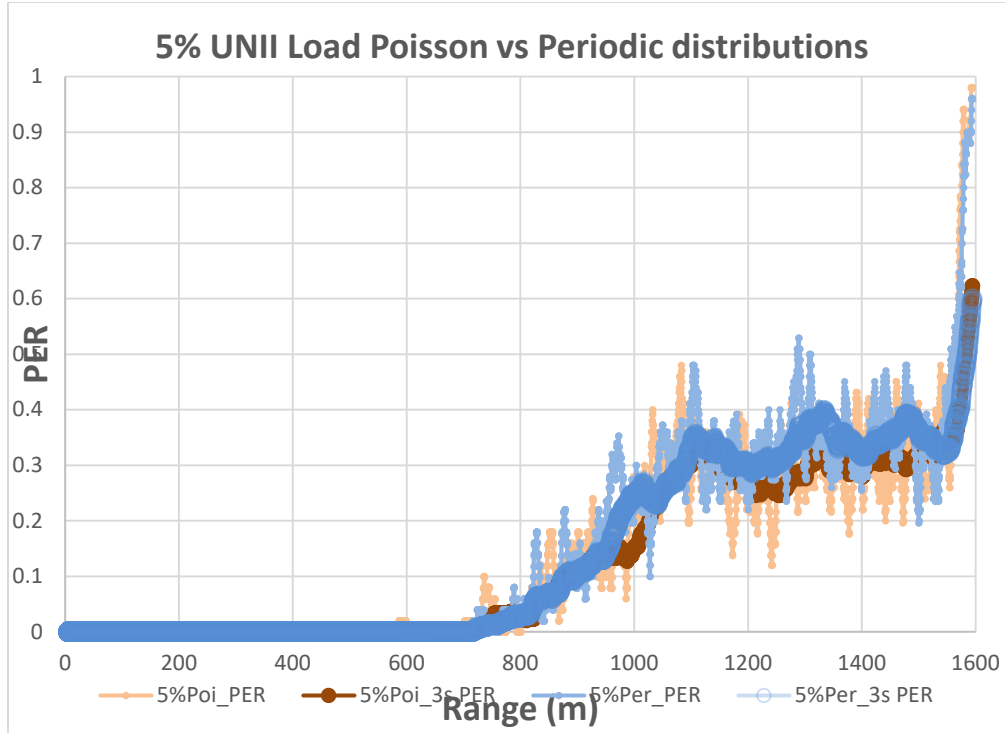


Figure 9-66. Comparison of Periodic and Poisson induced DSRC Packet Error Rate for 5% traffic load

At 5% traffic load it appears that the Poisson distribution is causing slightly fewer packet collisions (Figure 9-66). Even though Table 3 in Section 4.4 shows that the average gap for the Periodic distribution is 4.2 ms as opposed to 1.8 ms for the Poisson distribution at 5% load, it also shows that the maximum gap size appearing in the Poisson distribution is 30 ms wide. That seems to more than offset the Poisson distribution’s smaller average inter-packet gap.

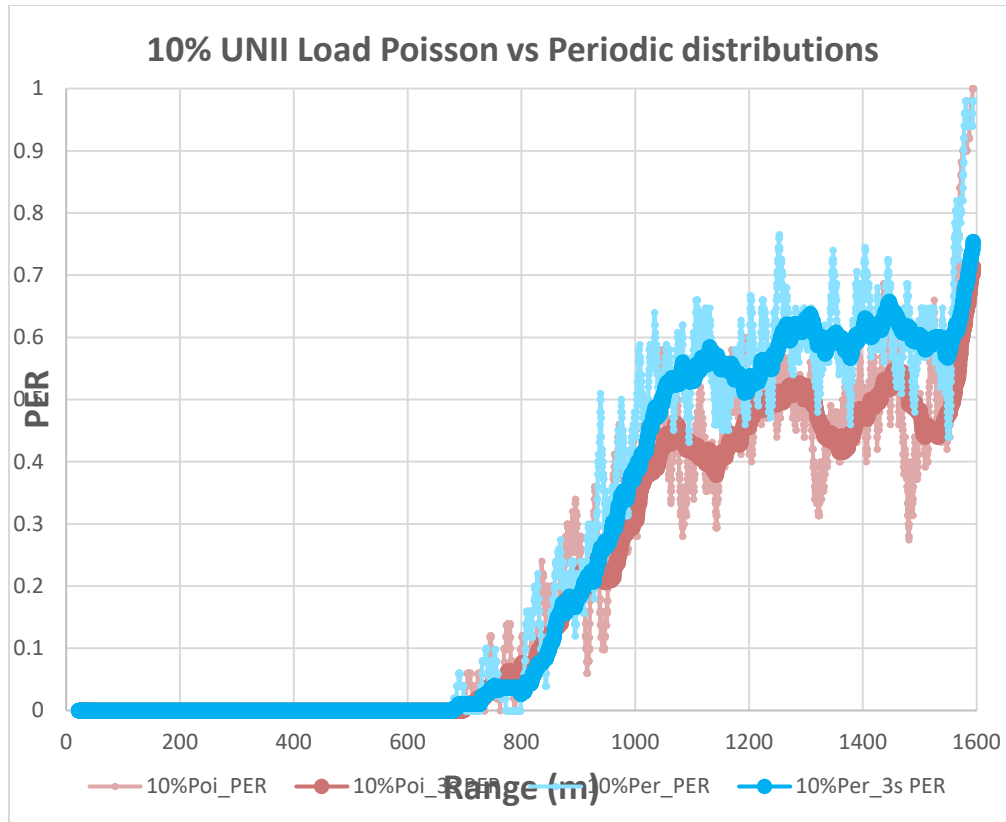


Figure 9-67. Comparison of Periodic and Poisson induced DSRC Packet Error Rate for 10% traffic load

Figures 9-67 and 9-68 show that at the moderate traffic loads of 10% and 15%, the Periodic distribution causes 10-20% higher packet error rate. A 10% load corresponds to a Periodic gap size of 2 ms and Poisson average gap size of 0.8 ms but with maximum Poisson gaps up to 19 ms (Table 4-3 in section 4.4.2). That means that the Periodic distribution gaps are roughly 4-5 times larger than a BSM whereas the average Poisson gap is barely twice as long as a BSM, but that long tail of larger gaps that can be up to 76 times larger than a BSM clearly lets 10-20% more BSMs slip through Poisson anyway. These actual interference measurements confirm the prediction of how the choice of Wi-Fi message traffic distribution would affect DSRC signals made by the lab measurements and calculations in Chapter 4.

Also note how much interference there is at these moderate traffic loadings. With 10% traffic load the PER ranges from 40-60%. So even with average gaps a bit larger than the BSMs, there are still plenty of collisions at this moderate traffic load. With 15% traffic load the PER for the two distributions range from 60-80% in the 600-meter space in front of the interferer.

Going back to the fence analogy presented in Chapter 4, this is like randomly throwing (not aiming) a ball at two fences, one with gaps 4 times wider than your ball, the other with gaps two times wider but random gaps up to 76 times larger. You are hitting a fence picket over half the time anyway.

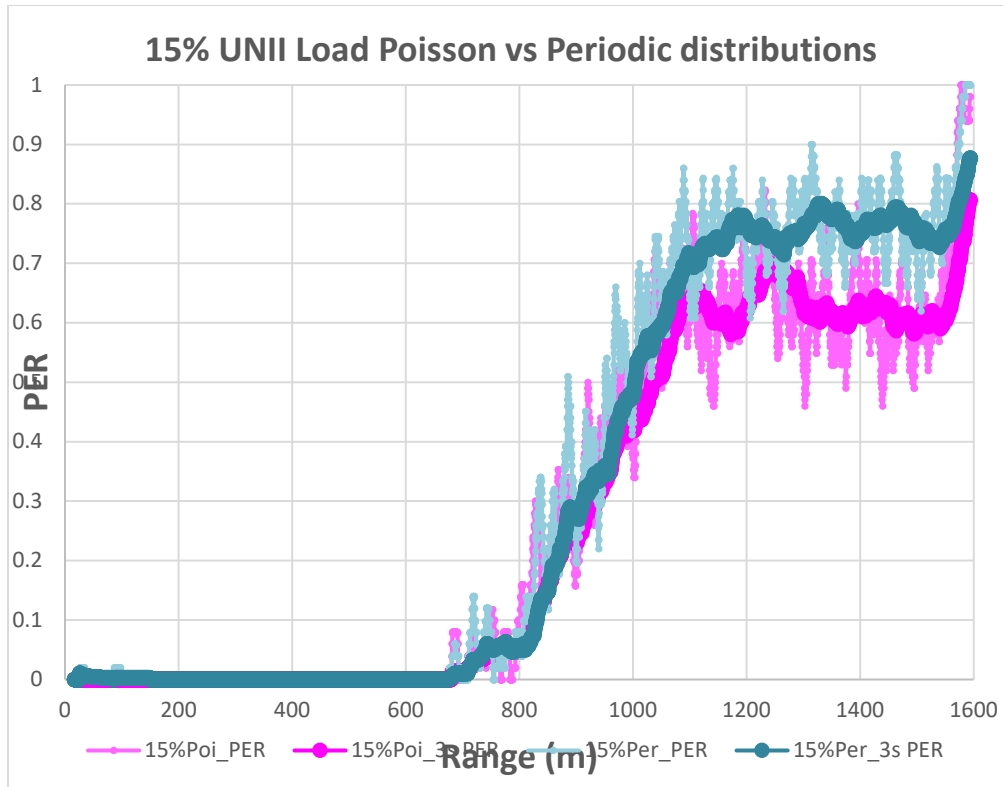


Figure 9-68. Comparison of Periodic and Poisson induced DSRC Packet Error Rate for 15% traffic load

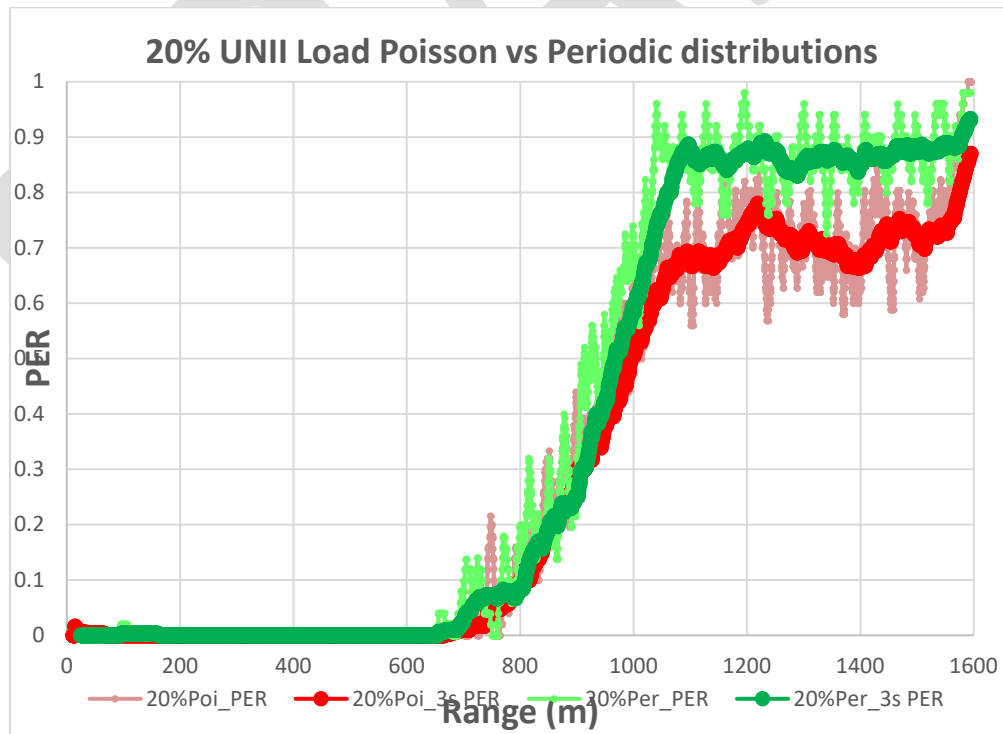


Figure 9-69. Comparison of Periodic and Poisson induced DSRC Packet Error Rate for 20% traffic load

Figures 9-69 and 9-70 show the results of the two higher load cases tested, 20% and 30% respectively. Again, the Poisson distribution let 10-20% more BSMs through than the Periodic distribution for both cases. At 20% load, the periodic distribution inter-packet gap is now just 0.9 ms, roughly twice as large as a BSM and essentially knocking 85% of them out in the 600-meter space in front of the interferer.

The average Poisson gap is now about the size of a BSM or less (0.4 ms), but the maximum Poisson gap at 2.4 ms is 5 times larger than a BSM. So Poisson at 20% load screens out roughly 70% of the BSMs in the 600-meter space in front of the interferer. So the Poisson distribution at 20% load interferes the same as the periodic distribution at 15% load (compare Figures 9-68 and 9-69).

At 30% load, the average inter-packet gap of the periodic distribution is now 0.5 ms and roughly the size of a BSM. Consistent with our initial sensitivity tests DSRC is completely blocked with 100% PER in the 500-meter space in front of the interferer. At any higher periodic loading there are no gaps large enough for a BSM to avoid collision.

The average Poisson inter-packet gap at 30% traffic load is now about half the size of a BSM but there are random gaps still larger than the BSM, hence the 10-15% of BSMs that still get through. Regardless 85-90% PER is untenable for DSRC communications.

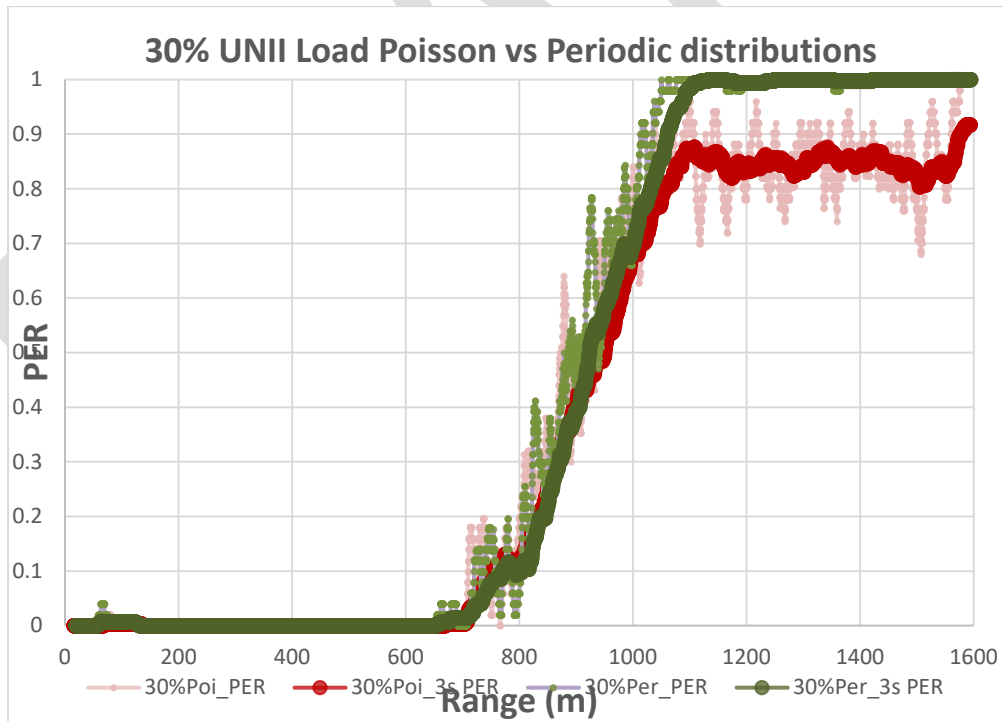


Figure 9-70. Comparison of Periodic and Poisson induced DSRC Packet Error Rate for 30% traffic load

Figure 9-71 shows DSRC packet error rate for periodic Wi-Fi traffic as a function of traffic load. Figure 9-72 shows the same for Poisson Wi-Fi traffic. Together these two plots provide a means to scale interference measurements made with periodic Wi-Fi traffic to what the equivalent result would be for Poisson, or randomly generated user traffic.

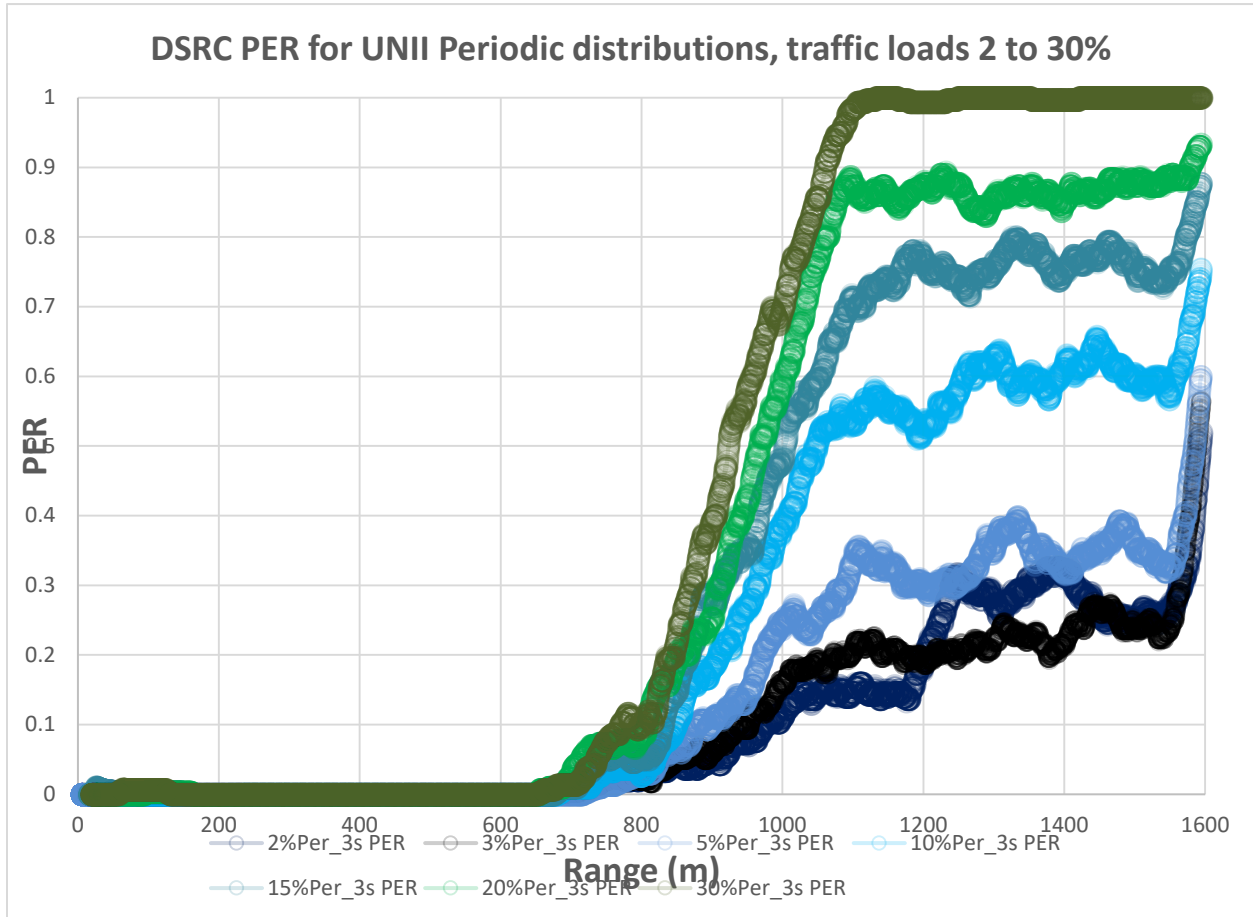


Figure 9-71. DSRC Packet Error Rate caused by Periodic distribution Wi-Fi traffic as a function of traffic load

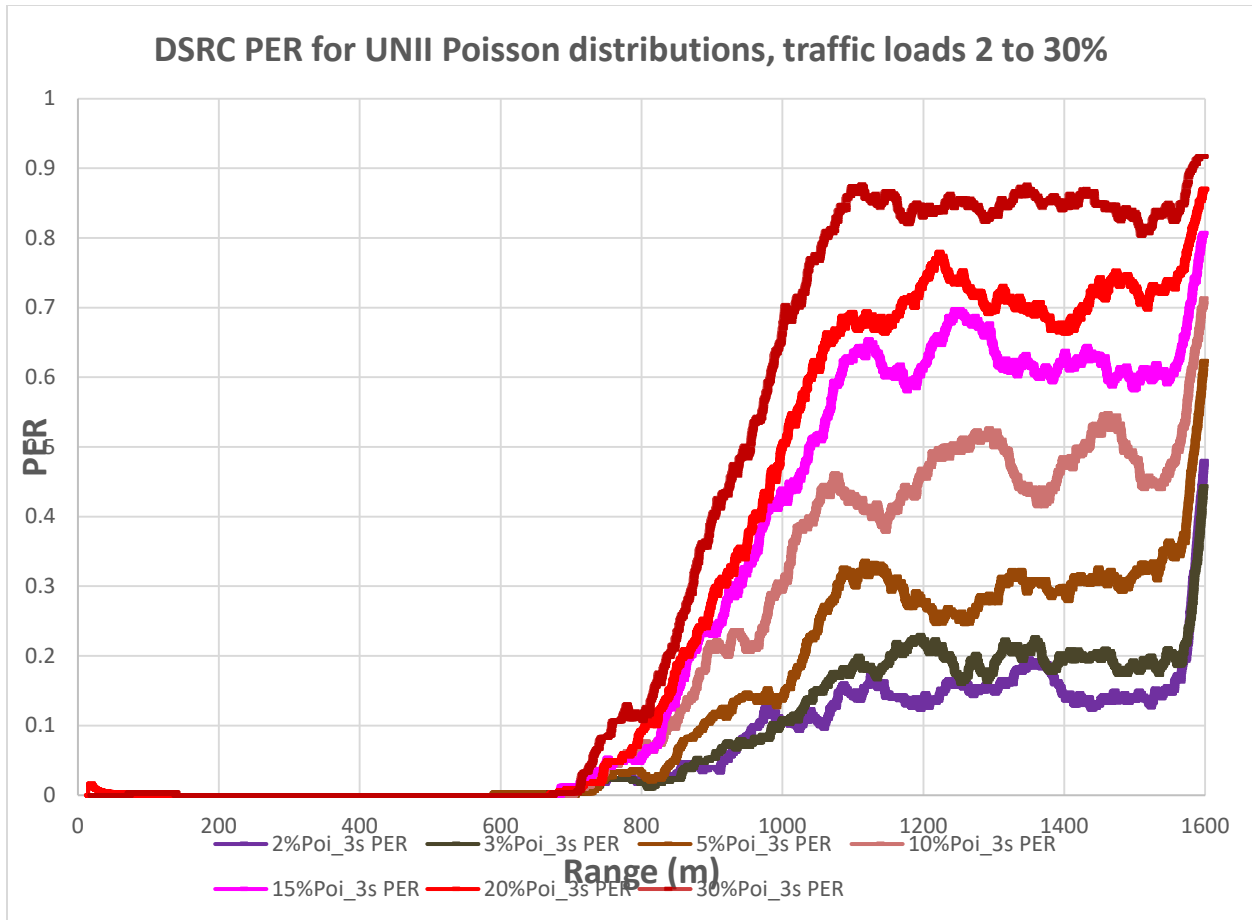


Figure 9-72. DSRC Packet Error Rate caused by Poisson distribution Wi-Fi traffic as a function of traffic load

Figure 9-73, shows the plots from Figures 9-71 and 9-72 layered together. It is hard to look at but you can use it to depreciate the DSRC PER due to a specific periodic Wi-Fi traffic distribution to its Poisson equivalent. Roughly speaking, at the higher loads (20-30%) the periodic distribution PER should be reduced about 15% for the Poisson equivalent, reduced about 10% for moderate loads (10-20%), no more than 5% for the 5% traffic load and not corrected for lower loads. These corrections are for the zone within 500 meters of the interferer with equivalently powered DSRC and UNII spaced half a mile apart. Some thought or additional measurements would be needed to scale in other conditions but this data provides ballpark results that bound the kind of corrections that would be made.

The most basic conclusion is that interference due to more realistic Poisson message traffic will be less than periodic traffic, but reduction on the order of 10-20% is not enough to materially affect conclusions about where the UNII interference will be untenable for DSRC. We provide a means to scale between periodic and Poisson traffic distributions here.

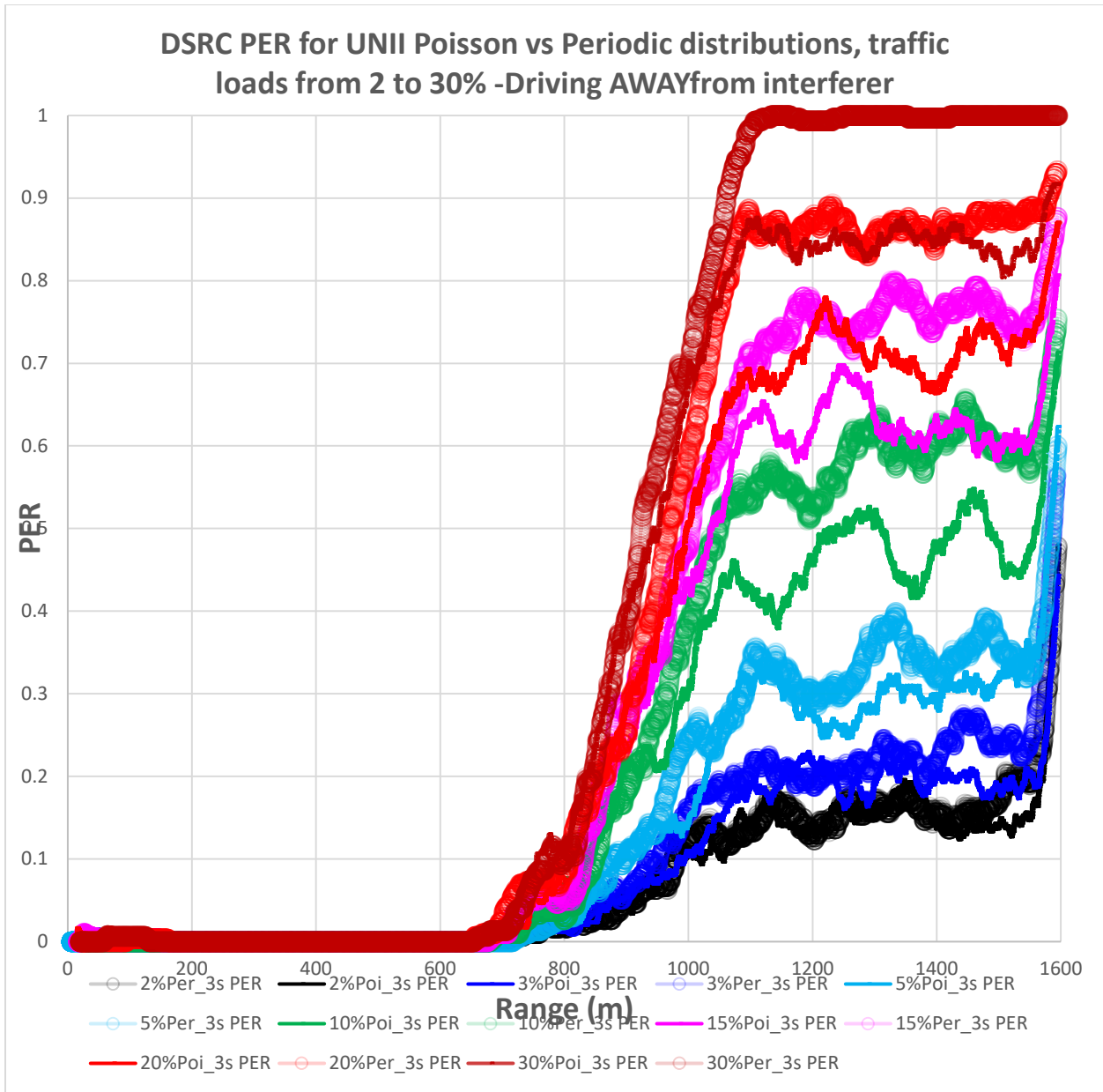


Figure 9-73. Comparison of the DSRC Packet Error Rates induced by Periodic and Poisson distributions as a function of traffic load vehicle driving away

Load	Periodic	Poisson
30%	[Red Solid]	[Red Dashed]
20%	[Red Solid]	[Red Dashed]
15%	[Magenta Solid]	[Magenta Dashed]
10%	[Green Solid]	[Green Dashed]
5%	[Cyan Solid]	[Cyan Dashed]
3%	[Blue Solid]	[Blue Dashed]
2%	[Black Solid]	[Black Dashed]

The other obvious conclusion is that even at moderate traffic loads the UNII causes significant interference to DSRC as far as 500 meters away with typical radio settings.

As an example, Figure 9-74 shows the specific interference measurements for Poisson distributed UNII message traffic at 10% traffic load. Note that SNR drops below the 12 dB safety app benchmark 500 meters from the UNII access point. The PER is mostly above 50% in that space, and safety critical gaps become prevalent 600 meters out.

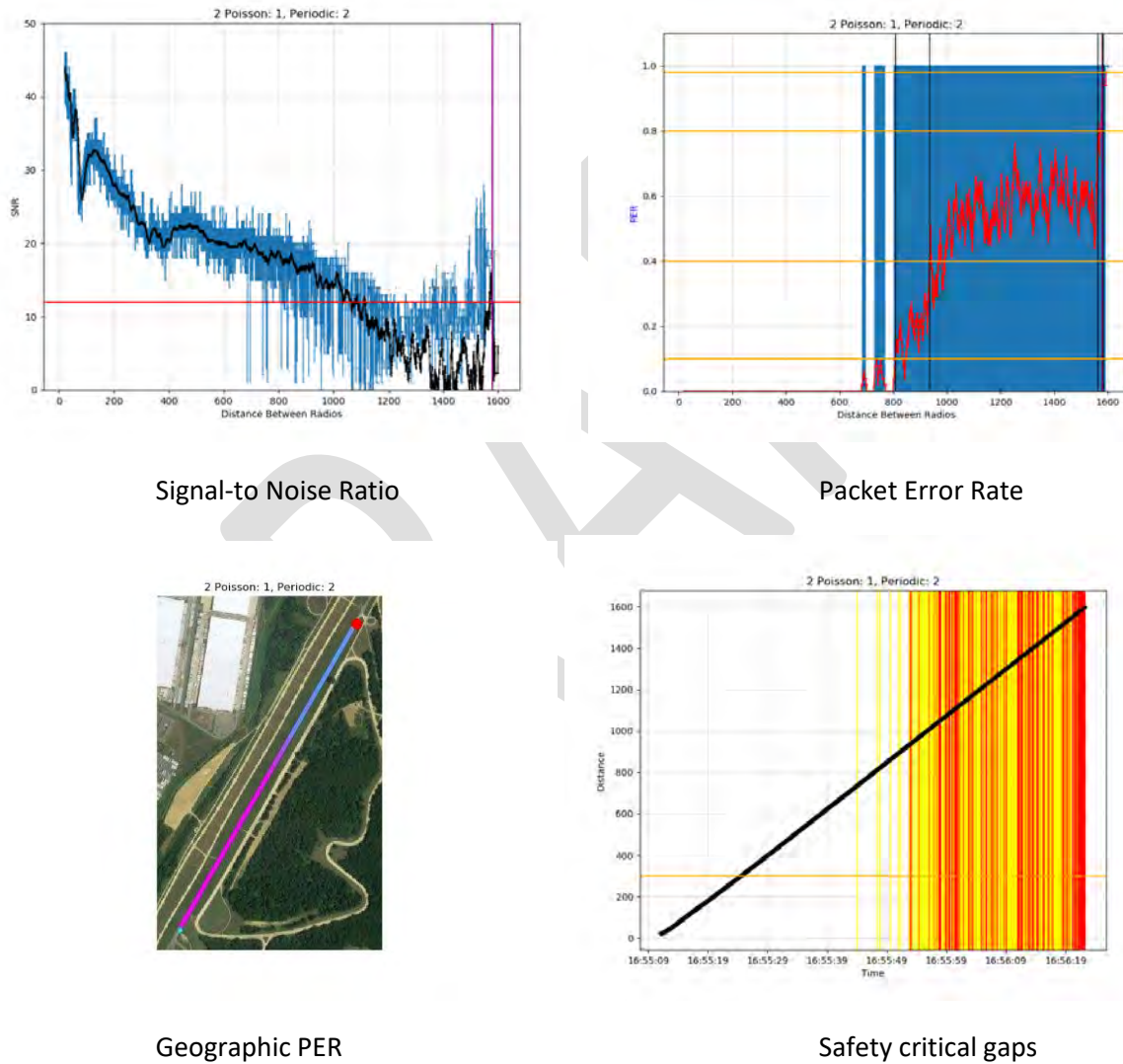


Figure 9-74. Interference to DSRC [EIRP=20 dBm] by UNII [EIRP=20 dBm, 10% Poisson traffic]

9.3 Packet suppression via EDCA

DSRC experienced packet suppression at the transmitter. DSRC was never completely shut out, but the UNII transmissions at a power of 9 dBm caused gaps serious enough to be problematic for safety applications, even when the UNII devices were at significant distances. Figure 9-75 illustrates this interference problem.

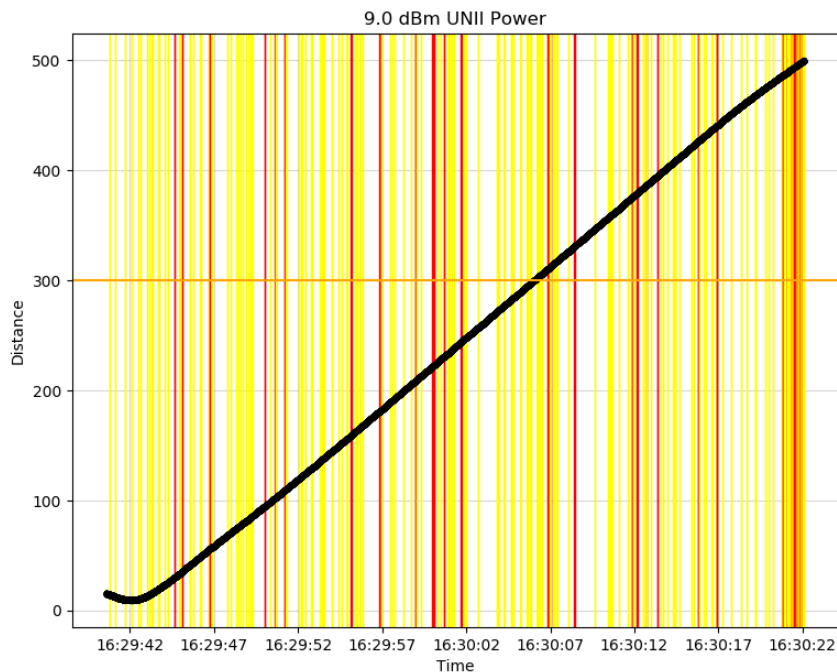


Figure 9-75 Serious gaps with interferer close to DSRC (50-100 meters); UNII EIRP at 17 dBm

Simulating DSRC and UNII handheld devices.

Setting the lowest UNII power (0 dBm) and DSRC at lowest transmit power of 0 dBm (so EIRPs of 5 dBm for both) simulates two devices operating with a few mW transmit power which is typical of handheld devices. UNII loading was high (70%).

Figure 9-76 shows DSRC transmissions were completely suppressed over 200 meters from the interferer (located by the purple line at 575m). The onset of interference develops very quickly going from insignificant to total interference in just 75 meters.

Note also that even though significant gaps develop and overwhelm the transmission in this region 200-300 meters in front of the interferer, there are still isolated instances of significant gaps much further out that do not correlate with the DSRC ground bounce nulls.

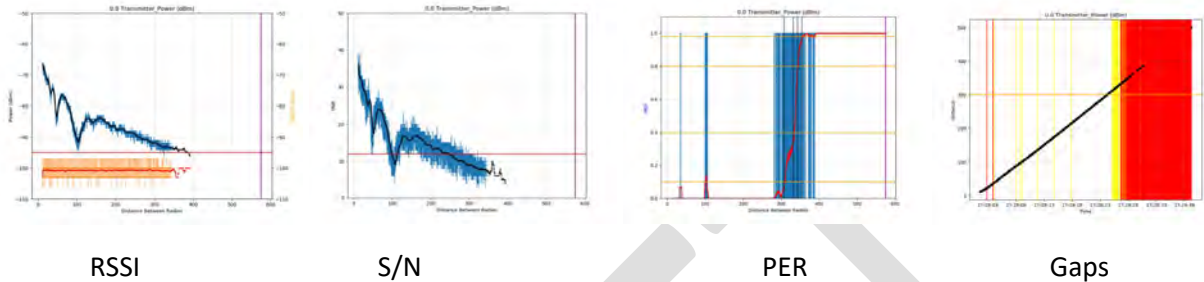


Figure 9-76. Interference by CCA suppression to DSRC handheld transmitting near a Wi-Fi handheld

Source: 20170821 Vary DSRC pwr --was Transmitter_Power_V3.xlsx; V2V mobile Tx tab

At the other extreme when the DSRC power was turned up to 15 dBm (EIRP 20 dBm) with the UNII still left at 0 dBm, more than ten times less power than DSRC, the DSRC is still affected when it is close to the interferer. Figure 9-77 shows PER climbing to 75% roughly 40 meters from the interferer. Notice also that even with the larger power differential, safety critical gaps pop up sporadically as far as 500 meters from the interferer.

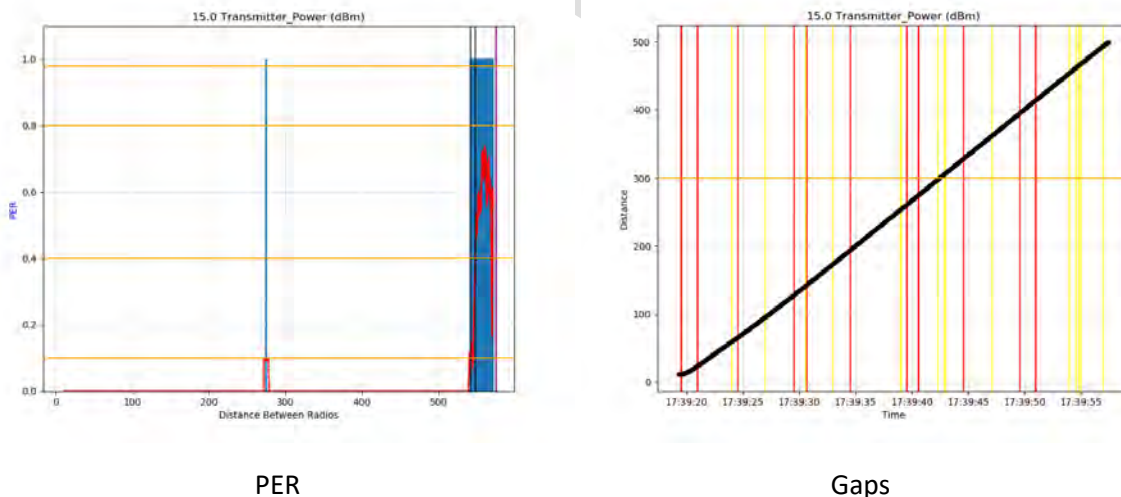


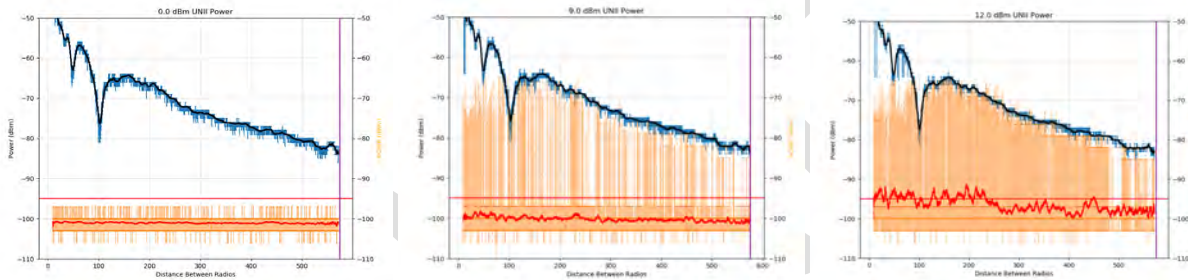
Figure 9-77. Interference by CCA suppression to full power DSRC transmitting near a Wi-Fi handheld

Source: 20170821 Vary DSRC pwr --was Transmitter_Power_V3.xlsx; V2V mobile Tx tab

packet RSSI values and the black trace is the 500 ms average. Similarly, the tan lines are the packet-by-packet noise measurements with the red trace being the 500 ms noise power average. That is, the average across 5 BSMs.

If you pick any distant point from the interferer (purple line) you can see how the noise power increases as the interferer transmit power increased from 0 dBm to 9 dBm and then 12 dBm. Also notice how the maximum tan individual packet noise measurements increase greatly, almost to the level of the DSRC signal. Moreover, as the UNII power increases the fraction of very high noise measurements increases as shown by the density of tan color. The red average noise trace creeps upward correspondingly as the UNII power increases.

Figure 9-81 plots DSRC signal-to-noise. The blue lines show the S/N for each packet received and the black trace is the 500 ms average. A close inspection shows how the S/N decreases as the interferer power increases even though it is a single interfering radio.



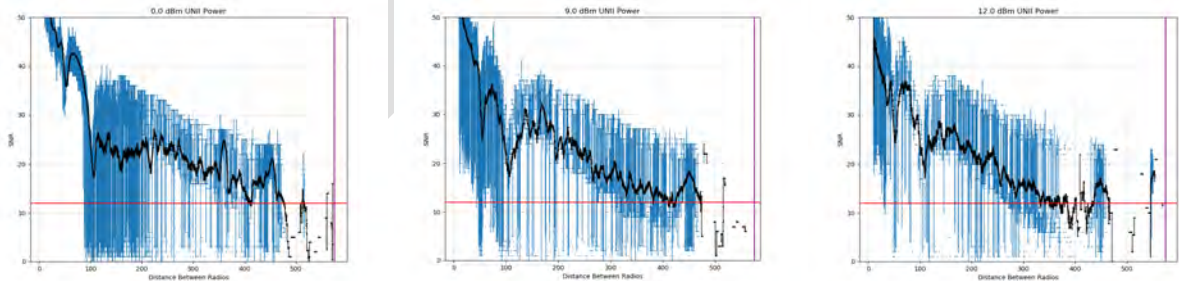
UNII EIRP: 5 dBm

14 dBm

17 dBm

Figure 9-80. DSRC RSSI and noise as UNII interferer power increases

Source: 20170821 Vary UNII pwr half ms avg V2 --was UNII_PowerV3.xlsx, Tab: V2V mobile Tx



UNII EIRP: 5 dBm

14 dBm

17 dBm

Figure 9-81. DSRC Signal-to-Noise as UNII interferer power increases

Source: 20170821 Vary UNII pwr half ms avg V2 --was UNII_PowerV3.xlsx, Tab: V2V mobile Tx

For a specific example, at a range of 200 meters down the test course, or 375 meters from the interferer, you can see from Figures 9-80 and 9-81 how the noise increases with UNII power in Table 9-2:

Table 9-2. Example noise contribution from a single co-channel Wi-Fi radio

UNII transmit power*	Noise†	S/N†
UNII off	xxx	xxx
0 dBm	-101 dBm	24 dB
9 dBm	-100 dBm	23 dB
12 dBm	-95 dBm	22 dB
* UNII load 70%, ¾ QAM64	† 375 meters from UNII	

9.5 Out-of-channel interference

Interference due to Wi-Fi energy leaking into an adjacent DSRC channel was measured both in the lab and in the field.

9.5.1 Lab Measurements -- Impact on signal-to-noise

9.5.1.1 Introduction

Signal to noise includes two different aspects of interference. First is receiver sensitivity and second is the impact different noise sources have on the DSRC receiver.

From a strict signal-to-noise approach, we have examined the receiver’s operation when no noise other than that of the background and that generated internally to the DSRC receiver is present. We then add two types of noise, Additive White Gaussian Noise (AWGN) and DSRC.

9.5.1.2 Receiver sensitivity.

Receiver sensitivity is a function of background noise that is always present as well as any noise generated within the receiver components. Fundamentally, it is the amount of signal energy that must be present in order for the receiver to understand the incoming signal. In other words, it is a measure of the signal strength of the incoming signal that is needed to overcome any background noise whether generated within the receiver or generated by the universe.

The base background noise (that generated by the universe and sometimes labeled thermal noise) can be calculated as follows:

$$N\left(\frac{dBw}{Hz}\right) = 10\text{Log}\left(\left(\frac{T_0}{k}\right) 1w\right)$$

Where:

T_0 = temperature = 290 kelvin

K = Boltzmann's constant = 1.38065×10^{-23} Joules/kelvin

1w is 1 watt.

Using these values, the background noise is:

$$N = 10\text{Log}\left(\frac{290}{1.38065 * 10^{23}}\right) = -204 \text{ dBw/Hz}$$

Since the DSRC receiver is nominally 10 MHz wide and power levels are typically expressed in terms of dBm, this converts to:

$$N\left(\frac{dBm}{10MHz}\right) = 204 + 10\text{Log}(1w/.001w) + 10\text{Log}(1Hz/10,000,000Hz) = -104 \text{ dBm/10MHz}$$

To determine receiver sensitivity, a DSRC transmitter and receiver were connected per Figure 9-82. Definitions for the abbreviations used in the figure are in Table 9-3. Note that Figure 9-82 is generic for all tests in this section and not all tests used all the equipment identified in the figure.

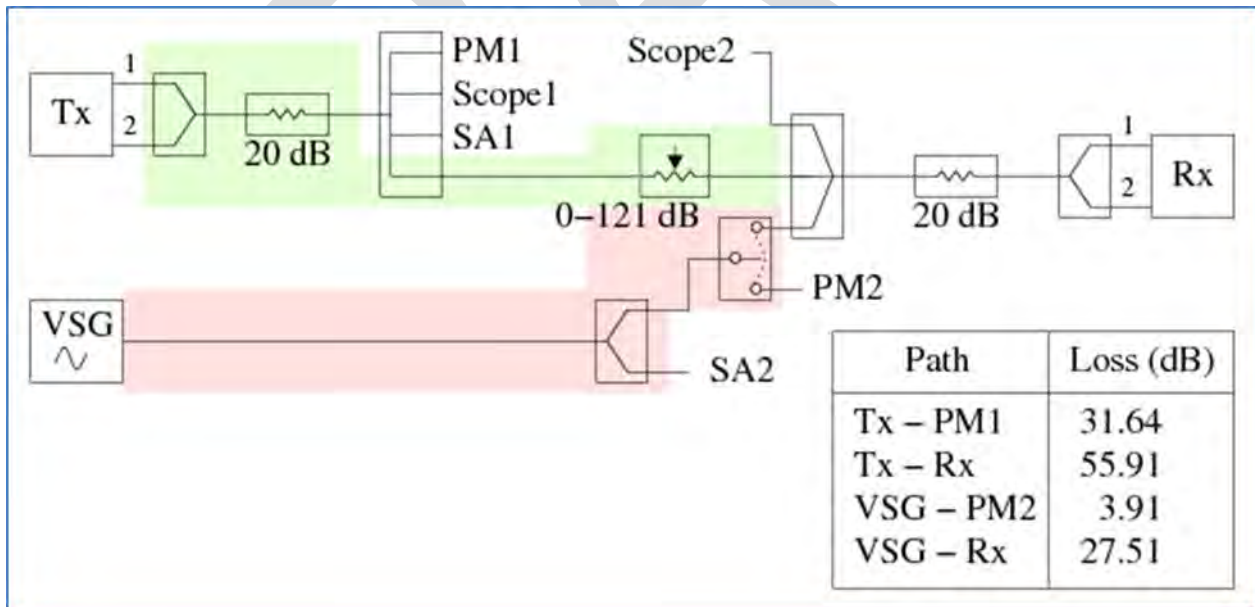


Figure 9-82 Block Diagram of Test Configuration

Table 9-3. Definitions for Figure 9-82

TX	DSRC Transmitter
RX	DSRC Receiver
PM1	Power Meter 1 measuring TX signal
PM2	Power meter 2 Measuring VSG signal
Scope 1	Oscilloscope monitoring TX signal
Scope 2	Oscilloscope monitoring signal at the receiver
SA1	Spectrum Analyzer 1 monitoring TX signal
SA2	Spectrum Analyzer 2 monitoring VSG signal
VSG	Vector Signal Generator transmitting an interfering signal

Note also, that signal loss occurs through cables and connectors. The table in the lower right hand corner of Figure 9-82 identifies specific losses due to cables and connectors. For example, the loss (or attenuation) that occurs between TX and RX is 55.91 dB.

The DSRC transmitting radio was set to output a QPSK rate ½ encoding signal at 24 dBm with 400 bytes per packet. To measure receiver sensitivity, the signal at the receiver was adjusted using the variable attenuator to be 20 dB above the calculated background noise. This ensured that an accurate measurement would be made. The signal was then decrease by 1 dB and the packet error rate (PER) measured at the receiver. 20,000 packets were generated so the power was decreased. This was completed for all seven channels in a DSRC radio. Figure 9-83 shows the seven curves.

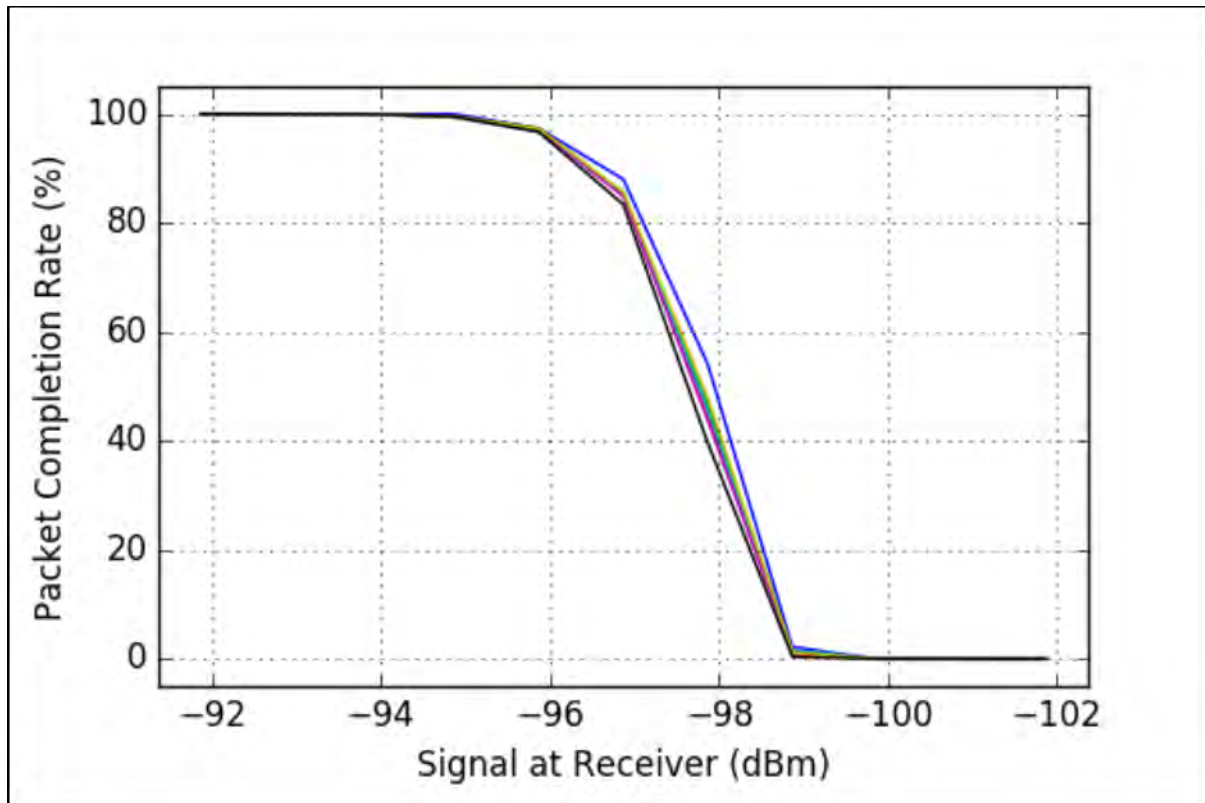


Figure 9-83. Receiver Sensitivity based on Packet Error Rate

IEEE 802.11-2012 indicates the PER shall be less than 10% (18.3.10.2 Receiver minimum sensitivity). This translates to a packet completion rate (PCR) of greater than 90%. Since all the curves in Figure 9-83 are similar, we will pull a single curve out and use that as an example to estimate the receiver sensitivity. Figure 9-84 shows the curve for channel 178. The 90% PCR is at approximately 96.5 dBm (at the intersection of the two lines). Thus, the incoming signal must be at least 7.5 dB above the background noise. Note this is also considered the receiver's noise figure (NF)⁴⁸.

⁴⁸ Noise Figure is (NF) is the measure of degradation of the signal-to-noise ratio (SNR), caused by components in a receiver's signal chain.

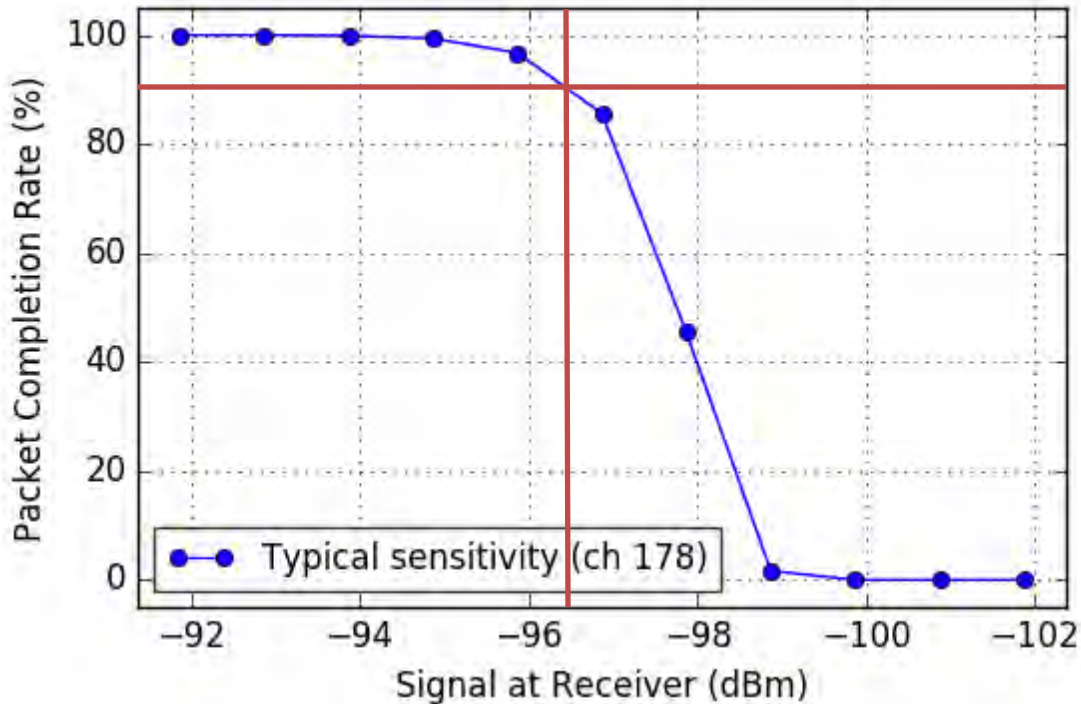


Figure 9-84 Packet Completion rate for Channel 178.

9.5.1.3 In channel noise.

Next, we determined the signal to jamming ratio. Beyond the NF, any interfering signal must be some number of dB below the desired signal. Under most circumstances, we would expect this to be similar to the NF.

9.4.1.3.1. Additive White Gaussian Noise

The standard approach to this is to inject white Gaussian noise into the channel, generally referred to as Additive White Gaussian Noise (AWGN). Rather than being a specific interfering signal, AWGN is meant to mimic a host of random processes, creating a uniform noise across the receiver's designated receive band. In this case, the AWGN generator creates noise across the 10 MHz of the DSRC receiver channel.

Referring to Figure 9-82, the vector signal generator (VSG) generates this noise and injects it into the receive channel. Note that the DSRC transmitter is still transmitting and is sufficiently isolated so that the energy detect function that would normally shut the transmitter down is not impacted.

Figure 9-85 shows the response to two potential interfering signals. The blue line is for the AWGN and indicated an SNR of approximately 7.6 dB. This is in keeping with the receiver's NF as previously calculated.

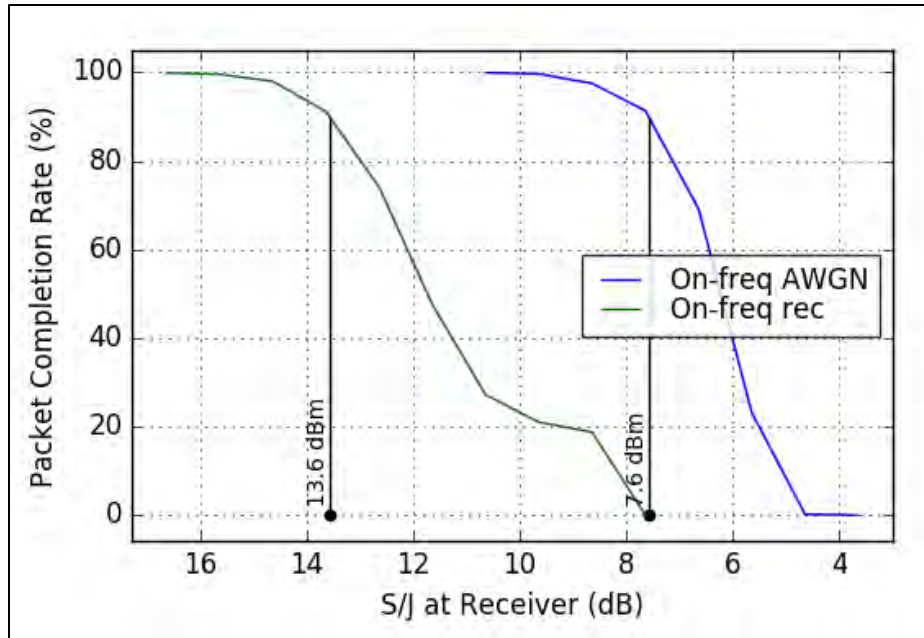


Figure 9-85. AWGN and Recorded DSRC impact on PER.

9.4.1.3.2. Recorded DSRC

In making the measurements of receiver sensitivity, we were concerned with both on channel interference from a DSRC device as well as adjacent channel interference from both an UNII device as well as a DSRC device.

The recorded DSRC was generated using the VSG. While the DSRC radio is transmitting, the signal is recorded as an I/Q waveform using Vector Signal Analysis software⁴⁹. Recordings are made on each of the protocol's seven channels. Once captured, the signal is edited to remove uninteresting "dead air" that precedes and follows the signal of interest. This is then loaded into the VSG and injected into the DSRC receive channel.

Referring again to Figure 9-85, the signal to noise ratio needed to achieve a better than 10% PER is 13.6 dB.

9.5.1.4 Adjacent Channel

9.4.1.4.1. AWGN on Adjacent channels

The same process used to examine co-channel interference was used to determine adjacent channel interference. Figure 9-86 shows the signal to jamming on channel 172 from channel 174, 176, and 178.

⁴⁹ There are several developers of this software. We had software available from Keysight for our testing.

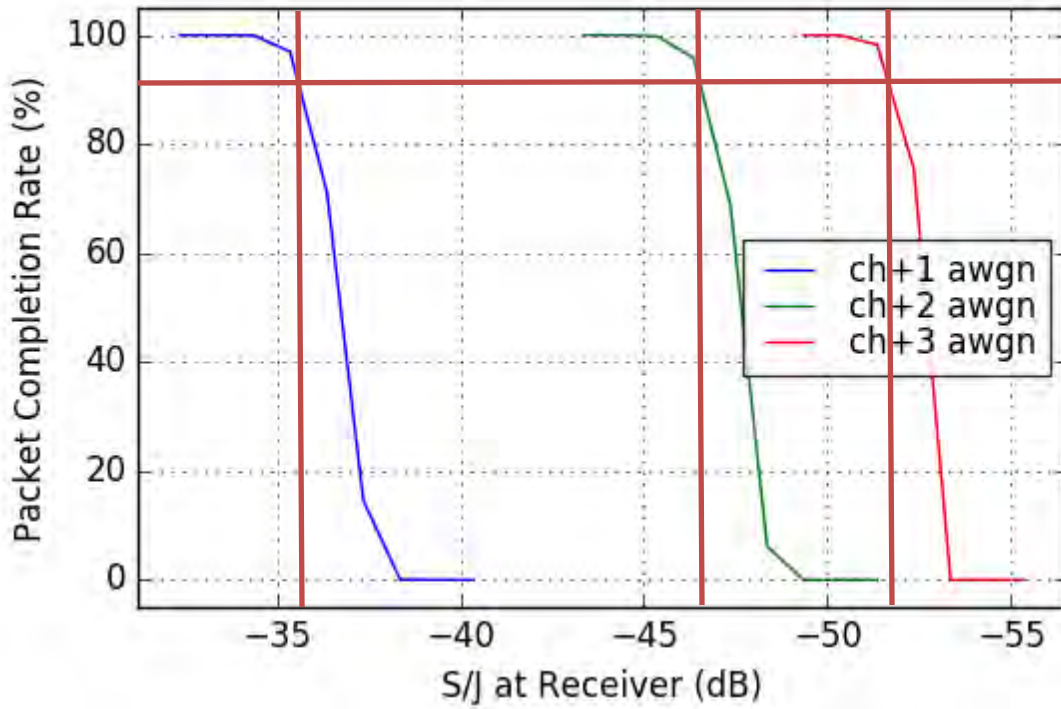


Figure 9-86, AWGN from channels 174, 176, and 178.

Table 9-4. Signal to Jamming for AWGN in dB.

Interfering Channel	S/J – AWGN (dB)
On Frequency	7.5
Adjacent (174)	-36
Adjacent +1 (176)	-47
Adjacent +2 (178)	-52

9.4.1.4.2. Recorded DSRC

Similar plots are available for recorded DSRC. The end result is shown in table 9-5.

Table 9-5. Signal to Jamming for Recorded DSRC in dB.

Interfering Channel	S/J – Recorded (dB)
On Frequency	13.6
Adjacent (174)	-28
Adjacent +1 (176)	--57
Adjacent +2 (178)	N/A

For the second adjacent channel, it was not possible to generate sufficient signal to measure any interference.

9.5.1.5 Out-of-Band Emissions (OOBE)

Our focus in this testing has been to understand the impact of UNII devices (notably IEEE 802.11ac compliant devices) on DSRC. The channel configuration for the UNII devices is such that the worst case at present is interference from channels 165 (20 MHz wide) and channel 159 (40 MHz wide). The VSG was configured to generate each of these and measurements were taken to determine the level of potential interference.

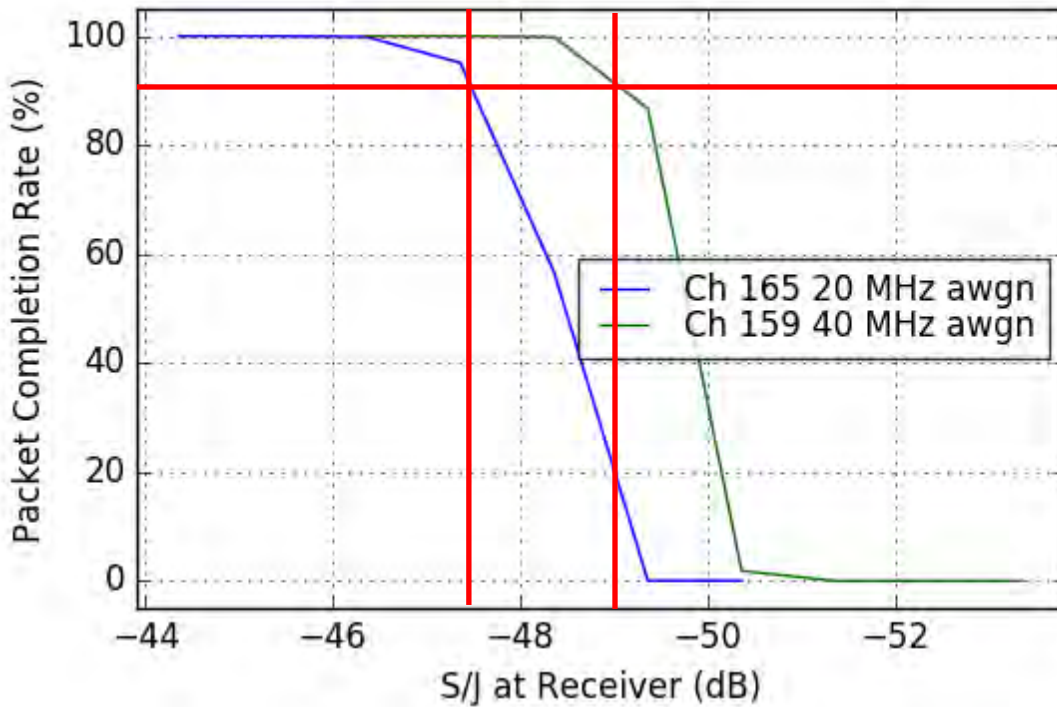


Figure 9-87. S/J for UNII into DSRC channel 172.

Table 9-6. Signal to Jamming for UNII channels in dB

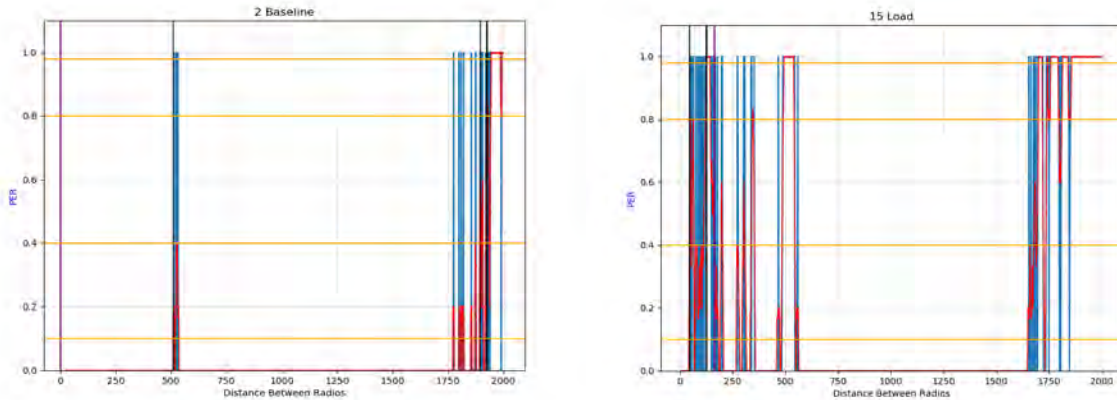
Interfering Channel	S/J – UNII (dB)
Channel 165	-47
Channel 159	-49

9.5.2 Field Measurements

A good bounding case came from I2V measurements with both radio services at their higher powers but the Wi-Fi traffic load only at a moderate 15%. The RSU transmitted to the mobile DSRC on channel 172

with an EIRP of 20 dBm, which is the maximum power specified by the SAE J2735 standard. The Wi-Fi access point was located 160 meters downrange of the RSU. It transmitted on adjacent channel 169 with an EIRP of 35 dBm and a traffic load of 15%. The mobile DSRC drove from the RSU past the access point until the DSRC signal was completely lost, then turned around and came back.

Figure 9-88 compares the baseline packet error rate before (left), and after (right), the Wi-Fi device was turned on. The purple line at 160 meters marks the position of the Wi-Fi access point. [As a reminder: Blue, each packet (1 or 0), Red is 0.5 sec average]



DSRC Baseline (EIRP=20 dBm) – channel 172

With UNII (EIRP=36 dBm, 15% load) – channel 169

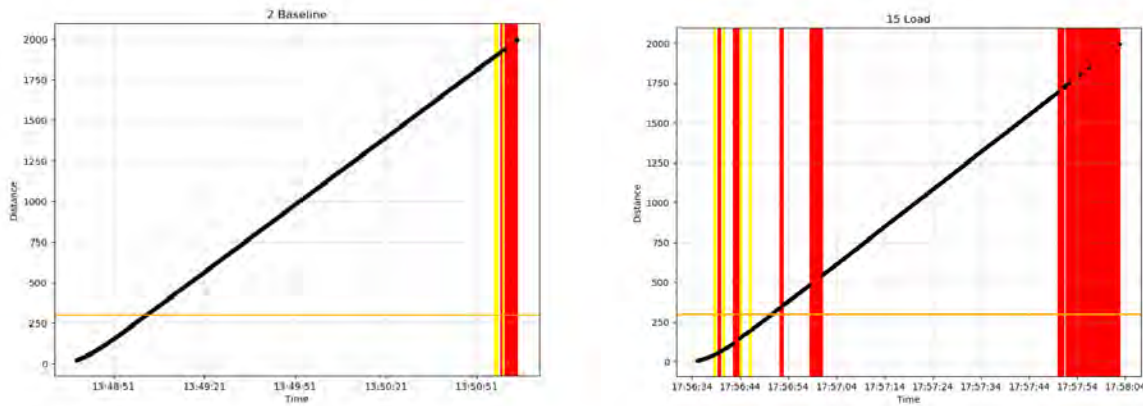
Figure 9-88. Packet error rate from adjacent channel interference, I2V

Source: 20190322 Adj channel tests away -- was exl_report_away.xlsx, Tabs: Baselines; V2I mobile Rx UNII@160meters 15%

The RSU was set at zero distance and the mobile DSRC drove from zero to 2000 meters in this segment. The baseline is clean except for a null at 500 meters. The larger error at 1750 meters in both plots is from driving out of range. In the right plot you can see the additional packet error out to about 350 meters. That is due to adjacent channel leakage.

Given that the safety applications are intended to work with a 300 meter safety radius, interference 150 meters from the Wi-Fi access point would have a safety impact.

Figure 9-89 displays the gaps showing how the packet errors clustered. As a reminder, Red marks gaps > 0.5 sec (safety critical) Yellow marks gaps 0.3-0.5s long (gaps of concern that may be safety critical for some vendors and apps but maybe not others). The black line is the vehicle trajectory in time and space. Orange line intersects trajectory at 300 meters.



DSRC Baseline (EIRP=20 dBm) – channel 172 With UNII (EIRP=36 dBm, 15% load) – channel 169

Figure 9-89. Gap analysis of adjacent channel interference, I2V

Source: 20190322 Adj channel tests away -- was exl_report_away.xlsx, Tabs: Baselines; V2I mobile Rx UNII@160meters 15%

The baseline plot on the left shows no gaps large enough to have safety implications until the vehicle drives out of range. With the access point turned on, the right plot shows that gaps of concern and safety critical gaps that occur out to 350 m, even with the access point on the adjacent channel. Those are essentially dead spots where the DSRC signal disappears for more than half a second. That means the packet errors are not uniformly distributed. Instead they cluster dangerously in places within the 300 meters safety warning zone.

Figure 9-90 displays the packet error rate geographically. As a reminder, **Magenta** signifies zero missing packets, **Aqua** signifies 100% packet error. The more reddish the purple the less packet error. The more bluish the purple, the higher the error. The RSU sits at the beginning of the trace at the upper left. The vehicle drove down and right. The **Red dot** is the UNII access point.



DSRC Baseline (EIRP=20 dBm) – channel 172 With UNII (EIRP=36 dBm, 15% load) – channel 169

Figure 9-90. Geographical distribution of Packet error rate from adjacent channel interference, I2V

Source: 20190322 Adj channel tests away -- was exl_report_away.xlsx, Tabs: Baselines; V2I mobile Rx UNII@160meters 15%

The Baseline (left) shows great signal until it suddenly disappears when driving out of range. The right plot clearly shows the dead spots caused by the adjacent channel interference (the blue and aqua regions that pop up on either side of the interferer).

Figure 9-91 is a close up of the adjacent channel interference plot. The yellow circle marks the 300 meter safety zone around the RSU. The red dot marks the position of the UNII access point in that zone. You can see a number of dead spots within the 300 meter radius of the RSU at the beginning of the trace.

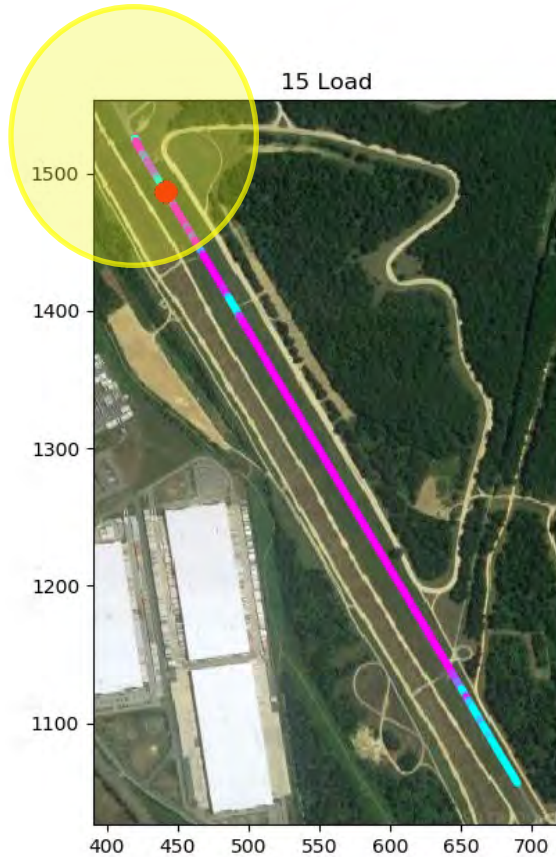
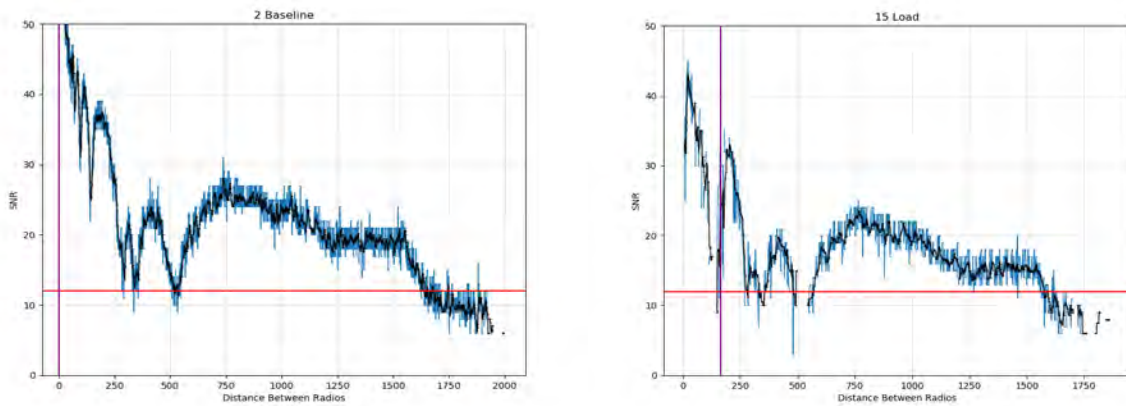


Figure 9-91. Geographical distribution of PER from adjacent channel interference, I2V close up

Source: 20190322 Adj channel tests away -- was exl_report_away.xlsx, Tabs: Baselines; V2I mobile Rx UNII@160meters 15%

Figure 9-92 compares the signal-to-noise ratio of the baseline and interference data for this case. As a reminder, blue is the SNR measurement at each packet and black is the 0.5 second rolling average SNR. The purple line in the right plot marks the position of the Wi-Fi access point. The horizontal red line is the 12 dB benchmark considered to be a minimum requirement for safety applications.



DSRC Baseline (EIRP=20 dBm) – channel 172

With UNII (EIRP=36 dBm, 15% load) – channel 169

Figure 9-92. Signal-to-Noise ratio with adjacent channel interference, I2V

Source: 20190322 Adj channel tests away -- was exl_report_away.xlsx, Tabs: Baselines; V2I mobile Rx UNII@160meters 15%

You can see in the baseline the nulls that make the DSRC signal vulnerable. They even get down to the 12 dB benchmark in a couple of places. The right plot shows how much worse the SNR becomes with the UNII in the adjacent channel. In fact, at one point there isn't enough signal to even measure the SNR for a distance longer than 50 meters at one point.

We have additional data that shows interference gets a bit worse as the Wi-Fi traffic load increases.

{Section still under development}

9.6 UNII in vehicle

To determine the impact of in-vehicle Wi-Fi devices we measured interference to DSRC communications from an RSU to two vehicles, and between the two vehicles, both approaching the RSU and each other at 50 mph. The vehicle closing speed was 100 mph. The vehicles crossed paths within 10-20 meters of the RSU for most runs. The Wi-Fi access point was located near the RSU to simulate an access point near an intersection on a rural highway.

{Section still under development}

10. Environmental Variation

We wrote the test plan before making the arrangement to test at APG. APG offered the possibility to test with multiple building types and to test on a track with a long and straight line-of-sight surrounded by dense woods. Both were opportunities to test for the effect of environmental conditions very different from the open field environments of the test tracks, but in a controlled fashion.

Key chapter takeaways

10.1 Building tests

Three types of buildings were tested with the surrogate-UNII testbed located inside and outside of the buildings to measure how different building materials affected interference to the DSRC. In each case, we operated the surrogate UNII testbed inside the building near the RSU and stationary vehicle as the mobile test vehicle passed by. We measured the impact of the UNII on the DSRC communications then moved the surrogate UNII testbed just outside the building and repeated the same interference tests. The difference in interference measures how much the different building materials impact the UNII transmissions.

We did the building tests at the highest and lowest UNII power levels (EIRP of 8 and 36 dBm) to bracket the range of possible effects for each type of building. We also compared the difference between interference to V2I and V2V communications.

10.1.1 Filled Cinderblock Building

The fire tower at the ATEF facility is used to train fire fighters at the Aberdeen Proving Grounds (Figure 10-1). It is constructed of filled cinderblock with few windows that were all sealed shut by steel shutters. There are several small ports near the floor on each level blocked by steel covers. This building offers the most RF attenuation of the three buildings tested. Figure 10-2 is a satellite image that shows lines of sight from the building and that it is positioned 50 meters from the ATEF test track

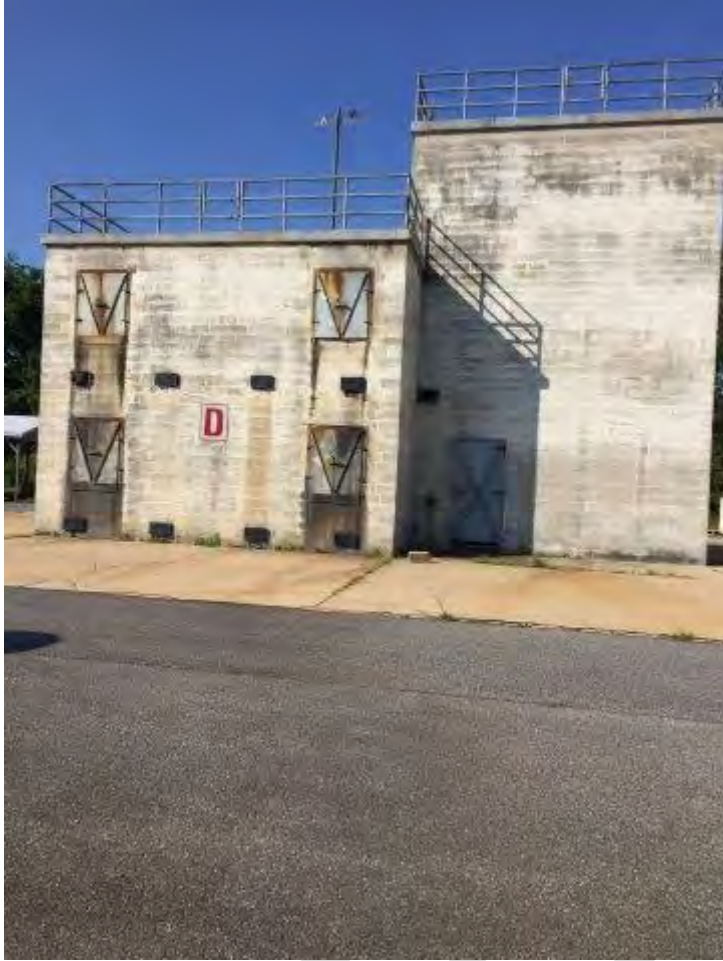


Figure 10-1. Filled cinderblock fire tower at ATEF



Figure 10-2. Aerial view of the fire tower near the ATEF test track.

10.1.1.1 V2I with highest UNII power

The satellite view of Figures 10-3 and 10-4 show the V2I baseline packet error rates geographically as the test vehicle approaches and departs the fire tower (red dot) in a counter clockwise direction. That means the motion of travel in the figures is right to left.

The surrogate UNII testbed was not turned on during these baseline tests. The color scale goes from hot pink for zero packet errors, to bright aqua for 100% PER.

You can see in Figure 10-3b that the mobile test vehicle doesn't come into an unobstructed view until it crosses the access road to the airfield. The RSU and static vehicle are on the test track, as close to the red spot marking the UNII location as we could get. You can also see, by blue and purple transition between the aqua and pink, that there is a region where some fraction of the DSRC signals get through the trees before the vehicle is directly in view. Figure 10-4b is a view of the approach through the trees.

The data trace in Figure 10-3a stops just after the abrupt cutoff of the DSRC signal by the trees in that direction (Figure 10-4a). There is no gradual transition in that direction. DSRC EIRP was 25 dBm and the UNII EIRP was 36 dBm. Note that this is a more robust DSRC link than would be commercially deployed. Hence, interference shown here would be worse for a deployed DSRC system.



Figure 10-3a. V2I Baseline PER departing Figure 10-3b. V2I Baseline PER approaching

Source: 20170912 Building-Cinderblock away – was exl_report_away_20170912.xlsx, Tab: V2I mobile Rx to UNII=31

Source: 20170912 Building-Cinderblock toward – was exl_report_toward_20170912.xlsx, Tab: V2I mobile Rx to UNII=31



Figure 10-4a. View south from fire tower

Figure 10-4b. View north from fire tower

The following data plots are for the approach segment shown in Figure 10-3b.

Figure 10-5 compares the RSSI and noise power plots for the baseline measurement, and the cases of the UNII inside, and then outside the building at the highest power level (EIRP=36 dBm). Blue shows the RSSI value of each BSM and black is the 0.5 sec average RSSI. Tan is the noise power of each BSM and red is the 0.5 sec average. The horizontal red line is a benchmark for the nominal DSRC receiver sensitivity of -95 dBm.

The first thing to notice is the more irregular shape of the RSSI curve compared to data from the clear and open sites at Zone 1 and Perryman. The more numerous and irregularly shaped peaks and nulls are due to multipath reflections in this more complicated environment.

The UNII inside figure shows noise received by the DSRC is noticeable 200 meters from the building but similar to the baseline further away. The UNII outside figure show much higher noise the whole way.

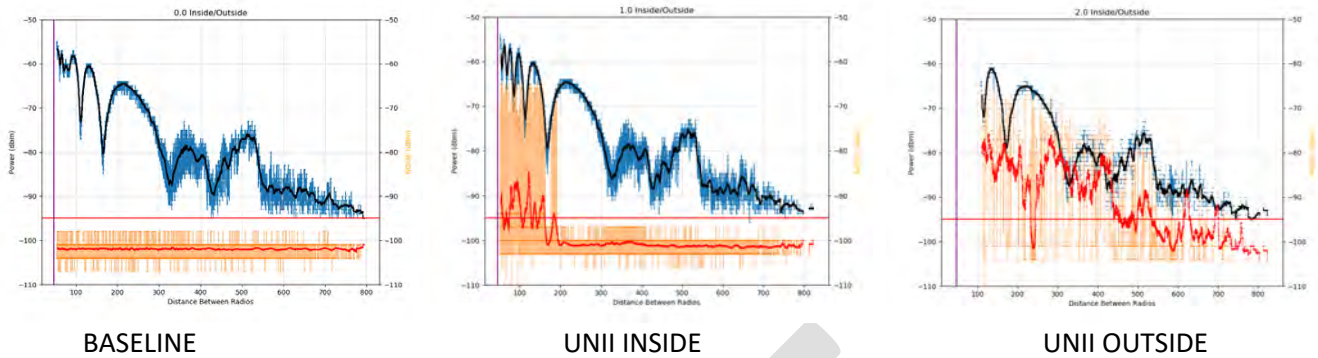


Figure 10-5. RSSI and noise power plots, V2I, UNII EIRP=36 dBm, approaching Cinderblock building

Source: 20170912 Building-Cinderblock toward – was exl_report_toward_20170912.xlsx, Tab: V2I mobile Rx to UNII=31

Figure 10-6 shows the signal-to-noise ratio directly. Blue is the SNR for each BSM and black is the 0.5 sec average. This figure shows more directly the deterioration of the SNR within 200 meters from the building when the UNII is inside, and the deterioration everywhere when the UNII is outside. The horizontal red line is the commonly used 12 dB SNR benchmark, which is thought to be the minimum required for safety applications to work.

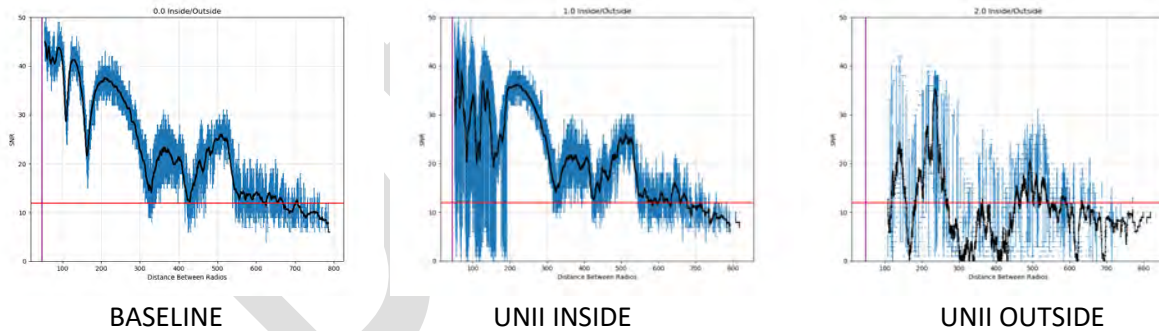


Figure 10-6. Signal-to-Noise plots, V2I, UNII EIRP=36 dBm, approaching Cinderblock building

Source: 20170912 Building-Cinderblock toward – was exl_report_toward_20170912.xlsx, Tab: V2I mobile Rx to UNII=31

Figure 10.7 compares the packet error rate measurements for this case. Blue records packet receptions and the red line is the 0.5 sec average PER. The plot resolution is not fine enough to show every reception, the line width for individual BSMs being so thin. The baseline plot shows how the PER

decreases gradually as the vehicle comes into view from 800 meters to around 550 meters. This corresponds to the transition region shown in Figure 10-4 as the color changes from aqua to hot pink. Once in view the PER is essentially zero except for multipath events that correlate with nulls seen in the RSSI plots.

Even with the UNII inside the building, you can see the PER rising from roughly 20% to over 40% as the vehicle approaches the building from the 200 meter range. Outside that range, even though no impact on SNR was visible, the PER is over 15%, and then an additional 15% above baseline during the region of partial obstruction.

When the UNII was moved outside, the PER was a steady 80-90% the entire time the vehicle was in view. The building essentially reduced packet losses caused by interference to one quarter or one third of that from direct exposure.

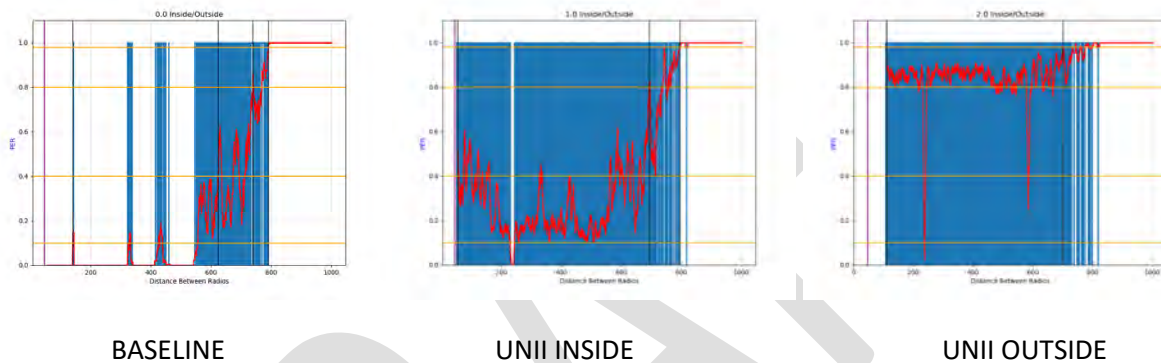


Figure 10-7. Packet Error Rate plots, V2I, UNII EIRP=36 dBm, approaching Cinderblock building
 Source: 20170912 Building-Cinderblock toward – was exl_report_toward_20170912.xlsx, Tab: V2I mobile Rx to UNII=31

Figure 10-8 conveys the distribution of the packet error rate shown in Figure 10-7. The plots in Figure 10-8 display gaps caused by consecutively missed packets. Yellow shows gaps of concern when 3 to 5 consecutive BSMs are missed. Red shows safety critical gaps due to the loss of more than 5 consecutive BSMs, which is a gap that is more than half a second long. The black line shows the distance of the vehicle from the building (y-axis) as a function of time (x-axis). The horizontal orange line marks the 300 meter distance, which is the intended operating range for DSRC safety applications.

The baseline plot essentially confirms that the vehicle isn't fully in view until about 550 meters from the building. Moreover, there are several instances when serious gaps occur, caused by multipath from the complex environment.

With the UNII inside there are about twice as many safety critical gaps as the baseline. In addition, there are about 10 times more gaps of concern (yellow) when the UNII is inside the building compared to the baseline. So even though the SNR plots make it appear that the inside case looks the same as the baseline beyond 200m, the gap plots not only show what the PER plots show, that many more packets

are lost, they further show that the packet losses occur in clumps that pose a greater threat to safety than if the losses were evenly distributed in time.

The UNII outside plot confirms earlier results that a full power UNII access point is totally disruptive to DSRC communications at least out to 800m.

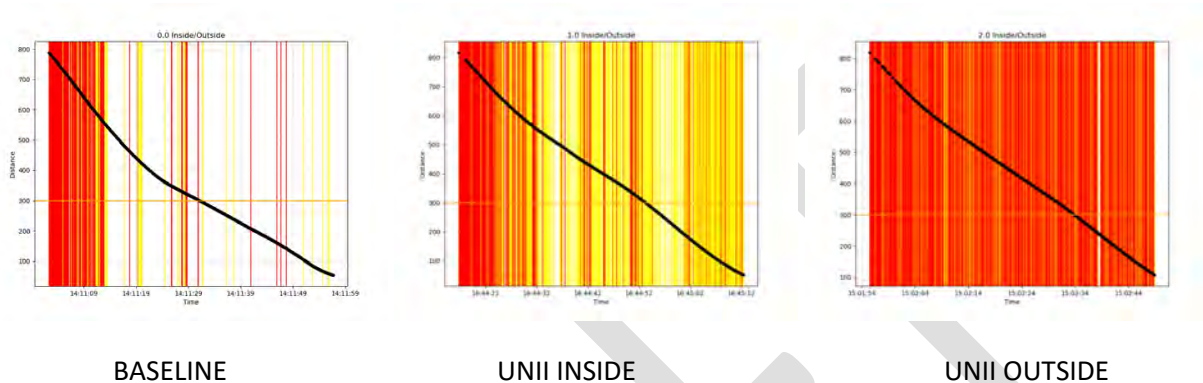


Figure 10-8. Packet gap plots, V2I, UNII EIRP=36 dBm, approaching Cinderblock building

Source: 20170912 Building-Cinderblock toward – was exl_report_toward_20170912.xlsx, Tab: V2I mobile Rx to UNII=31

Figure 10-9 aggregates the data from Figure 10-8 by showing percent of time spent in three gap conditions for the segment of data analyzed in Figures 10-4 to 10-8. The gap conditions are green for gaps less than 0.3s (only 1 or 2 missed packets between received packets), yellow for gaps of 0.3 to 0.5 (3 to 5 consecutively missed packets) “gaps of concern”, and red for gaps larger than 0.5 second (more than 5 BSMs in a row) “safety critical gaps.”

The baseline data shows that the first 9% of safety critical gaps was mostly due to the time the vehicle was out of view from obstruction by trees. Placing the UNII inside essentially doubled the fraction of safety critical gaps to 18%, meaning that adding the UNII inside the building caused safety critical gaps an additional 9% of the time. The UNII outside caused safety critical gaps an additional 70% of the time compared to the baseline, or a total of 80%.

As noted above, the high power access point outside the building completely disrupts DSRC communication. Putting it inside the filled-cinderblock building reduced safety critical gaps to about one seventh. That is much less but may still be considered unacceptable. If gaps down to 0.3s are considered unacceptable, that occurred essentially 20% of the time with the UNII inside the building, (90% outside).

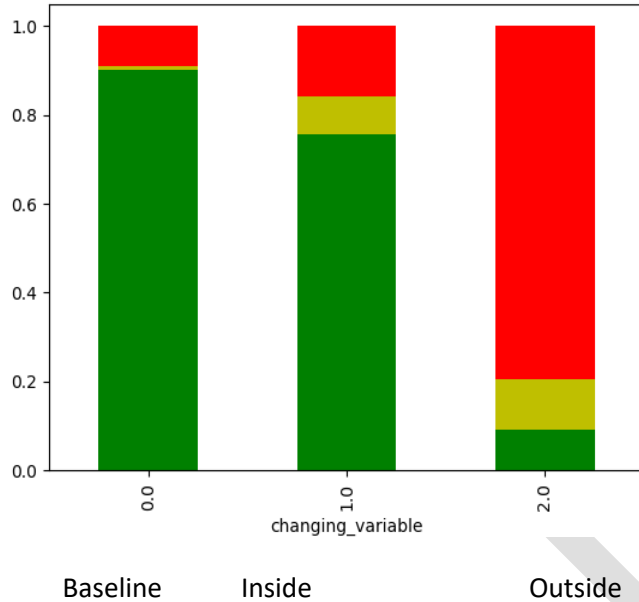


Figure 10-9. Summary of packet gaps, V2I, UNII EIRP=36 dBm, approaching Cinderblock building

Source: 20170912 Building-Cinderblock toward – was exl_report_toward_20170912.xlsx, Tab: V2I mobile Rx to UNII=31

Figure 10-10 is an aerial comparison of how PER is distributed on the approach to the fire tower. You can see how packets are lost near the building with the UNII inside and how disruptive it was outside the building. (Color scale: Aqua is 100% PER and hot pink zero PER. As color scales from blue toward purple and pink the PER decreases.)



Figure 10-10. Geographical distribution of PER, V2I, UNII EIRP=36 dBm, approaching Cinderblock building

Source: 20170912 Building-Cinderblock toward – was exl_report_toward_20170912.xlsx, Tab: V2I mobile Rx to UNII=31

Figure 10-11 compares the RSSI plots for the segments approaching and driving away from the fire tower and RSU. The very different power-over-distance profiles show how sensitive the RF environment is to simple changes in physical environment. What might look similar to the eye can be very different in terms of multipath distortion.

Note that though vehicle movement in the aerial images is right to left, movement in the departing plot below goes from zero to 1000m, left to right. In the approach plot the vehicle comes into view around 800 meters and motion in the plot is as the aerial images, right to left.

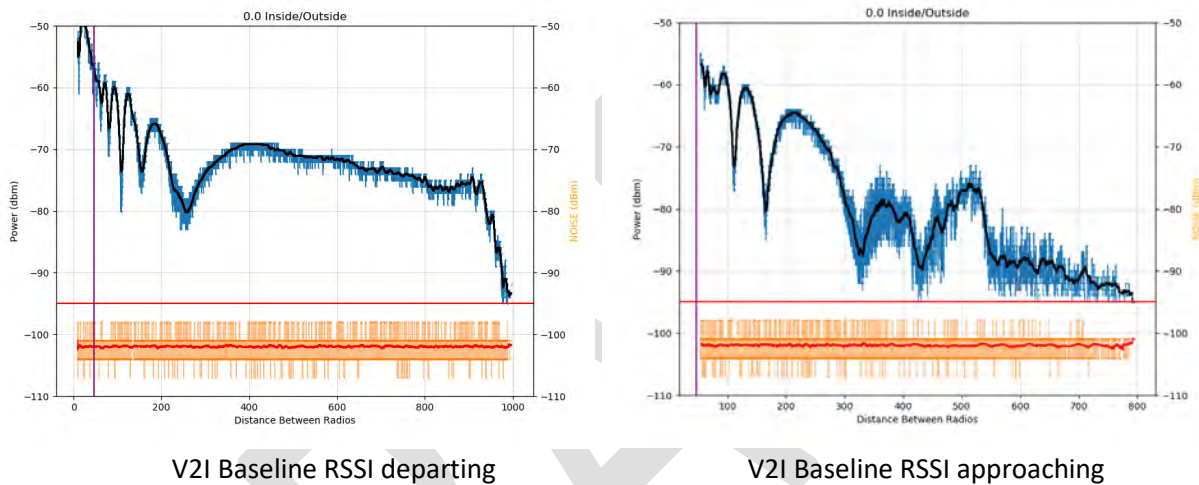


Figure 10-11. Comparing RSSI plots approaching and departing the fire tower, V2I EIRP=25 dBm

Source: 20170912 Building-Cinderblock away – was exl_report_away_20170912.xlsx, Tab: V2I mobile Rx to UNII=31

Source: 20170912 Building-Cinderblock toward – was exl_report_toward_20170912.xlsx, Tab: V2I mobile Rx to UNII=31

The departing data shows essentially the same result as the approaching data. Rather than repeat the above analysis in detail, we include the satellite view of PER in Figure 10-12. Compared with Figure 10-10 it makes the point more succinctly.



Figure 10-12. Geographical distribution of PER, V2I, UNII EIRP=36 dBm, departing Cinderblock building

Source: 20170912 Building-Cinderblock away – was exl_report_away_20170912.xlsx, Tab: V2I mobile Rx to UNII=31

Figure 10-13 directly compares the approach gap statistics of Figure 10-9 with the same statistics for the vehicle driving away. Both show the noticeable gaps caused by the Wi-Fi inside the building but the dramatic shielding the building provided to reduce the interference compared to direct exposure.

Note that there are more baseline safety critical gaps for the approach than departure due to the partial obstruction and more gradual transition described above. On departure, the cutoff was more sudden.

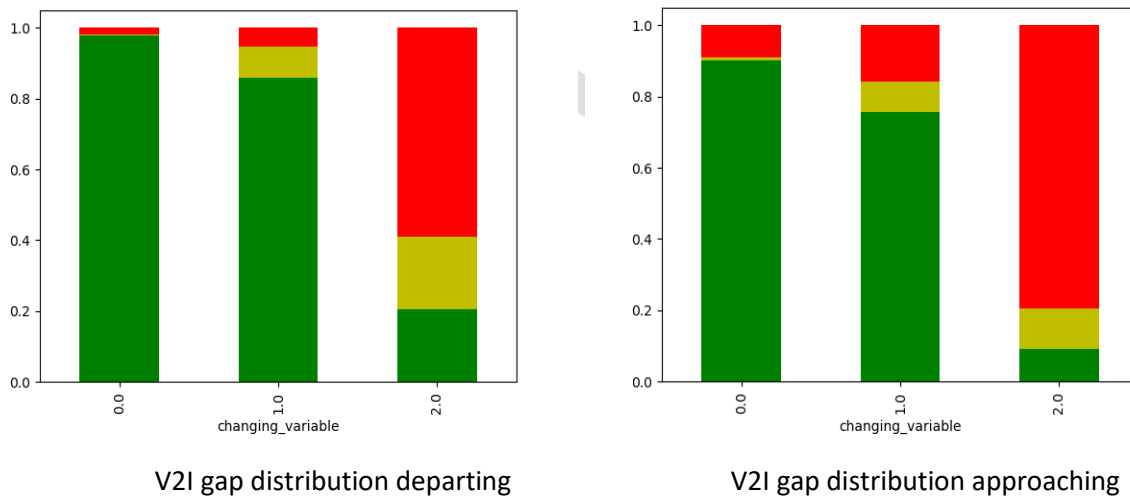


Figure 10-13. Comparing packet gaps, V2I EIRP=25 dBm, UNII EIRP=31 dBm, Cinderblock building

Source: 20170912 Building-Cinderblock away – was exl_report_away_20170912.xlsx, Tab: V2I mobile Rx to UNII=31

Source: 20170912 Building-Cinderblock toward – was exl_report_toward_20170912.xlsx, Tab: V2I mobile Rx to UNII=31

10.1.1.2 V2I with lowest UNII power

In this test case, DSRC EIRP was 25 dBm and the UNII EIRP was 8 dBm (note that this is a more robust DSRC link than would be commercially deployed). Hence, interference shown here would be worse for a deployed DSRC system. As before, the RSU was transmitting.

Figure 10-14 shows that the packet error rate with the lowest power UNII inside was essentially identical to the baseline. This indicates that the building completely shielded the DSRC from the Wi-Fi signals. Note that when moved outdoors, this low power UNII caused a 40% PER until about 200 meters away where it then rose to 75% at the closet point to the building (50m).

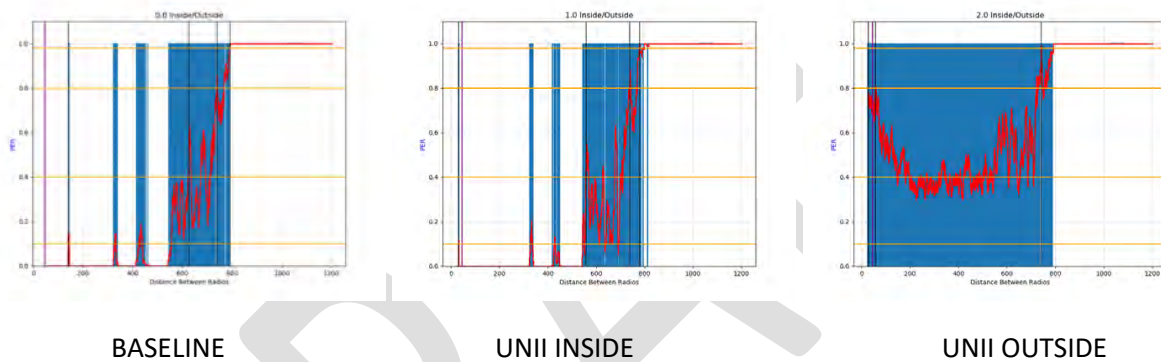


Figure 10-14. Packet Error Rate plots, V2I, UNII EIRP=8 dBm, approaching Cinderblock building

Source: 20170912 Building-Cinderblock toward – was exl_report_toward_20170912.xlsx, Tab: V2I mobile Rx to UNII=3

Figure 10-15, which shows the distribution of the missing packets in the serious and critical gap categories makes the same case. The building attenuated the low power Wi-Fi too much to affect the DSRC. But again, it is evident that even a low power access point outdoors would be untenable for DSRC.

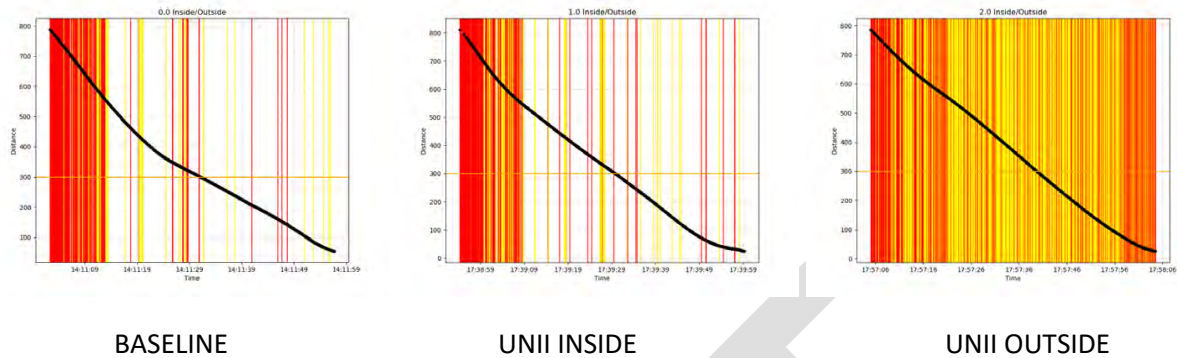


Figure 10-15. Packet gap plots, V2I, UNII EIRP=8 dBm, approaching Cinderblock building

Source: 20170912 Building-Cinderblock toward – was exl_report_toward_20170912.xlsx, Tab: V2I mobile Rx to UNII=3

These results demonstrate that a filled-cinderblock building with no windows can attenuate Wi-Fi sufficiently to prevent interference to DSRC if the Wi-Fi power is low enough. We would need to make measurements at additional EIRP values between 8 and 36 dBm to find the level at which the DSRC communication is first affected.

Any other UNII power level should produce interference at a level in between the bounding cases compared in Figure 10-16. Those bounding cases are the bars labelled 1.0 in the two plots as those are the high and low power cases when inside the building. Changing UNII power should provide a result in between.

The bars labeled 2.0 show how disruptive the access point was when located outside, especially at the high power. Again, any other power level should provide a result in between the two. Lastly this shows again how the low power inside result (1.0 bar in the second plot) looks like the baseline (0.0 bar in the first plot).

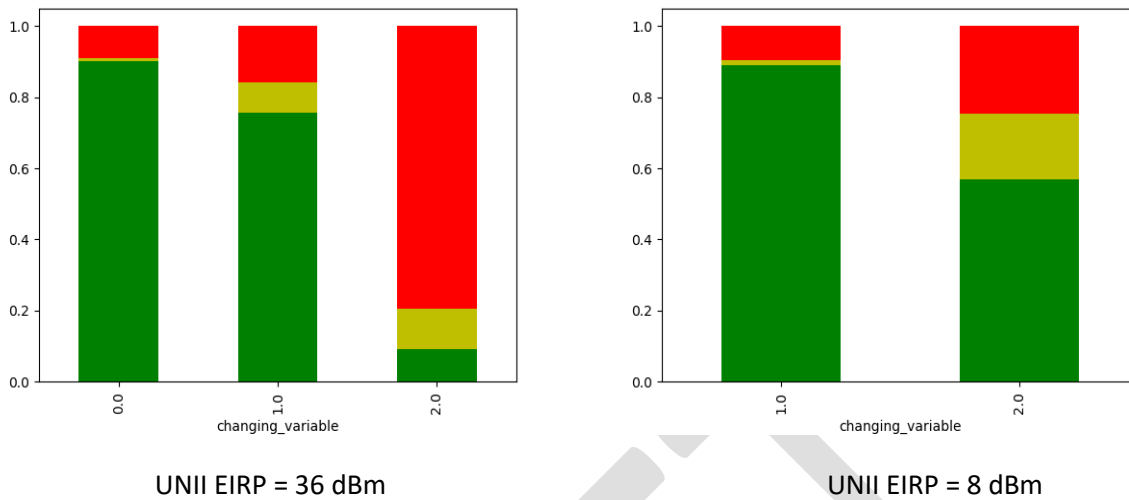


Figure 10-16. Effect of UNII power on packet gaps, V2I EIRP=25 dBm, approaching Cinderblock building

Source: 20170912 Building-Cinderblock toward – was exl_report_toward_20170912.xlsx, Tabs: V2I mobile Rx to UNII=31, and V2I mobile Rx to UNII=3

Because the driving away direction data provides the same result, just like in the high power case, we will leave it out as essentially redundant. The data will be provided in an appendix.

10.1.1.3 V2V with lowest UNII power

We also tested with the mobile vehicle transmitting and the static vehicle parked next to the RSU receiving. The V2V case with the lowest UNII power leads to the same basic conclusion as the V2I case: the filled-cinderblock building protected the DSRC communication from recognizable interference. Additionally, without the building, interference from the low power access point was untenable. Because that confirms the expected result, we will compare some V2V and V2I data rather than duplicate the V2I analysis for V2V.

To further emphasize the impact on environment and why the basic interference tests were done in the most open, multipath-free environments we could access, consider Figure 10-17. It shows the approaching and departing baselines to compare V2V and V2I directly.

Note the significant changes in the peaks, nulls and profiles, caused by just changing the height of one antenna or looking back versus forward toward the other radio. It would be too difficult to calculate predictions to validate our measurements, or to be certain when packets are lost due to multipath nulls rather than interference in a complex environment like this. Only the V2V departing looks like the expected $1/r^2$ 2-ray model with ground-bounce nulls. It may not be repeatable enough as well. As a

consequence, the results could not be easily generalized to other locations. So this data makes it clear why when looking for interference, rather than performance, we need to use a “clean” RF environment.

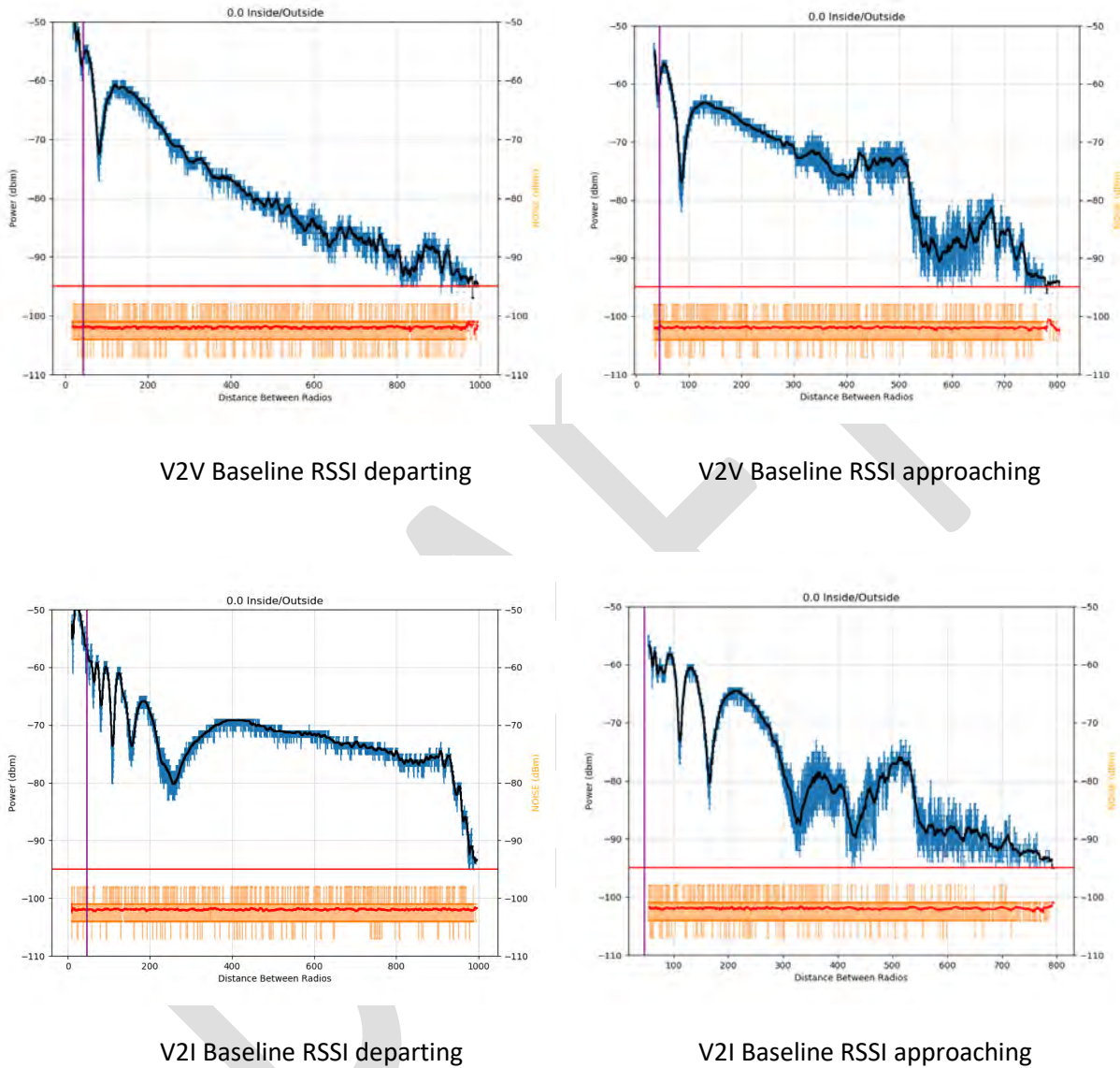


Figure 10-17. Comparing V2V and V2I RSSI plots both approaching and departing the fire tower, DSRC EIRP=25 dBm. Shows the complexity in simple power measurements due to multipath scatterers in the environment.

Source: 20170912 Building-Cinderblock away – was exl_report_away_20170912.xlsx, Tabs: V2I mobile Rx to UNII=31, and V2V mobile Tx to UNII=3

Source: 20170912 Building-Cinderblock toward – was exl_report_toward_20170912.xlsx, Tabs: V2I mobile Rx to UNII=31, and V2V mobile Tx to UNII=3

Turning to how the interferer played against V2V versus V2I, Figure 10-18 compares packet error rates for the lowest power UNII. As in the V2I case, with the UNII in the building, the V2V data was essentially the same as the baseline. So at that low power, the filled-cinderblock building effectively shielded the high power DSRC link from the lowest power UNII signals.

When this low power UNII was taken outside the building, you can see that the V2V communications suffered a packet loss about 50% higher than V2I. That is, over 60% PER as opposed ~40% PER.

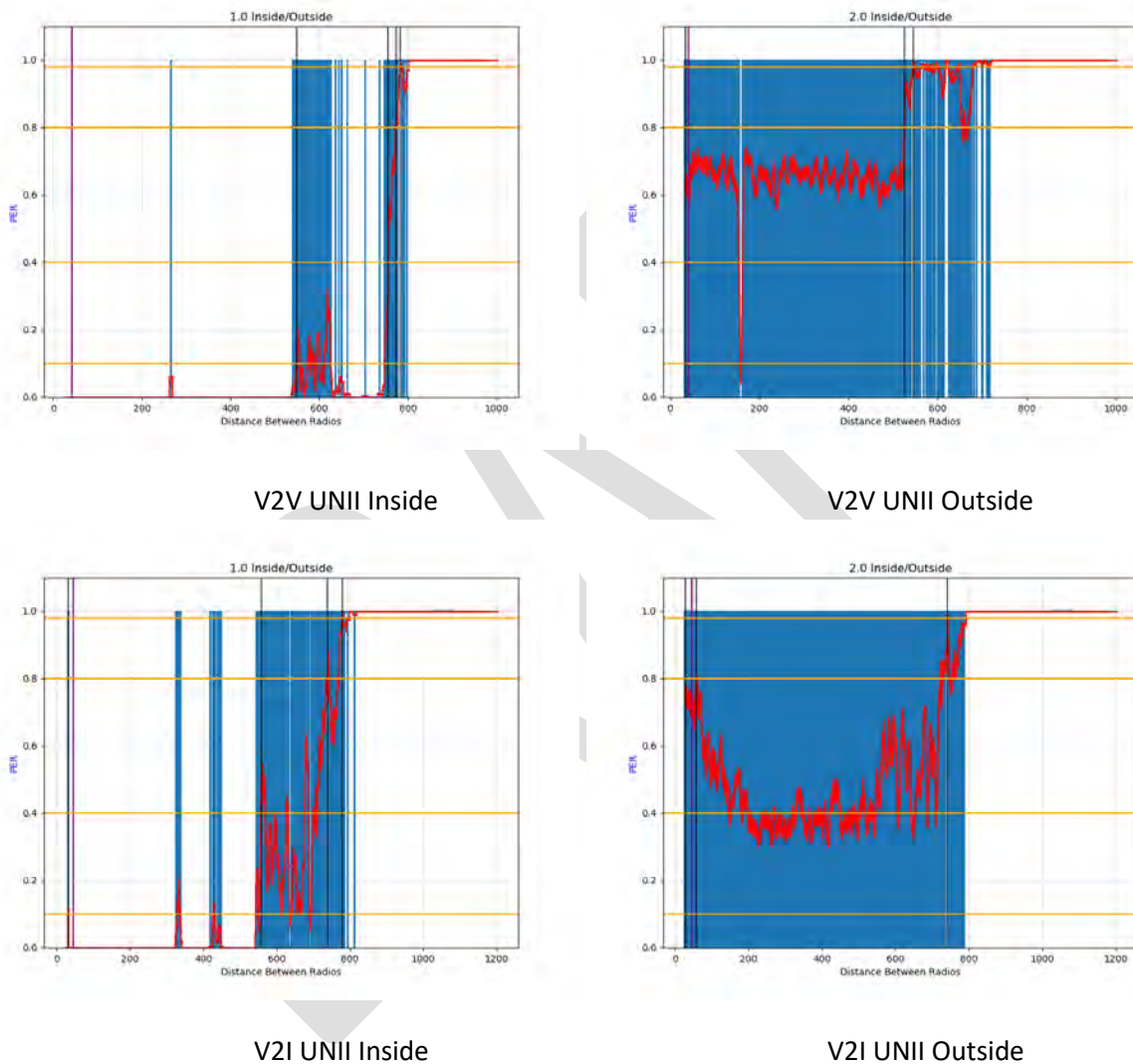


Figure 10-18. Comparing V2V and V2I PER, DSRC=25dBm, UNII EIRP=8 dBm, approaching Cinderblock building

Source: 20170912 Building-Cinderblock toward – was exl_report_toward_20170912.xlsx, Tabs: V2I mobile Rx to UNII=3, and V2V mobile Tx to UNII=3

We see the same thing in the packet gaps analysis of Figure 10-19. Inside looks like the baseline, and outside V2V fared worse. The difference is easier to quantify in the aggregate comparison of Figure 10-20.

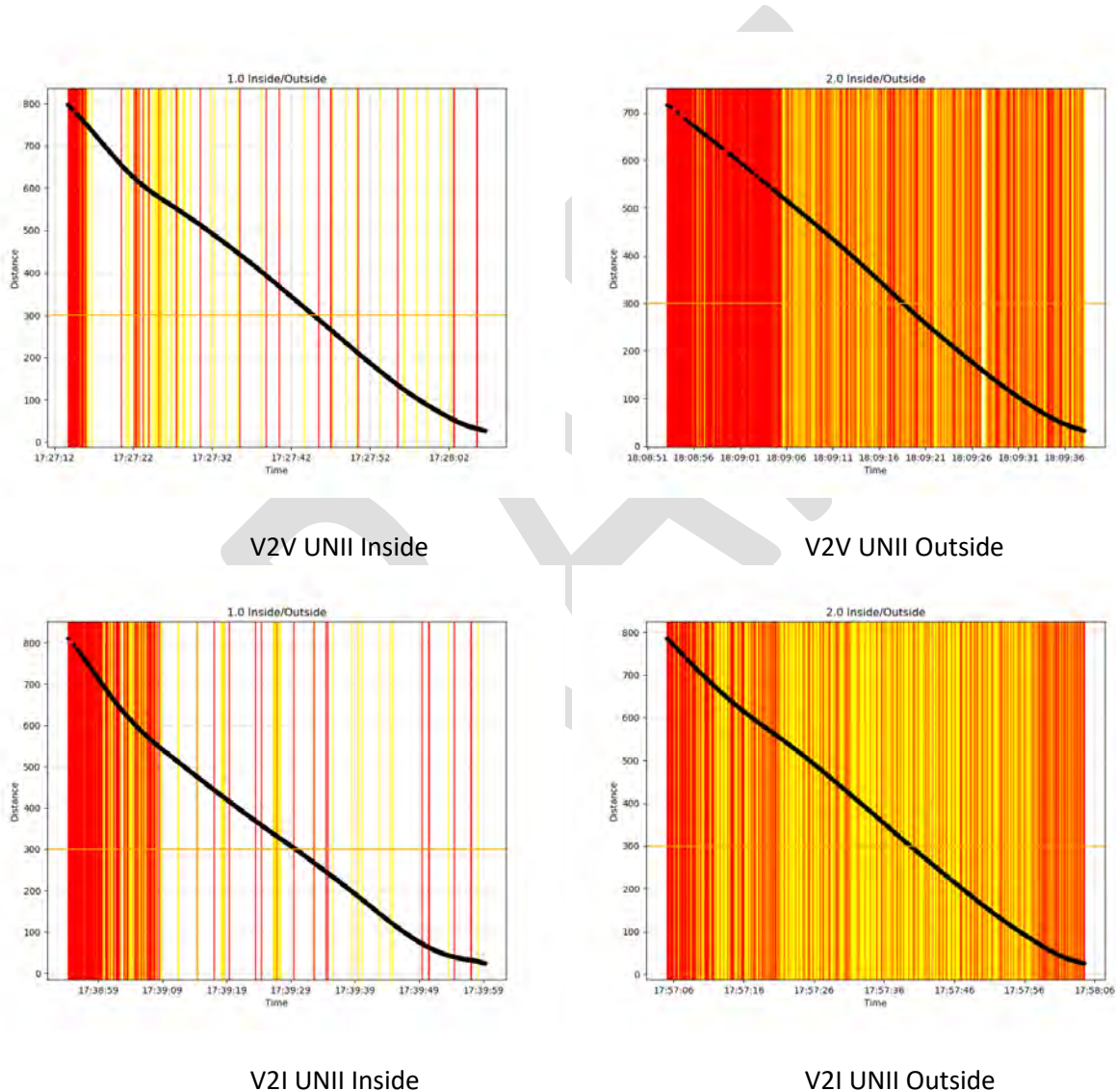


Figure 10-19. Comparing V2V and V2I Packet gap distribution, DSRC=25dBm, UNII EIRP=8 dBm, approaching Cinderblock building

Source: 20170912 Building-Cinderblock toward – was exl_report_toward_20170912.xlsx, Tabs: V2I mobile Rx to UNII=3, and V2V mobile Tx to UNII=3

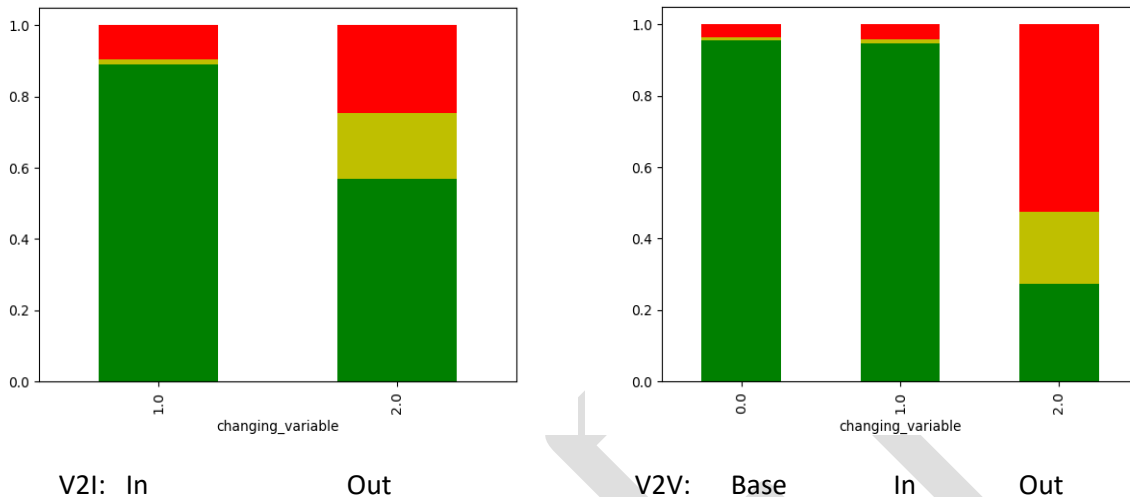


Figure 10-20. Comparing V2V and V2I Aggregate packet gap distribution, DSRC=25dBm, UNII EIRP=8 dBm, approaching Cinderblock building

Source: 20170912 Building-Cinderblock toward – was exl_report_toward_20170912.xlsx, Tabs: V2I mobile Rx to UNII=3, and V2V mobile Tx to UNII=3

The driving away data shows the same thing so will not be repeated here as redundant. See the appendix for all the data not included in this section. The satellite PER images provide a graphic visualization of the same result so will be left for the appendices as well.

10.1.2 Brick Building with Windows

Another class of building was the one story solid brick building with windows shown in Figures 10-21 and 10-22. There are other structures nearby that complicate the multipath environment even more so than the trees on the ATEF course by the cinderblock building (Figure 10-24). It is not a frame building with a brick veneer but actually brick, so its RF attenuation should be comparable to that of the cinderblock building. The brick is more dense but not as thick as the cinderblock material. As expected, both building types offered more attenuation than the wood building tested. More importantly the brick building test demonstrates the effect of windows on interference from inside a building. That is information we did not get from the other building tests.



Figure 10-21. Brick building with the surrogate UNII-4 interferer set up outside



Figure 10-22. Brick building with the surrogate UNII-4 interferer set up inside

The start point where the RSU and static vehicle were positioned was located roughly 100 meters to the west of the brick building. A data run consisted of the mobile vehicle driving 0.4 miles to the west from the starting point, turning around then continuing past the start point to drive by the building, turn a corner 100 meters further, and then turn around a couple hundred feet later to drive by the building a second time before returning to the start point. Figure 10-23 illustrates the geometry near the building.

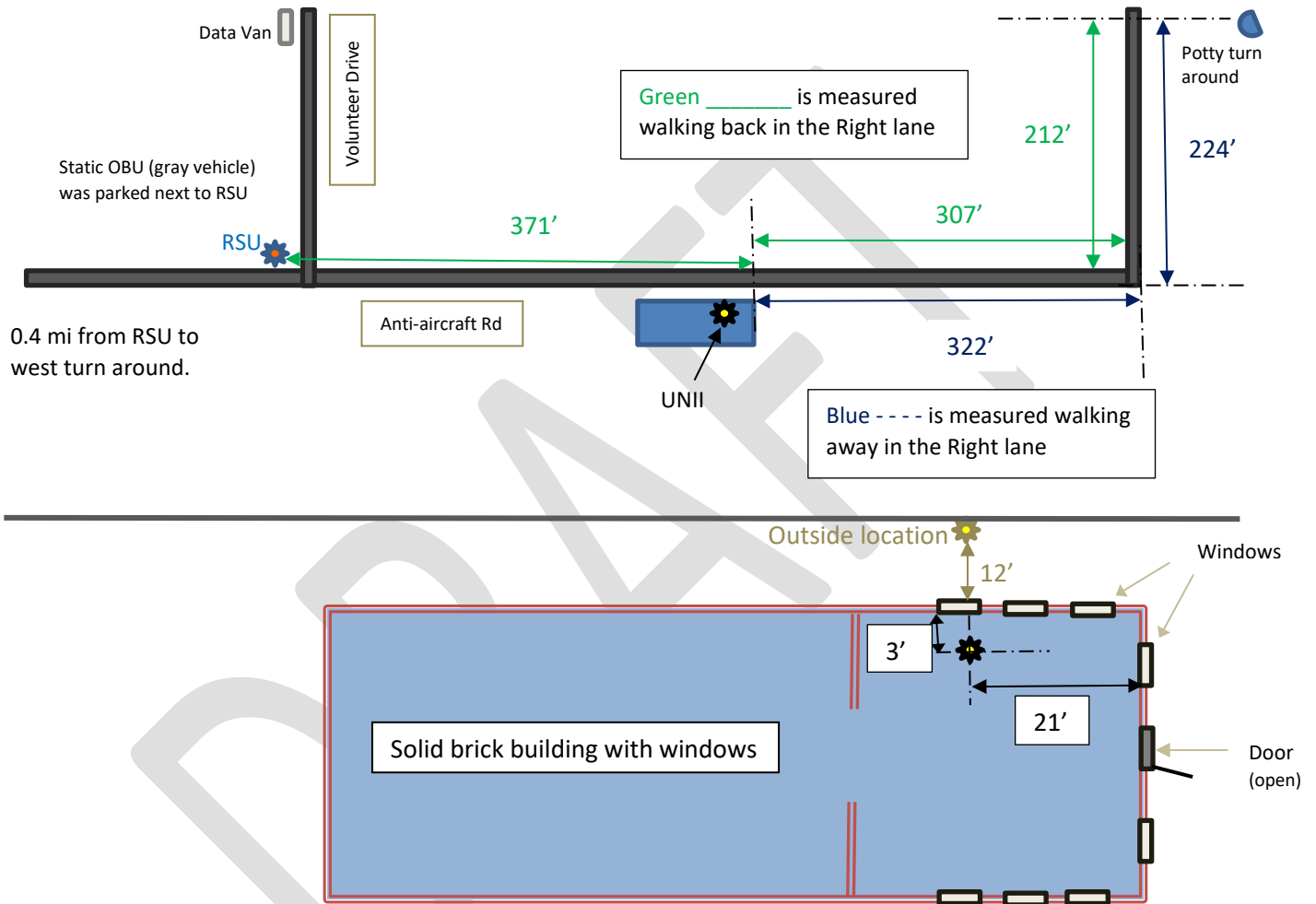


Figure 10-23. Layout of the brick building tests



Figure 10-24: The start point, RSU, and environment west of the brick building.

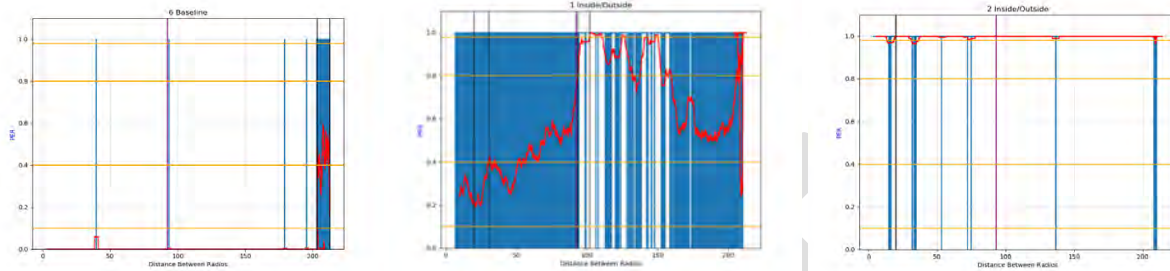
10.1.2.1 Effect of Windows

The effect of windows on how the Wi-Fi interfered with the DSRC was the most interesting result of the brick building tests. The wooden building also had windows but the RF attenuation of the wood was so low that it was impossible to discern any difference. The contrast in the attenuation by brick versus glass was much greater so it was obvious when the vehicle was exposed to the interferer through a window as it went by.

The most dramatic example comes from data taken with the RSU transmitting to the vehicle with the interferer at high power and a 70% traffic load. Recall from chapter 4 that the inter-packet gap between Wi-Fi packets is smaller than a BSM at this loading.

In Figure 10-25 you can see in the baseline plot (left) that there are essentially no packet errors until the vehicle reaches the turn around. With the UNII outside the building (right) PER is 100% almost the entire time and DSRC is completely shut down. With the UNII inside (center) you can see that the significant attenuation of the brick drops the packet error rate from 100% to the 40-60% range EXCEPT

by the windows where the PER shoots up to 100%. Even more interesting is that you can see the shadowing of the brick between the windows in the nulls that drop the PER to 80 or 90% before the vehicle is directly exposed by the next window.



BASELINE

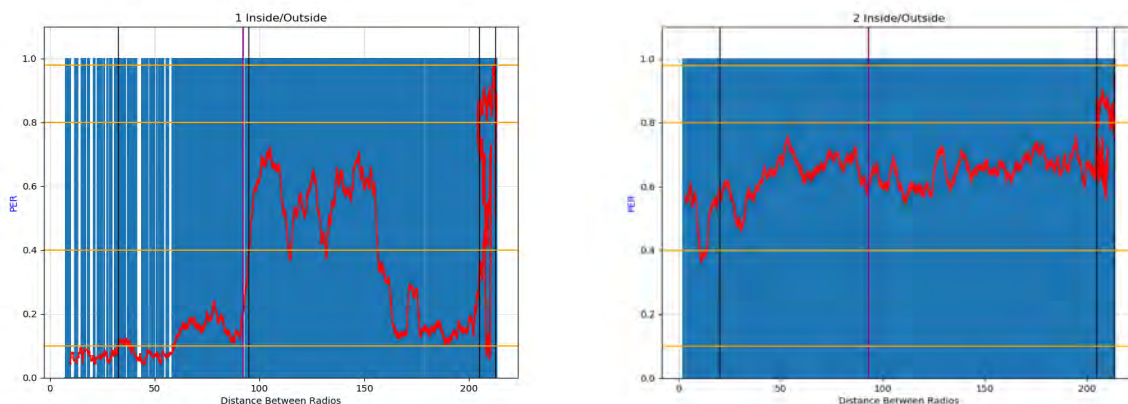
UNII INSIDE

UNII OUTSIDE

Figure 10-25. Packet Error Rate, I2V, UNII EIRP=35 dBm, 70% load, passing brick building shows effect of windows

Source: 20180208 Building-Brick drive-by toward V1 was -- exl_report_toward_2018020_side2.xlsx, Tab: V2I mobile Rx to UNII=30-70%

Figure 10-26 below shows the exact same case with one difference. That is, RSU to mobile OBU (I2V), DSRC EIRP of 25 dBm, UNII at 36 dBm, with the traffic loading turned down from 70% to 10%. The baseline is the same so not repeated here. There is significantly less interference across the board due to the lower traffic load, but it is still significant by the windows. The peaks in this data show how the interference increases significantly with direct exposure through the windows. Furthermore, the nulls in between the peaks show the shadowing, or partial shielding, by the brick in between the windows very clearly. The brick attenuates the interfering Wi-Fi signal allowing more DSRC signal to get through.



I2V UNII Inside

I2V UNII Outside

Figure 10-26. Packet Error Rate, I2V, UNII EIRP=35 dBm, 10% load, passing brick building shows effect of windows with light Wi-Fi traffic

Source: 20180208 Building-Brick drive-by toward V1 was -- exl_report_toward_2018020_side2.xlsx, Tab: V2I mobile Rx to UNII=30-10%

An important conclusion can be drawn from both Figures 10-24 and 10-25 by comparing the inside versus outside packet error rate for both cases. That is, direct exposure to the windows resulted in the same PER as when the UNII was outside. So when considering Wi-Fi inside buildings with windows, the outside data should be used to estimate the maximum interference to DSRC.

Figure 10-27 compares the packet error rates for the baseline, UNII inside, and UNII outside, geographically. The shielding provided by the building as well as the exposure through the windows and the shadowing of the windows stands out clearly and intuitively from these data images.

DRAFT



BASELINE



UNII INSIDE



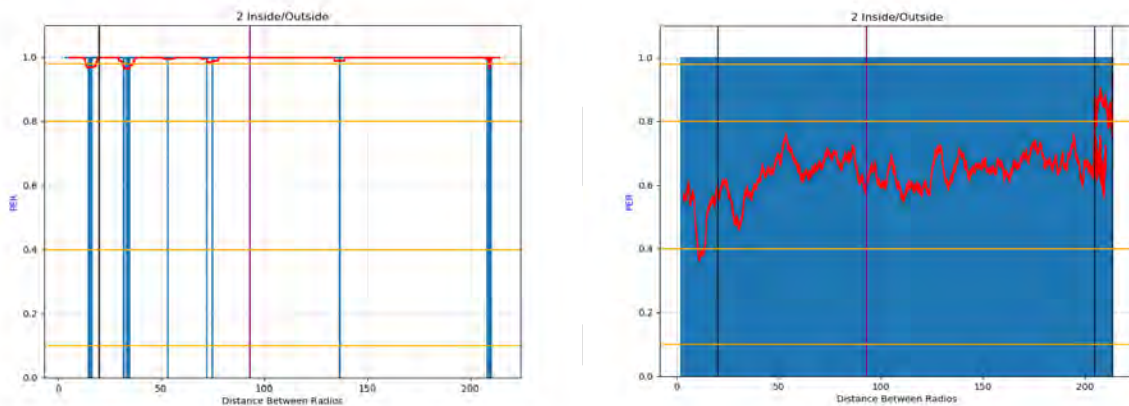
UNII OUTSIDE

Figure 10-27. Packet Error Rate, I2V, UNII EIRP=35 dBm, 10% load, passing brick building shows effect of windows with light Wi-Fi traffic

Source: 20180208 Building-Brick drive-by toward V1 was -- exl_report_toward_2018020_side2.xlsx, Tab: V2I mobile Rx to UNII=30-10%

From chapter 4 (Table 4-2) we know that the inter-packet gap for periodic packet generation increases from 100 ms at 70% load, much too small for a 400ms BSM to get by, to over 2000 ms, four times longer than a BSM, at 10 % load.

Figure 10-28 directly compares the outside the building data from Figures 10-24 and 10-25. The 70% traffic load on the left almost completely blocks the DSRC as is shown by the 100% PER. The plot on the right, shows the traffic load lowered to 10%, which made the inter-packet gaps much larger than a BSM. About a third of the DSRC packets are now received demonstrating the significant sensitivity of a DSRC receiver to the traffic load of nearby Wi-Fi transmitters. But not that even at 10% load the PER was more than 60%, meaning that more than half of the BSMs were knocked out by Wi-Fi packets.



UNII traffic load (inter-packet gap): 70% (~100 ms) 10% (2000 ms)

Figure 10-28. Packet Error Rate, I2V UNII outside, UNII EIRP=35 dBm, at short range

Source: 20180208 Building-Brick drive-by toward V1 was -- exl_report_toward_2018020_side2.xlsx,
 Tabs: V2I mobile Rx to UNII=30-70%, and V2I mobile Rx to UNII=30-10%

In another test we kept the same 10% traffic loading but lowered the UNII EIRP by a factor of 500, (from 35 to 8 dBm) to measure the sensitivity to UNII power. Figure 10-29 shows that this substantial decrease in power had little to no effect on the interference. The PER is about the same (60%) when the radiated power was 500 times higher.

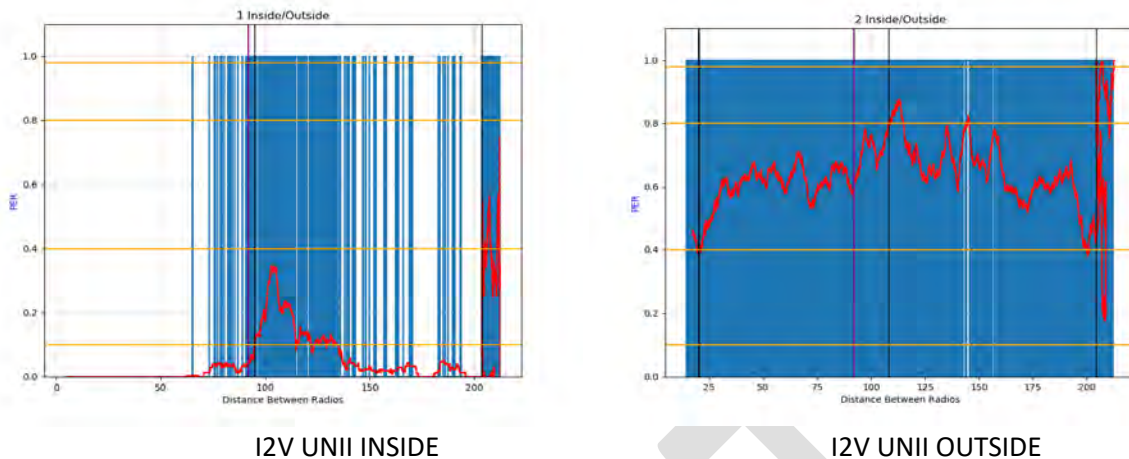


Figure 10-29. Packet Error Rate, I2V, UNII EIRP=8 dBm, 10% load, passing brick building shows effect of windows with light Wi-Fi traffic at very low power

Source: 20180208 Building-Brick drive-by toward V1 was -- exl_report_toward_2018020_side2.xlsx, Tab: V2I mobile Rx to UNII=30-10%

This result demonstrates at these relatively close ranges, (100 meters to the interferer and 0 to 200 meters between DSRC radios), even the lowest power Wi-Fi signal is enough to interfere. So the number of Wi-Fi packets in the air to collide with BSMs matters far more than their strength. Interference is highly sensitive to Wi-Fi traffic load and relatively insensitive to Wi-Fi power within the 300 meter safety radius needed by DSRC.

Note that shielding by the brick was the most effective at this low power, but still not enough as the vehicle passed the windows.

Another consideration is how missed packets are distributed. A 50% PER does not threaten safety if evenly distributed and not clustered. A vehicle will get an update from all other vehicles in 200 ms instead of 100 ms, which is adequate for safety. But if gaps are longer than half a second due to clustering that is a likely threat to safety. Figure 10-30 displays the packet gap distribution for lightly loaded, high power interferer of Figure 10-26. Large gaps appear at the same locations as high PER. When gaps size correlates with PER, the PER data can be taken as a measure of impact to safety as well.

Figure 10-30 shows that any Wi-Fi outside but lightly loaded (right) creates far too many safety critical gaps (red) to be tenable. Putting the UNII inside (center) creates far more gaps than the baseline (left) but acceptability away from the windows might depend on the sensitivity of the safety applications and the level of channel congestion. That depends on robustness to gaps 300-500 ms long (yellow). Safety critical gaps (red) in view of the windows are clearly untenable.

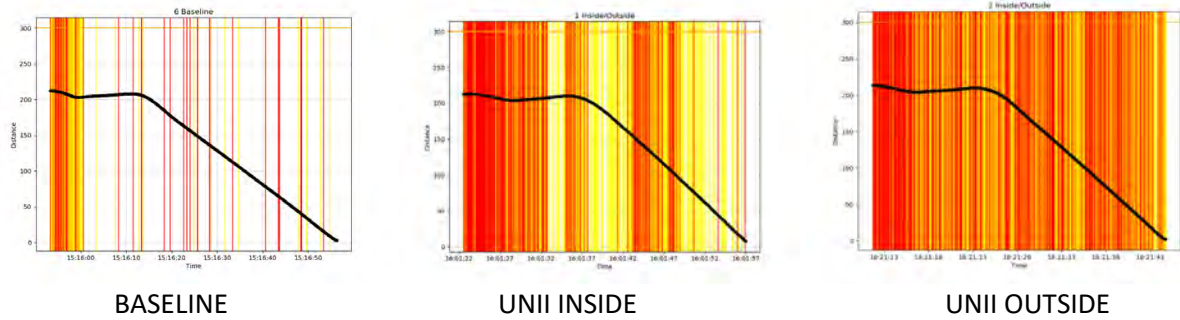
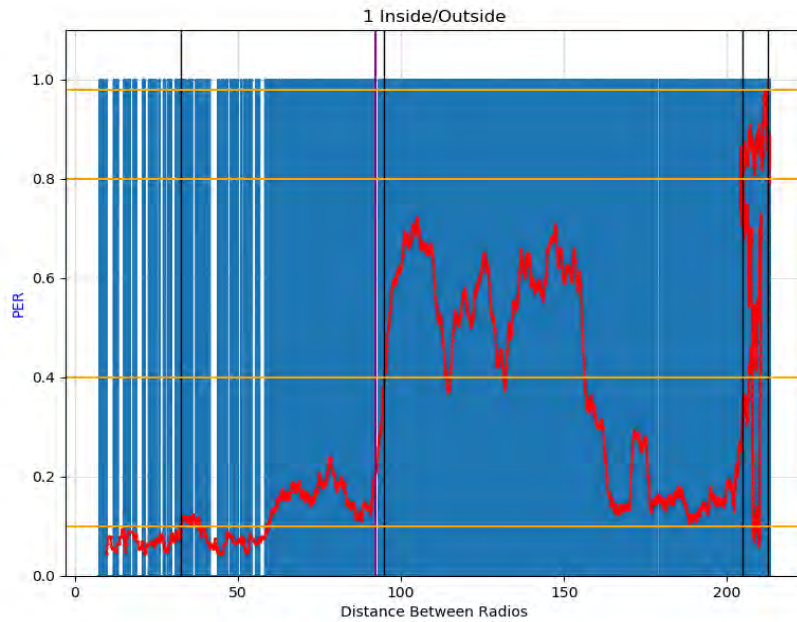


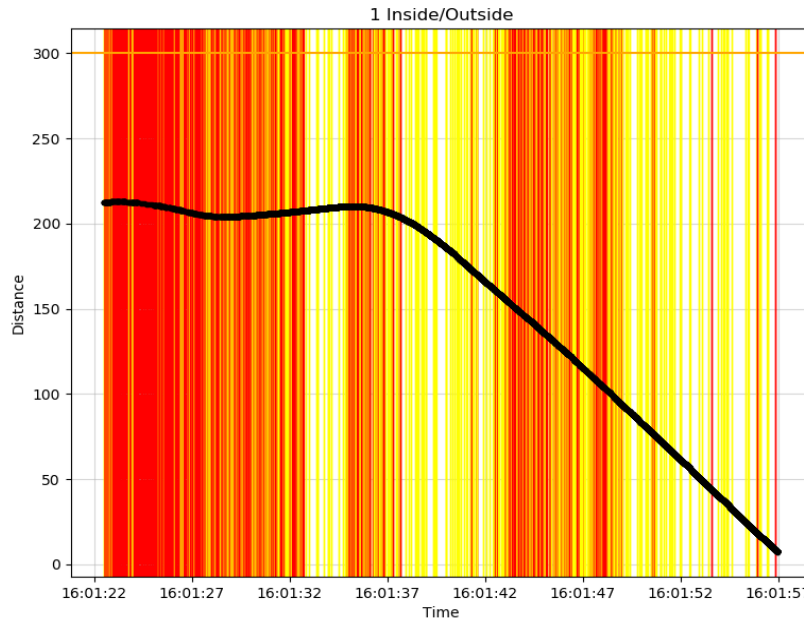
Figure 10-30. Packet gap distribution, I2V, UNII EIRP=35 dBm, 10% load, passing brick building shows that large PER correlates with large packet gaps

Source: 20180208 Building-Brick drive-by toward V1 was -- exl_report_toward_2018020_side2.xlsx, Tab: V2I mobile Rx to UNII=30-10%

Figure 10-31 is a close up of packet error rate and packet gap distribution for just the UNII inside the building to show better the correlation between them and the structure in the data caused by the windows. You can see the band of red safety critical gaps that occurs when the black trajectory line crosses through the 90 to 160 meter range from the start point, which is exactly the region where the PER shoots up by the building. The location of the interferer in the building is marked by the vertical purple line in the PER plot.



Packet error rate



Packet gap distribution

Figure 10-31. Correlation between PER and Packet gap distribution, I2V, UNII EIRP=35 dBm, 10% load, UNII inside brick building with windows

Source: 20180208 Building-Brick drive-by toward V1 was -- exl_report_toward_2018020_side2.xlsx, Tab: V2I mobile Rx to UNII=30-10%

Figure 10-32 shows another important discovery. The interference to a DSRC receiver is much greater than to a DSRC transmitter. You see no effect of the building windows as the transmitting DSRC drove by (bottom V2I plots). The flat PER data outside the building shows impact to the receiver at the start point, which remains the same with little or no suppression as the transmitter drove by.

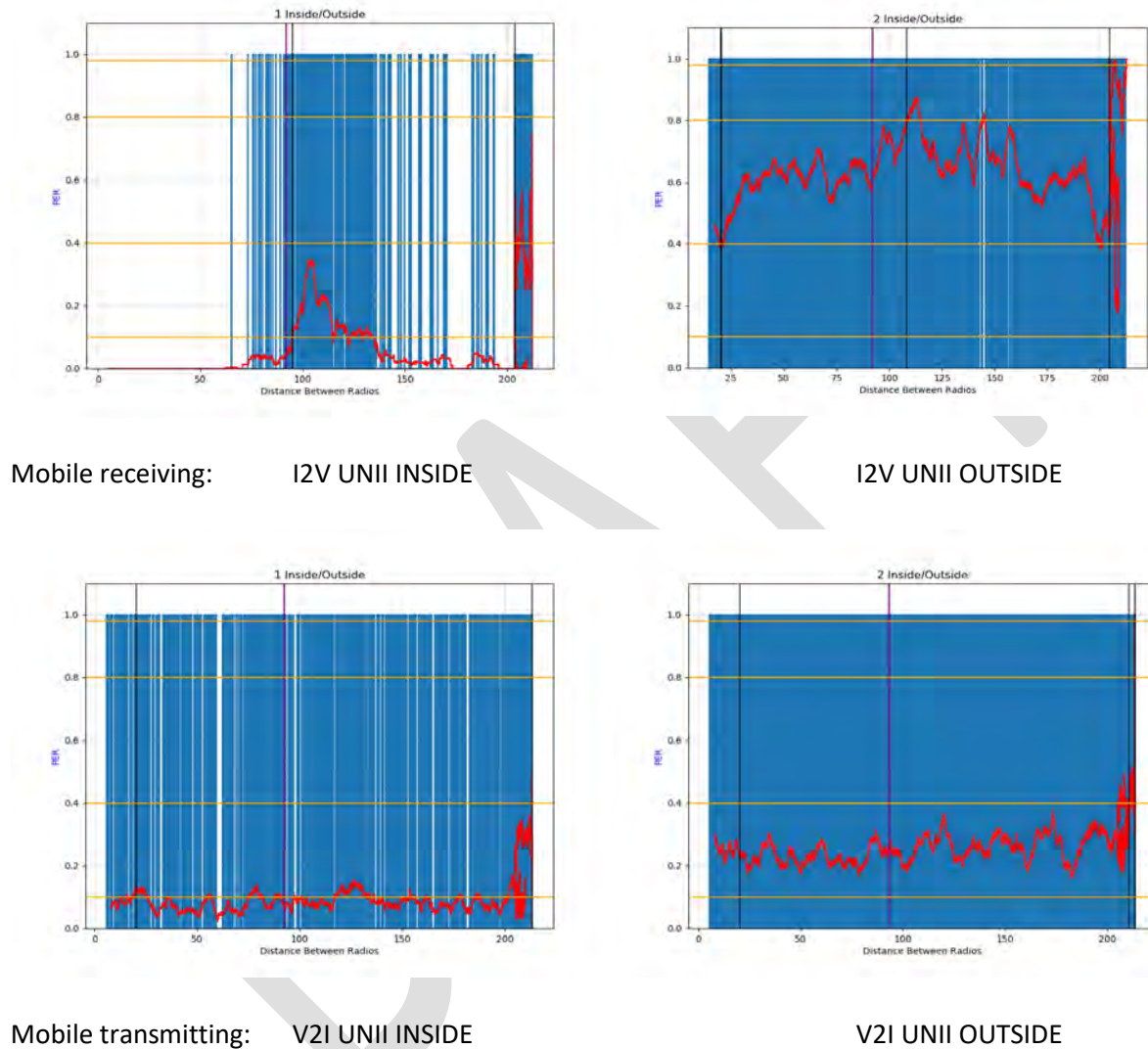


Figure 10-32. PER and Packet gap distribution, UNII EIRP=35 dBm, 10% load, drive by brick building with windows when mobile was transmitting (V2I) vs receiving (I2V)

Source: 20180208 Building-Brick drive-by toward V1 was -- exl_report_toward_2018020_side2.xlsx, Tabs: V2I mobile Rx to UNII=30-10% and V2I mobile Tx to UNII=30-10%

If the DSRC transmitter sensed the Wi-Fi energy and it was significant enough to activate the 802.11a clear channel access back-off mechanism you should see much greater latency, or time between the DSRC transmissions, when the vehicle drove by the interferer. Figure 10-33 plots the time between DSRC transmissions for the PER data in Figure 10-32.

Even when the mobile is transmitting and driving only a few meters from the Wi-Fi antenna (lower right) the latency data looks the same as the receive data and inside the building data. A spike in the time between sends should show when the vehicle drove by the interferer at around 100 meters. No suppression of transmission is evident. This buttresses the earlier conclusion that Wi-Fi interference to DSRC reception is far more significant than interference to DSRC transmission.

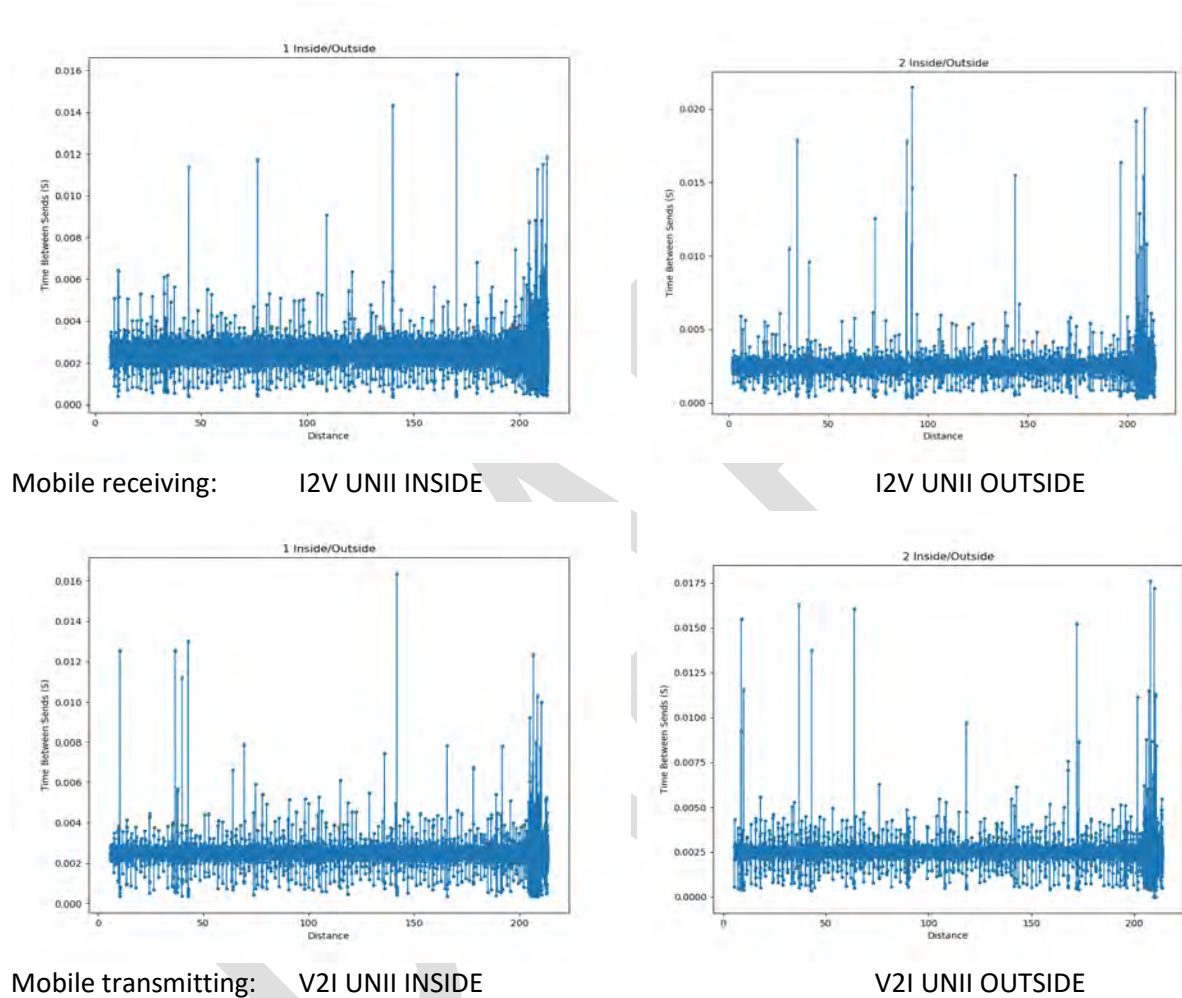


Figure 10-33 Time between transmissions, UNII EIRP=35 dBm, 10% load, drive by brick building with windows when mobile was transmitting (V2I) vs receiving (I2V)

Source: 20180208 Building-Brick drive-by toward V1 was -- exl_report_toward_2018020_side2.xlsx, Tabs: V2I mobile Rx to UNII=30-10% and V2I mobile Tx to UNII=30-10%

10.1.2.2 V2I with highest UNII power

In these runs the UNII operated at a high level of power (EIRP=36 dBm) and at a high traffic load (70%). In the following section, we will show the effect of lower the Wi-Fi traffic load. To be comparable with

the other building tests the data used in this section is strictly driving from the west where the vehicle was not exposed to the windows.

Figure 10-34 compares the RSSI and noise power plots for the baseline measurement, and the cases of the UNII inside, and then outside the building at the highest power level (EIRP=35 dBm). Blue shows the RSSI value of each BSM and black is the 0.5 sec average RSSI. Tan is the noise power of each BSM and red is the 0.5 sec average. The horizontal red line is a benchmark for the nominal DSRC receiver sensitivity of -95 dBm.

As with the other building measurements notice the more irregular shape of the RSSI curve compared to data from the clear and open sites at Zone 1 and Perryman. The more numerous and irregularly shaped peaks and nulls are due to multipath reflections in this more complicated environment.

The UNII inside plot shows noise received by DSRC ticks up a bit 200 meters from the building (purple vertical line at -100m). This was also 200 meters for the filled cinderblock building. The noise rises above the -95 dBm receiver sensitivity benchmark around 600 meters away. With the UNII outside the building, the noise is higher but more importantly the received DSRC power is disrupted the whole way.

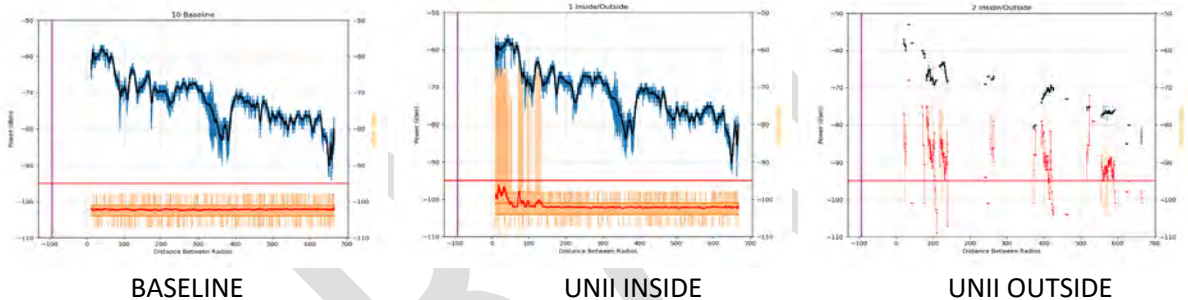


Figure 10- 34. RSSI and noise power plots, I2V, UNII EIRP=35 dBm, 70% load, approaching Brick building

Source: 20180208 Building-Brick W side toward V1 --was exl_report_toward_20180208.xlsx, Tab: V21 mobile Rx to UNII=30-70%

Figure 10-35 shows the signal-to-noise ratio directly. Blue is the SNR for each BSM and black is the 0.5 second average. Other than greater variation in the first 200 m, the SNR with interferer inside the brick building looks like the baseline, the same result as with the Cinderblock building. Not enough signal was received to evaluate the SNR when the UNII was outside the building. It is possible the Wi-Fi signal was more disruptive as the UNII radio was at the same elevation and less than 5 meters off the road as opposed to the 50 meter offset and higher elevation during the cinderblock building tests.

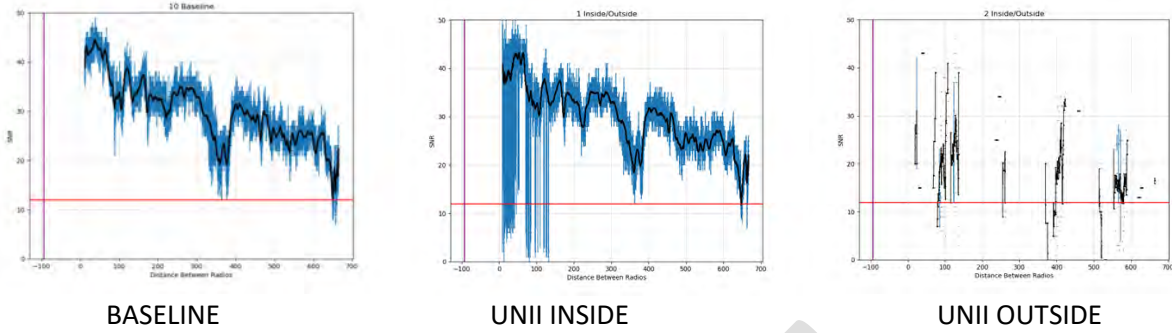


Figure 10-35. Signal-to-Noise plots, I2V, UNII EIRP=35 dBm, 70% load, approaching Brick building

Source: 20180208 Building-Brick W side toward V1 --was exl_report_toward_20180208.xlsx, Tab: V21 mobile Rx to UNII=30-70%

Figure 10-36 compares the packet error rate measurements for this case. Blue records individual packet receptions and the red line is the 0.5 sec average PER. This figure shows even more clearly how little the wood building reduces the interference. With the UNII inside the Cinderblock building PER ranged from 20-40%. With the brick building it is 10-20% within the first 200 meters and negligible after that. It appears that the brick building offered more shielding than the cinderblock. 60%.

When the UNII was moved outside, the PER was at 100% most of the time. That was even more than the steady 80-90% in the other building tests. Given that the interferer configuration for the brick building test seemed more potent, the results might slightly underestimate the already significant shielding provided by the brick.

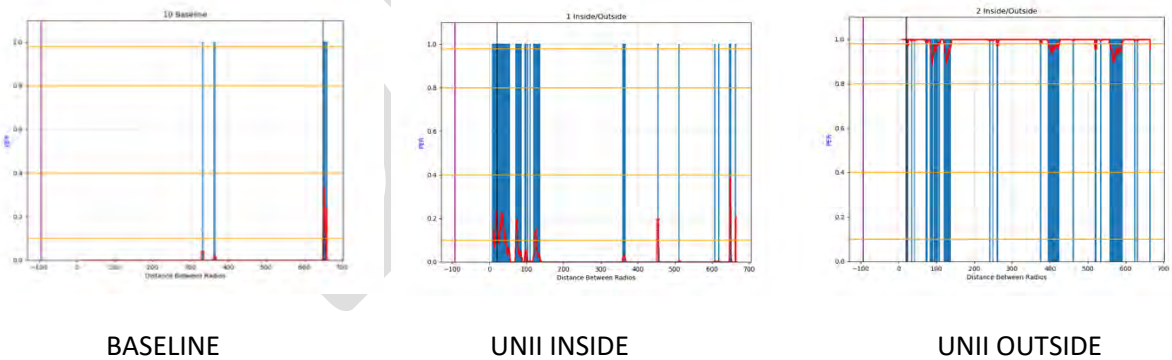


Figure 10- 36. Packet Error Rate plots, I2V, UNII EIRP=35 dBm, 70% load, approaching Brick building

Source: 20180208 Building-Brick W side toward V1 --was exl_report_toward_20180208.xlsx, Tab: V21 mobile Rx to UNII=30-70%

Figure 10-37 conveys the distribution of the packet error rate shown in Figure 10-36. The plots in Figure 10-37 display gaps caused by consecutively missed packets. Yellow indicates “gaps of concern” when no BSM is received in 300 to 500 ms. Red shows safety critical gaps due to the loss of consecutive BSMs for more than 500 ms, which is a gap that is more than half a second long. The black line shows the distance of the vehicle from the building (y-axis) as a function of time (x-axis). The horizontal orange line marks the 300-meter distance, which is the intended operating range for DSRC safety applications.

The baseline plot shows several safety critical gaps due to multipath from the complex environment. Unlike the Cinderblock building, which displayed more yellow than red, the UNII inside the brick building, shows a few gaps like the baseline with just a clustering of additional “gaps of concern” in the first 200 meters from the building. Again indicating the superior shielding of the brick. The solid red plot for the UNII outside with a few fragments of the trajectory line where occasional DSRC packets got through demonstrate how dramatically the Wi-Fi signal shutdown the DSRC without the shielding provided by the brick.

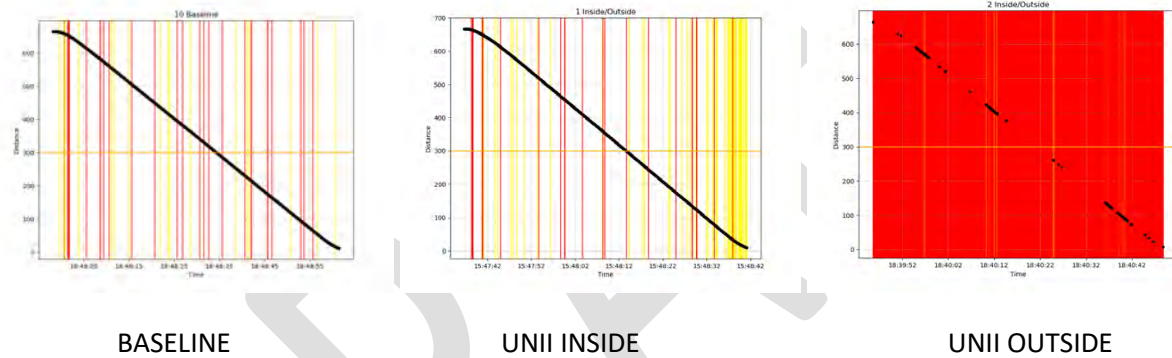


Figure 10-37. Packet gap plots, I2V, UNII EIRP=35 dBm, 70% load, approaching Brick building

Source: 20180208 Building-Brick W side toward V1 --was exl_report_toward_20180208.xlsx, Tab: V21 mobile Rx to UNII=30-70%

Figure 10-38 aggregates the data from Figure 10-37 by showing percent of time in three gap conditions for the segment of data analyzed in Figures 10-33 to 10-36. The gap conditions are green for gaps less than 0.3s (only 1 or 2 missed packets between received packets), yellow for gaps of 0.3 to 0.5 (3 to 5 consecutively missed packets) “gaps of concern”, and red for gaps larger than 0.5 second (more than 5 BSMs in a row) “safety critical gaps.”

The plot shows that putting the UNII inside the building meant less than 1% of the run time there were safety critical gaps, which was similar to the baseline. Outside of the building, the fraction time where gaps were less than half a second long is so small that the line of yellow is too thin to see in the plot.

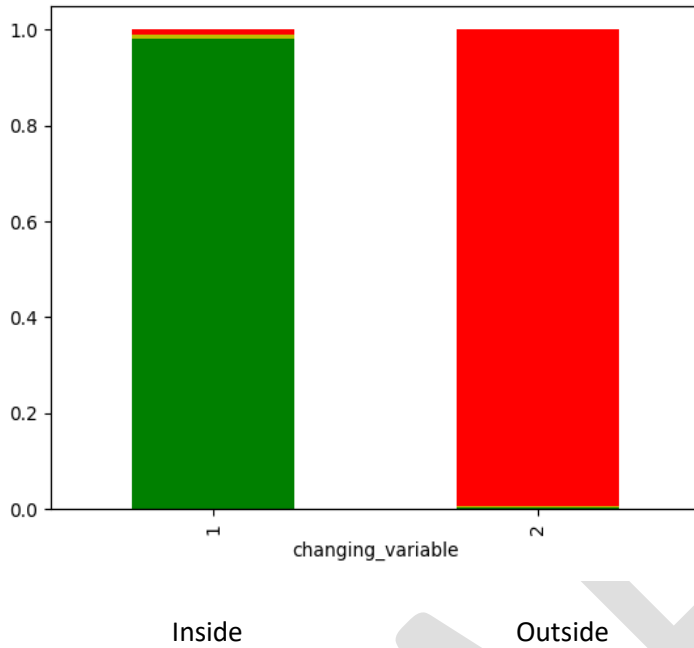


Figure 10-38. Summary of packet gaps, I2V, UNII EIRP=35 dBm, 70% load, approaching Brick building

Source: 20180208 Building-Brick W side toward V1 --was exl_report_toward_20180208.xlsx, Tab: V2I mobile Rx to UNII=30-70%

Figure 10-39 is an aerial comparison of how PER is distributed on the approach to the brick building. This figure makes it intuitively clear how effectively the brick prevented the Wi-Fi from interfering with the DSRC. Without the brick (UNII outside), DSRC communication was shut down completely by this high power, high traffic access point. (Color scale: Aqua is 100% PER and hot pink zero PER. As color scales from blue toward purple and pink the PER decreases. Red dot is the location of the Wi-Fi interferer and brick building.)



Figure 10-39. Geographical distribution of PER, I2V, UNII EIRP=35 dBm, 70% load,

approaching Brick building

Source: 20180208 Building-Brick W side toward V1 --was exl_report_toward_20180208.xlsx, Tab: V2I mobile Rx to UNII=30-70%

The departing data shows essentially the same result as the approaching data. Rather than repeat the above analysis in detail, we include the satellite view of departing packet error rate in Figure 10-40. The approaching PER data of Figure 10-39 is essentially the same as the departing data of Figure 10-40.



Figure 10-40. Geographical distribution of PER, I2V, UNII EIRP=35 dBm, 70% load, departing Brick building

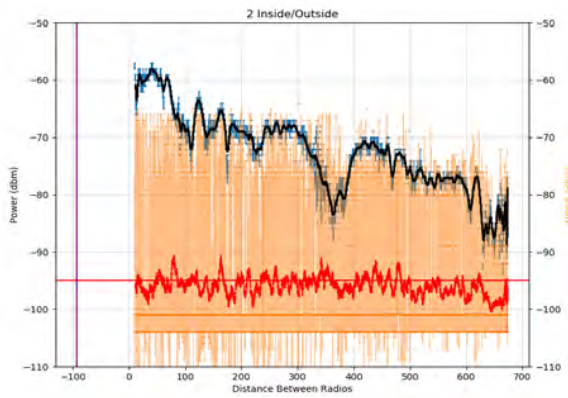
Source: 20180208 Building-Brick W side away V1 --was exl_report_away_20180208.xlsx, Tab: V2I mobile Rx to UNII=30-70%

10.1.2.3 V2I Highest UNII power but low traffic load

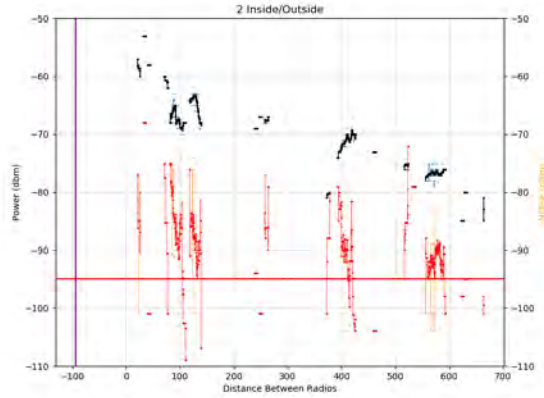
The same high power access point was tested inside and outside the brick building at a 10% traffic load. As shown in section 4 above, the inter-packet spacing for that Wi-Fi loading is large enough to allow some BSMs through without collision. These results show the sensitivity of interference to traffic loading.

The top row in Figure 10-41 shows the Wi-Fi access point outside the building, lowering the traffic load from 70% to 10% allowed DSRC communications. The DSRC detected noise around the -95 dB sensitivity benchmark up to 700 away from the building (vertical purple line) at 10% load.

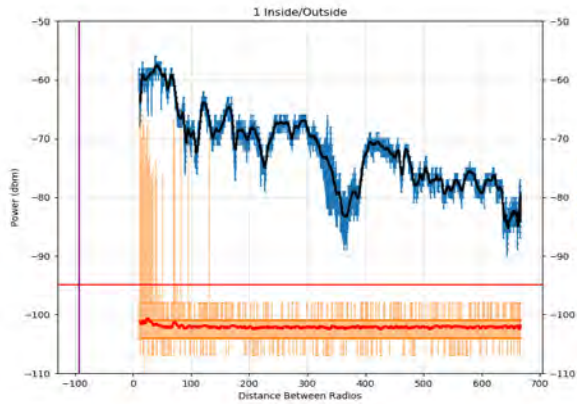
With the access point inside the brick building (bottom row) noise in the 70% loading tests is as much as 5 dB above the baseline within 200 meters but then diminishes to baseline. At the 10% load a ripple in the noise is perceptible over the same range but much smaller (~1 dBm).



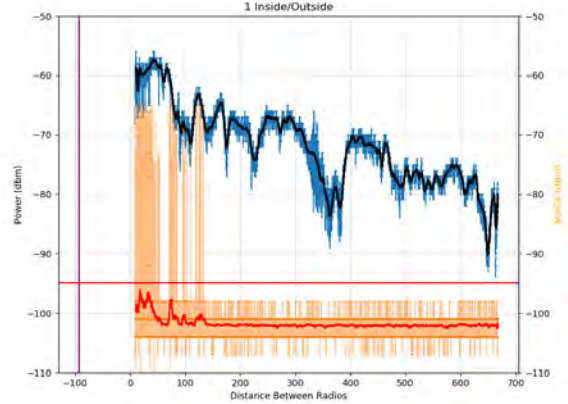
Outside UNII traffic load: 10%



70%



Inside UNII traffic load: 10%



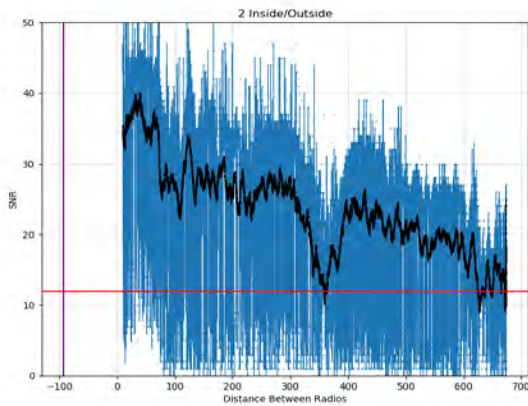
70%

Figure 10-41. Comparing RSSI plots as UNII traffic load changed, UNII EIRP=35 dBm, I2V EIRP=25 dBm, approaching Brick building

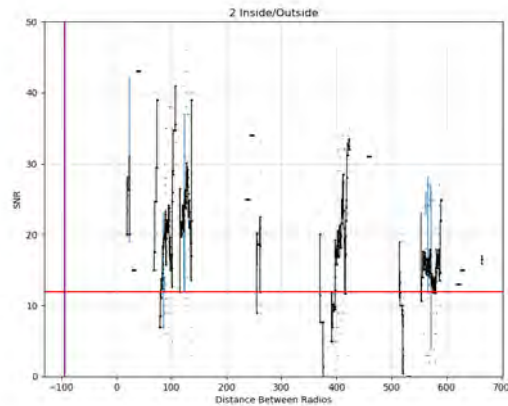
Source: 20180208 Building-Brick W side toward V1 --was exl_report_toward_20180208.xlsx, Tabs: V2I mobile Rx to UNII=30-10%; V2I mobile Rx to UNII=30-70%

Figure 10-42 shows this from the signal-to-noise perspective as well. Inside the brick building (bottom row) for both traffic loads the SNR is similar to the baseline but with more variability. At the higher load the variability is somewhat higher and lasts a little further.

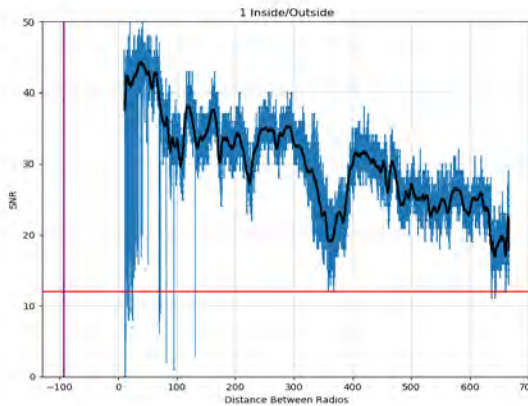
With the UNII outside (top row), the 10% load signal-to-noise curve averages about 5 dB less than the baseline. Not enough signal was received to analyze SNR for the 70% traffic load.



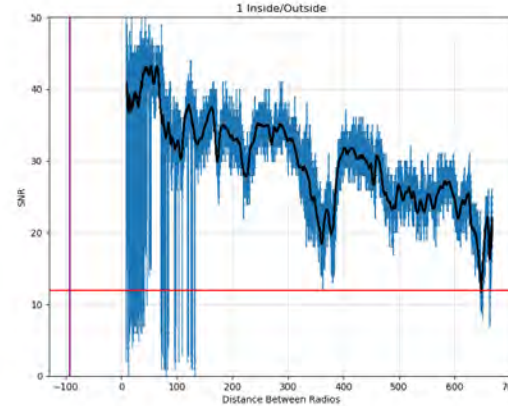
Outside UNII traffic load: 10%



70%



Inside UNII traffic load: 10%



70%

Figure 10-42. Comparing SNR plots as UNII traffic load changed, UNII EIRP=35 dBm, I2V EIRP=25 dBm, approaching Brick building

Source: 20180208 Building-Brick W side toward V1 --was exl_report_toward_20180208.xlsx, Tabs: V2I mobile Rx to UNII=30-10%; V2I mobile Rx to UNII=30-70%

Figure 10-43 shows packet error rate inside the brick building (bottom row). At the low 10% load packet losses barely peak at 10% and die out to baseline 150 meters from the building (vertical purple line). Turning the high power access point traffic load up to 70%, the packet errors double to 20% and take a bit longer—to 230 meters—to return back to baseline.

Two observations: One, compared to the plots on the upper row (UNII outside) the brick contains the Wi-Fi signal quite well. Two, the containment isn't perfect as increasing the loading did cause more interference within 200 meters. That is consistent with the increased noise observed in the inside building plots of Figure 10-41.

Outside the brick building (top row), the sensitivity of DSRC to Wi-Fi traffic load (hence inter-packet gap size) is apparent from the large change from 100% to 60% PER as the load was reduced from 70% to

10%. This data is consistent with the results of the window drive-by's presented in section 10.1.2.1 above. Also, note the substantial interference, 60% PER, more than 700 meters down range even the lightly loaded access point.

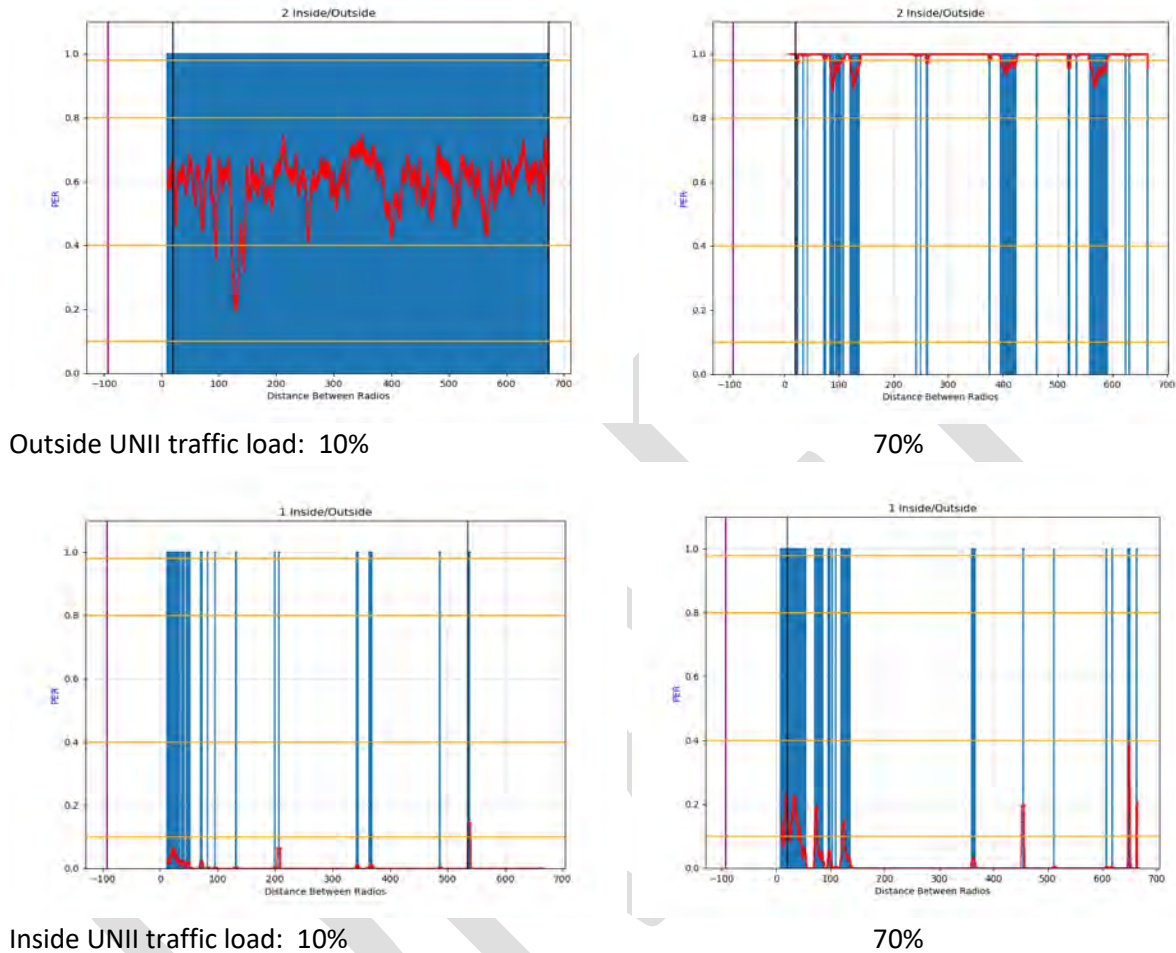


Figure 10-43. Comparing PER plots as UNII traffic load changed, UNII EIRP=35 dBm, 12V EIRP=25 dBm, approaching Brick building

Source: 20180208 Building-Brick W side toward V1 --was exl_report_toward_20180208.xlsx, Tabs: V2I mobile Rx to UNII=30-10%; V2I mobile Rx to UNII=30-70%

Figure 10-44 shows the distribution of the packet errors, in particular how they are clumped into larger gaps (yellow for concerning 300-500 ms gaps and red for safety critical gaps larger than 500 ms). Consistent with the PER plot you can see the UNII inside the building has a few more gaps of concern close in, several more at the higher loading, but otherwise similar to the baseline.

One conclusion is that a solid brick building with no windows may be able to reduce Wi-Fi interference to DSRC to an acceptable amount, even at high power. If necessary, a constraint on traffic load would be more effective than on Wi-Fi power to eliminate interference. In any case, that would ultimately

depend on the sensitivity of the most sensitive safety applications and the level of channel congestion so this is an area for further investigation.

Outside the brick building the gap data confirms the story told by the PER data. Interference to DSRC from a high power access point is untenable out to at least 700 meters at a light to moderate traffic load of 10% and devastating when at high power and high load (70%).

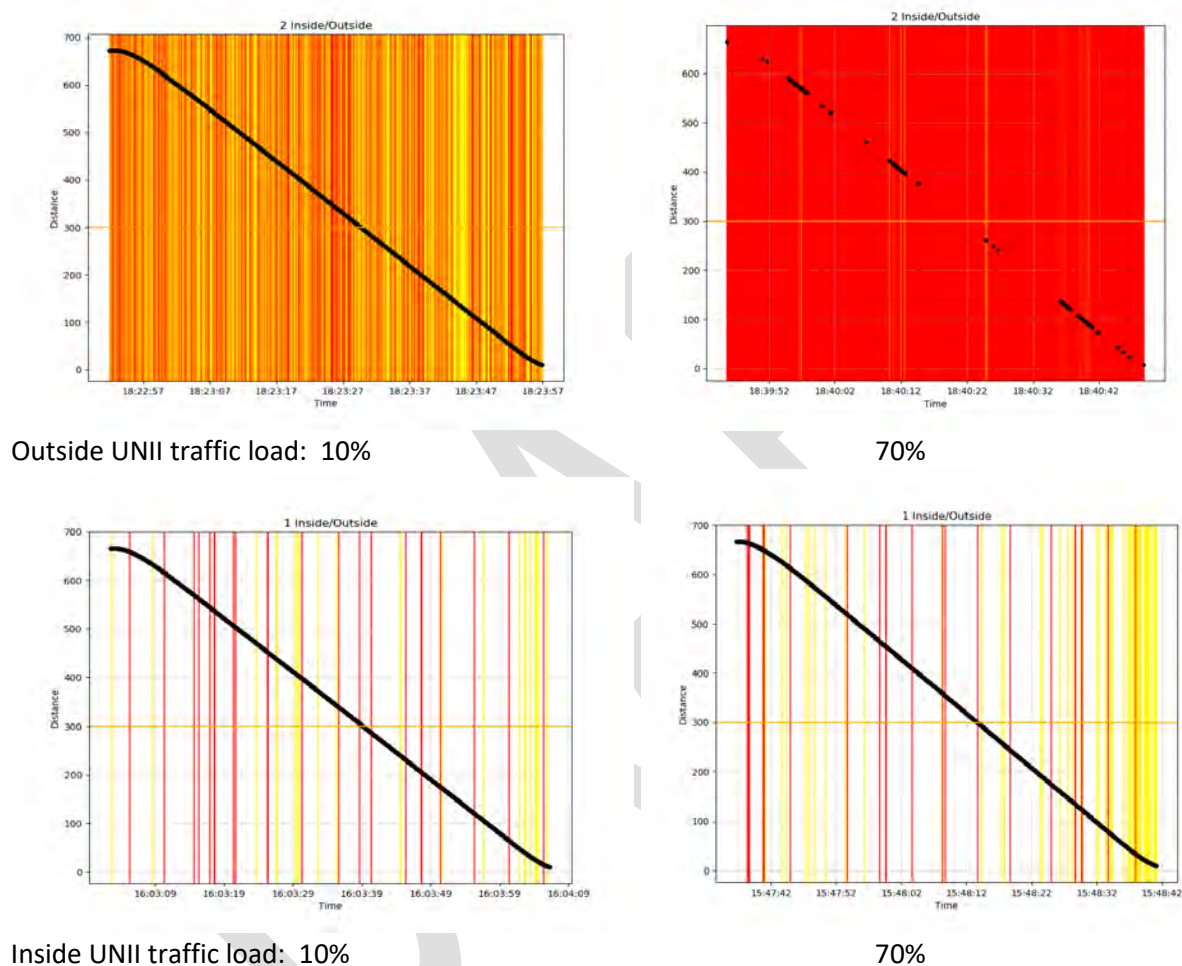


Figure 10-44. Comparing safety critical gaps as UNII traffic load changed, UNII EIRP=35 dBm, I2V, DSRC EIRP=25 dBm, approaching Brick building

Source: 20180208 Building-Brick W side toward V1 --was exl_report_toward_20180208.xlsx, Tabs: V2I mobile Rx to UNII=30-10%; V2I mobile Rx to UNII=30-70%

Figure 10-45 summarizes the percent of time the data runs spent in the three gap categories used in this analysis: Green for less than 300 ms, yellow for 300-500 ms gaps of concern, and red safety critical gaps longer than 500 ms. Figure 10-45 is the aggregate view of Figure 10-44. It provides a quantitative overall comparison of gaps that threaten safety while Figure 10-44 gives a better intuitive feel about how those gaps are spread out over the range.

It may be easier to see in Figure 10-45 just how dramatic the containment of the solid brick building is at lower interference when you compare the inside versus outside bars. Comparing the 10% and 70% outside bars clearly shows the effect of lower Wi-Fi traffic load and just how much of the time even a 10% load imposes concerning and threatening gaps in the DSRC communications. The data driving away from the building is the same as this approach data.

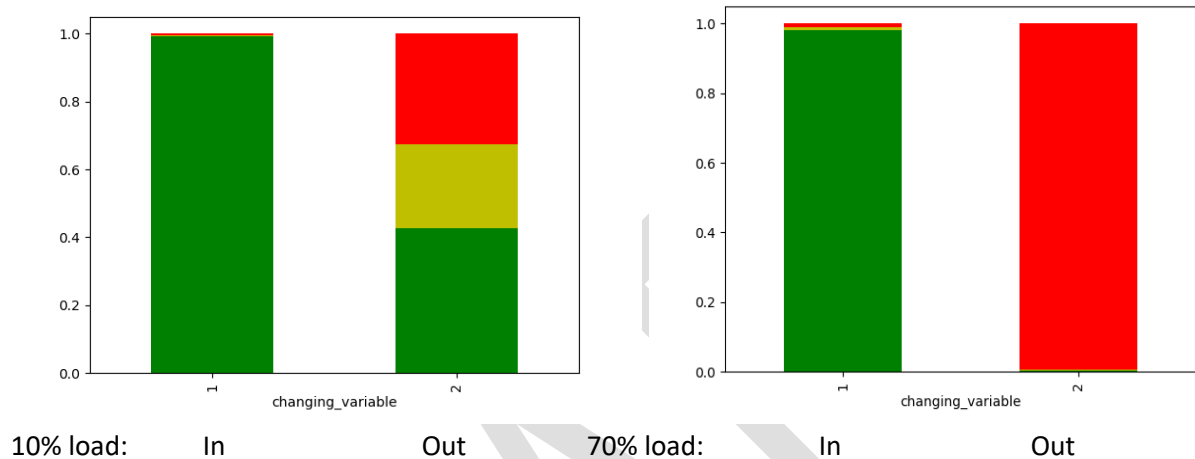


Figure 10-45. Summary of consecutive packet gaps as UNII traffic load changed, UNII EIRP=35 dBm, V2I EIRP=25 dBm, approaching Brick building

Source: 20180208 Building-Brick W side toward V1 --was exl_report_toward_20180208.xlsx, Tabs: V2I mobile Rx to UNII=30-10%; V2I mobile Rx to UNII=30-70%

The geographical representation of packet error rate that is Figure 10-46 shows more intuitively the shielding of DSRC from the Wi-Fi access point by the brick building. The outside data (top row) shows how reducing the traffic load allowed more DSRC packets through, though not enough for safety communications. These are the same results as the previous plots but this presentation is more intuitive.



Outside UNII traffic load: 10%



70%



Inside UNII traffic load: 10%



70%

Figure 10-46. Geographical distribution of PER, approaching Wood building as UNII traffic load changed, UNII EIRP=35 dBm, V2I EIRP=25 dBm, approaching Brick building

Source: 20180208 Building-Brick W side toward V1 --was exl_report_toward_20180208.xlsx, Tabs: V2I mobile Rx to UNII=30-10%; V2I mobile Rx to UNII=30-70%

10.1.2.4 I2V versus V2I (mobile receiving vs mobile transmitting) in the presence of Wi-Fi

Figure 10-47 compares I2V data (left) with the corresponding gaps and PER plots for the V2I runs (right) high load access point. The I2V data means the mobile was receiving DSRC transmissions from the RSU. This data has appears in the figures in the preceding sections of this chapter. The V2I data on the right where the mobile was transmitting and the RSU receiving is new.

What is clear comparing the right and left data, is that when the mobile was transmitting, the interference was not sensitive to where the vehicle was. The packet error rate and safety critical gaps are evenly distributed throughout the run, unlike when the mobile was receiving. When the mobile was receiving, the error was greatest closer to the building and interferer. As noted in section 10.1.2.1 above the DSRC radios don't "hear" the Wi-Fi loud enough at these ranges for them to suppress their

transmissions. Almost all the interference we see here is to the receiver, in this case, that is jamming of DSRC reception at the RSU.

The RSU is at the start point of zero and the brick building is at -100 meters on the plots below. The RSU is always close to the interferer, and its ability to receive from the mobile is compromised from the beginning. The only reason the communication isn't completely blocked is because of the shielding of the brick. It is curious though that the packet error rate is 40% so the brick is not shielding as well when the RSU is receiving. The PER is not seen that high when the mobile was receiving.

That might be because at 18 feet, the RSU antenna is better positioned to receive and transmit than the one on the vehicle. That might be a reason it competes better against the UNII. Moreover, the vehicle mounted antenna gain is reduced by 10 feet of cable loss that the RSU does not suffer. It is possible the gain of one of these antennas is not correctly accounted for, which might explain the imbalance. To get the same EIRP, perhaps the commanded power should not have been the same.

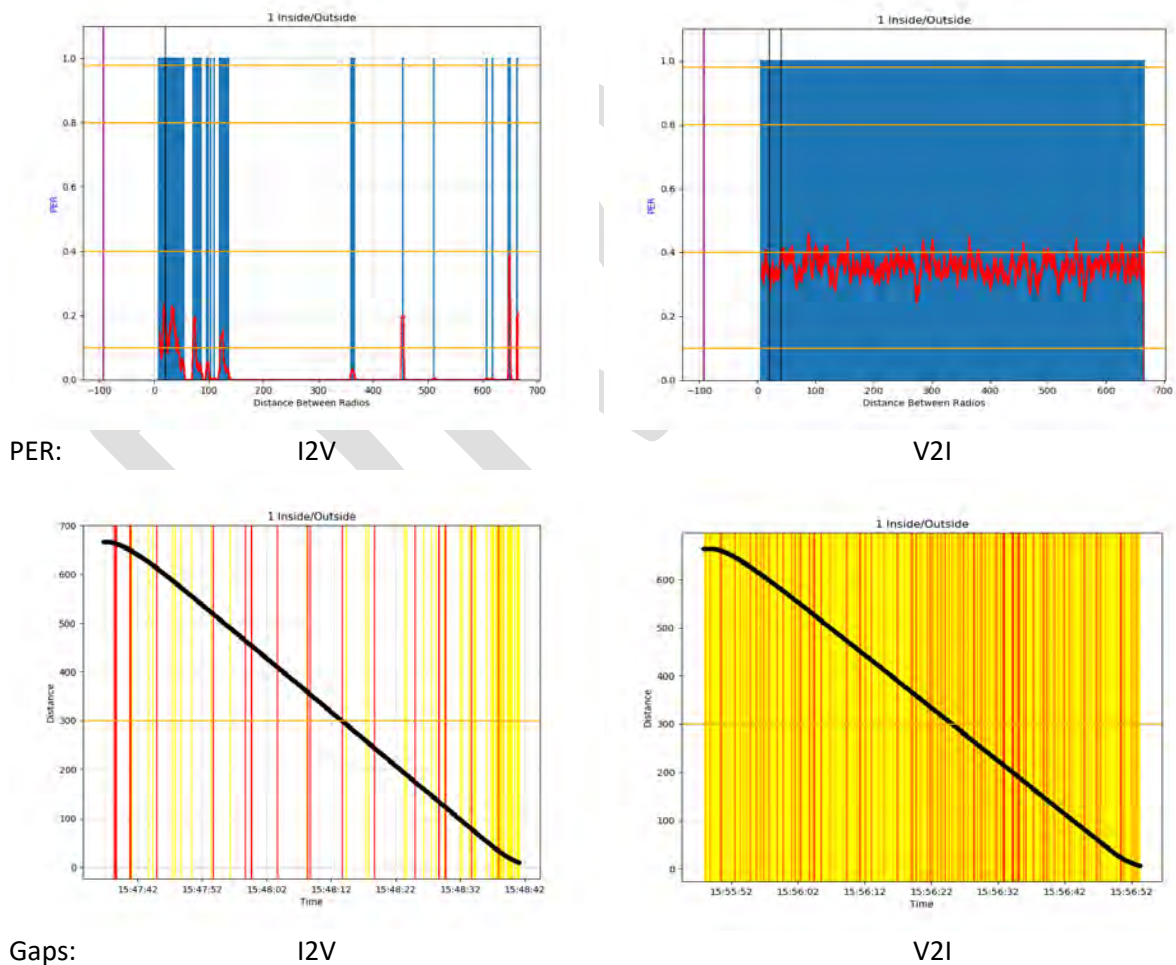


Figure 10-47. I2V versus V2I, approaching Brick building, UNII inside building with traffic load of 70%, UNII EIRP=35 dBm, DSRC EIRP=25 dBm

Source: 20180208 Building-Brick W side toward V1 --was exl_report_toward_20180208.xlsx, Tabs: V2I mobile Rx to UNII=30-70%; V2I mobile Tx to UNII=30-70%

Figure 10-48 shows the same results at a reduced level for the lightly loaded access point at high power.

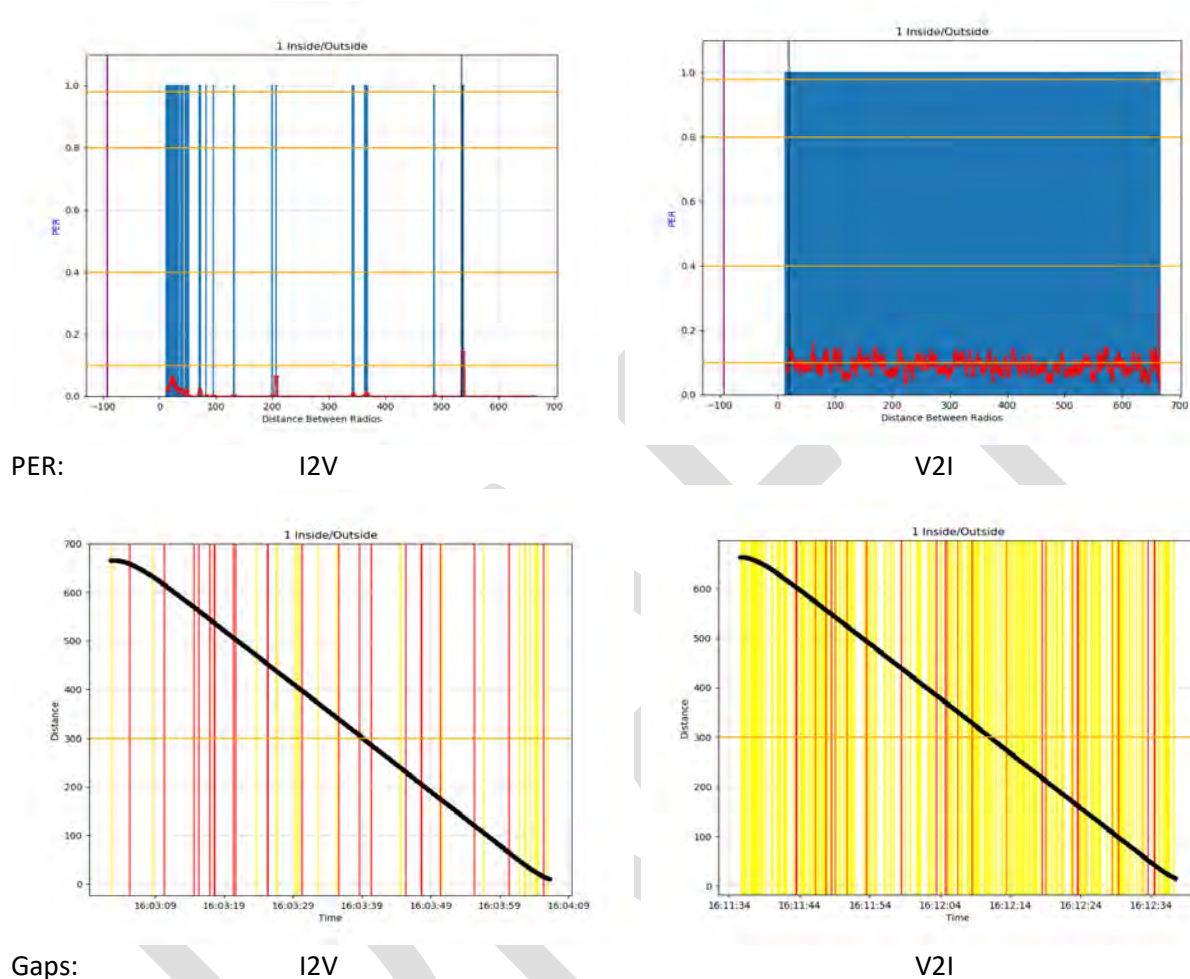


Figure 10-48. I2V versus V2I, approaching Brick building, UNII inside building with traffic load of 10%, UNII EIRP=35 dBm, DSRC EIRP=25 dBm

Source: 20180208 Building-Brick W side toward V1 --was exl_report_toward_20180208.xlsx, Tabs: V2I mobile Rx to UNII=30-10%; V2I mobile Tx to UNII=30-10%

10.1.2.5 Sensitivity to UNII power

Figure 10-49 shows the relative lack of sensitivity to changing the power of the UNII interferer compared to changing the traffic load as shown above. This was for a lightly to moderately loaded access point (10%). Raising the radiated power of the UNII inside the brick building by a factor 500 times (from 8 to 35 dBm) made little difference to the DSRC outside.

Raising the power of the access point when outside the building that same 500 times only moved the packet error rate by a factor of 2 to 3. Basically, even at the lowest power level tested, the Wi-Fi signals can interfere with the DSRC out to at least 700 meters. The number of Wi-Fi packets are in the air and the spacing in between them matters more for interfering with DSRC than power.

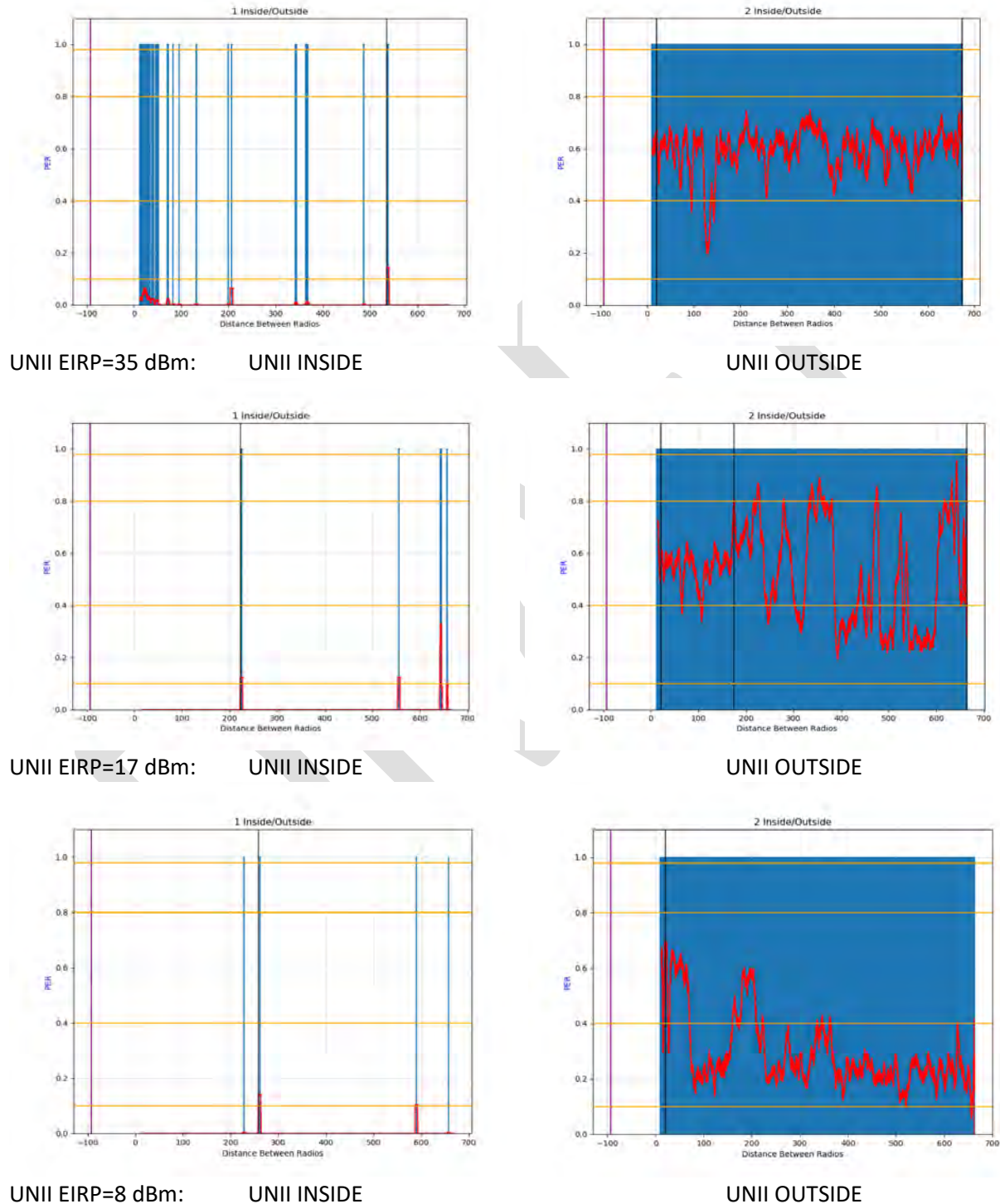


Figure 10-49. Sensitivity to UNII power, approaching Brick building, UNII traffic load of 10%, UNII EIRP=35 dBm, 12V

Source: 20180208 Building-Brick W side toward V1 --was exl_report_toward_20180208.xlsx, Tabs: V2I mobile Rx to UNII=30-120%; V2I mobile Rx to UNII=3-10%; V2I=20 mobile Rx to UNII=12-10%

For comparison Figure 10-50 shows the results for V2V with the mobile transmitting. That is two variables changed. Mobile is transmitting instead of receiving. DSRC antennas are both at the height of the access point antenna.

You can see that when the access point was outside, in this case, the 500 times reduction of power didn't affect the packet error rate much. It is interesting to see that the higher power did increase packet errors from none to ~10% when the access point was inside the brick building but affecting the static receiver 100 meters away rather than the moving vehicle.

Note that the DSRC was transmitting 4 times the power they would in actual deployment and the Wi-Fi traffic load was a moderate to light 10%. Hence, Figures 10-48 and 10-49 provide data points for bounding the minimum interference one can expect for different access point powers and traffic loads.

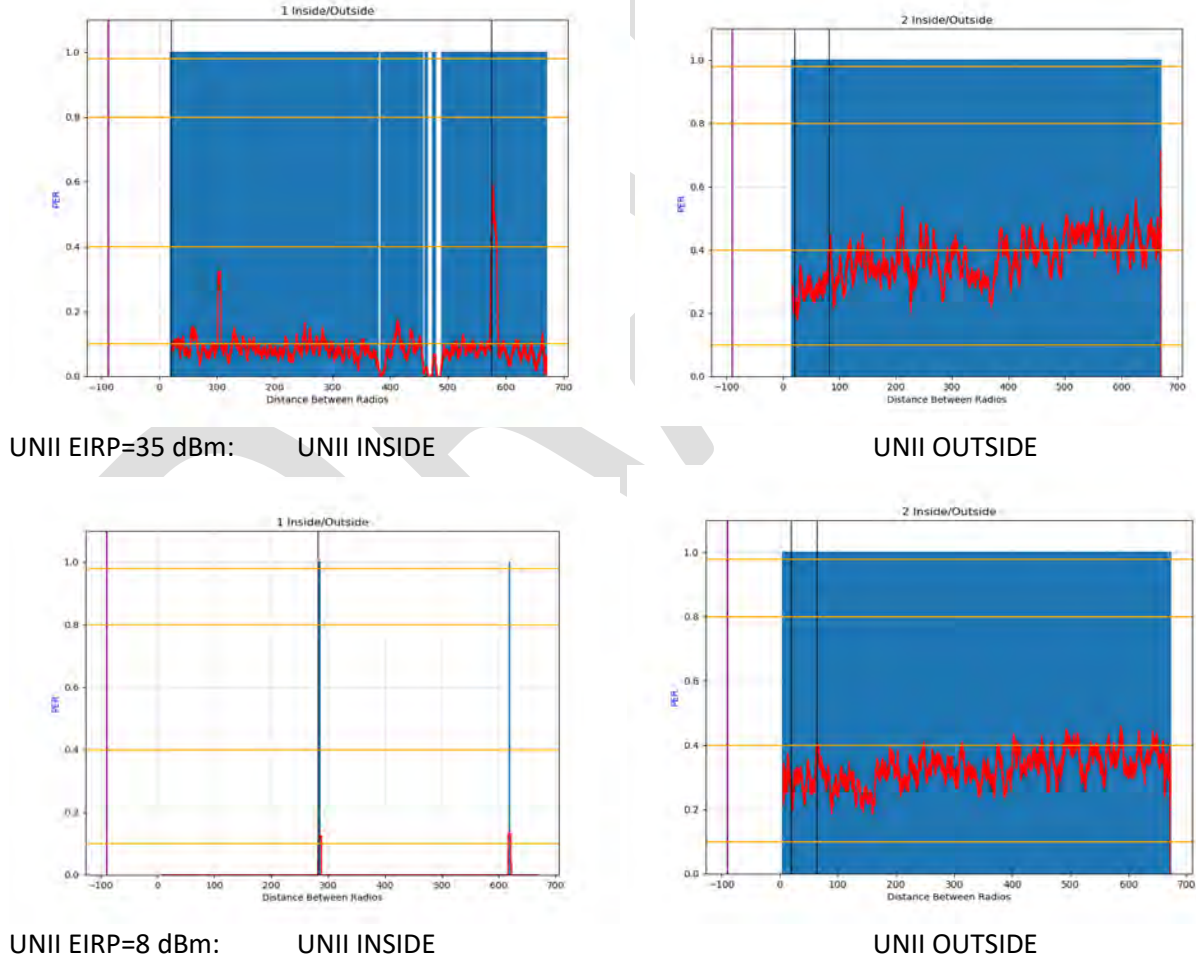


Figure 10-50. Sensitivity to UNII power, approaching Brick building, UNII traffic load of 10%, UNII EIRP=35 dBm, V2V EIRP=25 dBm

Source: 20180208 Building-Brick W side toward V1 --was exl_report_toward_20180208.xlsx, Tabs: V2V mobile Tx to UNII=30-10%; V2V mobile Tx to UNII=3-10%

10.1.2.6 V2V versus V2I

Figure 10-51 compares V2I data (left) with the corresponding gaps and PER plots for the V2V runs (right) with the high load, high power interferer inside the brick building. The top row of plots shows packet error rate the bottom row of plots shows time gaps between received BSMs distributed in time and space. Both sets of plots show untenable to interference to DSRC in either case but it was worse for V2V.

As noted before, almost all of this interference occurred at the receiver, either the RSU or static vehicle, which both remained 100 meters from the interferer the whole time. Even when the mobile DSRC drove by the start point, the PER didn't improve. The RSU at 18 feet has a height advantage over the UNII mounted at 6 feet high that may have allowed it to receive better than the static vehicle whose antenna was roughly 5 feet high.

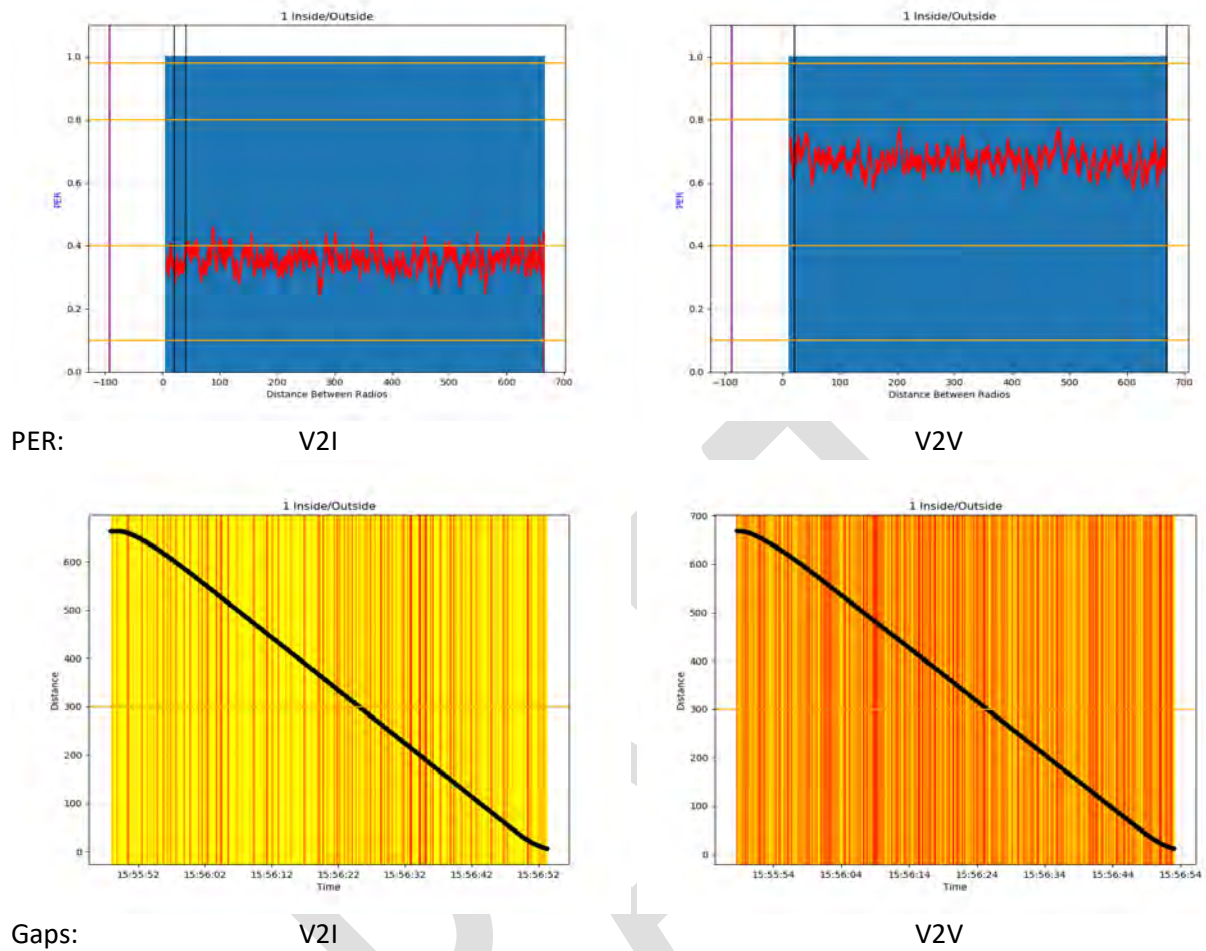


Figure 10-51. PER and gaps, V2V versus V2I, approaching Brick building, UNII inside building with traffic load of 70%, UNII EIRP=35 dBm, DSRC V2V and V2I EIRP=25 dBm, mobile transmitter

Source: 20180208 Building-Brick W side toward V1 --was exl_report_toward_20180208.xlsx, Tabs: V2I mobile Tx to UNII=30-70%; V2V mobile Tx to UNII=30-70%

Figure 10-52 similarly compares V2I and V2V for the interferer with the lower 10% traffic load. Unlike the high load case above, when the access point had a much lower traffic load, it interfered with the V2I and V2V DSRC about the same.

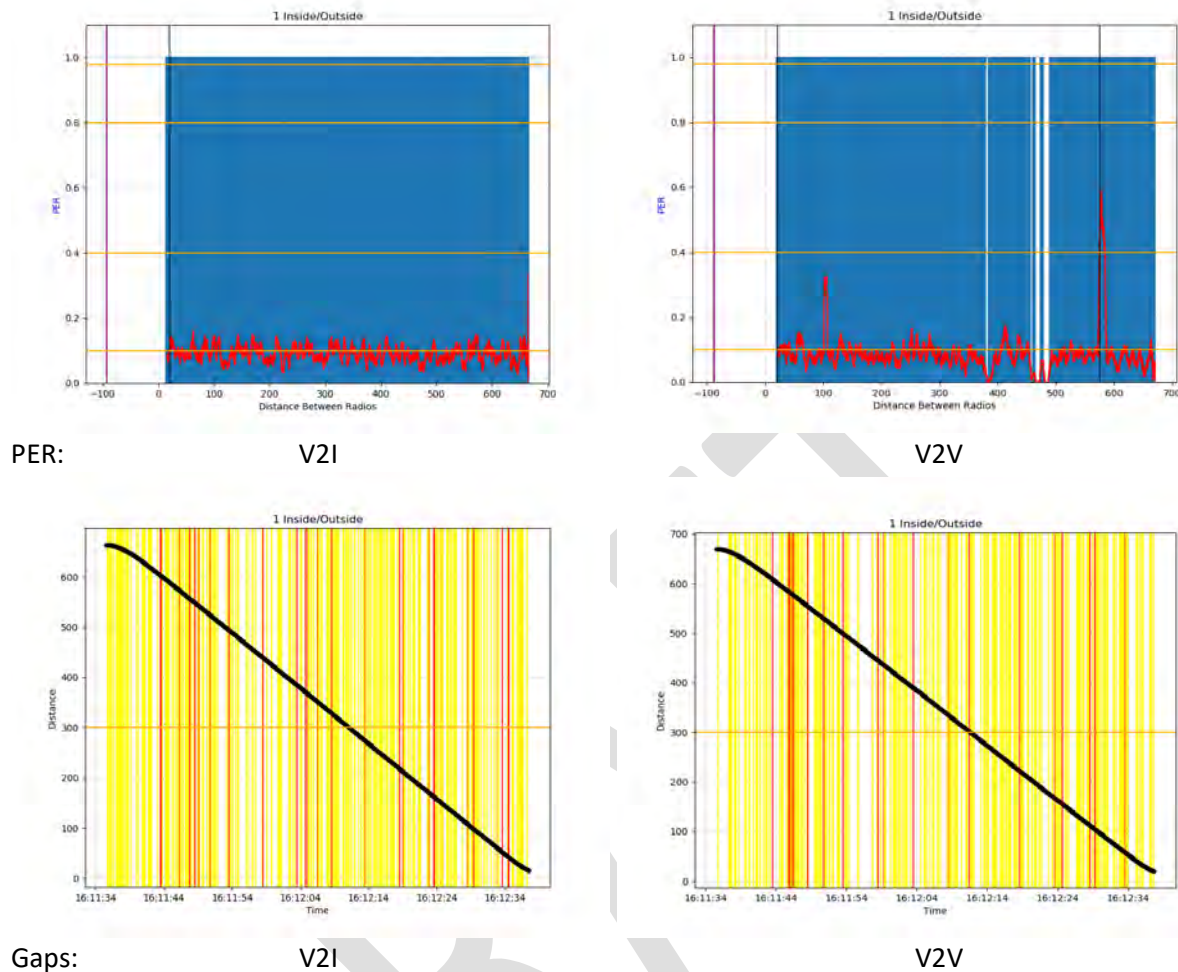


Figure 10-52. PER and gaps, V2V versus V2I, approaching Brick building, UNII inside building with traffic load of 10%, UNII EIRP=35 dBm, DSRC V2V and V2I EIRP=25 dBm, mobile transmitter

Source: 20180208 Building-Brick W side toward V1 --was exl_report_toward_20180208.xlsx, Tabs: V2I mobile Tx to UNII=30-10%; V2V mobile Tx to UNII=30-10%

The V2V data provided the same basic results as V2I leading to the same observations and conclusions so will not be repeated here. Consult the Appendices for those plots.

10.1.2.7 Deployment scenario

Most of the data in our tests were with the DSRC EIRP at 25 dBm, which is roughly 4 times more power than would be achieved by commercial equipment operating according to the SAE standard. The advantage in our tests might be even greater as our antennas likely have a higher gain and certainly a more uniform beam pattern than low profile, low cost commercial antennas for automobiles. As a result, our interference measurements underestimate the interference that would occur in real deployment. Thus, where we show interference, it is not questionable and likely to be worse.

On the other hand, the worst interference we measure is with the Wi-Fi access point transmitting at the maximum allowed EIRP. Some might argue that many access points aren't transmitting at maximum power and maximum load (like a jammer) all the time or even any of the time.

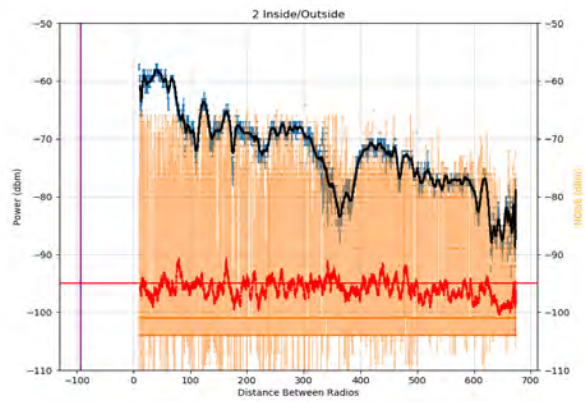
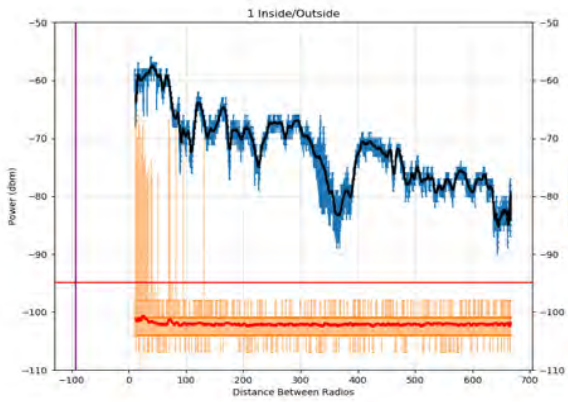
We ran an additional run during the brick building tests where we set the DSRC transmit power to what a non-ideal commercial device that "aspired" the SAE standard as an upper bound performance. That is an EIRP of 15 dBm or 4 times less power than the SAE upper limit.

Coupled with the lower powered DSRC is a "moderate" access point with the power turned down to an EIRP of 17 dBm. That is turned down by a factor of 63 times. At the same time we ran it with the light-moderate traffic load of 10%.

Figures 10-52 through 10-57 compare these deployment-like results with those where we ran both the DSRC and UNII at the high powers described above.

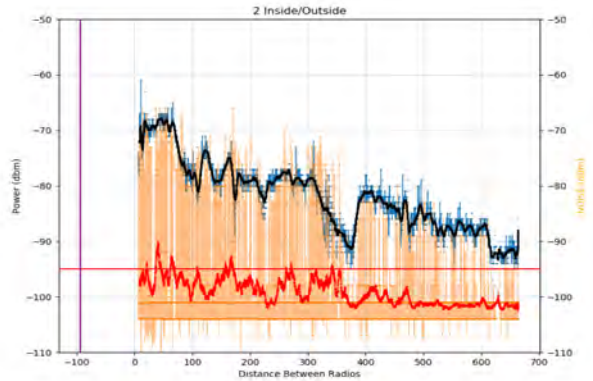
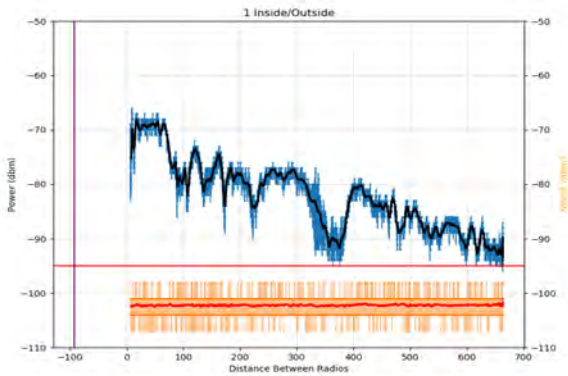
The primary observation from Figure 10-53 is that turning the DSRC power down 10 dBm lowers the RSSI curve 10 dBm as expected. The noise in the DSRC receiver with the access point outside is boosted up to the receiver sensitivity of -95 dBm in both cases.

Obviously with 10 dBm less signal power but the same noise floor you see the SNR plots for the deployment scenario down 10 dB as well in Figure 10-54. Both cases show much greater variation with the access point outside as expected from the greater variation in the noise signal (tan) in the RSSI/noise plots in Figure 10-53.



EIRP(dBm) UNII 35/ DSRC 25: UNII INSIDE

UNII OUTSIDE

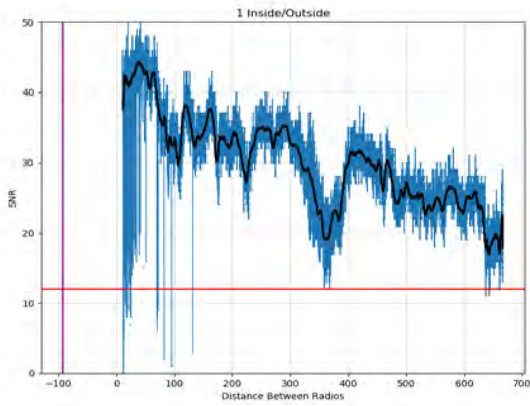


EIRP(dBm) UNII 17/ DSRC 15: UNII INSIDE

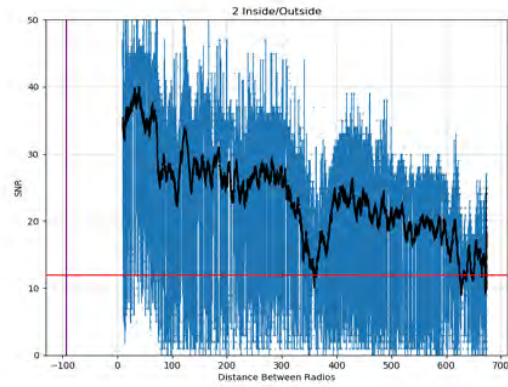
UNII OUTSIDE

Figure 10-53. Deployment versus high power scenarios, RSSI, approaching Brick building, UNII traffic load of 10%, I2V

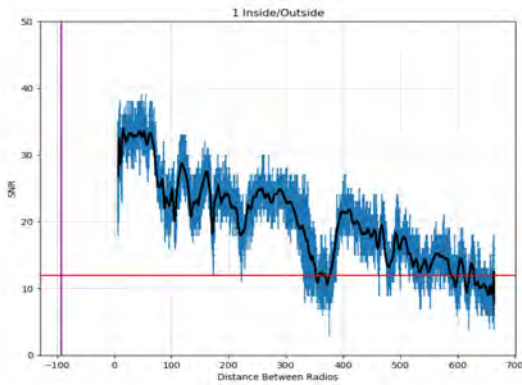
Source: 20180208 Building-Brick W side toward V1 --was exl_report_toward_20180208.xlsx, Tabs: V2I mobile Rx to UNII=30-10%; V2I=10 mobile Rx to UNII=12-10%



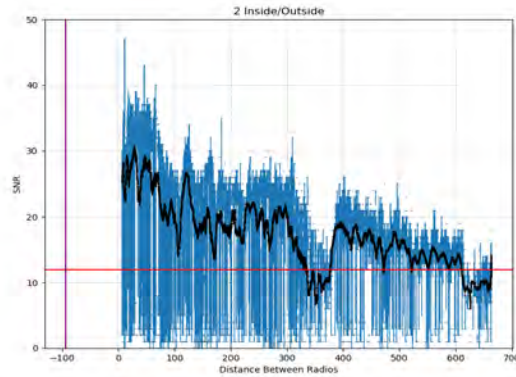
EIRP(dBm) UNII 35/ DSRC 25: UNII INSIDE



UNII OUTSIDE



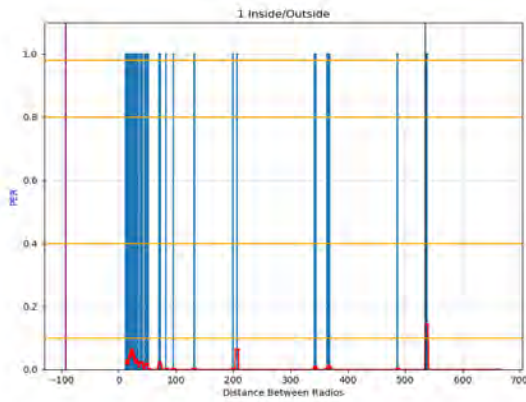
EIRP(dBm) UNII 17/ DSRC 15: UNII INSIDE



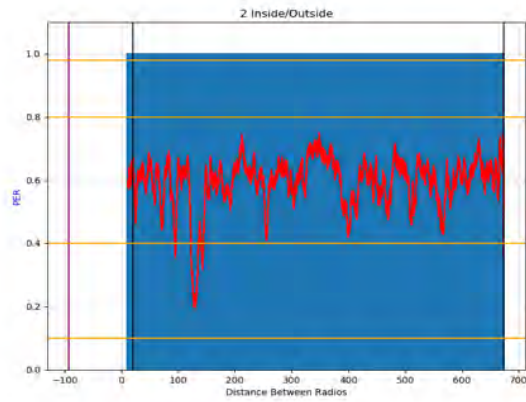
UNII OUTSIDE

Figure 10-54. Deployment versus high power scenarios, SNR, approaching Brick building, UNII traffic load of 10%, I2V

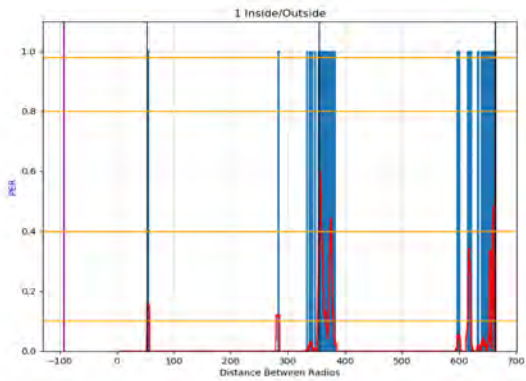
Source: 20180208 Building-Brick W side toward V1 --was exl_report_toward_20180208.xlsx, Tabs: V2I mobile Rx to UNII=30-10%; V2I=10 mobile Rx to UNII=12-10%



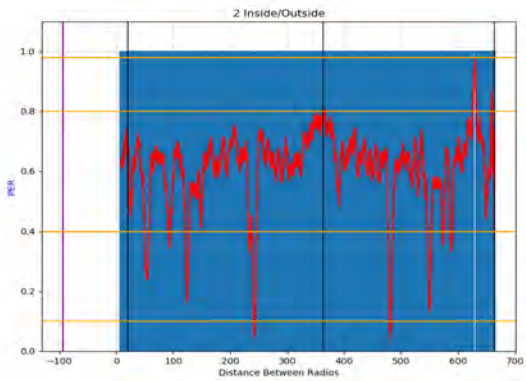
EIRP(dBm) UNII 35/ DSRC 25: UNII INSIDE



UNII OUTSIDE



EIRP(dBm) UNII 17/ DSRC 15: UNII INSIDE

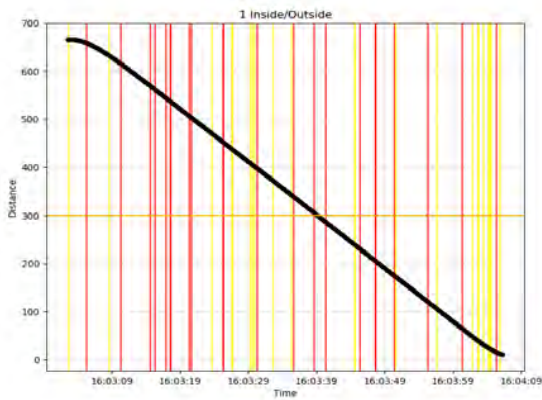


UNII OUTSIDE

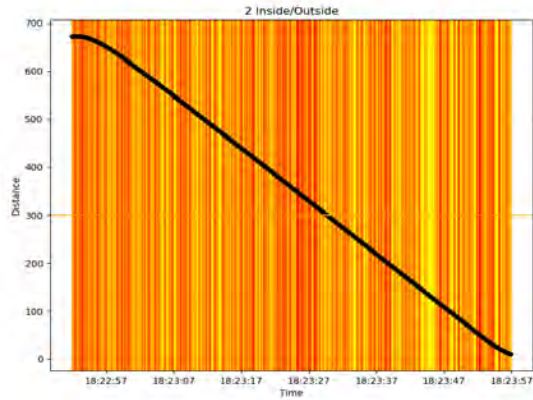
Figure 10-55. Deployment versus high power scenarios, PER, approaching Brick building, UNII traffic load of 10%, I2V

Source: 20180208 Building-Brick W side toward V1 --was exl_report_toward_20180208.xlsx, Tabs: V2I mobile Rx to UNII=30-10%; V2I=10 mobile Rx to UNII=12-10%

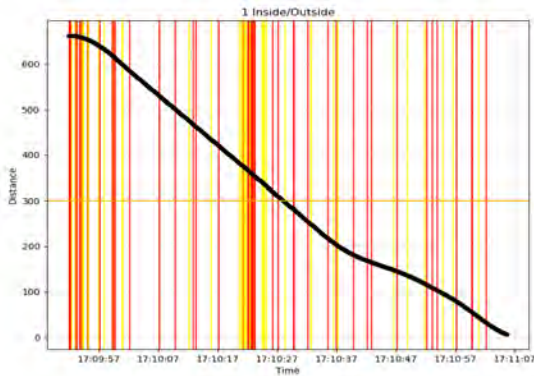
The packet error rate plots in Figure 10-55 show that the high power scenarios we have been testing give about the same results as the deployment scenario, especially for the outside access point. That indicates that much of the high power PER data we've collected tells us what to expect in the deployment scenario with both radio types turned down.



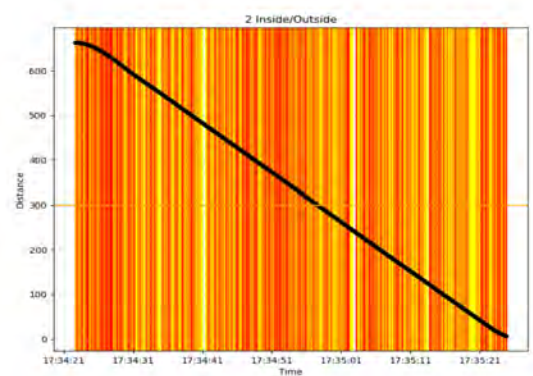
EIRP(dBm) UNII 35/ DSRC 25: UNII INSIDE



UNII OUTSIDE



EIRP(dBm) UNII 17/ DSRC 15: UNII INSIDE



UNII OUTSIDE

Figure 10-56. Deployment versus high power scenarios, Gaps, approaching Brick building, UNII traffic load of 10%, I2V

Source: 20180208 Building-Brick W side toward V1 --was exl_report_toward_20180208.xlsx, Tabs: V2I mobile Rx to UNII=30-10%; V2I=10 mobile Rx to UNII=12-10%

The safety critical gaps in Figure 10-56 show that the distribution of missing packets in the high power scenarios we have been testing give about the same results as the deployment scenario as well. That similarity further indicates that much of the high power PER data we've collected tells us what to expect in the deployment scenario with both radio types turned down.

As an exercise in reading these plots, note that the lower left plot (deployment inside) shows a cluster of safety critical gaps (red) that intersect the black trajectory line at around 350 m. If you look up to the corresponding plot in Figure 10-55 you see the spike in PER at the same location. That tells that even though the spike barely reached 60% and was mostly below 40%, the missing packets were clustered consecutively in long gaps that would represent a threat to safety at that point.

Also note that since the vertical purple line marks the position of the brick building and interferer, the range of 350 meters from start point and other DSRC radio is 450 meters from the interferer.

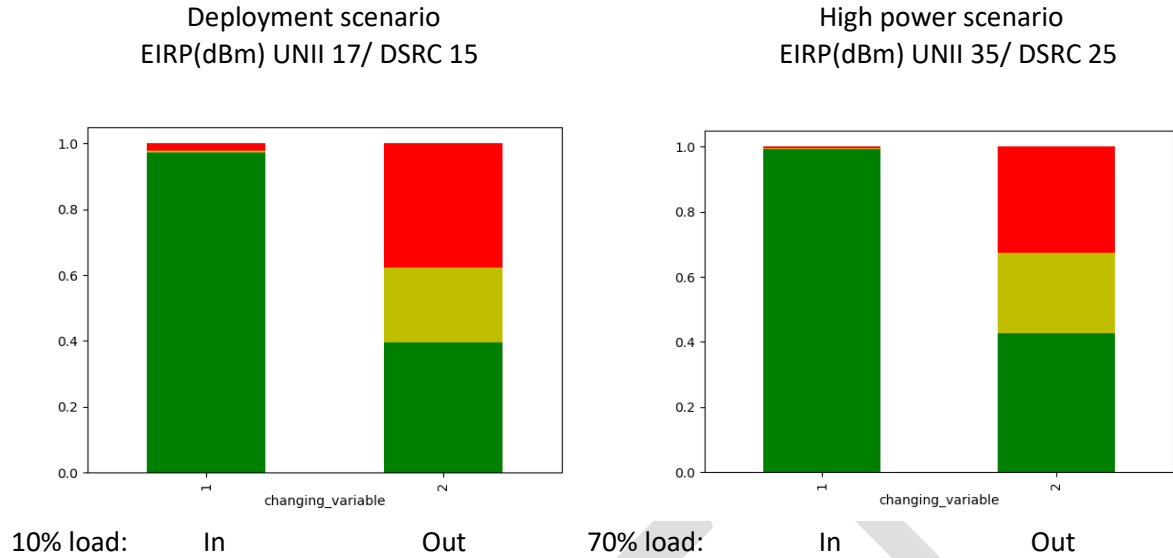


Figure 10-57. Summary of consecutive packet gaps in the deployment and high power scenarios, approaching Brick building, UNII traffic load of 10%, I2V

Source: 20180208 Building-Brick W side toward V1 --was exl_report_toward_20180208.xlsx, Tabs: V2I mobile Rx to UNII=30-10%; V2I=10 mobile Rx to UNII=12-10%

Figure 10-57 shows the cumulative distribution of gaps for the deployment and high power cases: safety critical gaps longer than half a second (red), gaps of concern 300 – 500 ms long (yellow), and gaps less than 300 ms. These plots also show that if anything, the high power scenario test if not the same, may underestimate the interference slightly. The conclusion is that the interference results with both the UNII and DSRC at high power is a good stand in for the interference when both radios are set with more moderate settings.



EIRP(dBm) UNII 35/ DSRC 25: UNII INSIDE



UNII OUTSIDE



EIRP(dBm) UNII 17/ DSRC 15: UNII INSIDE



UNII OUTSIDE

Figure 10-58. Deployment versus high power scenarios, Geographical distribution of PER, approaching Brick building, UNII traffic load of 10%, I2V

Source: 20180208 Building-Brick W side toward V1 --was exl_report_toward_20180208.xlsx, Tabs: V2I mobile Rx to UNII=30-10%; V2I=10 mobile Rx to UNII=12-10%

Figure 10-58 provides a more intuitive picture of the similarity between the deployment and high power scenarios.

This is the “approach” segment of the data. The vehicle drives from the lower left to the upper right. 100 meters further, the red dot marks the location of the brick building and Wi-Fi access point. The closer the color to magenta the closer the packet error rate is to zero. The closer the color is to aqua the closer the packet error rate is to 100%.

10.1.3 Wooden Building with Windows

The bounding case opposite the filled cinderblock was wooden building over 100 years old (Building 351 at the intersection of Lanyard Rd and Recoil Ave.). Figure 10-60 shows the RSU on its tower in the foreground and the wooden building in the background. The yellow tripod just to the left of the RSU held the static OBU since the vehicle usually used was out for repair. The static OBU antenna is 10 feet east of the RSU.

Figure 10-60 shows the UNII access point (foreground) and client (background) inside the building. Their location was 47 meters east of the RSU. Inside the building the access point (black tripod in foreground) was placed 9.5 feet from the front wall by the door and 44 feet from the west end wall that you see back and left in the picture. The two clients were positioned about ~15 from the access point. One client is visible in the center of the picture (orange tripod). For the outside runs the access point was moved straight out the door and placed about 15 feet from the building.



Figure 10-59 Wood building outside



Figure 10-60 Wood building UNII inside

Each run consisted of driving the white car to the east (“East route,” 120° on the compass) 0.5 miles to a turnaround. Figure 10-59 looks east so the vehicle would be seen driving away from the RSU in this picture. The vehicle with the mobile OBU is the white car in the center.

On the return, the vehicle would pass the RSU and continue west (“West route,” 300° on the compass) 0.75 miles to another turnaround and finish back at the RSU.

10.1.3.1 Environmental Effects

The wooden building was in perhaps the most varied and complex environment of the three buildings. The baseline measurements (without an interferer) provides some insight into the effects of trees and buildings. The satellite images in Figure 10-61 show the I2V PER baselines for the west side and east sides of the data run separately. As a reminder, hot pink means zero packet errors and aqua means total or 100% PER. The red circle is the position of the UNII interferer with the RSU and static OBU nearby where the data trace ends.



Figure 10-61. PER Baselines for RSU to WW (mobile), EIRP = 25 dBm

Source: 20180206 Building-Wood W-side away V1 -- was exl_report_away_20180206-2.xlsx, Tab: Baselines, and 20180206 Building-Wood E-side away V1 -- was exl_report_away_20180206_side2.xlsx, Tab: Baselines

To the west you can see the route jogs around trees after ~200 meters and then shortly curves around the track where more trees and a few buildings further blocked the signal. But notice that DSRC found a few gaps over the buildings and through the trees much further down the course where it wasn't expected.

The eastern part of the route was a straight shot down a road populated by several buildings out 800 meters to the turnaround point with very few packets lost. As shown in Section 9 this is just a fraction of the range DSRC achieve in our clean environment RSSI measurements.

Figure 10-62 shows the corresponding RSSI and noise plots. Notice how the simple ground bounce nulls are more difficult to see as they are partially filled in by energy from the many other reflections in the environment and at the same time many smaller nulls appear due to cancellations caused by many reflections. Note again how the west and east RSSI plots are different due to the significantly different environments on the two sides of the building. Most noticeable of course is how the signal on the west side is mostly cutoff once the vehicle starts driving behind the trees at roughly 250-300m. Also there is a small amount of signal leaking through the trees.

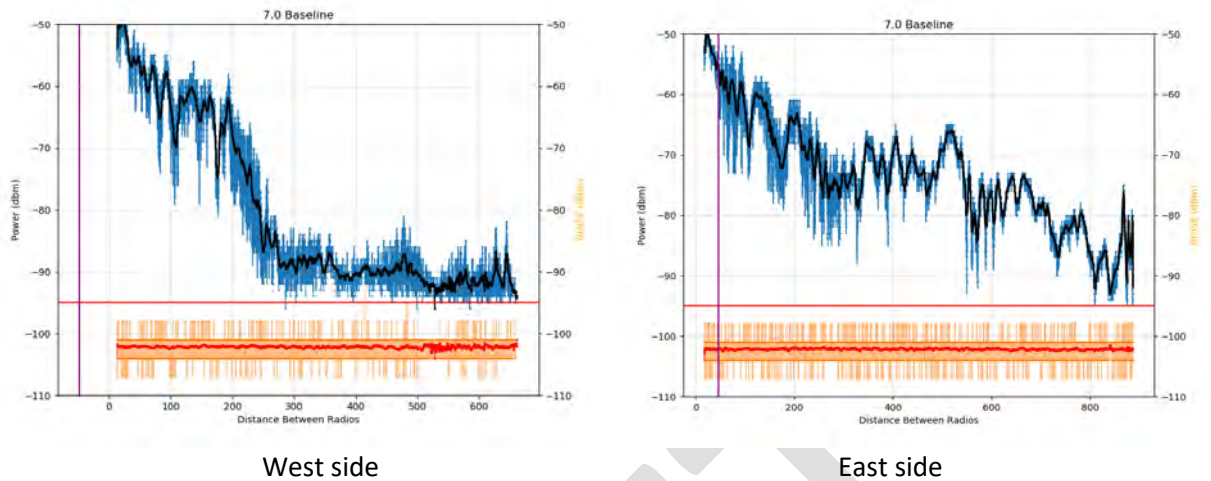


Figure 10-62. RSSI Baselines for RSU to WW (mobile), EIRP = 25 dBm

Source: 20180206 Building-Wood W-side away V1 -- was exl_report_away_20180206-2.xlsx, Tab: Baselines, and 20180206 Building-Wood E-side away V1 -- was exl_report_away_20180206_side2.xlsx, Tab: Baselines

Comparing the V2V and I2V baselines with trees and buildings on the west side shows another very interesting result (Figure 10-63). Look at where the route first circles left around the track in the two images. Notice how the V2V packet losses are much less than V2I for that portion. That is because the V2V antennas at the same low height shoot underneath the canopy of the trees there. Since the RSU is at 18 feet, its signal must pass through the canopy of the trees that you see at the first slight jog left, and so suffers more obstruction.

On the other hand, much later in the course (to the left), some I2V signal overtops the building and filters through gaps in the canopy while the V2V signal is completely blocked by the building and trees you see in the way. This illustrates the complexity of testing in actual urban and suburban environments that leads to results that may seem counterintuitive and unexpected at first. It becomes harder to separate interference caused by environment from interference caused by another radio. Baselineing for environmental effects is critical before making radio interference measurements.

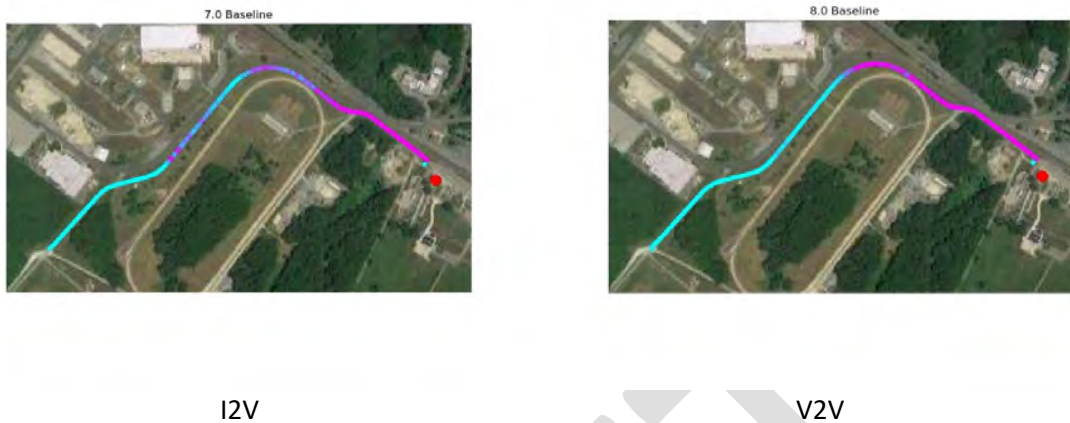
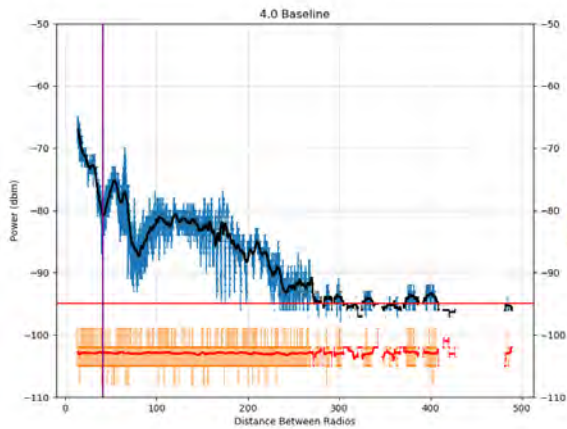


Figure 10-63. West side PER I2V and V2V Baselines, EIRP = 25 dBm

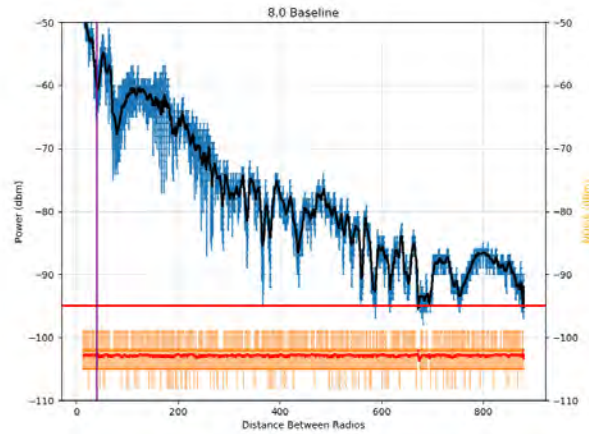
Source: 20180206 Building-Wood W-side away V1 -- was exl_report_away_20180206-2.xlsx, Tab: Baselines, and 20180206 Building-Wood E-side away V1 -- was exl_report_away_20180206_side2.xlsx, Tab: Baselines

A final interesting product of the baselining at this site was to compare DSRC baselines for the kind of power a handheld device might transmit with the vehicle power levels we have been using. Figure 10-64 compares the RSSI power and noise plots and the PER plots for V2V EIRP levels of 5 dBm and 25 dBm. The latter case (images on the right) is transmitting 100 times more power. The shorter range of the 5 dBm case is obvious. Less obvious is the more variable effect of the environment on the packet error rate.

This and the other data taken in these baselines allow predictions for use cases that employ low power short range applications next to high power DSRC channels to optimize band efficiency. These measured results provide the effect of lower power on parameters like noise level, SNR, PER, and the distribution of packet errors (gaps). The complete data sets can be found in the appendices.



5 dBm EIRP RSSI



25 dBm EIRP RSSI



5 dBm EIRP PER



25 dBm EIRP PER

Figure 10-64. Comparing low and high power V2V Baselines

Source: 20180206 Building-Wood E-side toward V1 -- was exl_report_toward_20180206_side2.xlsx, Tab: Baselines

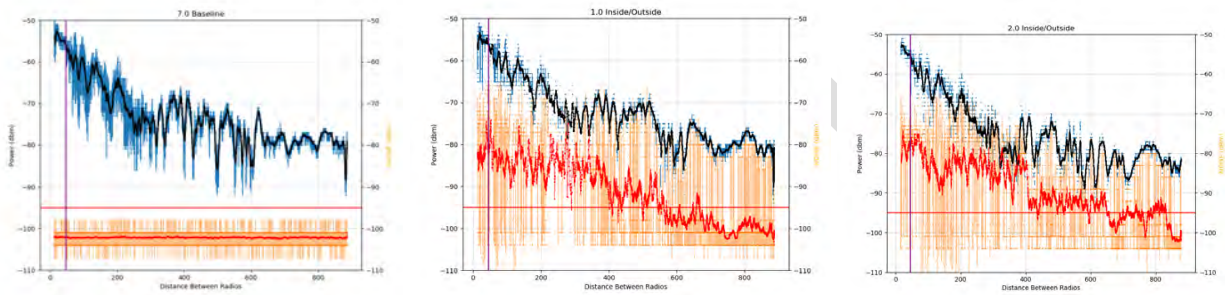
10.1.3.2 I2V with highest UNII power

In these runs the UNII operated at a high level of power (EIRP=36 dBm) and at a high traffic load (70%). In the following section we will show the effect of lower the Wi-Fi traffic load.

Figure 10-65 compares the RSSI and noise power plots for the baseline measurement, and the cases of the UNII inside, and then outside the building at the highest power level (EIRP=36 dBm). Blue shows the RSSI value of each BSM and black is the 0.5 sec average RSSI. Tan is the noise power of each BSM and red is the 0.5 sec average. The horizontal red line is a benchmark for the nominal DSRC receiver sensitivity of -95 dBm.

As with the other building measurements notice the more irregular shape of the RSSI curve compared to data from the clear and open sites at Zone 1 and Perryman. The more numerous and irregularly shaped peaks and nulls are due to multipath reflections in this more complicated environment.

The UNII inside figure shows noise received by DSRC is noticeable more than 900 meters from the building. This was 200 meters for the filled cinderblock building. The noise rises above the -95 dBm receiver sensitivity benchmark around 600 meters away. With the UNII outside the building, the noise is higher the whole way.



BASELINE

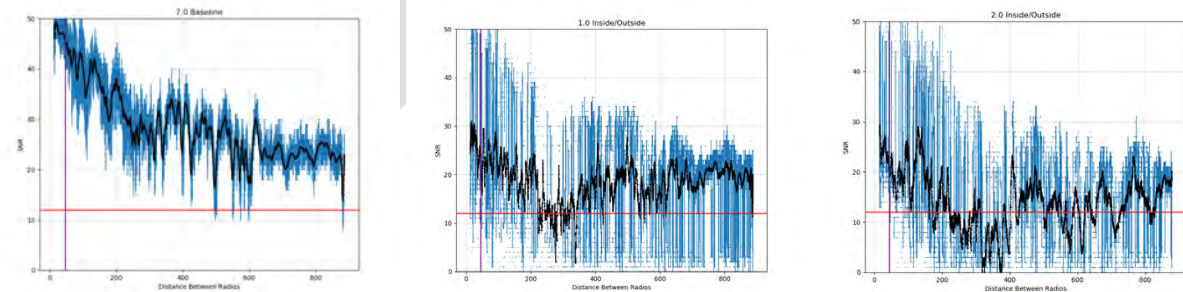
UNII INSIDE

UNII OUTSIDE

Figure 10-65. RSSI and noise power plots, I2V, UNII EIRP=35 dBm, approaching Wood building

Source: 20180206 Building-Wood E-side toward V1 -- was exl_report_toward_20180206_side2.xlsx, Tab: V2I mobile Rx to UNII=30-70%

Figure 10-66 shows the signal-to-noise ratio directly. Blue is the SNR for each BSM and black is the 0.5 sec average. Unlike the Cinderblock building that looked like the baseline beyond 200 meters, the wood building provides little shielding to the powerful high-traffic access point so the UNII inside SNR plot looks more like the UNII outside plot rather than the baseline. In fact, SNR is 10-20 dB worse than the baseline throughout. The horizontal red line is the commonly used 12 dB SNR benchmark, which is thought to be the minimum required for safety applications to work.



BASELINE

UNII INSIDE

UNII OUTSIDE

Figure 10-66. Signal-to-Noise plots, I2V, UNII EIRP=35 dBm, approaching Wood building

Source: 20180206 Building-Wood E-side toward V1 -- was exl_report_toward_20180206_side2.xlsx, Tab: V2I mobile Rx to UNII=30-70%

Figure 10-67 compares the packet error rate measurements for this case. Blue records individual packet receptions and the red line is the 0.5 sec average PER. This figure shows even more clearly how little the wood building reduces the interference. With the UNII inside the Cinderblock building PER ranged from 20-40% and inside the brick building it barely reached 20%. With the wood building it is above 80% until the vehicle is 600 meters away at which point the height advantage of the RSU comes into play. Even then the PER only drops to 60%.

As with the other buildings, when the UNII was moved outside, the PER was a steady 80-90% the entire time the vehicle was in view.

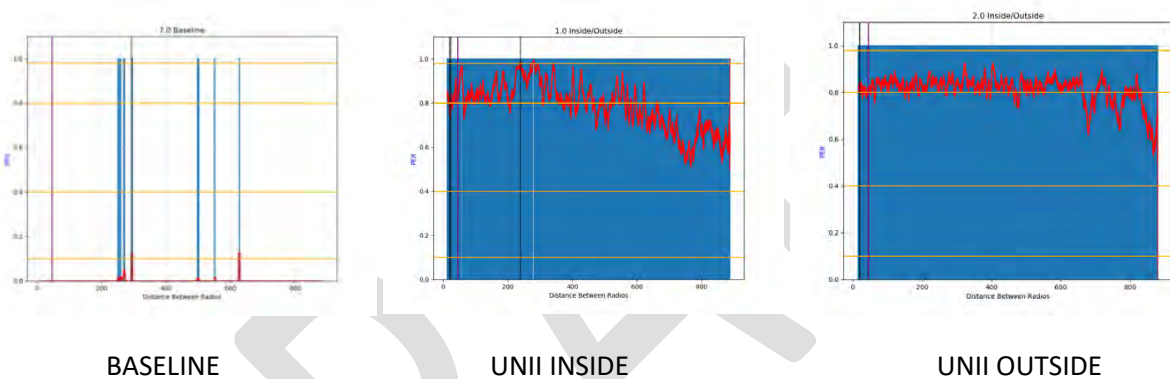


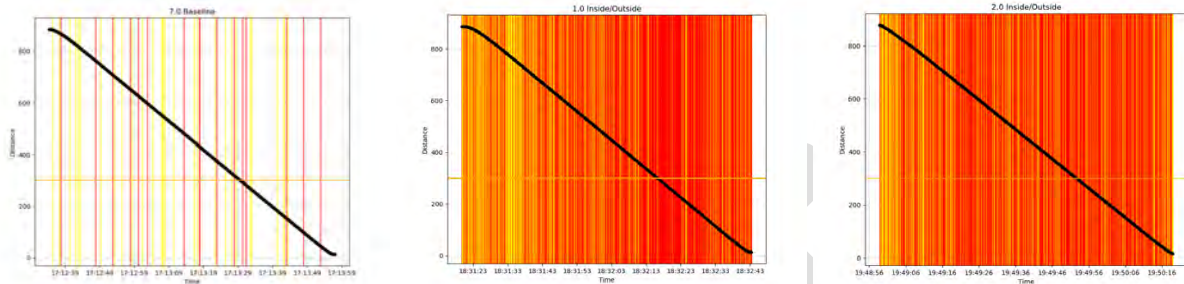
Figure 10-67. Packet Error Rate plots, I2V, UNII EIRP=35 dBm, approaching Wood building

Source: 20180206 Building-Wood E-side toward V1 -- was exl_report_toward_20180206_side2.xlsx, Tab: V2I mobile Rx to UNII=30-70%

Figure 10-68 conveys the distribution of the packet error rate shown in Figure 10-67. The plots in Figure 10-68 display gaps caused by consecutively missed packets. Yellow shows gaps of concern when consecutive BSMs are missed for 300 to 500 ms. Red shows safety critical gaps due to the loss of more consecutive BSMs for more than 500 ms, which is a gap that is more than half a second long. The black line shows the distance of the vehicle from the building (y-axis) as a function of time (x-axis). The horizontal orange line marks the 300-meter distance, which is the intended operating range for DSRC safety applications.

The baseline plot shows a few safety critical gaps due to multipath from the complex environment. Unlike the Cinderblock building, which displayed more yellow than red, the UNII inside the wooden building, similar to when it was outside, shows safety critical gaps most of the time. The slight easing in the PER after 600 meters shows up here as a band of yellow where majority of the gaps shrink to 300-

500 ms for a bit. In any case, DSRC communication is disrupted fatally whether or not the access point was inside or outside the wooden building.



BASELINE

UNII INSIDE

UNII OUTSIDE

Figure 10-68. Packet gap plots, I2V, UNII EIRP=35 dBm, approaching Wood building

Source: 20180206 Building-Wood E-side toward V1 -- was exl_report_toward_20180206_side2.xlsx, Tab: V2I mobile Rx to UNII=30-70%

Figure 10-69 aggregates the data from Figure 10-68 by showing percent of time in three gap conditions for the segment of data analyzed in Figures 10-65 to 10-68. The gap conditions are green for gaps less than 0.3s, yellow for gaps of 0.3 to 0.5s “gaps of concern”, and red for gaps larger than 0.5 second “safety critical gaps.”

The baseline data shows that gaps due to environmental interference occurred less than 0.5% of the time. That means almost all of the gaps with the UNII transmitting are due to the UNII. The plot shows that putting the UNII inside the building meant only 6% more of the run time did not have safety critical gaps than when it was outside. In either case, 60-70 percent of the run the DSRC experienced safety critical gaps. Only 16-19% of the time were gaps shorter than 3 ms.

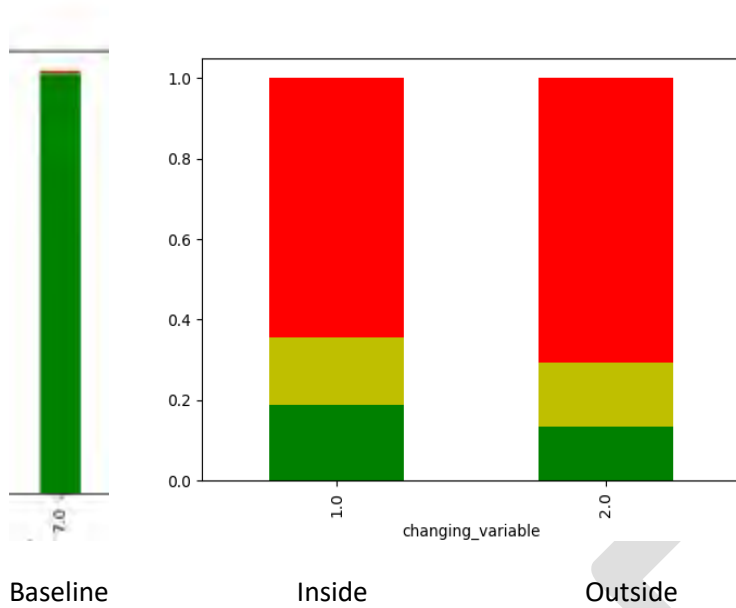


Figure 10-69. Summary of packet gaps, I2V, UNII EIRP=35 dBm, approaching Wood building

Source: 20180206 Building-Wood E-side toward V1 -- was exl_report_toward_20180206_side2.xlsx, Tab: V2I mobile Rx to UNII=30-70%

Figure 10-70 is an aerial comparison of how PER is distributed on the approach to the wooden building. This figure makes it intuitively clear how DSRC communication was shut down and what little difference the building made for a high power, high traffic Wi-Fi access point. (Color scale: Aqua is 100% PER and hot pink zero PER. As color scales from blue toward purple and pink the PER decreases.)

Note that the DSRC was operating with an EIRP 5 dB higher than the maximum EIRP to be deployed according to the SAE standard. Hence, interference for this case would be worse in a real deployment.



BASELINE

UNII INSIDE

UNII OUTSIDE

Figure 10-70. Geographical distribution of PER, I2V, UNII EIRP=35 dBm, approaching Wood building

Source: 20180206 Building-Wood E-side toward V1 -- was exl_report_toward_20180206_side2.xlsx, Tab: V2I mobile Rx to UNII=30-70%

The departing data shows essentially the same result as the approaching data. Rather than repeat the above analysis in detail, we include the satellite view of departing packet error rate in Figure 10-71. Compared with the approaching PER of Figure 10-70 the PER is slightly lower with the UNII inside in a few places but for all practical purposes the DSRC communication is similarly disrupted.



Figure 10-71. Geographical distribution of PER, I2V, UNII EIRP=35 dBm, departing Wood building

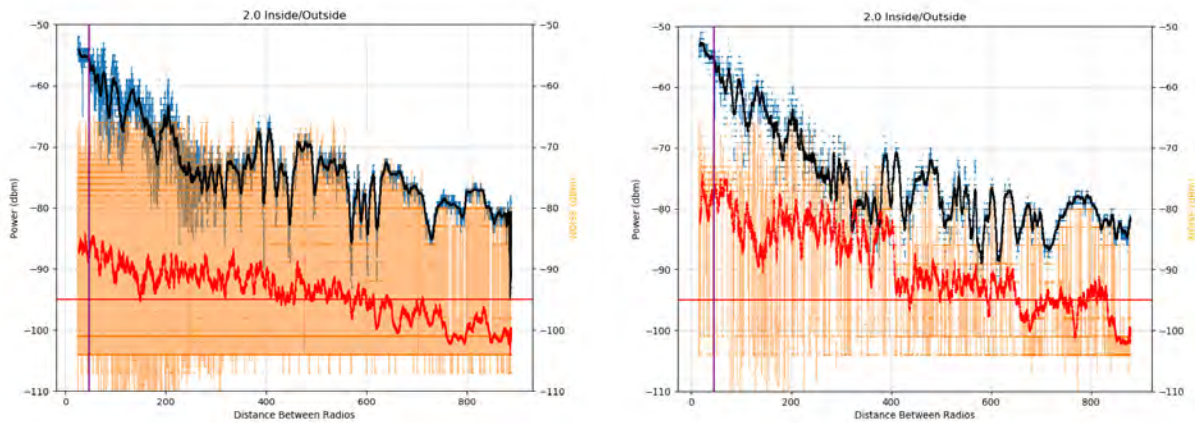
Source: 20180206 Building-Wood E-side away V1 -- was exl_report_away_20180206_side2.xlsx, Tab: V2I mobile Rx to UNII=30-70%

10.1.3.3 I2V Highest UNII power but low traffic load

The same high power access point was tested inside and outside the wooden building at a 10% traffic load. As shown in Table 4.2 above, the inter-packet spacing for that Wi-Fi loading is large enough to allow some BSMs through without collision. These results show the sensitivity of interference to traffic loading.

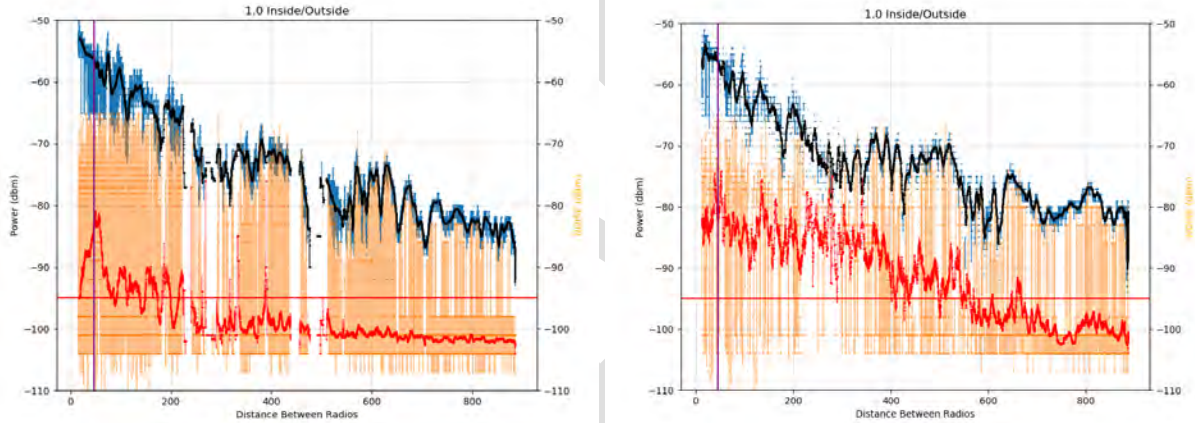
Figure 10-72 shows that DSRC still detected noise above baseline with an indoors UNII traffic load at 10% but at a lower level than at 70%. It crossed the -95 dB sensitivity benchmark 250 meters away from the building at 10% as opposed to 400 meters for 70%. That means the vehicle had to be 150 meters closer before that threshold was crossed due to the change in UNII traffic load.

The noise in the 70% loading tests look the same regardless of whether the access point was outside or inside. It appears that lowering the traffic load matters more for decreasing interference when the UNII access point was inside the building than outside.



Outside UNII traffic load: 10%

70%



Inside UNII traffic load: 10%

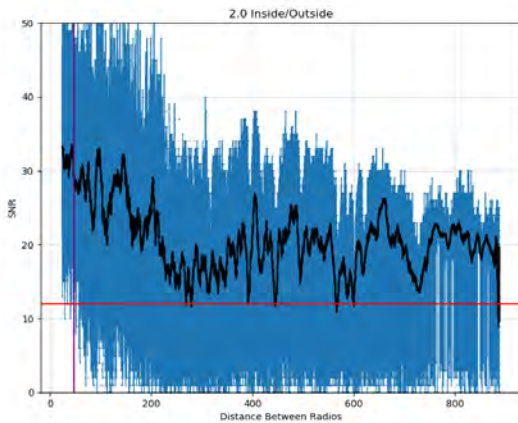
70%

Figure 10-72. Comparing RSSI plots as UNII traffic load changed, UNII EIRP=35 dBm, I2V EIRP=25 dBm

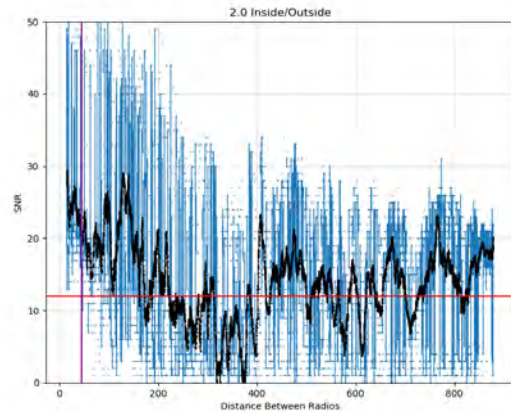
Source: 20180206 Building-Wood E-side toward V1 -- was exl_report_toward_20180206_side2.xlsx, Tabs: V2I mobile Rx to UNII=30-10%; V2I mobile Rx to UNII=30-70%

Figure 10-73 shows this from the signal-to-noise perspective as well. Inside the wooden building, at 10% load the SNR is about 10 dB worse than the baseline but noticeably better than at 70% load and it stays above the 12 dB benchmark the entire run.

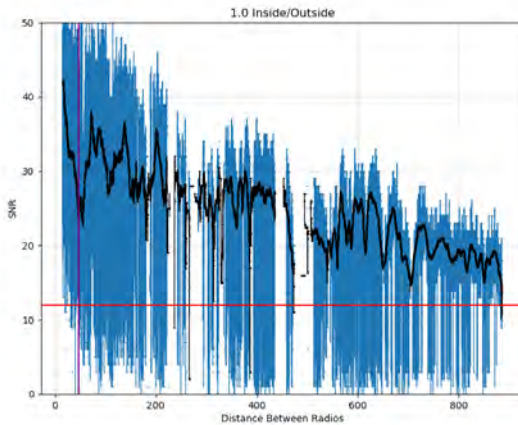
As expected, putting the UNII indoors with 10% load gave the best SNR, followed by outdoors at 10% which is noticeably lower. At 70% load the indoors/outdoors difference is less until about 500 meters and further away, where the outdoors case caused more interference.



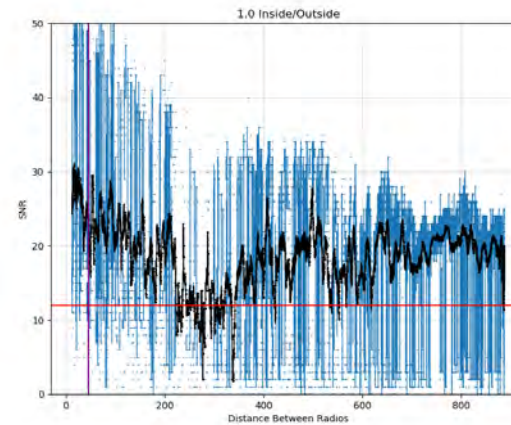
Outside UNII traffic load: 10%



70%



Inside UNII traffic load: 10%



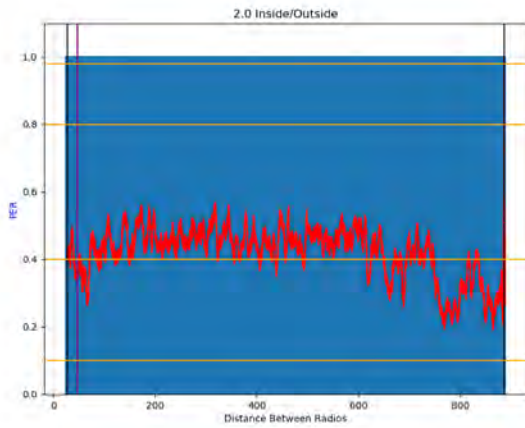
70%

Figure 10-73. Comparing SNR plots as UNII traffic load changed, UNII EIRP=35 dBm, I2V EIRP=25 dBm

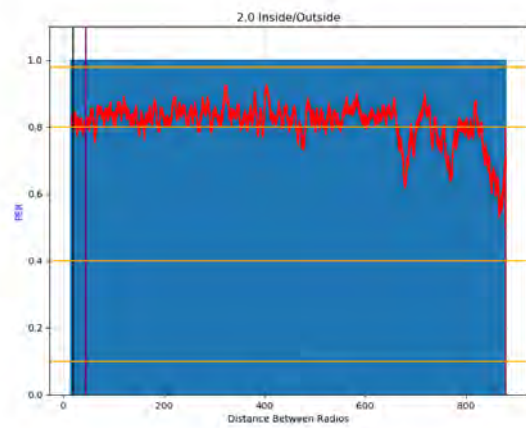
Source: 20180206 Building-Wood E-side toward V1 -- was exl_report_toward_20180206_side2.xlsx, Tabs: V2I mobile Rx to UNII=30-10%; V2I mobile Rx to UNII=30-70%

Figure 10-74 shows packet error rate inside the building, at the low 10% load, to vary wildly especially closer to the building perhaps due to the effect of the windows and door. This result is consistent with the noise measurement in Figure 10-72 that shows the noise increasing significantly only near the building.

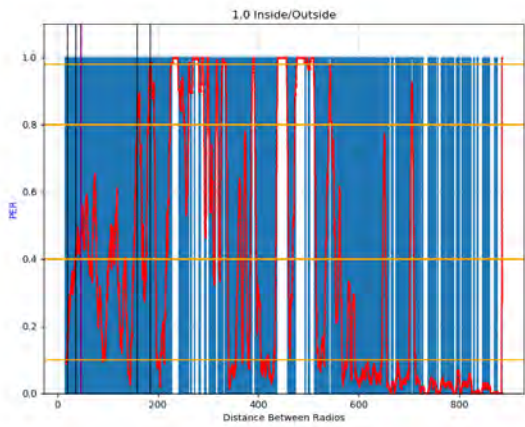
Outside the wooden building, at 10% load the PER is roughly steady 40-50% until it drops a bit at long range as the RSU's height advantage starts to manifest. This figure shows most clearly how with an access point running at fully power and so loaded that the inter-packet gaps are smaller than BSMs, the wooden building offers essentially no reduction in interference. The impact of the building increases as the Wi-Fi traffic load decreases.



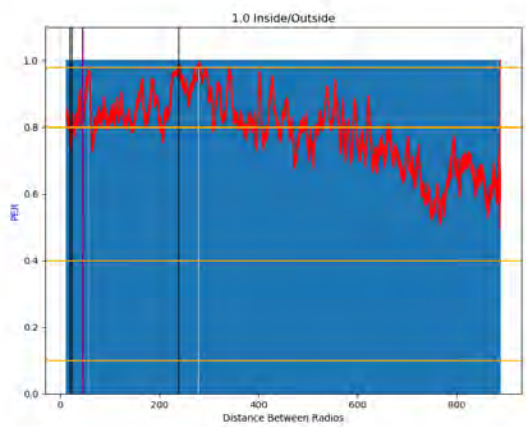
Outside UNII traffic load: 10%



70%



Inside UNII traffic load: 10%



70%

Figure 10-74. Comparing PER plots as UNII traffic load changed, UNII EIRP=35 dBm, I2V EIRP=25 dBm

Source: 20180206 Building-Wood E-side toward V1 -- was exl_report_toward_20180206_side2.xlsx, Tabs: V2I mobile Rx to UNII=30-10%; V2I mobile Rx to UNII=30-70%

Figure 10-75 shows the distribution of the packet errors, in particular how they are clumped into larger gaps (yellow for concerning 300-500 ms gaps and red for safety critical gaps larger than 500 ms). The erratic nature of the low load indoor PER plot above is evident here by the irregular distribution of gaps.

The most important observation to make is that in this least interfering case of the four shown (10% load inside), the disruption to DSRC is not tenable for safety communications. Pay attention to the red lines intersecting the black vehicle track below the orange 300-meter marker.

At 10% load, the gaps vary wildly especially closer to the building perhaps due to the effect of the windows and door. This result is consistent with the noise measurement in Figure 10-72 that shows the noise increasing significantly only near the building.

Outside the wooden building, at 10% load the safety critical gaps are more uniformly distributed but are far too frequent for tenable DSRC safety communications. Again, this figure also shows clearly how with an access point running at fully power and so loaded that the inter-packet gaps are smaller than BSMs, the wooden building offers essentially no reduction in interference. The building matters more as the Wi-Fi traffic load decreases.

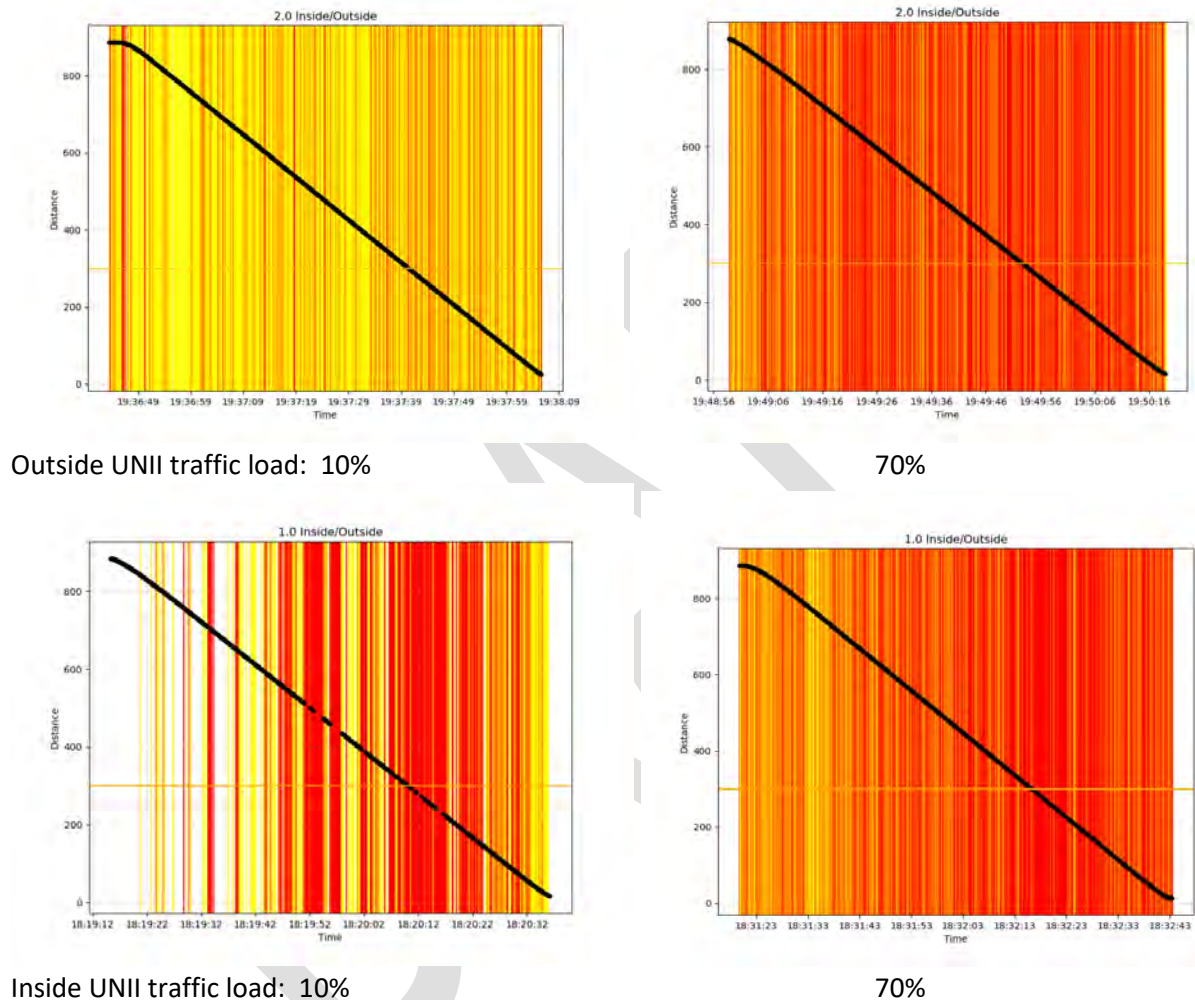


Figure 10-75. Comparing safety critical gaps as UNII traffic load changed, UNII EIRP=35 dBm, I2V EIRP=25 dBm

Source: 20180206 Building-Wood E-side toward V1 -- was exl_report_toward_20180206_side2.xlsx, Tabs: V2I mobile Rx to UNII=30-10%; V2I mobile Rx to UNII=30-70%

Figure 10-76 summarizes the percent of time the data runs spent in the three gap categories used in this analysis: Green for less than 300 ms, yellow for 300-500 ms gaps of concern, and red safety critical gaps longer than 500 ms. Interestingly, for the 10% load case, the bulk of the indoor gaps were safety critical, whereas the majority outdoors were gaps of concern. This is just the aggregate view of Figure 10-75.

The same result appeared in the departure data as well as this vehicle approaching data. Creating more serious interference from inside the building is counterintuitive. We don't have an explanation and would consider repeating this set of measurements.

Confirming the results above, at 70% UNII traffic load, the building made little difference to the interference.

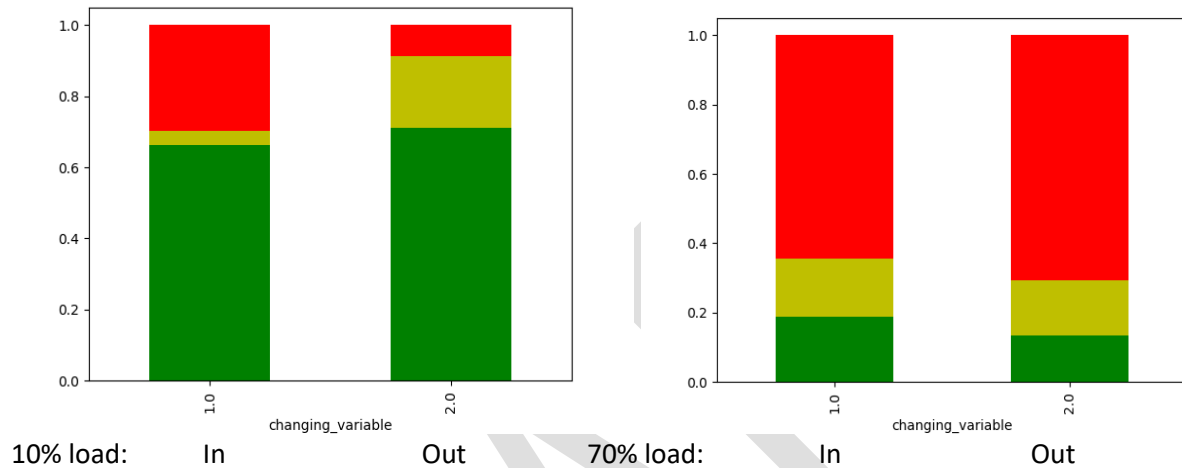


Figure 10-76. Summary of consecutive packet gaps as UNII traffic load changed, UNII EIRP=35 dBm, I2V EIRP=25 dBm

Source: 20180206 Building-Wood E-side toward V1 -- was exl_report_toward_20180206_side2.xlsx, Tabs: V2I mobile Rx to UNII=30-10%; V2I mobile Rx to UNII=30-70%

The geographical representation of PER that is Figure 10-77 shows more intuitively the hotspot and dead-spot nature of interference when the high power but low traffic load UNII access point was inside the building (lower left). Moving the UNII outside the wooden building at 10% load (upper left) shows, by the mostly purple color of the trace, that some DSRC BSMs get through but not enough to be tenable. At 70% Wi-Fi load, it doesn't matter whether the access point is in or out, very little DSRC gets through. Again, this figure also shows clearly how with an access point running at fully power and so loaded that the inter-packet gaps are smaller than BSMs, the wooden building offers essentially no reduction in interference. The building matters more as the Wi-Fi traffic load decreases. These are the same results as the previous plots but this presentation is more intuitive.

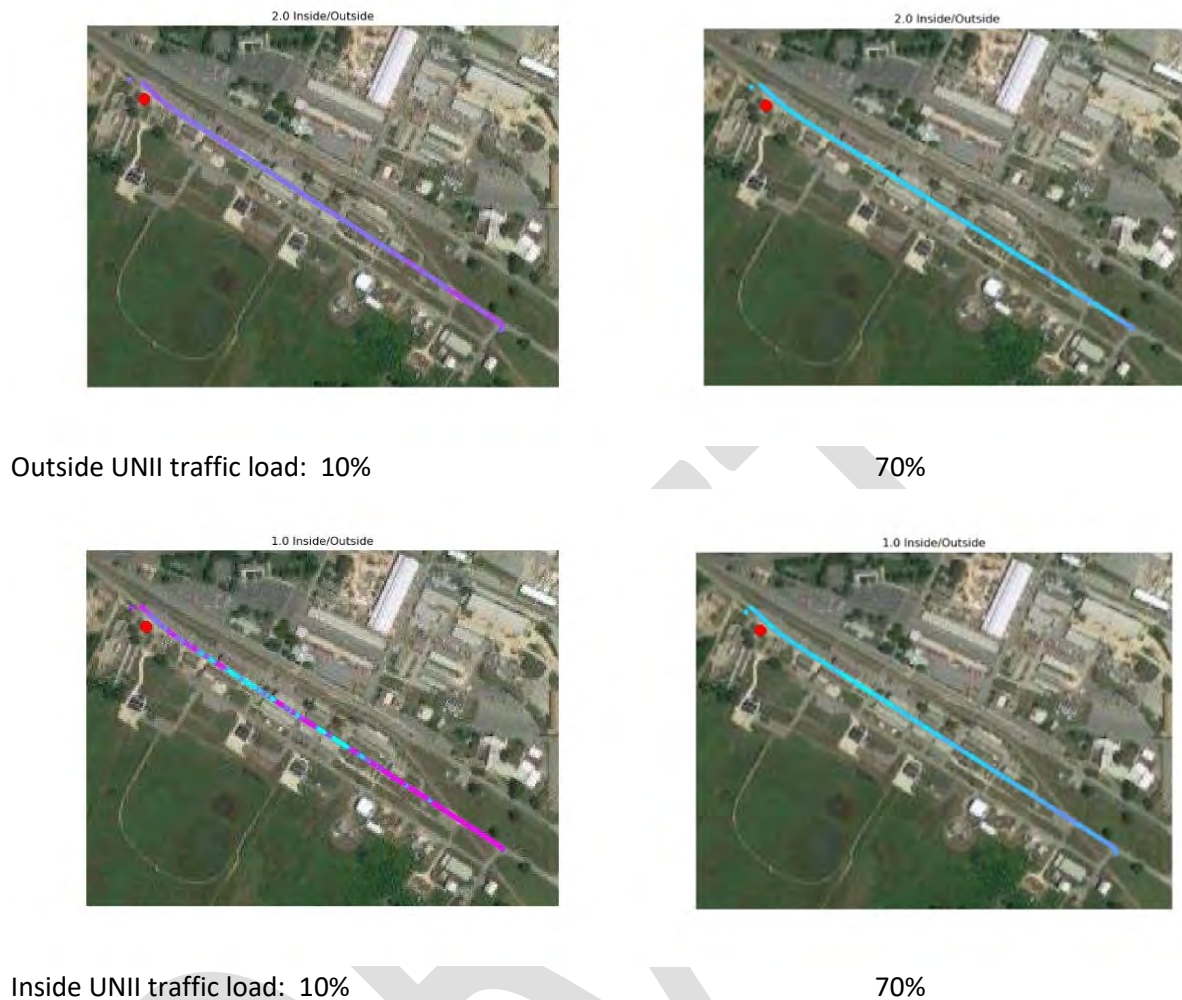


Figure 10-77. Geographical distribution of PER, approaching Wood building as UNII traffic load changed, UNII EIRP=35 dBm, I2V EIRP=25 dBm

Source: 20180206 Building-Wood E-side toward V1 -- was exl_report_toward_20180206_side2.xlsx, Tabs: V2I mobile Rx to UNII=30-10%; V2I mobile Rx to UNII=30-70%

10.1.3.4 V2V in presence of high power but low traffic load UNII

Figure 10-78 compares V2I data (left) with the corresponding gaps and PER plots for the V2V runs (right). The bottom row of plots shows PER distributed in space and the top row of plots shows PER distributed in time. Both sets of plots show that V2I suffered slightly more interference very near the building while V2V suffered more at long range (beyond 350m).

The RSU at 18 feet has a height advantage that gives it greater range to transmit or receive than the UNII mounted 6 feet high. In the V2V case both the UNII and DSRC are at roughly the same height taking away that advantage for DSRC.

Unlike the previous data shown in this section, which was for the mobile DSRC receiving, Figure 10-78 presents data when the mobile DSRC was transmitting. That is why the V2I plots below are somewhat different than the equivalent plots in Figures 10-75 and 10-77. In fact, the data here looks more like what was expected.

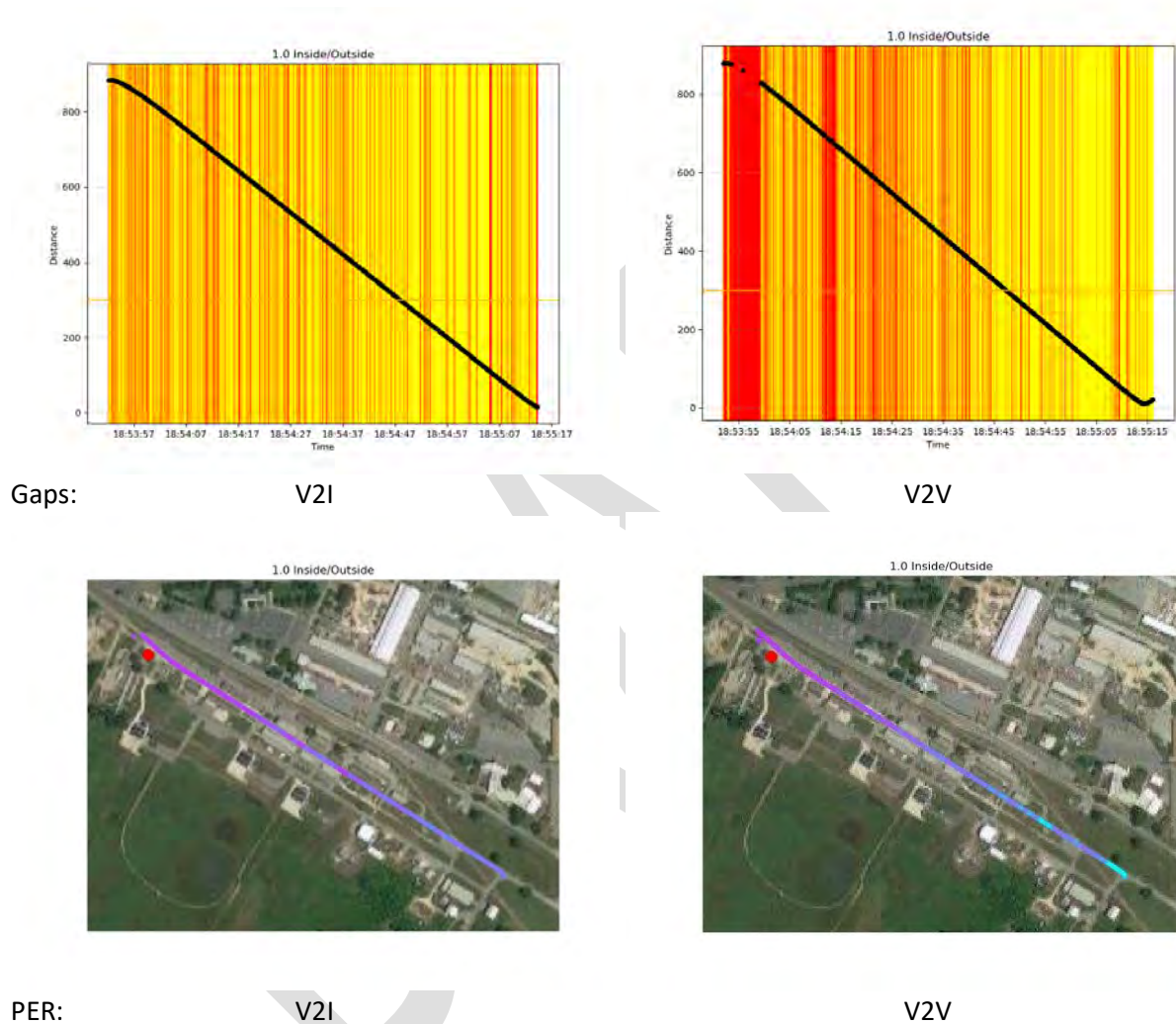


Figure 10-78. V2V versus V2I, approaching Wood building, UNII inside building with traffic load of 10%, UNII EIRP=35 dBm, V2V and V2I EIRP=25 dBm

Source: 20180206 Building-Wood E-side toward V1 -- was exl_report_toward_20180206_side2.xlsx, Tabs: V2I mobile Tx to UNII=30-10%; V2V mobile Tx to UNII=30-10%

The V2V data provided the same basic results as V2I leading to the same observations and conclusions so will not be repeated here. Consult the Appendices for those plots.

10.1.3.5 12V with the minimum UNII interferer

The last set of tests investigated a bounding case of minimum interference. The UNII was operated at both low power and at a low traffic load (EIRP=8 dBm at 10%). At the same time the DSRC was advantaged by running with roughly 3 times more power than actual deployment (EIRP=25 dBm). This looks at a low power access point, with little to moderate Wi-Fi traffic inside and outside a wood frame building.

The plots below directly compare the results of this minimum interferer with the maximum interferer tested in section 10.2.3.2 above. Any interference in the actual deployment of unmitigated UNII-4 Wi-Fi with DSRC would have to be worse than this minimum case and fall between these two bounding cases.

Figure 10-79 compares the RSSI and noise power plots for the baseline measurement, and the cases of the UNII inside, and then outside the building at the highest power level (EIRP=36 dBm). Blue shows the RSSI value of each BSM and black is the 0.5 sec average RSSI. Tan is the noise power of each BSM and red is the 0.5 sec average. The horizontal red line is a benchmark for the nominal DSRC receiver sensitivity of -95 dBm.

Even with the minimal interferer inside the wooden building, the DSRC receiver was sensitive to the UNII signals as far as 550 meters away. The noise level first breaks the -95 dBm benchmark 130 meters away. That happened with the maximal interferer 400 meters away. So expect a UNII interferer inside a wood building to breach this benchmark 130 to 400 meters away, and perhaps further given the advantaged DSRC in terms of height and power.

Taking the UNII outside the building, this benchmark was breached around 300 meters away in the minimal case (650 meters in the maximal case).

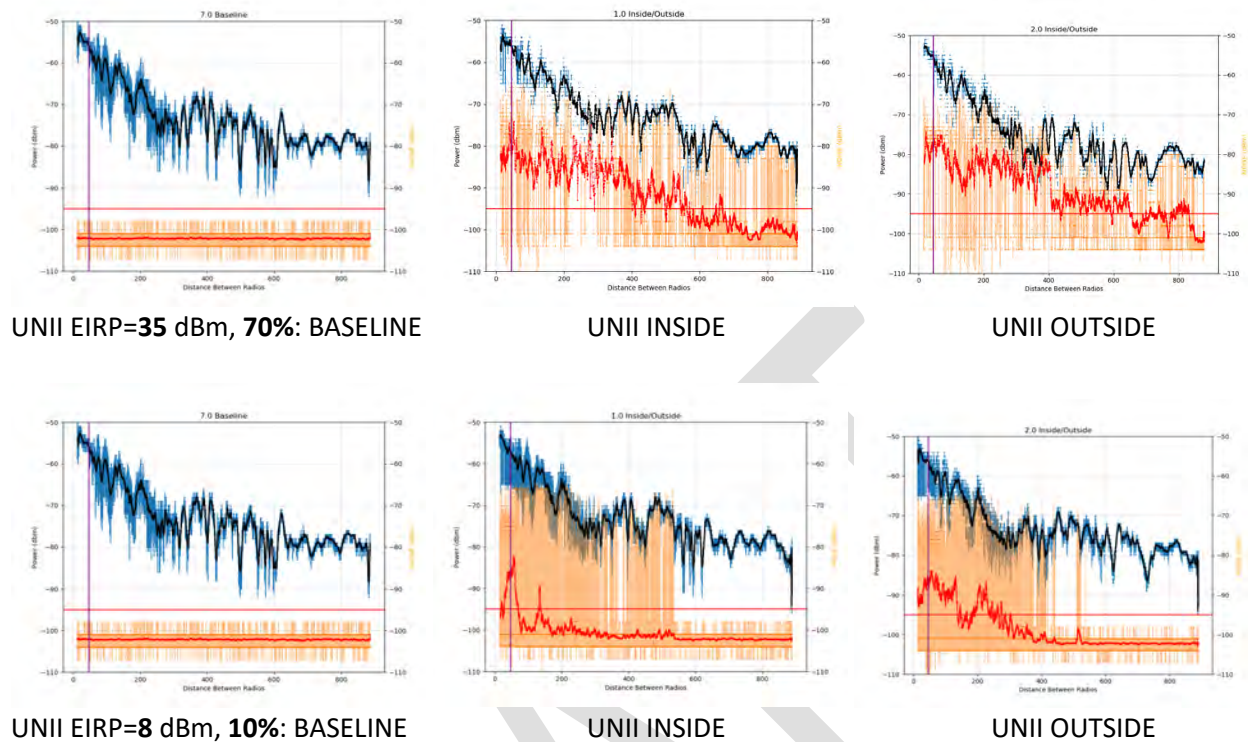


Figure 10-79. Comparing minimum and maximum interferer: RSSI and noise power plots, I2V, UNII EIRP=35 dBm, approaching Wood building

Source: 20180206 Building-Wood E-side toward V1 -- was exl_report_toward_20180206_side2.xlsx, Tabs: V2I mobile Rx to UNII=30-70% and V2I mobile Rx to UNII=3-10%

Figure 10-80 shows the signal-to-noise ratio directly. Blue is the SNR for each BSM and black is the 0.5 sec average. The minimal interferer caused the SNR to be a few dB worse close to the building but is similar to the baseline after 550 m. The greatest difference is the much greater variation in SNR within 550 meters. Contrast with the maximal interferer that caused the SNR to drop 15-20 dB, within 300 meters of the building.

Outside, the maximal interferer SNR varies from 10 to 20 dB worse than the minimal interferer with performance below the 12 dB benchmark most of the way. The SNR is never below 12 dB for the minimal interferer in either the inside or outside cases except perhaps where the vehicle turned around.

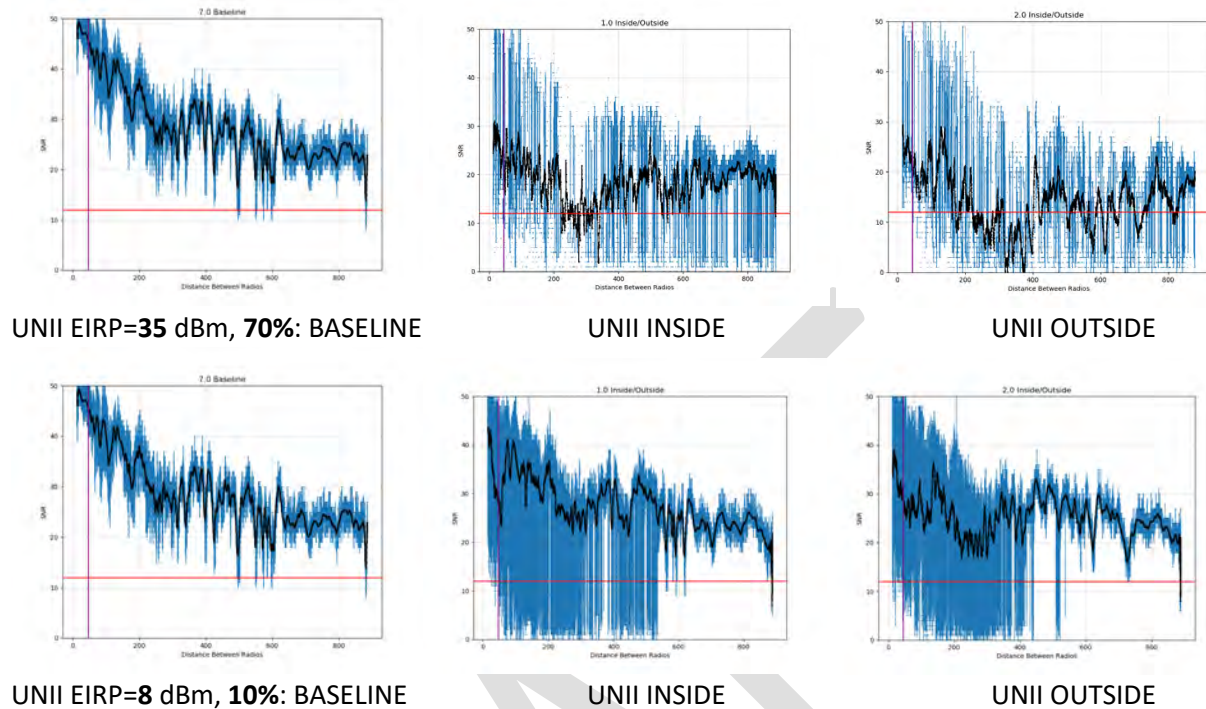


Figure 10-80. Comparing minimum and maximum interferer: Signal-to-Noise plots, I2V, UNII EIRP=35 dBm, approaching Wood building

Source: 20180206 Building-Wood E-side toward V1 -- was exl_report_toward_20180206_side2.xlsx, Tabs: V2I mobile Rx to UNII=30-70% and V2I mobile Rx to UNII=3-10%

Figure 10-81 compares the packet error rate measurements for this case. Blue records individual packet receptions and the red line is the 0.5 sec average PER. This figure shows even more clearly how influence of the wood building is greatest for the weakest UNII signals. It decreases as UNII power or load increases until it becomes irrelevant at some point before the maximal case where the PER is roughly the same whether or not the UNII is inside or out.

Even in the minimal case, the PER shoots up to serious levels (10-65%) at times within 300 meters of the building. The peaks are likely due to the windows, but even with the wood walls the PER is 10%. Any actual deployment would be worse since the DSRC would be transmitting 3 times less power. So between the two bounding cases, expect PER due to an access point within a wood building to be somewhere between 10% and 95%.

The other pertinent observation comes when the minimal UNII was taken outside the building. The PER jumped to 40-60% within 300 meters and kept it to 20% as far as 900 meters. As noted above, any actual interference would be worse. This leads to the conclusion that without mitigation that ensures that the UNII and DSRC transmissions never overlap, any outdoor Wi-Fi devices allowed in the band will interfere with DSRC safety communications. Indoor UNII will be discussed later when all three building results are compared.

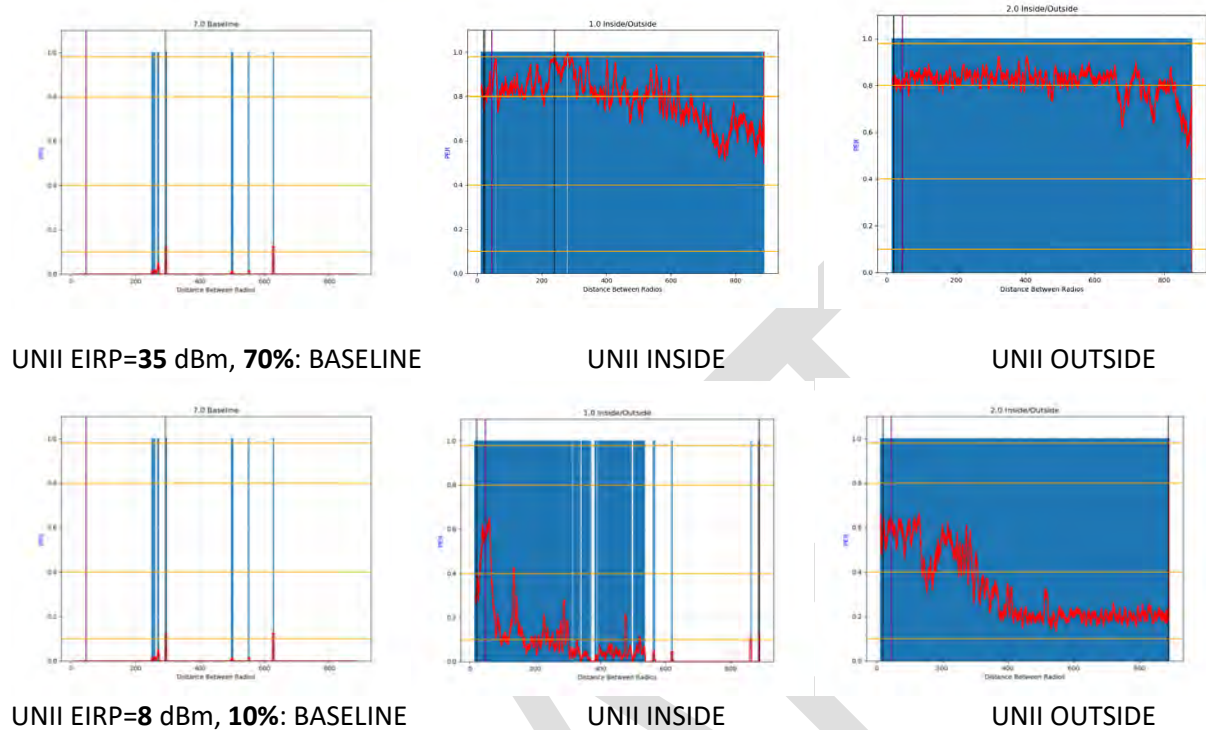


Figure 10-81. Comparing minimum and maximum interferer: Packet Error Rate plots, I2V, UNII EIRP=35 dBm, approaching Wood building

Source: 20180206 Building-Wood E-side toward V1 -- was exl_report_toward_20180206_side2.xlsx, Tabs: V2I mobile Rx to UNII=30-70% and V2I mobile Rx to UNII=3-10%

Figure 10-82 conveys the distribution of the packet error rate shown in Figure 10-81. The plots in Figure 10-82 display gaps caused by consecutively missed packets. Yellow shows gaps of concern when consecutive BSMs are missed for 300 to 500 ms. Red shows safety critical gaps due to the loss of consecutive BSMs for more than half a second. The black line shows the distance of the vehicle from the building (y-axis) as a function of time (x-axis). The horizontal orange line marks the 300-meter distance, which is the intended operating range for DSRC safety applications.

Even with the low power, low traffic UNII inside the wood building you can see quite a few more safety critical gaps (the red lines) and many more gaps of concern (yellow lines) within 300 meters than in the baseline. Given that this is an unrealistic best case for the DSRC, it is possible, that even inside a wooden building a low power UNII access point might be too disruptive for DSRC.

The high power, high load plots show how much worse the interference can get as UNII power and traffic increases. Taking the minimal UNII outside appears untenable out to 400 meter, with a definite easing after that. Increasing UNII power or traffic would push the zone of fatal interference out from 400 meter to beyond the range measured in this test as the maximal UNII plots show.

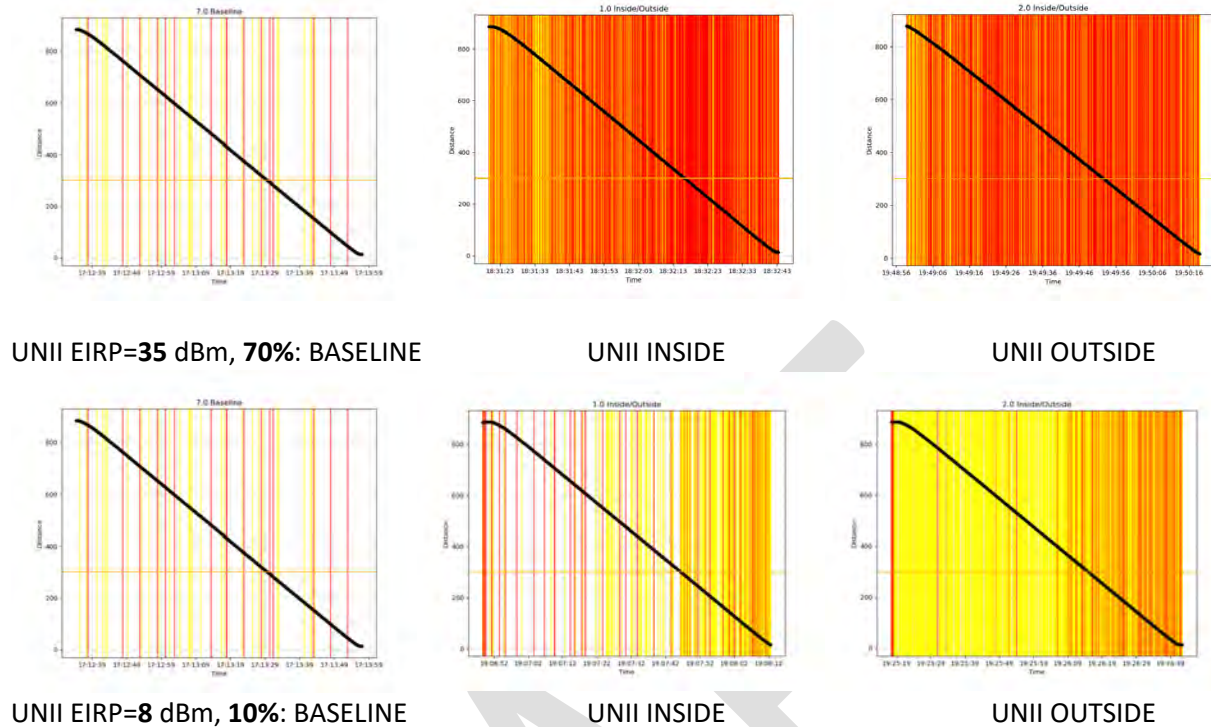


Figure 10-82. Comparing minimum and maximum interferer: Packet gap plots, V2I, UNII EIRP=35 dBm, approaching Wood building

Source: 20180206 Building-Wood E-side toward V1 -- was exl_report_toward_20180206_side2.xlsx, Tabs: V2I mobile Rx to UNII=30-70% and V2I mobile Rx to UNII=3-10%

Figure 10-83 aggregates the data from Figure 10-82 by showing percent of time in three gap conditions for the segment of data analyzed in Figures 10-79 to 10-82. The gap conditions are green for gaps less than 0.3s, yellow for gaps of 0.3 to 0.5s “gaps of concern”, and red for gaps larger than 0.5 second “safety critical gaps.”

The baseline data shows that gaps due to environmental interference occurred less than 0.5% of the time. That means almost all of the gaps with the UNII transmitting are due to the UNII. The bottom plots show that any real interference will cause safety critical gaps at least 2% of the time in the minimal case, inside a wood building. That seems small until you note that is aggregated over the full 900 meters of the run. Figure 10-82 shows that fraction would be higher if the analysis were limited to the first 300 meters.

With the minimal UNII outside, the DSRC was in a safety critical gap condition roughly 8% of the time. That means being safety critical for 5 seconds of every minute of operation. If that is unacceptable, then again, even the minimal outdoors UNII access point is unacceptable without iron-clad mitigation. Otherwise, this provides a benchmark to start searching for what UNII power and traffic limits might safely allow sharing. For safety apps sensitive to gaps of 0.3 to 0.5 seconds, the safety critical condition rises to 20% of the time, or 12 seconds per minute.

The upper plots show that saturated Wi-Fi traffic at the highest power resulted in a critical safety condition about 70% of the time and that rises to over 80% of the time for the most sensitive safety apps. That would be 40-50 seconds of every minute in a safety critical condition, which is clearly unacceptable. This is the case that any mitigation would have to tackle unless special conditions were ruled restricting Wi-Fi devices to the lowest power level, and perhaps restricting the allowed traffic load. But as shown, mitigation would still be required for that minimal case as well.

These results suggest additional measurements to determine if interference would increase linearly or non-linearly between the two bounding case results shown. If the interference during the minimal case is acceptable, then we need measurements at incrementally larger powers and traffic loads to find the tipping point where the interference becomes unacceptable. Is interference more sensitive to changes in power or load values when they are small (exponentially increasing curve)? Hence, interference develops rapidly and is a tougher problem to mitigate. Or is interference not as sensitive until higher powers or traffic loads (a flattening exponential)? In that case, power or load restrictions might make mitigation more tractable.

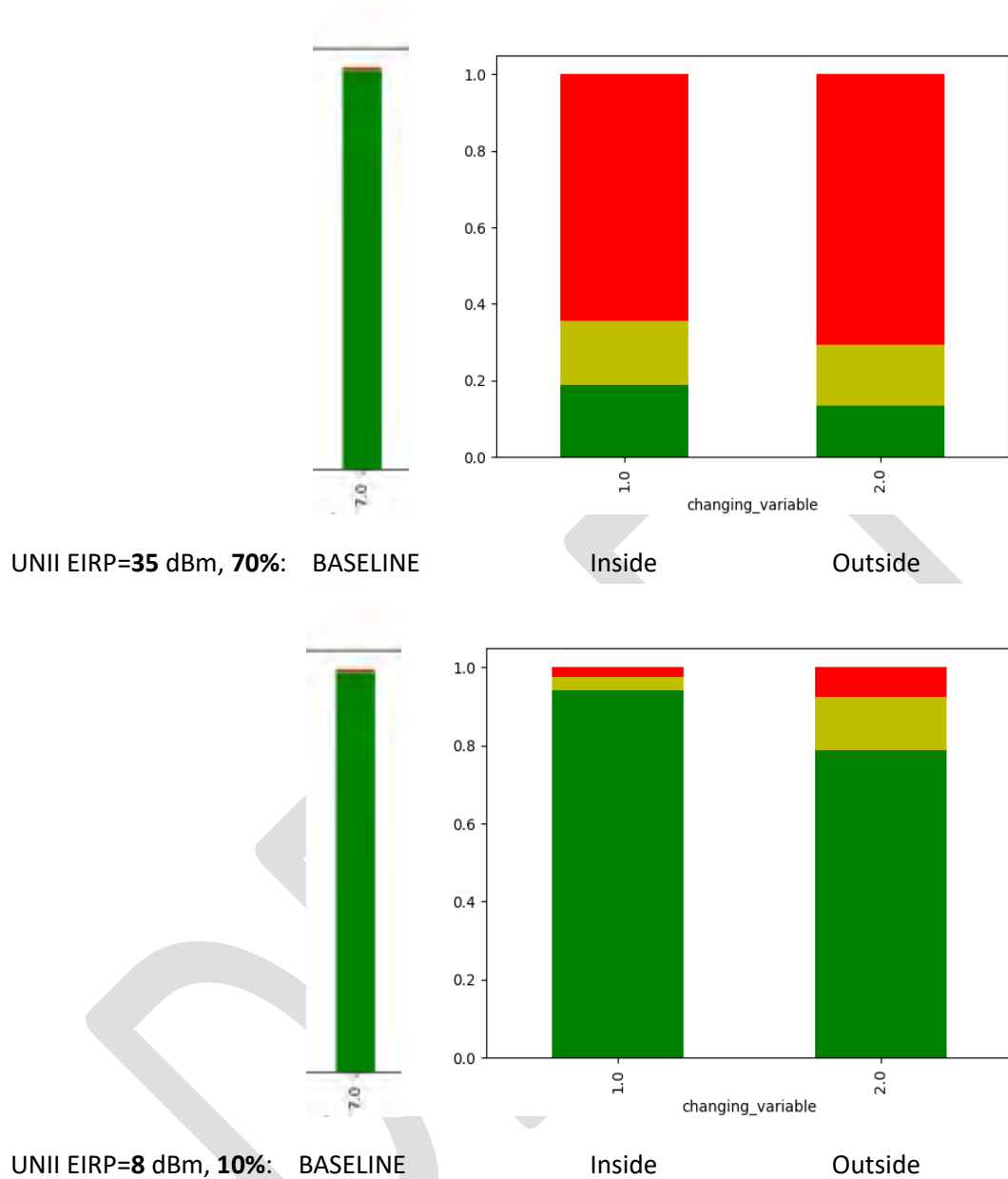


Figure 10-83. Comparing minimum and maximum interferer: Summary of packet gaps, V2I, UNII EIRP=35 dBm, approaching Wood building

Source: 20180206 Building-Wood E-side toward V1 -- was exl_report_toward_20180206_side2.xlsx, Tab: V2I mobile Rx to UNII=30-70%

Figure 10-84 is an aerial comparison of how PER is distributed spatially on the approach to the wooden building for the maximal case (top row) and the minimal case (bottom row). This figure shows more intuitively three important things. First, how DSRC communication was shut down in the maximal case regardless of the wooden building. Second, the size of the zone of disruption in the minimal case outdoors. Third, the kind of impact the building had to interference from the minimal UNII interferer.

You can see a small zone of disruption very near the building when the UNII was inside but you can also see that a large fraction of BSMs were received. The magenta of the minimal UNII inside with 10% PER is hard to distinguish from the hot magenta of the baseline at ~0% PER. (Color scale: Aqua is 100% PER and hot pink zero PER. As color scales from blue toward purple and pink the PER decreases.)

One needs to consider the specific information in Figures 10-80 to 10-82 above to determine if the distribution in time or space of the missing 10% of packets would impact safety. Moreover, whether the zone near the building is large enough and disrupted enough to again be untenable for safety. As discussed above, this case appears problematic for safety but a conclusive determination would require data at intermediate UNII power and load settings as well as more specific information about the sensitivity of safety applications to gaps in the DSRC traffic.

Note that the DSRC operated with an EIRP 5 dB higher than the maximum EIRP to be deployed according to the SAE standard. Hence, interference would be worse than shown here in a real deployment.

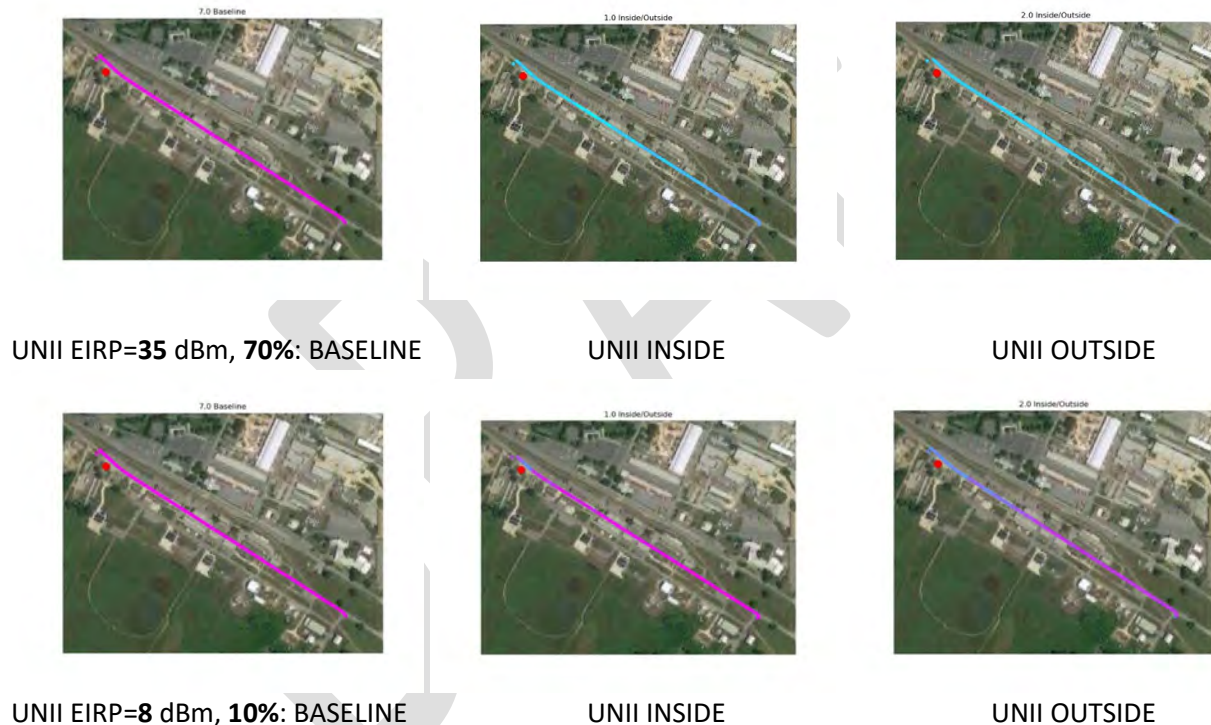


Figure 10-84. Comparing minimum and maximum interferer: Geographical distribution of PER, V2I, UNII EIRP=35 dBm, approaching Wood building

Source: 20180206 Building-Wood E-side toward V1 -- was exl_report_toward_20180206_side2.xlsx, Tabs: V2I mobile Rx to UNII=30-70% and V2I mobile Rx to UNII=3-10%

Distances and interference metrics vary a bit in the departing data and data from the west side where signals are cut off by trees and buildings. But because they lead to essentially the same conclusions we will not duplicate the above analysis for that data here. That data can be found in the appendices.

10.1.4 Impact of building material and type

{Section still under development}

10.1.4.1 USDOT field measurements

{Section still under development}

10.1.4.2 Correlation with NIST measurements of building materials.

As an analog we compare our packet error rate suppression with the attenuations measured by NIST. This provides a calibration point for anyone looking to translate lab measurements of materials to in the field effectiveness at isolating radio services in the same or adjacent channels. It should also help us in extrapolating material measurements into shielding effectiveness.

Table 10-1 directly compares the attenuation of PER that we measured with NIST measurements of attenuation by test materials. We don't expect the same values because of differences in materials, known and unknown. For example, our test building has filled cinderblocks rather than the normal hollow kind that NIST tested. We also did not measure wall thickness so those dimensions may not be the same. We were looking for macroscopic effects on interference and not to make a precise characterization of materials as was NIST's mission.

The NIST values in Table 10-1 come from data plots in NISTIR 6055, a report detailed in chapter 15. The red markings on the following plots place the USDOT in the same frequency and attenuation space as the NIST for a more visual comparison.

Table 10-1: Comparing USDOT building interference attenuation with NIST construction material RF measurements

Material	USDOT	NIST (attenuation compared to free space)
Cinderblock		-18 dB (8" hollow block)
Brick		-16 dB (89 mm holed red brick)
Wood		-4 dB (38 mm)

Figure 4.12d: Received Signal Magnitude (dB) for Masonry Block Walls (relative to free space).
Nominal thicknesses: CB1H = 203 mm; CB2H = 406 mm; CB3H = 610 mm
Dotted Curves represent +/- 1 standard deviation from mean (Solid Curves).
High Range Data: 3.0 to 8.0 GHz

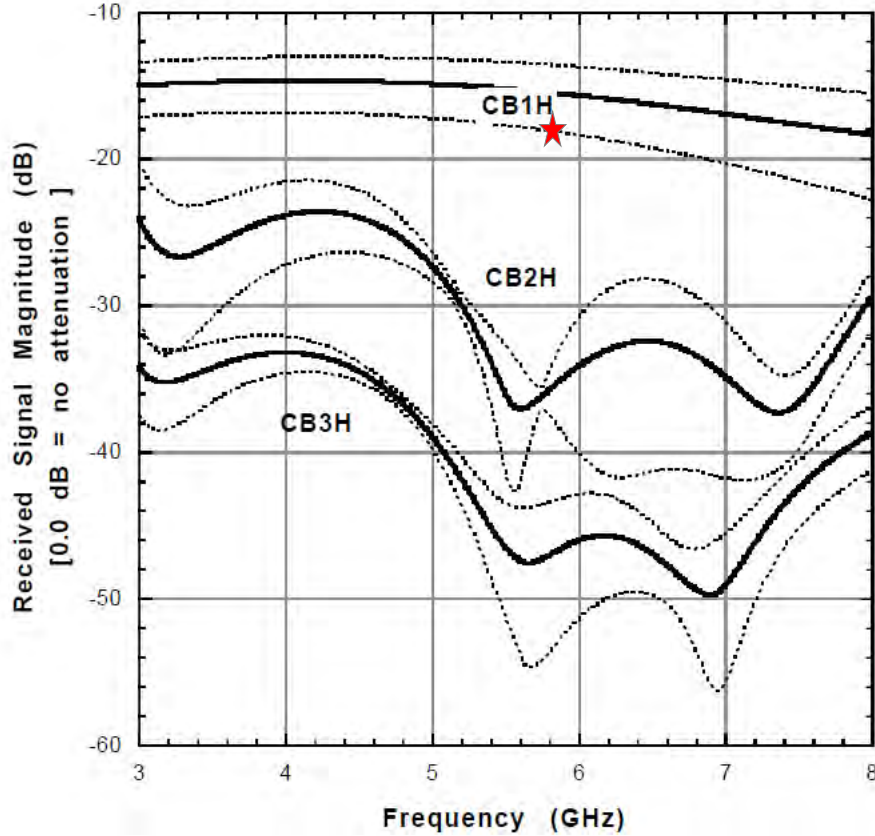


Figure 10-XXX1: Cinderblock attenuation⁵⁰

⁵⁰ NISTIR 6055, p133.



DRAFT

Figure 4.1d: Received Signal Magnitude for Brick (relative to free space)
B1L = 89 mm; B2L = 178 mm; B3L = 267 mm nominal Target Thickness.
Dotted Curves represent +/- 1 standard deviation from mean (Solid Curves).
High Range Data: 3.0-8.0 GHz. Amplitude Units: (dB)

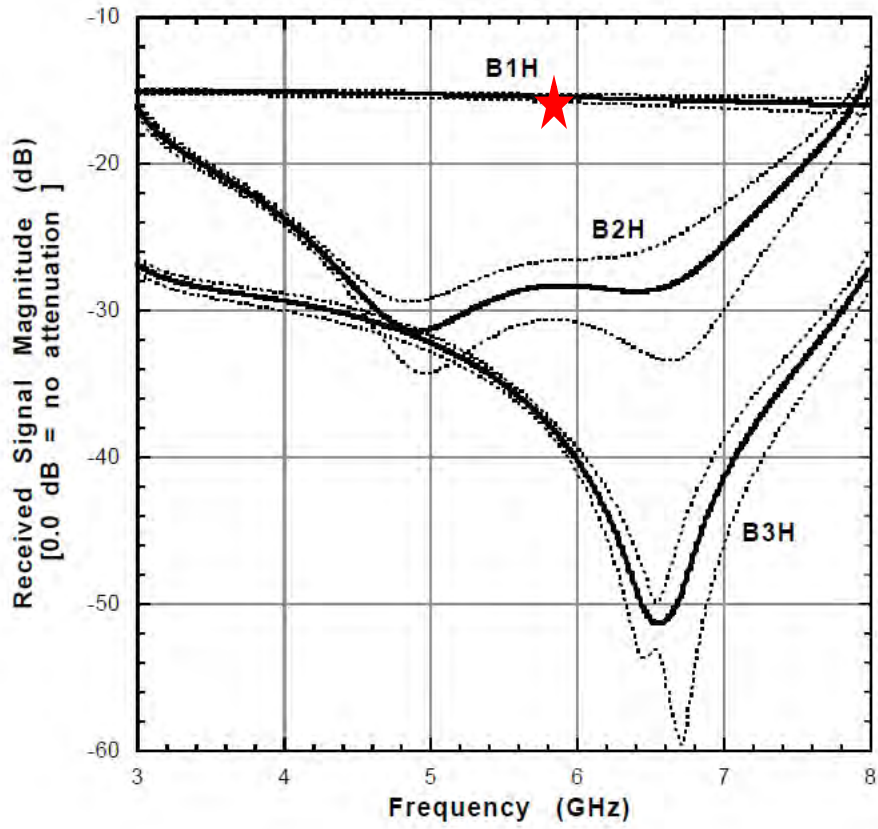


Figure 10-XXX2: Brick attenuation⁵¹

⁵¹ NISTIR 6055, p67.

Figure 4.15d: Received Signal Magnitude (dB) for Lumber (Spruce-Pine-Fir) (Dry) Panels (relative to free space).

L15DH = 38 mm; L30DH = 76 mm; L45DH = 114 mm; L60DH = 152 mm
Dotted Curves represent +/- 1 standard deviation from mean (Solid Curves).
High Range Data: 3.0 to 8.0 GHz

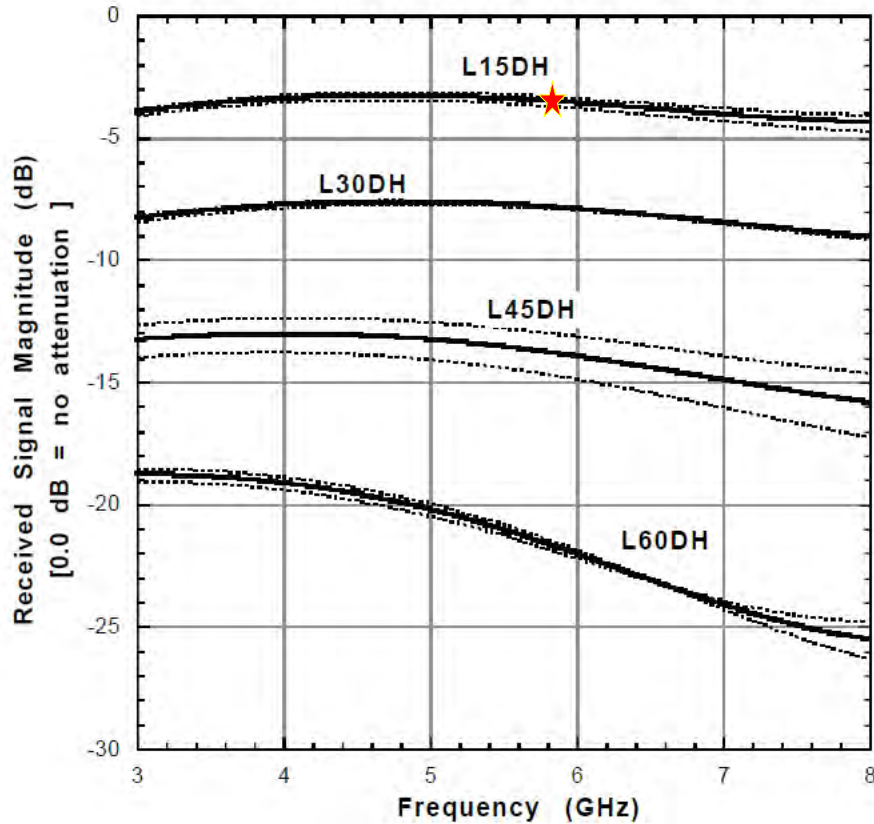


Figure 10-XXX3: Wood attenuation⁵²

⁵² NISTIR 6055, p151

Figure 4.12c: Transmission Coefficients for Masonry Block walls (relative to free space). Nominal thicknesses: CB1H = 203 mm; CB2H = 406 mm; CB3H = 610 mm. Dotted Curves represent +/- 1 standard deviation from mean (Solid Curves). High Range Data: 3.0 to 8.0 GHz

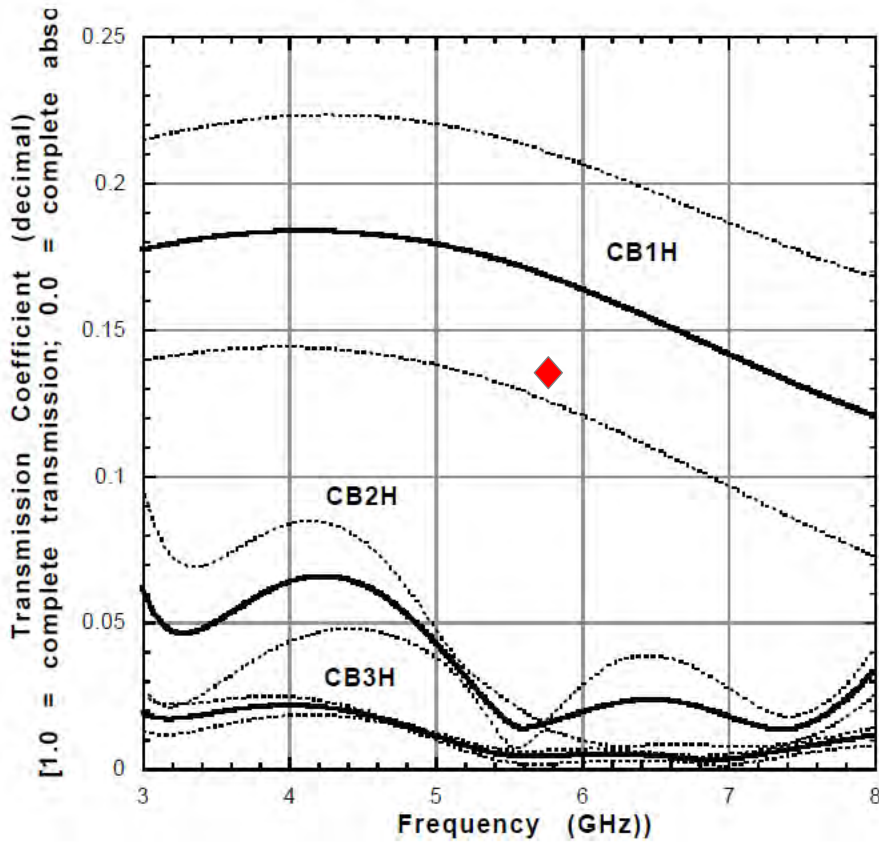


Figure 10-XXX4: RF transmission through Cinderblock⁵³

⁵³ NISTIR 6055, p132.

Figure 4.1c: Transmission Coefficients for Brick
B1L = 89 mm; B2L = 178 mm; B3L = 267 mm nominal Target Thickness.
Dotted Curves represent +/- 1 standard deviation from mean (Solid Curves).
High Range Data: 3.0-8.0 GHz. Amplitude Units: (decimal)

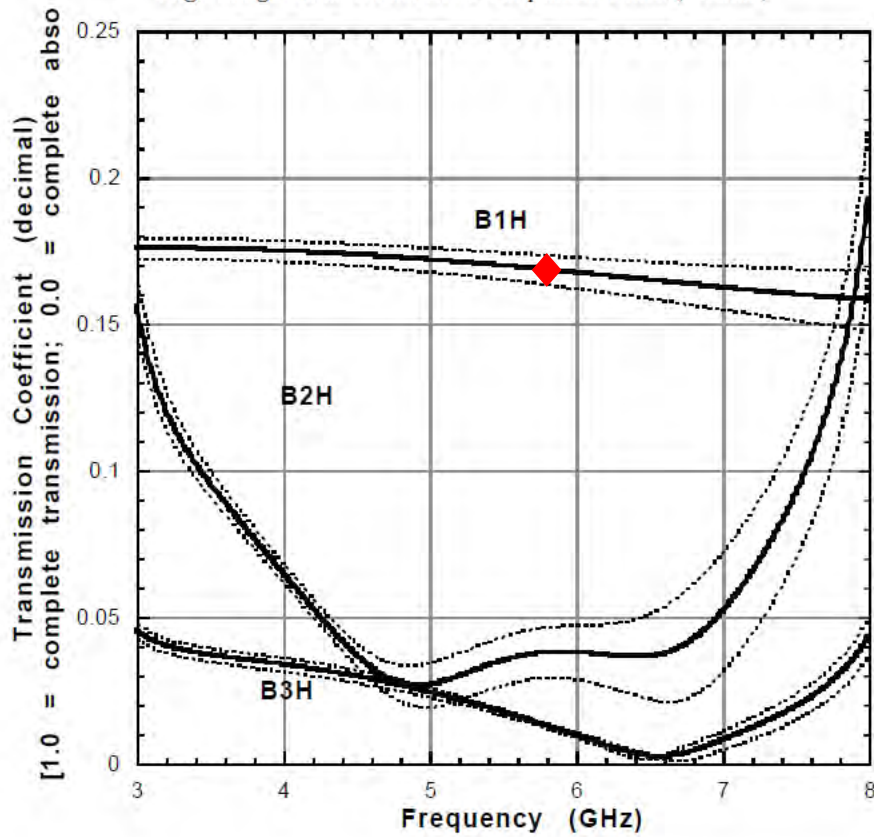


Figure 10-XXX5: RF transmission through Brick⁵⁴

⁵⁴ NISTIR 6055, p66.

Figure 4.15c: Transmission Coefficients for Lumber (Spruce-Pine-Fir) (Dry) Panels (relative to free space). Nominal thicknesses: L15DH = 38 mm; L30DH = 76 mm; L45DH = 114 mm; L60DH = 152 mm. Dotted Curves represent +/- 1 standard deviation from mean (Solid Curves). High Range Data: 3.0 to 8.0 GHz

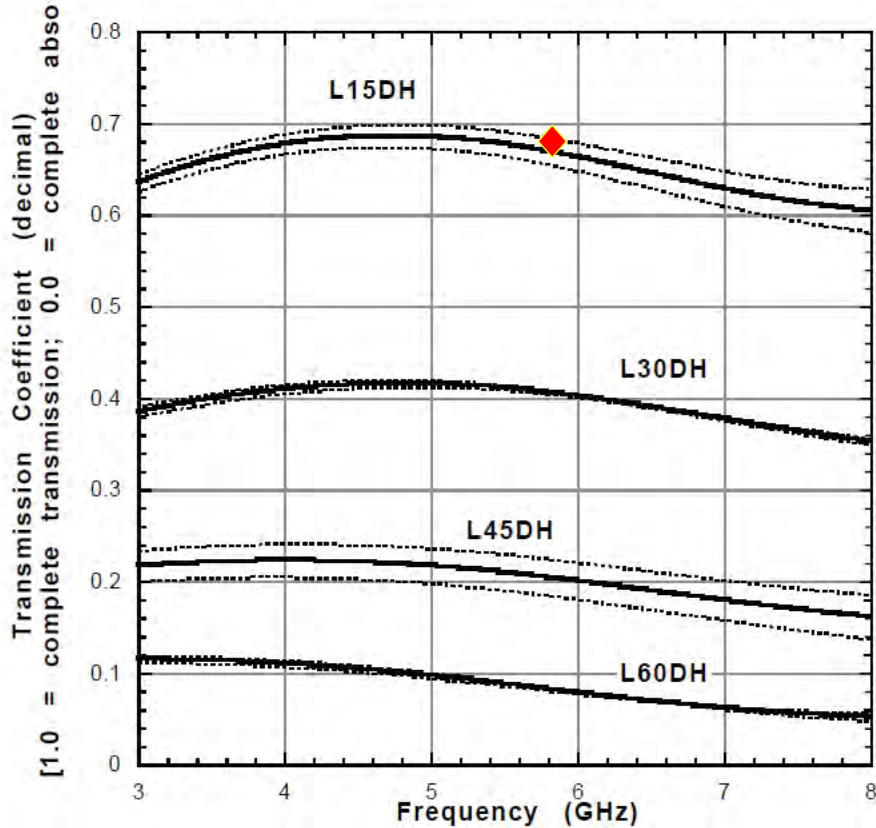


Figure 10-XXX5: RF transmission through Wood⁵⁵

The red clay brick used in this study was a common variety used in residential and commercial construction containing three circular weight-reduction holes along the longitudinal centerline (see Figure 3.1.1). The bricks had nominal lengths of 193 mm, a width of 90 mm, and a vertical thickness of 56 mm. The center holes differed in size with the center hole averaging 34 mm in diameter and the two end holes averaging 37 mm diameter. The brick is Grade MW, meeting specification ASTM C 652. wet on September 13, 2017

The concrete masonry block used in this study was also a common variety used in residential and commercial construction that included two large, approximately rectangular holes set towards either end of the block, a central thin rectangular slot; and a cutout on one end of the type typically used for window frame setting.⁵⁶

⁵⁵ NISTIR 6055, p150.

⁵⁶ NISTIR 6055, p37.

The U.S. Span Book for Major Lumber Species states that “more than 90%” of dimension lumber used in North America comes from four commercial species groups: Spruce-Pine-Fir; Douglas Fir-Larch; Hemlock-Fir, and Southern Pine. ... The specific type and grade obtained for the NLS Phase 2 tests was an off-the-rack “2x12x12-ft” (38 x 292 x 3658 mm) plank from the Lowe’s home improvement center in Gaithersburg, Maryland. The plank was manufactured by Finlay Forest Industries (Canada) with the specification KD-SPF #2 & Better, which stands for: “Kiln Dried, Spruce-Pine-Fir, Grade #2.”⁵⁷

10.2 Effect of Foliage

{Section still under development}

10.2.1 Dry Foliage

{Section still under development}

⁵⁷ NISTIR 6055, p52.



Figure 10-XXX1 Dynamometer course with dry foliage

10.2.2 Wet Foliage

{Section still under development}

10.2.3 Missing Foliage

{Section still under development}



Figure 10-XXX2 Dynamometer course after the foliage had fallen

10.3 Precipitation and pavement condition

{Section still under development}



Figure 10-YYY1. Snow at Perryman



Figure 10-YYY2. Testing in snowstorm

DRAFT

I 1. Comparison with other published results

{Section still under development}

I 2. Lessons Learned

{Section still under development}

I 3. Conclusions

{Section still under development}

I 4. Potential next steps

{Section still under development}

I 5. References

IEEE 802.11-2012, IEEE Standard for Information technology—Telecommunications and information exchange between systems Local and metropolitan area networks—Specific requirements, Part 11: Wireless LAN Medium Access Control (MAC) and Physical Layer (PHY) Specifications, IEEE Computer Society LAN/MAN Standards Committee, 29 March 2012. *Technical requirements for interoperability of Wi-Fi communications.*

IEEE P802.11ac™/D4.0, Draft STANDARD for Information Technology—Telecommunications and information exchange between systems—Local and metropolitan area networks—Specific requirements, Part 11: Wireless LAN Medium Access Control (MAC) and Physical Layer (PHY) specifications, Amendment 4: Enhancements for Very High Throughput for Operation in Bands below 6 GHz, Prepared by the 802.11 Working Group of the 802 Committee, October 2012. *Technical requirements for very high throughput Wi-Fi communications.*

FCC 99-305, FCC Report & Order, Adopted: October 21, 1999, Released: October 22, 1999. *Allocated 75 megahertz of spectrum at 5.850-5.925 GHz to the mobile service for use by Dedicated Short Range Communications ("DSRC") systems operating in the Intelligent Transportation System ("ITS") radio service.*

FCC 03-324, FCC Report & Order, Adopted: December 17, 2003, Released: February 10, 2004. *Adopted licensing and service rules for the Dedicated Short Range Communications Service (DSRCS) in the Intelligent Transportation Systems (ITS) Radio Service in the 5.850-5.925 GHz band (5.9 GHz band).*

FCC 06-110, FCC Memorandum & Order, Adopted: July 20, 2006, Released: July 26, 2006. *Provided new channel designations, site construction priorities, and altered power limitations in the DSRC band.*

SAE J2735, SAE International, Surface Vehicle Standard, Dedicated Short Range Communications (DSRC) Message Set Dictionary, March 2016. *Defines the data elements that compose DSRC messages as well as DSRC concepts.*

SAE J2945/1, SAE International, Surface Vehicle Standard, On-Board System Requirements for V2V Safety Communications, March 2016. *Defines concept of operations and minimum requirements for interoperable DSRC safety communications.*

NISTIR 6055, NIST Construction Automation Program, Report No. 3, Electromagnetic Signal Attenuation in Construction Materials, Building and Fire Research Laboratory Gaithersburg, Maryland 20899, United States Department of Commerce, Technology Administration, National Institute of Standards and Technology, William C. Stone, October 1997. *Electromagnetic power attenuation measurements to characterize various building material in two frequency bands (0.5-2 GHz and 3-8 GHz).*

Appendix A: DSRC Terminology

Term	Definition
After Market Device	An OBU that is not built into the vehicle by the OEM but purchased and installed after the vehicle has been sold.
BSM	Basic Safety Message – Messages from OBUs containing vehicle data including GPS location coordinates. With the communication and security overhead they can vary from roughly 170 – 470 octets long depending on how many points are in the path history variable.
DSRC	Dedicated Short Range Communication, microwave communications in the band 5850-5925 MHz governed by the IEEE 802.11p standard developed especially for mobile safety communications. IEEE 802.11p was folded into IEEE 802.11-2012.
Frame	In the OSI model of computer networking, a frame is the protocol data unit at the data link layer. Frames are the result of the final layer of encapsulation before the data is transmitted over the physical layer. [1] A frame is "the unit of transmission in a link layer protocol, and consists of a link layer header followed by a packet." [2] Each frame is separated from the next by an interframe gap. A frame is a series of bits generally composed of framing bits, the packet payload, and a frame check sequence. An example would be an Ethernet frame.
Handheld DSRC	Portable DSRC – DSRC radio in a handheld device such as a smartphone or tablet
MAP	Message that defines the geometry of an intersection. A companion to SPaT. Can be 1000-1500 octets long.
OBE	On-board Equipment – Electronic equipment in a vehicle that includes an OBU
OBU	Onboard Unit – DSRC radio, processors and memory that are necessary for DSRC communications mounted in a vehicle
Packet	A formatted unit of data carried by a packet-switched network. Computer communications links that do not support packets, such as traditional point-to-point telecommunications links, simply transmit data as a bit stream. When data is formatted into packets, the bandwidth of the communication medium can be better shared among users than if the network.
RSE	Roadside Equipment – Traffic equipment near a road, may contain an RSU
RSU	Roadside Unit – DSRC radio, processors and memory that are necessary for DSRC communications mounted to fixed or moveable but not mobile infrastructure
SPaT	Signal Phase and Timing – Data from a traffic signal controller giving signal status and the timing of upcoming state changes in all directions. Can be a few to a thousand octets long.
V2I	Vehicle-to-Infrastructure, DSRC communication between OBUs and RSUs. This entails a more varied range of message sizes and purposes.
V2V	Vehicle-to-Vehicle, DSRC communication between OBUs. This will be predominantly via the broadcast of BSMs.

Term	Definition
V2X	Vehicle-to-Other, This not defined consistently. Sometimes defined as an umbrella term for all DSRC communications, but defined by others as DSRC communications involving handheld and other devices that are not OBUs or RSUs. This document avoids use of the term but the authors subscribe to the latter definition.

DRAFT

Appendix B: Mapping this report to the test plan

{Section still under development}

DRAFT

Appendix C: Clear Channel Access Mechanism

Clear Channel Access (CCA) is a mechanism by which radios listen to the channel and wait until they hear it is clear before transmitting to avoid packet collisions. DSRC uses Enhanced Distributed Channel Access (EDCA) parameters to control its CCA mechanism. The following text are two excerpts from a whitepaper not yet published, "Radio Density versus Traffic Density," by Alan Chachich, USDOT/OST-R/Volpe Center, 2014.

C.1 First excerpt to explain what happens in the time between packets:

But that's not all. The total time a message ties up the channel has two components. Most obvious is the time the message is being sent. Less obvious is the forced idle time on the channel to keep transmitters from clashing. *Rockwell Collins/ARINC determined that was typically half as long as a BSM message or roughly a third of the total message time.*

This idle time is called the interframe spacing. See the following text box and figure B-1 below.

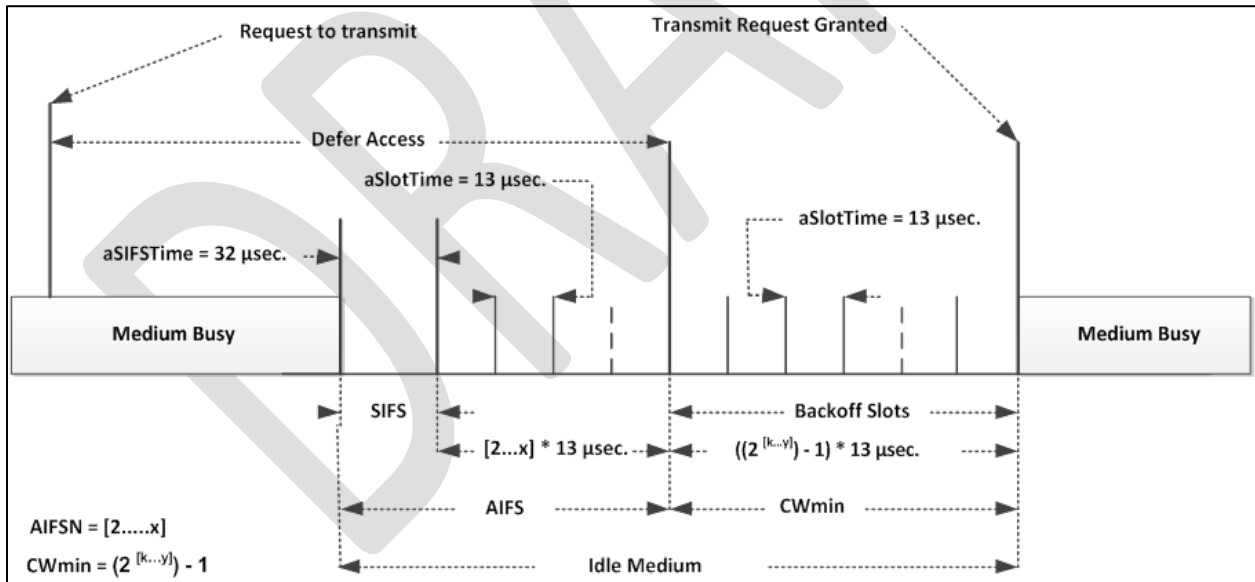


Figure C-1. Breakdown of Interframe Spacing

AIFS: Arbitration Interframe Spacing
 CWmin: Minimum contention window
 SIFS: Short Interframe Space

INTERFRAME SPACING

Interframe spacing has two parts.

The first is to make sure the channel is clear and the second is to avoid clashing with others also waiting for the channel to clear.

Part 1. Make sure the channel is clear

This is the AIFSN (Arbitration Interframe Space Number)

The AIFSN is composed of the SIFS (Short Interframe Space) + a certain number of slot times.

The Short Interframe Space gives the radio time to switch back into receive mode so it can receive the acknowledgement of the message frame it just sent. It is a constant determined by the appropriate 802.11 standard. *ARINC used 32 microseconds (μs) for 10 MHz since it is specified by the 802.11-2007 standard (see Table A-1).*

The Slot time is twice the time it should take a pulse to travel to the farthest node on the network. Waiting one slot time should allow the intended receiver to get the message before it can collide with the next transmission. *ARINC used 13 μs for 10 MHz since it is specified by the 802.11-2007 standard (see Table A-1).*

The default number of slot times waited is either, 2, 3, 6 or 9.

BSMs aren't acknowledged, so in the 802.11p standard the AIFSN is for prioritizing messages. The highest priority would be given the smallest AIFSN so it waits less.

Part 2. Avoid clashing with other transmitters who may also be waiting for the channel to clear

That is the CWmin (minimum Contention Window)

This is an additional random time delay added to the AIFSN so that all radios waiting to transmit do not start at the same time. It is an integer number of slot times chosen randomly from a range of numbers. *ARINC used the ranges specified in the VAD standard, $n=31$. See Table A-1. They based their calculation on the value in the middle of range to calculate the average wait time (i.e., half the maximum or $31/2 = 15.5$).*

C.2 Second excerpt to explain EDCA parameters:

Background

EDCA was added to the IEEE 802.11 standard in 2005 via 802.11e to introduce a way to prioritize messages that try to access the channel at the same time. The 802.11p WAVE (DSRC) standard that followed 5 years later built on it.

EDCA was introduced in 802.11 for typical mixed Wide Area Network (WAN) traffic. That includes video and voice which are delay sensitive but loss-tolerant and best effort or background data that tends to be delay tolerant but loss sensitive.

DSRC safety data is not like either of these two types of message traffic. It tends to be periodic and not streaming data. It is latency sensitive but not like real-time data. Delay in channel access of tens of milliseconds is OK, which is more than video or voice data can tolerate. It is more sensitive to delay than file transfer data but less sensitive than video and voice.

It is loss sensitive, but not as sensitive as file transfer data. So it is more sensitive to loss than video and more sensitive to delay than file transfer data. Table B-1 summarizes the different types of data assigned priority in 802.11p. Figure B-2 shows how the EDCA parameters implement priority in time.

Table C-1: Packet Data Types

Data type	Latency	Packet Loss	Characteristic
Video	Extremely sensitive	Tolerant	Streaming – real-time
Voice	Extremely sensitive	Tolerant	Streaming – real-time
Best effort data	Tolerant	Extremely sensitive	Streaming Large files
Background data	Tolerant	Extremely sensitive	Large files
DSRC BSMs	Tolerant to delay < 10's of ms Sensitive > 10's of ms	Sensitive	Periodic, smaller, not quite real-time

The optimum EDCA parameters for DSRC should minimize packet collisions and keep latencies to a few tens of milliseconds.

Figure C-2: Depiction of 802.11 default EDCA parameters

(Source: John Kenny, Toyota)

As described above, the mechanism to assign priority is the AIFSN. Remember that smaller AIFSN means shorter wait so preferential access to the channel. Assign this to higher priority packets.

The mechanism to avoid collision is the CWmin parameter that sets the contention window. Larger CWmin can reduce packet collisions, but if the channel is not congested it adds delay.

The 802.11 standard provides for 8 levels of priority, but half are essentially unused by DSRC. It suggests options for the values these parameters can take which are summarized in Table 2. But since channel 172 is just for safety traffic, that priority scheme isn't particularly helpful. The VAD and RSU specifications essentially say that AIFSN and CWmin can be determined by the chip set as provided by the vendor.⁵⁸

Concluding excerpts

Selecting the EDCA parameters is very complicated. Choosing the best values depend on whether or not the traffic in the channel is all at the same priority (homogeneous) or different priorities (heterogeneous) and the density (number of radios in range trying to access the channel). Those are factors that can change by time and location.

⁵⁸ USDOT, "System Requirement Description - 5.9GHz DSRC Vehicle Awareness Device Specification" V3.6, 1/24/2012 and v3.8, 3/18/2014; "DSRC Roadside Unit (RSU) Specifications Document" V4.0 4/15/2014

As a result, the selection of EDCA parameters for DSRC messages as well as the mechanism to define and enforce them is still a work in process.

The following table, also excerpted from the Volpe White paper, indicates the range of values that could be considered for DSRC. Note that these values are simply illustrative because the actual number of priority levels hasn't been decided and there are other schemes beside the virtual division scheme used as an example in this table.

Even though the selection of EDCA parameters for traffic internal to DSRC is still TBD, the detectability analysis described in section 5.4 of this analysis plan will experiment with different EDCA values for DSRC and unlicensed devices to determine how they might factor into potential sharing of the band.

Table C-2: Summary of Recommended EDCA Parameters

Access Category	IEEE 802.11p Default EDCA Parameter Set		Recommendation for homogenous traffic		Toyota's recommended defaults for heterogeneous traffic and virtual division with 3 priority levels	
	AIFSN	CW _{min}	AIFSN	CW _{min}	AIFSN	CW _{min}
AC0	9	15	X	X	x	x
AC1	6	15	X	X	14	15
AC2	3	7	X	X	6	7
AC3	2	3	2	15 or 31	2	3

Appendix D: Experimental License

Appendix E: Radio Calibrations

{Section still under development}

Appendix F: Antenna Patterns

{Section still under development}

Appendix G: DSRC Baselines

{Section still under development}

Appendix H: Surrogate UNII-4 Testbed Baselines

{Section still under development}

Appendix I: Sensitivity Testing

{Section still under development}

Appendix J: Effect of the Wi-Fi inter-packet space distribution on interference

{Section still under development}

Appendix K: Adjacent Channel Sensitivity and Interference

{Section still under development}

Appendix L: Transmission Suppression and EDCA configurations

{Section still under development}

Appendix M: EDCA channel access whitepaper

{Section still under development}

Appendix N: DSRC Radio Density Study

{Section still under development}

Appendix O: Outdoor Access Point Interference Data

{Section still under development}

Appendix P: Indoor Access Point Interference Data

{Section still under development}

Appendix Q: Wi-Fi In-Vehicle Access Point Interference Data

{Section still under development}

Appendix R: High Closing Speed near Access Point Interference Data

{Section still under development}

Appendix S: Maximum Range DSRC and UNII Data

{Section still under development}

Appendix T: 40 DSRC Radio Interference Data

{Section still under development}

Appendix U: Interference Data under Rain, Snow, and Pavement wet versus dry

{Section still under development}

U.S. Department of Transportation
Intelligent Transportation Systems Joint Program Office (ITS JPO)
1200 New Jersey Avenue, SE
Washington, D.C. 20590
202-366-9536